PAL
5811o

Palæontographica Americana

MCZ
LIBRARY
JUL 31 1991
HARVARD
UNIVERSITY

NUMBER 57 JUNE 28, 1991

Revised taxonomic procedures and paleoecological applications for some North American Mississippian Fenestellidae and Polyporidae (Bryozoa)

by

Edward McKinley Snyder

1989 Winner of the Osgood Prize

PALEONTOLOGICAL RESEARCH INSTITUTION

Officers

PRESIDENT	HARRY A. LEFFINGWELL
VICE-PRESIDENT	J. THOMAS DUTRO, JR.
SECRETARY	HENRY W. THEISEN
TREASURER	JAMES C. SHOWACRE
ASSISTANT TREASURER	ROGER J. HOWLEY
DIRECTOR	PETER R. HOOVER
LEGAL COUNSEL	HENRY W. THEISEN

Trustees

BRUCE M. BELL (to 6/30/93)
CARLTON E. BRETT (to 6/30/92)
J. THOMAS DUTRO, JR. (to 6/30/93)
HARRY A. LEFFINGWELL (to 6/30/93)
ROBERT M. LINSLEY (to 6/30/92)
CATHRYN NEWTON (to 6/30/91)
SAMUEL T. PEES (to 6/30/92)
EDWARD B. PICOU, JR. (to 6/30/92)
JAMES C. SHOWACRE (to 6/30/93)
JAMES E. SORAUF (to 6/30/91)
JOHN STEINMETZ (to 6/30/91)
HENRY W. THEISEN (to 6/30/92)
RAYMOND VAN HOUTTE (to 6/30/91)
WILLIAM P. S. VENTRESS (to 6/30/93)
A. D. WARREN, JR. (to 6/30/91)

BULLETINS OF AMERICAN PALEONTOLOGY

and

PALAEONTOGRAPHICA AMERICANA

PETER R. HOOVER .... EDITOR

Reviewers for this issue

A. HOROWITZ F. K. MCKINNEY

A list of titles in both series, and available numbers and volumes may be had on request. Volumes 1–23 of *Bulletins of American Paleontology* have been reprinted by Kraus Reprint Corporation, Route 100, Millwood, New York 10546 USA. Volume 1 of *Palaeontographica Americana* has been reprinted by Johnson Reprint Corporation, 111 Fifth Ave., New York, NY 10003 USA.

Subscriptions to *Bulletins of American Paleontology* may be started at any time, by volume or year. Current price is US $45.00 per volume. Numbers of *Palaeontographica Americana* are priced individually, and are invoiced separately on request.

for additional information, write or call:

Paleontological Research Institution
1259 Trumansburg Road
Ithaca, NY 14850 USA
(607) 273-6623

Table 7.—Definition of zoecial and zoarial characters used in species descriptions. The numbers preceding characters are used as abbreviations for those characters in Tables 10–46. They are defined in numerical order in Table 8a. **E** = in external view; **I** = in internal view; use of the symbol ≫ between these abbreviations indicates greater importance of the view abbreviated to the left.

A. Zoarial character

1. *branch width* (**WB**).—Measured perpendicular to direction of branch growth (in plane of frond); measurements are not made near dissepiments or branch bifurcations; exhibits high coefficients of variation in most species due to secondary or lamellar thickening of the branch (see Text-figs. 4A, 6A, 6B, 9A) .... **E or I**
2. *distance between branch centers* (**DBC**).—Measured between areas of branch bifurcation; has a high coefficient of variation among species (see Text-fig. 6A) .... **E or I**
3. *dissepiment width* (**WD**).—Measured parallel to direction of branch growth, in middle of dissepiment; has a high coefficient of variation due to secondary skeletal thickening (see Text-figs. 4A, 6C, 7B) .... **E ≫ I**
4. *length of fenestrule opening* (**LF**).—Measured parallel to direction of colony growth between dissepiment edges; used by Elias and Condra (1957) as one of the primary diagnostic characters of *Fenestella,* but coefficients of variation calculated herein raise questions as to its significance; decreasing fenestrule length is associated with secondary dissepiment thickening, and ontogenetic change in fenestrule length is a colony response to environmental pressures (see Text-figs. 4A, 6C, 7B) .... **E or I**
5. *width of fenestrule opening* (**WF**).—Measured perpendicular to growth axis between branch edges at maximum diameter of openings; moderately to highly variable due to correlation of decrease in fenestrule width with secondary branch thickening (see Text-fig. 4A) .... **E or I**
6. *number of aperture openings per fenestrule length* (**AF**).—Measured along one side of branch between dissepiment centers, counting complete apertures or those with greater than half of opening present in the interval between dissepiments; constant within most species, although some species have between two and four apertures per fenestrule, thus decreasing the usefulness of this character (see Text-fig. 4A) .... **E ≫ I**
12. *diameter of nodes along obverse branch surface* (**DN**).—Maximum node diameter; these features are highly symmetrical (see Text-fig. 4A) .... **E ≫ I**
13. *diameter of nodes on dissepiments* (**DND**).—Measured on obverse dissepiment surface (see Text-fig. 4A) .... **E ≫ I**
14. *distance between node centers along obverse branch surface* (**SNB**).—Included in the original meshwork formula of Ulrich (1890) [see p. 18]; high coefficients of variation for this character limit its usefulness (see Text-fig. 4A) .... **E or I**
15. *width of keel* (**WK**).—Measured perpendicular to direction of branch growth in plane of frond (see Text-fig. 4A) .... **E or I**
16. *diameter of stylets on obverse surface* (**DSO**).—Measured at maximum stylet diameter (see Text-fig. 4A) .... **E or I**
17. *spacing of stylets along obverse branch surface* (**SSO**).—Highly variable for most species; moderately constant for a few (see Text-fig. 4A) .... **E or I**
21. *diameter of macrostylets on reverse branch surface* (**RSL**).—Measured at maximum macrostylet diameter; highly variable (see Text-fig. 4B) .... **E or I**
22. *diameter of microstylets on reverse branch surface* (**RSS**).—Measured at maximum microstylet diameter (see Text-fig. 4B) ... **E ≫ I**
23. *spacing of macrostylets along reverse branch surface* (**SSL**).—Measured between macrostylet centers; has an extremely high coefficient of variation (see Text-fig. 4B) .... **E or I**
24. *spacing of microstylets along reverse branch surface* (**SSS**).—Measured between microstylet centers; both microstylet diameter and microstylet spacing have high coefficients of variation (see Text-fig. 4B) .... **E ≫ I**
25. *reticulate meshwork spacing parallel to direction of branch growth* (**LRM**).—Measured between mesh centers; closely correlated to spacing and number of apertures along obverse surface; used in *Hemitrypa* (see Text-fig. 5A, 5B) .... **E or I**
26. *reticulate meshwork spacing perpendicular to direction of branch growth* (**WRM**).—Measured between mesh centers; closely correlated to spacing and number of apertures along obverse surface; used in *Hemitrypa* (see Text-fig. 5A, 5B) .... **E or I**
27. *spacing of whorls along central axis* (**WSC**).—Measured between sites of maximum whorl expansion; corresponds to "number of volutions in 2 cm" of Ulrich (1890), but provides a more accurate determination of variability of the central axis of *Archimedes*; apparently strongly influenced by environment; used only in *Archimedes* (see Text-fig. 5C) .... **E or I**
28. *maximum diameter of central axis* (**DCA**).—Measured perpendicular to direction of axis emplacement at maximum whorl diameter; used only in *Archimedes* (see Text-fig. 5C) .... **E ≫ I**
29. *angle between distal end of axis and axial whorl* (**ACA**).—An acute angle; high coefficient of variation probably reflects environmental influence; used only in *Archimedes* (see Text-fig. 5C) .... **I ≫ E**
34. *thickness of front-wall (obverse-wall) laminated layer* (**FWT**).—Measured as thickness of laminated skeletal material between exterior side of obverse granular skeletal layer and outer edge of laminated skeleton on obverse exterior zoarial surface; shows pronounced increase with ontogeny (see Text-figs. 6B, 6D, 9C) .... **I**
35. *thickness of reverse-wall laminated layer* (**RWT**).—Measured as thickness of laminated skeletal material between exterior side of reverse granular skeletal layer and outer edge of laminated skeleton on reverse exterior zoarial surface; increases with ontogeny, producing high coefficients of variation (see Text-figs. 6B, 6D, 9A, 9C) .... **I**
43. *thickness of branch* (**TB**).—Measured across branch in obverse–reverse direction; pronounced increase with ontogeny (see Text-figs. 6A, 7A) .... **I**

Table 7.—Continued.

B. Zooecial features

7. *aperture length* (**AL**).—Inside diameter of apertural opening, measured parallel to direction of branch growth; measured on exterior surface where possible, due to problems in defining aperture orientation in shallow tangential sections (see Text-figs. 4A, 6C, 7B) .... **E ≫ I**
8. *aperture width* (**AW**).—Inside diameter of apertural opening, measured perpendicular to direction of branch growth; apertures inclined into fenestrules are measured in their apertural planes; measured on exterior surface where possible, due to problems in defining aperture orientation in shallow tangential sections (see Text-figs. 4A, 6C) .... **E ≫ I**
9. *distance between aperture centers along branch* (**ADB**).—Measured between closest apertures parallel to direction of branch growth (see Text-fig. 4A) .... **E ≫ I**
10. *distance between aperture centers across branch* (**AAB**).—Measured between closest apertures across branch; direction of measurement is frequently diagonal to branch length and width; often has means similar to **ABB** (see below) and low coefficients of variation, probably reflecting symmetrical areal coverage of lophophore feeding zones (see Text-fig. 4A) .... **E ≫ I**
11. *distance between aperture centers between branches* (**ABB**).—Measured between closest apertures between branches, across fenestrule opening or dissepiment; often has means similar to **AAB** (see above) and low coefficients of variation, probably reflecting symmetrical areal coverage of lophophore feeding zones (see Text-fig. 4A) .... **E ≫ I**
18. *width of peristome* (**WP**).—Measured at distal end of aperture; increases with colony ontogeny and can thicken to cap apertures on proximal end of the zoarium (see Text-fig. 4A) .... **E or I**
19. *number of stylets surrounding aperture* (**SA**).—Stylet number is very constant within a species, suggesting (where they are present, as they do not occur in all species) a possible function as tentacle guides for the polypide (see Text-fig. 4A) .... **E or I**
20. *diameter of stylets surrounding aperture* (**SAD**).—Measured as maximum diameter of apertural stylets (see Text-figs. 4A, 6C) .... **I ≫ E**
30. *ovicell length* (**OL**).—Inside diameter of enlarged polymorph exterior opening, measured parallel to direction of branch growth (see Text-fig. 4A) .... **E ≫ I**
31. *ovicell width* (**OW**).—Inside diameter of enlarged polymorph exterior opening, measured perpendicular to direction of branch growth; ovicells occur fairly rarely in most fenestrates, being most commonly found in *Hemitrypa* and polyporids (see Text-fig. 4A) . **E ≫ I**
44. *maximum width of ovicell in mid tangential view* (**WOT**).—Used only where enlarged polymorph chamber alters inner dimension of chamber width .... **I**
32. *thickness of reverse-wall granular layer* (**TRW**).—Measured across granular layer in longitudinal or transverse sectional view; granular skeletal material forms a complete lining of chambers in most fenestrates; has low coefficients of variation; much higher coefficients of variation are found in laminated skeletal characters; due to position of granular skeleton surrounding the zooecial chamber, granular skeletal material is considered to be zooecial (see Text-figs. 6B, 7A, 7C) .... **I**
33. *thickness of chamber lateral-wall granular layer* (**TLW**).—Measured in longitudinal view (see Text-figs. 6D, 7C) .... **I**
36. *autozooecial chamber length* (**CL**).—Maximum inside dimension of chamber measured subparallel to branch growth axis and parallel to long axis of chamber; measured in longitudinal view; may be taken between lateral chamber walls (Text-fig. 6) or between obverse and reverse chamber walls (Text-fig. 7); represents the maximum chamber length regardless of orientation of the measurement, although orientation must be included in the descriptive analysis; has great taxonomic and biologic significance (see Text-figs. 6D, 7C) .... **I**
37. *autozooecial chamber depth* (**CD**).—Inside diameter of chamber in longitudinal view, measured perpendicular to chamber length; measured only in longitudinal view (see Text-figs. 6D, 7C) .... **I**
38. *maximum chamber width* (**MAW**).—Measured across the branch; measured in a median tangential section taken parallel to the zoarial obverse surface (see Text-figs. 6C, 7B) .... **I**
39. *minimum chamber width* (**MIW**)—Measured across the branch; measured in a median tangential section taken parallel to the zoarial obverse surface; used for chambers that are polygonal or ovate-truncate in this view, but excludes those that are triangular, square, or rectangular (see Text-figs. 6C, 7B) .... **I**
40. *vestibule depth* (**VD**).—Measured perpendicular to plane of zoarial surface from outer edge of apertural opening to where vestibule opens into main chamber; measured in longitudinal section; the most variable of all chamber characters, due to increase in vestibule length as the obverse laminated skeletal material thickens (see Text-figs. 6D, 7C) .... **I**
41. *chamber reverse-wall budding-angle* (**RA**).—Measured at base of chamber, where lateral and reverse walls merge; measurement made from distal end of colony, in longitudinal view; represents angle of autozooecial chamber lateral-wall emplacement relative to direction of branch growth (typically an acute angle); has an extremely low coefficient of variation (see Text-figs. 6D, 7C) ..... **I**
42. *chamber lateral-wall budding-angle* (**LA**).—Measured in transverse view, this is the angle between a line perpendicular to the plane of the obverse surface and a line from the center of the aperture, through the middle of the chamber toward the reverse wall and intersecting with the line perpendicular with the obverse surface (see Text-figs. 6A, 7A) .... **I**

Table 8a.—Outlines of species diagnoses and descriptions, and definitions of measurements and terminology (in *italics*) employed therein. Definitions are either absolute or relative; in relative definitions, arrows [→] separate terms that indicate points in continua. Comparators of size may be further subdivided by the use of the terms "lower-end," "mid," and "upper-end," to indicate the bottom, middle, and top of the range, respectively. Abbreviations of measurements are explained in Table 8b. CV = coefficient of variation.

Outline of the **Diagnosis**

1. Zoarial characters
   - A. relative robustness (*delicate* [fragile, zoaria frequently broken and small] → *intermediate* [moderate number of large zoaria present, resist breakage better than delicate forms] → *robust* [zoaria typically large, highly resistant to breakage])
   - B. mesh spacing (*close* [**WF** < **WB**] → *intermediate* [**WF** ≅ **WB**] → *open* [**WF** > **WB**])
   - C. mesh uniformity (regular or irregular)
   - D. secondary zoarial features (*e.g.,* reticulate meshwork and central axis)
2. Branch characters
   - A. robustness (*delicate* [fragile, frequently crushed, thin width and depth] → *intermediate* [moderate preservation, width and depth intermediate] → *robust* [wide, thick, typically well-preserved])
   - B. width (*narrow* [<0.30 mm] → *intermediate* [0.30–0.39 mm] → *wide* [>0.39 mm])
   - C. branch thickness (*thin* [<0.30 mm] → *medium* [0.30–0.39 mm] → *thick* [>0.39 mm])
   - D. proximodistal trace (*e.g.,* straight, sinuous, broadly curved)
   - E. shape in transverse cross-section (*e.g.,* elliptical, ovate, circular, semicircular, rhombic, polygonal)
   - F. spacing (*close* [**DBC** < 2.0 × **WB**] → *intermediate* [**DBC** 2.0–2.5 × **WB**] → *wide* [**DBC** > 2.5 × **WB**])
3. Dissepiments
   - A. width (*thin* [<0.5 × **WB**] → *intermediate* [0.5–1.0 × **WB**] → *wide* [>1.0 × **WB**])
   - B. length (*short* [**WF** ≪ **WB**] → *intermediate* [**WF** ≅ **WB**] → *long* [**WF** ≫ **WB**])
   - C. placement (regular or irregular intervals)
4. Fenestrule
   - A. size (*small* [length <0.4 mm; width <0.24 mm] → *intermediate* [length 0.4–0.9 mm; width 0.24–0.34 mm] → *large* [length >0.9 mm; width >0.34 mm])
   - B. shape (*e.g.,* elliptical, ovate, rectangular, square, circular)
   - C. uniformity of shape (regular or variable)
5. Autozooecial apertures
   - A. relative size (*small* [length <0.09 mm; width <0.07 mm] → *intermediate* [length 0.09–0.15 mm; width 0.07–0.12 mm] → *large* [length >0.15 mm; width >0.12 mm])
   - B. shape (*e.g.,* circular, ovate [includes direction of elongation], elliptical [includes direction of elongation])
   - C. peristomal characters (width, degree of development, and completeness)
   - D. position of apertural stylets
   - E. number of apertures per fenestrule length
6. Branch surface ornamentation and features; placement and positioning along obverse and reverse branch surfaces
   - A. keel width (*narrow* [<0.05 mm] → *intermediate* [0.05–0.15 mm] → *wide* [>0.15 mm])
   - B. nodes (*small* [<0.7 mm] → *intermediate* [0.07–0.12 mm] → *large* [>0.12 mm])
7. Autozooecial chambers
   - A. relative size (*small* [length <0.20 mm; depth <0.10 mm; maximum width <0.10 mm; minimum width <0.07 mm] → *intermediate* [length 0.20–0.48 mm; depth 0.10–0.20 mm; maximum width 0.10–0.15 mm; minimum width 0.07–0.12 mm] → *large* [length >0.48 mm; depth >0.20 mm; maximum width >0.15 mm; minimum width >0.12 mm])
   - B. emplacement (monoserial, biserial, or in rows at and proximal to sites of branch bifurcation)
   - C. chamber outline
     1. near reverse wall (triangular, rectangular, square, ovate, elliptical, circular, parallelogram-shaped, or diamond-shaped)
     2. at mid chamber (triangular, rectangular, square, ovate, elliptical, circular, parallelogram-shaped, or diamond-shaped)
     3. near obverse surface (triangular, rectangular, square, ovate, elliptical, circular, parallelogram-shaped, diamond-shaped, or bilobate)
   - D. orientation of elongation
   - E. location of aperture relative to chamber
   - F. relative size of vestibules (if present)
   - G. degree of development of superior and/or inferior hemisepta (if present)
   - H. mean lateral-wall budding-angle (*constant* [CV < 10] or *variable* [CV > 10])
   - I. mean reverse-wall budding-angle (*constant* [CV < 10] or *variable* [CV > 10])
   - J. heterozooecia (if present, type and location on branch)

The Paleontological Research Institution
acknowledges with special thanks
the contributions of the following individuals and institutions

PATRONS

($1000 or more at the discretion of the contributor)

James E. Allen (1967)
American Oil Company (1976)
Atlantic Richfield Company (1978)
Christina L. Balk (1970, 1982, 1983)
Hans M. Bolli (1984)
Ruth G. Browne (1986)
Mr. & Mrs. Kenneth E. Caster (1967)
Chevron Oil Company (1978, 1982)
Exxon Company (1977 to date)
Lois S. Fogelsanger (1966)
Gulf Oil Corporation (1978)
Merrill W. Haas (1975)
Robert C. Hoerle (1974–1977)
Richard I. Johnson (1967, 1986)
J. M. McDonald Foundation (1972, 1978)
Mobil Oil Corporation (1977 to date)
Samuel T. Pees (1981)
Richard E. Petit (1983)
Robert A. Pohowsky (1982)
Texaco, Inc. (1978, 1982, 1987)
Union Oil of California (1982 to date)
United States Steel Foundation (1976)
Charles G. Ventress (1983 to date)
Christine C. Wakeley (1976–1984)

(continued overleaf)

LIFE MEMBERS

($200)

R. Tucker Abbott
James E. Allen
Elizabeth A. Balcells-Baldwin
Christina L. Balk
Bruce M. Bell
Robert A. Black
Richard S. Boardman
Hans Bolli
David John Bottjer
Ruth G. Browne
J. David Bukry
Sybil B. Burger
Lyle D. Campbell
John L. Carter
Anneliese S. Caster
Kenneth E. Caster
John E. DuPont
J. Thomas Dutro, Jr.
J. Mark Erickson
Richard J. Erickson
Lois S. Fogelsanger
A. Eugene Fritsche
Christopher L. Garvie
Ernest H. Gilmour
Merrill W. Haas
Anita G. Harris
Steven M. Herrick
Robert C. Hoerle
F. D. Holland, Jr.
Frederick H. C. Hotchkiss
David Jablonski
Richard I. Johnson
David B. Jones
Peter Jung
Tomoki Kase
David Garrett Kerr
Cecil H. Kindle
William F. Klose, II
Jiří Kříž
Ralph L. Langenheim, Jr.
Harry A. Leffingwell
Egbert G. Leigh, Jr.
Gerard A. Lenhard
Louie N. Marincovich, Jr.
Donald R. Moore
Shuji Niko
Hiroshi Noda
Sakae O'Hara
Samuel T. Pees
Richard E. Petit
Edward B. Picou, Jr.
Robert A. Pohowsky
John Pojeta, Jr.
John K. Pope
Anthony Reso
Arthur W. Rocker
Walter E. Sage, III
John B. Saunders
Judith Schiebout
Miriam W. Schriner
Edward S. Slagle
David H. Stansbery
Jorge P. Valdes
Charles G. Ventress
William P. S. Ventress
Emily H. Vokes
Harold E. Vokes
Christine C. Wakeley
Thomas R. Waller
Albert D. Warren, Jr.
Gary D. Webster
Ralph H. Willoughby
Armour C. Winslow
Victor A. Zullo

Membership dues, subscriptions, and contributions are all important sources of funding, and allow the Paleontological Research Institution to continue its existing programs and services. The P.R.I. publishes two series of respected paleontological monographs, *Bulletins of American Paleontology* and *Palaeontographica Americana,* that give authors a relatively inexpensive outlet for the publication of significant longer manuscripts. In addition, it reprints rare but important older works from the paleontological literature. The P.R.I. headquarters in Ithaca, New York, houses a collection of invertebrate type and figured specimens, among the five largest in North America; an extensive collection of well-documented and curated fossil specimens that can form the basis for significant future paleontologic research; and a comprehensive paleontological research library.

The Paleontological Research Institution is a non-profit, non-private corporation, and contributions may be U.S. income tax deductible. For more information on P.R.I. programs, memberships, or subscriptions to P.R.I. publications, call or write:

Peter R. Hoover
Director

Paleontological Research Institution
1259 Trumansburg Road
Ithaca, New York 14850 U.S.A.
607-273-6623

Palæontographica Americana

NUMBER 57 JUNE 28, 1991

Revised taxonomic procedures and paleoecological applications for some North American Mississippian Fenestellidae and Polyporidae (Bryozoa)

by

Edward McKinley Snyder

1989 Winner of the Osgood Prize

Paleontological Research Institution
1259 Trumansburg Road
Ithaca, New York, 14850 U.S.A.

Library of Congress Card Number: 91-61821

Printed in the United States of America
Allen Press, Inc.
Lawrence, KS 66044, U.S.A.

CONTENTS

Page

Abstract 7
Acknowledgments 7
Introduction 8
  Mississippian Stratigraphy and Structural Geology of the Upper Mississippi Valley 10
Taxonomy of Meshwork Fenestrate Bryozoa
  General Taxonomic Divisions of the Bryozoa 16
  Summary and Critique of Previous Approaches to the Taxonomy of Meshwork Fenestelloidea 17
  Historical Review and Approach to Taxonomic Divisions within the Form Genus *Fenestella* Lonsdale 22
  Biological Significance of Zooecial Chamber Shape 31
  Taxonomic Criteria for the Discrimination of Fenestellid and Polyporid Species 34
Systematic Paleontology
  Taxonomic Philosophy 36
  Abbreviations of Repository Institutions 40
  Systematics
    Family Fenestellidae King, 1849 40
      Genus *Rectifenestella* Morozova, 1974 40
        Rectifenestella tenax (Ulrich, 1888) 41
        Rectifenestella tenuissima (Cumings, 1906) 45
        Rectifenestella multispinosa (Ulrich, 1890) 47
      Genus *Laxifenestella* Morozova, 1974 49
        Laxifenestella coniunctistyla, n. sp. 50
        Laxifenestella maculasimilis, n. sp. 54
        Laxifenestella serratula (Ulrich, 1890) 56
        Laxifenestella fluctuata, n. sp. 58
      Genus *Minilya* Crockford, 1944 61
        Minilya sivonella, n. sp. 62
        Minilya paratriserialis, n. sp. 65
      Genus *Exfenestella* Morozova, 1974 67
        Exfenestella exigua (Ulrich, 1890) 68
      Genus *Banastella,* n. gen. 72
        Banastella guensburgi, n. sp. 73
        Banastella cingulata (Ulrich, 1890) 77
        Banastella mediocreforma, n. sp. 79
        Banastella limitaris (Ulrich, 1890) 81
        Banastella biseriata (Ulrich, 1890) 83
        Banastella delicata, n. sp. 86
      Genus *Cubifenestella,* n. gen. 88
        Cubifenestella rudis (Ulrich, 1890) 90
        Cubifenestella usitata, n. sp. 92
        Cubifenestella globodensata, n. sp. 95
      Genus *Apertostella,* n. gen. 97
        Apertostella foramenmajor, n. sp. 99
        Apertostella crassata, n. sp. 101
        Apertostella venusta, n. sp. 104
      Genus *Hemitrypa* Phillips, 1841 106
        Hemitrytpa perstriata Ulrich, 1890 108
        Hemitrypa hemitrypa (Prout, 1859) 111
        Hemitrypa aprilae, n. sp. 114
        Hemitrypa aspera Ulrich, 1890 116
        Hemitrypa vermifera (Ulrich, 1890) 119
      Genus *Archimedes* Hall, 1858 122
        Archimedes negligens Ulrich, 1890 124
        Archimedes owenanus (Hall, 1857b) 127
        Archimedes wortheni (Hall, 1857b) 130
        Archimedes valmeyeri, n. sp. 133

Family Polyporidae Vine, 1884 136
Genus *Fenestralia* Prout, 1858a 137
Fenestralia sanctiludovici Prout, 1858a 138
Genus *Polypora* McCoy, 1844 142
Polypora gracilis Prout, 1860 144
Polypora varsoviensis Prout, 1858a 146
Polypora spininodata Ulrich, 1890 149
Polypora simulatrix Ulrich, 1890 151
Polypora retrorsa Ulrich, 1890 154
Changing Distribution of Meshwork Fenestrate Species Throughout the Warsaw Study Area 156
Trophic Structure in Suspension-Feeding Communities
Introduction 160
Niche Differentiation Among Living and Fossil Species 160
Bryozoan Feeding Mechanism and Behavior 161
Food particle size 162
Morphological Features Governing Feeding Rates in Modern Bryozoan Species 163
Warsaw Environmental and Paleoecological Setting 163
Zoarial Emplacement and Feeding in Warsaw Meshwork Fenestrates 163
Parameters Used for Determining Niche Differentiation in Warsaw Fenestrates 165
Possible Niche Differentiation in Warsaw Fenestrate Bryozoa 166
Conclusions 170
Appendices
A. Descriptions of Warsaw Formation Sampled Outcrops and Localities 171
B. Columnar Sections for Localities Included in the Species Distribution Study 176
References Cited 186
Plates 192
Index 264

LIST OF ILLUSTRATIONS

Text-figure — Page
1. Warsaw Formation sample localities 9
2. Typical stratigraphic sections for the northern and southern portions of the study area 13
3. Comparison of interior sections of *Banastella guensburgi* and *Cubifenestella usitata* 21
4. Typical zoarial surficial features of meshwork fenestrates 35
5. Characters measured in the reticulate meshwork of *Hemitrypa* and the central spire or axis of *Archimedes* 36
6. Characters measured in the interior of *Banastella guensburgi* 37
7. Characters measured in the interior of *Cubifenestella usitata* 38
8. *Rectifenestella texax* and *Rectifenestella tenuissima* illustrated 43
9. *Laxifenestella coniunctistyla* illustrated 51
10. *Minilya sivonella* illustrated 63
11. *Exfenestella exigua* illustrated 69
12. *Banastella guensburgi* illustrated 75
13. *Cubifenestella rudis* illustrated 89
14. *Apertostella crassata* illustrated 99
15. *Hemitrypa perstriata* illustrated 107
16. *Archimedes wortheni* illustrated 123
17. *Fenestralia sanctiludovici* illustrated 139
18. *Polypora varsoviensis* illustrated 143
19. Measured sections used to determine species distribution 157
20. Changing species composition of localities in the Warsaw study area 159
21. Modern stenolaemate showing zooid with tentacles extended 161
22. Modern stenolaemate showing zooid with tentacles retracted 161
23. Schematic illustration of the obverse zoarial surface of *Cryptosula pallasiana* 165
24. Schematic illustration of the obverse surface of *Banastella guensburgi* 166
25. Range of aperture spacing over obverse zoarial surface for Warsaw meshwork fenestrates 167
26. Relationship of mouth diameter to lophophore diameter for some Warsaw meshwork fenestrates 168
27. Relationship between tentacle length and tentacle number for some Warsaw meshwork fenstrates 169
28. Relationship of maximum clearance rate and chamber volume for some Warsaw meshwork fenestrates 170
29. Relationship between inferred mouth diameter and calculated chamber volume for some Warsaw meshwork fenestrates 171
30. Relationship between lophophore diameter and chamber volume for some Warsaw meshwork fenestrates 172

LIST OF TABLES

Table — Page

1. Summary of stratigraphic nomenclature used for the Middle Mississippian of Illinois 11
2. Descriptive criteria for differentiation of species of *Fenestella* used by Morozova (1970b) 20
3. Characters used by Morozova (1974) for discrimination of 10 genera from the form genus *Fenestella*, here also applied to four genera of other authors 24, 25
4. Taxonomic criteria for generic divisions within the Warsaw fenestellids 26, 27

5a. Comparison of external taxonomic characters in 11 genera of fenestellid and polyporid bryozoans 28–31

5b. Comparison of internal taxonomic characters in 11 genera of fenestellid and polyporid bryozoans 32, 33

6. Key to Warsaw genera of the Fenestellidae and Polyporidae 34
7. Definition of zooecial and zoarial characters used in species descriptions .... foldout inside front cover

8a. Outlines of species diagnoses and descriptions, and definitions of measurements and terminology employed therein .... foldouts inside front and back covers

8b. Definitions and abbreviations of the 44 fenestellid and polyporid zooecial and zoarial characters measured in this study .... foldout inside back cover

9. Taxonomic list of Warsaw meshwork fenestrate species 39
10. Summary numerical analysis of *Rectifenestella tenax* (Ulrich, 1888) 42
11. Summary numerical analysis of *Rectifenestella tenuissima* (Cumings, 1906) 46
12. Summary numerical analysis of *Rectifenestella multispinosa* (Ulrich, 1890) 47
13. Summary numerical analysis of *Laxifenestella coniunctistyla,* n. sp. 52
14. Summary numerical analysis of *Laxifenestella maculasimilis,* n. sp. 54
15. Summary numerical analysis of *Laxifenestella serratula* (Ulrich, 1890) 57
16. Summary numerical analysis of *Laxifenestella fluctuata,* n. sp. 59
17. Summary numerical analysis of *Minilya sivonella,* n. sp. 62
18. Summary numerical analysis of *Minilya paratriserialis,* n. sp. 66
19. Summary numerical analysis of *Exfenestella exigua* (Ulrich, 1890) 70
20. Summary numerical analysis of *Banastella guensburgi,* n. sp. 74
21. Summary numerical analysis of *Banastella cingulata* (Ulrich, 1890) 77
22. Summary numerical analysis of *Banastella mediocreforma,* n. sp. 80
23. Summary numerical analysis of *Banastella limitaris* (Ulrich, 1890) 82
24. Summary numerical analysis of *Banastella biseriata* (Ulrich, 1890) 84
25. Summary numerical analysis of *Banastella delicata,* n. sp. 86
26. Summary numerical analysis of *Cubifenestella rudis* (Ulrich, 1890) 90
27. Summary numerical analysis of *Cubifenestella usitata,* n. sp. 93
28. Summary numerical analysis of *Cubifenestella globodensata,* n. sp. 95
29. Summary numerical analysis of *Apertostella foramenmajor,* n. sp. 98
30. Summary numerical analysis of *Apertostella crassata,* n. sp. 102
31. Summary numerical analysis of *Apertostella venusta,* n. sp. 104
32. Summary numerical analysis of *Hemitrypa perstriata* Ulrich, 1890 109
33. Summary numerical analysis of *Hemitrypa hemitrypa* (Prout, 1859) 111
34. Summary numerical analysis of *Hemitrypa aprilae,* n. sp. 114
35. Summary numerical analysis of *Hemitrypa aspera* Ulrich, 1890 117
36. Summary numerical analysis of *Hemitrypa vermifera* (Ulrich, 1890) 120
37. Summary numerical analysis of *Archimedes negligens* Ulrich, 1890 125
38. Summary numerical analysis of *Archimedes owenanus* (Hall, 1857b) 127
39. Summary numerical analysis of *Archimedes wortheni* (Hall, 1857b) 131
40. Summary numerical analysis of *Archimedes valmeyeri,* n. sp. 134
41. Summary numerical analysis of *Fenestralia sanctiludovici* Prout, 1858a 140
42. Summary numerical analysis of *Polypora gracilis* Prout, 1860 144
43. Summary numerical analysis of *Polypora varsoviensis* Prout, 1858a 147
44. Summary numerical analysis of *Polypora spininodata* Ulrich, 1890 149
45. Summary numerical analysis of *Polypora simulatrix* Ulrich, 1890 152
46. Summary numerical analysis of *Polypora retrorsa* Ulrich, 1890 154
47. Occurrence of meshwork fenestrate species throughout the Warsaw study area 156
48. Abundance of species of Warsaw Formation meshwork fenestrate bryozoans at each locality 158
49. Fenestrate characters used in niche differentiation 164
50. Calculated tentacle lengths, clearance rates, and chamber volumes for species with determinable tentacle numbers 171

The manuscript on which this monograph is based was awarded the Osgood Prize by the Paleontological Research Institution on November 7, 1989. The prize, a $500 cash award to the author(s) of an outstanding manuscript accepted for publication by the institution, is named in honor of the late Dr. R. G. Osgood. It is supported by an endowment initiated by his colleagues and enlarged by benefactors of the Paleontological Research Institution. Information on selection criteria is available from the institution.

REVISED TAXONOMIC PROCEDURES AND PALEOECOLOGICAL APPLICATIONS FOR SOME NORTH AMERICAN MISSISSIPPIAN FENESTELLIDAE AND POLYPORIDAE (BRYOZOA)

by

EDWARD McKINLEY SNYDER

Division of Science and Mathematics
Shepherd College
Shepherdstown, WV 25443

ABSTRACT

Fenestellid and polyporid Bryozoa of the lower Middle Mississippian Warsaw Formation of the Mississippi River outcrop belt are represented by nine genera of Fenestellidae (three of which are new: *Banastella*, *Cubifenestella*, and *Apertostella*) and two genera of Polyporidae. Twenty-two previously described species and fifteen new species are recognized. New species are: *Laxifenestella coniunctistyla*, *Laxifenestella maculasimilis*, *Laxifenestella fluctuata*, *Minilya sivonella*, *Minilya paratriserialis*, *Banastella guensburgi*, *Banastella mediocreforma*, *Banastella delicata*, *Cubifenestella usitata*, *Cubifenestella globodensata*, *Apertostella foramenmajor*, *Apertostella crassata*, *Apertostella venusta*, *Hemitrypa aprilae*, and *Archimedes valmeyeri*.

Exterior and interior analyses of bryozoan zoaria are employed in the classification of meshwork fenestrate Bryozoa, separating zoarial and zooecial features and emphasizing three-dimensional form, chamber size, and accessory features. The format presented in this study is designed to be employed as a thorough outline for classification.

Change of meshwork fenestrate species composition within the Warsaw from north to south within the study area could have been caused by environment or evolution; however, a significant change in faunal composition is evident.

Employing modern cheilostomes as analogues, possible niche differentiation of meshwork fenestrates is established for the Warsaw. Chamber volume, lophophore diameter, mouth diameter, interpreted maximum zooid clearance rate, tentacle number, and tentacle length are criteria used to infer fenestrate niche partitioning. These criteria, in conjunction with food particle size and efficiency of the feeding organ (lophophore), appear to be dominant factors governing niche partitioning within the meshwork fenestrates.

ACKNOWLEDGMENTS

This work is the culmination of more than 10 years of research into fenestrate Bryozoa, one result of which was completion of my Ph. D. degree at the University of Illinois. There have been numerous individuals, from farmers directing me to the most fossiliferous spots in the creek bed to fellow researchers offering constructive comments regarding my research, who have contributed to the content of this work. To all of these people I owe a sincere debt of gratitude.

I would, however, like to recognize several individuals whose assistance was instrumental in the evolution of this work. First and foremost I would like to thank Daniel B. Blake for initially introducing me to the spectacular fossils of the Warsaw Formation, for his helpful suggestions and wealth of ideas, and most of all for his patience and direction during my completion of this lengthy study. George deVries Klein, Ralph L. Langenheim, Philip Sandberg, and Daryl Sweeney, all of the University of Illinois, read the manuscript, offered helpful suggestions, and served as members of my dissertation committee. Ken McKinney of Appalachian State University, and Alan Horowitz of Indiana University reviewed the revised manuscript that was submitted for publication to the Paleontological Research Institution. Their extremely thorough and insightful reviews significantly improved the manuscript and their efforts are greatly appreciated.

Sincere thanks are due to Peter Hoover, for his patience, support, and thoughtful editorial recommendations, which have significantly improved the form and content of this work.

Assistance in the field was provided by Thomas Guensburg, Paul Sivon, Dan Blake, and numerous undergraduate students who contributed fossil Bryozoa for my use; the help and companionship while undertaking the extensive field work involved in the study is greatly appreciated.

A special thanks is due to Steve Hageman of the University of Illinois for his encouragement and assistance. His quantitative analysis (Hageman, 1987) of the morphometric data presented in this paper provided an important test of the taxonomic approach developed herein.

Richard S. Boardman and Alan H. Cheetham of the United States National Museum of Natural History (USNM), Washington, DC; Alan Horowitz, of Indiana University, Bloomington, IN; Lois Kent and Dennis R. Kolata, of the Illinois State Geological Survey (ISGS), Champaign, IL, arranged for the loan of specimens by their respective institutions.

The publication cost of a document of this size is a significant financial burden. In a very real sense, publication of this study has been made possible by the financial support of numerous institutions and individuals. Howard Carper and Donald Henry of Shep-

herd College, Shepherdstown, WV, provided both moral and, directly or indirectly, financial support; their efforts on my behalf are greatly appreciated. The Shepherd College Foundation and Shepherd College Faculty Minigrant Fund have both provided significant financial support; such assistance is not only appreciated, but is critical in a work of this size. I was fortunate to have the manuscript recognized by the Osgood Prize Committee and the Trustees of the Paleontological Research Institution (PRI), who awarded the 1989 Osgood Prize to this work. The $500 prize award was applied to the publication costs; further, the PRI contributed an additional $2,000 from the Osgood Fund toward publication costs. The remaining funds necessary were earned through revenues gained from teaching course overloads, elder hostels, and children's colleges, and through geologic consulting, archaeological site surveys, and other means as available; this makes the above financial assistance doubly appreciated.

I would also like to thank all those who have patiently tolerated my preoccupation with fenestrate Bryozoa, and especially I would like to thank my wife Cathy for her assistance and patience during this endeavor.

INTRODUCTION

General statement of investigation.—The primary goals of this study are twofold: (1) modernization of taxonomy of fenestrate Bryozoa; and (2) paleoecologic analyses based on the new taxonomy, resulting in functional morphologic interpretations for the fenestrates.

The Warsaw Formation (upper Osagean of U. S. Geological Survey terminology, or middle Valmeyeran of Illinois Geological Survey terminology) of the upper Mississippi Valley was selected for study because of its abundant, taxonomically diverse, well-preserved bryozoan fauna. Further, the Carboniferous represents the peak of fenestrate diversification at both the species and genus levels. The Warsaw is geographically widespread, flat-lying, and locally moderately well-exposed, and is part of the Mississippian stratotype. Lithologically, the Warsaw is composed of sequences of alternating argillaecous shale, calcareous shale, and biocalcarenite, some of which have been dolomitized and contain quartz and calcite geodes. This study was restricted to outcrops.

Fenestrate species concepts to date have been vague, even among species thought to be common. Varying emphasis on exterior or interior analyses, and primary reliance on two-dimensional tangential sections have led to a proliferation of unrecognizable species. Establishment herein of an outlined systematic approach to species delimitation clarifies taxon recognition, provides a comprehensive basis for generic groupings, and yields a taxonomic basis that can be applied to other faunas.

Although fenestrate bryozoans are a major component of the Warsaw fauna, the most recent taxonomic study of this unit is that of Ulrich (1890). Advances in fenestellid taxonomy (Termier and Termier, 1971; Morozova, 1974; McKinney, 1980) make Warsaw bryozoans appropriate subjects for taxonomic revision.

Specific and generic taxonomic assignments are based on recent conceptual advances including application of three-dimensional autozooecial chamber and zoarial reconstructions, study of populations, and employment of statistical analyses. Whether studies are biostratigraphic, paleoecologic, taphonomic, or evolutionary, their strengths and/or weaknesses are largely dependent on taxonomy. Conclusions of any nature using species defined on haphazard systematics or weak taxonomic concepts can be more misleading than useful.

Use of taxonomic data in conjunction with stratigraphic and sedimentologic data provides the basis for functional morphologic and paleoecologic interpretations of trophic structuring, niche differentiation, and faunal succession.

Location and extent of field area.—The Warsaw shale outcrop belt includes the Illinois and Mississippi River valleys extending from Nauvoo, Illinois in the north to Valmeyer, Illinois in the south, and as far northeast as Beardstown, Illinois along the Illinois River. The area also extends into eastern Iowa and Missouri (Text-fig. 1). Dimensions of the major part of the area are approximately 220 mi (352 km) in a north–south direction and from approximately 40 mi (64 km) to 85 mi (136 km) in the east–west direction. The one studied outcrop in Howard County, Missouri lies 120 mi (195 km) west of the main outcrop belt. In total, outcrops at 49 localities were examined and are described in *Appendix A*. Twenty-three localities were examined in detail and used for biostratigraphic and paleoenvironmental determinations. Stratigraphic columns and range charts for these 23 sections are presented in *Appendix B*. Other localities were used as data checks.

Because of low resistance to weathering, Warsaw outcrops are relatively poor. Throughout the area, topography is of low relief, and strata are overlain by Pleistocene till, thick soil profiles, and dense vegetation. Roadcuts and quarries usually provide the best-preserved material, as weathering and presence of lichen and mosses commonly obscure rock surfaces in stream valleys and along river cuts.

Field and laboratory methods.—Approximately six months were spent in measuring, describing, and sampling 49 stratigraphic sections during the summers of

Text-figure 1.—Warsaw Formation sample localities.

1977 through 1980. McKee and Weir's (1953) classification was used for recording bedding thickness; carbonate classification is after Carozzi (1972). Lithologic samples totalling over 4,500 lbs (approx. 2,000 kg) and consisting of both fossiliferous and unfossiliferous slabs were collected and returned to the laboratory. Approximately 200 thin-sections, supplemented by numerous acetate peels, were made from samples representative of the different facies present in the Warsaw. Polished slabs were prepared for the study of sedimentary features and textural analysis. Stratigraphic columns and lithologic descriptions were prepared for 23 of these measured sections; these were also analyzed for species distribution. The remaining localities provided stratigraphic control and are described briefly in the locality register (*Appendix A*).

Both exterior and interior analyses of fenestrate bryozoans are necessary, requiring extensive preparation. Shale samples and limestone surfaces were sieved and washed, respectively, to expose external zoarial surfaces. Zoaria were soaked in hot water and then placed in an ultrasonic bath for one to five minutes, depending on robustness of colonies, to remove surface debris. Internal bryozoan analyses are based solely on acetate peels. Peel preparation follows the procedures of Boardman and Utgaard (1964) and Nye, Dean, and Hinds (1972). Acetate peels are superior to thin-sections for description of skeletal structures because: (1) skeletal microstructure is shown in greater detail, as peels possess minimum relief, approaching a two-dimensional surface, whereas thin-sections are three dimensional slabs whose thickness frequently obscures many details; (2) many peels may be made of each zoarium, showing different orientations necessary for three-dimensional reconstruction; (3) serial peels can be taken at short intervals permitting three-dimensional reconstruction; (4) multiple peels of any surface can be made, providing duplicates for distribution to other workers; (5) plug surfaces from which peels are made can be studied with the Scanning Electron Microscope (SEM); (6) plug surfaces can more readily be reground to obtain the correct orientation, whereas thin-sections typically allow only one attempt at orientation; and (7) peel preparation is much more rapid. Subsequent to exterior analysis, specimens were embedded in epoxy (Epotuf® two-part resin and hardener with a mixture of 4.5 parts resin to 1 part harderer, by weight). Between 40 and 50 ml of propylene oxide were added to every 200 ml of mixed epoxy to thin the mixture for embedding. Specimens were placed in epoxy and vacuum-pumped to enhance epoxy penetration. Once the specimens were cut, 250- and 600-grit papers were used for grinding; the use of paper-backed abrasives minimized grit adherence. A final buffing on well-worn 600-grit paper helped prepare the plug surface for polishing.

Mirror-like polish was achieved with Buehler's microcloth and a slurry of 0.05 μm tin oxide polishing compound mixed with liquid detergent (Palmolive®), on a variable-speed polishing wheel. Best etch was attained by gentle agitation of polished specimens in dilute (0.5% to 1.0% by volume) formic acid for four to six seconds. Formic acid yields greater contrast peels than do hydrochloric or acetic acids. Short etching times were used for orientations illustrating closely packed laminae, such as transverse and shallow tangential orientations; longer etching times were necessary for orientations containing more granular calcite and greater spacing between laminae, particularly in longitudinal and deeper tangential sections. Some surfaces used for peels were then washed with acetone and gold-plated for SEM study.

High-contrast Kodak® D-19 developer was used for all film. Contact prints were made using AZO® 3 and 4 and 4×5 format negatives; 35 mm negatives were enlarged and printed on Kodabromide® 3 and 4. All steps of developing and printing were done in such a way as to enhance contrast in the final prints.

MISSISSIPPIAN STRATIGRAPHY AND STRUCTURAL GEOLOGY OF THE UPPER MISSISSIPPI VALLEY

Regional geologic setting.—During most of the Mississippian, the Illinois Basin (Eastern Interior Basin) slowly subsided along a north–south trend. The Transcontinental Arch and Mississippi River Arch to the west, the Wisconsin Arch to the north, the Cincinnati Arch–Nashville Dome trend to the east, and the Ozark Dome in the southwest could have contributed to the large amount of detrital material accumulated in the basin (Potter and Pryor, 1961; Walker, 1962). All these areas either were slightly positive or exposed during the Valmeyeran (Walker, 1962), as indicated by erosion of materials from them. Clastic sediments came predominantly from the delta-distributary system of the Michigan River, feeding into the Illinois Basin from the northeast during middle to late Valmeyeran time (Atherton and Palmer, 1979). Little material was introduced, but much autochthonous carbonate was provided by the indigenous fauna and flora. Bed thickness, cross-bedding, and the nature of facies distribution suggest a northwest–southeast shoreline trend (Atherton and Palmer, 1979).

In the early Valmeyeran (Osagean), sediment yield from the northeast greatly decreased, leaving the Illinois Basin relatively starved (Atherton and Palmer, 1979). During this time the widespread Burlington Limestone, a clean crinoidal biocalcarenite, was deposited. This unit represents a broad carbonate shelf throughout the Mississippian stratotype area (Atherton and Palmer, 1979). By middle Valmeyeran, the Borden Delta resulted in the resumption of supply of clastic

Table 1.—Summary of stratigraphic nomenclature used for the Middle Mississippian of Illinois. The leftmost column indicates the usage followed in this paper.

<table>
<tr><th>Formations</th><th>Worthen 1866</th><th>Ulrich 1904</th><th>S. Weller 1908</th><th>VanTuyl 1925</th><th colspan="2">Moore 1933</th><th colspan="2">J.M. Weller 1940</th><th>Laudon 1948</th><th>J.M. Weller 1948</th><th colspan="2">Swann 1963</th></tr>
<tr><td>St. Genevieve Formation</td><td rowspan="5">St. Louis Group</td><td rowspan="5">Meremec Group</td><td>St. Genevieve Group</td><td rowspan="5">Meremec Group</td><td rowspan="7">Valmeyer Series</td><td rowspan="4">Meremec Group</td><td rowspan="7">Iowa Series</td><td rowspan="4">Meremec Group</td><td rowspan="4">Meremec Group</td><td rowspan="5">Meremecian Group</td><td rowspan="7">Valmeyer Series</td><td>Genevieve Stage</td></tr>
<tr><td>St. Louis Limestone</td><td rowspan="3">Meremec Group</td><td rowspan="6">Unnamed</td></tr>
<tr><td>Salem Limestone</td></tr>
<tr><td>Sonora Formation</td></tr>
<tr><td>Warsaw Formation</td><td rowspan="3">Osage Group</td><td rowspan="3">Osage Group</td><td rowspan="3">Osage Group</td><td rowspan="3">Osage Group</td></tr>
<tr><td>Keokuk Limestone</td><td>Keokuk Group</td><td rowspan="2">Osage Group</td><td rowspan="2">Osage Group</td><td rowspan="2">Osagean Group</td></tr>
<tr><td>Burlington Limestone</td><td>Burlington Group</td></tr>
</table>

sediments from the northeast (Atherton and Palmer, 1979). Fine-grained clastics brought in by the Michigan River system began accumulating on the carbonate shelf to the west, resulting in shale in the Keokuk Limestone, which conformably overlies the Burlington Limestone. The carbonate shelf was covered finally by the clays and silts of the Warsaw Formation.

Valmeyeran Series (Osage–Meramec Series).—The U. S. Geological Survey (U. S. G. S.) and Illinois State Geological Survey (I. S. G. S.) employ different terminology for units lying between the Kinderhookian and Chesterian series. The U. S. G. S., the Missouri Geological Survey, and others use *Osage Series* to include rocks from the top of the Chouteau Limestone and Hannibal Shale through either the Keokuk Limestone (Ulrich, 1904; Van Tuyl, 1925; Weller *et al.*, 1948; Harris and Parker, 1964) or through and including the Warsaw Shale (Branner, 1888; Weller, 1914; Moore, 1933; Weller and Sutton, 1940; Laudon, 1948). The *Meramec Series* as so defined extends from the top of the Osage Series to the Renault Formation. The I. S. G. S. combines the two into the *Valmeyeran Series* (Weller and Sutton, 1940) with its stratotype in Dennis Hollow at Valmeyer in Monroe County, Illinois. Table 1 provides a summary of differences in stratigraphic classification. The Osage–Meramec Series are combined by the I. S. G. S. because of the difficulty in consistently delineating a boundary between the two series (Pryor and Sable, 1974). The boundary is not marked by a physical break (Weller and Sutton, 1940; Wanless, 1957; Baxter, 1972) and disagreement exists on the ages of fauna in the Warsaw and its supposed lateral equivalent, the Harrodsburg Formation (Pryor and Sable, 1974).

Continuous accumulation of sediment without evidence of a physical break in deposition could be a positive factor in recognizing a stratigraphic division between the Osage and Meramec Series at the Keokuk–Warsaw lithologic boundary, as the change in fauna used for biostratigraphic interpretation would be based on evolution, not on lack of depositional continuity. Complex facies and environmental factors resulting in interfingering of Keokuk-type material with the lower Warsaw lithologies, and Warsaw lithologies in the overlying Sonora and Salem lithologies provide no evidence of widespread lithologic unconformities in this stratigraphic interval, thus affirming continuity of deposition. Conclusions on the placement of this boundary based on lithostratigraphic and bryozoan biostratigraphic interpretations are presented on p. 156.

Middle Valmeyeran (Mississippian) formations.—Middle Valmeyeran lithostratigraphic units relevant to this investigation include the Keokuk Limestone, Warsaw Shale, Sonora Formation, Ullin Limestone, Salem Limestone, and St. Louis Limestone (see *Appendix B* and Text-fig. 2).

Keokuk Limestone: The Keokuk Limestone (Owen, 1852; Hall, 1857a; Van Tuyl, 1925) is 70 ft (21.3 m) of cherty biocalcarenitic limestone with shaly partings. The type section is along Soap Creek at Keokuk, Lee County, Iowa. The Keokuk ranges from 60 to 80 ft (18.3 to 24.4 m) thick throughout the study area, and conformably overlies the Burlington Formation. The lower 30 ft (9.1 m) of the Keokuk near the type section

is differentiated as the Montrose Chert Member (Keyes, 1895; Collinson, 1964) by its abundant chert. The Keokuk above this member consists of crinoidal, bryozoan, and brachiopod-rich biocalcarenite locally interbedded with fine-grained limestone, argillaceous dolomite, and calcareous medium- to dark-gray shale. South of St. Louis, the upper Keokuk consists of a thick oolitic lithology, termed the Short Creek Oolite Member of the Keokuk. The Keokuk–Warsaw contact is gradational, with a gradual upward increase in number and thickness of shale beds. The boundaries of the Keokuk Formation coincide with those of the *Gnathodus texanus–Taphrognathus* conodont Zone of Collinson, Scott, and Rexroad (1962). The brachiopod species *Spirifer logani* Hall, 1858, *Dictyoclostus crawfordsvillensis* (Hall, 1858), *Orthotetes keokuk* (Weller, 1914), and *Rotaia subtrigona* (Meek and Worthen, 1860) are confined to the Keokuk (Weller and Sutton, 1940). The first occurrences of several bryozoan genera, including *Worthenopora* Ulrich, 1890, *Cyclopora* Prout, 1858a, *Cycloporella* Ulrich, 1890, and *Proutella* Ulrich, 1890 are in the Keokuk. The Keokuk is conformably overlain by the Warsaw wherever the contact is exposed.

Warsaw Formation: The Warsaw Formation was named by Hall (1857a) for an exposure of approximately 50 ft (15.1 m) of shale lying between the Keokuk Limestone and the St. Louis Limestone in Geode Glen at Warsaw, Hancock County, Illinois. This section subsequently was designated the type section by Collinson (1964). Geode beds originally included in the upper Keokuk were reassigned to the basal Warsaw by Butts (1915) and Van Tuyl (1925). The areal extent of the Warsaw in southern Iowa, eastern Missouri, and western Illinois was also presented by these authors. Due to the accessible outcrops and abundant fauna of the Warsaw, the unit was intensively studied by many early stratigraphers and paleontologists of the Mississippi Valley region, including Ulrich (1890), Weller (1914; 1926), Worthen (1870), Worthen, Shaw, and Meek (1873), and Gordon (1895). Much of their stratigraphic work and many of their faunal descriptions are accurate and complete.

As defined, the Warsaw was considered equivalent to the Harrodsburg Limestone of Harrodsburg, Indiana (Butts, 1915). This led to abandonment of the name *Harrodsburg* because *Warsaw* had priority (Butts, 1915; Cumings, 1922). In Indiana, the base of the Warsaw was placed at the top of the Holtsclaw Sandstone. Three members were included in the Warsaw of Indiana and Kentucky. These are, in ascending order, the Wildie Sandstone, the Somerset Shale, and the Garret Mill Sandstone. Weller (1934) proposed restoration of the name *Harrodsburg* as it was originally used in Indiana and Kentucky, restricting the Warsaw Formation to its earlier status: all beds between the Keokuk and St. Louis limestones. Weller also suggested dividing the Warsaw into members in the type area, where such divisions seem applicable.

In a faunal study of the Keokuk, Warsaw, and Salem formations, Laudon (1948) found that of the 30 invertebrate species recovered, the Keokuk and Warsaw had 27 in common. The Warsaw and Salem were found to have very limited faunal similarity. In Laudon's investigation, the Salem, which had been removed from the upper Warsaw by Weller (1908), was once again recognized as a member of the Warsaw. Collinson (1964) redesignated the type section, preferring Weller's arrangement to that of Laudon. It is the type section as described by Collinson that is generally used in modern studies (Atherton and Palmer, 1979).

Parts of the Sonora Formation and Salem Limestone, once assumed to be younger than the Warsaw Formation, were found in this study to be equivalent in age, as indicated by bryozoan bioclasts. Several stratigraphic sections analyzed contain interbeds of both Sonora and Salem lithology within the middle and upper Warsaw, respectively. Sand Branch (loc. 15) contains upper Warsaw overlying the Salem, McKee Creek (loc. 21) contains upper Warsaw overlying the Salem, Versailles West (loc. 22) has interbeds of Salem (Sonora *of* Collinson, 1964) and Warsaw lithology, and Lacy Keosauqua (loc. 3) has beds of Warsaw lithology in the Sonora.

Collinson, Scott, and Rexroad (1962) and Rexroad and Collinson (1965) studied conodonts of the Keokuk, Warsaw, Salem, and St. Louis formations. They assigned the Warsaw, Salem, and lower St. Louis formations to the *Taphrognathus varians– Apatognathus* Zone. This zone is equivalent to the lower half of the *Taphrognathus varians–Cavusgnathus–Apatognathus* Zone of Rhodes, Austin, and Druce (1969), and the entire *Cavusgnathus unicornis–Apatognathus* Zone. Wills (1971) found the Sonora assignable to the *Taphrognathus varians–Apatognathus* Zone as defined by Collinson, Scott, and Rexroad (1962). Previous difficulties in separating the Warsaw, Salem, Sonora, and St. Louis formations support these conclusions.

The boundary between the Warsaw and Keokuk in the stratotype area has been a point of dispute among authors because of the variability in lithology and faunal content of the lower Warsaw. Some sections of the Warsaw consist of 25 to 45 ft (7.7 to 13.9 m) of unfossiliferous to scarcely fossiliferous gray to brownish-gray, fine-grained, geodiferous dolostone, with increased amounts of argillaceous shale toward the top. Other sections, some located within a mile of the first, show a similar thickness of highly fossiliferous cherty biocalcarenite lenses interspersed in fossiliferous shale, with no sign of dolomitization or presence of geodes.

The upper Warsaw is more uniform throughout the

area, consisting of from 20 to 32 ft (6.1 to 9.8 m) of locally highly fossiliferous bluish-gray shale interbedded with fossiliferous silty and dolomitic biocalcarenite. A general increase in clay particle size is observed up section (Wills, 1971). The total thickness of the Warsaw is as much as 300 ft (92.3 m), consisting mostly

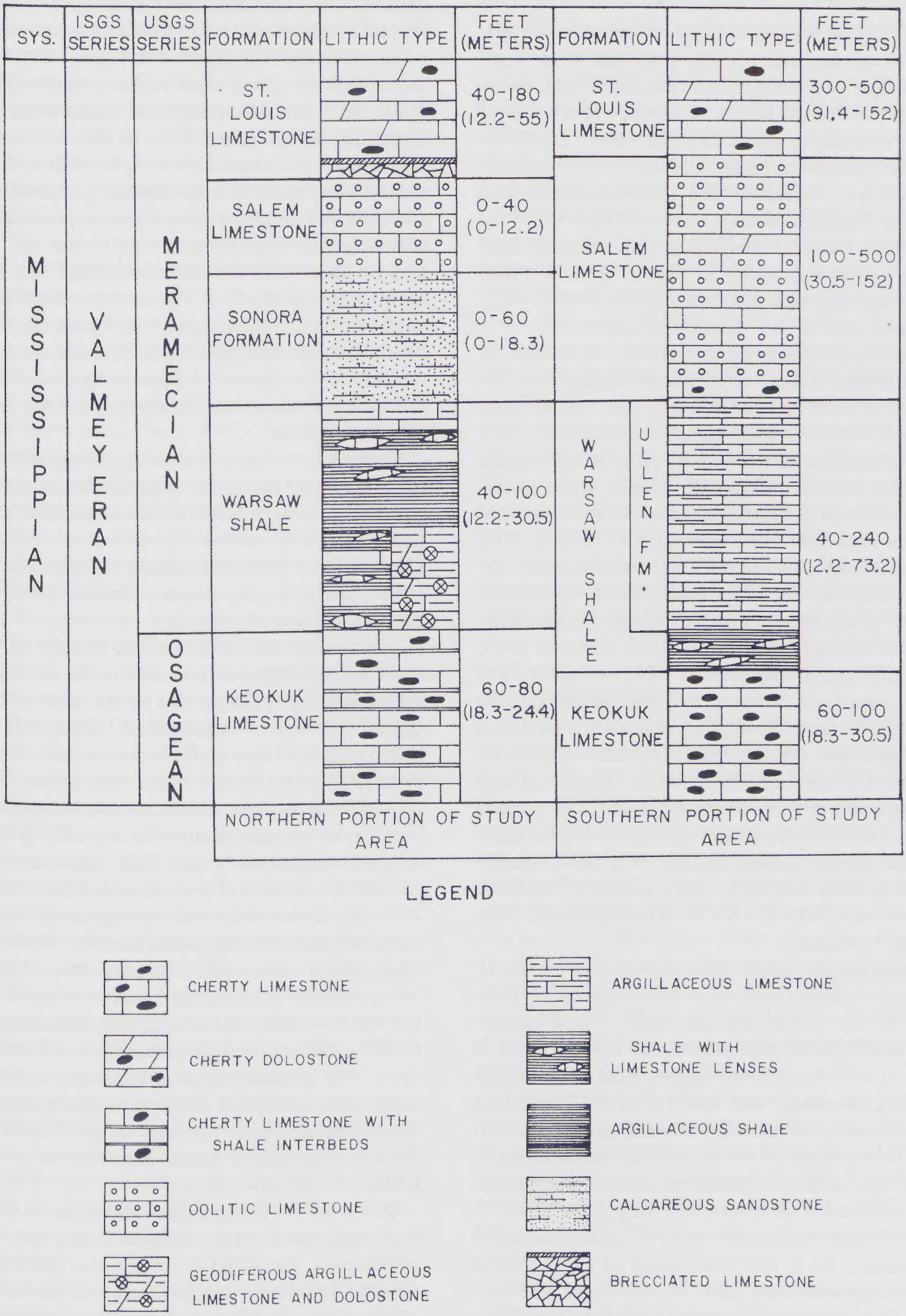

Text-figure 2.—Typical stratigraphic sections for the northern and southern portions of the study area.

of siltstone in west-central Illinois, and thins to less than 100 ft (30.7 m) in the outcrop area, where it consists of mostly shale and argillaceous biocalcarenite, with a small silty component near the top of some sections.

Lineback (1966), relying almost exclusively on drill cuttings and core and electric log data, analyzed Warsaw and younger Mississippian strata from their western edge into the Illinois Basin. Where the Keokuk and Burlington formations pinch out eastward, Lineback described the Warsaw as being separated from the Borden Siltstone by a vertical cutoff. The Bilyeu Member of the Borden Siltstone extends westward into the Warsaw Formation, thereby becoming a member shared by both formations (Lineback, 1966). The Warsaw Formation was thus most probably deposited coevally with the upper part of the Borden Siltstone.

The Warsaw is typically conformably overlain by the Sonora, Salem, Ullin, or St. Louis formations, although local unconformities between the Warsaw and overlying units are observed in some exposures.

Sonora Formation: Keyes (1895) named the Sonora Formation for approximately 20 ft (6.1 m) of cross-bedded dolomite to dolomitic sandstone in the Sonora Quarry, 5 mi (7.5 km) north of Nauvoo, Illinois. The Sonora varies over a spectrum from arenaceous or argillaceous dolomite through fine-grained dolomitic sandstone to greenish-gray sandy shale. Dolomitization tends to increase downward, and appears to be associated with grain size (Wills, 1971). Much of the Sonora is formed of dolomitized fenestellid debris. Conodonts (Collinson, Scott, and Rexroad, 1962) and the few megafossils (Wills, 1971) indicate equivalent age with the Warsaw and Salem; the Sonora grades laterally into these units (Collinson, 1964). The Sonora is overlain by both the St. Louis and Salem formations. Contact between the Sonora and Salem is conformable; between the Sonora and St. Louis, it is either conformable or erosional, with the St. Louis in the latter case being highly brecciated.

The unit crops out mainly in Adams and Hancock counties in Illinois and in the southeast corner of Iowa, and occurs in the subsurface of much of west-central Illinois. Weller (1908) designated the 8 ft (2.3 m) of cross-bedded limestone below the St. Louis Limestone as the Salem Limestone, and Van Tuyl (1925) assigned the name *Belfast* to arenaceous dolomite exposed south of Belfast, Iowa. Both of these units are equivalent to the Sonora Formation. Collinson (1964) resurrected the name *Sonora Sandstone sensu* Keyes, 1895.

Ullin Limestone: Lineback (1966) proposed the name Ullin Limestone for a unit composed of up to 800 ft (246.1 m) of light-colored, fine- to coarse-grained biocalcarenite. The type section was compiled from three exposures near Ullin, Pulaski County, Illinois. The Ullin Limestone, *sensu* Lineback, is a combination of two previously named formations: the upper Harrodsburg Limestone (Hopkins and Siebenthal, 1897; Stockdale, 1939) and the lower Ramp Creek Limestone (Stockdale, 1929). The units are lithologically distinct, the former composed of a light-colored coarse-grained biocalcarenite and the latter consisting of cherty, argillaceous biocalcarenite that contains glauconite in some horizons. Lineback combined these units because he could not differentiate them in about one-third of the Ullin area of occurrence (*e.g.*, Hamilton County, and on the crest of the Borden Delta). Lineback considered the Ullin Limestone a deep-water deposit, filling around the slopes of the Borden Delta and the deep-water tongue of the Fort Payne Formation. The Ullin Limestone overlies the Fort Payne Formation (or the Choteau Formation where the Fort Payne does not occur), or the Borden, Springville, or Warsaw formations, and underlies the Salem Limestone (Lineback, 1966). In western Illinois, the Ullin laterally grades into the Warsaw Formation.

Salem Limestone: The Salem Limestone was named by Cumings (1901) for Salem, Washington County, Indiana, near which it is quarried extensively for building stone. The names *Spergen Hill* or *Spergen* were also applied to this limestone in some later works. Hall (1864) includes the western Illinois bluffs and the Indiana localities in his work on the fauna of this unit. A maximum thickness for the Salem of over 500 ft (153.8 m) is attained in southeastern Illinois, with general thinning to the north. In the area of this investigation, the Salem ranges from 100 ft (30.7 m) in the south to a few feet thick in the north. At the Warsaw type section in Geode Glen, the Salem is about 5 ft (1.5 m) thick, and consists of cross-bedded brown, weathered biocalcarenite that laterally grades into calcareous sandstone. Equivalent material in southeastern Iowa consists of cross-bedded to massive biocalcarenite, dolomite, and fine-grained sandstone. In southern Illinois, the Salem is more uniform, coarsely crystalline, and may have an oolitic, biocalcarenitic composition. The varied nature of Salem facies along the entire extent of its northern exposure may relate to the shallow Salem depositional environment in this area. The presence of evaporites (anhydrite and gypsum) and sandstone tends to support this conclusion. The more uniform lithology of the Salem of southern Illinois is probably associated with deep-water deposition.

Baxter (1960) subdivided the Salem Limestone into four members. They include, from the basal to the uppermost, the Kidd Member, the Fults Member, the Chalfin Member, and the Rocher Member. Criteria on which these divisions are based are subtle, using bed thickness and slight differences in lithology. In the

northern outcrop, the Salem lies on either the Sonora Formation or the Warsaw Formation, whereas in the south the Salem overlies the Ullin Formation. Fairly abundant crinoids, bryozoans, and forminifera (particularly species of *Endothyra* Phillips, 1841) are predominant faunal components in the Salem. The St. Louis Limestone lies on top of the Salem.

St. Louis Limestone: The St. Louis Limestone was named by Engelmann (1847) for about 200 ft (61.2 m) of predominantly micritic or lithographic, fine-grained, cherty calcilutite exposed at St. Louis, Missouri. Lithologic variability is evident in the St. Louis, with rock types ranging from coarsely crystalline calcarenites to evaporites. The unit is exposed in the Mississippi and Illinois River valleys. Its maximum thickness is 500 ft (153.8 m) in southeastern Illinois, at the maximum depth of the Illinois Basin. In western Illinois, near Keokuk and Quincy, the St. Louis lies on either the Warsaw or the Sonora. The St. Louis generally overlies the Salem in southern Illinois, and underlies the Ste. Genevieve Limestone. The contact between the St. Louis and underlying units is typically conformable, although there is local evidence of an unconformity where collapse breccias are found.

Structural setting.—The study area lies on the western edge of the Illinois Basin. This basin possesses a NNW to SSE trend, and is egg-shaped in outline, having its more elongate end in Kentucky and Tennessee and its eastern edge in Indiana (Willman *et al.*, 1975). Downwarping of the Illinois Basin appears to have begun in Cambrian time and continued throughout most of the Paleozoic (Willman *et al.*, 1975). Seas advanced from the south and at times from the west, inundating the area intermittently until the late Pennsylvanian. Outcrops are typically associated with subtle structures within the Illinois Basin.

The northern half of the area, extending from Bentonsport, Iowa in the north to White Hall, Illinois in the south, is on the southern edge of the Mississippi Arch, a tectonically positive area separating the Illinois Basin and the Forest City Basin. Strata dip gently eastward, away from the Mississippi Arch and into the Illinois Basin. A secondary structural feature, named the Sangamon Arch (Whiting and Stevenson, 1965), probably corresponds with upwarping in this area. Movement began in the Late Silurian and lasted throughout the Devonian and Early Mississippian, as suggested by truncation of units at the edge of the Sangamon Arch and thinning of isopachs over this positive structure. Locations and trends of major structural features are thoroughly illustrated and described in Treworgy (1981).

The Warsaw Dome or Anticline, described by Bell (1932), is located approximately 3 mi NE of Warsaw, Illinois. Similar small anticlinal structures also occur in Brown, McDonough, Pike, and Greene counties. These structures include the Payson, Fishhook, Pittsfield, Drake–White Hall, Carrollton (a set of three: northern, middle, and southern), and Versailles anticlines. The Warsaw, Versailles, Drake–White Hall, and Carrollton anticlines are all associated with outcrops of Warsaw strata.

The southern half of the area, running from southern Calhoun County on the north to Valmeyer, Illinois in the south, shows much greater structural complexity. The Lincoln Fold extends through parts of Madison County, the southern edge of Jersey County, and across Calhoun County. This broad anticline trends northwestward, paralleling the Mississippi River, and extends through Missouri almost to the Iowa border. Initiation of the fold is associated with regional tilting away from the Ozark Uplift, starting during the Ordovician but not developing as a highly positive feature until the latest Devonian or Early Mississippian (Rubey, 1952). Final emergence occurred during or after the Late Pennsylvanian, contemporaneous with the Appalachian Revolution (McQueen, Hinchey, and Aid, 1941). The Cap au Gres Faulted Flexure occurs on the southern limb of this anticline. It is a narrow belt of strata that exhibits a southward dip, which locally approaches vertical and which is intersected by numerous discontinuous vertical faults. This flexure trends east-southeast, extends through Lincoln County, Missouri and parts of Calhoun, Jersey, and Madison counties in Illinois, and apparently terminates between Grafton and Alton, Illinois.

The Cap au Gres Faulted Flexure developed as the structural transition between the Lincoln Fold to the north and the Troy–Brussels Syncline to the south (Rubey, 1952). Beds dip gradually northward at low angles from the Ozark Dome in the extreme south of this flexure. North of the Lincoln Anticline and Cap au Gres Faulted Flexure, beds rise at shallow dips toward the Mississippi Arch, although in some areas this rise is interrupted by a series of minor folds (Rubey, 1952). Deformation of the flexure occurred during the Late Mississippian or Early Pennsylvanian, as evidenced by the steep folding of the St. Louis Limestone (Valmeyeran) and the overlapping of this structure by the Spoon Formation (Desmoinesian).

Associated with this flexure and the Lincoln Fold are numerous synclinal structures, some small but others attaining substantial size. These include (from north to south) the Hardin, Gilead, Kritesville, Otter Creek, Meepen, and Troy–Brussels synclines. The Nutwood, Deer Lick and Beltrees–Melville anticlines also occur in this area.

Outcrops of the Warsaw are associated frequently with some of these structural features, including the Cap au Gres Faulted Flexure, the Otter Creek Syncline,

the Beltrees–Melville Anticline, the Waterloo–Dupo Anticline, and the Valmeyer Anticline. Extension of the Cap au Gres Faulted Flexure into Missouri results in good exposures of Warsaw strata near Troy, Missouri.

The Waterloo–Dupo Anticline and associated Columbia Syncline, both located in Monroe and St. Clair counties, expose the Salem Limestone and upper Warsaw Formation along the Mississippi River bluff. Cole (1961), using geologic and geophysical evidence, suggested this anticline is an extension of the Lincoln Fold. In his structural model, the Cap au Gres Faulted Flexure is a left-lateral fault that offset the Waterloo–Dupo Anticline from the Lincoln Fold by a distance of approximately 30 mi (48 km). This contradicts Rubey's work, in which it was concluded that the Cap au Gres Faulted Flexure is primarily a fold and only subordinately faulted. The west sides of both the Lincoln Fold and Waterloo–Dupo Anticline show their steepest flanks. This and their overall similar shapes tend to support Cole's interpretation.

Farther south, in Monroe County, the Valmeyer Anticline and associated Monroe City Syncline expose most of the Valmeyeran Series in Dennis Hollow, near Valmeyer, Illinois and along the bluffs of the Mississippi River.

TAXONOMY OF MESHWORK FENESTRATE BRYOZOA

GENERAL TAXONOMIC DIVISIONS OF THE BRYOZOA

This paper deals taxonomically with members of one suborder of the classic Order Cryptostomata Vine, 1884, the Fenestelloidea Astrova and Morozova, 1956. The other two suborders of cryptostomes, the Rhabdomesoidea Astrova and Morozova, 1956, and Ptilodictyoidea Astrova and Morozova, 1956, are not covered.

McNair (1937) divided the cryptostomes into three morphologic groupings: fan-shaped and pinnate unilaminate forms, dendroid forms, and bifoliate forms. He stressed these were neither taxonomic nor phylogenetic groupings. Astrova and Morozova (1956) used these divisions to establish three suborders: the Fenestelloidea, Rhabdomesoidea, and Ptilodictyoidea. Elias and Condra (1957) removed the fenestrates completely from the cryptostomes, making them a separate order. Their primary argument was an inferred homology between the unlaminated granular calcite layer of the fenestrates (the "colonial plexus") and the zone of budding in modern stenolaemates, the so-called "common bud" of Borg (1926). This amounts to a return to Vine's (1884) original concept of Cryptostomata and away from Ulrich's (1890) concept. Elias and Condra also suggested that the fenestrates were ancestors to the Cheilostomata Busk, 1852, using the loss of "colonial plexus" in cheilostomes as the event marking the transition between the two groups. Waters (1891) concluded that if the fenestrates were ancestral to the cheilostomes, a missing link between Paleozoic and Cenozoic forms might be evident during Mesozoic, possibly in a family such as the Melicerititidae d'Orbigny, 1852. Workers with Mesozoic bryozoan faunas (Levinsen, 1925; Marcus, 1924) attempted unsuccessfully to recognize a connection between the fenestrates and cryptostomes and the Melicerititidae. Shishova (1968) accepted an ordinal ranking for the fenestrates, with taxonomic emphasis placed on zooecial shape, budding pattern, microstructure, and accessory features such as peristomes, lunaria, and ovicells.

Shishova (1968) also elevated the rhabdomesoids from subordinal (Astrova and Morozova, 1956) to ordinal rank. This left the bifoliates as the only major group in the Order Cryptostomata, a concept now highly altered from those of both Vine (1884) and Ulrich (1890).

Numerous workers have taken exception to the ordinal divisions of the classic cryptostomes. Tavener-Smith and Williams (1972), using microstructural skeletal considerations, adhered to Astrova and Morozova's subordinal placement. Cuffey (1973), using cluster analysis, found the three "orders" of cryptostomes grouped together, away from the Trepostomata Ulrich, 1882. Based on his work, Cuffey developed a strong argument for retention of the classic Cryptostomata.

In a comprehensive study, Blake (1975) supported the subordinal ranking of the fenestrates, rhabdomesoids, and ptilodictyoids, basing his interpretations on the similarities in skeletal development, budding patterns, zooecial and zoarial shapes, and overall symmetry between the suborders. His subordinal divisions are based on such characters as presence of ovicells in fenestellids, vesicles in bifoliates, and metapores in rhabdomesoids.

The taxonomic placement of phylloporinids has been somewhat controversial, but strong morphologic similarites suggest apparent close phylogenetic relationships between the Phylloporinidae Dunaeva and Morozova, 1974 and the fenestrates. Ulrich (1890) and Shulga-Nesterenko (1960) placed the phylloporinids with the Fenestelloidea because of their microstructure, whereas Bassler (1953) placed them with trepostomes, due to their elongate zooecia. Characters phylloporinids share with the Fenestellidae, reported by Ulrich (1890), Shulga-Nesterenko (1960), and Ross (1964), were used as strong criteria justifying their taxonomic placement in the Fenestellidae. Blake suggested probable derivation of the fenestellids from the

phylloporinids, with differences between the two families being a function of degree rather than of kind. Earlier, Dunaeva and Morozova (1974) removed the Phylloporinidae from the Fenestelloidea, citing as criteria the difference in zooecial shapes as well as the presence of "specific heterozooids" and the absence of ovicells in the phylloporinids.

In my view, historical considerations [Vine (1884) and Ulrich (1890)], phylogenetic affinities [Blake (1975)], numerical analyses [Cuffey (1973)], and polythetic character considerations [Ulrich (1890), Shulga-Nesterenko (1960), Ross (1964), and Morozova (1962)] endorse retention of the classic Cryptostomata with the three suborders of Fenestelloidea, Rhabdomesoidea, and Ptylodictyoidea: I have done so here. Such an arrangement stresses shared characters or similarities rather than dissimilarities. Microstructural and/or ultrastructural analyses of both fenestrates and rhabdomesoids indicate great similarities between these suborders [a view greatly contrasting with that of Condra and Elias (1944), but concurring with those of Tavener-Smith and Williams, 1972, and Blake, 1975].

King (1849) established the Family Fenestellidae for fanlike and pinnate Paleozoic bryozoans, including in his family *Fenestella* [type: *F. antiqua* Lonsdale, 1839], *Polypora*, and *Ptylopora* McCoy, 1844, and two new genera, *Synocladia* and *Phyllopora*. Zittel (1880) erected a new family for the pinnate forms, the Acanthocladiidae. Vine (1884) subdivided King's family Fenestellidae into three families: the Fenestellidae, Polyporidae, and Diploporidae. A similar division was made by Waagen and Pichl (1885), who subdivided the family Fenestellidae into three subfamilies: Fenestellinae, Polyporinae, and Goniocladiinae. Ulrich (1890, 1893) placed the fenestellids, acanthocladids, and polyporids within the cryptostomes [following the work of King (1849)], stressing a polythetic classification scheme and pointing out apparent phylogenetic relationships among taxa. His extensive work on Warsaw materials has proven invaluable in this study. Many of his taxonomic subdivisions and faunal interpretations show remarkable insight when one considers the techniques and equipment available at the time. Subdivision of the Fenestellidae into three groups was followed in the work of Cumings (1904, 1905), who further investigated the primary stages of colony development in *Fenestella* Lonsdale, 1839, and *Polypora* McCoy, 1844. From his studies, Cumings concluded that these genera should be assigned to different families. Vine (1884) established two of the dendroid families of cryptostomes: the Rhabdomesontidae (corrected to Rhabdomesidea by Bassler, 1953) and the Hyphasmoporidae. A third dendroid cryptostome family, the Arthrostylidae, was proposed by Ulrich (1888).

Overall similarity in symmetry and morphologic characters between the fenestellids and rhabdomesoids indicates a much closer affinity between these two groups than between them, either singularly or jointly, and the Trepostomata, Cystoporata, or Cyclostomata. Zooecial chambers in these two suborders are relatively short, highly symmetrical, and fixed in size and shape throughout the zoarium. Short symmetrical zooecia result in slender branches and delicate sheets and fans characteristic of the cryptostomes, contrasting with the commonly much more massive forms of the Trepostomata and Cystoporata. Budding loci for the Cryptostomata are restricted to one- or two-dimensional surfaces (very rarely three dimensions for a few species) for members of this order as opposed to the two- and predominantly three-dimensional surfaces characteristic of the other stenolaemates. Blake (1980) argued that the cryptostomes are an evolutionary clade whose establishment resulted from evolution of this restricted locus, which allowed colonies to grow out rapidly into the water column without needing to fill large amounts of lateral space, as is observed in the trepostomes and cystoporates. Many accessory features are common within the suborders of the cryptostomes. Some accessory features are also shared with the other orders, possibly as a result of homeomorphy, as illustrated by Blake in the rhabdomesoids and dendroid trepostomes. Such features include stylets, which are continuous with the internal granular layer that extends through the outer lamellar skeleton, both perforate and complete terminal diaphragms, and frequent symmetrically placed hemisepta within the zooecial chamber. The fenestrates and rhabdomesoids also lack the regenerative cycles evident and often common in the trepostomes and cystoporates.

Therefore, based on similarities in morphology, phylogeny, and use of historical considerations, the Order Cryptostomata is retained in this study, with Fenestelloidea grouped as a suborder under that order.

SUMMARY AND CRITIQUE OF PREVIOUS APPROACHES TO THE TAXONOMY OF MESHWORK FENESTELLOIDEA

Fenestrate bryozoans have been studied extensively since the mid-nineteenth century (Hall, 1847, 1852, 1857b, 1883, 1885; King, 1849, 1850; Lonsdale, 1839; McCoy, 1844; d'Orbigny, 1848–1852; Owen, 1838, 1842; Phillips, 1836, 1841; Prout, 1858a, 1858b, 1859, 1866; Vine, 1880, 1884, 1886). These authors presented illustrations and descriptions only of specimen exteriors; Ulrich (1888, 1890), Nicholson and Lydekker (1889) and Počta (1894) were apparently the first to publish thin-sectioned fossil Bryozoa. Ulrich (1890), in the most comprehensive work of the above, illustrated numerous views of fenestellids and other bry-

ozoans, providing detailed description of microstructure.

Ulrich (1882, 1888, 1890, 1893) made major contributions to descriptive and laboratory techniques, primarily concerning himself with the Silurian (as then conceived in North America) and Carboniferous bryozoan faunas of the Upper Mississippi Valley and surrounding areas. Ulrich emphasized the need for thin-sections as an important aspect of faunal analysis, and developed large collections. Many of Ulrich's remaining thin-sections are housed today at the U. S. National Museum of Natural History (Smithsonian Institution) and the Illinois State Museum. He also prepared and sold thin-sections to universities; some of these are still in collections at various institutions. Ulrich mounted his sections on windowpane glass taken from wrecked buildings in Washington, DC (Boardman, oral commun., 1978). In numerous publications, Ulrich illustrated thin-sections and exteriors, albeit at relatively low magnifications. He also recognized two microstructural skeletal components of the fenestrates: the granular skeletal layer, which he referred to as "original basal or germinal plate", and the lamellar skeletal layer called "subsequently added layers of calcareous tissue" (Ulrich, 1890, p. 352). He developed a diagnosis arrangement for the fenestrates that stressed almost all features considered important today. These include zooecial shapes, presence of a vestibule, presence of a well-developed, abruptly arising exozone, and presence of hemisepta; zoarial form and maximum zoarial length; branch character and nature of bifurcation; dissepiment character and width; fenestrule shape, including length and width; keel development; nodal development and spacing; aperture shape, positioning on branch surface, and relative size; number of apertures per fenestrule and spacing along branch; and reverse surface characters such as supports, dissepiment appearance and presence of longitudinal rows and stylets from external analysis. Lack of consideration of intraspecific variation is the primary weakness of Ulrich's work from a modern point of view.

A convention adopted by Ulrich to describe characters in terms of varying lengths in the proximodistal direction of branch growth has been adopted by many subsequent workers. These include branch bifurcations in 1 cm, fenestrules in 1 cm, nodes in 2 mm, and apertures in 5 mm. Nekhoroshev (1926) and later Condra and Elias (1944) refer to these characters as *meshwork formula* (really a listing, rather than an integrated formula), whereas Miller (1961a; 1961b) and Termier and Termier (1971) use the name *micrometric formula*. The formula applied by these authors dealt with colony exteriors, ignoring interior analyses entirely. Use of the meshwork formula has been a prime contributing factor in the extreme proliferation of species of *Fenestella* Lonsdale, 1839, because new species are based primarily on small quantitative differences. Thousands of species (Morozova, 1974) have been recognized through use of the meshwork or micrometric formula.

Condra and Elias (1944) and Elias and Condra (1957) worked with the predominantly Carboniferous genus *Archimedes* Hall, 1858 of the central United States and *Fenestella* from the Permian of West Texas. In their work on *Archimedes*, they dealt primarily with two topics: the central axes and means of species recognition. Further, they subdivided *Archimedes* into new species based almost exclusively on axial characteristics, which are primarily environmentally influenced. The effect of environmental influence is herein demonstrated by large coefficients of variation for the axis within species (Tables 37–40). Elias and Condra seemingly ignored mesh and zooecial characteristics in their analyses. Their approach to *Fenestella* resembled closely that of Ulrich (1890), and although strongly endorsing the use of thin-sections in bryozoan analysis, Condra and Elias used relatively few sections in their work. Standard meshwork formula measurements were applied and ranges were given, but no statistical analysis substantiates their data. The number of measurements made from different colonies was not provided, although they did indicate that single specimens were available for some species. Elias and Condra illustrated tangential and transverse (cross-sectional) interior views along with zoarial exteriors. No longitudinal sections were employed and, consequently, accurate three-dimensional reconstruction of the autozooecial chamber is not possible.

The meshwork formula, as used commonly and presented by Termier and Termier (1971) in their work on the upper Paleozoic of Afghanistan, appears as:

a / b / c / d / e

where **a** = range of number of branches in 10 mm; **b** = range of number of fenestrules in 10 mm; **c** = range of number of zooecia across the branch (two in the fenestellids [sometimes omitted in the formula]); **d** = range of number of zooecia in 5 mm; and **e** = range of number of nodes in 5 mm. Such a system records ranges, without providing a comprehensive system in which accepted statistical techniques used in comparing numerical data can be applied.

Tavener-Smith (1965, 1966, 1973), working with Visean fenestrates from Ireland, rejected the meshwork formula because of this lack of statistical credibility. Tavener-Smith restricted his work to colony exteriors because the fauna in his study area was primarily silicified. He greatly improved methods for analysis of fenestrate species by expanding the list of characters used and differentiating zooecial from zoarial charac-

ters. His criteria include, in outline form:

A. Zooecial features
  1. inter-apertural distance
  2. branch width
  3. apertural diameter
  4. zooecial chamber shape and size
B. Zoarial features
  1. fenestrule length
  2. fenestrule width
  3. number of apertures per fenestrule
  4. internodal distance
  5. dissepiment width

Tavener-Smith emphasized the written description, including features such as purported three-dimensional shape of the zooecia, aperture distribution at branch bifurcations, angle of newly formed branch, fenestrule shape, aperture position relative to branch and dissepiment surfaces, apertural features such as peristome, branch and dissepiment cross-sections, and reverse-wall striae. Even though Tavener-Smith recognized problems in species recognition due to secondary thickening of exterior lamellar skeleton and other morphologic changes during ontogeny, he apparently used only exteriors in his analyses. Although much of the fauna he analyzed was silicified, he did indicate the presence of non-altered specimens in his material. Tavener-Smith's major contribution was the introduction of a rigorous statistical approach, which included the range of specimen mean values, sample mean, standard deviation, and coefficient of variation for all characters except apertures per fenestrule — which are expressed in the range of specimen modes — and distribution of specimen modes. Other authors (Cuffey, 1967; Bork and Perry, 1967; Horowitz, 1968; Anstey and Perry, 1970, 1973) started employing more rigorous statistical analyses in their taxonomic works on Bryozoa shortly after Tavener-Smith.

Possible use of the internal skeleton and associated zooecial and zoarial features through thin-section analysis was recognized by the late 1800's (*e.g.*, Ulrich, 1890, 1893). Although aware of the significance of internal features for taxonomic interpretation, no subsequent workers until Nekhoroshev and Nikiforova, in the first half of the twentieth century, made extensive use of thin-sections for bryozoan taxomomy. Their attempt to express variation within a species in numerical form was an important contribution. Their work dealt with Upper Paleozoic bryozoans of the U. S. S. R.; Carboniferous bryozoans from the Altai, Kuzbass, Kazakhstan, and Turkestan; and Permian bryozoans from Bashkiria and Armenia, as well as eastern European materials. Nekhoroshev (1928, 1932, 1949, 1953, 1956), Nikiforova (1933, 1935, 1938), Shulga-Nesterenko (1936, 1941, 1949, 1951, 1952, 1955), Trizna (1939, 1950, 1958), and Trizna and Kautsan (1951) developed bryozoan faunas into useful biostratigraphic tools in the U. S. S. R. and surrounding countries.

Although more comprehensive in format than earlier works, the Soviet taxonomic approach possesses inherent problems stemming from the method of study. In Soviet fenestrate taxonomic work, tangential views are stressed, along with rare transverse views. Longitudinal views are essentially absent in Soviet studies of fenestrates. Further, there are few descriptions of obverse or reverse surface exterior details, which may be due to poor preservation of zoaria. Such a taxonomic approach, although more complete than typical studies in the West, allow little or no more accurate analysis than is possible from strictly exterior-oriented studies. A combination of both interior and exterior analyses is necessary to accurately determine taxonomic affinities and accurately delimit species. This conclusion is dealt with extensively on p. 22.

Morozova (1962, 1970a, 1970b, 1973, 1974) studied fenestrate bryozoans and provided suggestions for generic subdivisions of *Fenestella* in numerous taxonomic works. Her work represents the current Soviet approach to species within the fenestrates. The eight main criteria for differentiation of species of *Fenestella* used by Morozova (1970b) are outlined in Table 2 along with the principal measurements taken; these were not listed by Morozova, but were compiled by the writer from her text.

Morozova's approach, although including a greater number of measurements of characters, closely resembles that of Ulrich (1888, 1890). It differs from his work in recognizing a need for a more statistical approach and the use of zooecial shape in middle tangential section (referred to as *median section* by Morozova). Zooecial shape plays an important part in Morozova's specific and generic assignments of taxa. However, reconstruction of the zooecial chamber and, more importantly, three-dimensional chamber shape based only on tangential sections, is incomplete and misleading. Although this orientation is essential in chamber reconstruction, additional views are necessary, not only to accurately determine chamber shape and orientation relative to branch, but also to recognize various accessory features, such as inferior and superior hemisepta.

Banastella guensburgi, n. sp. (Text-fig. 3A) and *Cubifenestella usitata*, n. sp. (Text-fig. 3B) provide just two of many possible examples of how misleading it is to attempt to characterize internal anatomy of fenestrates based on mid tangential sections alone. Using mid tangential sections, as relied upon by Morozova, extreme similarity in zooecial chamber shape (arrow **a**) and only slight difference in size is evident between the

Table 2.—Descriptive criteria for differentiation of species of *Fenestella* used by Morozova (1970b). **D** = descriptive; **M** = measured (in mm).

1. mesh (regular or irregular)	D
2. branch	
a. width (narrow or wide) and depth (thin or thick)	D
b. width	M
c. distinctive changes in width (before or after bifurcation, or due to emplacement of accessory zooecia)	D
3. fenestrule	
a. shape (oval, round, or polygonal)	D
b. alterations in shape due to zooecial projection into opening	D
c. length	M
d. width	M
e. number in a 10 mm distance along colony	M
4. dissepiment	
a. width (narrow or wide)	D
b. width	M
5. zooecia	
a. shape (in median [tangential] section)	D
b. shape before and after a bifurcation	D
c. number in a 5 mm distance along branch	M
6. apertural characteristics	
a. degree and kind of projection into fenestrule	D
b. accessory features (*e.g.*, peristome, lunaria, stylets), and positioning of these features	D
c. length	M
d. width	M
e. peristome width	M
7. heterozooecia or polymorphs	
a. presence or absence	D
b. dimensions	M
8. other characteristics	
a. carinae, nodes, and tubercules	D
b. diameter of nodes and tubercules	M
c. number of nodes and tubercules in a 1 mm distance	M

two species; the ratios between length (arrow **b**) and width (arrow **c**) also appear moderately similar, as does placement of the autozooecial chamber within the branch. Some indication of different apertural-opening orientation (arrow **d**) is observed in shallow tangential section, although this is best presented in transverse section (arrow **e**), with apertures in *C. usitata* opening more into the fenestrule opening than apertures in *B. guensburgi*, whose opening approaches parallel to the obverse branch surface. Relying solely on tangential sections, we have two apparently similar species with similar chamber outlines, particularly in mid tangential view.

Comparing longitudinal and to a lesser degree, transverse sections of these two species, a much different conclusion is reached. A tangential section approximately follows the line marked by arrow **f** in longitudinal sections of both *B. guensburgi* and *C. usitata*. This length corresponds approximately to the measurement of chamber depth (arrow **g**) in *C. usitata*, which in turn equals approximately the chamber length (arrow **h**) in this species. In *B. guensburgi*, however, the line marked by arrow **f**, which corresponds to arrow **b** in the tangential section, does not represent either depth (arrow **g**) or length (arrow **h**) of the autozooecial chamber. The apparent length of the chamber as represented by the line marked by arrow **f** represents approximately 1.7 times the chamber depth (arrow **g**) and approximately one-half the chamber length (arrow **h**). Sole reliance on the tangential sections for measurements of chamber length and width can provide accurate information in some species, such as *C. usitata*, but provides no information about depth. In other species such as *B. guensburgi*, the tangential section provides only accurate chamber widths, but extremely misleading information concerning chamber lengths.

The angle subtended by the chamber's lateral and reverse walls (arrow **i**) is the character which causes the difference in applicability of tangential section in the two species illustrated. When the reverse-wall budding-angle approaches 90°, the length seen in tangential section will equal or closely approximate that seen in longitudinal section, as in the species *C. usitata*. In *B. guensburgi*, the reverse-wall budding-angle is quite low, approximately 38°, and thus the tangential section is of little use in determining chamber length. Although these two species appear similar in tangential section, a combination of sectional views demonstrates that differences between *B. guensburgi* and *C. usitata* are sufficient to justify assignment to different genera.

Among genera, there are similar problems with reverse-wall budding-angle, and the type, placement, and

degree of development of hemisepta. Until rigorous analyses using all necessary zoarial views are applied to the meshwork Fenestelloidea, it will not be possible to accurately identify species, and to compare species from different geographic areas.

Due to the problems in classification summarized below, species of *Fenestella* and members of most of the meshwork Fenestelloidea have been difficult to recognize. This difficulty has led to the proliferation of species names and the inability of workers to agree on phylogenetic affinities within genera. These difficulties seem to result from: (1) lack of work with populations; (2) dependence predominantly on either incomplete evaluation of interiors or exteriors rather than a thorough combination of the two; (3) insufficient statistical analyses of material (which are needed to determine true range of variation of characters); (4) adherence to the meshwork or micrometric formulas and similar approaches that deal with range and pattern instead of form (Similarity in mesh pattern may be extreme, even between members of different genera.); (5) two-dimensional treatment due to overdependence solely on tangential sections in analyses [Three-dimensional considerations and reconstructions, particularly of zooecial chambers, such as that of McKinney (1980) in his generic description of *Utropora* Počta, 1894, have not generally been used.]; (6) lack of consideration of astogenetic thickening as a factor causing pronounced variation in exterior zoarial morphology within a single species.

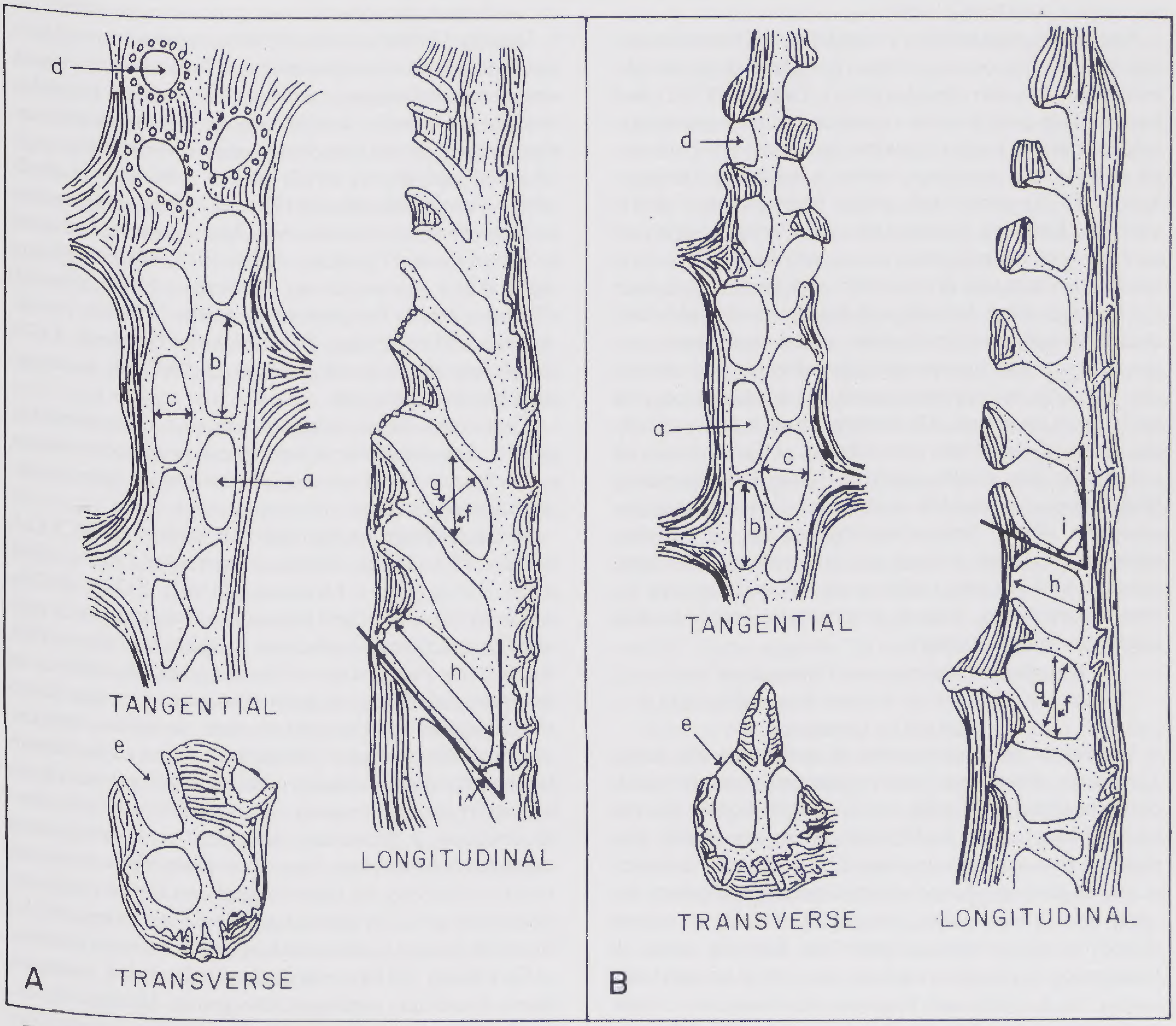

Text-figure 3.—Comparison of interior sections of *Banastella guensburgi* (**A**) and *Cubifenestella usitata* (**B**), illustrating significant similarities in chamber profile in tangential view and dissimilarities in longitudinal view.

A single taxonomic methodology can and should be employed throughout the Suborder Fenestelloidea. Within a species, members of the suborder exhibit pronounced similarity of certain zooecial characters, particularly with regard to chamber size, symmetry, and accessory features. Such common traits offer an ideal basis on which to develop a uniform taxonomic methodology. Because all zooids of a zoarium, excluding the ancestrula, were reproduced asexually and have a single genotype, phenotypic variations within a single zoarium can be assumed to be due to other than genetic factors (Gautier, 1970, 1972; Boardman and Cheetham, 1969, 1983; Cook, 1977). The advantage of the use of colonial animals for studies in variation, both ontogenetic and astogenetic, has been recognized by many workers, and was discussed in detail by Boardman and Cheetham (1969).

Secondary calcification or addition of lamellar calcite commonly occurs within the fenestrates, as observed by Tavener-Smith (1973), Gautier (1972) and herein. This calcification continued during colony astogeny, causing walls to thicken progressively from distal to proximal positions within a zoarium. Tavener-Smith (1973) concluded, solely from exterior observations, that such thickenings could be ignored if one carefully considered quantitative attributes. From my work, I believe this is incorrect, as I have found such thickenings affect branch and dissepiment width and thus fenestrule size, keel width, nodal appearance, exterior ornamentation on both the obverse and reverse zoarial surfaces, apparent aperture opening size, and peristomal thickness. This observation reduces greatly the value of six of the nine criteria of Tavener-Smith (1973): branch width, apertural diameter, fenestrule length, fenestrule width, internodal distance, and dissepiment width. Secondary thickenings of lamellar skeleton, at times enough to cover completely both obverse and reverse surfaces and completely fill fenestrule openings, suggest a structural response that increases colony strength.

HISTORICAL REVIEW AND APPROACH TO TAXONOMIC DIVISIONS WITHIN THE FORM GENUS *FENESTELLA* LONSDALE

Fenestrate bryozoans, and in particular the genus *Fenestella*, have long been recognized as major components of many Middle and Upper Paleozoic marine rocks. Many of the traditional genera are readily recognized because they are based on such exterior characters as fan- and funnel-shaped colonies; distinct obverse and reverse sides; straight to undular branches; dissepiments connecting branches, forming voids or fenestrules between branches; two rows of apertures across the branch; and frequent presence of a carina, keel, nodes, or other accessory features (Nickles and Bassler, 1900; Bassler, 1953; Nekhoroshev, 1960). Primary reliance on exterior analyses and provincial knowledge of literature have led to a great proliferation of species of *Fenestella* [over 1,200 to date (Morozova, 1974)] and extremely wide geographic and geologic ranges (Ordovician–Triassic): such ranges and abundance suggest the genus is heterogeneous.

In 1890, Ulrich, and later Nekhoroshev (1928), recognized the probable polyphyletic nature of *Fenestella*. These conclusions were based on exterior and thin-section analyses of transverse and tangential views in the case of Ulrich, and predominantly on tangential thin-sections in the case of Nekhoroshev. Both workers observed highly varied internal arrangement and structure for species which fit readily the then-current concept for the exterior of *Fenestella*. Neither Ulrich nor Nekhoroshev subdivided the genus, possibly to retain its usefulness for exterior recognition in the field.

Despite Ulrich's emphasis on a combination of both exterior and thin-section analyses for all bryozoan genera, many subsequent workers have relied on either interior or exterior analysis alone for taxonomic assignments. Species based only on exterior analysis (*e.g.*, Utgaard and Perry, 1960; Miller, 1961a; Campbell, 1961; Tavener-Smith, 1973), and new genera separated from *Fenestella* but based solely on exterior analysis (*Fenestrellina* d'Orbigny, 1849; *Flabelliporina* Simpson, 1895a; *Fenestrapora* Frederiks, 1915; *Cervella* Chronic, 1949; *Parafenestella* Miller, 1961b; *Levifenestella* Miller, 1961a, *Dogaddanella* Ganesan, 1972; *Polyfenestella* Bancroft, 1986a) are difficult to recognize beyond the types.

Taxonomy based solely on exterior characters (Engel, 1975) is justifiable where, due to poor preservation, only exterior views are available; however, general applications of such studies are limited.

Soviet workers, including Nekhoroshev (1928, 1932, 1949, 1953, 1956), Shulga-Nesterenko (1941, 1949, 1951, 1952, 1955), Morozova (1962, 1970a, 1970b, 1973, 1974), and others have done extensive work with interior microscopic analyses of species of *Fenestella*. Their early recognition of the extreme importance of autozooecial shape in both species and genus determination was a major contribution; however, their use of only cross-sectional (tangential) views of the chamber has resulted in much confusion of taxonomic assignment in the literature. This problem is discussed in detail on p. 30 in the context of a revised generic classification scheme. Taxonomic decisions based almost exclusively on interior analyses are nearly as seriously in error as those based only on exteriors, for they too ignore a great deal of available information.

Crockford (1944), working with Permian materials from Australia, separated the genus *Minilya* Crockford, 1944, from *Fenestella*. In her work, Crockford used triangular cross-sections of the autozooecial

chambers and alternating biserial arrangements of carinal nodes as criteria for separation. Wass (1966) rejected *Minilya* after his discovery of monoserial and biserial nodes on the same branch in two species assumed to belong to this genus. Morozova overturned Wass's conclusions, resurrecting *Minilya* based on her observations that Wass's analysis was "mistaken and connected with inadequate conditions of the material investigated by him." (Morozova, 1974, pp. 176–177). Triangular chamber shape, two rows of alternating nodes on a broad low carina, square fenestrule shape, and thin straight dissepiments are Morozova's main criteria for delimitation of this genus. Although Morozova's retention of the genus *Minilya* appears correct based on analysis of Warsaw materials, a more thorough justification both descriptively and numerically would be of great assistance to other workers.

Elias and Condra (1957), in a study of species of *Fenestella* from the Pennsylvanian of the midcontinent and the Permian of West Texas, argued that the genus was of polyphyletic origin. They divided the species of *Fenestella* studied into three sections or groups and thirteen subgroups. Group divisions were based on the following criteria: length of fenestrules, apertures per fenestrule length, and node distribution. The three groups include: (1) species with long fenestrules, 3.5 to 5.0 autozooecial apertures per fenestrule, and a single row of nodes; (2) species with long and short fenestrules and a double row of nodes; (3) species with short fenestrules, 2.0 to 3.5 autozooecial apertures per fenestrule, and a single row of nodes. The thirteen subgroups are divided on criteria ranging from chamber shape to number of zooecia per fenestrule, branch width, zoarial shape, and carinal development. Besides applying a primarily monothetic approach, the divisions of Elias and Condra (1957) are difficult to use because they employ few characters, and those used are not applied equally to all taxa (some involve interior chamber shape, others involve exterior features such as carina and even zoarial shape). *Loculiporina* Elias and Condra, 1957 is based on extremely poor material. Because there appear to be a relict superstructure and a mesh pattern similar to that of *Hemitrypa* Phillips, 1841, *Loculiporina* cannot be readily separated from *Hemitrypa* on the basis of information provided by Elias and Condra. Their use of group and subgroup and nonadherence to accepted taxonomic hierarchy and divisions make their work extremely difficult to apply or relate to earlier works.

The genus *Archaefenestella* was proposed by Miller (1962), based on material from the Lower Silurian of England. His genus is distinguished by quadrangular zooecial shape in tangential section and the presence of vesicular tabulae that intersect the zooecial chamber.

Termier and Termier (1971) recognized six new genera within the traditional *Fenestella* from the Late Paleozoic of Afghanistan. These genera include: *Rhombofenestella*, *Aequifenestella*, *Alternifenestella*, *Spinofenestella*, *Rugofenestella*, and *Mirandifenestella*. The Termiers based their genera primarily on the groups and subgroups of Elias and Condra (1957). Primary emphasis on the micrometric formula and an inadequate descriptive section for their species determinations handicapped the Termiers' conclusions. Type species were not designated for *Aequifenestella* or *Rugofenestella*, nor were diagnoses presented for any of the proposed genera. The short descriptions presented and the lack of throrough analysis make the Termiers' work of limited value.

Morozova (1974) acknowledged the heterogeneous nature of the traditional form genus *Fenestella* and subdivided it, retaining five established genera and establishing nine new genera, respectively: *Archaefenestella* Miller, 1962, *Mirifenestella* Morozova, 1974, *Laxifenestella* Morozova, 1974, *Exfenestella* Morozova, 1974, *Fabifenestella* Morozova, 1974, *Flexifenestella* Morozova, 1974, *Rarifenestella* Morozova, 1974, *Rectifenestella* Morozova, 1974, *Spinofenestella* Termier and Termier, 1971, *Minilya* Crockford, 1944, *Alternifenestella* Termier and Termier, 1971, *Ignotifenestella* Morozova, 1974, *Cavernella* Morozova, 1974, and *Permofenestella* Morozova, 1974, as well as retaining *Fenestella* Lonsdale, 1839. Believing "*Fenestella* consists of a large number of natural groupings of species that are connected by common origin and developed independently in different stages of the Paleozoic", Morozova (1974, p. 169) interpreted all her genera as phylogenetically linked groupings of species, many of which closely follow the inferred phylogenetic branchings of Shulga-Nesterenko (1951). Extreme differences in internal structure in zoaria, with mesh of nearly identical shape and structure, were interpreted by Morozova (1974, p. 169) as proof that "*Fenestella*" form species "arose independently in many genera of the family Fenestellidea," evidently as a result of parallel evolution.

Internal characteristics of the autozooecial chamber are stressed in her analyses, although she attempted to determine chamber shape from tangential section alone. Morozova's new genera are each based on the presence of a distinctive polymorphic type, with different polymorphs found in different genera. This often highly monothetic approach yields an apparent pattern of much parallel evolution. Examples of types of heterozooecia include the "parazooecia" used to delimit *Mirifenestella*, "cyclozooecia" delimiting *Ignotifenestella*, "caverns" delimiting *Cavernella*, and "microzooecia" delimiting *Permofenestella* (Morozova, 1974; pp. 170, 177, 178).

Table 3.—Characters used by Morozova (1974) for discrimination of 10 genera from the form genus *Fenestella,* here also applied to four genera of other authors. — = character absent or lacking in description.

	Fenestella Lonsdale, 1839 [Lower Silurian–Permian]	*Archaefenestella* Miller, 1962 [Lower Silurian]	*Mirifenestella* Morozova, 1974 [Middle Devonian]	*Spinofenestella* Termier and Termier, 1971 [Lower Devonian–Lower Permian]	*Minilya* Crockford, 1944 [Lower Devonian–Lower Permian]	*Alterni-fenestella* Termier and Termier, 1971 [Devonian–Lower Permian]	*Ignoti-fenestella* Morozova, 1974 [Lower Carboniferous]
1. colony mesh type	mesh-like	—	firm mesh	medium fine mesh	regular, mesh usually fine	—	coarse mesh
2. branch width and shape	wide	thin (straight)	very broad	straight, thick, broad	relatively broad	straight, thin	straight
3. dissepiment width and shape	thin	thin	very broad	comparatively slender	thin	thin	thin
4. number of rows of zooecia in deep cross-section and zooecial shape in median cross-section	two rows regular quadrangular	two rows quadrangular	two rows regular quadrangular	two rows triangular, triangular-pentagonal before bifurcation	two rows triangular, triangular-pentagonal before bifurcation	one row in deep cross-section, trapeziform or triangular-trapeziform	two rows, pentagonal and rounded pentagonal
5. presence or absence of carina, their size, shape, and emplacement	single straight narrow carina	straight, narrow	high, straight	narrow and high	broad and low	thin	low
6. presence or absence of nodes, their relative size, location, and emplacement	monoserial small nodes or carina	—	—	monoserial row of nodes on carina	biserial row of alternating nodes on carina	monoserial row of nodes on carina	monoserial row of nodes on carina
7. presence or absence of tubercles, and their size and location	—	monoserial tubercles	—	—	—	—	—
8. presence or absence of inferior and/or superior hemisepta	present	—	—	—	—	—	—
9. presence or absence of vesicular diaphragms	—	present, intersect zooecial cavities	—	—	—	—	—
10. presence or absence of heterozooecia	—	—	parazooecia	—	—	—	"cyclozooecia" on branch, and on interval between adjacent zooecia

Table 3 summarizes the ten characters Morozova used for generic differentiation of the form genus *Fenestella* and lists the genera recognized with their respective characters. Rather than providing discrete measurements or indicating presence or absence, Morozova applied descriptive modifiers to her characters. As opposed to giving an indication of presence/absence or of measurements and, as illustrated in the Table, those modifiers are frequently applied inconsistently. These problems led to descriptive ambiguities throughout her work. No definite means of comparison are given for such relative terms as *thin*, *wide*, *fine*, and *coarse*. For example, in two genera (*Mirifenestella* and *Flexifenestella*), the mesh is described as "firm"; it is not clear how this term fits in a scale of *fine*, *medium*, and *coarse*. Three genera (*Alternifenestella*, *Cavernella*, and *Permofenestella* lack any modifiers whatsoever concerning mesh type. Confusion of mesh symmetry and relative geometric placement of branches and dissepiments with mesh sturdiness or firmness could be a problem arising from translation of the original work into English from Russian; deletion of descriptive comparisons presumably is not.

Under branch width/shape, in some genera (*e.g.*, *Fenestella*, *Mirifenestella*, *Fabifenestella*, *Minilya*, and *Cavernella*), only width is considered, whereas only shape is touched upon in others (*e.g.*, *Laxifenestella*, *Exfenestella*, *Rectifenestella*, and *Ignotifenestella*). Similar problems can be observed in dissepiment width/shape, carina size and shape, and hemisepta development (*i.e.*, inferior or superior position).

Criteria selected by Morozova for generic differentiation, other than those emphasizing heterozooecia, appear to have value for delimiting divisions within the traditional genus *Fenestella*. Lack of three-dimensional reconstruction of the autozooecial chamber severely limits the usefulness of any bryozoan taxonomic work, including Morozova's. Further, chamber shape and related accessory features such as hemisepta and apertural stylets, as observed in the later section on

Table 3.—Continued.

Cavernella Morozova, 1974 [Carboniferous–Permian]	*Permofenestella* Morozova, 1974 [Permian]	*Laxifenestella* Morozova, 1974 [Devonian–Permian]	*Flexifenestella* Morozova, 1974 [Lower Carboniferous–Lower Permian]	*Exfenestella* Morozova, 1974 [Devonian–Permian]	*Fabifenestella* Morozova, 1974 [Devonian–Permian]	*Rarifenestella* Morozova, 1974 [Lower Devonian]	*Rectifenestella* Morozova, 1974 [Upper Silurian–Permian]
—	—	medium mesh	firm mesh	medium, fine mesh	firm, fine mesh	medium mesh	medium, fine mesh
moderately broad	broad, straight or weakly bending	straight or weakly bending	broad, undular curves	straight or weakly curved	broad	broad, straight	straight
moderately broad	short, broad	moderately broad	very short, reduced	straight	straight	very thin, straight	straight
two rows, rounded pentagonal	two rows, rounded pentagonal	two rows, tetragonal-pentagonal	two rows, tetragonal in deep section, tetragonal-pentagonal or fabiform near surface	two rows, fabiform	two rows, tetragonal in deep section, fabiform near surface	two rows, vermiform	two rows, pentagonal, becoming triangular-pentagonal before bifurcation
low	low	slightly curved	broad and low	narrow and slender	broad and low	narrow and high	present
monoserial row of nodes on carina	monoserial row of small nodes on carina	monoserial, small, frequently on carina	large monoserial nodes on carina	monoserial nodes on carina	two rows of alternating nodes on carina	single row of nodes on carina	monoserial row of nodes on carina
—	—	—	—	—	—	—	—
—	—	on branches in two rows	present	on branches in two rows	—	—	—
—	—	—	—	—	—	—	—
"caverns" on dorsal face of branches join with dissepiments	"microzooecia" in pairs, or singly between ordinary zooecia	—	—	—	—	—	—

species, are highly constant within a species and have significant application for generic level taxonomic comparisons.

McKinney (1980), in his redescription of the Devonian fenestrate genus *Utropora* Počta, 1894, clearly recognized and demonstrated the usefulness of three-dimensional chamber reconstructions when considering generic descriptions and affinities. McKinney illustrated reconstructed general chamber form in lateral, frontal, and distal views. McKinney observed that if zooecial shape is to be clearly understood, shallow, medium, and deep tangential views cut parallel to the branch surface are all necessary, as are transverse and longitudinal sections. Fortunately, single sections can provide more than one view; for example, an inclined tangential section over a large specimen provides shallow, medium, and deep tangential views.

In McKinney's work, comparison is made between the three-dimensionally reconstructed living chamber of *Utropora nobilis* (Barrande *in* Počta, 1894) and the type species of *Fenestella*, *Fenestella subantiqua* d'Orbigny, 1839. These reconstructions, along with detailed microstructural analysis showing relative position of granular and laminated skeletal material, offer great taxonomic potential. Unfortunately, although many of these ideas are well presented in the text of McKinney's article, they are not directly applied in his amended diagnosis. Many characters presented by Morozova, as well as those of other earlier workers, are used in McKinney's diagnoses, and although three-dimensional terminology is employed, the illustrations of chamber shape are not referred to therein. Such illustrations should be placed directly in the diagnosis to be of greatest value to subsequent workers. Positioning of the zooecial chamber relative to the branch orientation and other zooecia present, along with aperture positioning along the branch, is included in McKinney's analyses. These characters, neglected in the two-dimensional approach of the Soviets, have proven of prime importance in delimiting subdivisions within the traditional genus *Fenestella* in this study.

Bancroft (1986a) described the new fenestrate genus

Table 4.—Taxonomic criteria for generic divisions within the Warsaw fenestellids. See Table 7 for explanations of abbreviations.

Character Groupings (External)

- I. zoaria
  - A. robustness (*delicate* [fragile, small colony fragments] → *intermediate* [moderately complete zoaria present] → *robust* [zoaria large, thick, resist abrasion])
  - B. outward expansion (flat, obversely or reversely curved, undulating, cup-shaped, or spiralling from central axis)
  - C. mesh spacing (*close* [**WF** < **WB**] → *intermediate* [**WF** ≅ **WB**] → *open* [**WF** > **WB**])
  - D. mesh uniformity (regular[1] or irregular)
  - E. secondary features (*e.g.*, central axis, reticulate meshwork)
- II. branches
  - A. width (*narrow* [<0.30 mm] → *intermediate* [0.30–0.39 mm] → *wide* [>0.39 mm])
  - B. proximodistal trace (straight, sinuous, or broadly curved)
  - C. surface profile on obverse surface (round, flat, or angular)
  - D. keel (if present)
    - 1. number across branch surface (single or multiple)
    - 2. width (*narrow* [<0.05 mm] → *intermediate* [0.05–0.15 mm] → *wide* [>0.15 mm])
    - 3. emplacement (straight or anastomosing)
    - 4. astogenetic changes
  - E. nodes (if present)
    - 1. emplacement (monoserial or biserial)
    - 2. size (*small* [<0.07 mm] → *intermediate* [0.07–0.13 mm] → *large* [>0.13 mm])
    - 3. shape (circular, ovate, elliptical, or stellate)
    - 4. location on branch
    - 5. internode spacing (*close* [<0.24 mm] → *intermediate* [0.24–0.80 mm] → *wide* [>0.80 mm])
  - F. obverse stylets (if present)
    - 1. size (*small* [<0.01 mm] → *intermediate* [0.01–0.02 mm] → *large* [>0.02 mm])
    - 2. location on branch surface
  - G. reverse microstylets (if present)
    - 1. size (*small* [<0.018 mm] → *intermediate* [0.018–0.026 mm] → *large* [>0.026 mm])
    - 2. location on branch surface
  - H. reverse macrostylets (if present)
    - 1. size (*small* [<0.05 mm] → *intermediate* [0.05–0.08 mm] → *large* [>0.08 mm])
    - 2. location on branch surface
  - I. number of rows of autozooecia (two, two becoming three for a short distance proximal to branch bifurcations, or greater than two)
  - J. heterozooecia (if present)
    - 1. type (*e.g.*, ovicells, parazooecia[2], cyclozooecia[2], caverns[2], microzooecia[2])
- III. dissepiments
  - A. width (*thin* [<0.5 × **WB**] → *intermediate* [0.5 × **WB** − 1.0 × **WB**] → *wide* [>1.0 × **WB**])
  - B. length (*short* [**WF** ≪ **WB**] → *intermediate* [**WF** ≅ **WB**] → *long* [**WF** ≫ **WB**])
  - C. placement (regular or variable)
- IV. fenestrules
  - A. size (*small* [length <0.4 mm; width <0.24 mm] → *intermediate* [length 0.4–0.9 mm; width 0.24–0.34 mm] → *large* [length >0.9 mm; width >0.34 mm])
  - B. shape (elliptical, ovate, rectangular, square, or circular)
- V. apertures
  - A. relative size (*small* [length <0.09 mm; width <0.07 mm] → *intermediate* [length 0.09–0.15 mm; width 0.07–0.12 mm] → *large* [length >0.15 mm; width >0.12 mm])
  - B. shape (circular, ovate, or elliptical)
  - C. orientation of opening relative to plane of obverse surface (parallel, inclined into fenestrule, or perpendicular)
  - D. peristomes (if present) (complete or incomplete)
  - E. degree of development and emplacement of apertural stylets (if present)
  - F. terminal diaphragms (if present)
    - 1. location on zoarium (*e.g.*, proximal, middle, distal, throughout)

[1] Low coefficient of variation for length of fenestrule, width of fenestrule, and width of branch.

[2] *fide* Morozova (1974); not observed in Warsaw bryozoans.

Polyfenestella from the Midland Valley of Scotland. *Polyfenestella*, derived from *Synocladia*(?) *fenestelliformis* Young, 1881, is primarily distinguished on the basis of occurrence of two types of heterozooecia. Type **A** zooecia occur irregularly between autozooecia and type **B** zooecia occur on both the obverse and reverse branch surfaces.

Exterior analyses only were employed in Bancroft's work, with photographs of zoarial and zooecial features providing inadequate illustration. Bancroft recognizes

Table 4.—Continued.

Character Groupings (Internal)

- I. branches
  - A. outline in cross-section (*e.g.,* elliptical, ovate, circular, semicircular, rhombic, polygonal)
  - B. branch depth (thickness of others) (*shallow* [<0.30 mm] → *medium* [0.30–0.39 mm] → *thick* [>0.39 mm])
- II. autozooecial chambers
  - A. size (*small* [length <0.20 mm; depth <0.10 mm; maximum width <0.10 mm; minimum width <0.07 mm] → *intermediate* [length 0.20–0.48 mm; depth 0.10–0.20 mm; maximum width 0.10–0.15 mm; minimum width 0.07–0.12 mm] → *large* [length >0.48 mm; depth >0.20 mm; maximum width >0.15 mm; minimum width >0.12 mm])
  - B. emplacement (monoserial, biserial, or polyserial)
  - C. axial wall trace (*e.g.,* straight, sinuous, zigzag)
  - D. orientation of elongation (parallel to reverse wall, or parallel to proximal and distal lateral chamber walls)
  - E. outline
    - 1. near reverse wall (triangular, rectangular, square, ovate, elliptical, circular, pentagonal, parallelogram-shaped, or diamond-shaped)
    - 2. at mid chamber (triangular, rectangular, square, ovate, elliptical, circular, pentagonal, parallelogram-shaped, or diamond-shaped)
    - 3. near obverse surface (triangular, rectangular, square, ovate, elliptical, circular, pentagonal, parallelogram-shaped, diamond-shaped, or bilobate)
  - F. vestibules (if present)
    - 1. length (*short* [<0.06 mm] → *intermediate* [0.06–0.12 mm] → *long* [>0.12 mm])
  - G. degree of development and location of hemisepta (if present) (superior or inferior)
  - H. lateral-wall budding-angle (mean and range)
  - I. reverse-wall budding-angle (mean and range)
  - J. microstructure
    - 1. exterior lamellar skeleton
      - a. thickness (thin, intermediate, or thick)
      - b. secondary astogenetic thickening
    - 2. interior granular skeleton
      - a. thickness (thin, intermediate, or thick)
      - b. secondary astogenetic thickening
  - K. three-dimensional form
  - L. outline (shown in Text-figure) in longitudinal, transverse, and tangential views
  - M. three-dimensional reconstruction (shown in Text-figure) in lateral, distal, and frontal views
  - N. geologic range

the need for zooecial chamber reconstruction, ultrastructural analysis, and budding relationships as an essential part of a genus description; however, the interior analysis necessary to provide this information was not done due to "lack of adequate material for sectioning" (Bancroft, 1986a, p. 106). Interior sections must be provided in illustration and description of new genera, for without these little more is done than the establishment of more unrecognizable taxa. Bancroft (1986b), in a redescription of *Hemitrypa hibernicia* McCoy, 1844, employs interior sections and illustrations as well as measurements of autozooecial chambers. The thorough exterior and interior analyses in this work provide a much better model for bryozoan description, and a much more viable starting point for development of a format adequate for description of a new genus.

Based on analysis of Warsaw fenestellids, in conjunction with other meshwork bryozoans, a list of criteria for generic division within the Suborder Fenestelloidea has been established; these are listed in Table 4 along with modifiers and descriptors. Characters are adapted from the format used by McKinney (1980) for the genus *Utropora*, from Morozova's revision of the genus *Fenestella*, and from observations made on Warsaw materials. Application of this format has proven successful in delimiting new genera within the form genus *Fenestella*, as well as confirming the validity of established genera, including *Archimedes* Hall, 1858, *Hemitrypa* Phillips, 1841, *Polypora* McCoy, 1844, *Fenestralia* Prout, 1858a, *Rectifenestella* Morozova, 1974, *Laxifenestella* Morozova, 1974, and *Exfenestella* Morozova, 1974. The format adopted permits the addition of new characters as discovered, and it provides the means for comprehensive comparison of morphotypes.

Chamber form and orientation relative to the branch, as well as other chamber characters such as hemisepta and diaphragms, are highly consistent within these genera. In contrast, relative mesh size, branch and dissepiment dimensions and placement, chamber dimensions, and keel and node number and placement frequently show pronounced variation within any genus. Recognition of *Archimedes* and *Hemitrypa*, as well as other fenestellid genera, can therefore be made from small zoarial fragments, based on similarities in overall chamber shape within members of their respective genera.

Table 5a.—Comparison of external taxonomic characters in 11 genera of fenestellid and polyporid bryozoans.

	Rectifenestella Morozova, 1974 (Late Silurian–Permian)	*Laxifenestella* Morozova, 1974 (Devonian–Permian)	*Minilya* Crockford, 1944 (Early Devonian–Early Permian)	*Exfenestella* Morozova, 1974 (Devonian–Permian)	*Banastella,* n. gen. (Mississippian)
1. Zoaria					
A. robustness	delicate to intermediate	intermediate	intermediate to robust	robust	delicate to extremely robust
B. outward expansion from ancestrula	flat to slightly obversely curved	flat to obversely curved	flat to slightly obversely curved	obversely curved	flat, obversely or reversely curved, sinuous, or cupped
C. mesh type (spacing)	close to intermediate	close to intermediate	intermediate	intermediate	close to open
D. mesh uniformity	regular to irregular	extremely regular	regular to irregular	extremely regular	regular to irregular
E. secondary features	—	—	—	—	—
2. Branches					
A. width	narrow	narrow to wide	narrow	narrow	intermediate to extremely wide
B. proximodistal trace	straight to curved	straight, sinuous, or curved	straight, sinuous, or curved	straight, sinuous, or curved	straight, sinuous, or curved
C. surface profile on obverse surface	round to moderately flat	round to flat	rounded	rounded	rounded to angular
D. keel					
1. presence/absence	present	present	present	present	present
2. number	single	single	single	single	single or multiple
3. width	narrow to intermediate	narrow	narrow	intermediate	narrow to wide
4. astogenetic changes	width increasing, covering apertures	width increasing, covering apertures	width increasing, covering apertures	width increasing, covering apertures	width moderately to greatly increasing, covering apertures
E. nodes					
1. presence/absence	present	present	present or absent	present	present
2. emplacement	monoserial	monoserial	monoserial	monoserial	monoserial
3. size	intermediate	intermediate to large	intermediate	intermediate	large to intermediate
4. shape	circular to ovate	circular to ovate	ovate	circular to ovate	stellate or elliptical
5. location on branch	middle of keel	middle of keel in single alternating row	middle of keel	atop keel	middle of keel
6. internode spacing	close	close to intermediate	close	close	intermediate to wide
F. obverse stylets					
1. presence/absence	present	present	present	present	present or absent
2. size	small	small to extremely small	extremely small to intermediate	small	small to intermediate
3. location on branch surface	across obverse surface	across obverse surface	across obverse surface	across obverse surface	across obverse surface, on keel edge
G. reverse microstylets					
1. presence/absence	typically present	present	present	present	present
2. size	small to intermediate	small to large	extremely small to small	extremely small	small to intermediate
H. reverse macrostylets					
1. presence/absence	present in some species	present in some species	present in some species	present	absent
2. size	small to intermediate	large	large	large	—
3. location on branch surface	atop striae	typically at branch–dissepiment junctions	typically at branch–dissepiment junctions	typically at branch–dissepiment junctions	—
I. number of rows of autozooecia	two rows	two, rarely three rows proximal to branch bifurcation	two rows	two rows	two rows, three rows proximal to branch bifurcation
J. heterozooecia					
1. presence/absence	present in some species	present in some species	none observed	none observed	present
2. type	possible ovicells	possible ovicells	—	—	possible ovicells

Comparison with and adherence to already established genera is done wherever possible. Because most previous work, excluding that of McKinney (1980), has dealt with genera based on either solely exterior or two-dimensional interior interpretations, application of these works to a more modern three-dimensional ge-

Table 5a.—Continued.

Cubifenestella, n. gen. (Mississippian)	*Apertostella*, n. gen. (Mississippian)	*Hemitrypa* Phillips, 1841 (Silurian–Permian)	*Archimedes* Hall, 1858 (Mississippian–Permian)	*Fenestralia* Prout, 1858a (Mississippian)	*Polypora* McCoy, 1844 (Ordovician–Permian)
intermediate to robust	delicate to robust	delicate to robust	delicate to robust	robust	robust
flat to obversely or reversely curved	flat, undulating, or obversely curved	flat, undulating, or curved	cup-shaped to fan-shaped	flat to obversely curved	flat to cupped
intermediate to open	close to intermediate	close to intermediate	close	close to open	close to open
regular to irregular	regular	regular or irregular	regular	irregular	regular or irregular
—	—	reticulate meshwork	tightly coiled axis	—	—
narrow to intermediate	intermediate to wide	narrow to intermediate	narrow to intermediate	wide	wide
straight, sinuous, or curved	straight, sinuous, or curved	straight, sinuous, or curved	straight on obverse, sinuous on reverse surface	straight, sinuous, or curved	straight, slightly sinuous, or curved
round or angular	flat, angular, concave, or obversely curved	rounded to angular	flat to round	rounded	round, angular, or flat
present	present	present	present	present	absent
single	single	single	single	single	—
intermediate to wide	narrow to intermediate	intermediate	narrow	intermediate	—
pronounced thickening	slightly thickening, covering apertures	pronounced, forms reticulate meshwork	becoming covered by lamellar skeleton	thick, covering apertures	—
present	present	present	present	present	present or absent
monoserial	monoserial	monoserial	monoserial	monoserial	monoserial
large to intermediate	intermediate to large	intermediate	small to intermediate	large	intermediate to large
stellate, ovate, or circular	ovate to circular	stellate, ovate, or circular	circular, ovate, or stellate	ovate or elliptical	stellate or ovate
middle of keel	middle of keel	middle of keel	middle of keel	middle of keel	straight to anastomosing rows
intermediate	intermediate to wide	close to intermediate	close to intermediate	intermediate	intermediate to wide
present	present or absent	present	present	present	present or absent
intermediate	large	small to intermediate	small	intermediate	intermediate to large
across obverse surface and in rows between nodes	across obverse surface	across obverse surface	across obverse surface	across obverse surface	in rows, or across obverse surface
present	present	present	present	present	present or absent
small to intermediate	small to large	intermediate to large	small	small	intermediate to large
present in some species	present in some species	present in some species	absent	absent	present or absent
large	large	intermediate to large	—	—	large
typically at branch—dissepiment junctions	typically at branch–dissepiment junctions	at branch–dissepiment junction or irregularly across surface	—	—	atop striae or at branch–dissepiment junctions
two rows	two rows, three rows proximal to branch bifurcations	two rows, three to four rows proximal to branch bifurcations	two rows, three rows proximal to branch bifurcations	four rows, five to six rows at and proximal to bifurcation	three to five rows, five to seven prox. to branch bifurcations
none observed	none observed	present in some species	present in some species	present	present or absent
—	—	possible ovicells	possible ovicells	possible ovicells	possible ovicells

neric approach has proven difficult or impossible, particularly in regard to the work done by Morozova, whose material is accessible only if one can arrange and afford to travel to Moscow.

Eleven meshwork fenestellid genera are recognized in the Warsaw: nine genera from the Family Fenestel-

Table 5a.—Continued.

	Rectifenestella Morozova, 1974 (Late Silurian–Permian)	*Laxifenestella* Morozova, 1974 (Devonian–Permian)	*Minilya* Crockford, 1944 (Early Devonian–Early Permian)	*Exfenestella* Morozova, 1974 (Devonian–Permian)	*Banastella*, n. gen. (Mississippian)
3. Dissepiments					
A. width	thin to intermediate	intermediate	thin to intermediate	intermediate	thin to wide
B. length	short to intermediate	short to intermediate	short to intermediate	intermediate	short to long
C. placement	regular	regular to irregular	regular to variable	regular	regular to variable
4. Fenestrules					
A. size	small to intermediate	small to intermediate	intermediate	intermediate	intermediate to large
B. shape	rectangular, elliptical, square	ovate, elliptical, or approximately rectangular	rectangular, elliptical, or ovate	elliptical, rectangular, or ovate	elliptical, ovate, rectangular, or square
5. Apertures					
A. relative size	small to intermediate	small to intermediate	small to intermediate	small	large
B. shape	circular to ovate	circular to ovate	circular	circular to rarely ovate	circular to ovate
C. orientation of opening to plane of obverse surface	parallel, to inclined into fenestrules	parallel	parallel, or inclined into fenestrules	parallel, to inclined into fenestrules	parallel, to inclined into fenestrules
D. peristomes					
1. presence/absence	present	present	present	present	present
2. completeness	complete or incomplete	complete or incomplete	incomplete	complete	complete
E. apertural stylets					
1. presence/absence	present	absent	present, of two sizes	present	present or absent
2. emplacement	within the peristomal gap	—	small in peristomal gap, two large ones at adaxial–abaxial apertural edge	extension of peristomal edge	extension of peristomal edge
F. terminal diaphragms					
1. presence/absence	present	present	present	present	present
2. location on zoarium	proximal	proximal	proximal	proximal and middle	proximal and throughout

lidae, including *Rectifenestella* Morozova, 1974; *Laxifenestella* Morozova, 1974; *Minilya* Crockford, 1944; *Exfenestella* Morozova, 1974; *Banastella*, n. gen.; *Cubifenestella*, n. gen.; *Apertostella*, n. gen.; *Hemitrypa* Phillips, 1841; and *Archimedes* Hall, 1858; and two genera from the Family Polyporidae: *Fenestralia* Prout, 1858a; and *Polypora* McCoy, 1844. Tables 5a and 5b list these genera and their character descriptors. The genera are listed in order of character similarity, which is interpreted to represent phylogenetic positioning of genera relative to each other.

In analysis and description at the genus level, a broad set of characters should be applied for taxonomic differentiation. Some generic characters may show little or no variation throughout the genera (as *presence/absence of obverse stylets*) or may exhibit overlap of character size ranges (as frequently overlapping in *fenestrule opening size* or *autozooecial chamber size*), whereas others such as *hemiseptum type and placement* may be highly characteristic of a genus. To delete characters from a generic list because little variation is observed between genera is to invite misapplication of generic criteria, should variation in these characters occur in genera not considered within this faunal study. Deletion of viable characters solely because they do not allow ready taxonomic breaks based on variation between taxa is inviting establishment of a monothetic classification. Characters used in this study are those traditionally used in the literature, with the addition of increased emphasis on three-dimensional reconstruction of the chamber (Table 3). Numerical statistical approaches have not been applied in this study; however, it is hoped that by dealing with a broad, but significant generic character base, a truly polythetic classification scheme is developed.

Table 6 presents a key that can be used for generic assignment. It must be emphasized that a key of this nature, although useful in direction, should not be considered adequate or sufficient for generic determination, but merely useful as a guide. Once a genus has been assigned, a thorough review of *all* generic characters within that genus should be undertaken to accurately determine generic assignment. A key of this nature, and the very nature of keys, causes a trend toward development of monothetic classification. Properly applied, however, a key is a strong and useful directional device.

Zooecia frequently exhibit morphologic features that are characteristic of a single genus; zoaria frequently exhibit broadly overlapping morphologic features that may be found in different genera. For this reason, Tables 5a and 5b are based almost solely on zooecial

Table 5a.—Continued.

Cubifenestella, n. gen. (Mississippian)	*Apertostella,* n. gen. (Mississippian)	*Hemitrypa* Phillips, 1841 (Silurian–Permian)	*Archimedes* Hall, 1858 (Mississippian–Permian)	*Fenestralia* Prout, 1858a (Mississippian)	*Polypora* McCoy, 1844 (Ordovician–Permian)
intermediate	thin to intermediate	intermediate	intermediate	intermediate	thin to intermediate
intermediate to long	short to intermediate	short to intermediate	short	intermediate	short to long
regular or variable	regular	regular to variable	regular	regular	regular to irregular
intermediate to large	small to large	small to intermediate	intermediate	intermediate to large	intermediate to large
elliptical, ovate, rectangular, or polygonal	rectangular, elliptical, or ovate	rectangular on obverse, square, or polygonal on reverse surface	elliptical on obverse, elliptical, ovate, circular, or square on reverse	elliptical to ovate	ovate, circular, rectangular, parallelogram-shaped, elliptical, or polygonal
small to large	intermediate	intermediate to large	intermediate	intermediate	intermediate to large
ovate	ovate	elliptical, ovate, or rarely circular	circular, ovate, or elliptical	circular to ovate	ovate, elliptical, or circular
slight to pronounced inclination into fenestrule	parallel or slightly inclined into fenestrule	parallel, or inclined slightly into fenestrules	parallel	adaxially parallel, abaxially perpendicular	adaxially parallel, abaxially perpendicular or inclined into fenestrule
present or absent	present	present	present	present	present
complete where present	complete	complete	incomplete	complete	complete or incomplete
present	present or absent	absent	present or absent	absent	present
extension of apertural edge fused	on extension of peristomal edge	—	on extension of peristomal edge	—	on edge of peristome
present	present or absent	present	present	present	present
proximal throughout	proximal	proximal	proximal and near center of axis	throughout	proximal, to throughout

characters, with zoarial characters used only where such characters are highly diagnostic of a particular genus.

Establishing a generic taxonomic approach to any group of organisms based on the faunal assemblage from only a single area or stratigraphic interval has certain inherent risks, the dominant one being that the faunal assemblage analyzed is not characteristic of the group as a whole. This is apparently not the case in the Warsaw, where the fauna is typical of equivalent Valmeyeran age materials and environmentally similar assemblages.

Using a fenestrate fauna as rich and diverse as that of the Warsaw provides a starting point from which comparison with other similar faunas can develop, and an opportunity for establishing genera which have a thorough three-dimensional, statistically sound basis.

BIOLOGICAL SIGNIFICANCE OF ZOOECIAL CHAMBER SHAPE

A direct link between soft part morphology and zooecial shape in fenestrates is strongly indicated by extreme consistency of zooecial chamber shapes and dimensions within conspecific populations.

Boardman and Cheetham (1969) and Gautier (1970), in work with Paleozoic trepostomes, suggested a floor for the living chamber could have been provided by solid or perforate diaphragms, although the length of the chamber between these diaphragms and the colony surface is commonly variable, even within a single colony. Silen and Harmelin (1974) observed wide variability of peristome length of functioning zooids in modern cyclostomes, whereas Boardman (1975) observed high variability of soft part morphology in modern bryozoan colonies. Blake (1980) suggested that the very long zooecia of trepostomes need not mean relatively very long polypides, emphasizing the constructional needs of the zoarium over differences in development in the polypide and related organs. Blake (1983) argued for a unified Cryptostomata based on the basic constancy in chamber size and shape in members of this order.

My work with populations of numerous species of fenestrates and rhabdomesoids agrees with that of Blake, indicating that constancy of chamber shape and dimension in the cryptostomes relates directly to the polypide size and form, a relationship not observed in trepostome studies (see Tables 10–46, showing species dimensions and variability). Consistency of chamber dimensions (with resultant low coefficients of variation) and shape, however, indicate greater need for constancy of size and form than would be needed simply to satisfy structural constraints. Once formed,

Table 5b.—Comparison of internal taxonomic characters in 11 genera of fenestellid and polyporid bryozoans.

	Rectifenestella Morozova, 1974 (Late Silurian–Permian)	*Laxifenestella* Morozova, 1974 (Devonian–Permian)	*Minilya* Crockford, 1944 (Early Devonian–Early Permian)	*Exfenestella* Morozova, 1974 (Devonian–Permian)	*Banastella*, n. gen. (Mississippian)
1. Branches					
A. outline in cross-section	ovate, elliptical, circular, or semicircular	circular to ovate	circular to ovate	circular to ovate	circular, ovate, or elliptical
B. branch depth (thickness of others)	shallow to medium	shallow to thick	thick	medium	shallow to thick
2. Autozooecial chambers					
A. size	small to intermediate	intermediate	intermediate	intermediate	typically large, less commonly intermediate
B. emplacement	biserial	biserial	monoserial	biserial	biserial
C. axial wall trace	sinuous to zigzag	straight to sinuous	zigzag	sinuous	straight to slightly sinuous
D. orientation of elongation	parallel to reverse wall	parallel to reverse wall	parallel to reverse wall	parallel to proximodistal chamber axis	parallel to proximodistal lateral chamber wall
E. outline					
1. near reverse wall	triangular to irregularly pentagonal	irregularly ovate or elliptical	triangular	asymmetrical diamond-shaped	triangular, irregularly pentagonal, to ovate
2. at mid chamber	triangular to irregularly pentagonal	rectangular, parallelogram-shaped, irregularly pentagonal, or elliptical	triangular or irregularly pentagonal	asymmetrical parallelogram-shaped or rectangular	irregularly rectangular, parallelogram-shaped, to irregularly pentagonal
3. near obverse surface	bilobate-elliptical	bilobate-elliptical or bilobate-ovate	irregularly elliptical	bilobate-elliptical	irregularly ovate to elliptical
F. vestibules					
1. presence/absence	present	present	present	present	present
2. length	short to long	short to long	short to long	intermediate	short to long
G. hemisepta					
1. superior					
a. presence or absence	present	present	present	present	typically absent, present in one species
b. development and location	poor to intermediate	moderately to well-developed	poorly to well-developed	moderately well-developed	short, on proximal vestibular edge
2. inferior					
a. presence or absence	absent	present	absent	present	absent
b. development and location	—	well-developed on mid reverse, and proximal walls	—	well-developed on proximal side	—
H. lateral-wall budding-angle (mean and range)	23°–30° (means)	20°–27° (means)	22°–25° (means)	25° (mean)	16°–22° (means)
I. reverse-wall budding-angle (mean and range)	68°–71° (means)	57°–77° (means)	74°–89° (means)	71° (mean)	22°–55° (means)
J. microstructure					
1. exterior lamellar skeleton					
a. thickness	thin	thin to thick	thick	thick	thin to thick
b. secondary astogenetic thickening	moderate to pronounced	moderate to pronounced	pronounced	moderate	slight to pronounced
2. interior granular skeleton					
a. thickness	thin to intermediate	intermediate to thick	thick	thin	thin to thick
b. secondary astogenetic thickening	none	none	slight	none	slight
K. three-dimensional form	moderately to highly cuneate	box to rounded box with indentations	cuneate	rectangular box with indentations	irregular to slightly irregular rectangle to parallelogram

chambers exhibit minimal or no internal thickening by addition of lamellar or granular skeletal material. Highly symmetrical placement and often elaborate shapes of superior and inferior hemisepta in the fenestrates (shown in Pls. 6, 8–10, 12, 13, 16, 17) divide chambers in such ways as to suggest differential development of polypides among species. Uniform spacing of apertures along the branch, across the branch, and frequently between branches in many fenestrates and uniform closest packing of aperture centers in the rhabdomesoids reflect relatively symmetrical chamber positioning in both suborders. Symmetry of placement also indicates exploitation of a consistent area around the aperture opening for each lophophore and, therefore, a constant size for this feeding organ. Constant number and regular placement of apertural stylets in

Table 5b.—Continued.

Cubifenestella, n. gen. (Mississippian)	*Apertostella*, n. gen. (Mississippian)	*Hemitrypa* Phillips, 1841 (Silurian–Permian)	*Archimedes* Hall, 1858 (Mississippian–Permian)	*Fenestralia* Prout, 1858a (Mississippian)	*Polypora* McCoy, 1844 (Ordovician–Permian)
ovate, elliptical, or circular	polygonal, ovate, or elliptical	circular, ovate, or elliptical	circular, ovate, or elliptical	circular, ovate, or polygonal	elliptical, ovate, circular, or polygonal
thick to medium	medium to thick	medium to very thick	thin to thick	thick	thick
intermediate	intermediate	intermediate	small to intermediate	intermediate	intermediate to large
monoserial or biserial	biserial	biserial	biserial	quadriserial	triserial to quadriserial
sinuous to zigzag	sinuous to zigzag	straight to sinuous	sinuous	straight adaxially, straight to sinuous abaxially	straight to sinuous
depth and length of chamber approximately equal	parallel to reverse wall	parallel to reverse wall	parallel to reverse wall	parallel to proximodistal lateral chamber wall	parallel to proximodistal lateral chamber walls
triangular to ovate	triangular, polygonal, or irregularly pentagonal	ovate, elliptical, irregularly pentagonal, to triangular	irregularly pentagonal to triangular	ovate	ovate, diamond-shaped, circular, to pentagonal
irregularly pentagonal to rectangular	irregularly pentagonal, rectangular, to elliptical	irregularly pentagonal, rectangular, to parallelogram-shaped	irregularly pentagonal	irregularly pentagonal, rectangular, to parallelogram-shaped	elliptical, rectangular, hexagonal, ovate, to circular
pentagonal, rectangular, elliptical, square, or ovate	irregularly elliptical to ovate	ovate to elliptical	irregularly elliptical to irregularly ovate	bilobate-ovate	ovate, circular, bilobate-ovate, to elliptical
present	present	present	present	present	present
short to long	short to intermediate	short to long	short to intermediate	intermediate	intermediate to long
absent	absent	absent	absent	present	absent
—	—	—	—	poor, on vestibular edge	—
absent	absent	absent	absent	absent	absent
—	—	—	—	—	—
18°–37° (means)	22°–25° (means)	17°–23° (means)	20°–27° (means)	17° adaxially, 51° abaxially (means)	7°–12° adaxially, 25°–47° abaxially (means)
64°–81° (means)	67°–69° (means)	60°–77° (means)	58°–70° (means)	42° (mean)	18°–77° (means)
intermediate to thick	intermediate to thick	intermediate to thick	intermediate to thick	intermediate	intermediate to thick
moderate to pronounced	moderate to pronounced	moderate to pronounced	moderate to pronounced	moderate	slight to pronounced
intermediate to thick	intermediate to thick	intermediate to thick	intermediate to thick	intermediate	intermediate to thick
moderate	none	none	none	none	none
regular cubic to irregularly rectangular box	rectangular box	irregularly rectangular to cubic box	slightly irregularly rectangular box	slightly irregular cylinder	polygonal or irregular cylinder

some fenestrates suggest a functional interpretation of these structures as possible tentacle guides, as does the presence of such stylets as tentacle guides in modern species.

Jackson and Cheetham (1990, p. 579), in a work on cheilostome Bryozoa, justify the significance of a statistically rigorous approach to bryozoan taxonomy. Employing breeding experiments and protein electrophoresis, they observe that "skeletal characters of the kinds typically available in fossil material are indeed sufficient to discriminate biologic species of living cheilostome Bryozoa." With cheilostomes providing a good analogue for fenestrate Bryozoa, their work adds confidence to fossil studies of this nature.

Table 6.—Key to Warsaw genera of the Fenestellidae and Polyporidae.

1a.	typically two rows of autozooecia across branch, except proximal to sites of branch bifurcation where two, three, or four rows are present (=Family Fenestellidae)	go to 2
1b.	typically ranging from three to five rows of autozooecia across branch except proximal to sites of branch bifurcation, where five to seven rows are present (=Family Polyporidae)	go to 11
2a.	autozooecial chambers small to lower-end intermediate in size	go to 3
2b.	autozooecial chamber size intermediate to large	go to 4
3a.	superior hemiseptum absent, chamber form an irregular rectangular box, well-developed central axis of lamellar skeleton from which mesh projects in dextral or sinistral corkscrew fashion	*Archimedes*
3b.	superior hemiseptum poorly to intermediately developed at proximal vestibular edge, chamber form moderately to highly cuneate	*Rectifenestella*
4a.	reticulate meshwork develops atop obverse zoarial surface; each opening in mesh approximately covering one zooecial chamber	*Hemitrypa*
4b.	reticulate meshwork absent	go to 5
5a.	superior hemiseptum present	go to 6
5b.	superior hemiseptum absent	go to 9
6a.	inferior hemiseptum present	go to 7
6b.	inferior hemiseptum absent	go to 8
7a.	inferior hemiseptum well-developed, positioned between middle reverse and lateral proximal wall, apertural stylets absent, chamber elongate parallel to reverse wall proximodistally	*Laxifenestella*
7b.	inferior hemiseptum well-developed, positioned at proximal side of distal lateral chamber wall, apertural stylets present, chamber elongate parallel to proximal and distal lateral chamber walls	*Exfenestella*
8.	two sizes of apertural stylets present; small ones filling peristomal gap, large ones positioned one each on adaxial and abaxial edges of aperture extending either slightly proximally or distally	*Minilya*
9a.	reverse-wall budding-angle less than 55°, ranging to as low as 22°; apertures large; chamber elongate parallel to proximal and distal lateral chamber walls	*Banastella*
9b.	reverse-wall budding-angle greater than 55°	go to 10
10a.	chamber depth and length approximately equal; chambers open at a slight to pronounced angle toward and into the fenestrule, and two rows of autozooecia across branch proximal to sites of bifurcation, but can have third row at site of bifurcation	*Cubifenestella*
10b.	chamber elongate parallel to reverse wall; chambers open parallel or approximately parallel to plane of obverse surface, and third row of autozooecia at and proximal to sites of branch bifurcation	*Apertostella*
11a.	four rows of autozooecia across branch, two adaxial and two abaxial rows symmetrical across plane along midline of branch; adaxial chambers bud from reverse wall of branch, abaxial chambers bud from lateral wall of adaxial chambers, making this their reverse wall; poorly developed superior hemiseptum present; apertural stylets absent; keel present	*Fenestralia*
11b.	three to five rows of autozooecia across branch, lacking distinct branch midline separation; adaxial and abaxial chambers all bud from reverse wall of branch; superior hemiseptum absent; apertural stylets present; keel absent	*Polypora*

TAXONOMIC CRITERIA FOR THE DISCRIMINATION OF FENESTELLID AND POLYPORID SPECIES

Species definition within the fenestellids and polyporids has long been difficult, with concepts commonly based more on dissimilarities than similarities. Yet generic descriptions must be based on sound, biologically oriented species concepts. The preceding generic characters, criteria, and taxonomic approach were developed subsequent to determination of the following species concepts. The taxonomic approach herein emphasizes internal zooecial morphology and the statistical analysis of populations, including but de-emphasizing zoarial features. The traditional meshwork formula characters comprise one small part of species characterization.

Descriptive statistics including measures of central tendency (thus the typical development of a character) and measures of dispersion showing deviation from the typical are employed in this study; these measures include arithmetic mean, range, standard deviation, and coefficient of variation. The value of the latter depends on character variability; the greater the consistency of the character, the lower the value of the coefficient of variation and potentially the higher its diagnostic value (Anstey and Perry, 1970, 1973; Tavener-Smith, 1965; Cuffey, 1967; Bork and Perry, 1967). Higher coefficients of variation for characters reflect generally nongenetic factors, *i.e.*, microhabitat and changes related to astogeny (Anstey and Perry, 1970). Previous studies stressing statistical comparisons (Tavener-Smith, 1965; Bork and Perry, 1967; Horowitz, 1968) of the more consistent zooecial and zoarial characters range in coefficient of variation from 4.87 to 38.62, corresponding quite well to those observed in Warsaw species (see Tables 10–46). The charts are based on more than 10,000 measurements. Even a casual viewing verifies the consistently lower coefficients of variation for zooecial characters than zoarial characters. The least variable characters are autozooecial chamber measurements of length, depth and width, and the reverse-wall budding-angle (*e.g.*, numbers 36–39 and 41); the most variable characters are those of zoarial pattern and ontogenetic skeletal accretion (*e.g.*, numbers 2–5, 14, 15). The spread of values within each of these characters can be an order of magnitude or greater. Character lists and their associated morpho-

logic statistics are arranged to facilitate use of biometric tests such as the t-test or chi-square goodness of fit.

As considered earlier, zooecial characters presumably reflect polypide morphologies. Because zooecia are conservative within taxa but highly distinctive between taxa, zooids presumably were as well (for greater detail, see pp. 31–33). Zoarial characters exhibit a much broader range of phenotypic variability than do zooecial characters. The more consistent the interspecific character's expression (*i.e.*, the lower the coefficient of variation), the potentially greater that character's use in species differentiation.

Taxon concepts were evolved in the following sequence:

(1) Shales and calcareous interbeds of the Warsaw were collected by horizon. Samples were washed and sieved in the laboratory and bryozoans were picked.

(2) Specimens were grouped based on exterior similarities, thus grouping similar morphs. Obverse surfaces were relied upon almost exclusively, as homeomorphy between reverse surfaces of species in the fenestrates is pronounced.

(3) Where material was available, 12 zoarial fragments from each group were photographed on both exterior surfaces and impregnated in epoxy. Where fossil fragments were incorporated in calcareous slabs, photographs of the specimen with obverse surfaces exposed were taken and the specimen was subsequently impregnated in epoxy.

(4) Oriented acetate peels were made of all fragments, providing tangential, transverse, and longitudinal interior views; serial peels were frequently taken to assist in determination of zooecial chamber shape.

(5) Many specimens and orientations were photographed at both low magnification (×20 and ×40) and high magnification (×70), allowing more immediate comparison between zoarial fragments.

(6) Specimens were then resorted based on both exterior and interior zoarial and zooecial appearance. Interior characters necessitated realignment of groupings as some taxa have very similar obverse and reverse exteriors, but significantly different interiors.

(7) Statistical analysis of both zoarial and zooecial exterior and interior characters was made; including arithmetic mean, standard deviation, coefficient of variation, range of character variation (maximum and minimum), and number of measurements. Readjustment of tentative species groups was made following these statistical tests.

(8) Detailed descriptions were prepared based on all information, with zooecial and zoarial features described three-dimensionally.

Characters used for taxon determination are divided into zoarial and zooecial groups; this allows ready comparison between characters concerned with colonial development, both ontogenetic and astogenetic, and those related to individual development, which are primarily ontogenetic in the fenestrates (McKinney, 1980). Quantitative features on which numerical analyses are based are listed and defined in the following section and are illustrated in Text-figures 4–7. Text-

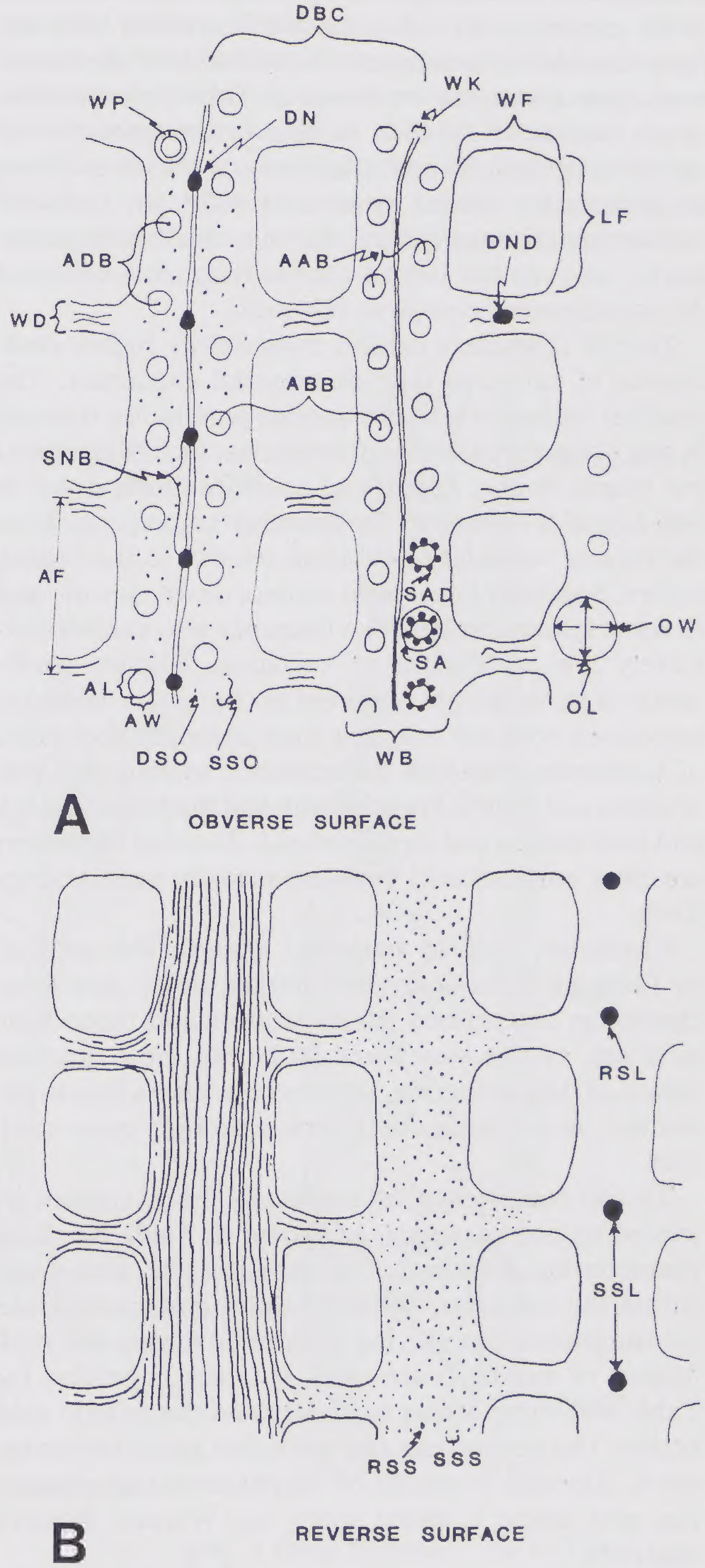

Text-figure 4.—Typical zoarial surficial features of meshwork fenestrates. Obverse (**A**) and reverse (**B**) surfaces are illustrated. Abbreviations of characters are defined in Tables 7 and 8 (foldouts).

figure 4 provides typical measured zoarial and zooecial surface features of an idealized meshwork fenestrate. Text-figure 5 illustrates specialized skeletal features found in *Hemitrypa* Phillips, 1841, and *Archimedes* Hall, 1858, along with the measured dimensions of these features. Text-figures 6 and 7 provide interior measured features for two different meshwork fenestrate species exhibiting the major characteristics found in all species. A list of measured characters with appropriate abbreviations and definitions for the meshwork fenestrates can be found in Table 7; an outline of the format of Table 7, to help in interpretation of species descriptions and diagnoses, is shown in Table 8a. Maximum zoarial length and width are included in the written descriptions, but not dealt with statistically, as even the largest zoarial fragments collected do not represent complete colonies.

Zoarial characters exhibit consistently higher coefficients of variation than do zooecial characters. The smallest variation within a species population is found in autozooecial chamber dimensions, including chamber length, width, depth, and aperture dimensions; as well as angles formed by the chamber's emergence from the reverse wall and orientation relative to the branch center. Spacing of apertural centers down, across, and in some specimens between branches also exhibits relatively low coefficients of variation. Highest coefficients of variation are observed in characters definitely associated with the zoarium such as length and width of fenestrule, width of dissepiment, spacing and size of nodes and stylets, branch width and thickness (depth), and keel and carinal development. Zooecial characters are thus emphasized, both empirically and descriptively.

Characters used in statistical analysis are outlined in Table 8a. This analysis is broken down into those characters determined from exteriors and those from interiors, as this was found to be the most practical means of data gathering. Species data sheets follow this outline, as grouping characters separately eases analysis.

To add consistency, all characters for all species are treated in one sequence, as shown in Table 8b. Each character has a delimiter for range of size, shape, *etc.* within the character. Where possible and appropriate, measurements (employing arithmetic mean) and coefficients of variation are used. It is my hope that the Table will allow others to understand the criteria used herein. The outline can also provide a guide for further work, although it should be emphasized that range of size and shape is based solely on Warsaw Bryozoa analyzed.

Table 9 provides a taxonomic list of Warsaw species analyzed in the order in which they are presented in the systematics section.

SYSTEMATIC PALEONTOLOGY

TAXONOMIC PHILOSOPHY

Modern biological and paleontological concepts of species are significantly different, basically due to the nature of available data. Biologists can apply breeding experiments and/or protein electrophoresis to discriminate biologic species of living Bryozoa. Through observation, it is possible for biologists to determine if they are dealing with members of the same biological species as well as to delimit, through analysis of individuals, the boundaries of phenotypic expression of the genotype. In spite of the paucity of comparable data available to the paleontologist, it is imperative that fossils be classified in the most biologically correct fashion possible.

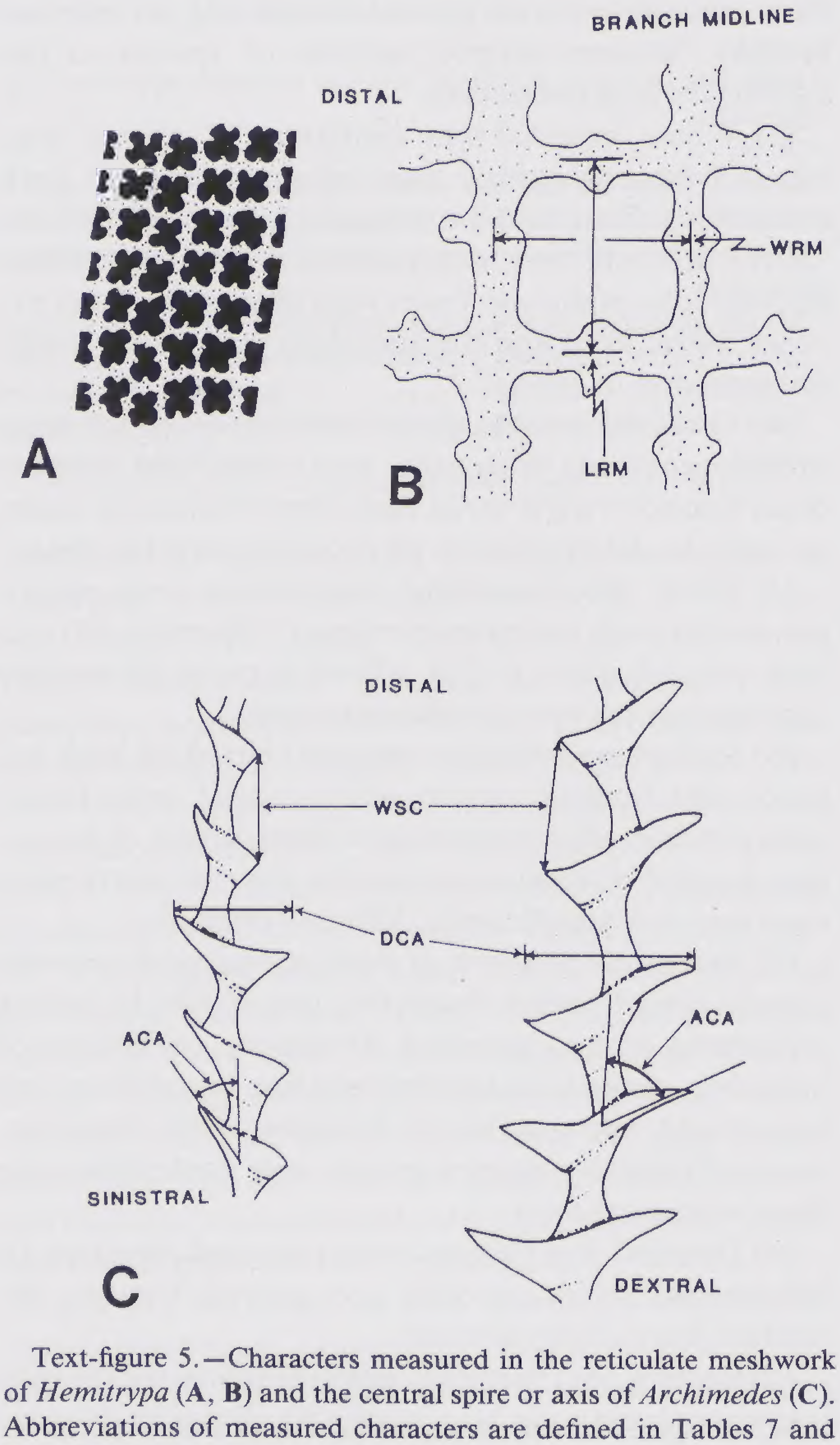

Text-figure 5.—Characters measured in the reticulate meshwork of *Hemitrypa* (**A**, **B**) and the central spire or axis of *Archimedes* (**C**). Abbreviations of measured characters are defined in Tables 7 and 8 (foldouts).

For paleontologists to emphasize features of biological significance in their classification schemes requires, in a real sense, working in reverse, compared to the way a biologist analyzes species. Biologists employ soft-part analysis as a major aspect of systematic description, with skeletal components significant but in many respects occupying a supportive role. In Warsaw Bryozoa, the phenotypic expression of the genotype is locked in the superbly preserved skeletal remains.

The task of the paleontologist is to attempt to reproduce soft body structures through interpretation of the preserved skeletal remains. In the Warsaw fenestrates, this can be accomplished in several ways. The first is to employ modern analogs, such as the cheilostome Bryozoa, for comparison with the Paleozoic fenestrates. Although it is not possible to reproduce the appearance of the polypide in the fenestrates, we can assume that the size and shape of the polypide is as consistent as it is in modern cheilostomes. Second, through careful measurement of zooecial chambers, it was found that chambers exhibit extremely consistent sizes and through reconstruction of chambers it was also determined that within species they have highly constant shapes. Thus, we now have not only determined skeletal physical dimensions, but have, through interpretation of these measurements and comparison with modern species, been able to reconstruct interpreted soft-part sizes and shapes. Through such a combination, we satisfy not only classic paleontological prerequisites, but also provide a more accurate bio-

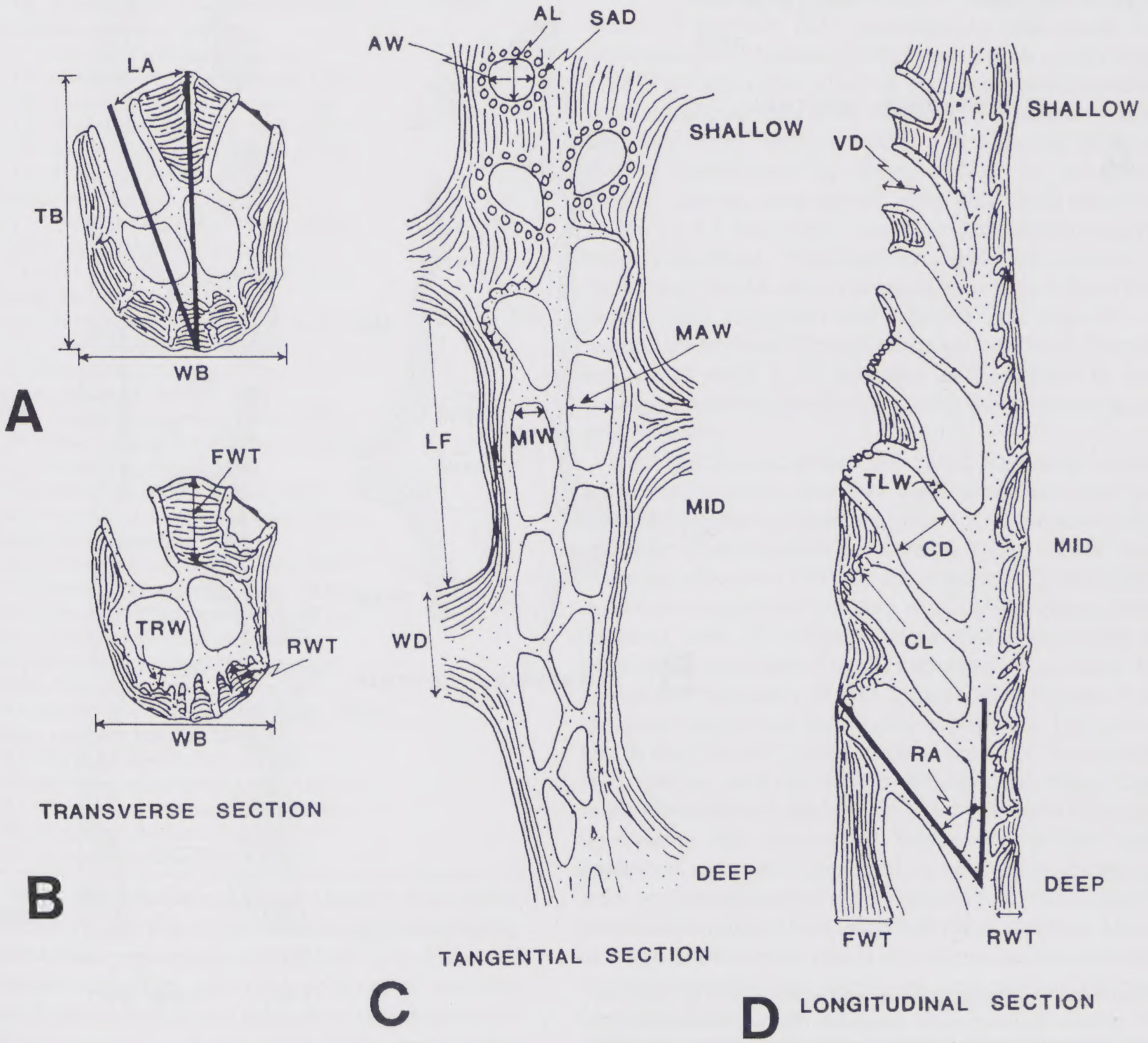

Text-figure 6.—Characters measured in the interior of *Banastella guensburgi*. Transverse (**A**, **B**), tangential (**C**), and longitudinal (**D**) section views are shown. Abbreviations of measured characters are defined in Tables 7 and 8 (foldouts).

logical interpretation of fossil species. Biologically significant characteristics are emphasized in the taxonomic descriptions and diagnoses of fenestrate Bryozoa herein, as such characters assist in establishing a less artificially constructed classification.

The species concepts applied herein are a significant departure from those of most previous workers, excluding McKinney (1980). Whether such a departure is necessary is a question answered by the numerous problems encountered when attempting to classify a fenestrate species. I became interested in taxonomic difficulties in the fenestrates while analyzing bryozoan

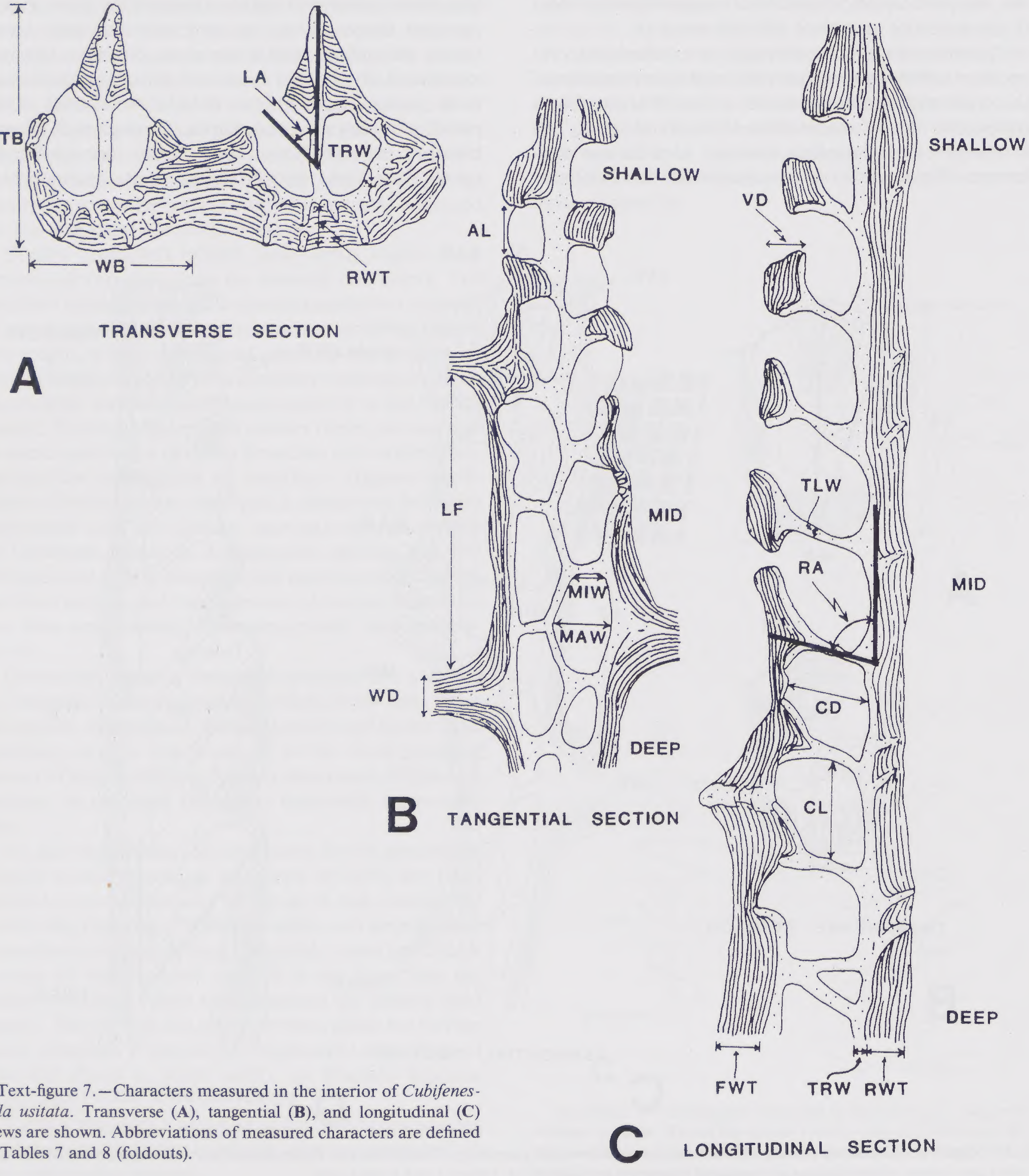

Text-figure 7.—Characters measured in the interior of *Cubifenestella usitata*. Transverse (A), tangential (B), and longitudinal (C) views are shown. Abbreviations of measured characters are defined in Tables 7 and 8 (foldouts).

Table 9.—Taxonomic list of Warsaw meshwork fenestrate species. Numbers assigned to species are used in illustrations elsewhere in this paper.

Order Cryptostomata Vine, 1884
  Suborder Fenestelloidea Astrova and Morozova, 1956
    Family Fenestellidae King, 1849
      Genus *Rectifenestella* Morozova, 1974
        1. *Rectifenestella tenax* (Ulrich, 1888)
        2. *Rectifenestella tenuissima* (Cumings, 1906)
        3. *Rectifenestella multispinosa* (Ulrich, 1890)
      Genus *Laxifenestella* Morozova, 1974
        4. *Laxifenestella coniunctistyla,* n. sp.
        5. *Laxifenestella maculasimilis,* n. sp.
        6. *Laxifenestella serratula* (Ulrich, 1890)
        7. *Laxifenestella fluctuata,* n. sp.
      Genus *Minilya* Crockford, 1944
        8. *Minilya sivonella,* n. sp.
        9. *Minilya paratriserialis,* n. sp.
      Genus *Exfenestella* Morozova, 1974
        10. *Exfenestella exigua* (Ulrich, 1890)
      Genus *Banastella,* n. gen.
        11. *Banastella guensburgi,* n. sp.
        12. *Banastella cingulata* (Ulrich, 1890)
        13. *Banastella mediocreforma,* n. sp.
        14. *Banastella limitaris* (Ulrich, 1890)
        15. *Banastella biseriata* (Ulrich, 1890)
        16. *Banastella delicata,* n. sp.
      Genus *Cubifenestella,* n. gen.
        17. *Cubifenestella rudis* (Ulrich, 1890)
        18. *Cubifenestella usitata,* n. sp.
        19. *Cubifenestella globodensata,* n. sp.
      Genus *Apertostella,* n. gen.
        20. *Apertostella foramenmajor,* n. sp.
        21. *Apertostella crassata,* n. sp.
        22. *Apertostella venusta,* n. sp.
      Genus *Hemitrypa* Phillips, 1841
        23. *Hemitrypa perstriata* Ulrich, 1890
        24. *Hemitrypa hemitrypa* (Prout, 1859)
        25. *Hemitrypa aprilae,* n. sp.
        26. *Hemitrypa aspera* Ulrich, 1890
        27. *Hemitrypa vermifera* (Ulrich, 1890)
      Genus *Archimedes* Hall, 1858
        28. *Archimedes negligens* Ulrich, 1890
        29. *Archimedes owenanus* (Hall, 1857b)
        30. *Archimedes wortheni* (Hall, 1857b)
        31. *Archimedes valmeyeri,* n. sp.
    Family Polyporidae Vine, 1884
      Genus *Fenestralia* Prout, 1858a
        32. *Fenestralia sanctiludovici* Prout, 1858a
      Genus *Polypora* McCoy, 1844
        33. *Polypora gracilis* Prout, 1860
        34. *Polypora varsoviensis* Prout, 1858a
        35. *Polypora spininodata* Ulrich, 1890
        36. *Polypora simulatrix* Ulrich, 1890
        37. *Polypora retrorsa* Ulrich, 1890

fossils from the Guadalupian age Gerster Formation of northeastern Nevada in 1972. Although challenging, the trepostomes, cystoporates, and other cryptostomes were recognizable from previous works or at least describable from materials and references that were available. The fenestrates, on the other hand, were seemingly impossible to work with employing existing techniques. It was this difficulty, and my introduction to the superbly preserved Warsaw fenestrates by Dan Blake, that led me to undertake this project.

Thorough specimen analysis is critical for accurate species assignment and taxonomic analysis. As indicated throughout the text, reliance on methods that measure and/or describe symmetry of the fossil, frequently ignoring characters that have taxonomic significance, has been a major problem in fenestrate taxonomy. *A priori* determination of significant taxonomic characteristics, without benefit of complete and detailed comparison of those characters within and between species has been a common failing of taxonomic works, and has been a major weakness in the Bryozoa. The great number of characters employed herein reflects the numerous significant taxonomic characteristics present in the fenestrates. Numerical manipulation of the raw data generated by this study was undertaken by Hageman (1987) and Snyder and Kepler (1987) to determine which of the measured characters were significant and if the number of characters could be significantly reduced while still allowing accurate species determination. Based solely on numerical means, species assignments were well confirmed with as few as 15 characters, zooecial characters being the most significant. Although this reduced number of characters would allow recognition within a described fauna, both Hageman and I found that virtually *all* characters had significance at the species level. Further numerical work is in progress, and analysis to date strongly supports detailed character measurements and descriptions.

New species and genera are based on readily distinguishable zooecial chamber differences between species; differences in shape, size, apertural characteristics, accessory features such as hemisepta, and variation in chamber placement within the zoarium. Zoarial characters are employed, but to a much lesser degree than zooecial ones. A difficulty arises with comparison to previously established species and genera, as their descriptions frequently do not contain what appear to be the most significant taxonomic characters. This problem is due, in part, to incomplete sections, inadequate descriptions, and use of two-dimensional rather than three-dimensional analyses in most previous works on fenestrates. For this reason, Warsaw fenestrates were separated into what appeared to be species groupings *prior* to comparison of the Warsaw fauna with species previously assigned by Ulrich and other workers. Many new species were the result of exterior homeomorphy between species that exhibited pronounced interior dissimilarities.

Finally, once measurements and significant features have been determined, it is imperative to present such

information in a consistent format that allows accurate comparison within and between species.

ABBREVIATIONS OF REPOSITORY INSTITUTIONS

Specimens and lithologic samples collected for this study are all reposited in the collections of the Department of Geology, University of Illinois. Addresses and acronyms of this and other specimen repositories are listed below. It is unfortunate that, in spite of extensive searching, so few of Ulrich's original types could be located. The quality of specimen illustration and thin-section reproduction in his published works proved invaluable for species recognition.

AMNH: American Museum of Natural History, New York, NY.
ISGS (ISM): Illinois State Geological Survey, Urbana, IL.
USNM: United States National Museum of Natural History, Smithsonian Institution, Washington, DC.
UI X: University of Illinois, Urbana, IL.

Materials from this study housed at the University of Illinois have type numbers (UI-X . . .) assigned to the fossil fragment. One number is assigned to each fragment. Many fragments were embedded in epoxy, and acetate peels were prepared to illustrate chamber and colony characteristics in different sectional views. An alphanumeric designator is given to each peel following the appropriate UI X number. For example, in the explanation of Plate 1, figure 5 (p. 192), **UI X-6799** is followed by the peel designator **FF-69**. This designator indicates that the photograph was taken from peel **#69**, stored in box **FF**, and belongs to hypotype **UI X-6799**. This procedure protected peels by housing them in dust-proof peel [=thin-section] boxes while research continued, and the same storage procedure was followed when type assignments were made. Should readers desire access to specific peels, use of peel designators in the above fashion will facilitate their rapid retrieval.

The information enclosed in brackets in taxonomic synonymies indicates the stratigraphic and geographic locations of the specimen or specimens referred to by the indicated authors.

In photographic plates, dashed lines are employed to add continuity to portions of the same colony that would otherwise appear disjunct.

SYSTEMATICS

Family **FENESTELLIDAE** King, 1849

Zoaria fan-shaped, constructed of branches that bifurcate at regular to variable intervals. Branches connected at varying distances by dissepiments (transverse links lacking autozooecial chambers), which may or may not have apertures opening onto the dissepiment edge. Each individual (autozooecium) of the zoarium has single apertural opening; openings occur only on the front or obverse surface of the fan, the back or reverse surface being without apertural openings. Two rows of zooecia typically are present across each branch. Exterior obverse ornamentation can consist of longitudinal keels (referred to as *carinae* by some authors); nodes of various forms positioned along branch surfaces and/or on dissepiments; stylets positioned down the branch, on dissepiments, and/or around apertures; peristomal structures; and heterozooecial features. Reverse exterior surfaces commonly exhibit longitudinal striae, microstylets and macrostylets of varying sizes, zoarial supports, and show pronounced character changes with astogeny. Interior features include autozooecial chamber shape and orientation, presence of superior hemiseptum (adjacent to obverse interior wall) or inferior hemiseptum (adjacent to reverse interior or lateral chamber walls), vestibule and terminal diaphragms. Interior characters are considered in detail under the species and genera.

Range.—Ordovician to Triassic. Many genera are long-ranging and abundant.

The Warsaw genera *Rectifenestella* Morozova, 1974, *Laxifenestella* Morozova, 1974, *Minilya* Crockford, 1944, *Exfenestella* Morozova, 1974, *Banastella*, n. gen., *Cubifenestella*, n. gen., *Apertostella*, n. gen., *Hemitrypa* Phillips, 1841, and *Archimedes* Hall, 1858 are included in this family. The genus *Fenestella* Lonsdale, 1839 should also be included, but needs redefinition from the type materials. As currently defined, *Fenestella* does not appear to be present in the Warsaw, but this genus does belong in the Fenestellidae.

Genus **RECTIFENESTELLA** Morozova, 1974
Text-figure 8

Type species.—*Fenestella medvedkensis* Shulga-Nesterenko, 1951. [Upper Carboniferous, Kasimovian Stage; Russian Platform]; Morozova, 1974. pp. 175–176; pl. 4–1.

Typical Warsaw species.—*Fenestella tenax* Ulrich, 1888, p. 71. [Waverly Group, Devonian, Ohio].

Diagnosis.—Zoarium robustness delicate to intermediate, mesh close to intermediate; characteristic triangular to pentagonal chamber outline in mid tangential section, chamber size small to intermediate, aperture size small to intermediate, poorly developed superior hemiseptum present, chamber reverse-wall budding-angle approximately 70°.

Three-dimensionally reconstructed chamber form moderately to highly cuneate.

Description.—Zoarium robustness delicate to inter-

mediate, expansion flat to slightly obversely curved with mesh spacing close to intermediate, mesh uniformity regular to irregular.

Branches narrow, straight to curved, surface profile rounded to moderately flat. Keel present, single, narrow to intermediate width, straight to anastomosing; width increases and keel frequently covered by lamellar skeleton during astogeny. Nodes present, monoserially emplaced, intermediate in size, circular to ovate in shape, located atop middle of keel, closely spaced. Obverse stylets present, small, occurring across obverse branch surface. Reverse surface typically bearing microstylets, small to intermediate in size, developed atop longitudinal striae. Autozooecia in two rows, third row at sites of branch bifurcation. Heterozooecia (ovicells?) present in some species.

Dissepiment width thin to intermediate; short to intermediate in length and regularly emplaced.

Fenestrule size small to intermediate, shape ranging from rectangular to elliptical to square.

Aperture size small to intermediate, circular to ovate in shape, oriented parallel to plane of obverse surface or at a low angle toward fenestrule. Peristome present, complete or incomplete, open at proximal edge; apertural stylets occurring in peristomal gap. Terminal diaphragms present, most commonly occurring toward proximal end of zoarium.

Branches ovate, elliptical, circular to semicircular in cross-section; shallow to medium in depth.

Autozooecial chambers small to intermediate in size, biserially emplaced, axial wall trace sinuous to zigzag. Maximum chamber length parallel to reverse wall in proximodistal direction. Chamber outline in tangential view triangular to irregularly pentagonal near reverse wall and throughout mid chamber, bilobate elliptical near obverse surface (Text-fig. 10). Vestibule present, short to long. Superior hemiseptum present, poorly to intermediately developed at proximal vestibular edge; inferior hemiseptum absent. Lateral-wall budding-angle varying between 23° and 30° (means); reverse-wall budding-angle varying between 68° and 71° (means). Lamellar skeletal layer thin, exhibiting moderate to pronounced astogenetic thickening; granular skeletal layer thin to intermediate, exhibiting no astogenetic thickening.

Three-dimensionally reconstructed chamber form moderately to highly cuneate.

Text-figure 8 illustrates zoarial outlines in longitudinal, tangential, and transverse orientations, and three-dimensional chamber reconstructions from distal, abaxial branch edge, and obverse surface views.

Remarks.—General chamber shape is quite similar to that of *Minilya* Crockford, 1944, as are development of superior hemisepta and general autozooecial chamber size. *Rectifenestella* is distinguished by typically having a less cuneate chamber shape, by lacking the large biserially arranged apertural stylets that are characteristic of *Minilya*, and by having a generally lower reverse-wall budding-angle.

The generic concept is expanded from that of Morozova through use of a three-dimensional approach; this genus is readily recognized among Warsaw fenestellids. The age of species (Late Silurian to Permian) assigned to this genus by Morozova easily encompasses the age of the Warsaw.

Assignment of *F. serratula* Ulrich, 1890, and *F. rudis* Ulrich, 1890, to this genus is incorrect according to three-dimensional study of autozooecial chamber shape and placement of hemisepta. *F. serratula*, herein assigned to *Laxifenestella* Morozova, 1974, has a box-like rather than cuneate chamber form in three-dimensional view and well-developed superior and inferior hemisepta, whereas species of *Rectifenestella* lack inferior hemisepta. *F. rudis*, herein assigned to *Cubifenestella*, n. gen., has a box-like chamber form in three-dimensional view and lacks both superior and inferior hemisepta. *R. multispinosa* Ulrich, 1890, is correctly assigned to this genus, as suggested by Morozova.

Problems with Morozova's assignment of species to this genus are due largely, if not solely, to the lack of adequate three-dimensional analysis. Her work, based almost exclusively on obverse surficial view, does not allow for recognition of chamber form and hemiseptal development, two of the characters most critical for generic assignment.

Specific composition.—Over 100 species were recognized by Morozova (1974); this number would be reduced by following emended diagnosis provided here. Three Warsaw species are included in this genus: *R. tenax* (Ulrich, 1888), *R. tenuissima* (Cumings, 1906), and *R. multispinosa* (Ulrich, 1890).

Range.—Late Silurian to Permian (Morozova, 1974).

Rectifenestella tenax (Ulrich, 1888)

Plates 1, figures 1–12, Plate 2, figures 1–3; Table 10

Fenestella tenax Ulrich, 1888, p. 71; Ulrich, 1890, p. 546, pl. 51, figs. 2–23; Nekhoroshev, 1926, p. 1248, pl. 19, fig. 12; Condra and Elias, 1944, pp. 99–102, pl. 21, figs. 1–4; Elias and Condra, 1957, pp. 106–107, pl. 10, figs. 1, 2; Trizna, 1958, p. 132, pl. 38, figs. 1–4; Burckle, 1960, pp. 1084–1085, pl. 131, fig. 2.

Fenestella tenax Ulrich (?). Cumings, 1906, p. 1279, pl. 30, fig. 1; pl. 21, figs. 1–1a.

Fenestella submicroporata Shulga-Nesterenko, 1952, pp. 35–36, fig. 15; pl. 4, fig. 2.

Diagnosis.—Zoarium delicate, mesh close, pattern irregular; branches delicate, width narrow, thickness thin, straight to slightly curved in trace, transversely ovate, moderately closely spaced; branches joined at highly regular intervals by thin, short dissepiments.

Table 10.—Summary numerical analysis of *Rectifenestella tenax* (Ulrich, 1888). For explanation of abbreviations of characters (left column), see Table 8b (foldout inside back cover).

	number of measurements	mean	standard deviation	coefficient of variation	observed range
1. **WB**	24	0.2641	0.0498	18.86	0.190–0.350
2. **DBC**	24	0.4612	0.0533	16.56	0.380–0.548
3. **WD**	24	0.1268	0.0283	22.32	0.093–0.187
4. **LF**	24	0.3368	0.0504	14.96	0.228–0.413
5. **WF**	24	0.2143	0.0332	14.93	0.158–0.283
6. **AF**	24	2.25	0.51	20.43	2–3
7. **AL**	24	0.0644	0.0074	11.49	0.050–0.082
9. **ADB**	24	0.2307	0.0211	9.15	0.195–0.278
10. **AAB**	24	0.2821	0.0443	15.70	0.220–0.355
11. **ABB**	24	0.3014	0.0714	23.69	0.213–0.499
12. **DN**	24	0.0954	0.0180	18.87	0.065–0.143
14. **SNB**	24	0.2248	0.0360	16.01	0.167–0.293
15. **WK**	24	0.0781	0.0163	20.87	0.048–0.100
16. **DSO**	24	0.0081	0.0012	14.81	0.006–0.011
17. **SSO**	24	0.0419	0.0170	40.57	0.020–0.077
18. **WP**	24	0.0208	0.0075	36.06	0.011–0.038
19. **SA**	24	6.42	1.02	15.86	5–8
20. **SAD**	24	0.0306	0.0088	28.76	0.018–0.058
21. **RSL**	24	0.0609	0.0261	42.86	0.022–0.112
23. **SSL**	24	0.0919	0.0361	39.28	0.042–0.227
30. **OL**	15	0.1306	0.0240	18.38	0.090–0.178
31. **OW**	15	0.1213	0.0215	17.72	0.083–0.167
32. **TRW**	24	0.0071	0.0012	16.90	0.005–0.009
33. **TLW**	24	0.0076	0.0011	14.48	0.005–0.009
34. **FWT**	24	0.0295	0.0169	57.29	0.009–0.066
35. **RWT**	24	0.0535	0.0367	68.60	0.018–0.149
36. **CL**	24	0.1840	0.0041	2.23	0.179–0.195
37. **CD**	24	0.1003	0.0061	6.08	0.092–0.114
38. **MAW**	24	0.1037	0.0080	7.71	0.089–0.122
40. **VD**	24	0.0449	0.0168	37.42	0.027–0.076
41. **RA**	24	70.75	5.42	7.67	62–82
42. **LA**	24	30.63	4.74	15.49	19–39
43. **TB**	24	0.2170	0.0300	13.82	0.159–0.271

Fenestrules small; shape rectangular, elliptical to rarely square, moderately regular in shape. Autozooecial apertures very small, shape circular, surrounded by well-developed incomplete peristome open only at proximal-adaxial edge; two to three (most commonly two) apertures per fenestrule. Single intermediate-width keel along middle of obverse branch, atop which are positioned intermediate-size, circular to ovate nodes. Autozooecial chamber size upper-end small, emplaced in two rows, except third row at sites of branch bifurcation; outline triangular to irregularly pentagonal near reverse wall and throughout most of chamber, becoming irregularly bilobate-elliptical near obverse surface. Chambers elongate proximodistally, parallel to reverse wall. Aperture at distal-abaxial end of chamber connected to chamber by short vestibule of variable length. Intermediately developed short superior hemiseptum present, inferior hemiseptum lacking. Lateral-wall budding-angle moderately variable (mean of 30°); reverse-wall budding-angle highly constant (mean of 71°). Heterozooecia between nodes along middle of obverse branch surface.

Table 10 presents statistical criteria used in delimiting this species.

Exterior description.—Zoarium delicate; expansion flat to slightly obversely curved, fan-shaped; mesh close; pronounced astogenetic thickening observed in both obverse and reverse zoarial lamellar skeleton; external zoarial pattern irregular, partially as a result of astogenetic thickening. Probable mature widths 10 to 15 mm; lengths 20 to 30 mm.

Branches delicate; narrow, moderately variable in width; most commonly straight, some very slightly curving toward lateral edge of zoarium. Branches moderately closely spaced, distance between adjacent branch centers regular. Obverse surface slightly granular in texture, becoming increasingly so with astogeny; surface rounded except for single intermediate-width, moderately well-developed keel; keel relatively continuous, straight to slightly anastomosing, extending along branch midline and causing positive inflection on obverse surface. With astogeny, keel frequently covered by lamellar skeleton. Single row of well-developed intermediate-size nodes, shape circular to ovate, elongate proximodistally; size and shape of nodes moderately regular; nodes project from middle of keel in straight line; one to three nodes per fenestrule length, two most common; closely and evenly spaced; node diameter increasing with astogeny. Small, regularly

Text-figure 8.—*Rectifenestella tenax* and *Rectifenestella tenuissima* illustrated. 1, diagrammatic longitudinal section of *R. tenax* showing chamber outline from deep section near middle of branch (bottom of figure) to shallow section near adaxial edge of branch (top of figure), ×70; 2, diagrammatic tangential section of *R. tenax* illustrating change in chamber outline from deep section near reverse-wall budding-site (bottom of figure) to shallow section near obverse surface (top of figure) [Note presence of superior hemiseptum at proximal vestibular edge (arrow).], ×70; 3, diagrammatic transverse sections across branch of *R. tenax* illustrating short superior hemiseptum (arrow) and orientation of the aperture to the obverse surface, ×70; 4, diagrammatic longitudinal section of *R. tenuissima* showing chamber outline from deep section (bottom of figure) to shallow (top of figure) [Note pronounced similarity in chamber outline between this species and *R. tenax*.], ×70; 5, diagrammatic tangential section of *R. tenuissima* from deep (bottom of figure) to shallow (top of figure sectional view [Superior hemiseptum (arrow) is more reduced in this species than in *R. tenax*.], ×70; 6, diagrammatic transverse section of *R. tenuissima*, ×70; 7, reconstruction of typical *Rectifenestella* chamber shape (three-dimensional) as viewed from abaxial edge of branch, showing slight inflection of superior hemiseptum into chamber (arrow), ×140 [*R. tenax* is used as a representative rectifenestellid in this reconstruction.]; 8, reconstruction of typical *Rectifenestella* chamber shape (three-dimensional) as viewed from obverse surface; chamber reconstructed is from the right side of branch [Moderate displacement of apertures toward abaxial edge of chamber is exhibited.], ×140; 9, reconstruction of typical chamber shape (three-dimensional) as viewed from distal end of branch; chamber reconstructed is from the right side of branch, ×140.

sized and variably positioned stylets across obverse branch surface. Reverse surface texture relatively granular, becoming more coarsely granular with astogeny; bearing a moderate number of rows of closely spaced longitudinal striae atop which are positioned closely spaced rows of small to intermediate-size macrostylets; macrostylet size and shape highly variable. Macrostylets increase in diameter with astogeny, becoming more irregularly positioned along reverse branch surface; longitudinal striae becoming covered through astogenetic thickening of lamellar skeleton. Autozooecia arranged in two rows, except third row at sites of branch

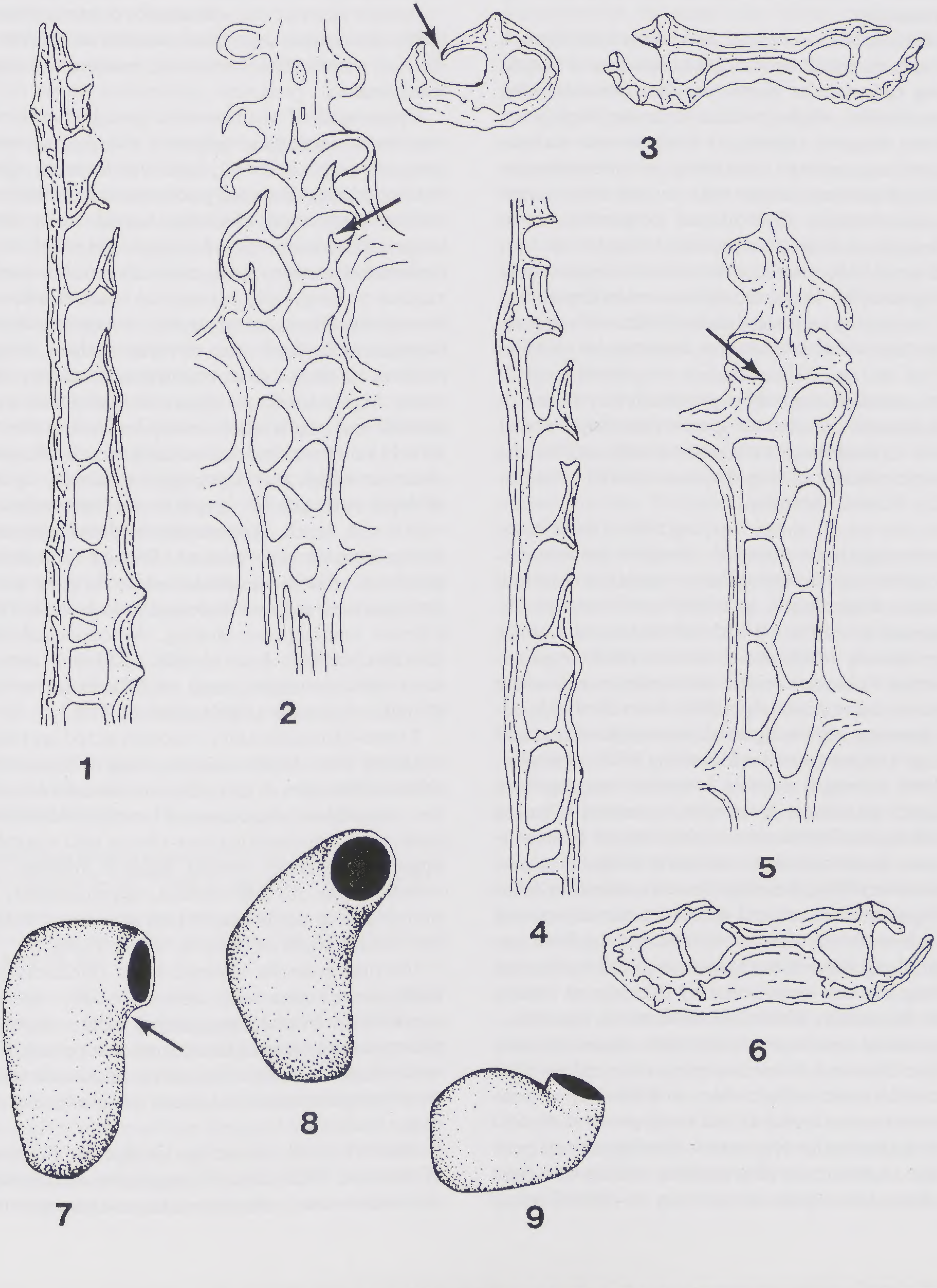

bifurcation where middle autozooecium evidently shared by both branches; pronounced thickening of branches proximal, thinning distal to sites of branch bifurcation. Circular to slightly ovate depressions (ovicells?) occurring between nodes along middle of obverse branch surface; mean diameter of polymorphs approximately twice that of autozooecial apertures; no direct connection evident between apertural opening and polymorphs.

Dissepiments thin, slightly less than half branch width, width variable; short, quite constant in length; connecting branches at highly regular intervals. Dissepiments barlike, slight medial thinning; highly recessed from obverse, slightly so from reverse surface. Pronounced astogenetic thickening of dissepiments. Obverse dissepiment surface with two to three longitudinal striae across dissepiment perpendicular to branch length; reverse dissepiment surface with longitudinal striae atop which occur rows of stylets; striae covered by lamellar skeleton, stylet number decreasing and size increasing as dissepiment thickens during astogeny; both obverse and reverse dissepiment surfaces granular in texture. Dissepiments emplaced perpendicular to or at slight angle from perpendicular to branch length. Apertures commonly open on proximal or distal edge or in middle of dissepiment edge at branch–dissepiment contact; arranged symmetrically or asymmetrically between branches.

Fenestrules small; shape varying from (most commonly) rectangular to elliptical, elongate proximodistally, to rarely square; moderately regular in size and shape; expanding slightly in width and length in obverse–reverse direction. Width of fenestrule slightly less than branch width on obverse surface, approximately equal to branch width on reverse, mean width of fenestrule approximately 1.28× branch width; fenestrule opening becoming small toward proximal end of zoarium with astogenetic thickening of lamellar skeleton. Width to length ratio of fenestrule ranging from 1:1 to slightly less than 1:2, variable; constancy of length and width equal. Two to three apertures per fenestrule length, two most common; distance between closest aperture centers along branch approximately four-fifths of spacing across branch and across fenestrule, spacing of aperture centers across fenestrules varying from less than that along branch to twice that distance; spacing along branch much more constant than across branch or across fenestrule, which are moderately variable.

Autozooecial apertures very small, shape circular, uniform in size and shape; opening oriented parallel to plane of obverse surface; thin, well-developed peristome continuous around all but small portion of most proximal-adaxial edge of aperture, leaving a small peristomal gap. Apertural stylets present, with five to eight intermediate-size stylets developing as extensions of vestibule outer edge; apertural stylets moderately constant in number. Aperture margin extends into fenestrule, causing pronounced inflections in fenestrule outline in obverse surface. Centrally thickened terminal diaphragms present, occurring moderately infrequently, confined to most proximal end of zoarium.

Zoarial supports well-developed, as extension of reverse zoarial surface and lateral edge of zoarium.

Interior description.—Branches ovate or elliptical in transverse section, elongate parallel to zoarial surface (*i.e.*, in width). Branches thin, moderately regular in thickness.

Upper end of autozooecial living chamber small, chambers biserially arranged in alternating rows along planar branch axial wall; axial wall forming zigzag pattern extending diagonally across entire branch or connecting with short chamber lateral walls. Chamber longest dimension paralleling reverse wall in proximodistal direction. Autozooecial chamber outline triangular or irregularly pentagonal near reverse wall and throughout most of chamber; becoming irregularly biolobate-elliptical near obverse surface, longest direction of ellipse oriented distal-abaxially; chamber shape highly uniform. Aperture positioned at distal-abaxial end of chamber, connected to chamber by relatively short vestibule of variable length. Autozooecial chamber width and depth approximately equal; ratio of depth to length 5:9; length much more constant than width and depth. Intermediately developed short superior hemiseptum present, formed as extension of proximal-adaxial vestibular edge, forming partial restriction between vestibule and autozooecial chamber; inferior hemiseptum lacking. Autozooecial chamber diverges laterally from middle of branch at a moderately variable angle (mean of 30°); from reverse wall at highly constant angle (mean of 71°).

Three-dimensionally reconstructed autozooecial chamber form highly cuneate, long in horizontal view with acute angles at proximal and distal ends of chamber, and obtuse angle toward branch midline; near reverse wall, approaching box-like in mid chamber with angular extension toward branch midline; long as viewed from obverse surface, approximately equidimensional in depth and width as viewed from distal and lateral edges of branch, respectively.

Internal granular skeletal layer thickness intermediate, continuous with obverse nodes, stylets, keel, peristome, reverse longitudinal striae, stylets across dissepiments, in middle of zoarial supports. Outer lamellar layer initially thin, with pronounced astogenetic thickening of skeleton toward proximal end of zoarium.

Remarks.—*R. tenax* is similar to *R. tenuissima* (Cumings, 1906) and *R. multispinosa* (Ulrich, 1890) in autozooecial chamber shape and orientation of

chambers relative to the branch. However, *R. tenax* differs moderately to substantially from the above two species in chamber dimensions, aperture size and shape (circular in *R. tenax* but not in *R. tenuissima* or *R. multispinosa*), and exterior accessory characters such as node placement and dissepiment ornamentation. Similarities in chamber shape and orientation are characteristic of generic level taxonomic groupings within the fenestellids and polyporids.

Fenestella submicroporata Shulga-Nesterenko, 1952 was placed in synonymy with *R. tenax* due to similarities in mesh symmetry, accessory features, and chamber size and shape between the two species.

Externally, *R. tenax* is similar in appearance to *Laxifenestella serratula* (Ulrich, 1890), however pronounced differences are observed in internal chamber shape and orientation. Such similar patterns in exterior view most probably represent geometric constraints of zoarial growth, and do not appear to denote close taxonomic affinities.

The moderately variable appearance of both obverse and reverse zoarial exteriors as a result of astogenetic thickening of lamellar skeleon makes interior analysis mandatory for recognition of this species.

Material studied.—Forty exterior fragments, 20 sectioned specimens; largest zoarial fragment 11×18 mm (width to length). Most fragments examined were moderately well-preserved, although compaction of some autozooecial chambers was evident.

Occurrence.—*R. tenax* is common thoughout the Warsaw study area, occurring primarily in facies thought to have been deposited in a lower energy environment.

Syntypes.—ISGS(ISM) 4486-4. USNM 43756, 43757. Several specimens from various localities are illustrated in Ulrich (1890, pl. 51, figs. 2, 2a, 2b, 2c, 2d, 2e).

Figured and/or measured specimens.—UI X-6797–6807 (loc. 49B, samples 10, 12), UI X-6889, 6890, 6892–6897, 6899 (loc. 10, samples 27, 31).

Rectifenestella tenuissima (Cumings, 1906)
Plate 2, figures 4–10, Plate 3, figures 1–8; Table 11

Fenestella tenuissima Cumings, 1906, p. 1279.
Fenestella stocktonensis Condra and Elias, 1944, pp. 162–163, pl. 35, fig. 5; pl. 36, figs. 1, 2.

Diagnosis.—Zoarium delicate, mesh intermediate and regular; branches delicate, width narrow, thickness thin, straight to broadly curved in trace; transversely ovate to semicircular, elongate in plane of zoarial surface; distance between branches intermediate. Intermediate-width, intermediate-length dissepiments connect branches at highly regular intervals. Fenestrule size intermediate, rectangular to elliptical, moderately variable in shape. Autozooecial apertures of intermediate size, ovate, elongate proximodistally; peristome well-developed, incomplete, open only at proximoadaxial edge; three to six small stylets occurring in peristomal gap, large apertural stylet at distal-abaxial edge of aperture; two to four (most commonly three) apertures per fenestrule length. Single narrow keel along middle of obverse branch, nodes of intermediate size, ovate, proximodistally elongate, positioned atop keel. Autozooecial chamber size lower-end intermediate, chambers emplaced in two rows, except third row at sites of branch bifurcation; chamber outline irregularly pentagonal throughout most of chamber depth, becoming elliptical, then irregularly bilobate-elliptical near obverse surface. Chambers elongate proximodistally, parallel to reverse wall. Aperture at distal-abaxial end of chamber, connected to chamber by short vestibule of variable length. Short superior hemiseptum present, inferior hemiseptum absent. Lateral-wall budding-angle highly variable (mean of 23°); reverse-wall budding-angle constant (mean of 68°). Large heterozooecia (ovicells?) rarely present.

Table 11 presents statistical criteria used in species delimitation.

Exterior description.—Zoarium delicate, expansion flat to slightly obversely curved, fan-shaped; mesh intermediate; slight to moderate astogenetic thickening of both obverse and reverse lamellar skeleton; zoarial pattern regular. Probable mature widths 20 to 25 mm, lengths 30 to 40 mm.

Branches delicate, narrow, relatively constant in width; straight to broadly curved toward lateral edge of zoarium. Branch spacing intermediate, distance between adjacent branch centers moderately regular. Obverse surface texture moderately granular, surface rounded or moderately flat; except single narrow, continuous keel anastomosing around autozooecial apertures, extending along branch midline, causing positive inflection. Keel widens, becomes covered by lamellar skeleton, and obverse surface becomes increasingly granular in texture with astogeny. Single row of intermediately developed, intermediate-size nodes; nodes ovate, elongate proximodistally, size and shape moderately regular, projecting from middle of keel; two to four nodes per fenestrule length, three most common; nodes intermediately, moderately unevenly spaced; node diameter increasing with astogeny. Extremely small, irregularly spaced stylets occurring between nodes and across obverse branch surface. Reverse surface texture granular, becoming more coarsely granular with astogeny, bearing numerous rows of longitudinal striae atop which are positioned closely spaced rows of small microstylets; longitudinal striae become covered by lamellar skeleton; stylets become larger, less regularly positioned along branch surface with astogeny. Two rows of autozooecia across branch, except

third row at site of branch bifurcation where middle autozooecium evidently shared by both branches; pronounced proximal thickening of branches, thinning distal to sites of branch bifurcation.

Dissepiments of intermediate width, two-thirds that of branch, moderately constant; length intermediate, moderately constant; connecting branches at highly regular intervals. Dissepiments relatively barlike, slight medial thinning; slightly to moderately recessed from obverse surface, even with reverse; pronounced astogenetic thickening of dissepiments toward proximal end of zoarium. Obverse dissepiment surface with two to five longitudinal striae across dissepiment, oriented perpendicular to branch length; reverse dissepiment surface with longitudinal striae oriented perpendicular to branch length, atop which occur rows of small microstylets; dissepiment surfaces granular, texture similar in appearance to obverse and reverse branch surfaces. Dissepiment emplacement primarily perpendicular to branch length, less frequently at acute angle trending either proximally or distally. Apertures commonly open on proximal or distal edge or in middle of dissepiment edge at branch–dissepiment contact; arranged symmetrically or assymmetrically between branches.

Fenestrules of intermediate size, rectangular to elliptical in tangential view, elongate proximodistally; moderately variable in shape, regular in size; opening constant in size and shape on both obverse and reverse surfaces. Mean width of fenestrule slightly less than that of branch; fenestrule opening becoming slightly smaller toward proximal end of zoarium with astogenetic thickening of lamellar skeleton. Width to length ratio of fenestrule 2:5, relatively constant, length much more constant than width. Two to four apertures per fenestrule length, three most common; distance between closest aperture centers along branch and across branch approximately equal; spacing of aperture centers across fenestrule 1.3× greater than across branch, much more variable.

Autozooecial apertures of intermediate size, ovate, slightly elongate proximodistally and enlarged at distal end, width to length ratio 9:10, size and shape uniform; opening oriented parallel to plane of obverse surface; thin, well-developed, incomplete peristome with small gap at most proximal-adaxial edge, three to six small stylets occurring in peristomal gap. Large apertural stylet at distal-abaxial edge of each aperture, forms as a peristomal extension. Aperture margin extends into fenestrule, causing slight inflections in fenestrule outline in obverse view. Centrally thickened terminal diaphragms rare, confined to most proximal end of zoarium.

Zoarial supports develop as extensions of reverse zoarial surface and lateral edge of zoarium, relatively poorly developed.

Table 11.—Summary numerical analysis of *Rectifenestella tenuissima* (Cumings, 1906). For explanation of abbreviations of characters (left column), see Table 8b (foldout inside back cover).

	number of measurements	*mean*	*standard deviation*	*coefficient of variation*	*observed range*
1. **WB**	24	0.2615	0.0319	12.20	0.195–0.350
2. **DBC**	24	0.5023	0.0804	16.01	0.333–0.678
3. **WD**	24	0.1774	0.0353	19.90	0.127–0.255
4. **LF**	24	0.6335	0.0736	11.62	0.500–0.777
5. **WF**	24	0.2513	0.0467	18.58	0.153–0.343
6. **AF**	24	3.25	0.61	18.70	2–4
7. **AL**	24	0.1006	0.0035	3.48	0.094–0.109
8. **AW**	24	0.0895	0.0044	4.92	0.080–0.096
9. **ADB**	24	0.2304	0.0252	10.94	0.188–0.295
10. **AAB**	24	0.2302	0.0248	10.77	0.187–0.283
11. **ABB**	24	0.2974	0.0501	16.85	0.198–0.397
12. **DN**	24	0.0756	0.0155	20.50	0.048–0.113
14. **SNB**	24	0.3258	0.1038	31.86	0.178–0.527
15. **WK**	24	0.0400	0.0110	27.50	0.010–0.059
16. **DSO**	24	0.0060	0.0012	20.00	0.004–0.009
17. **SSO**	24	0.0468	0.0156	33.33	0.022–0.067
18. **WP**	24	0.0226	0.0032	14.16	0.017–0.030
19. **SA**	24	4.33	0.89	20.48	3–6
20. **SAD**	24	0.0065	0.0019	29.23	0.004–0.011
22. **RSS**	24	0.0167	0.0026	15.57	0.012–0.021
24. **SSS**	24	0.0500	0.0112	22.40	0.022–0.088
30. **OL**	12	0.2500	0.0211	8.44	0.222–0.267
31. **OW**	12	0.2000	0.0183	9.15	0.187–0.225
32. **TRW**	24	0.0071	0.0020	28.17	0.004–0.011
33. **TLW**	24	0.0138	0.0026	18.84	0.009–0.018
35. **RWT**	24	0.0442	0.0284	64.25	0.007–0.123
36. **CL**	24	0.2153	0.0110	5.11	0.197–0.238
37. **CD**	24	0.1052	0.0102	9.70	0.089–0.126
38. **MAW**	24	0.1055	0.0079	7.49	0.091–0.118
39. **MIW**	24	0.0635	0.0071	11.18	0.050–0.074
40. **VD**	24	0.0431	0.0124	28.77	0.019–0.062
41. **RA**	24	67.79	5.52	8.15	55–78
42. **LA**	24	23.42	4.53	19.34	17–33
43. **TB**	24	0.1957	0.0316	16.15	0.150–0.257

Interior description.—Branches ovate to semicircular in transverse view, flattened on obverse surface, elongate parallel to plane of zoarial surface. Branch thin, moderately regular in thickness.

Autozooecial living chamber size lower-end intermediate, chambers biserially arranged in alternating rows along planar branch axial wall; axial wall anastomosing toward sites of lateral-wall emplacement near reverse wall; axial wall becoming relatively straight with moderate inflections toward lateral walls in mid chamber and near obverse surface. Chamber longest dimension paralleling reverse wall in proximodistal direction. Autozooecial chamber outline irregularly pentagonal near reverse wall and toward mid chamber, becoming irregularly elliptical near obverse side of chamber; ellipse bilobate near obverse surface due to initiation of superior hemiseptum at proximal-abaxial edge of vestibule, longest direction of ellipse oriented distal-abaxially; chamber shape highly uniform. Ap-

erture positioned at distal-abaxial end of chamber, connected to chamber by relatively short vestibule of variable length. Ratio of autozooecial chamber minimum width to maximum width 3:5; dimensions of maximum width and depth equal; ratio of depth to length of chamber approximately 1:2. Inferior hemiseptum lacking; small, reduced superior hemiseptum formed as slight extension of proximal-adaxial vestibular edge, forming very slight restriction between vestibule and autozooecial chamber. Autozooecial chamber diverges laterally from middle of branch at highly variable angle (mean of 23°); from reverse wall at constant angle (mean of 68°). Heterozooecia rare, probably ovicells; slightly longer than autozooecia and twice autozooecial width.

Three-dimensionally reconstructed autozooecial chamber form moderately cuneate with rounded acute angles at proximal and distal ends of chamber, obtuse angle toward branch midline; elongate as viewed from obverse surface, approximately equi-dimensional in depth and width as viewed from distal and lateral edges of branch respectively.

Internal granular skeletal layer thin, continuous with obverse nodes, stylets, keel, peristome, apertural stylets, reverse longitudinal striae, stylets across dissepiment, in middle of zoarial supports. Moderate astogenetic thickening of lamellar skeleton toward proximal end of zoarium.

Remarks.—Autozooecial chamber shape in this species is quite similar to that of *R. multispinosa* (Ulrich, 1890), indicating close affinities. Dimensions of the chamber are different, as are the general mesh dimensions and symmetry. Chamber dimensions are similar to those of *R. tenax* (Ulrich, 1888). Exterior similarities are greatest between *R. tenuissima* and *R. tenax*. Evidence supporting emphasis on internal features for taxonomic assignment is strong.

Fenestella stocktonensis Condra and Elias, 1944 was separated from *Fenestella tenuissima* Cumings, 1906 by Condra and Elias. My analysis of *stocktonensis* indicated it was insufficiently different from *tenuissima* to justify separation as a new species, and it is therefore placed in synonymy here.

R. tenuissima is separated from other rectifenestellids by larger aperture size, ovate shape of aperture, slightly larger autozooecial chambers, slightly different shape of autozooecial chambers, and mesh dimensions and symmetry.

Material studied.—Twenty-five exterior fragments; six sectioned specimens; largest zoarial fragment 12 × 22 mm (width to length). Fragments examined were moderately well-preserved, although many zoarial fragments were broken due to their delicate nature.

Occurrence.—*R. tenuissima* is relatively rare at the Valmeyer, St. Louis, and White Hall localities, with occurrence restricted to the Lower Warsaw. It occurs in both limestones and shale, and is more frequent in the latter.

Type Material.—Unknown.

Hypotypes.—UI X-6832–6836, 6891 (loc. 49B, samples 8, 10, 15).

Table 12.—Summary numerical analysis of *Rectifenestella multispinosa* (Ulrich, 1890). For explanation of abbreviations of characters (left column), see Table 8b (foldout inside back cover).

	number of measurements	*mean*	*standard deviation*	*coefficient of variation*	*observed range*
1. **WB**	24	0.2606	0.0437	16.77	0.200–0.356
2. **DBC**	24	0.4096	0.0629	15.36	0.294–0.540
3. **WD**	24	0.1218	0.0226	18.56	0.085–0.188
4. **LF**	24	0.3576	0.0478	13.37	0.290–0.468
5. **WF**	24	0.2101	0.0307	14.61	0.140–0.266
6. **AF**	24	2.25	0.44	16.77	2–3
7. **AL**	24	0.1174	0.0071	6.05	0.102–0.129
8. **AW**	24	0.0968	0.0057	5.89	0.086–0.110
9. **ADB**	24	0.2342	0.0190	8.11	0.184–0.260
10. **AAB**	24	0.2248	0.0222	9.88	0.191–0.278
11. **ABB**	24	0.2135	0.0419	19.63	0.122–0.308
12. **DN**	24	0.0834	0.0182	21.82	0.056–0.125
14. **SNB**	24	0.1743	0.0300	17.21	0.112–0.234
15. **WK**	24	0.0326	0.0059	18.10	0.021–0.044
16. **DSO**	24	0.0076	0.0018	23.68	0.005–0.011
17. **SSO**	24	0.0514	0.0197	38.33	0.029–0.164
18. **WP**	24	0.0119	0.0029	24.37	0.008–0.015
22. **RSS**	24	0.0081	0.0027	33.33	0.005–0.014
24. **SSS**	24	0.0324	0.0083	25.62	0.020–0.046
32. **TRW**	24	0.0063	0.0009	13.65	0.005–0.009
33. **TLW**	24	0.0065	0.0009	13.54	0.005–0.009
34. **FWT**	24	0.0880	0.0398	45.23	0.036–0.171
35. **RWT**	24	0.0684	0.0268	39.18	0.012–0.124
36. **CL**	24	0.2605	0.0117	4.49	0.234–0.286
37. **CD**	24	0.1511	0.0080	5.29	0.136–0.167
38. **MAW**	24	0.1461	0.0159	10.88	0.118–0.188
39. **MIW**	24	0.0887	0.0165	18.60	0.061–0.130
40. **VD**	24	0.0811	0.0250	30.83	0.041–0.126
41. **RA**	24	69.92	5.18	7.40	62–81
42. **LA**	24	23.25	3.51	15.08	17–31
43. **TB**	24	0.3436	0.0460	13.39	0.249–0.411

Rectifenestella multispinosa (Ulrich, 1890)

Plate 4, figures 1–13, Plate 5, figures 1–3; Table 12

Fenestella multispinosa Ulrich, 1890, pp. 540–541, pl. 50, figs. 3–3c; Cumings, 1906, pp. 1278–1279, pl. 29, figs. 1, 1a, 1b, 1d; Nekhoroshev, 1926, pp. 1245–1246, pl. 19, figs. 5–6; pl. 20, fig. 3; Nikiforova, 1927, pl. 178; Nikiforova, 1933, p. 16; Kaisin, 1942, p. 93; Condra and Elias, 1944, pp. 110–112, pl. 33, figs. 1–4; Shulga-Nesterenko, 1951, p. 85; Trizna, 1958, p. 129, pl. 36, fig. 4; pl. 37, figs. 1–5; Miller, 1962, p. 121; Tavener-Smith, 1973, pp. 416–418, pl. 3, figs. 1–9.

Fenestrellina multispinosa (Ulrich). McFarlan, 1942, p. 444.

Diagnosis.—Zoarium robustness intermediate, mesh close, pattern regular; branches delicate, width narrow, thickness intermediate, straight to broadly curved; transversely circular to ovate, closely spaced; branches

joined at regular intervals by thin, short dissepiments; dissepiments emplaced at highly regular intervals. Fenestrules small; shape rectangular to elliptical, moderately variable in shape. Autozooecial aperture size intermediate, shape circular to ovate, elongate proximodistally; peristome thin, well-developed, complete; two to three (most commonly two) apertures per fenestrule. Single narrow, continuous keel along middle of obverse branch, atop which are positioned intermediate-size circular to ovate nodes. Autozooecial chamber size intermediate, emplaced in two rows, except third row at sites of branch bifurcation; chamber outline attaining an irregularly pentagonal shape throughout most of chamber depth, becoming bilobate-elliptical near obverse surface. Chambers elongate proximodistally, parallel to reverse wall. Aperture at distal-abaxial end of chamber, connected to chamber by relatively long, variable-length vestibule. Short superior hemiseptum at proximal vestibular edge, inferior hemiseptum absent. Lateral-wall budding-angle moderately variable (mean of 23°); reverse-wall budding-angle highly constant (mean of 70°).

Table 12 presents statistical criteria used in species delimitation.

Exterior description.—Zoarium robustness intermediate, expansion flat, planar to slightly obversely curved, fan-shaped; mesh close; pronounced astogenetic thickening of both obverse and reverse zoarial skeleton; external zoarial pattern regular. Probable mature widths 12 to 15 mm, lengths 18 to 25 mm.

Branches delicate; width narrow, relatively variable; branches most commonly straight, although locally broadly curved toward lateral edge of zoarium. Branches closely spaced, distance between adjacent branch centers regular. Obverse surface slightly granular in texture, becoming increasingly so with astogeny, surface rounded; except for presence of single keel which is narrow, well-developed, continuous, relatively straight, extending along branch midline causing positive inflection in obverse surface profile. Keel width increasing with astogeny. Nodes monoserially emplaced, well-developed and of intermediate size; node shape circular to ovate, elongate proximodistally when ovate; size and shape relatively regular; nodes develop as projections from middle of keel; two to three per fenestrule length, three most common; nodes evenly, closely spaced; diameter increasing with astogeny. Small, variable-size stylets irregularly positioned along obverse surface. Reverse surface texture relatively granular, coarsening with astogeny, bearing numerous intermediately spaced longitudinal striae which become covered by astogenetic thickening of lamellar skeleton; rows of closely spaced small microstylets become larger, more irregularly positioned along reverse branch surface with astogeny. Two rows of autozooecia across branch, except third row at sites of branch bifurcation where middle autozooecium evidently shared by both branches; pronounced thickening proximal, thinning distal to sites of branch bifurcation. Heterozooecia absent in all zoarial fragments observed.

Dissepiments thin, slightly less than half branch width, moderately constant in width; short, relatively constant in length; connect branches at highly regular intervals. Dissepiments barlike, with moderate medial thinning; highly recessed from obverse surface, even with reverse. Moderate to pronounced astogenetic thickening of dissepiments. Obverse dissepiment surface lacking ornamentation; reverse surface with longitudinal striae atop which are emplaced closely spaced rows of small microstylets; striae becoming obscured by thickened lamellar skeleton with astogeny, microstylets increase in diameter. Obverse dissepiment surface texture slightly granular, reverse relatively granular, both coarsening with astogeny. Dissepiment emplacement ranging from perpendicular to up to 20° from perpendicular to branch length. Apertures commonly open on proximal or distal edge or in middle of dissepiment edge at branch–dissepiment contact; arranged symmetrically or asymmetrically between branches.

Fenestrules small, shape rectangular to elliptical, elongate proximodistally; moderately variable in shape, regular in size; expanding in width and length in obverse–reverse direction. Mean width of fenestrule slightly less than branch width on obverse surface, approximately equal on reverse; fenestrule opening becoming smaller toward proximal end of zoarium with astogenetic thickening of lamellar skeleton. Ratio of mean fenestrule width to length approximately 3:5; constancy of length and width approximately equal. Two to three apertures per fenestrule length, two most common; distance between closest aperture centers along branch, across branch, across fenestrule approximately equal, forming relatively uniform grid of aperture openings over obverse surface; spacing along branch and across branch constant, spacing across fenestrule variable.

Autozooecial apertures intermediate in size, shape circular to ovate, elongate proximodistally and slightly enlarged at distal end; opening most commonly oriented parallel to obverse surface, in some tilting toward fenestrule at slight angle; thin, well-developed complete peristome present. Aperture margin with pronounced extension into fenestrule, causing extreme inflections in fenestrule outline on obverse surface. In late astogeny toward proximal end of zoarium, some apertures become capped by thin terminal diaphragm.

Well-developed zoarial supports form as extensions of reverse zoarial surface and lateral edge of zoarium.

Interior description.—Branches circular to ovate in

transverse section, asymmetrically thickened on obverse surface through astogenetic thickening of lamellar skeleton and presence of keel and nodes; elongate parallel to zoarial surface. Branches intermediate, moderately constant in thickness.

Autozooecial living chambers of intermediate size, biserially arranged in alternating rows along planar branch axial wall; axial wall sinuous, anastomosing toward and connecting with chamber lateral walls; axial wall sinuous throughout chamber depth. Chamber longest dimension parallels reverse wall in proximodistal direction. Autozooecial chamber outline irregularly pentagonal near reverse wall and throughout most of chamber depth, becoming bilobate-elliptical near obverse surface, curved abaxially; chamber shape highly uniform. Aperture positioned at distal-abaxial end of chamber, connected to chamber by relatively long, well-developed vestibule of variable length. Ratio of autozooecial chamber minimum width to maximum width 3:5; maximum chamber width and depth approximately equal; ratio of chamber depth to length approximately 3:5; chamber length and depth highly constant, minimum and maximum widths slightly variable. Short superior hemiseptum at proximal vestibular edge; inferior hemiseptum lacking. Autozooecial chambers diverge laterally from middle of branch at moderately variable angle (mean of 23°); from reverse wall at highly constant angle (70°).

Three-dimensionally reconstructed chamber form moderately cuneate with pronounced angular extension toward branch midline; long dimension as viewed from obverse surface, approximately equidimensional in depth and width as viewed from distal and lateral edges of branch respectively.

Internal granular skeleton relatively thin, continuous with obverse keel, nodes, stylets, and peristomes; reverse longitudinal striae and microstylets, across dissepiments and in the middle of zoarial supports. Astogenetic thickening of lamellar skeletal layer pronounced, most pronounced toward proximal end of zoarium.

Remarks.—*R. multispinosa* can be readily differentiated from *R. tenax* (Ulrich, 1888) and *R. tenuissima* (Cumings, 1906) by the much greater size of its autozooecial chamber, although chamber shape closely resembles that of the two other rectifenestellids. Aperture size is also greater in *R. multispinosa* than in the other rectifenestellid species. Interior appearance alone allows differentiation of *R. multispinosa* from *R. tenuissima*, but separation of these species based solely on exterior features is almost impossible because of similarity in symmetry of mesh and associated characters.

This species has been reported from geographically widely separated areas, suggesting misidentification due to reliance on exterior characters. To determine whether all species have been accurately assigned to *R. multispinosa* requires section and reanalysis of all specimens.

Material studied.—Thirty exterior fragments, five sectioned specimens; largest zoarial fragment 10×12 mm (width to length). Preservation excellent in some fragments, poor due to crushing in others.

Occurrence.—Common in Warsaw study area; most abundant in shaly beds, although not restricted to this facies.

Syntypes.—USNM 43349, 43350. Several specimens are illustrated in Ulrich (1890, pl. 50, figs. 3, 3a, 3b, 3c, 3d).

Figured and/or measured specimens.—UI X-6734, 6872, 6874, 6870 (loc. 10, samples 16, 31), 6949 (loc. 49B, sample 12).

Genus **LAXIFENESTELLA** Morozova, 1974
Text-figure 9

Type species.—*Fenestella sarytshevae* (Shulga-Nesterenko, 1951) [Lower Carboniferous, Namurian Stage; Russian Platform]. Morozova, 1974, pp. 173–174; pls. 3–2.

Typical Warsaw species.—*Laxifenestella coniunctistyla*, n. sp. Osagean–Meramecian throughout Mississippi River Valley outcrop area.

Diagnosis.—Zoarium robustness intermediate, mesh spacing close to intermediate; rectangular, parallelogram-shaped, irregularly pentagonal to elliptical chamber outline in mid tangential section, chamber size intermediate; aperture size small to intermediate; moderate to well-developed superior hemiseptum, well-developed inferior hemiseptum present; chamber reverse-wall budding-angle means vary between 57° and 77°.

Three-dimensionally reconstructed chamber form rounded box- to box-like with indentations caused by hemiseptal positioning (Text-fig. 9).

Description.—Zoarium robustness intermediate, expansion flat to obversely curved, mesh spacing close to intermediate, extremely regular.

Branch width narrow to wide, straight to sinuous in trace with lateral branches broadly curved toward edge of zoarium; branch surface flat to rounded. Keel present, single, width narrow, increasing with astogeny and frequently covered by lamellar skeleton. Nodes present, emplacement monoserial, size intermediate to large, shape circular to ovate, located atop keel in single or alternating rows, spacing close to intermediate. Obverse stylets present, size small to extremely small, occurring across obverse surface. Microstylets present, ranging in size from small to large. Macrostylets present in some species, large, typically located at site of

branch–dissepiment junction. Autozooecia in two rows, third row at site of branch bifurcation or three rows for distance along branch proximal to branch bifurcation. Heterozooecia (ovicells?) present in some species.

Dissepiments of intermediate width, length short to intermediate, connect branches at regular to variable intervals.

Fenestrule size small to intermediate, shape ovate to elliptical to approaching rectangular.

Aperture size small to intermediate, shape circular to ovate, oriented parallel to plane of obverse surface. Peristome present, either complete or incomplete; apertural stylets absent; terminal diaphragms present, primarily occurring toward proximal end of zoarium.

Branch shape in cross-section ranging from circular to ovate, shallow to thick in depth.

Autozooecial chamber size intermediate, chambers biserially emplaced along straight to sinuous axial wall; maximum chamber length extending proximodistally, parallel to reverse wall. Chamber outline irregularly ovate to elliptical near reverse wall, becoming a rectangle, parallelogram, irregular pentagon to elliptical in mid and throughout most of chamber depth, bilobate-elliptical to bilobate-ovate near obverse surface. Vestibule present, varying in length from short to long. Superior hemiseptum present, moderately to well-developed, positioned at proximal vestibular edge; inferior hemiseptum present, well-developed, positioned on middle of reverse and lateral proximal wall, superior and inferior hemisepta frequently fused in mid chamber. Lateral-wall budding-angle means ranging from 20° to 27°; reverse-wall budding-angle means from 57° to 77°. Lamellar skeletal layer thin to thick, exhibiting moderate to pronounced astogenetic thickening; granular skeletal layer thickness intermediate to thick, exhibiting no astogenetic thickening.

Three-dimensionally reconstructed chamber form rounded box- to box-like, with indentations in "box" caused by hemiseptal positioning near mid chamber.

Text-figure 9 illustrates zoarial outlines in longitudinal, tangential, and transverse orientations and three-dimensional chamber reconstructions from distal, abaxial branch edge, and obverse surface views.

Remarks.—This genus is readily characterized by fused inferior and superior hemisepta in conjunction with chamber shape, anastomosing keel, and closely to intermediately spaced intermediate-size nodes. The limited diagnosis and illustrations available in Morozova (1974) seem to agree with a generic grouping established in the Warsaw materials studied, and thus I use her genus herein. The general age of species she assigned to this genus also agree with my own materials. The use of the generic name is somewhat tentative because of Morozova's lack of three-dimensional approach in the establishment of the genus and the inaccessibility of her study samples.

The more highly anastomosing nature of branches and short, wide dissepiments in *Laxifenestella fluctuata*, n. sp. correspond with characters of *Flexifenestella* Morozova, 1974. However, internal analysis of *L. fluctuata* shows no appreciable difference between this species and the rest of the species of *Laxifenestella* found in the Warsaw, thus suggesting the genus *Flexifenestella* is probably synonymous with *Laxifenestella*. Detailed three-dimensional analysis of the type species of these two genera could lead to conclusive determination as to whether they are indeed synonymous.

Specific composition.—Approximately 70 species of *Laxifenestella* were recognized by Morozova. Herein, four species are assigned to this genus: *L. coniunctistyla*, *L. maculasimilis*, n. sp., *L. serratula* (Ulrich, 1890), and *L. fluctuata*.

Range.—Devonian–Lower Mississippian–Permian(?); Permian species differ greatly from those in the Lower Mississippian, and might be better assigned to a separate genus (Morozova, 1974).

Laxifenestella coniunctistyla, new species
Plate 5, figures 4–12, Plate 6, figures 1–8, Plate 7, figures 1, 2; Table 13

Etymology of name.—Named for the occurrence of the stylet in the middle of the dissepiment.

Diagnosis.—Zoarium robustness intermediate, mesh spacing close, pattern extremely regular; branch robustness and width intermediate, thickness medium, trace straight to rarely broadly curved, transversely circular to rarely elliptical, closely spaced. Branches

Text-figure 9.—*Laxifenestella coniunctistyla* illustrated. 1, diagrammatic longitudinal section illustrating changing chamber outline from deep section near middle of branch (bottom of figure) to shallow section near abaxial edge of branch (top of figure) [Inferior hemisepta well-developed, bridging reverse to obverse chamber walls (arrow) near the obverse surface in this species.], ×70; 2, diagrammatic tangential section showing changing chamber outline from deep section near reverse-wall budding-site (bottom of figure) to shallow section near obverse surface (top of figure) [Well-developed superior hemiseptum is illustrated in this view (arrow).], ×70; 3, diagrammatic transverse section across branch showing typical orientation of aperture relative to plane of obverse surface (arrow), ×70; 4, diagrammatic transverse section illustrating well-developed inferior hemiseptum (arrow), ×70; 5, reconstruction of typical chamber shape (three-dimensional) as viewed from distal end of branch; chamber reconstructed is from the right side of the branch [Observe indentation caused by near connection of inferior and superior hemisepta (arrow).], ×140; 6, reconstruction of typical chamber shape (three-dimensional) as viewed from abaxial edge of branch, showing indentation caused by the inferior and superior hemisepta (arrow), ×140; 7, reconstruction of typical chamber shape (three-dimensional) as viewed from the obverse surface; chamber reconstructed is from the right side of the branch [Hemiseptal inflections into chamber outline are evident in this view (arrow).], ×140.

connected at highly regular intervals by lower-end intermediate width, short dissepiments. Fenestrule size intermediate; shape elliptical to approaching rectangular, moderately regular. Autozooecial aperture size intermediate, shape circular, surrounded by well-developed complete peristome; two to four (most commonly three) apertures per fenestrule. Single narrow keel along middle of obverse branch, atop which are positioned intermediate-size, circular to ovate nodes. Autozooecial chamber size intermediate, chambers

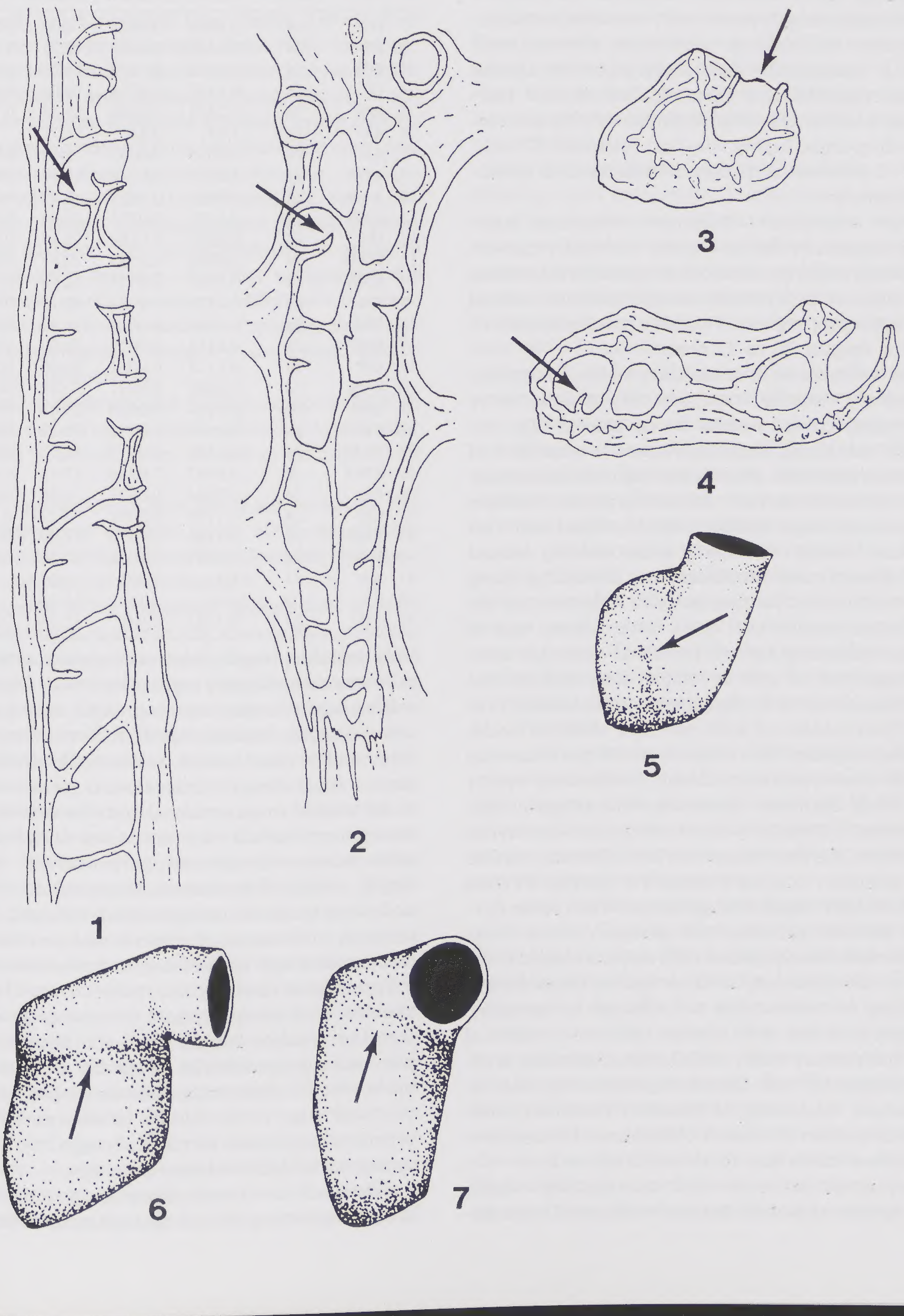

emplaced in two rows, except third row at sites of branch bifurcation; outline elliptical near reverse wall, rapidly becoming a rectangle to parallelogram throughout mid and most of chamber, irregularly bilobate-elliptical near obverse surface. Chambers elongate proximodistally, parallel to reverse wall. Aperture at distal-abaxial end of chamber, connected to chamber by intermediate-length moderately variable vestibule. Both superior and inferior hemisepta present, well-developed, occasionally fuse along chamber abaxial wall restricting chamber opening. Lateral-wall budding-angle moderately variable (mean of 20°); reverse-wall budding-angle highly constant (mean of 57°).

Table 13 presents statistical criteria used in delimiting this species.

Exterior description.—Zoarium robustness intermediate; expansion flat to broadly obversely curved; mesh spacing close; pronounced astogenetic thickening of both obverse and reverse zoarial skeleton; zoarial pattern extremely regular. Probable mature widths 15 to 25 mm, lengths 20 to 35 mm.

Branch robustness intermediate; width intermediate, relatively variable; trace generally straight, more rarely broadly curved toward lateral zoarial edge, occasionally exhibiting slight inflections toward sites of dissepiment insertion. Branch spacing close, extremely regular. Obverse surface texture granular; surface rounded except single narrow, well-developed keel; keel continuous, straight to slightly anastomosing toward sites of dissepiment emplacement, extending along branch midline and causing positive inflection on obverse surface profile; keel thins toward distal end of zoarium, thickening toward proximal end with astogeny. Single row of well-developed intermediate size nodes, circular to ovate, elongate proximodistally, projecting from middle of keel; size and shape of nodes moderately regular; four to seven nodes per fenestrule length, five most common; closely, moderately evenly spaced; node diameter increasing with astogeny. Extremely small, irregularly sized and positioned stylets across entire obverse branch surface. Reverse surface texture granular, bearing a moderate number of rows of intermediately spaced longitudinal striae; striae covered by lamellar skeleton with astogeny; rows of extremely small, closely spaced microstylets extend along branch surface; microstylet size irregular, diameter and positioning of microstylets not affected by astogeny. Autozooecia in two rows, except third row at sites of branch bifurcation where middle autozooecium is evidently shared by both developing branches; slight to intermediate thickening of branches proximal, thinning distal to sites of branch bifurcation. Heterozooecia not observed in any specimen examined.

Dissepiments of lower-end intermediate width, slightly greater than half branch width, width moderately variable; length short, moderately variable; connect branches at highly regular intervals. Dissepiments exhibit slight medial thinning, slight flaring at dissepiment–branch contact; slightly recessed from both obverse and reverse zoarial surfaces. Pronounced astogenetic thickening of dissepiments, nearly tripling in width toward most proximal end of zoarium. Obverse dissepiment surface with one or two thick longitudinal striae across dissepiment perpendicular to branch length; one well-developed, intermediate size, ovate node atop longitudinal striae, node elongate parallel to striae in mid center of dissepiment; reverse dissepiment surface with rows of longitudinal striae atop which are positioned small stylets, stylets covered by lamellar skeleton with astogeny; both obverse and reverse dissepiment surface texture granular. Dissepiment emplacement perpendicular or nearly perpendicular to branch length. Apertures commonly open on proximal or distal edge or in middle of dissepiment edge at branch–dissepiment contact; arranged symmetrically or asymmetrically between branches.

Fenestrule size intermediate; shape elliptical to approaching rectangular, elongate proximodistally; mod-

Table 13.—Summary numerical analysis of *Laxifenestella coniunctistyla*, n. sp. For explanation of abbreviations of characters (left column), see Table 8b (foldout inside back cover).

	number of measurements	*mean*	*standard deviation*	*coefficient of variation*	*observed range*
1. **WB**	24	0.3453	0.0553	16.02	0.263–0.456
2. **DBC**	24	0.5430	0.0690	12.71	0.456–0.719
3. **WD**	24	0.1882	0.0542	28.80	0.119–0.300
4. **LF**	24	0.7337	0.0738	10.06	0.563–0.875
5. **WF**	24	0.2429	0.0608	25.03	0.150–0.388
6. **AF**	24	3.08	0.65	21.21	2–4
7. **AL**	24	0.1035	0.0037	3.57	0.098–0.110
9. **ADB**	24	0.2995	0.0178	5.94	0.268–0.337
10. **AAB**	24	0.2890	0.0257	8.89	0.236–0.328
11. **ABB**	24	0.3779	0.0591	15.64	0.278–0.497
12. **DN**	24	0.0961	0.0184	19.15	0.065–0.130
13. **DND**	24	0.0882	0.0185	20.98	0.060–0.125
14. **SNB**	24	0.2087	0.0473	22.66	0.128–0.287
15. **WK**	24	0.0139	0.0021	15.11	0.012–0.018
16. **DSO**	24	0.0029	0.0010	34.48	0.002–0.005
17. **SSO**	24	0.0113	0.0039	30.00	0.007–0.020
18. **WP**	24	0.0125	0.0021	16.80	0.008–0.016
22. **RSS**	24	0.0036	0.0011	30.56	0.002–0.005
24. **SSS**	24	0.0124	0.0036	29.03	0.009–0.029
32. **TRW**	24	0.0102	0.0016	15.29	0.007–0.014
33. **TLW**	24	0.0106	0.0017	16.13	0.007–0.014
34. **FWT**	24	0.0463	0.0266	57.45	0.014–0.103
36. **CL**	24	0.2634	0.0078	2.96	0.251–0.278
37. **CD**	24	0.1709	0.0091	5.32	0.157–0.189
38. **MAW**	24	0.1480	0.0173	11.69	0.119–0.185
40. **VD**	24	0.0844	0.0170	20.14	0.046–0.123
41. **RA**	24	56.83	4.03	7.09	50–64
42. **LA**	24	20.00	3.13	15.64	15–28
43. **TB**	24	0.3233	0.0407	12.64	0.271–0.381

erately regular in shape; expanding slightly in width and length in obverse–reverse direction. Mean width of fenestrule seven-tenths branch width; fenestrule width and length decreasing toward proximal end of zoarium due to astogenetic thickening of lamellar skeleton. Ratio of fenestrule width to length ranging from 1:5 to 1:2, variable; mean ratio of 1:3 most common; length much more constant than width. Two to four apertures per fenestrule length, three most common; distance between closest aperture centers along branch and across branch approximately equal, spacing of aperture centers across fenestrule normally much greater, variable, ranging from slightly less than that along and across branch to almost twice that distance.

Autozooecial aperture size intermediate, shape circular, highly uniform; opening oriented parallel to plane of obverse surface; thin, well-developed continuous peristome around aperture. Aperture margin extends into fenestrule, causing moderate inflections in fenestrule outline on obverse surface. Centrally thickened terminal diaphragms commonly occurring toward proximal end of zoarium.

Extremely well-developed zoarial supports develop as extensions of reverse zoarial surface and lateral edge of zoarium; most common toward proximal end of zoarium.

Interior description.—Branches approximately circular in transverse section, rarely elliptical, slightly elongate parallel to zoarial surface. Branches medium, relatively constant in thickness.

Autozooecial living chambers intermediate in size, biserially arranged in alternating rows along a predominantly straight, planar to slightly sinuous branch axial wall, with inflections extending toward and connecting with lateral wall. Chamber maximum dimension parallel to reverse wall in proximodistal direction. Autozooecial chamber outline elliptical near reverse wall; rapidly becoming a rectangle to parallelogram, with longest dimension toward outer edge of chamber, in the middle and throughout most of chamber; chamber irregularly bilobate-elliptical near obverse surface, longest direction of ellipse oriented slightly distal-abaxially; chamber shape regular. Aperture located at distal-abaxial end of chamber, connected to chamber by intermediate-length, moderately regular vestibule. Ratio of chamber width to depth approximately 7:8; depth to length ratio 5:8; length and depth much more consistent than width. Well-developed superior hemiseptum forms as extension of proximal interior vestibular edge; superior hemiseptum directed toward the reverse wall in a distal direction, curves around the vestibule inner edge. Inferior hemiseptum located in mid chamber along reverse wall, extending across entire chamber width; toward obverse surface, inferior hemiseptum extends as a ridge along abaxial edge of chamber wall. Superior and inferior hemisepta occasionally fuse along chamber abaxial wall; positioning of these hemisepta restricts opening between autozooecial chamber and inner vestibule edge. Autozooecial chamber diverges laterally from mid chamber at a moderately variable angle (mean of 20°); from reverse wall at a highly constant angle (mean of 57°).

Three-dimensionally reconstructed chamber form box-like with indentations in "box" caused by hemiseptal positioning; long dimension as viewed from obverse surface, depth as viewed from distal end of zoarium slightly greater than width as viewed from lateral edge of branch.

Internal granular skeletal layer moderately thick, exhibiting slight astogenetic thickening in autozooecial chamber, continuous with obverse nodes, stylets, peristome and keel; reverse longitudinal striae and stylets; across dissepiments and in the middle of zoarial supports. Outer lamellar layer initially thin, with extreme thickening during astogeny as observed toward proximal end of zoarium.

Remarks.—General autozooecial chamber shape and presence of inferior and superior hemisepta in this species are also typical of several other Warsaw species including *L. serratula* (Ulrich, 1890), *L. maculasimilis*, n. sp., and *L. fluctuata*, n. sp. Hemisepta provide a chamber which offers protection against predators and adverse environmental conditions. Similar hemiseptal shapes, and the way in which they restrict the chamber, suggest physical similarities among the polypides of different species. Phylogenetic affinities between these species would seem close, probably closer than between groups of fenestellids that do not have such extensive hemiseptal development. For these among other reasons, these species are herein all assigned to *Laxifenestella*.

L. coniunctistyla is readily distinguished from the other laxifenestellids by the presence of a well-developed, intermediate-size node occurring in the middle of each dissepiment, a larger apertural opening, distinctive mesh dimensions, and characteristic autozooecial chamber dimensions.

A very similar species was discovered in material collected by Cumings from the Salem Formation at Dark Hollow near Bloomington, Indiana and contained in collections at Indiana University. This species was not described in suites collected by Ulrich.

Material studied.—Forty-four exterior fragments; nine sectioned specimens; largest zoarial fragment 18 × 28 mm (width to length). Excellent preservation observed in collected specimens.

Occurrence.—*Laxifenestella coniunctistyla*, n. sp. is abundant in the Warsaw throughout the study area. Slight differences do exist between northern and southern specimens. Northern specimens consistently have

a slightly tighter mesh, but this difference is not adequate for species separation as it does not affect the internal chamber dimensions. The species is found in both calcarenite and shale facies.

Holotype.—UI X-6790 (loc. 49B, sample 12).

Paratypes.—UI X-6784–6789 and 6801 (loc. 49B, samples 12, 13, 17) UI X-6791, 6792 (loc. 10, sample 25).

Laxifenestella maculasimilis, new species
Plate 7, figures 3–9, Plate 8, figures 1–10, Plate 9, figures 1, 2; Table 14

Etymology of name.—The name refers to the similar external mesh symmetry between this species and species of *Archimedes*.

Diagnosis.—Zoarium robustness intermediate, mesh intermediate, pattern extremely regular; branch robustness intermediate, width narrow to lower-end intermediate, thickness medium, branches straight to slightly sinuous toward sites of dissepiment emplacement, lateral branches often broadly curved toward edge of zoarium; branches transversely circular to ovate, closely spaced. Branches joined at highly regular intervals by intermediate-width, intermediate-length dissepiments. Fenestrule size intermediate, shape elliptical to approaching rectangular, moderately irregular. Autozooecial apertures small, circular, surrounded by thin, well-developed incomplete peristome open only at proximal-adaxial edge; two to four (most commonly three) apertures per fenestrule. Single narrow keel along middle of obverse branch, atop which are positioned intermediate-size, ovate nodes. Autozooecial chamber size intermediate, chambers emplaced in two rows, except third row at sites of branch bifurcation; outline irregularly ovate near reverse-wall budding-site; rapidly expanding, becoming a parallelogram throughout mid chamber; bilobate-ovate near obverse surface. Chambers elongate proximodistally, parallel to reverse wall. Apertures at distal-abaxial end of chamber, connected to chamber by short, variable-length vestibule. Superior hemiseptum moderately well-developed, inferior hemiseptum well-developed, occasionally both fuse along chamber abaxial wall, restricting chamber opening. Lateral-wall budding-angle relatively constant (mean of 23°); reverse-wall budding-angle highly constant (mean of 66°). Heterozooecia (ovicells?) occurring as intermediate size enlargements between apertures.

Table 14 presents statistical criteria used in delimiting this species.

Exterior description.—Zoarium robustness intermediate; generally forming a flat fan-shaped expansion, rarely slightly obversely curved; mesh spacing intermediate; moderate astogenetic thickening of both obverse and reverse zoarial skeleton; zoarial mesh pattern extremely regular. Probable mature widths of 10 to 25 mm; lengths 15 to 40 mm.

Branch robustness intermediate; width narrow to lower-end intermediate, moderately variable; branches straight to slightly sinuous, bending toward sites of dissepiment emplacement, frequently lateral branches broadly curving toward edge of zoarium. Branches closely spaced, distance between adjacent branch centers extremely regular. Obverse surface texture granular; surface rounded except for presence of single narrow, well-developed keel; keel continuous, straight, extending along branch midline, causing slight positive inflection on obverse surface profile. Keel frequently becomes covered by lamellar skeleton during astogeny, obverse surface texture becomes increasingly granular. Single row of well-developed intermediate size nodes, ovate in shape, elongate proximodistally, size and shape moderately regular, projecting from middle of keel; one to three nodes per fenestrule length, two most common, spacing intermediate, moderately uneven; node

Table 14.—Summary numerical analysis of *Laxifenestella maculasimilis*, n. sp. For explanation of abbreviations of characters (left column), see Table 8b (foldout inside back cover).

	number of measurements	mean	standard deviation	coefficient of variation	observed range
1. **WB**	24	0.2997	0.0724	24.16	0.169–0.481
2. **DBC**	24	0.5203	0.0513	9.86	0.450–0.650
3. **WD**	24	0.1676	0.0226	13.48	0.138–0.223
4. **LF**	24	0.6196	0.0646	10.43	0.457–0.730
5. **WF**	24	0.3118	0.0692	22.19	0.213–0.444
6. **AF**	24	3.08	0.50	16.33	2–4
7. **AL**	24	0.0759	0.0048	6.32	0.062–0.082
9. **ADB**	24	0.2552	0.0224	8.78	0.205–0.300
10. **AAB**	24	0.3010	0.0283	9.40	0.250–0.373
11. **ABB**	24	0.2567	0.0310	12.08	0.207–0.400
12. **DN**	24	0.1066	0.0250	23.45	0.060–0.163
14. **SNB**	24	0.5084	0.1416	27.85	0.288–0.747
15. **WK**	24	0.0199	0.0046	23.12	0.014–0.030
16. **DSO**	24	0.0085	0.0014	16.47	0.006–0.020
17. **SSO**	24	0.0163	0.0053	32.52	0.012–0.037
18. **WP**	24	0.0094	0.0019	20.21	0.006–0.014
21. **RSL**	24	0.1421	0.0267	18.79	0.100–0.208
22. **RSS**	24	0.0283	0.0072	25.44	0.012–0.063
23. **SSL**	24	0.7627	0.2582	33.85	0.223–1.300
24. **SSS**	24	0.0467	0.0159	34.05	0.019–0.142
30. **OL**	14	0.1315	0.0112	8.52	0.117–0.153
31. **OW**	14	0.1302	0.0110	8.45	0.116–0.149
32. **TRW**	24	0.0076	0.0010	13.16	0.006–0.010
33. **TLW**	24	0.0080	0.0012	15.00	0.006–0.011
34. **FWT**	24	0.0444	0.0310	69.82	0.009–0.104
35. **RWT**	24	0.0411	0.0176	42.82	0.008–0.076
36. **CL**	24	0.2299	0.0137	5.96	0.203–0.267
37. **CD**	24	0.1540	0.0099	6.43	0.132–0.167
38. **MAW**	24	0.1396	0.0115	10.74	0.121–0.168
40. **VD**	24	0.0698	0.0170	24.36	0.039–0.099
41. **RA**	24	65.54	4.36	6.66	59–77
42. **LA**	24	23.14	2.80	12.09	19–27
43. **TB**	24	0.3654	0.0804	22.00	0.250–0.500

diameter slightly to moderately increasing with astogeny. Small stylets, moderately regular in size, variably emplaced along obverse branch surface, increasing in size during astogeny. Reverse surface texture granular, becoming more coarsely granular with astogeny; bearing a moderate number of rows of intermediately spaced longitudinal striae which become overgrown during astogenetic thickening of lamellar skeleton. Numerous large microstylets positioned atop striae; microstylet size, shape and positioning atop striae moderately irregular, with size and irregularity increasing during astogeny. Large macrostylets present along reverse branch midline; shape circular or ovate, elongate proximodistally, with size and shape moderately regular; one to two macrostylets per fenestrule length, with most common placement at branch–dissepiment contact; macrostylet spacing highly irregular, with size of macrostylets greatly increasing during astogeny. Autozooecia arranged in two rows, except third row only at sites of branch bifurcation where middle autozooecium evidently shared by both branches; branch diameter thickens proximal and thins slightly distal to sites of branch bifurcation; otherwise diameters moderately constant. Heterozooecia (ovicells?) occurring as intermediate size enlargements positioned between apertures; mean width and length of polymorphs approximately twice that of autozooecial apertures; connection between polymorph and autozooecial chamber probable; polymorphs primarily situated toward proximal end of zoarium.

Dissepiment width intermediate, slightly greater than half branch width, width constant; length intermediate, constant; dissepiments connect branches at highly regular intervals. Dissepiments thin medially, flare at dissepiment–branch contact; highly recessed from obverse, approximately even with reverse surface. Moderate astogenetic thickening of dissepiments. Obverse dissepiment surface with one to three longitudinal striae across dissepiment perpendicular to direction of branch length; reverse dissepiment surface with numerous rows of longitudinal striae atop which occur closely spaced rows of small microstylets; microstylet number decreasing, size increasing during astogenetic thickening of dissepiments; both obverse and reverse dissepiment surfaces granular in texture. Emplacement of dissepiments perpendicular or at small angle from perpendicular to branch length. Apertures commonly open on proximal or distal edge of dissepiments, rarely in middle of dissepiment edge at branch–dissepiment contact; apertures arranged symmetrically or asymmetrically between branches.

Fenestrule size intermediate; shape most commonly elliptical to approaching rectangular, elongate proximodistally; irregular in size, moderately irregular in shape; expanding in length and width in obverse–reverse direction. Mean width of fenestrule slightly less than mean branch width on obverse surface, slightly greater on reverse; fenestrule opening decreasing in size toward proximal end of zoarium due to astogenetic thickening of lamellar skeleton. Width to length ratio of fenestrule approximately 1:2; length much more constant than width. Two to four apertures per fenestrule length, three most common; distance between closest aperture centers along branch, across branch, and across fenestrule all approximately equal, resulting in an evenly spaced grid of apertures across obverse zoarial surface.

Autozooecial apertures small, circular, sometimes irregular in outline; size uniform, shape moderately variable, opening oriented parallel to plane of obverse surface. Thin, well-developed incomplete peristome, continuous around all but most proximal-adaxial edge of aperture, leaving a small to intermediate size peristomal gap. Aperture margin extends into fenestrule, causing pronounced inflections in fenestrule outline on obverse surface. Centrally thickened terminal diaphragm commonly present toward proximal end of zoarium.

Zoarial supports rare, when present develop as extensions of reverse zoarial surface and lateral edge of zoarium.

Interior description.—Branches circular to ovate in cross-section, elongate parallel to zoarial surface. Branches medium in thickness, variable.

Autozooecial living chamber size intermediate, chambers biserially arranged in alternating rows along a planar branch axial wall; axial wall straight to slightly sinuous, extending toward and connecting with moderately long chamber lateral walls. Chambers elongate proximodistally, parallel to reverse wall. Autozooecial chamber outline irregularly ovate near reverse-wall budding-site; expanding rapidly, becoming a parallelogram, with distal edge of parallelogram near branch edge, throughout most of chamber; bilobate-ovate appearance to chamber near obverse surface, longest direction of ovoid oriented distal-abaxially; chamber shape highly uniform. Aperture positioned at distal-abaxial end of chamber, connected to chamber by well-developed short vestibule of variable length. Ratio of chamber width to depth 9:10; depth to length ratio approximately 2:3; depth and length more constant than width. Superior hemiseptum moderately well-developed, forms as extension of proximal vestibular adaxial edge and front chamber wall; well-developed inferior hemiseptum positioned in mid chamber along reverse wall and extending across entire chamber perpendicular to chamber length; hemisepta restrict chamber opening size between autozooecial chamber and inner vestibule edge; occasionally fusing of superior and inferior hemisepta observed. Autozooecial

chamber diverges laterally from middle of branch at relatively constant angle (mean of 23°); from reverse wall at a highly constant angle (mean of 66°). Length and depth of enlarged polymorphs (ovicells?) approximately equal to those of standard autozooecial chambers; width slightly greater.

Three-dimensionally reconstructed chamber form box-like with indentations in "box" caused by hemiseptal positioning; long dimension as viewed from obverse surface, approximately equidimensional in depth and width, as viewed from distal and lateral edges of branch, respectively.

Internal granular skeletal layer moderately thick, exhibiting slight astogenetic thickening, continuous with obverse nodes, keel and peristome; reverse longitudinal striae and both macrostylets and microstylets; across dissepiments and in the middle of zoarial supports. Outer lamellar layer thickness intermediate to thin, with moderate astogenetic thickening.

Remarks.—*Laxifenestella maculasimilis* is similar to other laxifenestellids in development of superior and inferior hemisepta and fusion of these hemisepta across the autozooecial chamber, as well as characteristic indented box-like shape of the chamber. It can be distinguished from other laxifenestellids by presence of reverse macrostylets and smaller aperture size than all other laxifenestellids, along with significantly smaller autozooecial chambers than the other coarsely meshed laxifenestellids, *L. fluctuata*, n. sp. and *L. coniunctistyla*, n. sp.

Although present in suites of the Warsaw fauna collected by Ulrich, this species was placed with *Archimedes* Hall, 1858 on the basis of close general exterior appearance. Examination of oriented peels shows distinctive features such as presence of superior and inferior hemisepta present in *L. maculasimilis*, but absent in *Archimedes*.

Material studied.—Thirty-two exterior fragments, 14 sectioned specimens; largest zoarial fragment 16×21 mm (width to length). Preservation of the zoarial fragments excellent, as observed in the microstructural detail evident.

Occurrence.—*Laxifenestella maculasimilis* is common throughout the Warsaw study area; occurring in both calcarenites and shales.

Holotype.—UI X-6811 (loc. 49B, sample 8).

Paratypes.—UI X-6808–6810, 6812–6815, 6759, 6760 (loc. 49B, samples 8, 10, 11, 17), 6944, 6945, 6767 (loc. 47A, sample 32), 6732, 6733 (loc. 49B, samples 12, 16).

Laxifenestella serratula (Ulrich, 1890)
Plate 9, figures 3–11, Plate 10, figures 1–8,
Plate 11, figure 1; Table 15

Fenestella serratula Ulrich, 1890, p. 544, pl. 50, figs. 5–5c [Keokuk Group, Nauvoo, Illinois; Warsaw Beds, Monroe County and Warsaw, Illinois; St. Louis Limestone, Caldwell, Lyon, and Crittenden counties, Kentucky; Chester Group, Sloan's Valley, Kentucky]; Keyes, 1894, p. 23 [Keokuk Limestone, Keokuk, Iowa]; Cumings, 1906, p. 1280, pl. 30, figs. 2–2c, 3–3a; Condra and Elias, 1944, pp. 72–76, pl. 13, figs. 6–8; pl. 21, figs. 4, 5; pl. 36, fig. 3; Elias and Condra, 1957, p. 409, pl. 45, fig. 2; pl. 46, figs. 7–9; pl. 48, fig. 1; Koenig, 1958, pp. 137–138, pl. 21, fig. 5; Trizna, 1958, p. 135, pl. 39, figs. 1–5; pl. 40, figs. 1–3; Burckle, 1960, pp. 1082–1083, pl. 131, figs. 4, 6.

Diagnosis.—Zoarium robustness intermediate, mesh close, pattern extremely regular; branches delicate, width narrow, thickness thin; branches most commonly straight, lateral branches frequently broadly curved toward edge of zoarium; branches usually transversely ovate, rarely circular, closely spaced. Intermediate width, short dissepiments connect branches at highly regular intervals. Fenestrules small, shape elliptical to approximately rectangular, regular. Autozooecial aperture size lower-end intermediate, predominantly ovate, elongate proximoabaxially, rarely circular, surrounded by well-developed incomplete peristome open only at proximal-adaxial edge; two to three (most commonly two) apertures per fenestrule. Single narrow keel along obverse branch midline, atop which are positioned intermediate size, ovate nodes. Autozooecial chamber size lower-end intermediate, chambers emplaced in two rows, except third row at sites of branch bifurcation; outline irregularly ovate to elliptical near reverse-wall budding-site; rapidly expanding, becoming irregularly pentagonal throughout mid chamber; bilobate-elliptical near obverse surface. Chambers elongate proximodistally, parallel to reverse wall. Apertures at distal-abaxial end of chamber, connected to chamber by short, variable-length vestibule. Superior and inferior hemisepta present, both well-developed, frequently hemisepta fuse in mid chamber, partitioning chamber and restricting chamber opening. Lateral-wall budding-angle moderately variable (mean of 22°); reverse-wall budding-angle highly constant (mean of 71°).

Table 15 presents statistical criteria used in delimiting this species.

Exterior description.—Zoarium robustness intermediate; expansion flat to slightly obversely curved, fan-shaped; mesh close; moderate to slight astogenetic thickening of both obverse and reverse zoarial lamellar skeleton; zoarial mesh pattern extremely regular. Probable mature widths 15 to 20 mm, lengths 15 to 25 mm.

Branches delicate; width narrow, relatively variable; most commonly straight, outer branches frequently broadly curved toward lateral edge of zoarium. Branches closely spaced, with distance between adjacent branch centers highly regular. Obverse surface texture granular; surface flat to slightly rounded, except

Table 15.—Summary numerical analysis of *Laxifenestella serratula* (Ulrich, 1890). For explanation of abbreviations of characters (left column), see Table 8b (foldout inside back cover).

	number of measurements	mean	standard deviation	coefficient of variation	observed range
1. WB	24	0.2744	0.0434	15.82	0.193–0.343
2. DBC	24	0.4420	0.0330	7.47	0.380–0.513
3. WD	24	0.1559	0.0328	20.63	0.115–0.260
4. LF	24	0.3354	0.0398	11.87	0.257–0.415
5. WF	24	0.2008	0.0259	12.90	0.150–0.096
6. AF	24	2.25	0.44	19.66	2–3
7. AL	24	0.0995	0.0029	2.91	0.093–0.104
8. AW	24	0.0844	0.0040	4.74	0.073–0.096
9. ADB	24	0.2354	0.0144	6.12	0.192–0.258
10. AAB	24	0.2418	0.0167	6.91	0.210–0.273
11. ABB	24	0.2493	0.0241	9.67	0.192–0.295
12. DN	24	0.0885	0.0174	19.66	0.057–0.123
14. SNB	24	0.1659	0.0601	36.23	0.098–0.307
15. WK	24	0.0223	0.0048	21.52	0.014–0.033
16. DSO	24	0.0052	0.0009	17.31	0.004–0.006
17. SSO	24	0.0267	0.0091	34.08	0.011–0.043
18. WP	24	0.0129	0.0024	18.60	0.008–0.016
22. RSS	24	0.0064	0.0011	17.19	0.005–0.009
24. SSS	24	0.0286	0.0083	29.02	0.023–0.040
32. TRW	24	0.0065	0.0007	10.77	0.005–0.008
33. TLW	24	0.0064	0.0007	10.94	0.005–0.008
34. FWT	24	0.0341	0.0244	71.56	0.005–0.093
35. RWT	24	0.0417	0.0222	53.24	0.010–0.081
36. CL	24	0.2185	0.0078	3.57	0.209–0.230
37. CD	24	0.1386	0.0056	4.04	0.131–0.148
38. MAW	24	0.1433	0.0189	13.19	0.111–0.187
39. MIW	24	0.0939	0.0144	15.36	0.071–0.118
40. VD	24	0.0596	0.0190	31.88	0.035–0.088
41. RA	24	71.04	3.57	5.02	64–80
42. LA	24	22.17	2.26	10.19	19–27
43. TB	24	0.2525	0.0303	12.12	0.171–0.312

single, narrow, moderately well-developed keel; keel continuous, straight to slightly anastomosing, extending along branch midline and causing positive inflection on obverse surface. Keel exhibiting pronounced thickening toward proximal end of zoarium due to astogenetic thickening of lamellar skeleton. Single row of alternately emplaced, well-developed, intermediate-size nodes; shape ovate, proximodistally elongate, size and shape of nodes moderately regular, formed as projections from middle of keel; two to four nodes per fenestrule length, three most common; nodes closely, moderately unevenly spaced; node diameter increasing with astogeny. Small stylets, moderately regularly sized, variably emplaced along obverse branch surface, increasing in size and frequently fusing with astogeny. Reverse surface texture granular, coarsening with astogeny; bearing a moderate number of rows of closely spaced longitudinal striae atop which are positioned closely spaced rows of small microstylets; stylet size moderately regular, stylets increasing in diameter slightly with astogeny, frequently overgrowing and obscuring longitudinal striae toward proximal end of zoarium. Autozooecia arranged in two rows, except third row only at sites of branch bifurcation where middle autozooecium evidently shared by both branches; branch diameter thickens proximal and thins moderately distal to sites of branch bifurcation; otherwise diameters highly constant. Heterozooecia not observed in any specimen examined.

Dissepiments of intermediate width, slightly greater than half branch width, width moderately variable; length short, constant; connect branches at highly regular intervals. Dissepiments moderately barlike, flare slightly at dissepiment–branch contact; slightly recessed from obverse, approximately even with reverse surface. Moderate astogenetic thickening of dissepiment. Obverse dissepiment surface with one to three longitudinal striae across dissepiment perpendicular to direction of branch length; reverse dissepiment surface with moderate number of rows of longitudinal striae atop which occur intermediately spaced rows of small stylets; striae becoming obscured during astogeny; both obverse and reverse dissepiment surface texture granular. Emplacement of dissepiments perpendicular or nearly perpendicular to branch length. Apertures open on proximal edge, distal edge, or in middle of dissepiment at dissepiment–branch contact; apertures arranged symmetrically or asymmetrically between branches.

Fenestrule size small; shape most commonly elliptical to approximately rectangular, elongate proximodistally; both size and shape regular; moderately expanding in width and length in obverse–reverse direction. Mean width of fenestrule approximately three-fourths that of branch on obverse surface, about equal on reverse; fenestrule opening decreasing in size toward proximal end of zoarium due to astogenetic thickening of lamellar skeleton. Width to length ratio of fenestrule approximately 2:3; width and length both moderately constant. Two to three apertures per fenestrule length, two most common; distance between closest aperture centers along branch, across branch, and across fenestrule all approximately equal, resulting in an evenly spaced grid of apertures across obverse zoarial surface.

Autozooecial aperture size lower-end intermediate, apertures predominantly ovate, elongate proximoabaxially, rarely circular; opening moderately large relative to branch diameter, size and shape both highly consistent; oriented parallel to plane of obverse surface. Peristome thin, well-developed; incomplete, continuous around all but most proximal-adaxial edge of aperture, leaving a small peristomal gap. Aperture margin extends into fenestrule, causing pronounced inflections in outline on obverse surface. Apertures commonly capped by centrally thickened terminal diaphragms toward proximal end of zoarium.

Zoarial supports common, develop as extensions of reverse zoarial surface and lateral edge of zoarium.

Interior description.—Branches most commonly ovate in cross-section, elongate parallel to zoarial surface, rarely circular in cross-section. Branches shallow, moderately regular in thickness.

Autozooecial living chamber size lower-end intermediate, chambers biserially arranged in alternating rows along a planar branch axial wall; axial wall sinuous, extending toward and connecting with proximal and distal chamber lateral walls. Chambers elongate parallel to reverse wall in proximodistal direction. Autozooecial outline irregularly ovate to elliptical near reverse-wall budding-site; expanding rapidly, becoming irregularly pentagonal throughout most of chamber depth; chamber bilobate-elliptical near obverse surface, with separation between proximal-adaxial and distal-abaxial ends of the chamber; shape of chamber highly uniform. Aperture positioned at distal-abaxial end of chamber, connected to chamber by well-developed short vestibule of variable length. Ratio of chamber minimum width to maximum width approximately 2:3; maximum width and depth approximately equal; depth to length ratio 5:8; depth and length more constant than width. Superior hemiseptum well-developed, forms as extension of proximal vestibular interior edge and front chamber wall, extending across width of entire chamber; well-developed, curved inferior hemiseptum, emerging from junction of lateral and reverse wall, divides chamber in half transversely and longitudinally from proximal end of vestibule to middle of chamber reverse wall; frequent fusing of superior and inferior hemisepta to form a partial to nearly complete partition across chamber and between chamber and inner vestibule edge. Autozooecial chamber diverges laterally from middle of branch at a moderately variable angle (mean of 22°); from reverse wall at a highly constant angle (mean of 71°).

Three-dimensionally reconstructed chamber form box-like with pronounced indentations in "box" caused by hemiseptal partitioning; longest dimension of "box" as viewed from obverse surface, approximately equidimensional in depth and width as viewed from distal and lateral edges of branch, respectively.

Internal granular skeletal layer thickness intermediate, continuous with obverse nodes, stylets, keel, and peristome; reverse longitudinal striae and microstylets; across dissepiments and in the middle of zoarial supports. Outer lamellar thickness intermediate to thin, with moderate astogenetic thickening.

Remarks.—Superior and inferior hemiseptal development, in conjunction with three-dimensional autozooecial chamber shape, readily place *Laxifenestella serratula* with the other laxifenestellids. *L. serratula* is, however, distinguished by closer mesh spacing, closely spaced, slightly alternating obverse nodal development, smaller chamber size, and smaller branch width than the other laxifenestellids.

Close external similarity exists between *L. serratula* and *R. tenax* (Ulrich, 1888) in mesh spacing, branch dimensions, nodal size and placement, and aperture placement. However, comparison of interior characters in these two species shows moderate to extreme differences in autozooecial chamber size and shape, and illustrates lack of inferior hemisepta with only presence of short superior hemiseptal development in *R. tenax* when compared to the well-developed superior and inferior hemisepta in *L. serratula*. Using the micrometric (meshwork) formula, one would probably place *L. serratula* and *R. tenax* in the same species; when based on internal and external characters combined, they are placed under separate genera.

Recognition of *L. serratula* in numerous localities covering a long time range probably reflects reliance on the meshwork formula or similar approaches.

Material studied.—Thirty-five exterior fragments, 11 sectioned specimens; largest zoarial fragment 11×16 mm (width to length). The preservation of many zoarial fragments is excellent, although materials are frequently crushed, obscuring internal details.

Occurrence.—*Laxifenestella serratula* is common throughout the Warsaw study area, occurring both in shaly and calcarenitic facies. Zoarial mesh varies slightly from north to south with slight coarsening of mesh in the south. However, size and shape of internal characters are constant and apparently not dependent on mesh variation.

Syntypes.—USNM 44079, ISGS (ISM) 2745–2/4. Several specimens are illustrated in Ulrich (1890, pl. 50, figs. 5, 5a, 5b, 5c).

Figured and/or measured specimens.—UI X-6741 (loc. 11, sample 61), 6837–6843 (loc. 49B, samples 12, 13), 6765 (loc. 47A, sample 32).

Laxifenestella fluctuata, new species
Plate 11, figures 2–11, Plate 12, figures 1–8, Plate 13, figure 1; Table 16

Etymology of name.—The name refers to the fluctuating or anastomosing nature of the branches that characterizes this species.

Diagnosis.—Zoarium robustness intermediate, mesh intermediate, pattern highly variable; branches robust, lower-end wide in width, upper-end intermediate in thickness; branches ranging from straight to highly sinuous toward sites of dissepiment emplacement, lateral branches frequently broadly curved toward edge of zoarium; branches transversely ovate, closely spaced. Branches joined at moderately irregular intervals by

Table 16.—Summary numerical analysis of *Laxifenestella fluctuata*, n. sp. For explanation of abbreviations of characters (left column), see Table 8b (foldout inside back cover).

	number of measurements	mean	standard deviation	coefficient of variation	observed range
1. WB	24	0.3941	0.0800	20.30	0.263–0.567
2. DBC	24	0.6724	0.1302	19.36	0.363–0.973
3. WD	24	0.3780	0.1304	34.50	0.194–0.673
4. LF	24	0.6873	0.1973	28.71	0.270–1.100
5. WF	24	0.3630	0.0842	23.20	0.240–0.531
6. AF	24	3.50	0.78	22.29	2–5
7. AL	24	0.0913	0.0107	11.72	0.075–0.117
8. AW	24	0.0740	0.0073	9.86	0.060–0.088
9. ADB	24	0.2617	0.0316	12.07	0.177–0.323
10. AAB	24	0.2945	0.0377	12.80	0.231–0.364
11. ABB	24	0.3986	0.0848	21.27	0.270–0.590
12. DN	24	0.1308	0.0380	29.05	0.078–0.219
14. SNB	24	0.6309	0.1966	31.16	0.187–1.020
15. WK	24	0.0461	0.0078	16.92	0.032–0.059
16. DSO	24	0.0086	0.0020	23.26	0.004–0.018
17. SSO	24	0.0196	0.0059	30.10	0.014–0.039
18. WP	24	0.0196	0.0039	19.90	0.016–0.034
30. OL	17	0.1821	0.0266	14.61	0.138–0.240
31. OW	17	0.1525	0.0209	13.70	0.127–0.192
32. TRW	24	0.0078	0.0009	11.54	0.006–0.010
33. TLW	24	0.0143	0.0053	36.96	0.008–0.027
34. FWT	24	0.0636	0.0272	42.77	0.024–0.129
35. RWT	24	0.0894	0.0323	36.13	0.029–0.141
36. CL	24	0.2807	0.0165	5.88	0.260–0.314
37. CD	24	0.1466	0.0135	9.21	0.121–0.176
38. MAW	24	0.1622	0.0151	9.31	0.129–0.185
40. VD	24	0.0606	0.0134	22.11	0.040–0.082
41. RA	24	76.75	8.50	11.08	64–95
42. LA	24	27.42	3.59	13.08	18–34
43. TB	24	0.1979	0.0116	5.86	0.179–0.225

intermediate-width, intermediate-length dissepiments. Fenestrule size intermediate, shape ovate to elliptical, variable. Autozooecial aperture size lower-end intermediate, ovate; surrounded by thin, intermediately developed complete peristome; two to five (three or four most common) apertures per fenestrule. Single upper-end narrow keel along middle of obverse branch, atop which are positioned large, ovate nodes. Autozooecial chamber size intermediate, chambers most commonly emplaced in two rows, occasionally three rows for short to intermediate distances immediately proximal to sites of branch bifurcation; outline irregularly elliptical to ovate near reverse-wall budding-site; rapidly expanding, becoming an irregular parallelogram to ellipse throughout mid chamber; bilobate-ovate near obverse surface. Chambers elongate proximodistally, parallel to reverse wall. Apertures at distal-abaxial end of chamber, connected to chamber by intermediate and variable-length vestibule. Superior and inferior hemisepta present, well-developed, frequently fuse causing restriction in chamber opening at proximal vestibular edge. Lateral-wall budding-angle variable (mean of 27°); reverse-wall budding-angle moderately variable (mean of 77°). Heterozooecia (ovicells?) occurring as intermediate size enlargements of some chambers.

Table 16 presents statistical criteria used in delimiting this species.

Exterior description.—Zoarium robustness intermediate; forming a flat to slight obversely curved fan-shaped expansion; mesh spacing intermediate; distributed across zoarial surface, most frequently positioned at or near site of branch–dissepiment contact.

Dissepiments of intermediate width, slightly less than branch width, width highly variable; length intermediate, moderately variable; connect branches at moderately irregular intervals. Dissepiments thin medially, flare at dissepiment–branch contact; moderately recessed from obverse, less so from reverse surface. Pronounced astogenetic thickening of dissepiments. Obverse and reverse dissepiment surfaces highly granular, granularity increasing with astogeny; otherwise dissepiment surfaces lack ornamentaion. Emplacement of dissepiments approximately perpendicular to branch length. Apertures commonly open on proximal or distal edge or in middle of dissepiment edge at branch–dissepiment contact; apertures arranged symmetrically or asymmetrically between branches.

Fenestrule size intermediate; shape ovate to elliptical, elongate proximodistally; variable in both size and shape; width and length the same on both obverse and reverse surfaces. Mean width of fenestrule slightly less than mean branch width, slight decrease in size of fenestrule opening toward proximal end of zoarium due to astogenetic thickening of lamellar skeleton. Ratio of fenestrule width to length approximately 1:2; both width and length moderately variable. Two to five apertures per fenestrule length, three to four most common; distance between closest aperture centers along branch and across branch approximately equal; distance between closest aperture centers across fenestrule 1.4 times greater.

Autozooecial aperture size lower-end intermediate; apertures ovate, elongate proximodistally or proximoabaxially, frequently irregular in outline, shape variable; opening ranging from parallel to plane of obverse surface to attaining slight angle toward fenestrule. Thin, intermediately developed continuous peristomes surround apertures. Minor extension of aperture into fenestrule, causing very slight inflections in fenestrule outline on obverse surface. Centrally thickened terminal diaphragms present, most common toward end of zoarium, moderate astogenetic thickening of both obverse and reverse zoarial skeleton; zoarial pattern highly variable. Probable mature widths of 25 to 30 mm; lengths 35 to 45 mm.

Branches robust; lower-end wide in width, variable; ranging from straight to highly sinuous, with pronounced inflections toward sites of dissepiment emplacement, frequently lateral branches broadly curved toward edge of zoarium. Branches closely spaced, distance between adjacent branch centers moderately regular. Obverse surface texture granular; surface rounded, except for presence of single upper-end narrow, poorly developed keel; keel intermittent, moderately straight, extending along branch midline, causing moderate positive inflection on obverse surface. During astogeny lamellar skeleton frequently develops to cover keel and granularity of obverse surface texture increases. Single row of well-developed large nodes present, ovate in shape, proximodistally elongate, size and shape moderately variable, projecting from middle of keel; one to two nodes per fenestrule length, one most common, spacing intermediate, highly uneven; node diameter greatly increasing with astogeny. Small variable size stylets irregularly positioned across obverse surface. Reverse surface texture highly granular, coarsening with astogeny; moderate number of rows of closely spaced longitudinal striae at most distal end of zoarium atop which occur rows of small, irregular size and shape microstylets. Both striae and microstylets covered by secondary lamellar skeleton at middle and proximal end of zoarium. Autozooecia most commonly in two rows across branch, occasionally three rows for short to intermediate distances immediately proximal to sites of branch bifurcation; branch diameter thickens proximal, exhibits pronounced thinning distal to sites of branch bifurcation, branch diameters moderately variable. Heterozooecia (ovicells?) occurring as moderate enlargements of some apertures; shape ovate, mean diameter of polymorphs approximately twice that of autozooecial apertures, polymorph width-to-length ratio approximately 4:5.

Zoarial supports common, develop as extensions of reverse zoarial surface and lateral edge of zoarium.

Interior description.—Branches ovate in cross-section, moderately elongate parallel to plane of zoarial surface. Branch thickness upper-end medium, moderately variable.

Autozooecial living chamber size intermediate, chambers biserially arranged in alternating rows along a straight to slightly sinuous branch axial wall, extending toward and connecting with moderately long chamber lateral walls. Chambers elongate proximodistally, parallel to reverse wall. Autozooecial chamber outline irregularly elliptical to ovate near reverse-wall budding-sites; rapidly expanding, becoming an irregular parallelogram to ellipse in mid and throughout most of chamber depth; bilobate-ovate appearance to chamber near obverse surface, with longest direction of ovoid oriented proximodistally or proximoabaxially; chamber shape moderately uniform. Aperture positioned at distal-abaxial end of chamber, connected to chamber by extremely well-developed intermediate length vestibule of variable length. Ratio of chamber width to depth approximately 10:9; depth to length ratio approximately 1:2; chamber length more constant than width and depth. Well-developed superior hemiseptum forms as proximal extension of adaxial vestibular edge, extends across almost entire depth of chamber; well-developed short inferior hemiseptum extends across reverse-wall width two-thirds the way distally from chamber proximal edge; superior and inferior hemisepta frequently fuse, greatly restricting opening between autozooecial chamber and inner vestibular edge. Autozooecial chambers diverge laterally from middle of branch at variable angle (mean of 27°); from reverse wall at a moderately variable angle (mean of 77°). Length and depth of enlarged polymorphs (ovicells?) approximately equal to those of standard autozooecial chambers; width 1.2 times greater.

Three-dimensionally reconstructed chamber form box-like, rounded, with pronounced indentations in "box" caused by hemiseptal partitioning; longest dimension of "box" as viewed from obverse surface, approximately equidimensional in depth and width as viewed from distal and lateral edges of branch respectively.

Internal granular skeleton thick, continuous with obverse nodes, keel, and peristome; reverse longitudinal striae; across dissepiments and in the middle of zoarial supports. Outer lamellar layer intermediate to thick, showing moderate astogenetic thickening.

Remarks.—*Laxifenestella fluctuata* is differentiated from other laxifenestellids by the presence of three rows of autozooecia for distances proximal to sites of branch bifurcation, whereas other laxifenestellids only have the third row at site of bifurcation; by greater chamber width than depth, whereas all other laxifenestellids observed have greater depth than width; by generally anastomosing nature of branches; and by greater width and depth of branches.

Interior characters including autozooecial chamber shape and symmetry, and development of superior and inferior hemisepta in this species closely resemble those found in other laxifenestellids. Exterior differences between species are often quite pronounced.

Material studied.—Twenty-five exterior fragments, 14 sectioned specimens; largest zoarial fragment 16×18 mm (width to length). Excellent preservation is observed in almost all zoarial fragments collected.

Occurrence.—*Laxifenestella fluctuata* is a relatively rare component of the Warsaw fauna at the Valmeyer and St. Louis localities, but occurs throughout the formation in both limestones and shales at these localities.

Holotype.—UI X-6778 (loc. 49B, sample 12).

Paratypes.—UI X-6724–6729, 6771–6777 (loc. 49B, samples 8, 11, 12, 17).

Genus **MINILYA** Crockford, 1944
Text-figure 10

Minilya Crockford, 1944, pp. 165–185, pl. 1, figs. 5, 7; text-figs. 1c, d.
Rhombofenestella Termier and Termier, 1971, p. 39.

Type species.—*Minilya duplaris* Crockford, 1944; [Lower Permian, Australia].

Typical Warsaw species.—*Minilya sivonella*, n. sp. [Osage–Meramec, Warsaw, Illinois].

Diagnosis.—Zoarium robustness intermediate to robust, mesh spacing intermediate; triangular to irregularly pentagonal chamber outline in mid tangential section, chamber size intermediate; poorly to well-developed superior hemiseptum present, inferior hemiseptum absent, reverse-wall budding-angle high (means of 74° to 89°); alternating rows of large stylets along obverse surface formed as extensions of apertural peristomal ring.

Three-dimensionally reconstructed chamber form cuneate.

Description.—Zoarium robustness intermediate to robust, expansion flat to slightly obversely curved, mesh spacing intermediate, regular to variable in uniformity.

Branch width narrow to intermediate, straight to sinuous in trace with lateral branches broadly curved toward edge of zoarium, branch surface rounded. Keel present, single, narrow, width increases with astogeny and keel becomes covered. Nodes present or absent, emplacement monoserial, size intermediate, shape ovate, located in middle of keel, closely spaced. Obverse stylets present, size extremely small to intermediate, occurring across obverse surface. Microstylets present, size small to extremely small. Macrostylets present in some species, large, typically occurring at branch–dissepiment junction. Autozooecia in two rows, third row at sites of branch bifurcation. Heterozooecia absent.

Dissepiment width thin to intermediate, length short to intermediate, placement regular to variable.

Fenestrule size intermediate, shape rectangular, elliptical to ovate.

Aperture size small to intermediate, shape circular, oriented parallel to plane of obverse surface or at slight angle toward fenestrule; peristome present, incomplete; two sizes of apertural stylets, small apertural stylets filling peristomal gap and two large apertural stylets developing from adaxial and abaxial apertural edge; terminal diaphragms present, primarily occurring toward proximal end of zoarium.

Branch shape in cross-section ranging from circular to ovate. Branches thick in depth.

Autozooecial chamber size intermediate, chambers monoserially emplaced, becoming biserially arranged along zigzagged axial wall; maximum chamber length extending proximodistally, parallel to reverse wall. Chamber outline triangular near reverse wall, triangular to rarely irregularly pentagonal in mid chamber, becoming irregularly elliptical near obverse surface. Vestibule present, length short to long. Superior hemiseptum present, poorly to well-developed at proximal vestibular edge, inferior hemiseptum absent. Lateral-wall budding-angle approximately 22° to 25° (means); reverse-wall budding-angle approximately 74° to 89° (means). Lamellar skeletal layer thick, exhibiting pronounced astogenetic thickening; granular skeletal layer thick, exhibiting slight astogenetic thickening.

Three-dimensionally reconstructed chamber form cuneate.

Text-figure 10 illustrates zoarial outlines in longitudinal, tangential, and transverse orientations and three-dimensional chamber reconstructions from distal, abaxial branch edge, and obverse surface views.

Remarks.—Acceptance of this genus has been slow in coming. Crockford (1944) introduced the genus, using the following diagnosis:

> Fenestrellinae in which the branches show two rows of alternating zooecia, one on each side of a slight median carina; nodes small, in two rows on the carina, placed so that one node is lateral to each zooecial aperture; zooecia sub-triangular; structure of the reverse surface as in *Fenestrellina* (Crockford, 1944, p. 172).

Elias and Condra (1957, p. 66) considered *Minilya* to be of subgeneric status because they doubted the taxonomic significance of biserial nodes adjacent to autozooecial apertures and the consistency of triangular zooecial chamber shapes; the main criteria used by Crockford in distinguishing the genus. Nekhoroshev (1960) placed *Minilya* in synonymy with *Fenestella* Lonsdale, 1839, for the same reasons as those of Elias and Condra.

Both monoserial and biserial arrangement of nodes were found by Wass (1966) on the same zoaria and were considered nonspecific based on general meshwork similarities. Wass also placed *Minilya* in synonymy with *Fenestella*. Morozova (1974), relying on tangential chamber outline, fenestrule shape, dissepiment size and shape, nodal number and placement, recognized *Minilya* and assigned 20 species to the genus.

Biserial nature of nodal placement can be achieved in several ways: as nodal extensions, nodes positioned across obverse surface without keel, large stylets that develop as extensions of peristome with one adaxially and one abaxially positioned stylet per aperture, biserial nature of aperture placement resulting in biserial nature of stylet placement. The latter characterizes *Minilya* as found in the Warsaw, and appears to be consistent with *Minilya* as described and illustrated by Crockford. Such stylet positioning associated with ap-

Table 17.—Summary numerical analysis of *Minilya sivonella*, n. sp. For explanation of abbreviations of characters (left column), see Table 8b (foldout inside back cover).

	number of mea-sure-ments	*mean*	*standard deviation*	*coeffi-cient of variation*	*observed range*
1. **WB**	24	0.3773	0.1034	27.41	0.225–0.600
2. **DBC**	24	0.7054	0.1215	17.22	0.500–0.875
3. **WD**	24	0.1745	0.0485	27.79	0.113–0.275
4. **LF**	24	0.8662	0.1765	20.38	0.500–1.125
5. **WF**	24	0.3336	0.0585	17.54	0.250–0.438
6. **AF**	24	3.50	0.78	22.29	2–5
7. **AL**	24	0.1056	0.0107	10.13	0.080–0.120
9. **ADB**	24	0.3936	0.0366	9.30	0.350–0.500
10. **AAB**	24	0.3793	0.0319	8.41	0.320–0.440
11. **ABB**	24	0.3914	0.0517	12.20	0.344–0.550
12. **DN**	24	0.1139	0.0173	15.19	0.075–0.160
14. **SNB**	24	0.2393	0.0428	17.89	0.128–0.300
15. **WK**	24	0.0408	0.0080	19.61	0.030–0.055
16. **DSO**	24	0.0102	0.0039	38.24	0.004–0.020
17. **SSO**	24	0.0592	0.0211	35.64	0.030–0.100
18. **WP**	24	0.0222	0.0051	22.97	0.012–0.032
19. **SA**	24	10.42	0.67	7.42	10–12
20. **SAD**	24	0.0094	0.0044	46.32	0.003–0.023
21. **RSL**	24	0.1292	0.0498	38.54	0.050–0.250
22. **RSS**	24	0.0097	0.0027	28.72	0.007–0.015
23. **SSL**	24	0.8500	0.3754	44.16	0.675–1.350
24. **SSS**	24	0.0333	0.0123	36.94	0.020–0.063
32. **TRW**	24	0.0158	0.0045	28.48	0.010–0.025
33. **TLW**	24	0.0150	0.0045	30.00	0.010–0.025
34. **FWT**	24	0.1215	0.0340	27.98	0.053–0.167
35. **RWT**	24	0.1219	0.0386	31.67	0.056–0.180
36. **CL**	24	0.3693	0.0194	5.25	0.343–0.405
37. **CD**	24	0.1580	0.0175	11.08	0.125–0.180
38. **MAW**	24	0.1394	0.0130	9.33	0.120–0.175
40. **VD**	24	0.1628	0.0190	11.67	0.133–0.200
41. **RA**	24	88.50	4.49	5.07	80–93
42. **LA**	24	21.75	4.73	21.75	14–32
43. **TB**	24	0.5133	0.0858	16.72	0.363–0.650

ertural development suggests greater phylogenetic significance than nodes associated with keel or obverse surface development. Stylet development in conjunction with chamber shape, superior hemisepta, high reverse-wall budding-angle, and monoserial chamber emplacement endorse retention of *Minilya* as a valid genus.

Species composition.—The type species, *Minilya duplaris* Crockford, 1944, and two additional species are herein assigned to this genus: *M. sivonella*, n. sp., and *M. paratriserialis*, n. sp. Morozova (1974) assigned 20 additional species.

Range.—Lower Mississippian to Lower Permian; species included by other workers have a greater range.

Minilya sivonella, new species

Plate 13, figures 2–12, Plate 14, figures 1–5; Text-figure 10; Table 17

Etymology of name.—Named for Paul Sivon, whose input into concepts of taxonomy and research while I was preparing the manuscript was appreciated.

Diagnosis.—Zoarium robust, mesh spacing lower-end intermediate, pattern moderately irregular; branches robust, width upper-end intermediate, thick in depth, predominantly sinuous to rarely straight, transversely circular to ovate, branch spacing moderately close; joined at moderately irregular intervals by thin, short to intermediate length dissepiments. Fenestrule size upper-end intermediate; shape elliptical to rarely ovate, moderately irregular. Autozooecial aperture size lower-end intermediate, shape circular, surrounded by thin, well-developed incomplete peristome open at proximal or distal edge of aperture, nine to 14 small stylets fill opening; two to five (most commonly three or four) apertures per fenestrule. Single narrow keel along middle of obverse branch. Biserially arranged large stylets along obverse surface; stylets form as extensions of either proximal or distal-adaxial peristomal edge. Autozooecial chamber size intermediate, monoserially emplaced, rapidly becoming two rows toward obverse surface throughout zoarium, except third row at sites of branch bifurcation; outline rounded triangle near reverse-wall budding-site and throughout most of chamber; becoming irregularly elliptical near obverse surface. Chambers elongate proximodistally, parallel to reverse wall. Aperture at distal-abaxial end of chamber, connected to chamber by long vestibule of moderately constant length. Superior hemiseptum well-developed, short to intermediate in length; inferior hemiseptum absent. Lateral-wall budding-angle highly variable (mean of approximately 22°); reverse-wall budding-angle highly constant (mean of approximately 89°).

Table 17 presents statistical criteria used in delimiting this species.

Exterior description.—Zoarium robust, expansion flat or slightly curved in obverse direction, less frequently curved in reverse direction or undulating, fan-

Text-figure 10.—*Minilya sivonella* illustrated. 1, diagrammatic longitudinal section illustrating changing chamber outline from deep section near middle of branch (bottom of figure) to shallow section near abaxial edge of branch (top of figure) [Superior hemiseptum (arrow) is shown in this illustration.], ×70; 2, diagrammatic tangential section showing changing chamber outline from deep section near reverse-wall budding-site (bottom of figure) to shallow section near obverse surface (top of figure) [Observe large apertural stylet at proximoadaxial edge of aperture (arrow).], ×10; 3, diagrammatic transverse section across branch, ×70; 4, diagrammatic transverse section across branch illustrating typical orientation of apertures (arrow) relative to plane of obverse surface, ×70; 5, reconstruction of chamber shape (three-dimensional) as viewed from distal end of branch, chamber reconstructed from right side of branch, ×140; 6, reconstruction of chamber shape (three-dimensional) as viewed from abaxial edge of branch [Observe inflection in chamber outline caused by superior hemiseptum (arrow).], ×140; 7, reconstruction of chamber shape (three-dimensional) as viewed from obverse surface, ×140.

shaped; mesh lower-end intermediate; pronounced astogenetic thickening of both obverse and reverse zoarial lamellar skeleton; zoarial pattern moderately irregular. Probable mature widths 20 to 35 mm; lengths 30 to 45 mm.

Branches robust; width upper-end intermediate, variable; most commonly sinuous, extending toward sites of dissepiment insertion, rarely straight, lateral branches exhibiting large-scale curvature toward edge of zoarium. Branch spacing moderately close, distance between adjacent branch centers regular. Obverse surface smooth to slightly granular in texture; surface

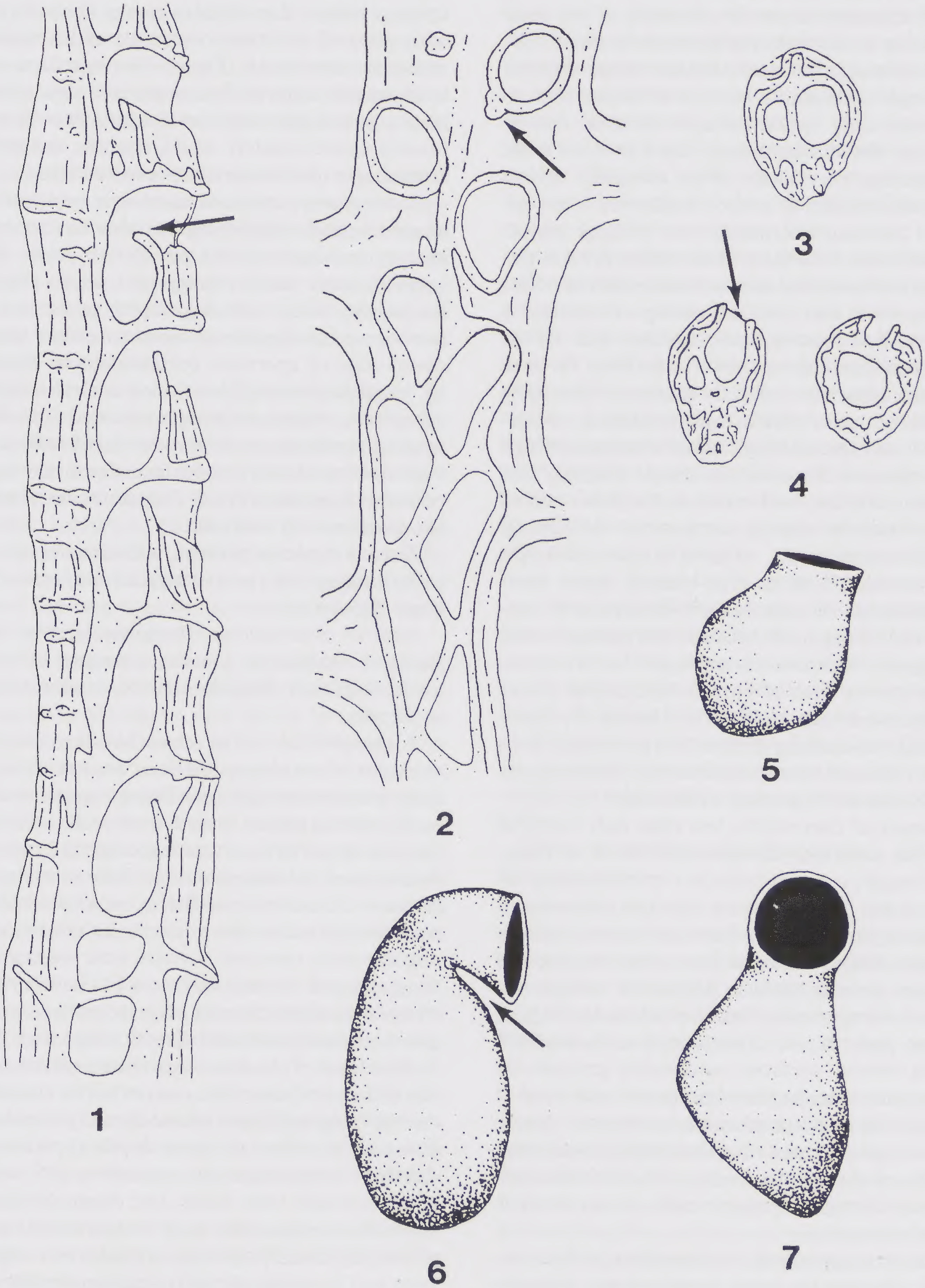

rounded except for single, narrow, well-developed keel; keel continuous, straight or anastomosing, extending along branch midline and causing very slight inflection on obverse surface. With astogeny, keel becomes covered by lamellar skeleton and obverse surface texture becomes increasingly granular. A single large stylet develops on either proximal or distal adaxial edge of each autozooecial aperture, forms as extension of the peristome, resulting in biserial emplacement pattern. Stylets well-developed, size intermediate; shape circular to ovate, elongate proximodistally, less frequently stellate; size moderately regular, shape variable; two to five stylets per fenestrule length, three or four most common, spacing very even. With astogeny, stylets migrate toward middle of branch and away from apertural edge, forming alternating row of large stylets along obverse branch surface; these stylets are not positioned atop keel and thus cannot be considered nodes by definition; stylet diameter increasing with astogeny as well. Lower-end intermediate, variable-size stylets irregularly positioned across obverse surface. Reverse surface texture smooth to slightly granular, becoming more coarsely granular with astogeny; bearing numerous rows of closely spaced longitudinal striae atop which are positioned rows of extremely small, irregular size and shape microstylets; both striae and stylets covered by lamellar skeleton during astogenetic thickening. Large circular macrostylets, variable in size and shape, positioned in middle of reverse branch; most commonly occurring at or near branch–dissepiment contact; moderately irregularly spaced, increasing in size during astogeny. Autozooecia arranged in two rows, except third row at sites of branch bifurcation where middle autozooecium evidently shared by both branches; slight thickening of branches proximal, thinning distal to sites of branch bifurcation. Heterozooecia absent in zoarial fragments examined.

Dissepiments of thin width, less than half width of branch, width variable; dissepiments short to intermediate in length, connect branches at moderately irregular intervals. Dissepiments exhibit pronounced medial thinning, moderately flared at branch–dissepiment contact; highly recessed from obverse, moderately so from reverse surface. Moderate astogenetic thickening of dissepiment. Ornamentation lacking on both obverse and reverse dissepiment surfaces; both obverse and reverse surfaces moderately granular in texture. Dissepiments emplaced perpendicular to or at a slight angle from perpendicular to branch length. Apertures commonly open on proximal or distal edge, or in middle of dissepiment edge at branch–dissepiment contact; arranged symmetrically or asymmetrically between branches.

Fenestrule size upper-end intermediate; shape predominantly elliptical to more rarely ovate, elongate proximodistally; moderately irregular in shape; expanding slightly in width and length in obverse–reverse direction. Mean width of fenestrule slightly less than branch on obverse surface, approximately equal on reverse; fenestrule opening decreasing in size toward proximal end of zoarium due to astogenetic thickening of lamellar skeleton. Width to length ratio of fenestrule ranging from 1:2 to slightly greater than 1:4, variable, with ratio of 1:3 most common; width slightly more constant than length. Two to five apertures per fenestrule length, three to four most common; distance between closest aperture centers along branch and across branch approximately equal, slightly less than that of closest aperture centers between branches.

Autozooecial aperture size lower-end intermediate, shape circular, moderately variable in size, constant in shape; opening oriented parallel to plane of obverse surface, more rarely attaining a slight angle toward fenestrule; thin, well-developed peristome present; peristome incomplete, formed at either proximal or distal edge of aperture; peristomal gap filled by nine to 14 small, evenly positioned stylets which form a semicircle. Aperture margins extend into fenestrule, causing moderate to pronounced inflections in fenestrule outline on obverse surface. Terminal diaphragms commonly present, most frequently occurring toward proximal end of zoarium.

Zoarial supports present, well-developed, occurring as extensions of reverse zoarial surfaces and lateral edge of zoarium.

Interior description.—Branches circular to slightly ovate in transverse section, elongate in obverse–reverse direction. Branches thick, moderately variable in depth.

Autozooecial living chamber size intermediate, monoserial emplacement at or near reverse-wall budding-site, becoming biserially arranged toward obverse surface along planar branch axial wall; axial wall forming zigzag pattern, extending diagonally across entire branch and forming chamber lateral walls. Chamber longest dimension paralleling reverse wall in proximodistal direction. Autozooecial chamber outline triangular with rounded corners near reverse-wall budding-site and throughout most of chamber; becoming irregularly elliptical near obverse surface, ellipse elongate in proximal-abaxial direction and slightly enlarged at distal end of chamber. Aperture positioned at distal-abaxial end of chamber, connected to chamber by relatively long vestibule of moderately constant length. Ratio of chamber width to depth approximately 8:9; depth to length ratio approximately 2:5; length much more constant than width and depth. Well-developed superior hemiseptum, short to intermediate in length, extending distally from proximal inner edge of vestibule and forming partial restriction between vestibule

and autozooecial chamber; inferior hemiseptum absent. Autozooecial chamber diverges laterally from middle of branch at a highly variable angle (mean of approximately 22°); from reverse wall at a highly constant angle (mean of approximately 89°).

Three-dimensionally reconstructed chamber form cuneate with acute angles oriented proximally and distally, and obtuse angle toward branch midline; moderate indentation in chamber form caused by superior hemiseptum; longest dimension as viewed from obverse surface; smaller, approximately equidimensional in depth and width as viewed from distal and lateral edges of branch respectively.

Inner granular skeletal material thick, continuous with obverse large stylets, small stylets, peristome, apertural stylets, and keel; reverse longitudinal striae and both large and small stylets; across dissepiments and in the middle of zoarial supports. Outer lamellar layer thick, with pronounced astogenetic thickening on both obverse and reverse zoarial surfaces; thickest toward proximal end of zoarium.

Remarks.—*M. sivonella* is differentiated from *M. paratriserialis*, n. sp., the only other species of *Minilya* Crockford, 1944 in the Warsaw, by a substantially larger autozooecial chamber, better developed superior hemiseptum, much coarser meshwork, and substantially thicker branches. Similarities in autozooecial chamber shape and inflection in chambers caused by superior hemiseptum suggest close phylogenetic affinity between the two species, as does the large stylet developed at the peristomal edge.

M. sivonella appears similar to an unnamed species contained in a faunal suite collected by Ulrich from Kings Mountain, Kentucky and stored in collections at the U. S. National Museum of Natural History. The restriction of occurrence of this species to the southern half of the study area (an area not extensively dealt with by Ulrich, who concentrated on the northern portion of the area included in this study), could account for Ulrich's not describing this species in his extensive works. Another reason could be that he did not deal in great detail with much of the material collected from Kings Mountain.

Material studied.—Forty-four exterior fragments; 12 sectioned specimens; largest zoarial fragment 21 × 30 mm (width to length). There is little skeletal alteration or crushing in the zoaria collected.

Occurrence.—*Minilya sivonella* is common at the Valmeyer and St. Louis localities, although it occurs primarily in the Lower Warsaw. It is also infrequently found in the Upper Warsaw. It is present in both calcarenites and shales.

Holotype.—UI X-6905 (loc. 49B, sample 12).

Paratypes.—UI X-6904, 6906, 6876–6879, 6951–6955 (loc. 49B, samples 8, 10, 15, 16).

Minilya paratriserialis, new species
Plate 14, figures 6–10, Plate 15, figures 1–9; Table 18

Etymology of name.—Named for its similarity in appearance to *F. triserialis* Ulrich, 1890.

Diagnosis.—Zoarium robustness intermediate, mesh spacing intermediate, pattern extremely regular; branches moderately robust, narrow in width, thick in depth; branches straight to slightly curved, transversely irregularly ovate or circular, closely spaced; connected at highly regular intervals by intermediate width and length dissepiments. Fenestrule size lower-end intermediate; shape approaching rectangular to less commonly elliptical, highly regular. Autozooecial aperture size small, shape circular, surrounded by well-developed incomplete peristome from or near to which two intermediate-size apertural stylets, one abaxial and the other adaxial, originate and form an alternating biserial arrangement across the keel; two to four (most commonly three) apertures per fenestrule. Single upper-end narrow width keel along middle of obverse branch, atop which are positioned intermediate-size ovate nodes. Autozooecial chamber size lower-end intermediate, monoserially emplaced, rapidly becoming two rows toward obverse surface and throughout zoarium, except third row at sites of branch bifurcation; outline rounded triangle near reverse-wall budding-site; usually remaining triangular throughout mid chamber, more rarely becoming irregularly pentagonal; becoming irregularly elliptical near obverse surface. Chambers elongate proximodistally, parallel to reverse wall. Aperture at distal-abaxial end of chamber, connected to chamber by short vestibule of moderately variable length. Superior hemiseptum poorly developed, short; inferior hemiseptum absent. Lateral-wall budding-angle variable (mean of approximately 25°); reverse-wall budding-angle highly constant (mean of approximately 74°).

Table 18 presents statistical criteria used in delimiting this species.

Exterior description.—Zoarium robustness intermediate; expansion flat to slightly obversely curved, fan-shaped; mesh spacing intermediate; pronounced astogenetic thickening of both obverse and reverse lamellar skeleton; zoarial pattern extremely regular. Probable mature widths 15 to 20 mm; lengths 20 to 30 mm.

Branches moderately robust; narrow in width, moderately variable; most commonly straight, some lateral branches slightly curved toward edge of zoarium. Branches closely spaced, distance between adjacent branch centers extremely regular. Obverse surface texture granular; surface rounded except for single upper-end narrow width well-developed keel; keel continuous, predominantly straight to more rarely anas-

tomosing, positioned along branch midline and causing positive inflection along obverse surface. With astogeny, keel exhibits pronounced astogenetic thickening, primarily toward proximal end of zoarium. Single row of well-developed intermediate-size nodes, shape ovate, elongate proximodistally; size and shape of node moderately variable; projecting from middle of keel; one to three nodes per fenestrule length, two most common; node spacing even, intermediate; node diameter greatly increasing with astogeny. Extremely small, regular-size, variably positioned stylets emplaced across obverse branch surface. Two intermediate-size apertural stylets form as extensions of the apertural peristome; one at the mid-distal adaxial edge, positioned abaxial to keel and forming an alternating biserial arrangment across the keel; the other at the mid-distal abaxial edge, extending into the fenestrule opening; during astogeny these stylets migrate away from sites of origin along peristomal edge, the first toward the branch edge and the second into the fenestrule opening. Reverse surface texture granular, coarsening with astogeny; bearing numerous rows of closely spaced longitudinal striae atop which are positioned small microstylets variable in both size and shape; both striae and microstylets frequently become covered during astogenetic thickening of lamellar skeleton. Autozooecia arranged in two rows, except third row at sites of branch bifurcation where middle autozooecium evidently shared by both branches; branches exhibit slight thickening proximal, slight thinning distal to sites of branch bifurcation. Heterozooecia absent in zoarial fragments examined.

Dissepiments of intermediate width, two-thirds width of branch, width relatively constant; length intermediate, relatively constant; connect branches at highly regular intervals. Dissepiments exhibit slight medial thinning, moderately barlike in appearance; highly recessed from obverse, less so from reverse surface. Pronounced astogenetic thickening of dissepiments. Obverse dissepiment surface with one to three longitudinal striae across dissepiment perpendicular to branch length; both obverse and reverse dissepiment surfaces containing rows of small stylets and granular in texture. Emplacement of dissepiments either perpendicular or at an angle of 10° to 15° from perpendicular to branch length. Apertures commonly open on proximal or distal edge or in middle of dissepiment at branch–dissepiment contact; arranged symmetrically or asymmetrically between branches.

Fenestrule size lower-end intermediate; shape approaching rectangular to less commonly elliptical, elongate proximodistally; highly regular in size and shape; expanding slightly in width and length in obverse–reverse direction. Mean width of fenestrule slightly less than branch width on obverse surface, approximately equal on reverse; fenestrule opening decreasing in size toward proximal end of zoarium due to astogenetic thickening of lamellar skeleton. Width to length ratio of fenestrule approximately 1:2, length more constant than width. Two to four apertures per fenestrule length, three most common; distance between closest aperture centers along branch approximately three-fourths of spacing either across branch or across fenestrule, which are approximately equal; spacing along branch much more constant than spacing across branch or across fenestrule.

Autozooecial apertures small, shape circular, uniform; opening oriented parallel to plane of obverse surface or at slight angle toward fenestrule; thin, well-developed peristome present, incomplete with peristomal gap at proximal edge, peristome site from which two previously described intermediate size stylets originate. Aperture margin extends into fenestrule, causing pronounced inflections in fenestrule outline on obverse surface. Centrally thickened terminal diaphragms pres-

Table 18.—Summary numerical analysis of *Minilya paratriserialis*, n. sp. For explanation of abbreviations of characters (left column), see Table 8b (foldout inside back cover).

	number of measurements	*mean*	*standard deviation*	*coefficient of variation*	*observed range*
1. **WB**	24	0.2567	0.0427	16.63	0.184–0.356
2. **DBC**	24	0.4766	0.0560	11.75	0.359–0.581
3. **WD**	24	0.1654	0.0305	18.44	0.114–0.248
4. **LF**	24	0.4783	0.0715	14.95	0.311–0.587
5. **WF**	24	0.2708	0.0512	18.91	0.156–0.362
6. **AF**	24	3.00	0.42	13.90	2–4
7. **AL**	24	0.0712	0.0035	4.92	0.064–0.079
9. **ADB**	24	0.2272	0.0136	5.99	0.207–0.257
10. **AAB**	24	0.3115	0.0439	14.09	0.236–0.401
11. **ABB**	24	0.3212	0.0450	15.15	0.231–0.422
12. **DN**	24	0.1088	0.0284	26.10	0.064–0.159
14. **SNB**	24	0.3527	0.0472	13.38	0.269–0.467
15. **WK**	24	0.0480	0.0102	21.25	0.032–0.065
16. **DSO**	24	0.0033	0.0053	16.31	0.002–0.005
17. **SSO**	24	0.2105	0.0139	6.60	0.188–0.234
18. **WP**	24	0.0165	0.0033	20.00	0.014–0.022
19. **SA**	24	2.00	0.00	0.00	2
20. **SAD**	24	0.0262	0.0064	24.43	0.019–0.044
22. **RSS**	24	0.0172	0.0041	23.84	0.010–0.024
24. **SSS**	24	0.1077	0.0272	25.26	0.073–0.156
32. **TRW**	24	0.0114	0.0035	30.70	0.006–0.018
33. **TLW**	24	0.0175	0.0040	22.86	0.010–0.026
34. **FWT**	24	0.0405	0.0165	40.74	0.016–0.071
35. **RWT**	24	0.0942	0.0422	44.80	0.028–0.186
36. **CL**	24	0.2104	0.0107	5.09	0.194–0.229
37. **CD**	24	0.1516	0.0076	5.01	0.139–0.167
38. **MAW**	24	0.1269	0.1084	6.62	0.115–0.148
39. **MIW**	24	0.0618	0.0084	13.59	0.049–0.078
40. **VD**	24	0.0766	0.0107	13.97	0.065–0.103
41. **RA**	24	73.67	5.44	7.39	62–82
42. **LA**	24	24.67	3.45	13.97	20–32
43. **TB**	24	0.3951	0.0451	11.41	0.292–0.483

ent, moderately uncommon; occurring predominantly at proximal end of zoarium.

Zoarial supports extremely well-developed, form as extensions of reverse zoarial surfaces and lateral edge of zoarium.

Interior description.—Branches irregularly ovate, elongate in obverse–reverse direction, to approximately circular in transverse section, slightly expanded on obverse side. Branches thick, regular in depth.

Autozooecial living chamber size lower-end intermediate, chambers monoserially emplaced at or near reverse-wall budding-site, becoming biserially arranged toward obverse surface along planar branch axial wall; axial wall forming zigzag pattern, extending diagonally across entire branch and forming chamber lateral walls. Chamber maximum dimension extending proximodistally, parallel to chamber reverse wall. Autozooecial chamber outline triangular with rounded corners near reverse-wall budding-site; remaining primarily triangular, less frequently irregularly pentagonal, throughout mid chamber; becoming irregularly elliptical near obverse surface, ellipse elongate in proximal-abaxial direction and slightly enlarged at distal end of chamber. Aperture positioned at distal-abaxial end of chamber, connected to chamber by short vestibule of moderately variable length. Ratio of chamber minimum to maximum width approximately 1:2; maximum width to depth ratio 5:6; depth to length ratio approximately 7:10; chamber length, depth, and maximum width much more constant than minimum width. Superior hemiseptum poorly developed, positioned at inner proximal vestibular edge; inferior hemiseptum absent. Autozooecial chamber diverges laterally from middle of branch at a variable angle (mean of 25°); from reverse wall at a highly constant angle (mean of 74°).

Three-dimensionally reconstructed chamber form cuneate with acute angles oriented proximally and distally and obtuse angle toward branch midline; slight indentation in chamber form caused by superior hemiseptum; longest dimension as viewed from obverse surface, depth smaller than length as viewed from distal end of branch; width smallest, viewed from lateral edge of branch.

Inner granular skeletal layer thick, continuous with obverse nodes, small stylets, peristome, apertural stylets, and keel; reverse longitudinal striae and stylets; across dissepiments and in the middle of zoarial supports. Outer lamellar layer extremely thick on reverse, thinner on obverse side of branch, with pronounced astogenetic thickening evident on both surfaces; thickest toward proximal end of zoarium.

Remarks.—*M. paratriserialis* is readily distinguished from *M. sivonella*, n. sp. by its finer mesh, smaller autozooecial chamber, nodal development atop keel, reduced hemiseptal development, and smaller aperture opening. Close phylogenetic relationships appear to exist between them based on similar cuneate three-dimensional chamber shape, presence of superior hemisepta, and relatively large apertural stylet development at the peristomal edge.

M. paratriserialis is similar in appearance to *Fenestella triserialis* Ulrich, 1890 which occurs in the Lower Keokuk Limestone near Keokuk, Iowa. Biserially arranged stylets are positioned across a central keel in both species; however *M. paratriserialis* is distinguished from *F. triserialis* by a finer mesh, smaller autozooecial chambers, thinner branches, less distinct rows of stylets, and more pronounced nodes.

Material studied.—Thirty-eight exterior fragments; six sectioned specimens; largest zoarial fragment 14 × 22 mm (width to length). Intermediate robustness of the zoarium normally results in excellent preservation of this species.

Occurrence.—*Minilya paratriserialis* is common throughout the Warsaw study area. It occurs in both calcarenites and shales, but is more common in the latter.

Holotype.—UI X-6871 (loc. 10, sample 35).

Paratypes.—UI X-7023 (loc. 49B, sample 12), 7024, 6948, 6947, 6950 (loc. 10, samples 28, 35, 42).

Genus **EXFENESTELLA** Morozova, 1974
Text-figure 11

Type species.—*Fenestella erkovae* (Shulga-Nesterenko, 1951); [Lower Carboniferous, Namurian Stage; Russian Platform]: Morozova, 1974, p. 174, pl. 3–3.

Typical Warsaw species.—*Exfenestella exigua* (Ulrich, 1890) [Warsaw Beds, Monroe County, Illinois].

Diagnosis.—Zoarium robust, mesh spacing intermediate; chamber outline an assymetrical rectangle to parallelogram in mid tangential section, chamber size intermediate, aperture size small; well-developed superior hemiseptum present on proximal vestibular edge, well-developed inferior hemiseptum present on proximal side of distal lateral chamber wall approximately halfway up wall, extending across entire width of chamber and half chamber depth; chamber reverse-wall budding-angle approximately 71° (mean).

Three-dimensionally reconstructed chamber form a rectangular box exhibiting inflections in mid chamber due to hemiseptal emplacement.

Description.—Zoarium robust, expansion obversely curved, mesh spacing intermediate, extremely regular.

Branch width narrow to intermediate, straight to sinuous in trace with lateral branches broadly curved toward edge of zoarium; branch surface rounded. Keel present, single, width intermediate, increasing with astogeny and in many covered by lamellar skeleton. Nodes present, emplacement monoserial, size intermediate,

shape circular to ovate, located atop keel, closely spaced. Obverse stylets present, small, occurring across obverse branch surface. Microstylets present, extremely small in size. Macrostylets present, large, typically located at site of branch–dissepiment junction. Autozooecia in two rows, third row at sites of branch bifurcation. Heterozooecia not observed.

Dissepiments of intermediate width, length intermediate, connect branches at highly regular intervals.

Fenestrule size intermediate, shape regularly to irregularly elliptical, less frequently rectangular to ovate.

Aperture size small, shape circular to rarely ovate, oriented parallel to plane of obverse surface or at slight angle toward fenestrule. Peristome present, complete; apertural stylets present, developed as extensions of peristomal edge; terminal diaphragms present, occurring toward proximal edge and in middle of zoarium.

Branches circular to ovate in cross-section; medium in thickness.

Autozooecial chamber size intermediate, chambers biserially emplaced along sinuous axial wall; maximum chamber length parallel to proximal and distal lateral chamber walls. Chamber outline an asymmetrical diamond near reverse wall, becoming an asymmetrical parallelogram to rectangle in mid chamber and throughout most of chamber depth, bilobate-elliptical near obverse surface. Vestibule present, length intermediate. Superior hemiseptum present, positioned at proximal vestibular edge, inferior hemiseptum present, well-developed at proximal side of distal lateral chamber wall. Lateral-wall budding-angle approximately 25° (mean); reverse-wall budding-angle approximately 71° (mean). Lamellar skeletal layer thick, exhibiting moderate astogenetic thickening; granular skeletal layer thin, exhibiting no astogenetic thickening.

Three-dimensionally reconstructed chamber form a rectangular box exhibiting inflections in middle of box length due to hemiseptal emplacement.

Text-figure 11 illustrates zoarial outlines in longitudinal, tangential, and transverse orientations and three-dimensional chamber reconstructions from distal, abaxial branch edge and obverse surface views.

Remarks.—Morozova (1974, p. 174) based the genus *Exfenestella* on "hemisepta located on branches in two rows", a fabiform (irregular parallelogram-shaped) chamber shape, carina size, and rows of nodes. Hemiseptal positions are unclear from Morozova's illustrations; however, general chamber shape allows assignment of *Fenestella exigua* Ulrich, 1890 to her genus, assuming proximal inflections in chamber lateral walls represent locations of inferior septal emplacement, thus forming the two rows used in Morozova's diagnosis. Because of the variable form of the autozooecial chamber within and between specimens of *E. exigua* and because these shapes most consistently approach that of a parallelogram to rectangle throughout the majority of the chamber depth, I have found use of the term "fabiform" to be unnecessary. The general age of species assigned this genus, Lower Carboniferous for the type species and Devonian to Permian for the genus overall, readily overlaps the age of the Warsaw.

Exfenestella is similar in some characters to *Banastella*, n. gen.; however, the former is distinguished by the presence of hemisepta, different chamber outline, presence of a pronounced keel, and stellate nodal shape. Similarities of the two genera include apertural stylets, relatively low angle at which chamber emerges from the reverse wall, and longest chamber direction paralleling lateral chamber walls.

Species composition.—Approximately 30 species were recognized by Morozova. *E. exigua* is the only Warsaw species assigned to this genus.

Range.—Devonian to Permian.

Exfenestella exigua (Ulrich, 1890)
Plate 16, figures 1–8, Plate 17, figures 1–7,
Plate 18, figure 1; Text-figure 11; Table 19

Fenestella exigua Ulrich, 1890, p. 545, pl. 51, figs. 1, 1a [Warsaw Beds: Monroe County, Illinois]; Cumings, 1906, p. 1278, pl. 38, figs. 3–3a; Trizna, 1958, p. 121, pl. 33, figs. 4–5.

Fenestella exigua var. *springerensis* Elias and Condra, 1957, pp. 406–407, pl. 42, figs. 13–15.

Diagnosis.—Zoarium robust, mesh spacing intermediate, pattern extremely regular; branches moderately robust, width narrow to intermediate, medium in thickness; straight, sinuous to broadly curved in trace, transversely circular to ovate, spacing intermediate; branches joined at highly regular intervals by intermediate width and length dissepiments. Fenes-

Text-figure 11.—*Exfenestella exigua* illustrated. 1, diagrammatic longitudinal view showing changing chamber outline from deep section near middle of branch (bottom of figure) to shallow section near adaxial edge of branch (top of figure) [Observe presence of well-developed inferior hemiseptum on proximal side of distal lateral wall (arrow).], ×70; 2, diagrammatic tangential section showing changing outline of chamber from deep section near reverse wall (bottom of figure) to shallow section near obverse surface (top of figure) [Extension of inferior hemisepta across chambers (arrow) and short superior hemisepta at proximal vestigular edges typical of this genus are illustrated.], ×70; 3, diagrammatic transverse section across branch illustrating aperture orientation to obverse surface, ×70; 4, diagrammatic transverse section showing inferior hemiseptum development (arrow), ×70; 5, reconstruction of typical chamber shape (three-dimensional) as viewed from distal end of branch; chamber reconstructed from right side of branch [Observe inflection of inferior hemiseptum into adaxial edge of chamber (arrow).], ×140; 6, reconstruction of typical chamber shape (three-dimensional) as viewed from abaxial edge of branch; inflection of inferior hemiseptum into distal part of chamber is shown (arrow), ×140; 7, reconstruction of typical chamber shape (three-dimensional) as viewed from obverse zoarial surface [Extension of inferior hemiseptum across chamber (arrow) and superior hemiseptum causing inflections in chamber shape are illustrated.], ×140.

trule size intermediate; shape regularly to irregularly elliptical, less frequently rectangular to ovate, highly regular. Autozooecial apertures small, shape circular to rarely ovate, surrounded by well-developed complete peristome; seven to 11 (mean of nine) small stylets form as extension of peristome, fuse during astogeny; two to four (most commonly three) apertures per fenestrule. Single, intermediate-width keel along middle of obverse branch surface; single row of intermediate-size, circular to ovate nodes along middle of ob-

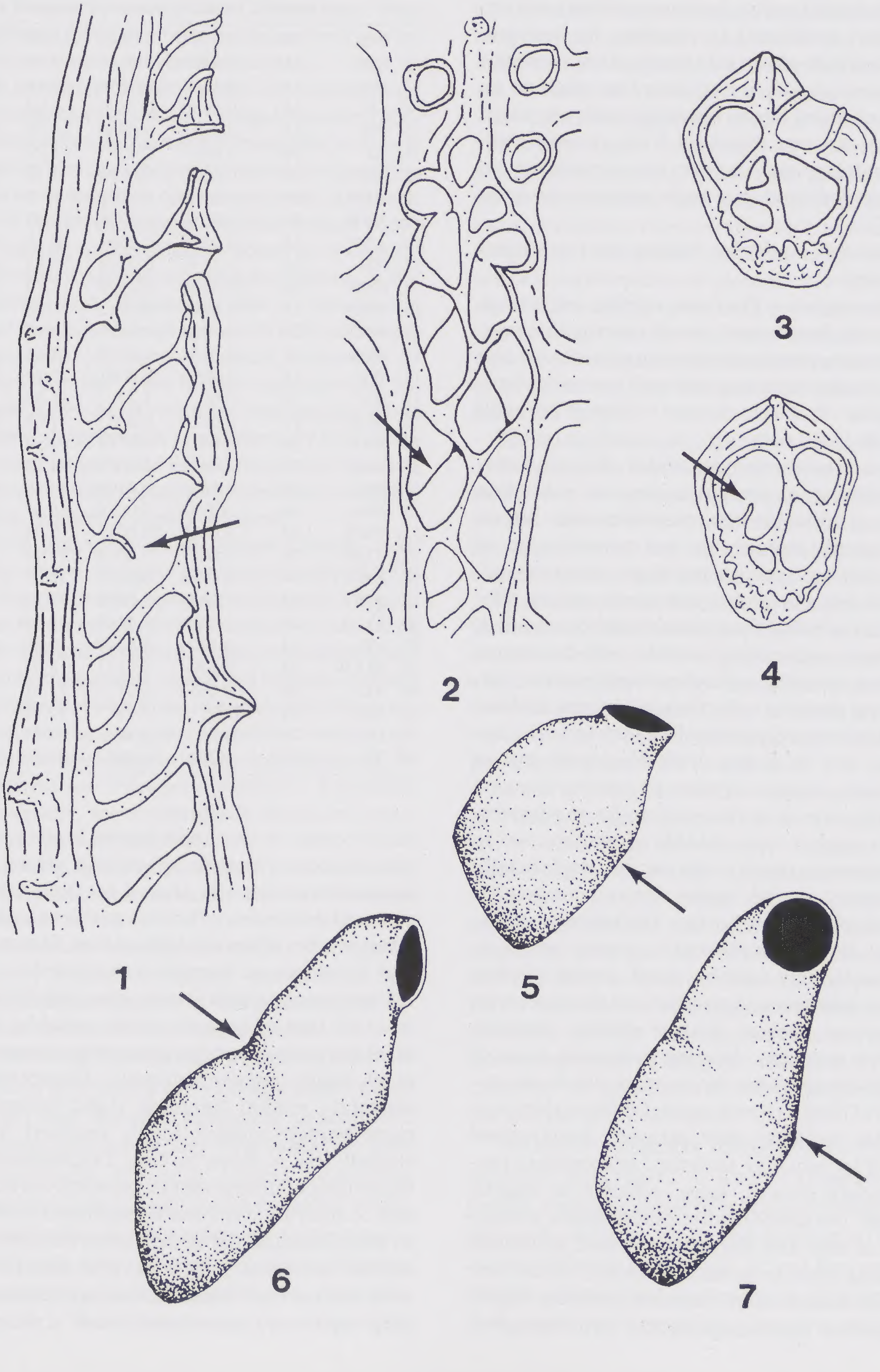

verse branch surface. Autozooecial chamber size intermediate, emplaced in two rows, except third row at sites of branch bifurcation; outline asymmetrical parallelogram-shaped to rectangular throughout mid chamber, irregularly bilobate-elliptical near obverse surface. Chambers elongate parallel to proximal and distal chamber lateral walls. Aperture at distal-abaxial end of chamber, connected to chamber by intermediate-length vestibule of variable length. Short superior hemiseptum present, inferior hemiseptum situated on proximal side of distal lateral chamber wall, one-third the distance in obverse direction from reverse wall. Lateral-wall budding-angle moderately variable (mean of 25°); reverse-wall budding-angle moderately variable (mean of 71°).

Table 19 presents statistical criteria used in delimiting this species.

Exterior description.—Zoarium robust; expansion obversely curved, fan-shaped; mesh spacing intermediate; moderate astogenetic thickening of both obverse and reverse lamellar skeleton; external zoarial pattern extremely regular. Probable mature widths of 20 to 30 mm; lengths 30 to 40 mm.

Branches moderately robust; width thin to intermediate, variable; trace straight or sinuous, extending toward sites of dissepiment emplacement; lateral branches frequently broadly curved toward edge of zoarium. Branch spacing intermediate, distance between adjacent branch centers extremely regular. Obverse surface texture slightly granular; surface rounded, except for single intermediate-width, well-developed keel, continuous, straight, extending along branch midline and causing positive inflection in obverse surface. Keel frequently covered by lamellar skeleton with astogeny. Single row of nodes, well-developed and of intermediate-size, shape circular to ovate, elongate proximodistally; size and shape of nodes moderately regular; nodes project from middle of branch, two to four (most commonly three) nodes per fenestrule length, moderately evenly spaced; nodes and surrounding lamellar skeleton on obverse surface thickening with astogeny. Small stylets, moderately closely, unevenly spaced and moderately variably sized, across obverse branch surface, increasing in number and diameter with astogeny. Reverse surface texture slightly granular, coarsening with astogeny; bearing numerous rows of closely spaced longitudinal striae atop which are positioned rows of small, closely spaced microstylets; size of microstylets variable; with astogeny longitudinal striae covered by lamellar skeleton, microstylets persist. Macrostylets present, large, circular to slightly ovate, elongate proximodistally; macrostylets moderately regular in size and shape, positioned in middle of branch along reverse surface primarily at or near site of branch–dissepiment junction, spacing highly variable; diameter increasing slightly with astogeny.

Table 19.—Summary numerical analysis of *Exfenestella exigua* (Ulrich, 1890). For explanation of abbreviations of characters (left column), see Table 8b (foldout inside back cover).

	number of measurements	*mean*	*standard deviation*	*coefficient of variation*	*observed range*
1. **WB**	24	0.2958	0.0543	18.36	0.214–0.399
2. **DBC**	24	0.5603	0.0683	12.19	0.406–0.676
3. **WD**	24	0.1663	0.0346	20.81	0.123–0.254
4. **LF**	24	0.5600	0.0506	9.04	0.464–0.660
5. **WF**	24	0.2801	0.0302	10.78	0.220–0.327
6. **AF**	24	3.00	0.42	13.90	2–4
7. **AL**	24	0.0887	0.0028	3.16	0.083–0.093
9. **ADB**	24	0.2389	0.0090	3.77	0.220–0.254
10. **AAB**	24	0.3012	0.0315	10.46	0.252–0.359
11. **ABB**	24	0.2955	0.0596	20.17	0.181–0.388
12. **DN**	24	0.1191	0.0204	17.13	0.089–0.152
14. **SNB**	24	0.3430	0.0590	17.20	0.174–0.429
15. **WK**	24	0.0985	0.0212	21.52	0.061–0.132
16. **DSO**	24	0.0083	0.0020	24.10	0.006–0.120
17. **SSO**	24	0.0462	0.0122	26.41	0.024–0.071
18. **WP**	24	0.0101	0.0021	20.79	0.007–0.014
19. **SA**	24	9.00	1.22	13.51	7–11
20. **SAD**	24	0.0119	0.0037	31.09	0.007–0.022
21. **RSL**	24	0.0919	0.0216	23.50	0.059–0.149
22. **RSS**	24	0.0111	0.0029	26.13	0.005–0.016
23. **SSL**	24	0.5667	0.2504	44.19	0.320–0.867
24. **SSS**	24	0.0241	0.0088	36.37	0.013–0.036
32. **TRW**	24	0.0079	0.0015	18.99	0.005–0.011
33. **TLW**	24	0.0071	0.0015	21.13	0.005–0.010
34. **FWT**	24	0.0588	0.0212	36.05	0.027–0.088
35. **RWT**	24	0.0854	0.0370	43.33	0.024–0.170
36. **CL**	24	0.2869	0.0106	3.69	0.267–0.310
37. **CD**	24	0.1401	0.0147	10.49	0.115–0.164
38. **MAW**	24	0.1384	0.0111	8.02	0.123–0.168
40. **VD**	24	0.0652	0.0137	21.01	0.039–0.080
41. **RA**	24	43.17	5.26	12.19	33–55
42. **LA**	24	25.04	3.48	13.91	19–33
43. **TB**	24	0.3701	0.0802	21.67	0.249–0.527

Autozooecia in two rows across branch, except third row at sites of branch bifurcation where middle autozooecium evidently shared by both branches; pronounced thickening of branch proximal, slight thinning distal to sites of branch bifurcation. Heterozooecia absent in all zoarial fragments examined.

Dissepiment width intermediate, slightly greater than one-half that of branch, width variable; length intermediate, quite constant; dissepiments connect branches at highly regular intervals. Dissepiments exhibit moderate medial thinning, slight flaring at dissepiment–branch contact; highly recessed from obverse surface, less so from reverse. Pronounced astogenetic thickening of dissepiments, primarily toward proximal end of zoarium. Obverse dissepiment surface with one to three longitudinal striae across dissepiment perpendicular to branch length; reverse dissepiment surface with similar but more numerous longitudinal striae atop which are positioned small stylets; number of

striae covered by lamellar skeleton and stylet size slightly increasing with dissepiment thickening during astogeny; both obverse and reverse dissepiment surfaces slightly granular in texture. Emplacement of dissepiments approximately perpendicular to branch length. Apertures commonly open on proximal or distal edge, less frequently in middle of dissepiment edge at branch–dissepiment contact; arranged symmetrically or asymmetrically between branches.

Fenestrule size intermediate; shape most commonly regularly to irregularly elliptical, elongate proximodistally, less frequently approaching rectangular to ovate; highly regular in size and shape; moderately expanding in width, less so in length in obverse–reverse direction. Mean width of fenestrule slightly less than branch width on obverse surface, approximately equal to or slightly greater on reverse; fenestrule opening decreasing in size toward proximal end of zoarium due to astogenetic thickening of the lamellar skeleton. Width to length ratio of fenestrule 1:2, highly constant; constancy of width and length equal. Two to four apertures per fenestrule length, three most common; spacing of closest aperture centers along branch approximately four-fifths of spacing across branch and across fenestrule; spacing along and across branch highly to moderately constant, spacing across fenestrule highly variable.

Autozooecial apertures small, shape circular, very rarely slightly ovate, elongate proximodistally, highly uniform in size and shape; opening orientation ranging from parallel to plane of obverse surface to attaining a slight angle toward fenestrule; thin, well-developed complete peristome present, seven to 11 (mean of nine) small stylets form as extensions of peristome, frequently stylets fuse during astogeny. Aperture margin extends into fenestrule, causing slight inflections in fenestrule outline on obverse surface. Terminal diaphragms present, most commonly found in proximal and central part of zoarium.

Zoarial supports develop moderately infrequently, form as extensions of reverse zoarial surface and lateral edge of zoarium.

Interior description.—Branches circular to ovate in transverse view, frequently slightly enlarged on obverse side of branch, elongate in obverse–reverse direction. Branch thickness medium, variable.

Autozooecial living chamber size intermediate, biserially arranged in alternating rows along planar branch axial wall; axial wall sinuous, exhibiting pronounced inflections toward and connecting with relatively long chamber lateral walls. Chamber longest dimension paralleling proximal and distal chamber lateral walls. Autozooecial chamber outline attaining an asymmetrical diamond shape near reverse wall; rapidly becoming an asymmetrical parallelogram to rectangle throughout most of mid chamber; outline irregularly bilobate-elliptical near obverse surface, longest direction of ellipse oriented distal-abaxially; chamber shape highly regular. Aperture positioned at distal-abaxial end of chamber, connected to chamber by well-developed, intermediate-length vestibule of variable length. Autozooecial chamber width and depth approximately equal; ratio of depth to length approximately 1:2; length much more constant than width and depth. Moderately well-developed short, superior hemiseptum present, formed as extension of proximal-adaxial vestibular edge, forming partial restriction between vestibule and autozooecial chamber; well-developed inferior hemiseptum present, situated on proximal side of distal lateral chamber wall one-third the distance in obverse direction from reverse wall; lateral wall exhibiting slight inflection into chamber toward site of inferior hemiseptum emplacement, with inferior hemiseptum extending up to half the diameter of chamber depth. Autozooecial chamber diverges laterally from middle of branch at a moderately variable angle (mean of 25°); from reverse wall at a moderately variable angle (mean of 71°).

Three-dimensionally reconstructed chamber form a rectangular box exhibiting inflections in middle of box length due to hemiseptal emplacement; long dimension as viewed from lateral edge of branch; width and depth approximately equidimensional as viewed from obverse surface and distal end of branch, respectively.

Internal granular skeletal layer relatively thin, continuous with obverse nodes, stylets, peristome and apertural stylets; reverse longitudinal striae and both large and small stylets; across dissepiments and in the middle of zoarial supports. Outer lamellar layer thick, with moderate to pronounced astogenetic thickening, most prevalent toward end of zoarium.

Remarks.—*Exfenestella exigua* was first recognized as *Fenestella* Lonsdale, 1839, by Ulrich (1890) from the Warsaw Beds near Warsaw, Illinois. The exterior appearance of *E. exigua* closely resembles that of *Archimedes wortheni* (Hall, 1857b), with traditional meshwork formula and number of apertural stylets similar in both species. However, *E. exigua* is readily distinguished in interior view by the presence of superior and inferior hemisepta, which are lacking in *A. wortheni*, and by having an asymmetrical parallelogram-shaped to rectangular chamber outline in mid chamber, as opposed to the irregular pentagonal chamber outline in *A. wortheni*.

The relative chamber dimensions in *E. exigua*, particularly with regard to longest chamber dimension, closely resemble those of species of *Banastella*, n. gen., although chamber shape and hemiseptal development is very different between *E. exigua* and species of *Banastella*. Hemiseptal placement in *E. exigua* resembles that in the laxifenestellids, however chamber shapes

and direction of chamber elongation are significantly different.

Placement within the genus *Exfenestella* by Morozova (1974) appears appropriate, although access to her type materials would definitely be desirable. From Morozova's illustrations, the outline of chambers in tangential views and hemiseptal emplacement for *Exfenestella* are the critical criteria used for placement of this species herein.

Material studied.—Twenty-eight exterior fragments, 19 sectioned specimens; largest zoarial fragment 18 × 26 mm (width to length). The thin internal granular skeletal layer, particularly in the lateral walls, results in poor preservation with many fragments being crushed and of little use for internal analysis.

Occurrence.—*Exfenestella exigua* is relatively rare in the Warsaw study area. It is most common in the Valmeyer, St. Louis, and associated localities, and is restricted to Warsaw Beds in the north.

Figures and/or measured specimens.—UI X-6873 (loc. 11, sample 57), 6749, 6898, 6761–6764, 6716, 6810, 6816–6818, 6735, 6736 (loc. 49B, samples 12, 13, 15), 6769, 6768, 6759, 6868, 6942, 7021 (loc. 47A, samples 32, 37).

Genus **BANASTELLA**, new genus

Etymology of name.—Named for Champaign–Urbana, where the work leading to recognition of this genus took place.

Type species.—*Banastella guensburgi*, n. sp.

Diagnosis.—Zoarium ranging from delicate to extremely robust, mesh ranging from close to open; chamber outline irregularly rectangular, parallelogram-shaped to irregularly pentagonal in mid tangential section, chamber size typically large to less commonly intermediate; aperture size large, apertural stylets present in most species; three rows of autozooecia present for prolonged distances proximal to branch bifurcation; chamber reverse-wall budding-angle low, means vary between 22° and 55°. Three-dimensionally reconstructed chamber form a rectangular to parallelogram-shaped box.

Description.—Zoarium robustness ranging from delicate to extremely robust, expansion flat, obversely to reversely curved, slightly sinuous or cupped; mesh spacing variable, ranging from close to open, regular to irregular.

Branch width intermediate to more commonly wide, straight to sinuous in trace with lateral branches broadly curved toward edge of zoarium; branch surface rounded to angular. Keel present, typically single to rarely multiple, width varying from narrow to wide, straight to anastomosing, moderately to greatly increasing with astogeny and frequently covered by lamellar skeleton. Nodes present, emplacement monoserial, size large to intermediate, shape typically stellate to more rarely elliptical, located atop middle of keel, spacing ranging from intermediate to wide. Obverse stylets present or absent, size small to intermediate, occurring across obverse surface, however, most common at keel edge and between nodes. Microstylets present, size small to intermediate. Macrostylets absent. Autozooecia in two rows, third row at sites of branch bifurcation or for moderate to pronounced distances along branch proximal to sites of branch bifurcation. Heterozooecia (ovicells?) present in some species.

Dissepiment width ranging from thin to wide, length varying from short to long, placement regular to variable.

Fenestrule size intermediate to large, shape varying from elliptical, ovate, rectangular, to approaching square.

Aperture size large, shape ovate to more rarely circular, oriented parallel to plane of obverse surface or at slight angle toward fenestrule. Peristome present, complete; apertural stylets either present or absent, when present well-developed, form as extensions of peristomal edge; terminal diaphragms present, positioned at proximal end and throughout zoarium.

Branch shape in cross-section from circular to ovate to elliptical, shallow to thick in depth.

Autozooecial chamber size typically large, less commonly intermediate, chambers biserially emplaced along straight to slightly sinuous axial wall; maximum chamber length parallel to proximal and distal lateral chamber walls in most species, rarely parallel to reverse wall at proximal and curving to become parallel to lateral walls toward distal end of chamber. Chamber outline varying from triangular to irregularly pentagonal to ovate near reverse wall; becoming a parallelogram, irregular rectangle to irregular pentagon in mid chamber and throughout most of chamber depth; irregularly ovate to elliptical near obverse surface. Vestibule present, varying from short to long. Superior hemiseptum typically absent, although short superior hemiseptum present in one species analyzed; present at proximal vestibular edge; inferior hemiseptum absent. Lateral-wall budding-angle means ranging from 16° to 22°; reverse-wall budding-angle means from 22° to 55°. Lamellar skeletal layer varying from thin to thick, exhibiting slight to pronounced astogenetic thickening; granular skeletal layer thin to thick, exhibiting slight astogenetic thickening.

Three-dimensionally reconstructed chamber form an irregular to slightly irregular, rectangular to parallelogram-shaped box, frequently with tubular extension at distal obverse end caused by the vestibule.

Text-figure 12 illustrates zoarial outlines in longitudinal, tangential, and transverse orientations, and three-dimensional chamber reconstructions from ab-

axial branch edge, obverse surface, and distal views.

Remarks.—This genus includes a significant percentage of fenestellid species found in the Warsaw. Its members are typically well-preserved due to their robust nature.

Species of *Banastella* can be separated from other fenestellids by the following combination of characters: frequent presence of well-developed apertural stylets, which fuse during ontogeny to form a peristome; large aperture opening, complete lack of inferior and rare superior hemisepta, typically large to less commonly intermediate autozooecial chamber size, elongate shape parallel to proximal and distal lateral chamber walls, low reverse-wall budding-angle, and typically stellate nodes.

Autozooecial chambers occurring in more than two rows across the branch appear directly related to low chamber budding angles from the reverse wall; such low angles are present in both *Banastella* and *Polypora* McCoy, 1844, the latter being recognized by typically having more than two rows of autozooecia across the branch proximal to sites of branch bifurcation. A possible close phylogenetic connection between *Banastella* and *Polypora* is suggested by the presence of stellate nodes, well-developed apertural stylets, and similar chamber outlines and low reverse-wall budding-angles.

Ulrich (1890) assigned *Polypora biseriata* Ulrich, 1890 to the polyporids based on pronounced external similarities even though *P. biseriata* had two rows of zooecia across the branch, a criterion that should have excluded placement in that genus. Herein. *P. biseriata* is placed in *Banastella* which, as stated above, appears phylogenetically close to *Polypora*. Ulrich's insight into taxonomy of fenestellids, based significantly on exterior analysis of a great volume of material, is impressive even after 100 years.

Species composition.—Six Warsaw species are assigned to this genus: *Banastella guensburgi*, n. sp., *Banastella cingulata* (Ulrich, 1890), *Banastella mediocreforma*, n. sp., *Banastella limitaris* (Ulrich, 1890), *Banastella biseriata* (Ulrich, 1890), and *Banastella delicata*, n. sp.

Range.—Lower Mississippian (Valmeyeran), present in the Keokuk, Warsaw, Salem and St. Louis formations.

Banastella guensburgi, new species
Plates 18, figures 2–9, Plate 19, figures 1–10, Plate 20, figure 1; Text-figure 12; Table 20

Etymology of name.—Named for Tom Guensburg, who assisted greatly in developing techniques for working with these bryozoans.

Diagnosis.—Zoarium extremely robust, mesh spacing close, pattern moderately regular; branches robust, wide, extremely thick in depth; straight to sinuous, broadly curved at lateral zoarial edge; transversely elliptical, spacing moderately close; branches joined at moderately constant intervals by intermediate-width, short dissepiments. Fenestrules large; shape irregularly ovate to more rarely irregularly elliptical, moderately variable. Autozooecial apertures large, shape circular to slightly ovate, surrounded by well-developed, wide, complete peristome formed from fusion of 15 to 25 large stylets regularly positioned around aperture; three to five (most commonly four) apertures per fenestrule. Single wide, continuous keel along middle of obverse branch, atop which are positioned large, stellate, four- to eight-lobed nodes. Autozooecial chambers large, emplaced in two rows, except three rows occurring for pronounced distances proximal to sites of branch bifurcation; outline irregularly pentagonal near reverse wall, rapidly becoming a rectangle to parallelogram in mid and throughout most of chamber length, irregularly ovate near obverse surface, slightly enlarged at distal end. Chamber longest dimension parallel to proximal and distal lateral chamber walls. Aperture at distal and slightly abaxial end of chamber, connected to chamber by long vestibule of variable length. Superior and inferior hemisepta both absent, Lateral-wall budding-angle highly variable (mean of approximately 19°); reverse-wall budding-angle moderately constant (mean of approximately 38°). Enlarged apertural openings, possibly representing ovicells.

Table 20 presents statistical criteria used in delimiting this species.

Exterior description.—Zoarium extremely robust, expansion flat to slightly obversely curved, fan-shaped; mesh spacing close; pronounced astogenetic thickening of both obverse and reverse lamellar skeleton; zoarial pattern moderately regular. Probable mature widths 30 to 45 mm; lengths 30 to 50 mm.

Branches robust; wide, moderately variable in width; straight to slightly sinuous, with inflections toward sites of dissepiment insertion; lateral branches frequently broadly curved toward edge of zoarium. Branch spacing moderately close, distance between adjacent branch centers regular. Obverse surface texture smooth, becoming slightly granular with astogeny; surface rounded; except single wide, extremely well-developed keel; keel continuous, straight to slightly anastomosing, extending along branch midline and causing pronounced positive inflection on obverse surface. With astogeny pronounced thickening of keel occurs; keel forming a ropy expansion across most of obverse surface toward proximal end of zoarium, frequently extending over adaxial edge of aperture; lamellar skeleton covering much of keel with astogeny. Single row of extremely well-developed, large stellate nodes with four to eight pronounced lobes; node size regular, shape moderately variable; nodes projecting from middle of keel; one to

two per fenestrule length; widely, moderately evenly spaced, most commonly located at or near branch–dissepiment junction; with astogeny node diameter increases and nodes frequently become covered by thickened secondary lamellar skeleton of the keel. Intermediate, highly variable size stylets in single row along middle of keel, located between nodes and along abaxial edges of keel. Reverse surface texture highly granular, becoming more coarsely granular with astogeny; bearing an intermediate number of closely spaced longitudinal striae atop which are positioned rows of small, closely spaced, variable-size microstylets. With astogeny longitudinal striae disappear, becoming covered by lamellar skeleton, and microstylets become larger, more unevenly positioned across surface. Autozooecia arranged in two rows, except third row at site of, or three rows occurring for pronounced distances proximal to sites of branch bifurcation; branches with pronounced thickening proximal, thinning distal to sites of branch bifurcation. Enlarged apertural openings, possibly representing ovicells, infrequently occurring at most proximal end of zoarium.

Dissepiments of intermediate width, approximately one-half width of branch, width highly variable; short, variable in length; connect branches at moderately constant intervals. Dissepiments with pronounced medial thinning, flaring at branch–dissepiment contact; slightly recessed from both obverse and reverse surfaces. Moderate to pronounced astogenetic thickening of dissepiments. Obverse dissepiment surface lacking ornamentation; reverse dissepiment surface with longitudinal striae oriented perpendicular to branch length, atop which occur rows of small microstylets; striae covered by lamellar skeleton and microstylet size increasing with astogeny; obverse dissepiment texture smooth, reverse surface highly granular, both coarsening with astogeny. Emplacement of dissepiments approximately perpendicular to branch length. Apertures commonly open on proximal or distal edge, or in middle of dissepiment edge at branch–dissepiment contact; arranged symmetrically or asymmetrically between branches.

Fenestrules large; shape most commonly irregularly ovate to more rarely irregularly elliptical, highly elongate proximodistally; moderately irregular in size and shape; expanding moderately in width and length in obverse–reverse direction. Mean width of fenestrule appreciably less than branch width on obverse surface, approaching equal to branch width on reverse; fenestrule opening decreasing in size toward proximal end of zoarium due to astogenetic thickening of lamellar skeleton. Width to length ratio of fenestrule ranging from 1:3 to 1:5, moderately variable; mean ratio of width to length approximately 1:4; length of fenestrule more constant than width. Three to five (most com-

Table 20.—Summary numerical analysis of *Banastella guensburgi*, n. sp. For explanation of abbreviations of characters (left column), see Table 8b (foldout inside back cover).

	number of measurements	*mean*	*standard deviation*	*coefficient of variation*	*observed range*
1. **WB**	24	0.4568	0.0969	21.02	0.257–0.600
2. **DBC**	24	0.8121	0.1433	17.65	0.563–1.063
3. **WD**	24	0.3145	0.1378	43.82	0.200–0.820
4. **LF**	24	1.2151	0.2227	18.33	0.813–1.625
5. **WF**	24	0.3458	0.0891	25.11	0.200–0.500
6. **AF**	24	4.21	0.59	13.78	3–5
7. **AL**	24	0.1958	0.0087	4.44	0.180–0.210
8. **AW**	24	0.1647	0.0204	12.39	0.120–0.200
9. **ADB**	24	0.4367	0.0523	11.98	0.360–0.560
10. **AAB**	24	0.4188	0.0529	12.63	0.320–0.520
11. **ABB**	24	0.4524	0.0852	18.83	0.343–0.660
12. **DN**	24	0.1929	0.0306	15.86	0.110–0.250
14. **SNB**	24	1.4579	0.2368	16.24	1.050–2.130
15. **WK**	24	0.2133	0.0756	35.44	0.110–0.375
16. **DSO**	24	0.0101	0.0035	34.65	0.006–0.017
17. **SSO**	24	0.1144	0.0438	38.29	0.050–0.200
18. **WP**	24	0.0523	0.0134	25.62	0.036–0.080
19. **SA**	24	18.29	2.44	13.34	15–25
20. **SAD**	24	0.0185	0.0126	68.11	0.007–0.038
22. **RSS**	24	0.0176	0.0045	25.57	0.011–0.028
24. **SSS**	24	0.0412	0.0174	42.23	0.024–0.073
32. **TRW**	24	0.0074	0.0014	18.92	0.005–0.010
33. **TLW**	24	0.0078	0.0014	17.95	0.005–0.010
34. **FWT**	24	0.1296	0.0396	30.56	0.070–0.175
35. **RWT**	24	0.0839	0.0251	29.92	0.050–0.140
36. **CL**	24	0.5890	0.0466	7.91	0.500–0.675
37. **CD**	24	0.2243	0.0185	8.25	0.200–0.250
38. **MAW**	24	0.1743	0.0191	10.96	0.150–0.210
40. **VD**	24	0.1140	0.0280	24.56	0.093–0.158
41. **RA**	24	38.17	3.50	9.16	33–48
42. **LA**	24	18.67	4.44	23.78	9–30
43. **TB**	24	1.0096	0.1667	16.51	0.750–1.380

Text-figure 12.—*Banastella guensburgi* illustrated. 1, diagrammatic longitudinal section showing changing chamber outline from deep section near middle of branch (bottom of figure) to shallow section near abaxial edge of branch (top of figure) [Observe moderately low reverse-wall budding-angle (arrow) characteristic of this genus.], ×70; 2, diagrammatic tangential section showing changing chamber outline from deep section near reverse-wall budding-site (bottom of figure) to shallow section near obverse surface (top of figure) [Apertural stylets are well-developed in this example (arrow).], ×70; 3, diagrammatic transverse section across branch showing typical aperture orientation to obverse surface (arrow), ×70; 4, diagrammatic transverse section illustrating reverse stylet development as an extension of granular skeleton (arrow), ×70; 5, reconstruction of typical chamber shape (three-dimensional) as viewed from abaxial edge of branch [Observe much greater length than width or depth typical of this genus.], ×140; 6, reconstruction of typical chamber shape (three-dimensional) as viewed from obverse surface; chamber reconstructed is from right side of branch, ×140; 7, reconstruction of typical chamber shape (three-dimensional) as viewed from distal end of branch; chamber reconstructed is from right side of branch [Observe slight inflection into vestibule by apertural stylets (arrow).], ×140.

monly four) apertures per fenestrule length; distance between closest aperture centers along, across branch, and across fenestrule all approximately equal; spacing along and across branch slightly more constant than

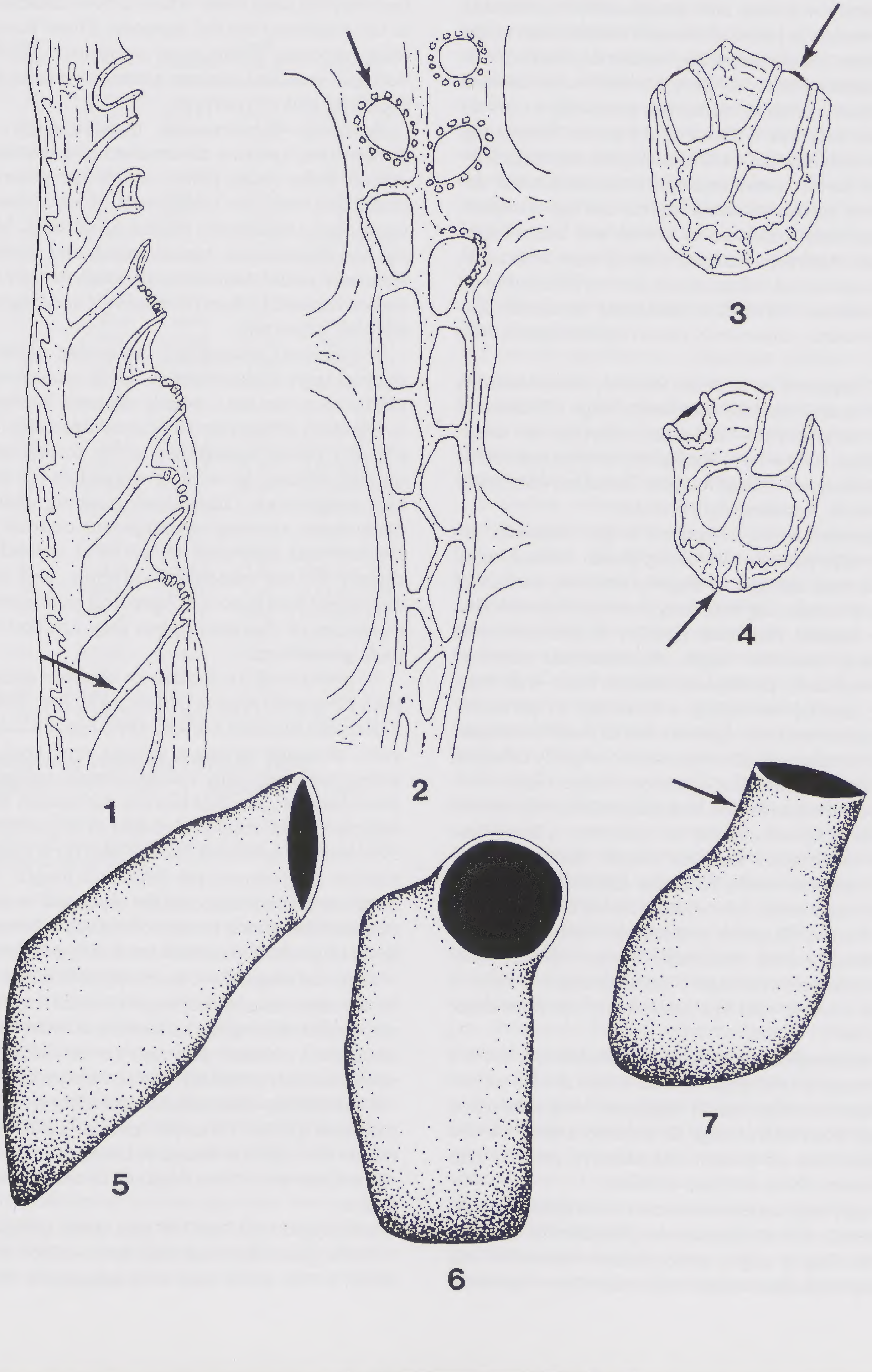

across fenestrule; all moderately constant.

Autozooecial apertures large, shape circular to slightly ovate, elongate proximoabaxially; width to length ratio approximately 4:5, size and shape uniform; opening oriented parallel to plane of obverse surface or at slight angle toward fenestrule; wide, extremely well-developed peristome frequently present, continuous around aperture where present, occurring primarily at proximal end of zoarium. Fifteen to 25 (most commonly 18) large, variable-size, well-developed, and regularly positioned stylets surround aperture; peristome develops from fusion of these stylets during astogeny, with stylets most common at lateral and distal edges of zoarium. Aperture margins extend into fenestrule, causing pronounced inflections in fenestrule outline on obverse surface. Centrally thickened terminal diaphragms present, commonly occurring throughout the zoarium.

Zoarial supports commonly develop as extensions of reverse zoarial surface and lateral edge of zoarium.

Interior description.—Branches elliptical in transverse section, moderately flaring on obverse side, elongate in obverse–reverse direction. Branches extremely thick in depth, moderately variable.

Autozooecial living chambers large, biserially arranged in alternating rows along planar branch axial wall; axial wall straight to slightly sinuous, extending toward and connecting with long chamber lateral walls. Chamber longest direction parallel to proximal and distal lateral chamber walls. Autozooecial chamber outline irregularly pentagonal near reverse-wall budding-site; rapidly becoming a rectangle to parallelogram in middle and throughout most of chamber length, irregularly ovate near obverse surface, slightly enlarged at distal end of chamber; chamber shape highly uniform. Aperture positioned at distal and slightly abaxial end of chamber, connected to chamber by long vestibule of moderately variable length. Ratio of autozooecial chamber width to depth approximately 3:4; depth to length ratio 3:8; width, depth, and length all highly constant. Superior and inferior hemisepta both absent. Autozooecial chambers diverge laterally from middle of branch at a highly variable angle (mean of 19°); from reverse wall at a moderately constant angle (mean of 38°).

Three-dimensionally reconstructed chamber form a slightly irregular rectangular box with tubular extension at distal-obverse end of vestibule; long dimension as viewed from lateral edge of branch; depth, viewed from distal end of branch, moderately greater than width, viewed from obverse surface.

Large apertural stylets connect to inner granular skeletal material; stylets increase in diameter in the vestibule, forming a slight to moderate restriction immediately chamberward from aperture opening. Internal granular skeletal layer moderately thick, well-developed; continuous with obverse nodes, stylets, peristome, and keel; reverse longitudinal striae and microstylets atop these striae; across dissepiments and in the middle of zoarial supports. Outer lamellar layer thick, showing pronounced astogenetic thickening on both obverse and reverse exterior surface, greatest at proximal end of zoarium.

Remarks.—Reverse-wall budding-angle, chamber dimensions, aperture dimensions and spacing, and apertural stylet count (when stylets are present) are all characters with low coefficients of variation and high taxonomic importance within *Banastella*. Mesh spacing and dimensions, branch width and thickness, and stylet and nodal diameters, although usually exhibiting higher variability than reverse-wall budding-angle, *etc.*, are also important.

Pronounced astogenetic thickening of the lamellar skeletal layer is characteristic of *B. guensburgi*, particularly over the keel, which expands to form a ropy overgrowth which partially covers apertures. This gives a highly varied appearance to the zoarial exterior, requiring reliance on interior characters for proper species assignment. Other distinguishing characters include large aperture openings surrounded by highly symmetrical apertural stylets that extend into and slightly fill the middle of vestibule, and large, well-developed lobate nodes. Apertural stylets occur in other species of *Banastella*, but they are best developed in *B. guensburgi*.

B. guensburgi is similar in exterior appearance to both *Fenestella regalis* Ulrich, 1890 [pp. 538–539] and *Fenestella funicula* Ulrich, 1890 [pp. 542–543]. *F. regalis*, although having a similar ropy keel, has much wider branches and coarser mesh pattern than *B. guensburgi*. *F. funicula* has similar branch width, mesh symmetry, and ropy keel to that in *B. guensburgi*, however smaller apertures, lack of apertural stylets, greater number of apertures per fenestrule length, and lack of three rows of autozooecia for moderate to pronounced distances proximal to sites of branch bifurcation readily distinguish *F. funicula* from *B. guensburgi*.

Material studied.—Fourty-eight exterior fragments, 16 sectioned specimens; largest zoarial fragment 27 × 58 mm (width to length). Little skeletal alteration of these colonies is evident, although several sectioned zoaria were crushed, probably due to compacting of mud.

Occurrence.—*Banastella guensburgi* is extremely common at the Valmeyer and St. Louis localities; it ranges through the Warsaw, but is much less common toward the top. It is abundant in both limestones and shales.

Holotype.—UI X-6779 (loc. 49B, sample 12).

Paratypes.—UI X-6748, 6794–6796, 6780, 7016, 6941, 6959– 6966 (loc. 49B, samples 8, 12, 13).

Table 21.—Summary numerical analysis of *Banastella cingulata* (Ulrich, 1890). For explanation of abbreviations of characters (left column), see Table 8b (foldout inside back cover).

	number of measurements	mean	standard deviation	coefficient of variation	observed range
1. **WB**	24	0.3150	0.0744	23.62	0.188–0.456
2. **DBC**	24	0.4820	0.0595	12.34	0.375–0.580
3. **WD**	24	0.2091	0.0417	19.94	0.125–0.288
4. **LF**	24	0.5611	0.0980	17.47	0.356–0.675
5. **WF**	24	0.3061	0.0723	23.62	0.219–0.433
6. **AF**	24	3.00	0.67	22.30	2–4
7. **AL**	24	0.1697	0.0111	6.54	0.148–0.188
8. **AW**	24	0.1484	0.0169	11.39	0.129–0.188
9. **ADB**	24	0.3144	0.0578	18.38	0.260–0.450
10. **AAB**	24	0.2757	0.0379	13.75	0.243–0.320
11. **ABB**	24	0.3228	0.0540	16.73	0.240–0.400
12. **DN**	24	0.0955	0.0288	30.16	0.060–0.163
14. **SNB**	24	0.3812	0.0766	20.09	0.275–0.533
15. **WK**	24	0.0250	0.0087	34.80	0.012–0.043
18. **WP**	24	0.0342	0.0096	28.07	0.021–0.071
19. **SA**	24	21.08	3.42	16.24	16–28
20. **SAD**	24	0.0158	0.0034	2.52	0.012–0.024
22. **RSS**	24	0.0117	0.0025	21.37	0.009–0.018
24. **SSS**	24	0.0541	0.0162	29.94	0.029–0.086
32. **TRW**	24	0.0101	0.0022	21.78	0.006–0.014
33. **TLW**	24	0.0187	0.0078	41.71	0.010–0.034
34. **FWT**	24	0.1242	0.0633	50.97	0.049–0.245
35. **RWT**	24	0.1619	0.0689	42.56	0.069–0.286
36. **CL**	24	0.4894	0.0291	5.95	0.449–0.554
37. **CD**	24	0.2122	0.0171	8.06	0.185–0.243
38. **MAW**	24	0.1475	0.0183	12.41	0.122–0.863
40. **VD**	24	0.1280	0.0413	32.27	0.072–0.214
41. **RA**	24	55.00	4.79	8.70	46–62
42. **LA**	24	15.83	2.97	18.77	10–22
43. **TB**	24	0.5457	0.1282	23.49	0.328–0.715

Banastella cingulata (Ulrich, 1890)
Plate 20, figures 2–10, Plate 21, figures 1–6; Table 21

Fenestella cingulata Ulrich, 1890, p. 543, pl. 52, figs. 1–1d [Keokuk Group: Nauvoo, Illinois; Keokuk, Iowa]; Keyes, 1894, p. 23 [Keokuk Limestone; Keokuk, Iowa].

Diagnosis.—Zoarium robust, mesh spacing intermediate, pattern regular; branches robust, width lower-end intermediate, thick in depth; branches sinuous, lateral branches frequently broadly curved toward zoarial edge; transversely elliptical, spacing close; branches joined at moderately regular intervals by intermediate-width, very short dissepiments. Fenestrule size intermediate; shape ranging from ovate to elliptical, moderately variable. Autozooecial apertures large, shape circular to slightly ovate, surrounded by intermediate-size well-developed, complete peristome formed from fusion of 16 to 28 intermediate-size stylets regularly positioned around aperture; two to four (most commonly three) apertures per fenestrule. Single narrow, intermittent keel along middle of obverse branch, from which project intermediate-size, stellate multilobed nodes. Autozooecial chambers large, emplaced in two rows, except three rows occurring for pronounced distances proximal to sites of branch bifurcation; outline irregularly pentagonal near reverse wall, rapidly becoming irregularly rectangular to more rarely slightly irregularly pentagonal throughout most of chamber, irregularly ovate to elliptical near obverse surface, slightly enlarged at distal end. Chambers elongate parallel to proximal and distal lateral chamber walls. Aperture at distal-abaxial end of chamber, connected to chamber by long vestibule of highly variable length. Superior and inferior hemisepta both absent. Lateral-wall budding-angle highly variable (mean of 16°); reverse-wall budding-angle moderately constant (mean of 55°).

Table 21 presents statistical criteria used in delimiting this species.

Exterior description.—Zoarium robust; expansion curving slightly toward obverse surface, rarely cupped, fan-shaped; mesh spacing intermediate; pronounced astogenetic thickening of obverse and reverse lamellar skeleton; external zoarial pattern regular. Probable mature widths 20 to 25 mm; lengths 20 to 30 mm.

Branches robust; width lower-end intermediate, variable; generally sinuous, exhibiting slight inflections toward sites of dissepiment emplacement, lateral branches frequently broadly curved toward edge of zoarium. Branches closely spaced, distance between adjacent branch centers extremely regular. Obverse surface texture granular; surface moderately angular as a result of close spacing of large apertures; single narrow, poorly developed, intermittent, highly anastomosing keel curving around apertures on obverse branch surface, causing very slight inflection on obverse surface. Keel covered by lamellar skeleton during astogenetic thickening and obverse surface becomes increasingly granular in texture. Nodes monoserially emplaced and well-developed, size intermediate, shape stellate, multilobed, generally elongate proximodistally, highly irregular in size and shape, positioned in slightly anastomosing way along middle of obverse branch surface, projecting from keel and most commonly occurring between two apertural openings across the branch surface; two to three (most commonly two) per fenestrule length, intermediately evenly spaced, node diameter greatly increasing with astogeny. Reverse surface texture moderately granular, coarsening with astogeny; bearing an intermediate number of intermediately spaced longitudinal striae which become covered by lamellar skeleton with astogeny; closely spaced rows of small microstylets positioned atop striae; microstylets increase in diameter and become scattered across reverse zoarial surface with astogeny. Autozooecia arranged in two rows, except three rows frequently occurring for pronounced distances proxi-

mal to sites of branch bifurcation; pronounced thickening of branches proximal, thinning distal to sites of branch bifurcation.

Dissepiments of intermediate width, two-thirds that of branch, width moderately constant; very short, moderately variable in length; connect branches at moderately regular intervals. Pronounced astogenetic thickening of dissepiments. Dissepiments exhibiting pronounced medial thinning, flaring at branch–dissepiment contact; highly recessed from obverse, approximately even with reverse surface. Obverse dissepiment surface lacking ornamentation; reverse surface with rows of poorly developed longitudinal striae oriented perpendicular to branch length, atop which project rows of small stylets; striae covered by lamellar skeleton, stylet diameter increasing as dissepiments thicken during astogeny; both obverse and reverse dissepiment surfaces granular in texture. Emplacement of dissepiments perpendicular or approximately perpendicular to branch length. Apertures commonly open on proximal or distal edge, less frequently in middle of dissepiment at branch–dissepiment contact; arranged symmetrically or asymmetrically between branches.

Fenestrule size intermediate; shape ranging from ovate to elliptical, elongate proximodistally, to rarely approaching square; moderately regular in size, moderately variable in shape; greatly expanding in width and length in obverse–reverse direction. Mean width of fenestrule much less than branch width on obverse surface, approximately equal on reverse; fenestrule opening decreasing in size toward proximal end of zoarium with astogenetic thickening of lamellar skeleton. Width to length ratio of fenestrule ranging from 1:1 to approximately 1:3, variable; mean width to length ratio approximately 1:2; length more constant than width. Two to four (most commonly three) apertures per fenestrule length; distance between closest aperture centers along branch and across branch approximately equal, slightly less than spacing of aperture centers across fenestrule; spacing along branch, across branch, and across fenestrule all moderately variable.

Autozooecial apertures large, shape circular to slightly ovate, elongate proximodistally, width to length ratio approximately 7:8, size uniform, shape moderately uniform; opening oriented parallel to plane of obverse surface; intermediate-size, well-developed peristome present, continuous around aperture at proximal end of zoarium. Sixteen to 28 (most commonly 21) stylets, intermediate in size, well-developed and regularly positioned, surrounding aperture; peristome develops from fusion of these stylets during astogeny, with stylets present at middle and distal edges of zoarium. Aperture margins exhibit pronounced extension into fenestrule, causing pronounced inflections in fenestrule outline on obverse surface. Centrally thickened terminal diaphragms commonly occurring throughout the zoarium.

Large zoarial supports develop as extensions of reverse zoarial surface and lateral edge of zoarium.

Interior description.—Branches elliptical in transverse section, moderately flaring on obverse side, elongate in obverse–reverse direction. Branches thick, variable in depth.

Autozooecial living chambers large, biserially arranged in alternating rows along planar branch axial wall; axial wall straight to slightly sinuous, extending toward and connecting with long chamber lateral walls. Chamber longest direction parallel to proximal and distal lateral chamber walls. Autozooecial chamber outline irregularly pentagonal near reverse-wall budding-site; rapidly becoming irregularly rectangular to more rarely slightly irregularly pentagonal throughout most of chamber depth; irregularly ovate to elliptical near obverse surface, slightly enlarged at distal end of chamber; chamber shape moderately regular. Aperture located at distal-abaxial end of chamber, connected to chamber by long vestibule of highly variable length. Ratio of autozooecial chamber width to depth approximately 7:10; depth to length ratio approximately 4:9; chamber length and depth more constant than width. Superior and inferior hemisepta both absent. Autozoocial chamber diverges laterally from middle of branch at a highly variable angle (mean of 16°); from reverse wall at a moderately constant angle (mean of 55°).

Three-dimensionally reconstructed chamber form an irregular rectangular box, with slight tubular extension of vestibule; long dimension as viewed from lateral edge of branch; depth, viewed from distal end of branch, moderately greater than width, viewed from obverse surface.

Intermediate-size apertural stylets connect to inner granular skeletal material; stylets increase in diameter in the vestibule, forming a slight restriction immediately chamberward from aperture opening. Internal granular skeletal layer extremely thick; continuous with obverse keel, nodes, and apertural stylets; reverse longitudinal striae and stylets; across dissepiments and in the middle of zoarial supports; granular layer exhibiting secondary astogenetic thickening slightly filling chamber. Outer lamellar layer thick, exhibiting pronounced astogenetic thickening on both obverse and reverse exterior surfaces at proximal end of zoarium.

Remarks.—Ulrich (1890, p. 543) described the apertural stylets in *B. cingulata* as "a ring of minute tubules around the zooecial aperture." A longitudinal section through one of the stylets (Pl. 20, figs. 7a, 8b) illustrates the granular skeletal composition and their connection with the internal granular skeleton.

Characters typical of species of *Banastella* include autozooecial chamber shape and great chamber elongation, direction of maximum elongation paralleling lateral chamber walls, apertural stylets and their fusion to form a peristome, stellate nodes, and centrally thickened terminal diaphragms. *B. cingulata* is distinguished from other species of *Banastella* by its closer mesh spacing, moderately high reverse-wall budding-angle compared to other species of this genus, and characteristic autozooecial chamber dimensions.

Material studied.—Twenty-two exterior fragments, five sectioned specimens; largest zoarial fragment 24×28 mm (width to length). The robust nature of the colonies leads to preservation of nearly complete zoaria, although some secondary alteration of microstructure is evident.

Occurrence.—*Banastella cingulata* is moderately common at the Valmeyer and St. Louis localities, and ranges throughout the Warsaw. It is present in both limestone and shale.

Figured and/or measured specimens.—UI X-6719, 6720 (loc. 49B, sample 12), 6747, 7025, 7026 (loc. 47A, sample 37).

Banastella mediocreforma, new species

Plate 22, figures 1–11, Plate 23, figures 1–6; Table 22

Etymology of name.—Named for the moderately indistinct exterior appearance that characterizes this species.

Diagnosis.—Zoarium extremely robust, mesh spacing lower-end intermediate, pattern moderately regular; branches robust, wide, thick, straight to sinuous, transversely circular, spacing lower-end intermediate; branches joined at moderately variable intervals by wide, short dissepiments. Fenestrules large; shape elliptical to more rarely ovate, moderately variable. Autozooecial apertures large, shape ovate, surrounded by well-developed, intermediate-width, complete peristome formed from fusion of nine to 17 small stylets irregularly positioned around aperture; three to four (mean of 3.5) apertures per fenestrule. Single narrow, intermittent keel along middle of obverse branch, atop which are positioned large, stellate, four- to 10-lobed nodes. Autozooecial chambers large, emplaced in two rows, except three rows occurring for pronounced distances proximal to sites of branch bifurcation; outline irregularly pentagonal near reverse wall, rapidly becoming a rectangle to parallelogram in mid and throughout most of chamber, ovate near obverse surface, slightly enlarged at distal end. Chamber elongate parallel to proximal and distal lateral chamber walls. Aperture at distal and slightly abaxial end of chamber, connected to chamber by short vestibule of moderately variable length. Superior and inferior hemisepta both absent. Lateral-wall budding-angle highly variable (mean of 22°); reverse-wall budding-angle slightly variable (mean of 36°).

Table 22 presents statistical criteria used in delimiting this species.

Exterior description.—Zoarium extremely robust, expansion flat to rarely slightly obversely curved, fan-shaped; mesh spacing lower-end intermediate; pronounced astogenetic thickening of both obverse and reverse lamellar skeleton; zoarial pattern moderately irregular. Probable mature widths 20 to 35 mm, lengths 30 to 45 mm.

Branches robust; wide, slightly variable in width; relatively straight, however frequently with slight inflections toward sites of dissepiment insertion. Branch spacing lower-end intermediate, distance between adjacent branch centers extremely regular. Obverse surface texture highly granular, becoming more coarsely granular with astogeny; surface rounded, except single narrow, poorly developed keel; keel intermittent, highly anastomosing, extending along branch midline and causing slight positive inflection on obverse surface. Keel becomes covered by lamellar skeleton with astogeny, completely obscuring keel on obverse surface. Single row of well-developed, large irregularly stellate nodes with four to 10 lobes; nodes elongate proximodistally, size moderately regular, shape highly variable; nodes projecting from keel, one to two per fenestrule length, widely and evenly spaced, commonly opening at or near branch–dissepiment junction; node diameter increases with astogeny, with nodes frequently covered by secondary lamellar skeleton and becoming no longer visible on obverse surface. Small to upper-end small regularly sized stylets variably positioned across obverse surface. Reverse surface texture granular, becoming increasingly granular with astogeny; intermediate number of closely spaced longitudinal striae atop which are positioned rows of intermediately spaced small, variable-size microstylets. With astogeny longitudinal striae disappear and stylets increase in size, becoming more unevenly positioned across surface; striae visible on reverse exterior of zoarium only at most distal end of zoarium. Autozooecia arranged in two rows, except three rows frequently occurring for pronounced distances proximal to sites of branch bifurcation; branches exhibit pronounced thickening proximal, thinning distal to sites of branch bifurcation. Heterozooecia absent in all zoarial fragments analyzed.

Dissepiments wide, width greater than that of branch, moderately variable; length short, moderately variable; connect branches at moderately variable intervals. Dissepiments thin medially, exhibit moderate flaring at branch–dissepiment contact; approximately even with both obverse and reverse surfaces. Pronounced astogenetic thickening of dissepiments. Obverse dissepiment surface lacking ornamentation; re-

verse dissepiment surface with longitudinal striae oriented perpendicular to branch length, atop which occur rows of small stylets; with astogeny striae covered by lamellar skeleton and stylet size increases along with increasingly irregular placement of stylets across reverse surface; both obverse and reverse dissepiment surface textures granular, becoming increasingly granular with astogeny. Emplacement of dissepiments varying from approximately perpendicular to branch length to a slight angle toward fenestrule. Apertures commonly open on proximal or distal edge, or in middle of dissepiment edge at branch–dissepiment contact; arranged symmetrically or asymmetrically between branches.

Fenestrule large; shape primarily elliptical, more rarely irregularly ovate, highly elongate proximodistally; irregular in both size and shape; very slight expansion in width and length in obverse–reverse direction. Mean width of fenestrule approximately five-sixths that of branch; slight decrease in fenestrule opening size toward proximal end of zoarium due to astogenetic thickening of lamellar skeleton. Width to length ratio of fenestrule ranging from 1:3 to 1:2, mean width to length ratio approximately 2:5; equally variable width and length of fenestrule. Three to four (mean of 3.5) apertures per fenestrule length; distance between closest aperture centers along branch and across branch approximately equal, approximately seven-eighths spacing across fenestrule; constancy of spacing along and across branch approximately equal, much more constant than spacing across fenestrule, which is moderately variable.

Autozooecial apertures large, shape ovate, elongate proximoabaxially, width to length ratio approximately 3:4; opening most commonly oriented parallel to plane of obverse surface, more rarely at a slight angle toward fenestrule; peristome width intermediate, well-developed, continuous around aperture where present toward proximal end of zoarium. Nine to 17 (most commonly 13) small, well-developed, and irregularly positioned stylets surround aperture; peristome develops from fusion of these stylets during astogeny, with stylets present at lateral and distal edge of zoarium. Aperture margin exhibiting slight extension into fenestrule, causing slight inflections in fenestrule outline on obverse surface. Apertures covered toward proximal end of zoarium by astogenetically thickened lamellar skeleton.

Large zoarial supports commonly develop as extensions of reverse zoarial surface and lateral edge of zoarium.

Interior description.—Branches a near-perfect to slightly irregular circle in transverse section, moderately flaring on obverse side. Branch thick, moderately regular in depth.

Table 22.—Summary numerical analysis of *Banastella mediocreforma*, n. sp. For explanation of abbreviations of characters (left column), see Table 8b (foldout inside back cover).

	number of measurements	*mean*	*standard deviation*	*coefficient of variation*	*observed range*
1. **WB**	24	0.4543	0.0854	18.80	0.321–0.725
2. **DBC**	24	0.8261	0.0934	11.31	0.670–1.042
3. **WD**	24	0.4711	0.1086	23.05	0.317–0.783
4. **LF**	24	1.0410	0.2274	21.84	0.879–1.296
5. **WF**	24	0.3803	0.0944	24.82	0.246–0.625
6. **AF**	24	3.50	0.51	14.59	3–4
7. **AL**	24	0.2235	0.0081	3.62	0.209–0.240
8. **AW**	24	0.1705	0.0081	4.75	0.152–0.190
9. **ADB**	24	0.3832	0.0340	8.87	0.296–0.463
10. **AAB**	24	0.3758	0.0291	7.74	0.321–0.428
11. **ABB**	24	0.4408	0.0763	17.31	0.283–0.558
12. **DN**	24	0.1446	0.0208	14.38	0.107–0.188
14. **SNB**	24	0.8788	0.2052	23.35	0.438–1.183
15. **WK**	24	0.0365	0.0132	36.16	0.020–0.064
16. **DSO**	24	0.0078	0.0015	19.23	0.005–0.008
17. **SSO**	24	0.0981	0.0284	28.95	0.048–0.138
18. **WP**	24	0.0324	0.0037	11.42	0.027–0.040
19. **SA**	24	12.96	1.83	14.11	9–17
20. **SAD**	24	0.0141	0.0052	36.88	0.005–0.028
22. **RSS**	24	0.0126	0.0026	20.63	0.009–0.018
24. **SSS**	24	0.1209	0.0363	30.02	0.078–0.179
32. **TRW**	24	0.0057	0.0008	14.04	0.004–0.008
33. **TLW**	24	0.0061	0.0009	14.75	0.004–0.008
34. **FWT**	24	0.0937	0.0334	35.65	0.043–0.155
35. **RWT**	24	0.0750	0.0278	37.07	0.028–0.124
36. **CL**	24	0.5574	0.0123	2.21	0.535–0.583
37. **CD**	24	0.2295	0.0210	9.15	0.193–0.265
38. **MAW**	24	0.2083	0.0137	6.58	0.192–0.250
40. **VD**	24	0.0926	0.0183	19.76	0.049–0.138
41. **RA**	24	35.54	5.52	15.54	23–46
42. **LA**	24	21.54	4.32	20.07	14–32
43. **TB**	24	0.4964	0.0566	11.40	0.357–0.566

Autozooecial living chamber large, biserially arranged in alternating rows along planar branch axial wall; axial wall straight, slightly sinuous near reverse wall of chamber, curving toward sites of long lateral-wall emplacement. Chamber longest dimension parallel to proximal and distal lateral chamber walls. Autozooecial chamber outline irregularly pentagonal near reverse-wall budding-site; rapidly becoming a rectangle to parallelogram in the mid and throughout most of chamber; ovate near obverse surface, slightly enlarged at distal end of chamber; chamber shape highly regular. Aperture positioned at distal-abaxial end of chamber, connected to chamber by short vestibule of moderately variable length. Ratio of autozooecial chamber width to depth approximately 9:10; depth to length ratio approximately 2:5; length more constant than width or depth, however all regular. Superior and inferior hemisepta both absent. Autozooecial chamber diverges laterally from middle of branch at highly vari-

able angle (mean of 22°); from reverse wall at a slightly variable angle (mean of 36°).

Three-dimensionally reconstructed chamber form a slightly irregular rectangular box; long dimension as viewed from lateral edge branch; depth, viewed from distal end of branch, slightly greater than width, viewed from obverse surface.

Internal granular layer thickness intermediate; continuous with obverse keel, nodes, stylets, peristome, and apertural stylets; reverse longitudinal striae and microstylets atop these striae; across dissepiment and in the middle of zoarial supports. Outer lamellar layer thick, exhibiting pronounced astogenetic thickening on both obverse and reverse exterior surfaces, most pronounced at proximal end of zoarium.

Remarks.—*Banastella mediocreforma* is distinguished from the closely similar species, *B. limitaris* (Ulrich, 1890), by having lower-end intermediate mesh spacing rather than intermediate spacing, single as compared to multiple keels, autozooecial chamber slightly shorter in length and smaller in volume, fewer apertural stylets, and a smaller reverse-wall budding-angle, one of the lowest for any of the species of *Banastella*. A highly granular zoarial exterior is also highly characteristic of *B. mediocreforma*.

Material studied.—Twenty-eight exterior fragments; four sectioned specimens; largest zoarial fragment 20×25 mm (width to length). The highly robust nature of this species results in the presence of nearly complete colonies that exhibit little secondary skeletal alteration.

Occurrence.—*Banastella mediocreforma* is relatively rare, and is present at the Valmeyer and St. Louis localities. It ranges throughout the Warsaw, and is present in both limestones and shales.

Holotype.—UI X-6717 (loc. 49B, sample 12).

Paratypes.—UI X-6916, 6917, 6746 (loc. 49B, samples 120, 12, 13).

Banastella limitaris (Ulrich, 1890)

Plate 24, figures 1–10, Plate 25, figures 1–8; Table 23

Fenestella limitaris Ulrich, 1890, p. 538, pl. 49, figs. 4, 4a [Keokuk Group: Bentonsport and Keokuk, Iowa]; Keyes, 1894, p. 23 [Keokuk Limestone: Keokuk, Iowa].

Diagnosis.—Zoarium robustness intermediate, mesh spacing intermediate, pattern regular; branches moderately robust, wide, depth thick; straight to sinuous, frequently broadly curved at lateral zoarial edge; transversely irregularly ovate to elliptical, spacing close; branches joined at regular intervals by lower-end intermediate width, short to lower-end intermediate length dissepiments. Fenestrules large; shape elliptical to ovate, variable. Autozooecial apertures large, shape ovate, elongate proximoabaxially; surrounded by well-developed, intermediate-width, complete peristome formed from fusion of 16 to 26 small stylets regularly positioned around aperture; three to four (mean of 3.67) apertures per fenestrule. Single to multiple intermediate-width intermittent keel(s), straight to anastomosing around autozooecial apertures along middle of obverse branch, atop which are positioned large, stellate nodes. Autozooecial chambers large, emplaced in two rows, except third row at sites of branch bifurcaion or three rows for pronounced distances proximal to sites of branch bifurcation; outline irregularly ovate to rounded triangle near reverse wall, rapidly becoming irregularly pentagonal immediately obverse from reverse wall, a rectangle to parallelogram throughout mid and most of chamber length, elliptical to ovate near obverse surface, slightly enlarged at distal end of chamber. Chamber longest dimension parallel to proximal and distal lateral chamber walls. Aperture at distal-abaxial end of chamber, connected to chamber by long vestibule of variable length. Superior and inferior hemisepta both absent. Lateral-wall budding-angle variable (mean of 21°); reverse-wall budding-angle constant (mean of 47°).

Table 23 presents statistical criteria used in delimiting this species.

Exterior description.—Zoarium robustness intermediate, expansion flat, flaring at distal end, fan-shaped; mesh spacing intermediate; slight to moderate astogenetic thickening of both obverse and reverse lamellar skeleton; zoarial pattern regular. Probable mature widths 40 to 50 mm; lengths 30 to 45 mm.

Branches moderately robust; wide, slightly variable in width; ranging from straight to sinuous, with inflections toward sites of dissepiment insertion; lateral branches frequently broadly curved toward edge of zoarium. Branch spacing close, distance between adjacent branch centers moderately regular. Obverse surface texture slightly granular; surface profile angular with single to multiple intermediate-width, well-developed keel(s); keel(s) intermittent, varying from straight to moderately anastomosing, curving around autozooecial apertures; keel(s) extending along branch midline, causing moderate positive inflection(s) on obverse surface. Slight thickening of keel(s) occurring with astogeny, due to covering of keel(s) by lamellar skeleton; near proximal end of zoarium partially covering adaxial edge of aperture. Single row of extremely well-developed, large elliptical to slightly stellate, proximodistally elongate nodes; node size moderately regular, shape variable; nodes projecting from middle of keel; most commonly one, rarely two nodes per fenestrule length, widely, evenly spaced, most frequently located at or near branch–dissepiment junction; node diameter increases with astogeny. Extremely small stylets in rows along middle of keel(s) positioned between nodes. Reverse surface texture highly granular, becom-

ing more coarsely granular with astogeny; bearing an intermediate number of closely spaced longitudinal striae atop which are positioned rows of intermediate-size, closely spaced, variable microstylets. With astogeny longitudinal striae disappear and microstylets become larger, more scattered across surface. Autozooecia arranged in two rows, except third row at site of branch bifurcation or three rows extending for pronounced distances proximal to branch bifurcation; branches exhibiting pronounced thickening proximal, thinning distal to sites of branch bifurcation. Enlarged apertural openings, possibly representing ovicells, infrequently occurring at most proximal end of zoarium.

Dissepiments of lower-end intermediate width, approximately three-fifths branch width, width highly variable; short to lower-end intermediate in length, moderately constant; connect branches at regular intervals. Dissepiments exhibit pronounced medial thinning, flaring at branch–dissepiment contact; moderately recessed from obverse, approximately even with reverse surface. Slight to moderate astogenetic thickening of dissepiments. Obverse dissepiment surface with two to five barlike longitudinal striae located across dissepiment surface, oriented perpendicular to branch length, extremely small stylets positioned atop striae; reverse dissepiment surface with less pronounced longitudinal striae across dissepiment surface, oriented perpendicular to branch length, small to intermediate-size microstylets project from these striae; with astogeny reverse striae disappear, microstylets become larger, more scattered across dissepiment surface; obverse dissepiment texture slightly granular, reverse surface highly granular. Emplacement of dissepiments most commonly at a slight angle from perpendicular to branch length, more rarely emplaced perpendicular thereto. Apertures commonly open on proximal or distal edge, or in middle of dissepiment at branch–dissepiment contact; predominantly arranged symmetrically, less commonly arranged asymmetrically between branches.

Fenestrules large; shape elliptical to ovate, elongate proximodistally; moderately regular in size, variable in shape; expanding slightly in width and length in obverse–reverse direction. Mean width of fenestrule approximately equal to branch width on obverse, slightly greater on reverse surface; very slight decrease in size of fenestrule opening toward proximal end of zoarium due to astogenetic thickening of lamellar skeleton. Ratio of mean fenestrule width to length approximately 1:3, moderately constant; length of fenestrule more constant than width. Three to four (mean of 3.67) apertures per fenestrule length; distance between closest aperture centers across branch nine-tenths of that along branch; aperture center spacing along branch four-fifths of that across fenestrule; spacing along and across branch and across fenestrule all variable.

Table 23.—Summary numerical analysis of *Banastella limitaris* (Ulrich, 1890). For explanation of abbreviations of characters (left column), see Table 8b (foldout inside back cover).

	number of measurements	*mean*	*standard deviation*	*coefficient of variation*	*observed range*
1. **WB**	24	0.4851	0.0854	17.60	0.369–0.619
2. **DBC**	24	0.7810	0.1248	15.98	0.581–1.038
3. **WD**	24	0.2898	0.0749	25.86	0.213–0.456
4. **LF**	24	1.2220	0.1598	13.08	0.981–1.500
5. **WF**	24	0.4420	0.0851	19.25	0.350–0.625
6. **AF**	24	3.67	0.49	13.43	3–4
7. **AL**	24	0.2040	0.0184	9.02	0.178–0.240
8. **AW**	24	0.1615	0.0192	11.89	0.135–0.193
9. **ADB**	24	0.3979	0.0668	16.79	0.331–0.550
10. **AAB**	24	0.3653	0.0496	13.58	0.265–0.455
11. **ABB**	24	0.4908	0.1009	20.56	0.350–0.700
12. **DN**	24	0.1338	0.0297	22.20	0.098–0.170
14. **SNB**	24	1.3820	0.2100	15.20	1.100–1.825
15. **WK**	24	0.0745	0.0248	33.29	0.043–0.130
16. **DSO**	24	0.0145	0.0035	24.14	0.011–0.031
17. **SSO**	24	0.0348	0.0110	31.61	0.029–0.086
18. **WP**	24	0.0254	0.0045	17.72	0.018–0.033
19. **SA**	24	20.25	2.90	14.30	16–26
20. **SAD**	24	0.0162	0.0032	19.75	0.013–0.023
22. **RSS**	24	0.0182	0.0050	27.47	0.011–0.031
24. **SSS**	24	0.0515	0.0131	25.44	0.030–0.075
32. **TRW**	24	0.0129	0.0033	25.58	0.008–0.020
33. **TLW**	24	0.0188	0.0038	20.21	0.012–0.025
34. **FWT**	24	0.0960	0.0305	31.77	0.037–0.147
35. **RWT**	24	0.0984	0.0491	49.90	0.023–0.180
36. **CL**	24	0.6915	0.0377	5.45	0.600–0.750
37. **CD**	24	0.1950	0.0187	9.59	0.160–0.225
38. **MAW**	24	0.2055	0.0253	12.31	0.175–0.250
40. **VD**	24	0.1236	0.0304	24.60	0.074–0.181
41. **RA**	24	47.15	4.04	8.56	40–54
42. **LA**	24	21.17	3.59	16.95	15–28
43. **TB**	24	0.5603	0.0883	15.76	0.425–0.718

Autozooecial apertures large, shape ovate, elongate proximoabaxially, width to length ratio 4:5, shape moderately uniform; opening oriented parallel to plane of obverse surface, more rarely at slight angle toward fenestrule; intermediate-width, well-developed peristome present, complete, continuous around aperture, best developed toward proximal end of zoarium. Sixteen to 26 (most commonly 20) small, variable-size stylets, well-developed and regularly positioned around aperture; peristome develops from fusion of these stylets during astogeny, with stylets most common at lateral and distal edges of zoarium. Slight to moderate extension of aperture margin into fenestrule, causing inflections in fenestrule outline on obverse surface. Centrally thickened terminal diaphragm rarely present, capping apertural openings in late astogeny toward proximal end of zoarium.

Zoarial supports occurring infrequently, develop as extensions of reverse zoarial surface and from lateral edge of zoarium.

Interior description.—Branches irregularly ovate to irregularly elliptical in transverse section, most commonly flaring on obverse surface, elongate either in obverse–reverse direction or parallel to zoarial surface; branches thick, moderately variable in depth.

Autozooecial living chambers large, biserially arranged in alternating rows along planar branch axial wall; axial wall highly sinuous near reverse wall, curving toward sites of lateral wall emplacment connecting with intermediate-length lateral walls, becoming straight toward obverse surface. Chamber longest dimension parallel to proximal and distal lateral chamber walls. Autozooecial chamber outline irregularly ovate to rounded triangular near reverse-wall budding-site; rapidly becoming irregularly pentagonal immediately toward obverse surface from reverse wall; becoming a rectangle to parallelogram through mid chamber and most of chamber length; elliptical to ovate, slightly enlarged at distal end of chamber near obverse surface; chamber shape moderately regular. Aperture positioned at distal-abaxial end of chamber, connected to chamber by long, well-developed vestibule of variable length. Autozooecial chamber width approximately equal to depth; depth to length ratio approximately 3:10; length more constant than depth or width, all moderately constant. Superior and inferior hemisepta both absent. Autozooecial chambers diverge laterally from middle of branch at variable angle (mean of 21°); from reverse wall at a constant angle (mean of 47°).

Three-dimensionally reconstructed chamber form an irregular rectangular or parallelogram-shaped box; long dimension as viewed from lateral edge of branch; approximately equidimensional in depth and width, as viewed from the distal end of branch and obverse surface, respectively.

Internal granular layer thick, well-developed; continuous with obverse nodes, stylets, keel, apertural stylets, and peristome; reverse longitudinal striae and microstylets atop these striae; across dissepiments and in the middle of zoarial supports. Outer lamellar layer of intermediate thickness, exhibiting slight astogenetic thickening on both obverse and reverse exterior zoarial surfaces.

Remarks.—The intermittent, "faint" nature of the keel was observed by Ulrich (1890, p. 538), and is moderately characteristic of *B. limitaris*. Ulrich compared this species to *Fenestella rudis* (Ulrich, 1890), indicating the two species to be phylogenetically closely related. Interior analysis indicates pronounced differences in chamber shape between these two species, with *B. limitaris* having a much larger chamber that is elongate parallel to chamber lateral walls and *C. rudis* having a smaller chamber elongate parallel to the reverse wall.

Many characteristics are common to *B. limitaris* and the other species of the genus, *B. guensburgi*, n. sp., *B. cingulata* (Ulrich, 1890), and *B. mediocreforma*, n. sp. These include fusion of apertural stylets to form the peristome, autozooecial chamber shape and placement, and nodal development. Such similarities indicate probable close phylogenetic association among these species.

B. limitaris is distinguished from the closest other species of *Banastella*, *B. mediocreforma*, by a slightly longer autozooecial chamber, multiple rather than single keel, greater reverse-wall chamber budding-angle, and greater number of apertural stylets.

Exquisite preservation of specimens of this species makes them some of the most visually elegant to be found in the Warsaw.

Material studied.—Twelve exterior fragments; three sectioned specimens; largest zoarial fragment 28 × 30 mm (width to length). The robust nature of this species results in its frequent excellent preservation.

Occurrence.—*Banastella limitaris* is restricted to the Upper Keokuk and Lower Warsaw in the northern part of the study area near Warsaw, Illinois and Keokuk, Iowa; it ranges as far south as Mt. Sterling, Illinois. It is rare, found most frequently in shaly facies.

Lectotype of F. limitaris (*herein designated*)—ISGS (ISM) 2770.

Hypotypes.—UI X-7015, 7027 (loc. 10, sample 31).

Banastella biseriata (Ulrich, 1890)

Plate 26, figures 1–10, Plate 27, figure 1; Table 24

Polypora biseriata Ulrich, 1890, p. 592, pl. 60, figs. 4–4b [Warsaw Beds: Monroe County, Illinois; Warsaw, Illinois. ?St. Louis Limestone: ?Barrett's Station, Missouri]; Keyes, 1894, p. 2a [St. Louis Limestone: Barrett's Station, Missouri]; Trizna, 1958, p. 166, pl. 46, figs. 2–4.

Diagnosis.—Zoarium robustness intermediate, mesh spacing close, pattern moderately regular; branches moderately robust, depth thin, wide; branches straight to broadly curved at lateral zoarial edge; transversely circular to ovate, spacing close; branches joined at fairly regular intervals by thin, short dissepiments. Fenestrule size intermediate, shape irregularly elliptical to rarely irregularly ovate, fairly regular. Autozooecial apertures large, shape ovate, surrounded by intermediate-width, well-developed complete peristome; two to four (most commonly three) apertures per fenestrule. Single intermediate-width intermittent keel anastomosing along branch midline and curving around apertures; lower-end intermediate size slightly stellate nodes positioned atop keel. Autozooecial chamber size intermediate, chambers emplaced in two rows, except three rows occurring for moderately to extremely pronounced distances proximal to sites of branch bifurcation; outline irregularly triangular to pentagonal near reverse wall, rapidly becoming an irregular rectangle to parallelogram in mid and throughout most of cham-

ber length, irregularly ovate to elliptical near obverse surface, slightly enlarged at distal end. Chamber longest dimension parallel to proximal and distal lateral chamber walls. Aperture positioned at distal or distal-abaxial end of chamber, connected to chamber by short vestibule of variable length. Short superior hemiseptum present; inferior hemiseptum absent. Lateral-wall budding-angle variable (mean of 22°); reverse-wall budding-angle constant (mean of 39°).

Table 24 presents statistical criteria used in delimiting this species.

Exterior description.—Zoarium robustness intermediate, expansion most commonly flat, less frequently obversely or reversely curved, fan-shaped; mesh spacing close; slight astogenetic thickening of both obverse and reverse lamellar skeleton; zoarial pattern moderately regular. Probable mature widths 18 to 25 mm; lengths 30 to 40 mm.

Branches moderately robust; wide, highly variable in width; straight, except lateral branches broadly curved toward edge of zoarium. Branch spacing close, distance between adjacent branch centers moderately regular. Obverse surface texture smooth; surface rounded except single intermediate-width, poorly developed keel; keel intermittent, anastomosing, extending along branch midline and curving around autozooecial apertures, causing slight positive inflection in obverse surface profile. Keel covered during astogenetic thickening of lamellar skeleton, exhibiting slight increase in width; obverse branch surface becoming slightly granular with astogeny. Single row of well-developed, lower-end intermediate size, slightly stellate nodes; node size and shape regular; nodes anastomosing, project from middle of keel; two to four per fenestrule length, most commonly one per pair of apertures across branch, intermediately unevenly spaced; with astogeny, node diameter increases and nodes frequently become covered by thickened secondary lamellar skeleton of keel. Reverse surface texture moderately smooth, becoming slightly granular with astogeny; bearing numerous rows of closely spaced longitudinal striae atop which are positioned rows of small, closely spaced, variable-size microstylets. With astogeny striae become more pronounced and microstylet diameters increase. Autozooecia arranged in two rows, except three rows frequently occurring for moderate to extremely pronounced distances proximal to sites of branch bifurcation; branches exhibit pronounced thickening proximal, thinning distal to sites of branch bifurcation. Heterozooecia not found in any zoaria analyzed.

Dissepiments of thin width, slightly less than half branch width, width moderately variable; short, moderately variable in length; connect branches at fairly regular intervals. Dissepiments thin medially, flaring

Table 24.—Summary numerical analysis of *Banastella biseriata* (Ulrich, 1890). For explanation of abbreviations of characters (left column), see Table 8b (foldout inside back cover).

	number of measurements	*mean*	*standard deviation*	*coefficient of variation*	*observed range*
1. **WB**	24	0.4823	0.1293	26.81	0.300–0.738
2. **DBC**	24	0.6859	0.1033	15.06	0.525–0.880
3. **WD**	24	0.2128	0.0489	22.98	0.144–0.312
4. **LF**	24	0.7468	0.0874	11.70	0.575–0.831
5. **WF**	24	0.2644	0.0638	24.13	0.175–0.356
6. **AF**	24	3.00	0.60	20.10	2–4
7. **AL**	24	0.1610	0.0093	5.78	0.144–0.178
8. **AW**	24	0.1338	0.0136	10.32	0.116–0.156
9. **ADB**	24	0.3239	0.0439	13.55	0.264–0.390
10. **AAB**	24	0.2923	0.0281	9.61	0.234–0.328
11. **ABB**	24	0.3869	0.0737	19.05	0.238–0.500
12. **DN**	24	0.0729	0.0082	11.25	0.058–0.088
14. **SNB**	24	0.3494	0.0944	27.02	0.148–0.508
15. **WK**	24	0.0617	0.0091	14.75	0.048–0.080
18. **WP**	24	0.0435	0.0068	15.63	0.034–0.056
22. **RSS**	24	0.0099	0.0021	21.21	0.007–0.014
32. **TRW**	24	0.0103	0.0016	15.53	0.008–0.014
33. **TLW**	24	0.0093	0.0018	19.35	0.007–0.012
34. **FWT**	24	0.0396	0.0214	54.04	0.018–0.086
35. **RWT**	24	0.0302	0.0166	54.97	0.011–0.061
36. **CL**	24	0.3293	0.0102	3.10	0.311–0.347
37. **CD**	24	0.2102	0.0136	16.47	0.189–0.235
38. **MAW**	24	0.1604	0.0120	7.18	0.139–0.187
40. **VD**	24	0.0615	0.0132	21.46	0.042–0.094
41. **RA**	24	39.0	3.01	7.73	34–44
42. **LA**	24	22.00	3.77	16.90	14–27
43. **TB**	24	0.2917	0.0614	21.05	0.204–0.395

at branch–dissepiment contact; both obverse and reverse dissepiment surfaces recessed from respective branch surfaces. Slight astogenetic thickening of dissepiments. Obverse dissepiment surface with one to four rows of longitudinal striae oriented perpendicular to branch length; reverse dissepiment surface with numerous rows of longitudinal striae oriented perpendicular to branch length, atop which occur small microstylets similar in all respects to those found on branch reverse surface; both obverse and reverse dissepiment surfaces smooth, becoming slightly granular with astogeny. Emplacement of dissepiments approximately perpendicular to branch length. Apertures open on proximal or distal edge, or in middle of dissepiment edge at branch–dissepiment contact; most commonly arranged asymmetrically between branches, more rarely arranged symmetrically.

Fenestrule size intermediate; shape irregularly elliptical to rarely irregularly ovate, moderately elongate proximodistally; size and shape both fairly regular; expanding in width and length in obverse–reverse direction. Mean width of fenestrule slightly greater than half branch width on obverse surface, slightly greater than half branch width on reverse; fenestrule opening de-

creasing in size toward proximal end of zoarium due to astogenetic thickening of lamellar skeleton. Mean width to length ratio approximately 1:3. Two to four (most commonly three) apertures per fenestrule length; distance between closest aperture centers along branch slightly greater than across branch, ratio approximately 10:9, spacing across branch appreciably less than that across fenestrule, ratio of approximately 7:10; spacing along and across branch fairly constant, much more regular than spacing across fenestrule, which is highly variable.

Autozooecial apertures large; shape ovate, elongate proximodistally to proximoabaxially, width to length ratio approximately 4:5, size and shape highly uniform; opening most commonly oriented parallel to plane of obverse surface, less frequently at slight angle toward fenestrule; intermediate-width, well-developed complete peristome present; peristome width increasing with astogeny toward proximal end of zoarium. Aperture margin extends into fenestrule, causing pronounced inflection in fenestrule outline on obverse surface. Centrally thickened terminal diaphragms present, occurring toward proximal end of zoarium.

Zoarial supports rare, develop as extensions of reverse zoarial surface.

Interior description.—Branches circular to ovate in transverse section, slightly flaring on obverse side, elongate parallel to zoarial surface. Branches shallow, moderately variable in depth.

Autozooecial living chamber size intermediate, chambers biserially arranged in alternating rows along planar branch axial wall; axial wall exhibiting pronounced inflections toward and connecting with intermediate-length lateral walls near reverse wall, becoming straight in mid and shallow tangential sections. Chamber maximum dimension parallel to proximal and distal lateral chamber walls. Autozooecial chamber outline irregularly triangular to pentagonal near reverse-wall budding-site; rapidly becoming an irregular rectangle to parallelogram in middle and throughout most of chamber length; irregularly ovate to elliptical near obverse surface, with slightly enlarged distal end of chamber; chamber shape highly regular. Aperture positioned at distal or distal-abaxial end of chamber, connected to chamber by short vestibule of variable length. Ratio of autozooecial chamber width to depth approximately 3:4; depth to length ratio approximately 5:8; length slightly more constant than width or depth, all dimensions highly constant. Short superior hemiseptum present at proximal apertural edge; inferior hemiseptum absent. Autozooecial chamber diverges laterally from middle of branch at a variable angle (mean of 22°); from reverse wall at constant angle (mean of 39°).

Three-dimensionally reconstructed chamber form an irregular rectangular box, long dimension as viewed from lateral edge of branch; depth, viewed from distal end of branch, slightly greater than width, viewed from obverse surface.

Internal granular skeletal layer thin, continuous with obverse nodes, keel, and peristome; reverse longitudinal striae and microstylets atop these striae; across dissepiments and in the middle of zoarial supports. Outer lamellar skeleton thin, exhibiting slight astogenetic thickening.

Remarks.—This species was originally assigned to *Polypora* McCoy, 1844 by Ulrich (1890, p. 592) based on the presence of three rows of autozooecia "at a point 2 or 3 mm below branch divisions," and appearance similar to that of *P. varsoviensis* Prout, 1858a, although the latter species typically has "one row of cells more to the branch, and larger fenestrules." (Ulrich, 1890, p. 593) Ulrich's inclusion in *Polypora* of a species that has two rows of autozooecia across the branch — traditionally the standard criterion for placement in the fenestellids — seems to indicate that Ulrich was aware of the problem of number of apertural rows in fenestellid taxonomy.

Banastella, a genus exhibiting characters of both the traditional fenestellids (*i.e.*, two rows of autozooecia across branch) and polyporids (*i.e.*, long autozooecial chambers having small reverse-wall budding-angles and three rows of autozooecia proximal to branch bifurcation), apparently lies between *Fenestella* Lonsdale, 1839 and *Polypora*.

Banastella biseriata is herein assigned to *Banastella* because of chamber shape, low reverse-wall budding-angle, large aperture size, and presence of two rows of autozooecia along branch with three rows present for moderate to prolonged distances proximal to sites of branch bifurcation. Separation of *B. biseriata* from other species of the genus is based on smaller chamber size, close mesh spacing, and lack of apertural stylets.

Material studied.—Eighteen exterior fragments, three sectioned specimens; largest zoarial fragment 8 × 23 mm (width to length). Little secondary skeletal alteration of this species is evident. The thin nature of the internal granular skeleton results in frequent mechanical crushing of this species, particularly common in shales.

Occurrence.—*Banastella biseriata* is rare, and is restricted to the Lower Warsaw in the southern portion of the outcrop area near St. Louis, Missouri, and Valmeyer, Illinois.

Syntypes.—ISGS(ISM) 2805 (10 fragments).

Figured and/or measured specimens.—UI X-6742, 6743, 6915 (loc. 11, sample 55).

Banastella delicata, new species

Plate 27, figures 2–10, Plate 28, figures 1–5; Table 25

Etymology of name.—Named for the characteristic delicate growth habit.

Diagnosis.—Zoarium delicate, mesh spacing highly open, pattern highly irregular; branches moderately delicate, width intermediate, thickness medium; straight, sharply curved to broadly curved at zoarial edge in trace; transversely circular, spacing wide; branches joined at moderately variable intervals by thin, long dissepiments. Fenestrules extremely large; shape regularly to irregularly rectangular, variable. Autozooecial apertures large, shape ovate to rarely circular, surrounded by thin, well-developed complete peristome formed from fusion of 13 to 17 small stylets regularly positioned around aperture; five to nine (most commonly seven) apertures per fenestrule. Single intermediate-width continuous keel along middle of obverse branch, atop which are positioned large irregularly stellate nodes. Autozooecial chambers large, emplaced in two rows, except third row at sites of branch bifurcation; outline irregularly pentagonal near reverse wall, rapidly becoming an irregular rectangle to parallelogram in mid and throughout most of chamber, irregularly elliptical near obverse surface, slightly enlarged at distal end. Chamber longest dimension paralleling proximodistal direction for proximal two-thirds of chamber, most distal third of chamber paralleling proximal and distal chamber lateral walls. Aperture at distal and slightly abaxial end of chamber, connected to chamber by short vestibule of variable length. Short superior hemiseptum present; inferior hemiseptum absent. Lateral-wall budding-angle highly variable (mean of 21°); reverse-wall budding-angle variable (mean of 22°).

Table 25 presents statistical criteria used in delimiting this species.

Exterior description.—Zoarium delicate, expansion flat to slightly sinuous, lateral branches broadly curved toward edge of zoarium, fan-shaped; mesh highly open; slight astogenetic thickening of both obverse and reverse lamellar skeleton; zoarial pattern highly irregular. Probable mature widths 20 to 40 mm, lengths 30 to 60 mm.

Branches moderately delicate; width intermediate, moderately consistent; straight or slightly curved, sharply curved distal to sites of branch bifurcation, lateral branches commonly broadly curved toward edge of zoarium. Branch spacing wide, distance between adjacent branch centers moderately regular. Obverse surface texture smooth, becoming slightly granular with astogeny; surface well rounded, except for single intermediate-width, extremely well-developed keel; keel continuous, straight to slightly anastomosing, curving around autozooecial apertures, extending along branch midline and causing slight positive inflection on obverse surface. Keel thickens slightly with astogeny due to partial covering by lamellar skeleton, most common toward proximal end of zoarium. Single row of intermediately developed, large, irregularly stellate nodes present; size and shape fairly regular; nodes project from middle of keel; one to two per fenestrule length, widely, moderately evenly spaced, most frequently located at or near branch–dissepiment junction; with astogeny, node diameters exhibit slight increase due to partial covering by lamellar skeleton. Small, variable-size stylets positioned along obverse branch surface, most commonly occurring atop or on lateral edge of keel. Reverse surface texture finely granular, coarsening with astogeny; bearing numerous rows of closely spaced longitudinal striae atop which are positioned rows of very small, closely spaced, variable-size microstylets. With astogeny, longitudinal striae become covered by lamellar skeleton and disappear, microstylets increase in size, become unevenly positioned

Table 25.—Summary numerical analysis of *Banastella delicata*, n. sp. For explanation of abbreviations of characters (left column), see Table 8b (foldout inside back cover).

	number of measurements	*mean*	*standard deviation*	*coefficient of variation*	*observed range*
1. **WB**	24	0.3411	0.0480	14.07	0.250–0.438
2. **DBC**	24	0.9005	0.1567	17.40	0.625–1.213
3. **WD**	24	0.1452	0.0259	17.84	0.105–0.200
4. **LF**	24	1.8116	0.2578	14.23	1.375–2.225
5. **WF**	24	0.5155	0.1308	25.37	0.325–0.750
6. **AF**	24	6.96	1.16	16.67	5–9
7. **AL**	24	0.1982	0.0232	11.71	0.165–0.225
8. **AW**	24	0.1578	0.0153	9.70	0.130–0.195
9. **ADB**	24	0.4364	0.00352	8.07	0.388–0.525
10. **AAB**	24	0.3468	0.0270	7.79	0.300–0.400
11. **ABB**	24	0.5813	0.1051	18.08	0.231–0.919
12. **DN**	24	0.1555	0.0374	24.05	0.100–0.250
13. **DND**	24	0.0228	0.0064	27.93	0.013–0.031
14. **SNB**	24	1.1900	0.2009	16.88	0.813–1.625
15. **WK**	24	0.0583	0.0152	26.07	0.038–0.084
16. **DSO**	24	0.0092	0.0027	29.35	0.005–0.014
17. **SSO**	24	0.1055	0.0246	13.32	0.071–0.152
18. **WP**	24	0.0156	0.0045	28.85	0.010–0.025
19. **SA**	24	15.21	0.97	6.41	13–17
20. **SAD**	24	0.0107	0.0039	36.45	0.004–0.019
22. **RSS**	24	0.0150	0.0043	28.67	0.011–0.028
24. **SSS**	24	0.0314	0.0125	39.81	0.020–0.069
32. **TRW**	24	0.0045	0.0008	17.78	0.004–0.006
33. **TLW**	24	0.0047	0.0009	19.15	0.004–0.006
34. **FWT**	24	0.0073	0.0217	38.07	0.050–0.114
35. **RWT**	24	0.0602	0.0201	33.39	0.023–0.089
36. **CL**	24	0.6389	0.0351	5.49	0.595–0.720
37. **CD**	24	0.1699	0.0230	13.54	0.138–0.225
38. **MAW**	24	0.1544	0.0162	10.49	0.130–0.200
40. **VD**	24	0.0607	0.0103	16.97	0.040–0.075
41. **RA**	24	22.25	3.57	16.05	18–30
42. **LA**	24	20.92	4.44	21.23	12–27
43. **TB**	24	0.3564	0.0563	15.80	0.257–0.436

across branch surface. Autozooecia arranged in two rows, except third row at sites of branch bifurcation where middle autozooecium is evidently shared by both branches; branches with little or no thickening proximal or thinning distal to sites of branch bifurcation. Heterozooecia not present on any zoarial fragments observed.

Dissepiments of thin width, approximately two-fifths width of branch, width fairly regular; long, variable in length; connect branches at moderately variable intervals. Dissepiments barlike, exhibit slight flaring at branch–dissepiment contact; slightly recessed from both obverse and reverse surfaces. Little or slight astogenetic thickening of dissepiment. Obverse dissepiment surface with one to three longitudinal striae across dissepiment perpendicular to direction of branch length; median ridge pronounced, forming elongate node-like projection along entire dissepiment length, continuous with peristome or apertural stylets where aperture occurs at middle edge of dissepiment; reverse dissepiment surface with longitudinal striae oriented perpendicular to branch length, atop which occur rows of small microstylets; striae covered by lamellar skeleton and microstylets increase in size with astogeny; obverse dissepiment surface texturally smooth, reverse texture finely granular, coarsening with astogeny. Emplacement of dissepiments oriented approximately perpendicular to branch length, although deviation from perpendicular by angles of up to 15° is observed. Apertures open on proximal or distal edge or in middle of dissepiment edge at branch–dissepiment contact; arranged symmetrically or asymmetrically between branches.

Fenestrules extremely large; shape regularly to irregularly rectangular, highly elongate proximodistally, regular in length, variable in width; variable in shape; exhibiting little or no expansion in width or length in obverse–reverse direction. Width of fenestrule variable, ranging from equal to 2.5 times branch width; slight decrease in size of fenestrule opening toward proximal end of zoarium due to astogenetic thickening of lamellar skeleton. Width to length ratio of fenestrule ranging from 1:2 to 1:7, highly variable, mean ratio 1:3.5; length of fenestrule much more constant than width. Five to nine (most commonly seven) apertures per fenestrule length; distance between closest aperture centers along branch five-fourths that of spacing across branch; spacing across branch three-fifths that across fenestrule; spacing along and across branch constant, spacing across fenestrule highly variable.

Autozooecial apertures large, shape ovate, elongate proximal to slightly abaxially, to rarely circular; width to length ratio approximately 4:5, size and shape moderately uniform; opening most commonly oriented parallel to plane of obverse surface, more rarely at slight angle toward fenestrule; thin, well-developed peristome present, continuous around aperture where present at proximal end of zoarium. Thirteen to 17 (most commonly 15) small, variable-size well-developed and moderately regularly positioned stylets surround aperture; peristome develops from fusion of these stylets during astogeny, with stylets most commonly occurring at lateral and distal edges of zoarium. Aperture margin extends into fenestrule, causing slight inflection in fenestrule outline on obverse surface. Centrally thickened terminal diaphragms present, most common at proximal end of zoarium.

Zoarial supports lacking on all zoarial fragments analyzed.

Interior description.—Branches a nearly perfect circle in transverse section, slightly flaring on obverse side. Branches medium, slightly variable in thickness.

Autozooecial living chambers large, biserially arranged in alternating rows along planar branch axial wall; axial wall straight throughout most of chamber except near reverse wall, where axial wall exhibits inflections toward and connects with relatively long lateral walls. Chamber maximum dimension parallel to proximodistal direction of branch growth paralleling reverse wall from proximal end of chamber to near distal end; curving obversely two-thirds of distance up the chamber and becoming parallel to proximal and distal lateral chamber walls. Autozooecial chamber outline irregularly pentagonal near reverse-wall budding-site; rapidly becoming an irregular rectangle to parallelogram, with distalmost edge of parallelogram occurring at outer branch edge, in the mid and throughout most of chamber; irregularly elliptical near obverse surface, slightly enlarged at distal end of chamber; chamber shape moderately regular. Aperture positioned at distal and slightly abaxial end of chamber, connected to chamber by short vestibule of moderately variable length. Ratio of autozooecial chamber width to depth approximately 9:10; depth to length ratio approximately 1:4; length much more constant than width or depth, which are moderately constant. Short superior hemiseptum present at vestibular proximal edge, inferior hemiseptum absent. Autozooecial chambers diverge laterally from middle of branch at a highly variable angle (mean of 21°); from reverse wall at a variable angle (mean of 22°).

Three-dimensionally reconstructed chamber form a slightly irregular rectangular box; long dimension as viewed from lateral edge of branch, approximately equidimensional in depth and width, as viewed from distal end of branch and obverse surface, respectively.

Internal granular layer thin, continuous with obverse nodes, stylets, keel, apertural stylets, and peristome; reverse longitudinal striae and microstylets atop these striae; and across dissepiments. Outer lamellar layer

moderately thin, exhibiting slight astogenetic thickening toward proximal end of zoarium.

Remarks.—In many respects, the exterior of *B. delicata* closely resembles that of *Fenestella filistriata* Ulrich, 1890, described from the Burlington Limestone near Burlington, Iowa. The two species can be readily separated on the basis of exterior analysis (no interior views of *F. filistriata* were available) by the more delicate nature of branches and zoaria in *B. delicata*, its larger apertures ringed by apertural stylets, and the presence of a more pronounced keel from which stellate nodes project. *Fenestella regalis* Ulrich, 1890, from materials collected at Kings Mountain, Kentucky, also exhibits many characters in common with *B. delicata*, but can be readily distinguished by its much wider branches, almost twice those of *B. delicata*, and its extreme robustness.

This species is distinguished from other species of *Banastella*, n. gen. by its much more open mesh, elongate nodes occurring lengthwise across the dissepiment obverse surface, longest chamber dimension which parallels the reverse wall proximally and curves toward the obverse surface distally, and measured chamber dimensions. The open, loosely knit mesh found in *B. delicata* is moderately rare in Warsaw fenestrates, with a closer mesh pattern more typical.

Material studied.—Twenty-six exterior fragments, eight sectioned specimens; largest zoarial fragment 11×20 mm (width to length). The delicate nature of this species results in infrequent preservation of uncrushed complete zoaria, although disarticulated fragments in various states of preservation are common.

Occurrence.—*Banastella delicata* is relatively rare at the Valmeyer and St. Louis localities; it occurs primarily in the Lower Warsaw, where it is present in both limestones and shales.

Holotype.—UI X-6793 (loc. 49B, sample 12).

Paratypes.—UI X-6781, 6782, 6783, 6967–6970 (loc. 49B, samples 8, 13).

Genus **CUBIFENESTELLA**, new genus

Etymology of name.—Named for the approximately cubic form characteristic of autozooecial chambers in this genus.

Type species.—*Fenestella rudis* Ulrich, 1890; p. 537, pl. 49, figs. 3–3d [Lower Carboniferous, Valmeyeran Stage; Keokuk Limestone; Illinois Basin].

Diagnosis.—Zoarium robustness intermediate to robust, mesh spacing intermediate to open; chamber outline an irregular pentagon to rectangle in mid tangential section, chamber size intermediate; aperture size variable, small to large, opening at slight to pronounced angle toward and into fenestrule; superior and inferior hemisepta absent; chamber reverse-wall budding-angle varies between 64° and 81° (means).

Three-dimensionally reconstructed chamber form a regular cubic to irregular rectangular box.

Description.—Zoarium robustness intermediate to robust, expansion flat to obversely or reversely curved, mesh spacing intermediate to open, ranging from regular to irregular.

Branch width narrow to intermediate, straight to sinuous in trace with lateral branches broadly curved toward edge of zoarium; branch surface rounded to angular. Keel present, single, width intermediate to wide, straight to slightly anastomosing, exhibiting pronounced astogenetic thickening. Nodes present, emplacement monoserial, size large to intermediate, shape stellate, ovate to circular, located in middle of keel, spacing intermediate. Obverse stylets present, size intermediate, occurring across obverse surface or between nodes along keel. Microstylets present, size small to intermediate, occurring across obverse surface or between nodes along keel. Macrostylets present in some species, large, typically located at sites of branch–dissepiment junction. Autozooecia in two rows, third row at site of branch bifurcation. Heterozooecia absent.

Dissepiments of intermediate width, length intermediate to long, connect branches at regular to variable intervals.

Fenestrule size intermediate to large, shape elliptical, ovate, rectangular to polygonal.

Aperture size ranging from small to large, shape ovate, orientation ranging from slight to pronounced angle toward and into fenestrule. Peristome present or absent, complete where present. Apertural stylets present, develop as extension of aperture end, fuse to form peristome. Terminal diaphragms present, occurring toward proximal end and throughout zoarium.

Branch shape in cross-section ranging from ovate to elliptical to circular, thick to medium in depth.

Autozooecial chamber size intermediate, chamber emplacement monoserial or biserial along sinuous to zigzagged axial wall; chamber length and depth approximately equal. Chamber outline triangular to ovate

Text-figure 13.—*Cubifenestella rudis* illustrated. 1, diagrammatic longitudinal section illustrating chamber outline from deep section near middle of branch (bottom of figure) to shallow section near abaxial edge of branch (top of figure) [Observe approximately equal length and depth of chambers typical in this genus.], ×70; 2, diagrammatic tangential section showing changing chamber outline from deep section near reverse-wall budding-site (bottom of figure) to shallow section near obverse surface (top of figure), ×70; 3, diagrammatic transverse section illustrating orientation of aperture openings to plane of obverse surface (arrow) and continuity of granular skeleton across the dissepiment between branches, ×70; 4, reconstruction of typical chamber shape (three-dimensional) as viewed from distal end of branch; chamber reconstructed is from right side of branch, ×140; 5, reconstruction of typical chamber shape (three-dimensional) as viewed from abaxial edge of branch, ×140; 6, reconstruction of typical chamber shape (three-dimensional) as viewed from obverse surface; chamber reconstructed is from the right side of branch [Observe ovate shape of aperture (arrow), which is positioned on distal–abaxial edge of chamber.], ×140.

near reverse wall; becoming irregularly pentagonal to rectangular in mid chamber and throughout most of chamber depth; pentagonal, rectangular, elliptical, square to ovate near obverse surface. Vestibule present, varying in length from short to long. Superior and inferior hemisepta both absent. Lateral-wall budding-angle ranging from 18° to 37° (means); reverse-wall budding-angle ranging from 64° to 81° (means). Lamellar skeletal layer thickness intermediate to thick, exhibiting moderate to pronounced astogenetic thickening; granular skeletal layer thickness intermediate to thick, exhibiting moderate astogenetic thickening.

Three-dimensionally reconstructed chamber form a regular cubic to irregular rectangular box.

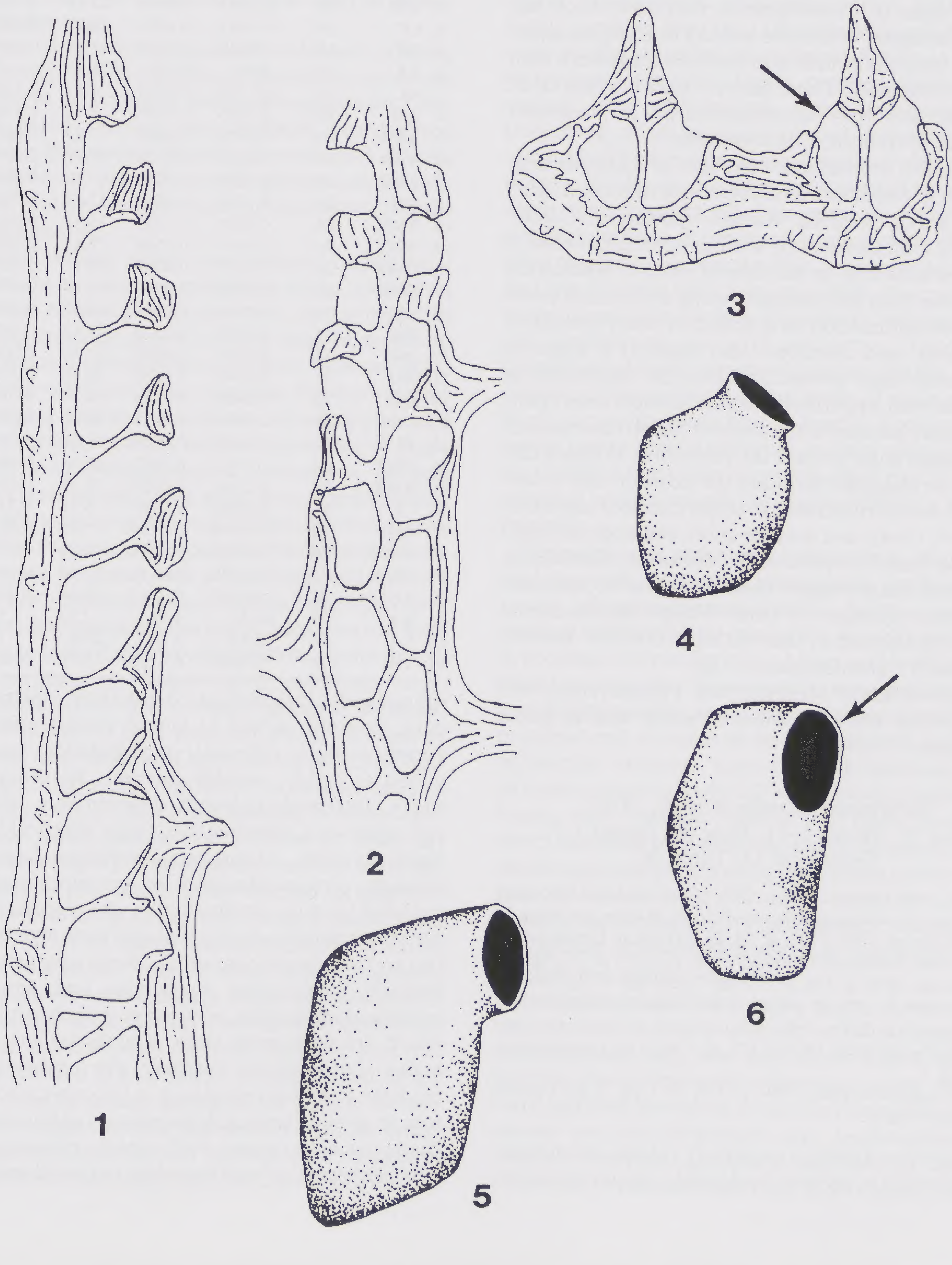

Text-figure 13 illustrates zoarial outlines in longitudinal, tangential, and transverse orientations, and three-dimensional reconstructions from distal, abaxial edge of branch, and obverse surfaces.

Remarks.—Morozova (1974) assigned *Fenestella rudis* Ulrich, 1890, herein designated the type species of *Cubifenestella*, to the genus *Rectifenestella* Morozova, 1974. Species of *Rectifenestella* typically have a chamber form that is more cuneate, compared to the box-like form in *Cubifenestella*, they have short superior hemisepta, which are lacking in *Cubifenestella*, and they typically exhibit a much finer meshwork than does *Cubifenestella*. These factors result in removal of *Fenestella rudis* from *Rectifenestella* and its placement in a genus of its own, *Cubifenestella*.

Among the fenestellids, members of *Cubifenestella* most closely resemble members of *Apertostella*, n. gen., another genus based on Warsaw specimens. *Cubifenestella* is distinguished by a more open meshwork, a third apertural row at the site of branch bifurcation only, rather than for distances along the branch proximal to the bifurcation as is found in many species of *Apertostella*, and chambers that open at a slight to pronounced angle toward and into the fenestrule, as compared with *Apertostella*, which has apertures opening generally parallel to the plane of the obverse surface or at a slight angle toward the fenestrule. Primary differences in chamber form are the position and orientation of the aperture relative to the chamber (see Text-figs. 16-4, 17-4); and a more cubic chamber in *Cubifenestella* than in *Apertostella*. However, similarities in chamber shape suggest close phylogenetic affinities.

Species composition.—Three Warsaw species are assigned to the genus: *C. rudis* (Ulrich, 1890), *C. usitata*, n. sp., and *C. globodensata*, n. sp.

Range.—Middle Mississippian (Valmeyeran), occurring in the Keokuk, Warsaw, Salem and St. Louis formations.

Cubifenestella rudis (Ulrich, 1890)
Plate 29, figures 1–11, Plate 30, figures 1–7;
Text-figure 13; Table 26

Fenestella rudis Ulrich, 1890, p. 537, pl. 49, figs. 3–3d [Keokuk Limestone, Keokuk and Bentonsport, Iowa; Warsaw and Nauvoo, Illinois]; Keyes, 1894, p. 23, pl. 34, fig. 5 [Keokuk Limestone, St. Francisville, Missouri]; Cumings, 1906, p. 1277, pl. 27, figs. 3–3d; Koenig, 1958, p. 136, pl. 21, fig. 7, text-figs. 1i, 1jj, table 8; Trizna, 1958, p. 127, pl. 34, fig. 5; pl. 35, figs. 1–4; Elias, 1964, p. 377, fig. 1; pl. 2, figs. 1–3.

Fenestella iowensis Elias, 1964, p. 378, pl. 1, fig. 2; pl. 3 [entire plate]; pl. 5, fig. 1.

Fenestella rudiformis Elias, 1964, p. 379, pl. 1, fig. 3; pl. 4 [entire plate]; pl. 5, fig. 2.

Diagnosis.—Zoarium extremely robust, mesh spacing intermediate, pattern moderately regular; branches robust, width intermediate, depth thick; straight to sinuous, broadly curved at lateral zoarial edge; transversely ovate to elliptical, intermediately spaced and joined at highly variable intervals by intermediate-width, intermediate-length dissepiments. Fenestrule size upper-end intermediate; shape elliptical to ovate, highly variable. Autozooecial apertures large, ovate, elongate proximoabaxially to proximodistally; surrounded by thin, intermediately developed, complete peristome across which small apertural stylets project; two to four (most commonly three) apertures per fenestrule. Single wide, continuous keel; straight, extending along middle of obverse branch surface, atop which are positioned large, slightly stellate to ovate nodes. Autozooecial chamber size upper-end intermediate, chambers emplaced in two rows, except third row at sites of branch bifurcation; outline irregularly triangular near reverse wall, rapidly becoming irregularly pentagonal in mid chamber, outline changing from

Table 26.—Summary numerical analysis of *Cubifenestella rudis* (Ulrich, 1890). For explanation of abbreviations of characters (left column), see Table 8b (foldout inside back cover).

	number of measurements	mean	standard deviation	coefficient of variation	observed range
1. **WB**	24	0.3504	0.1559	44.49	0.144–0.775
2. **DBC**	24	0.6671	0.1495	22.41	0.369–0.960
3. **WD**	24	0.2388	0.0969	23.88	0.131–0.475
4. **LF**	24	0.7455	0.1990	26.69	0.300–1.125
5. **WF**	24	0.3619	0.0645	17.82	0.269–0.490
6. **AF**	24	3.08	0.78	25.15	2–4
7. **AL**	24	0.1759	0.0081	4.61	0.166–0.198
8. **AW**	24	0.1435	0.0054	3.76	0.130–0.154
9. **ADB**	24	0.3058	0.0221	7.23	0.266–0.355
10. **AAB**	24	0.3259	0.0358	10.98	0.255–0.393
11. **ABB**	24	0.4388	0.0774	17.64	0.304–0.549
12. **DN**	24	0.1785	0.0560	31.37	0.102–0.300
14. **SNB**	24	0.6614	0.1205	18.22	0.421–0.964
15. **WK**	24	0.1815	0.0534	29.42	0.088–0.273
16. **DSO**	24	0.0137	0.0055	40.15	0.007–0.028
17. **SSO**	24	0.0452	0.0209	46.24	0.013–0.096
18. **WP**	24	0.0129	0.0024	18.60	0.009–0.029
21. **RSL**	24	0.0799	0.0173	21.65	0.047–0.119
22. **RSS**	24	0.0131	0.0041	31.30	0.008–0.023
23. **SSL**	24	0.6543	0.3238	49.49	0.313–1.313
24. **SSS**	24	0.0426	0.0148	34.74	0.014–0.074
32. **TRW**	24	0.0091	0.0028	30.77	0.005–0.016
33. **TLW**	24	0.0089	0.0033	37.08	0.006–0.014
34. **FWT**	24	0.1812	0.1077	59.44	0.066–0.447
35. **RWT**	24	0.2199	0.2029	92.37	0.050–0.859
36. **CL**	24	0.2832	0.0149	5.26	0.255–0.316
37. **CD**	24	0.2699	0.0139	5.15	0.241–0.295
38. **MAW**	24	0.1874	0.0154	8.22	0.163–0.221
39. **MIW**	24	0.1298	0.0150	11.56	0.108–0.166
40. **VD**	24	0.1567	0.0712	45.44	0.085–0.357
41. **RA**	24	64.46	4.98	7.72	55–74
42. **LA**	24	18.42	3.84	20.87	12–26
43. **TB**	24	0.6899	0.0738	10.70	0.569–0.819

pentagonal to rectangular approaching obverse surface; near obverse surface irregularly ovate. Chambers elongate parallel to proximal and distal lateral chamber walls. Aperture at distal-abaxial end of chamber, connected to chamber by extremely long vestibule of highly variable length. Superior and inferior hemisepta both absent. Lateral-wall budding-angle highly variable (mean of 18°); reverse-wall budding-angle constant (mean of 64°).

Table 26 presents statistical criteria used in delimiting this species.

Exterior description.—Zoarium extremely robust, expansion flat, exhibiting little or no obverse or reverse curvature in any zoarial fragments examined, fan-shaped; mesh spacing intermediate; pronounced astogenetic thickening of both obverse and reverse zoarial skeleton; external zoarial pattern moderately irregular. Probable mature widths 20 to 30 mm, lengths 35 to 45 mm.

Branches robust, width intermediate, highly variable; straight to sinuous, exhibiting slight inflections toward sites of dissepiment insertion, lateral branches commonly broadly curved toward edge of zoarium. Branch spacing intermediate, distance between adjacent branch centers slightly irregular. Obverse surface texture highly granular, becoming increasingly so with astogeny; surface rounded, except for presence of single keel; keel wide, well-developed, continuous, straight to slightly sinuous extending along branch midline and causing pronounced positive inflection in obverse surface profile. Pronounced astogenetic thickening of keel; toward most proximal end of zoarium keel extends across entire obverse surface, nearly to completely covering apertural openings, starting at most adaxial edge and filling in toward the abaxial direction. Nodes monoserially emplaced, well-developed, extremely large, slightly stellate to ovate in shape, elongate proximodistally; variable in both size and shape; develop as projections from middle of keel; one to two per fenestrule length, frequently positioned at or near sites of branch–dissepiment junction; spacing intermediate, moderately even; pronounced increase of node diameter with astogeny. Intermediate, variably sized stylets irregularly positioned along obverse surface. Reverse surface texture granular, coarsening with astogeny, bearing few rows of widely spaced longitudinal striae, occurring in exterior view at distal end of zoarium, becoming covered immediately proximal from zoarial distal edge due to pronounced astogenetic thickening of lamellar skeleton; rows of small, closely spaced microstylets develop as extensions of longitudinal striae, become variably spaced across entire reverse surface and exhibit slight increase in diameter with astogeny. Large, approximately circular macrostylets, moderately regular in size and shape and variable in placement, located at or near sites of branch–dissepiment junction on reverse surface. Autozooecia in two rows across branch, except third row at sites of branch bifurcation where middle autozooecium evidently shared by both branches; pronounced thickening proximal, thinning distal to sites of branch bifurcation. Heterozooecia absent in all zoarial fragments observed.

Dissepiments of intermediate width, approximately two-thirds that of branch, slightly variable in width; length intermediate, constant; connect branches at highly variable intervals. Dissepiments exhibit moderate medial thinning, pronounced flaring at branch–dissepiment junction; highly recessed from obverse surface, even with reverse. Pronounced astogenetic thickening of dissepiment toward proximal end of zoarium. Obverse dissepiment surface with medially thickened ridge atop which occur rows of small, irregularly spaced stylets which increase in diameter with astogeny; reverse dissepiment surface with small stylets irregularly positioned across surface, stylet number and size increase with astogeny. Both obverse and reverse dissepiment surfaces granular in texture, becoming increasingly so with astogeny. Dissepiment emplacement most commonly approximately perpendicular to branch length, more rarely at angle up to 20° from perpendicular to branch length. Apertures commonly positioned on proximal or distal edge or in middle of dissepiment edge at branch–dissepiment contact; arranged symmetrically or asymmetrically between branches.

Fenestrule size upper-end intermediate, shape elliptical to ovate, becoming increasingly ovate with astogeny, elongate proximodistally; highly variable in size and shape; slightly expanding in width and length in obverse–reverse direction. Mean width of fenestrule slightly greater than branch width; fenestrule becoming appreciably smaller, at times completely closed toward proximal end of zoarium with astogenetic thickening of lamellar skeleton. Ratio of mean fenestrule width to length approximately 1:2; width more constant than length, both variable. Two to four (most commonly three) apertures per fenestrule length; distance between closest aperture centers along branch and across branch approximately equal, spacing of apertures across fenestrule approximately 1.5 times greater; spacing along branch and across branch constant, spacing across fenestrule moderately variable.

Autozooecial apertures large, ovate, elongate proximoabaxially to proximodistally, width to length ratio approximately 4:5; size and shape highly uniform; opening most commonly oriented at slight angle toward and into fenestrule or rarely at pronounced angle toward and into fenestrule; thin, intermediately developed complete peristome surrounding aperture, commonly with small apertural stylets projecting from

peristome toward proximal end of zoarium, forming through secondary overgrown lamellar skeletal layer and having the same dimensions as small obverse stylets. Aperture margins extend into fenestrule, causing pronounced inflections in fenestrule outline on obverse surface. In late astogeny apertures become covered by centrally thickened terminal diaphragms.

Large, well-developed zoarial supports develop as extensions of reverse zoarial surface and lateral edge of zoarium.

Interior description.—Branches ovate to elliptical in transverse section, commonly slightly enlarged on obverse surface, elongate in obverse–reverse direction. Branches thick, regular in depth.

Autozooecial living chamber size upper-end intermediate, chambers biserially arranged in alternating rows along planar branch axial wall; axial wall highly sinuous, exhibiting inflections toward and connecting with chamber lateral walls near reverse wall and throughout chamber; inflections become less pronounced near obverse surface. Chamber longest dimension only slightly greater than depth, elongate parallel to proximal and distal lateral chamber walls. Autozooecial chamber outline rounded, irregularly triangular near reverse wall; rapidly becoming irregularly pentagonal throughout most of chamber length, outline changing from pentagonal to rectangular approaching obverse surface; near obverse surface chambers irregularly ovate; chamber shape highly uniform. Aperture positioned at distal-abaxial end of chamber, connected to chamber by extremely long, well-developed, highly variable-length vestibule. Ratio of autozooecial chamber minimum width to maximum width approximately 7:10; maximum width to depth ratio about 7:10; dimensions of depth to length of chamber approximately equal, length only very slightly greater than depth; chamber length and depth highly constant, maximum and minimum widths moderately constant. Superior and inferior hemisepta both absent. Autozooecial chambers diverge laterally from middle of branch at highly variable angle (mean of 18°); from reverse wall at a constant angle (mean of 64°).

Three-dimensionally reconstructed chamber form a regular box; approximately equidimensional in length and depth as viewed from lateral edge and distal end of branch respectively; width as viewed from obverse surface moderately less than length or depth.

Internal granular skeletal layer thick, well-developed; continuous with obverse nodes, stylets, keel, peristome; reverse longitudinal striae, microstylets and macrostylets; across dissepiments and in the middle of zoarial supports. Outer lamellar layer extremely thick, exhibiting pronounced astogenetic thickening on both obverse and reverse exterior zoarial surfaces.

Remarks.—*Fenestella rudis* Ulrich, 1890 was first described from the Keokuk Limestone and Warsaw Beds near Keokuk, Iowa, and Warsaw, Illinois. Ulrich (1890, p. 537) noted marked variation within this species, caused in his opinion by varying "age and state of preservation." Based on my observations, astogenetic variability of exterior appearance is greater than in most other fenestellids.

The assignment of Ulrich's syntypes of *Fenestella rudis* into two species, *Fenestella iowensis* Elias, 1964, and *Fenestella rudiformis* Elias, 1964, is not justified by internal analyses. Interior and exterior dimensions for both *F. iowensis* and *F. rudiformis* are within the observed range for *C. rudis*, and I therefore place these species in synonymy with *C. rudis*.

Characteristic astogenetic thickening, chamber shape, presence of apertural stylets, mesh pattern, and aperture orientation are similar in *C. rudis*, *C. usitata*, and *C. globodensata*, suggesting close taxonomic affinities. Variability of mesh symmetry due to astogenetic thickening makes recognition of *C. rudis* heavily dependent on use of internal characteristics such as autozooecial chamber dimensions and reverse-wall budding-angle. *C. rudis* is distinguished from other species of *Cubifenestella* by a finer mesh, larger autozooecial chamber, and thicker branches.

Material studied.—Fourty-four exterior fragments, 14 sectioned specimens; largest zoarial fragment 32 × 26 mm (width to length). Microstructural and whole specimen preservation is good to excellent in all material collected.

Occurrence.—*Cubifenestella rudis* is common throughout the Warsaw Formation: it is also reported from the Keokuk and Salem formations in the study area. Observation suggests the zoarial mesh is more open in shaly facies, and becomes coarser with thicker branches in calcarenitic facies; internal characters remain the same regardless of exterior mesh variation.

Syntypes.—ISGS(ISM) 2745–1, 2776–1/2; USNM 43759. One specimen is illustrated in Ulrich (1890, pl. 49, figs. 3, 3a, 3b, 3c, 3d).

Figured and/or measured specimens.—UI X-6718, 6744, 6752, 6754 (loc. 10, samples 28, 31), 6900–6903, 6753, 6755–6758 (loc. 49B, samples 8, 12, 13).

Cubifenestella usitata, new species

Plate 31, figures 1–12, Plate 32, figures 1–6; Table 27

Etymology of name.—Named for the lack of distinctive distinguishing characteristics in exterior view, this species exhibits a typical fenestellid fan shape.

Diagnosis.—Zoarium robustness intermediate, mesh intermediate, pattern moderately regular; branch robustness and width intermediate, branches thick in depth; branches straight to broadly curved; transversely ovate to approaching circular, spacing intermediate, branches joined at regular intervals by intermediate

Table 27.—Summary numerical analysis of *Cubifenestella usitata*, n. sp. For explanation of abbreviations of characters (left column), see Table 8b (foldout inside back cover).

	number of measurements	mean	standard deviation	coefficient of variation	observed range
1. WB	24	0.3189	0.0816	25.59	0.219–0.500
2. DBC	24	0.6244	0.1149	18.40	0.403–0.853
3. WD	24	0.2018	0.0288	14.27	0.150–0.263
4. LF	24	0.8459	0.0743	8.78	0.673–0.973
5. WF	24	0.3199	0.0765	23.91	0.167–0.463
6. AF	24	3.96	0.46	11.73	3–5
7. AL	24	0.1434	0.0066	4.60	0.125–0.155
8. AW	24	0.1043	0.0086	8.25	0.088–0.128
9. ADB	24	0.2715	0.0184	6.78	0.243–0.313
10. AAB	24	0.2624	0.0339	12.92	0.203–0.337
11. ABB	24	0.4178	0.0990	23.70	0.223–0.565
12. DN	24	0.1456	0.0243	16.69	0.101–0.203
14. SNB	24	0.7747	0.1611	20.80	0.413–1.150
15. WK	24	0.1177	0.0377	32.03	0.071–0.200
16. DSO	24	0.0119	0.0028	23.53	0.008–0.019
17. SSO	24	0.0524	0.0131	25.00	0.026–0.088
19. SA	24	8.58	0.88	10.26	7–11
20. SAD	24	0.0110	0.0019	17.36	0.008–0.013
22. RSS	24	0.0189	0.0032	16.85	0.034–0.026
24. SSS	24	0.0571	0.0130	22.77	0.033–0.091
32. TRW	24	0.0085	0.0013	15.70	0.006–0.011
33. TLW	24	0.0111	0.0017	15.56	0.008–0.014
34. FWT	24	0.0838	0.0388	46.28	0.026–0.166
35. RWT	24	0.0720	0.0304	42.24	0.014–0.123
36. CL	24	0.2454	0.0100	4.07	0.221–0.264
37. CD	24	0.1834	0.0123	6.71	0.160–0.209
38. MAW	24	0.1450	0.0174	12.00	0.116–0.184
39. MIW	24	0.0868	0.0123	14.17	0.068–0.121
40. VD	24	0.0505	0.0190	37.77	0.030–0.082
41. RA	24	67.87	4.87	7.17	58–77
42. LA	24	37.29	5.43	14.57	28–49
43. TB	24	0.4117	0.0798	19.38	0.294–0.596

width and length dissepiments. Fenestrule size intermediate, shape elliptical to approaching rectangular, highly regular. Autozooecial aperture size intermediate, shape ovate, elongate proximodistally; surrounded by seven to 11 (mean of nine) small stylets; three to five (most commonly four) apertures per fenestrule. Single intermediate-width, continuous keel; straight, extending along middle of obverse branch surface, atop which are positioned large, circular to ovate nodes. Autozooecial chamber size intermediate, emplaced in two rows, except third row at sites of branch bifurcation; outline irregular–ovate to rounded-triangle near reverse wall, rapidly becoming irregularly pentagonal throughout chamber, shape becoming increasingly rectangular toward obverse surface; near obverse surface chamber rectangular to elliptical, nearest obverse surface chamber approximately square. Chambers elongate parallel to proximal and distal lateral chamber walls. Aperture at distal and highly abaxial edge of chamber, connected to chamber by short, variable-length vestibule. Superior and inferior hemisepta absent. Lateral-wall budding-angle moderately variable (mean of 37°); reverse-wall budding-angle constant (mean of 68°).

Table 27 presents statistical criteria used in species delimitation.

Exterior description.—Zoarium robustness intermediate, expansion flat, planar to slightly obversely curved, fan-shaped; mesh spacing intermediate; moderate astogenetic thickening of both obverse and reverse zoarial lamellar skeleton; external zoarial pattern moderately regular. Probable mature widths 20 to 35 mm, lengths 35 to 50 mm.

Branch robustness intermediate; width intermediate, variable; straight in trace, lateral branches frequently broadly curved toward edge of zoarium. Branch spacing intermediate, distance between adjacent branch centers moderately regular. Obverse surface texture granular, becoming increasingly so with astogeny, surface profile angular to slightly rounded; except for presence of single keel of intermediate width, extremely well-developed, continuous, straight, positioned along branch midline causing pronounced positive inflection in obverse surface profile. Pronounced astogenetic thickening of keel, which develops to extend across entire obverse surface between apertures and frequently covers most adaxial edge of aperture. Nodes emplaced in single row, extremely well-developed, large; shape circular to ovate, elongate proximodistally when ovate; size and shape moderately regular; one to two nodes per fenestrule length, frequently positioned at or near sites of branch–dissepiment junction; node spacing upper-end intermediate, moderately even; diameter increasing with astogeny. Intermediate-size stylets, variable in size and positioning, located across obverse branch surface, increasing in number and diameter with astogeny. Reverse surface texture granular, coarsening with astogeny; bearing relatively few rows of intermediately spaced longitudinal striae which become covered by astogenetic thickening of lamellar skeleton; rows of closely spaced intermediate-size microstylets atop striae along reverse surface, microstylet size moderately regular; with astogeny microstylets increase in diameter and become more irregularly positioned across reverse branch surface. Two rows of autozooecia across branch, except third row at sites of branch bifurcation where middle autozooecium evidently shared by both branches; moderate to pronounced thickening of branches proximal, thinning distal to sites of branch bifurcation. Heterozooecia not present in any zoarial fragments examined.

Dissepiments of intermediate width, approximately two-thirds that of branch; constant in width; length intermediate, moderately variable; connect branches at regular intervals. Dissepiments barlike, exhibiting

slight medial thinning and moderate flaring at branch–dissepiment contact; highly recessed from obverse surface, moderately recessed from reverse. Moderate to pronounced astogenetic thickening toward proximal end of zoarium. Obverse dissepiment surface with thickened barlike expansion positioned longitudinally across dissepiment and oriented approximately perpendicular to branch length; small, irregularly spaced stylets occurring across obverse dissepiment surface; reverse surface with longitudinal striae oriented perpendicular to branch length, atop which occur rows of small to intermediate-size stylets; both obverse and reverse dissepiment surfaces granular, becoming increasingly so with astogeny. Dissepiments most commonly emplaced approximately perpendicular to branch length. Apertures commonly open on proximal or distal edge or in middle of dissepiment edge at branch–dissepiment contact; arranged symmetrically or asymmetrically between branches.

Fenestrule size intermediate, shape elliptical to approaching rectangular, elongate proximodistally; highly regular in shape, overall size variable; exhibiting little or no expansion in length and width in obverse–reverse direction. Mean width of fenestrule approximately equal to branch width; fenestrule opening becoming moderately to appreciably smaller toward proximal end of zoarium with astogenetic thickening of lamellar skeleton. Ratio of mean fenestrule width to length approximately 3:8; length constant, much more so than width, which is highly variable. Three to five (most commonly four) apertures per fenestrule length; distance between closest aperture centers along branch and across branch approximately equal, spacing of apertures across fenestrule 1.6 times greater; spacing along branch and across branch constant, spacing across fenestrule moderately variable.

Autozooecial aperture size intermediate, shape ovate, elongate proximodistally and slightly enlarged at distal end; aperture opening oriented approximately 45° into fenestrule from parallel to plane of obverse surface, rarely approaching parallel to plane of obverse surface; peristome lacking. Seven to 11 (mean of nine) small stylets fairly constant in size and moderately variable in number, surround aperture; stylet diameter exhibiting slight increase in diameter with astogeny. Apertures even with branch surface, causing no inflections in fenestrule outline. Centrally thickened terminal diaphragms frequently occurring at most proximal end of zoarium, less frequently distally.

Well-developed zoarial supports present as extensions of reverse zoarial surface.

Interior description.—Branches ovate to approaching circular in transverse view, moderately symmetrical, elongate in obverse–reverse direction. Branches thick, variable in depth.

Autozooecial living chambers of intermediate size, monoserially emplaced at or near reverse-wall budding-site, become biserially arranged in alternating rows along a planar branch axial wall; axial wall sinuous, exhibiting pronounced inflections toward and connecting with chamber lateral walls near reverse surface and throughout most of chamber length, toward obverse surface sinuous nature is reduced and axial wall becomes nearly straight. Chamber longest dimension parallel to proximal and distal lateral chamber walls. Autozooecial chamber outline irregular ovate to rounded triangle near reverse wall; rapidly becoming irregularly pentagonal throughout most of chamber length, with outline becoming increasingly rectangular toward obverse surface; approaching obverse surface chamber outline rectangular to elliptical, nearest obverse surface chamber approximately square; chamber shape highly uniform. Aperture positioned at distal and highly abaxial edge of chamber, connected to chamber by short, intermediately developed variable-length vestibule. Ratio of autozooecial chamber minimum width to maximum width approximately 3:5; maximum width to depth ratio about 4:5; ratio of depth to length of chamber approximately 3:4; chamber length and depth highly constant, minimum and maximum widths slightly variable. Superior and inferior hemisepta both lacking. Autozooecial chambers diverge laterally from middle of branch at moderately variable angle (mean of 37°); from reverse wall at a constant angle (mean of 68°).

Three-dimensionally reconstructed chamber form a rectangular irregular box; length as viewed from lateral edge of branch; depth as viewed from distal end of branch; width as viewed from obverse surface.

Internal granular skeletal layer width intermediate, continuous with obverse nodes, stylets, keel, and apertural stylets; reverse striae and stylets; across dissepiments and in the middle of zoarial supports. Moderate to pronounced thickening of lamellar skeleton toward proximal end of zoarium with astogeny.

Remarks.—Differentiation between *C. usitata*, n. sp. and *C. globodensata*, n. sp. based on exterior characteristics is difficult due to similarity in mesh pattern, astogenetic thickening, aperture orientation, and presence of apertural stylets. *C. usitata* differs from *C. globodensata* by its larger chamber size, more widely spaced obverse nodes, wide branches, and more closely spaced mesh. Pronounced differences in positioning of the chamber relative to the branch exist between the two species as well. Internal similarity to *C. rudis* (Ulrich, 1890) suggests strong affinities among the three species; differences include chamber dimensions and general mesh symmetry.

C. usitata exhibits slight similarity in exterior appearance with *Fenestella funicula* Ulrich, 1890. It differs in having narrower branches, tighter mesh, and

Table 28.—Summary numerical analysis of *Cubifenestella globodensata*, n. sp. For explanation of abbreviations of characters (left column), see Table 8b (foldout inside back cover).

	number of measurements	mean	standard deviation	coefficient of variation	observed range
1. WB	24	0.2777	0.0601	21.64	0.188–0.407
2. DBC	24	0.7034	0.1873	26.63	0.400–1.133
3. WD	24	0.2110	0.0676	32.04	0.102–0.367
4. LF	24	0.9753	0.1664	17.06	0.667–1.267
5. WF	24	0.4104	0.1400	34.11	0.222–0.760
6. AF	24	4.25	0.85	19.93	3–6
7. AL	24	0.0835	0.0075	8.98	0.069–0.100
8. AW	24	0.0671	0.0061	9.03	0.057–0.083
9. ADB	24	0.2799	0.0269	9.61	0.238–0.340
10. AAB	24	0.2946	0.0293	9.95	0.247–0.343
11. ABB	24	0.5333	0.0964	18.08	0.313–0.903
12. DN	24	0.1247	0.0336	26.94	0.072–0.213
14. SNB	24	0.4451	0.0956	21.48	0.214–0.600
15. WK	24	0.1277	0.0429	33.59	0.067–0.216
16. DSO	24	0.0188	0.0041	34.75	0.006–0.023
17. SSO	24	0.0534	0.0165	30.90	0.021–0.089
18. WP	24	0.0211	0.0051	24.17	0.015–0.039
19. SA	24	16.28	3.55	21.81	14–22
20. SAD	24	0.0107	0.0045	42.06	0.007–0.017
22. RSS	24	0.0249	0.0065	26.10	0.016–0.043
24. SSS	24	0.0529	0.0168	31.76	0.027–0.096
32. TRW	24	0.0069	0.0010	13.91	0.006–0.009
33. TLW	24	0.0107	0.0013	12.06	0.008–0.013
34. FWT	24	0.0592	0.0337	56.93	0.015–0.150
35. RWT	24	0.0988	0.0507	51.32	0.017–0.200
36. CL	24	0.2133	0.0083	3.89	0.199–0.229
37. CD	24	0.1546	0.0071	4.59	0.143–0.169
38. MAW	24	0.1288	0.0129	10.02	0.112–0.154
39. MIW	24	0.0415	0.0143	34.46	0.016–0.068
40. VD	24	0.0757	0.0212	38.01	0.048–0.110
41. RA	24	81.04	7.67	9.46	69–94
42. LA	24	33.96	6.13	18.04	20–44
43. TB	24	0.3238	0.0364	11.24	0.265–0.371

more pronounced orientation of aperture opening into fenestrule opening than was reported and observed by Ulrich in *F. funicula*.

Material studied.—Twenty-two exterior fragments; seven sectioned specimens; largest zoarial fragment 27×38 mm (width to length). Excellent microstructural and whole specimen preservation is observed in all material collected.

Occurrence.—*Cubifenestella usitata* is common at the Valmeyer, St. Louis and associated localities in the southern part of study area. It occurs throughout the Warsaw Formation, and is equally common in limestones and shales.

Holotype.—UI X-6709 (loc. 49B, sample 12).

Paratypes.—UI X-6704, 6708, 6712 (loc. 49B, samples 12, 13, 15), 6723, 6831 (loc. 10, samples 24, 29), 6869 (loc. 47A, sample 27).

Cubifenestella globodensata, new species

Plate 33, figures 1–11, Plate 34, figures 1–6; Table 28

Etymology of name.—Named for the globularly thickened obverse surface, resulting from overgrowth of the keel and obverse surface by the external lamellar skeletal layer, resulting in infilling of apertural openings during astogeny.

Diagnosis.—Zoarium robustness intermediate, mesh open, pattern highly variable; branches moderately robust, width thin, depth intermediate; straight to anastomosing to broadly curved; branches transversely circular to irregularly ovate, widely spaced; branches joined at variable intervals by intermediate-width, long dissepiments. Fenestrules large; shape elliptical, irregularly polygonal to ovoid, moderately irregular. Autozooecial apertures small, shape ovate, elongate proximodistally, surrounded by moderately well-developed, thin, complete peristome formed from fusion of 14 to 22 small stylets irregularly positioned around aperture; three to six (most comonly four) apertures per fenestrule. Single intermediate-width, continuous keel along middle of obverse branch, atop which are positioned lower-end large, irregularly ovate to slightly stellate nodes. Autozooecial chamber size lower-end intermediate, emplaced in two rows, except third row at sites of branch bifurcation; outline irregularly ovate to rounded triangular near reverse wall, rapidly becoming irregularly pentagonal throughout most of chamber depth, outline irregularly elliptical near obverse surface, slightly enlarged at distal end. Chamber longest dimension parallel to reverse wall in proximodistal direction. Aperture positioned at distal-abaxial end of chamber, connected to chamber by intermediate, variable-length vestibule. Superior and inferior hemisepta both absent. Lateral-wall budding-angle variable (mean of 34°); reverse-wall budding-angle moderately constant (mean of 81°).

Table 28 presents statistical criteria used in delimiting this species.

Exterior description.—Zoarium robustness intermediate, expansion flat, planar to rarely slightly obversely or reversely curved, fan-shaped; mesh spacing open; pronounced astogenetic thickening of both obverse and reverse zoarial lamellar skeleton, external zoarial pattern highly variable within and between zoaria. Probable mature widths 25 to 35 mm, lengths 35 to 60 mm.

Branches moderately robust; thin, variable in width; straight to slightly anastomosing toward sites of dissepiment emplacement, lateral branches frequently broadly curved toward edge of zoarium. Branches widely spaced, distance between adjacent branch centers moderately irregular. Obverse surface texture granular, becoming increasingly so with astogeny, surface rounded, except for presence of single, moderately well-developed positive inflection in obverse surface profile. Pronounced thickening of keel occurs with as-

togeny; keel forming a ropy expansion across most of obverse surface toward proximal end of zoarium, frequently extending over adaxial edge of aperture to completely overgrow aperture; lamellar skeleton covering much of keel with astogeny. Nodes emplaced in single row, well-developed, size lower-end large; irregularly ovate to slightly stellate in shape, elongate proximodistally; size and shape both highly variable; one to five nodes per fenestrule length; spacing intermediate, moderately evenly spaced; diameter greatly increasing with astogeny. Intermediate-size stylets, variable in size, typically variably positioned in rows, located along obverse surface between nodes; increasing in diameter and number with astogeny. Reverse surface texture granular, coarsening with astogeny; bearing few rows of widely spaced longitudinal striae; with astogeny striae covered by thickening of lamellar skeleton, most prominent toward proximal end of zoarium; rows of intermediate size microstylets, closely spaced, located atop striae along reverse surface, microstylet size moderately variable; with astogeny microstylets greatly increase in diameter and become more irregularly positioned across reverse branch surface. Autozooecia in two rows across branch, except third row at sites of branch bifurcation where middle autozooecium evidently shared by both branches; slight to moderate thickening of branches proximal, thinning distal to site of branch bifurcation. Heterozooecia not present in any zoarial fragments examined.

Dissepiments of intermediate width, approximately three-fourths that of branch; highly variable in width; dissepiments long, highly variable in length; connect branches at variable intervals. Dissepiments moderately barlike, exhibiting slight medial thinning and intermediate flaring at branch–dissepiment contact; moderately recessed from obverse, approximately even with reverse surface. Moderate to pronounced astogenetic thickening, most pronounced toward proximal end of zoarium. Obverse dissepiment surface with two to four thickened barlike expansions oriented longitudinally across dissepiment and emplaced perpendicular to branch length; small, irregularly spaced stylets occurring in rows atop striae; reverse dissepiment surface with two to four thickened barlike expanions, oriented perpendicular to branch length, atop which are positioned rows of small to intermediate-size stylets; both obverse and reverse dissepiment surfaces granular in texture, coarsening with astogeny. Dissepiments typically emplaced perpendicular to branch length, more rarely at a small angle from perpendicular. Apertures commonly open on proximal or distal edge, more rarely in middle of dissepiment edge at branch–dissepiment contact; arranged symmetrically or asymmetrically between branches.

Fenestrules large, typically elliptical, but also asymmetrically polygonal to ovoid in shape, elongate proximodistally; moderately irregular in shape, overall size variable; exhibiting no change in size or shape of opening from obverse to reverse surface. Mean width of fenestrule 1.5 times that of branch; fenestrule opening exhibiting slight decrease in size toward proximal end of zoarium due to astogenetic thickening of lamellar skeleton. Ratio of mean fenestrule width to length approximately 2:5; length moderately constant, much more so than width, which is highly variable. Three to six (most commonly four) apertures per fenestrule length; distance between closest aperture centers along branch and across branch approximately equal, spacing of aperture centers across fenestrule approximately three times greater; spacing along branch and across branch moderately constant, spacing across fenestrule variable.

Autozooecial apertures small, shape ovate, elongate proximodistally and slightly enlarged at distal end; aperture openings typically at a moderate to pronounced angle into fenestrule, rarely parallel to plane of obverse surface; thin, moderately well-developed complete peristome present. Fourteen to 22 (most commonly 16) small, variable-size, moderately well-developed and irregularly positioned stylets surround aperture; peristome develops from fusion of these stylets during astogeny, with stylets most common at lateral and distal edges of zoarium. Aperture margins extend into fenestrule, causing very slight inflections in fenestrule outline on obverse surface. In late astogeny apertures frequently capped by centrally thickened terminal diaphragms.

Well-developed zoarial supports present as extensions of reverse zoarial surface and lateral edge of zoarium.

Interior description.—Branches circular to irregularly ovate in transverse view, moderately symmetrical, elongate either parallel to plane of zoarium or in obverse–reverse direction. Branches intermediate, moderately regular in thickness.

Autozooecial living chamber size lower-end intermediate, chambers monoserially emplaced at or near reverse-wall budding-site, rapidly becoming biserially arranged toward obverse surface along planar branch axial wall; axial wall forming zigzag pattern, extending diagonally across entire branch and forming chamber lateral walls; inflections reduced in mid chamber, axial wall connecting with short lateral walls; inflections further reduced near obverse surface. Chamber longest dimension parallel to reverse wall in proximodistal direction. Autozooecial chamber outline irregularly ovate to rounded triangular near reverse wall; rapidly becoming irregularly pentagonal throughout most of chamber depth; outline irregularly elliptical near obverse surface, slightly enlarged at distal-abaxial end of

chamber; chamber shape moderately uniform. Apertures positioned at distal-abaxial edge of chamber, connect to chamber by well-developed, intermediate-length vestibules; vestibules variable in length. Ratio of autozooecial chamber minimum width to maximum width approximately 1:3; maximum width to depth ratio about 5:6; ratio of depth to length of chamber approximately 5:7; chamber length and depth highly constant, maximum width slightly variable and minimum width highly variable. Superior and inferior hemisepta both absent. Autozooecial chamber diverges laterally from middle of branch at a variable angle (mean of 34°); from reverse wall at a moderately constant angle (mean of 81°).

Three-dimensionally reconstructed chamber form an irregular slightly rectangular box, length as viewed from lateral edge of branch; depth as viewed from distal end of branch, width as viewed from obverse surface.

Internal granular skeletal layer thick, exhibiting pronounced astogenetic thickening resulting in partial to complete infilling of autozooecial chambers toward most proximal end of zoarium; granular skeletal layer continuous with obverse nodes, stylets, keel, peristome, and apertural stylets; reverse striae and microstylets; across dissepiments including dissepiment longitudinal striae and stylets, and in the middle of zoarial supports. Pronounced thickening of lamellar skeleton, moderate thickening of granular skeleton with astogeny.

Remarks.—The initial monoserial chamber emplacement in *Cubifenestella globodensata*, n. sp. is similar to that found in species of *Minilya* Crockford, 1944 (*e.g.*, *M. sivonella*, n. sp.); however, all other internal chamber and most external characters closely match those found in species of *Cubifenestella*, n. gen. Marked similarities in appearance between *C. globodensata* and *C. usitata*, n. sp. suggest close phylogenetic affinity. Smaller chamber and aperture size, and highly variable nature of node placement and mesh pattern of *C. globodensata* allow ready separation of this species from *C. usitata*, the most similar congeneric species. Sole reliance on external characters and mesh patterns for differentiation of these two species is not effective because of their overlapping external dimensions and similarity in external characters.

Cubifenestella globodensata moderately closely resembles *Fenestella compressa* Ulrich, 1890 from Kings Mountain, Kentucky in its large fenestrules, small and widely separated apertures, numerous nodes on a well-developed keel, and apertures facing into the fenestrule. It is clearly separated by its much narrower branches, more closely spaced apertures, and finer mesh. Internal sections of *F. compressa* would be beneficial in species comparison, but were unavailable.

Material studied.—Thirty-four exterior fragments; 26 sectioned specimens; largest zoarial fragment 20 × 36 mm (width to length). Excellent microstructural and whole specimen preservation is observed in most material collected.

Occurrence.—*Cubifenestella globodensata* is common at the Valmeyer, St. Louis, and associated localities in the southern part of the study area, south of White Hall. It occurs throughout the Warsaw and into the Lower Salem Formation at these localities, and is equally abundant in both limestones and shales.

Holotype.—UI X-6702 (loc. 49B, sample 15).

Paratypes.—UI X-6819–6830, 6705–6707, 6710, 6711, 6715, 6713, 6714 (loc. 49B, samples 13, 15, 16), 6703, 6700, 6701 (loc. 47A, samples 32, 35), 6750, 6751 (loc. 20, sample 10).

Genus **APERTOSTELLA**, new genus

Etymology of name.—Named for the distinctive, irregularly ovate, intermediate-size apertures characteristic of the genus.

Type species.—*Apertostella crassata*, n. sp.

Diagnosis.—Zoarium robustness ranging from delicate to robust, mesh spacing close to intermediate; chamber outline irregularly pentagonal, rectangular to elliptical in mid tangential section, chamber size intermediate; aperture size intermediate, opening typically oriented parallel to plane of obverse surface or infrequently at slight angle toward fenestrule, superior and inferior hemisepta absent, chamber reverse-wall budding-angle varies between 67° and 69° (means).

Three-dimensionally reconstructed chamber form a rectangular box.

Description.—Zoarium robustness variable, ranging from delicate to robust, expansion flat, undulating to slightly obversely curved, mesh spacing close to intermediate, regular.

Branch width intermediate to wide, straight to sinuous in trace with lateral branches curved toward edge of zoarium; branch surface ranging from flat, slightly concave, angular to slightly rounded. Keel present, single, width narrow to intermediate, straight to slightly anastomosing, slightly thickening with astogeny and frequently covered by lamellar skeleton. Nodes present, emplacement monoserial, size intermediate to large, shape ovate to circular, located atop middle of keel, spacing intermediate to wide. Obverse stylets present or absent; where present, size large, occurring across obverse surface. Microstylets present, ranging in size from small to large, emplaced in rows, becoming variably placed with astogeny. Macrostylets present in some species, large, typically located at site of branch–dissepiment junction. Autozooecia in two rows, third row at sites of branch bifurcation or three rows for distance along branch proximal to branch bifurcation.

Heterozooecia absent.

Dissepiments of thin to intermediate width, length short to intermediate, connect branches at regular intervals.

Fenestrule size variable, ranging from small to large, shape rectangular to elliptical to ovate.

Aperture size intermediate, shape ovate, oriented parallel to plane of obverse surface or infrequently at slight angle toward fenestrule. Peristome present, complete; apertural stylets either present or absent, develop as extension of peristomal edge; terminal diaphragms present, primarily occurring toward proximal end of zoarium.

Branch shape in cross-section ranging from polygonal to ovate to elliptical, medium to deep in thickness.

Autozooecial chamber size intermediate, chambers biserially emplaced along sinuous to zigzagged axial wall; maximum chamber dimension (length) extending proximodistally, parallel to reverse wall. Chamber outline triangular, polygonal to irregularly pentagonal near reverse wall; becoming irregularly pentagonal, rectangular to elliptical in mid chamber and throughout most of chamber depth; irregularly elliptical to ovate near obverse surface. Vestibule present, ranging in length from short to intermediate. Superior and inferior hemisepta both absent. Lateral-wall budding-angle ranging from 22° to 25° (means); reverse-wall budding-angle from 67° to 69° (means). Lamellar skeletal layer thickness intermediate to thick, exhibiting moderate to pronounced astogenetic thickening; granular skeletal layer thickness intermediate to thick, exhibiting no astogenetic thickening.

Three-dimensionally reconstructed chamber form a rectangular box.

Text-figure 14 illustrates zoarial outlines in longitudinal, tangential, and transverse orientations, and three-dimensional chamber reconstructions from distal, abaxial edge of branch, and obverse surfaces.

Remarks.—Moderate similarities exist between species of *Apertostella* and *Cubifenestella* n. gen. Species of *Apertostella* are distinguished by a typically more closed meshwork, third row of autozooecia at sites of branch bifurcation and for pronounced distances along the branch proximal to sites of branch bifurcation, and chambers that open generally parallel to the plane of obverse surface. Species of *Apertostella* also typically exhibit a less cubic and more rectangular chamber shape than species of *Cubifenestella*, and have a more highly ovate apertural shape.

Similarities between the two genera suggest close phylogenetic affinities, however difference in chamber orientation to the obverse surface is consistently present between them. The orientation of the chamber relative to the zoarial surface, which is very different in *Cubifenestella* and *Apertostella*, apparently would have had a great effect on polypide feeding.

Table 29.—Summary numerical analysis of *Apertostella foramenmajor*, n. sp. For explanation of abbreviations of characters (left column), see Table 8b (foldout inside back cover).

	number of measurements	mean	standard deviation	coefficient of variation	observed range
1. **WB**	24	0.3030	0.0608	20.07	0.213–0.488
2. **DBC**	24	0.5033	0.0678	13.47	0.313–0.612
3. **WD**	24	0.1591	0.2063	16.53	0.107–0.212
4. **LF**	24	0.5627	0.0793	14.09	0.433–0.740
5. **WF**	24	0.2571	0.0425	16.53	0.133–0.333
6. **AF**	24	3.33	0.48	14.45	3–4
7. **AL**	24	0.1246	0.0108	8.67	0.105–0.145
8. **AW**	24	0.0718	0.0070	9.75	0.063–0.093
9. **ADB**	24	0.2457	0.0255	10.38	0.208–0.295
10. **AAB**	24	0.2376	0.0246	10.35	0.188–0.290
11. **ABB**	24	0.2981	0.0645	21.64	0.137–0.425
12. **DN**	24	0.0969	0.0144	14.86	0.073–0.132
14. **SNB**	24	0.4867	0.1097	22.54	0.317–0.655
15. **WK**	24	0.0099	0.0015	15.15	0.008–0.013
18. **WP**	24	0.0170	0.0091	11.18	0.014–0.022
21. **RSL**	24	0.1128	0.0347	30.76	0.063–0.167
22. **RSS**	24	0.0383	0.0131	34.20	0.027–0.088
23. **SSL**	24	0.5790	0.2514	43.42	0.206–1.047
24. **SSS**	24	0.0767	0.0239	31.16	0.042–0.141
32. **TRW**	24	0.0080	0.0020	25.00	0.005–0.011
33. **TLW**	24	0.0070	0.0010	14.29	0.005–0.009
34. **FWT**	24	0.0432	0.0194	44.91	0.019–0.084
35. **RWT**	24	0.0650	0.0353	54.22	0.018–0.131
36. **CL**	24	0.1979	0.0063	3.18	0.189–0.210
37. **CD**	24	0.1592	0.0062	3.89	0.146–0.175
38. **MAW**	24	0.1338	0.0082	6.13	0.116–0.146
39. **MIW**	24	0.0967	0.0069	7.14	0.086–0.112
40. **VD**	24	0.0494	0.0115	23.28	0.036–0.072
41. **RA**	24	67.79	4.42	6.52	59–77
42. **LA**	24	25.33	3.96	15.65	18–34
43. **TB**	24	0.3083	0.0365	11.84	0.259–0.378

Species composition.—Three species are assigned to this genus: *A. foramenmajor*, n. sp., *A. crassata*, n. sp., and *A. venusta*, n. sp.

Range.—Lower Mississippian (Valmeyeran); present in the Keokuk, Warsaw, Salem and St. Louis formations.

Text-figure 14.—*Apertostella crassata* illustrated. 1, diagrammatic longitudinal section illustrating changing chamber outline from deep section near middle of branch (bottom of figure) to shallow section near abaxial edge of branch (top of figure) [Observe lack of hemisepta characteristic of this genus.], ×70; 2, diagrammatic tangential section illustrating changing chamber outline from deep section near reverse-wall budding-site (bottom of figure) to shallow section near obverse surface (top of figure) [Typical ovate aperture opening is shown (arrow).], ×70; 3, diagrammatic transverse section across branch, ×70; 4, reconstruction of typical chamber shape (three-dimensional) as viewed from distal end of branch; chamber reconstructed is from the right side of branch, ×140; 5, reconstruction of typical chamber shape (three-dimensional) as viewed from abaxial edge of branch, ×140; 6, reconstruction of typical chamber shape (three-dimensional) as viewed from obverse surface; chamber reconstructed is from the right side of branch [Observe slight displacement of aperture opening toward abaxial edge of chamber.], ×140.

Apertostella foramenmajor, new species
Plate 35, figures 1–12, Plate 36, figures 1–3; Table 29

Etymology of name.—Named for the relatively large apertural openings that characterize the species.

Diagnosis.—Zoarium robustness intermediate, mesh spacing lower-end intermediate, pattern regular; branch robustness intermediate, width lower-end intermediate, depth lower-end medium; branches straight to broadly curved toward zoarial edge; transversely asymmetrically ovate, flattened on obverse surface, branches moderately closely spaced and joined at regular intervals by thin to lower-end intermediate width, relatively short dissepiments. Fenestrule size intermediate; shape more elliptical on obverse, more rect-

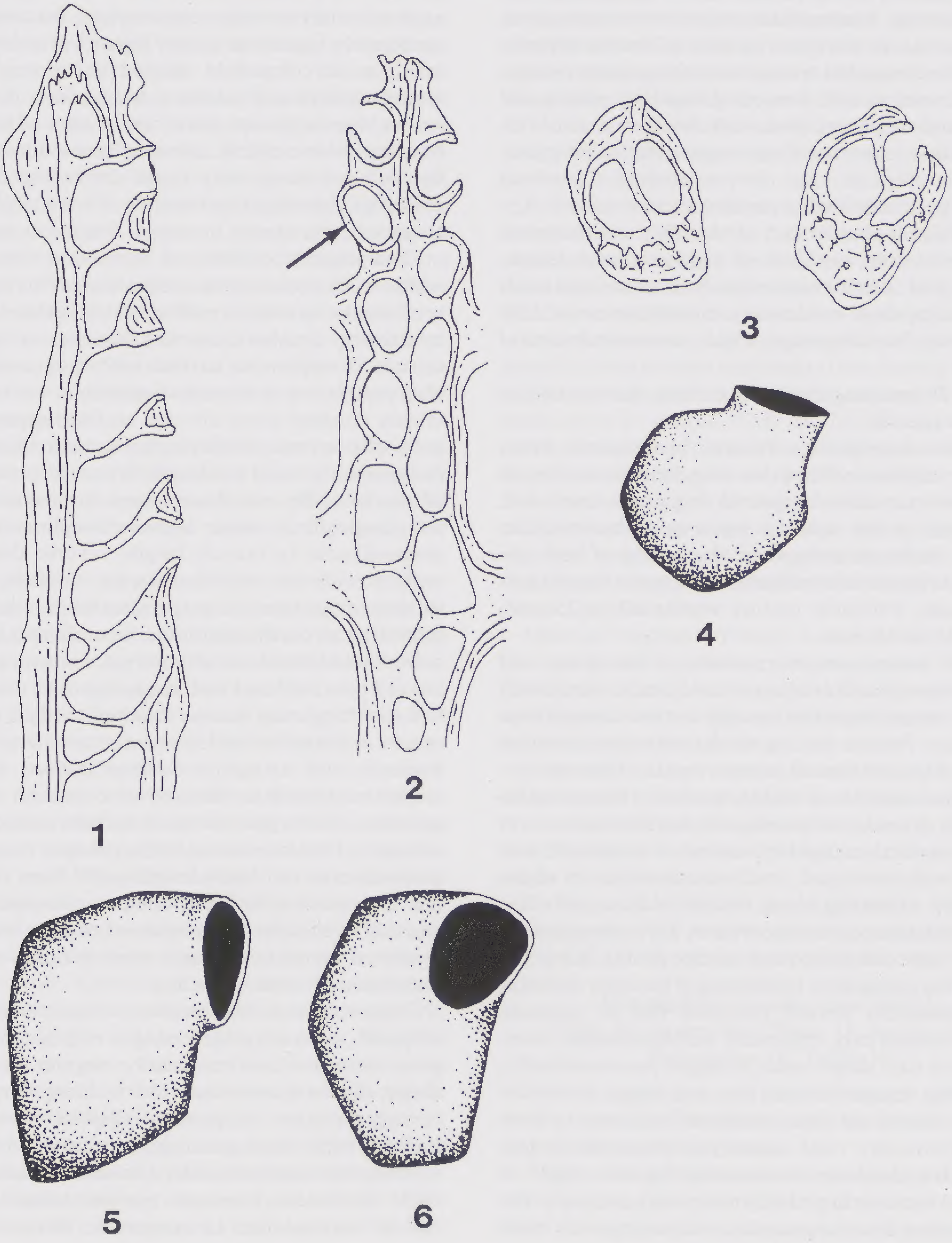

angular on reverse surface, regular. Autozooecial aperture size upper-end intermediate, large relative to branch width, shape ovate, elongate proximodistally; surrounded by thin, extremely well-developed complete peristome; three to four (most commonly three) apertures per fenestrule. Single narrow, continuous keel; straight to slightly sinuous, extending along middle of obverse branch surface, atop which are positioned intermediate-size, ovate nodes. Autozooecial chamber size lower-end intermediate, chambers emplaced in two rows, except third row at sites of branch bifurcation; outline rounded triangular to irregularly pentagonal near reverse wall, becoming angularly pentagonal toward mid chamber; from mid chamber toward obverse surface, chamber shape rectangular to elliptical, irregularly elliptical near obverse surface. Chambers elongate proximodistally, parallel to reverse wall. Aperture at distal-abaxial end of chamber, connected to chamber by short vestibule of highly variable length. Superior and inferior hemisepta both absent. Lateral-wall budding-angle moderately variable (mean of 25°); reverse-wall budding-angle highly constant (mean of 68°).

Table 29 presents statistical criteria used in delimiting this species.

Exterior description.—Zoarium robustness intermediate, expansion flat, exhibiting little or no obverse or reverse curvature in zoarial fragments examined, fan-shaped; mesh spacing lower-end intermediate; slight to moderate astogenetic thickening of both obverse and reverse zoarial skeleton; external zoarial pattern regular. Probable mature widths 20 to 25 mm, lengths 30 to 40 mm.

Branch robustness intermediate, width lower-end intermediate, moderately variable; most frequently straight, lateral branches broadly curved toward edge of zoarium. Branch spacing moderately close, distance between adjacent branch centers regular. Obverse surface texture smooth to slightly granular, becoming increasingly granular with astogeny; surface flat or very slightly rounded, except for presence of single keel; keel narrow, well-developed, continuous, straight to slightly sinuous, extending along branch midline and curving around autozooecial apertures; keel causing slight positive inflection in obverse surface profile. Keel covered during astogenetic thickening of lamellar skeleton, most prominent toward proximal end of zoarium. Nodes monoserially emplaced, well-developed, intermediate in size, shape ovate, elongate proximodistally; moderately regular in both size and shape; nodes develop as extensions from middle of keel; two to three (most commonly two) nodes per fenestrule length; spacing intermediate, moderately regular; slight to moderate increase in node diameter with astogeny. Reverse surface texture granular, coarsening with astogeny, bearing an intermediate number of moderately closely spaced longitudinal striae, evident in exterior view at most distal end of zoarium, becoming covered by astogenetically thickened lamellar skeleton toward proximal end of zoarium; large microstylets positioned atop striae, emplaced in rows, closely spaced; microstylets highly variable in size and placement, increasing in diameter and becoming more irregularly positioned across reverse branch surface with astogeny. Large, approximately circular macrostylets, variable in size, moderately regular in shape, highly variable in placement, most commonly located at or near sites of branch–dissepiment junction. Autozooecia in two rows across branch, except third row at sites of branch bifurcation where middle autozooecium evidently shared by both branches, very slight thickening of branch proximal, thinning distal to sites of branch bifurcation. Heterozooecia absent in zoarial fragments analyzed.

Dissepiments of thin to lower-end intermediate width, width approximately equal to half that of branch, moderately variable in width; relatively short in length, moderately constant; connect branches at regular intervals. Dissepiments barlike, with slight medial thinning and flaring at branch–dissepiment contact; moderately recessed from obverse surface, approximately even with reverse. Moderate astogenetic thickening of dissepiments, most pronounced toward proximal end of zoarium. Obverse dissepiment surface with two to five longitudinal striae across dissepiment oriented perpendicular to branch length; reverse dissepiment surface with one well-developed, medially located, thickened bar oriented perpendicular to branch length extending across dissepiments; dissepiments highly angular toward distal end of zoarium, becoming rounded toward proximal end with astogeny; rows of small stylets occurring atop reverse dissepiment bar, stylets increase in diameter and become more irregularly positioned with astogeny. Surface texture similar to respective branch surface; obverse smooth to slightly granular, reverse granular; both surfaces coarsening with astogeny. Emplacement of dissepiments ranging from perpendicular to branch length to 20° from perpendicular. Apertures commonly open on proximal or distal edge, or in middle of dissepiment edge at branch–dissepiment contact; arranged symmetrically or asymmetrically between branches.

Fenestrule size intermediate; shape rectangular to elliptical, becoming increasingly elliptical with astogeny, elongate proximodistally; regular in size and shape; slight expansion of width and length in obverse–reverse direction, shape more elliptical from obverse surface, more rectangular from reverse. Mean width of fenestrule approximately two-thirds branch width; slight decrease in fenestrule opening toward proximal end of zoarium due to astogenetic thickening of la-

mellar skeleton. Ratio of fenestrule mean width to length approximately 1:2; width and length both moderately constant. Three to four (most commonly three) apertures per fenestrule length; distance between closest aperture centers along branch and across branch approximately equal, spacing of aperture centers across fenestrule 1.3 times greater; spacing along and across branch constant, spacing across fenestrule moderately variable.

Autozooecial aperture size upper-end intermediate, large relative to branch width; apertures ovate, elongate proximodistally, width to length ratio approximately 4:7; size and shape moderately uniform; opening orientation most commonly at a slight angle toward fenestrule, more rarely parallel to plane of obverse surface; surrounded by thin, extremely well-developed, complete peristome; peristome exhibiting slight thinning at proximal end. Aperture margins exhibiting no or slight extension into fenestrule, the latter causing very slight inflections in fenestrule outline on obverse surface. Centrally thickened terminal diaphragms present, rare; most common at proximal end of zoarium.

Zoarial supports develop as extensions of reverse zoarial surface and lateral edge of zoarium, moderately rare in occurrence.

Interior description.—Branches asymmetrically ovate in transverse section, flattened and slightly enlarged on obverse surface, elongate parallel to plane of zoarial surface. Branches lower-end medium, highly regular in depth.

Autozooecial living chamber size lower-end intermediate, chambers arranged in alternating rows along planar axial wall; axial wall highly sinuous, extending toward and connecting with chamber lateral walls near reverse wall of zoarium, becoming relatively straight with only slight inflections toward lateral walls in mid chamber and near obverse surface. Chamber longest dimension paralleling reverse wall in proximodistal direction. Autozooecial chamber outline rounded triangular to irregularly pentagonal near reverse wall, becoming more angularly pentagonal toward mid chamber; from mid chamber toward obverse surface, chamber shape rectangular to elliptical; in shallow obverse section, chamber becomes irregularly elliptical, slightly enlarged at distal-abaxial end; chamber shape highly uniform. Aperture positioned at distal-abaxial end of chamber, connected to chamber by short, poorly developed, highly variable length vestibule. Ratio of autozooecial chamber minimum width to maximum width approximately 3:4; maximum width to depth ratio 5:6; ratio of depth to length of chamber approximately 4:5; chamber length and depth slightly more constant than minimum and maximum widths, all dimensions highly constant. Superior and inferior hemisepta both absent. Autozooecial chambers diverge laterally from middle of branch at variable angle (mean of 25°); from reverse wall at a highly uniform angle (mean of 68°).

Three-dimensionally reconstructed chamber form a rectangular box; length as viewed from lateral edge of branch; depth as viewed from distal end of branch slightly greater than width as viewed from obverse surface.

Internal granular skeletal layer thin to intermediate, continuous with obverse nodes, keel, peristome, and dissepiment striae; reverse longitudinal striae, microstylets and macrostylets; across dissepiments and in the middle of zoarial supports. Outer lamellar layer thickness intermediate, exhibiting slight to moderate astogenetic thickening, most pronounced toward proximal end of zoarium.

Remarks.—The exterior pattern of *Exfenestella exigua* (Ulrich, 1890) is very similar to that of *Apertostella foramenmajor*, n. sp. However, *A. foramenmajor* has a much smaller chamber than does *E. exigua*, lacks hemisepta (whereas the latter has both superior and inferior hemisepta), and has chambers whose length is parallel to the reverse wall rather than having the longest chamber dimension paralleling the lateral chamber walls, as in *E. exigua*. This species-pair provides yet another example of taxonomic problems that can result from excessive reliance on specimen exteriors.

A. foramenmajor is distinguished from other species of *Apertostella* by a larger chamber and aperture openings that are large relative to branch width. Interior chamber dimensions are highly characteristic for species of *Apertostella*.

Material studied.—Twenty-two exterior fragments, five sectioned specimens; largest zoarial fragment 20×28 mm (width to length). Although microstructurally unaltered, many zoarial fragments are crushed due to compaction of shales.

Occurrence.—*Apertostella foramenmajor* is moderately common at the Keokuk and Warsaw localities. It occurs as far south as Jerseyville, and is most frequently found in shales, although some fragments occur in biocalcarenites.

Holotype.—UI X-6766 (loc. 11, sample 53).

Paratypes.—UI X-6745 (loc. 11, samples 53, 57), 6721, 6722, 6770 (loc. 10, samples 28, 33).

Apertostella crassata, new species
Plate 36, figures 4–9, Plate 37, figures 1–9;
Text-figure 14; Table 30

Etymology of name.—The species name refers to the closely spaced mesh and small fenestrule openings characteristic of this species.

Diagnosis.—Zoarium robust, mesh spacing extremely close, pattern highly regular; branches moderately robust, width intermediate, moderately deep in

thickness, straight to sinuous, broadly curved at lateral zoarial edge; transversely irregularly polygonal to approaching ovate, very closely spaced and joined at highly regular intervals by intermediate-width, short dissepiments. Fenestrule size small; shape ovate on obverse surface, becoming elliptical on reverse, moderately regular. Autozooecial aperture size upper-end intermediate, shape ovate, highly elongate proximo-abaxially; surrounded by thin, intermediately developed, complete peristome; two to three (most commonly three) apertures per fenestrule. Single moderately narrow, continuous keel; straight to slightly anastomosing, extending along middle of obverse branch surface, atop which are positioned intermediate-size ovate nodes. Autozooecial chamber size lower-end intermediate, chambers emplaced in two rows, except third row at sites of branch bifurcation, rarely three rows for short distances proximal to sites of branch bifurcation; outline irregular rounded-triangular to polygonal near reverse wall, rapidly becoming irregularly pentagonal in mid and throughout most of chamber, ovate to elliptical in shape near obverse surface. Chambers elongate parallel to reverse wall in proximodistal direction. Aperture at distal-abaxial end of chamber, connected to chamber by intermediate-length vestibule; vestibule length variable. Superior and inferior hemisepta both absent. Lateral-wall budding-angle variable (mean of 22°); reverse-wall budding-angle constant (mean of 67°).

Table 30 presents statistical criteria used in delimiting this species.

Exterior description.—Zoarium robust, expansion flat to slightly undulating, fan-shaped; mesh spacing extremely close; pronounced astogenetic thickening of both obverse and reverse zoarial skeleton; external zoarial pattern highly regular. Probable mature widths 40 to 50 mm, lengths up to 60 mm.

Branches moderately robust, width intermediate, constant; straight to slightly sinuous in trace, with inflections toward sites of dissepiment insertion, lateral branches commonly broadly curved toward edge of zoarium. Branch spacing very close, distance between adjacent branch centers highly regular. Obverse surface texture slightly granular, remaining texturally the same throughout astogeny; surface regularly angular to slightly rounded, except for presence of single keel; keel moderately narrow, well-developed, continuous, straight to slightly anastomosing extending along branch midline and causing moderate positive inflection in obverse surface profile. Keel becomes covered by lamellar skeleton during astogeny. Nodes monoserially emplaced, poorly developed, intermediate in size, highly ovate, elongate proximodistally; regular in both size and shape; develop as projections from middle of keel; one to two per fenestrule length, spacing intermediate, constant; nodes partially to completely covered by lamellar skeleton with astogeny. Reverse surface texture granular, coarsening with astogeny, bearing few rows of widely spaced longitudinal striae, evident in exterior view at most distal end of zoarium, becoming covered immediately proximal from zoarial distal edge due to astogenetic thickening of lamellar skeleton; rows of very small microstylets develop atop longitudinal striae; microstylets closely spaced, become variably positioned across entire reverse surface and exhibit slight increase in diameter with astogeny. Autozooecia in two rows across branch; except third row at sites of branch bifurcation where middle autozooecium evidently shared by both branches, rarely three rows for short distances proximal to sites of branch bifurcation; pronounced thickening proximal, thinning distal to sites of branch bifurcation. Heterozooecia absent in all zoarial fragments examined.

Dissepiments of intermediate width, approximately seven-eighths width of branch, moderately constant; short in length, constant; connect branches at highly regular intervals. Dissepiments thin medially, exhibit pronounced flaring at branch–dissepiment contact;

Table 30.—Summary numerical analysis of *Apertostella crassata*, n. sp. For explanation of abbreviations of characters (left column), see Table 8b (foldout inside back cover).

	number of measurements	*mean*	*standard deviation*	*coefficient of variation*	*observed range*
1. **WB**	24	0.3471	0.0436	12.56	0.283–0.480
2. **DBC**	24	0.5067	0.0536	10.58	0.413–0.603
3. **WD**	24	0.2976	0.0475	15.96	0.191–0.410
4. **LF**	24	0.4053	0.0680	16.78	0.238–0.505
5. **WF**	24	0.1567	0.0206	17.05	0.125–0.200
6. **AF**	24	2.83	0.38	13.44	2–3
7. **AL**	24	0.1401	0.0069	4.93	0.127–0.154
8. **AW**	24	0.0962	0.0046	4.78	0.086–0.108
9. **ADB**	24	0.2158	0.0167	7.74	0.184–0.253
10. **AAB**	24	0.2218	0.0190	8.57	0.192–0.262
11. **ABB**	24	0.2970	0.0351	11.82	0.228–0.365
12. **DN**	24	0.0852	0.0122	14.32	0.069–0.115
14. **SNB**	24	0.3761	0.0574	15.26	0.239–0.464
15. **WK**	24	0.0470	0.0087	18.51	0.039–0.068
18. **WP**	24	0.0090	0.0021	23.80	0.005–0.012
22. **RSS**	24	0.0087	0.0020	23.09	0.006–0.011
24. **SSS**	24	0.0286	0.0109	38.11	0.018–0.060
32. **TRW**	24	0.0093	0.0020	21.51	0.005–0.013
33. **TLW**	24	0.0081	0.0019	22.96	0.006–0.102
34. **FWT**	24	0.0594	0.0222	37.37	0.029–0.143
35. **RWT**	24	0.1208	0.0616	50.99	0.034–0.280
36. **CL**	24	0.2015	0.0070	3.47	0.189–0.214
37. **CD**	24	0.1767	0.0072	4.07	0.165–0.193
38. **MAW**	24	0.1363	0.0177	12.99	0.115–0.193
39. **MIW**	24	0.0764	0.0141	18.46	0.052–0.104
40. **VD**	24	0.0661	0.0115	17.40	0.051–0.091
41. **RA**	24	67.04	5.84	8.71	53–78
42. **LA**	24	21.58	3.50	16.22	17–31
43. **TB**	24	0.4157	0.0715	17.20	0.326–0.587

highly recessed from obverse, approximately even with reverse surface. Moderate to pronounced astogenetic thickening of dissepiments toward proximal end of zoarium. Obverse dissepiment surface lacking ornamentation; reverse surface with longitudinal striae oriented perpendicular to branch length atop which are positioned small stylets; striae covered and stylets increase in diameter, become more irregularly positioned with astogeny. Obverse dissepiment surface texture slightly granular, remaining the same with astogeny; reverse surface texture granular, coarsening with astogeny. Emplacement of dissepiments ranging from perpendicular to branch length to angles deviating up to 20° from perpendicular. Apertures commonly positioned on proximal or distal edge or in middle of dissepiment edge at branch–dissepiment contact; arranged symmetrically or asymmetrically between branches.

Fenestrule size small; shape ovate on obverse surface, becoming elliptical on reverse, elongate proximodistally; moderately regular in size and shape; slight to moderate expansion of fenestrule width and length in obverse–reverse direction. Mean width of fenestrule slightly less than half branch width on obverse surface, greater than half branch width on reverse; fenestrule opening decreasing in size, becoming appreciably smaller to completely closed toward proximal end of zoarium with astogenetic thickening of lamellar skeleton. Ratio of fenestrule mean width to length approximately 3:10; width slightly more constant than length, both moderately constant. Two to three (most commonly three) apertures per fenestrule length; distance between closest aperture centers along branch and across branch approximately equal; distance between apertures across fenestrule approximately 1.35 times greater; spacing along and across branch constant, spacing across fenestrule slightly variable.

Autozooecial aperture size upper-end intermediate, shape ovate, highly elongate proximoabaxially, width to length ratio approximately 2:3; size highly uniform, shape moderately uniform; opening most commonly oriented parallel to plane of obverse surface, rarely at slight angle toward fenestrule; thin, intermediately developed complete peristome surrounding aperture. No extension of aperture margin into fenestrule, apertures even with obverse branch surface. Thin, uniform thickness terminal diaphragms cover some apertures, most common near proximal end of zoarium.

Zoarial supports develop near proximal end of zoarium, form as extension of lateral zoarial edge and reverse zoarial surface.

Interior description.—Branches irregularly polygonal to approaching ovate in transverse section, irregular shape due to astogenetic thickening of lamellar skeleton; branches commonly slightly flaring on obverse surface, elongate either in obverse–reverse direction or parallel to plane of obverse surface. Branches moderately deep, variable in thickness.

Autozooecial chamber size lower-end intermediate, chambers biserially arranged in alternating rows along planar branch axial wall; axial wall sinuous, anastomosing toward sites of lateral-wall emplacement near reverse wall, becoming relatively straight, exhibiting slight inflections toward lateral walls from mid chamber to obverse surface. Chamber longest dimension only slightly greater than depth, elongate parallel to reverse wall in proximal–distal direction. Autozooecial chamber outline irregular, rounded triangular to polygonal near reverse wall; rapidly becoming irregularly pentagonal in shape throughout mid chamber and toward obverse surface; ovate to elliptical in shape near obverse surface, slightly enlarged at distal end; chamber shape moderately uniform. Aperture positioned at distal-abaxial end of chamber, connected to chamber by well-developed, intermediate-length vestibule; vestibule length variable. Ratio of autozooecial chamber minimum width to maximum width approximately 5:9; maximum width to depth ratio about 7:9; depth to length ratio about 7:8. Superior and inferior hemisepta both absent. Autozooecial chambers diverge laterally from middle of branch at a variable angle (mean of 22°); from reverse wall at a constant angle (mean of 67°).

Three-dimensionally reconstructed chamber form a rectangular box; length as viewed from lateral edge of branch; depth as viewed from distal end of branch, and width as viewed from obverse surface.

Internal granular layer width intermediate, well-developed; continuous with obverse nodes, keel, and peristome; reverse longitudinal striae and microstylets; across dissepiments and in the middle of zoarial supports. Outer lamellar skeletal layer usually thick, exhibiting pronounced astogenetic thickening on both obverse and reverse exterior surfaces, most pronounced thickening occurring at proximal end of zoarium.

Remarks.—The robust fan, close mesh, and small fenestrule openings allow relatively easy exterior recognition of *Apertostella crassata*, n. sp. Although exteriors of this species are similar to those of species of *Hemitrypa* Phillips, 1841, *A. crassata* is readily assigned to *Apertostella* by its lack of exterior secondary reticulate structure, difference in fenestrule shape and size, and interior characters such as autozooecial chamber size and shape.

A. crassata is distinguished from other species of *Apertostella* by having the largest chamber size, most closely spaced mesh, fewest number of apertures per fenestrule, and largest size aperture opening. All species of *Apertostella* have extremely similar reverse-wall and

lateral-wall budding-angles, characters extremely constant within this genus.

Material studied.—Twenty-eight exterior fragments; four sectioned specimens; largest zoarial fragment 30×38 mm (width to length). The robust fan in this species resulted in the collection of many large, nearly complete zoarial fragments. The preservation of fragments is also good, although some colonies have been crushed by shale compaction.

Occurrence.—*Apertostella crassata* is present in the Warsaw Formation and Upper Keokuk Formation in the northern half of the study area. It is most common near Keokuk, Iowa and Warsaw, Illinois, but occurs as far south as White Hall, and is found in both limestones and shales.

Holotype.—UI X-6737 (loc. 10, sample 28).

Paratypes.—UI X-6738–6740 (loc. 10, samples 28, 35).

Apertostella venusta, new species

Plate 38, figures 1–9, Plate 39, figures 1–5; Table 31

Etymology of name.—Name refers to the pleasing exterior appearance of this species.

Diagnosis.—Zoarium delicate, mesh spacing upper-end intermediate, pattern moderately regular; branches robust, width lower-end wide, medium in thickness; straight to broadly curved toward lateral zoarial edge; transversely irregularly ovate to elliptical, flattened or slightly concave on obverse surface, intermediately spaced and joined at highly regular intervals by intermediate width and length dissepiments. Fenestrules large; shape elliptical to approaching rectangular, moderately constant. Autozooecial aperture size intermediate, ovate, elongate proximodistally; surrounded by thin, well-developed, complete peristome with very small stylets projecting from peristome outer edge; five to six apertures per fenestrule. Single intermediate-width, continuous keel, straight to slightly sinuous, extending along middle of obverse branch surface, atop which are positioned lower-end large size, circular or ovate nodes. Autozooecial chamber size intermediate, chambers emplaced in two rows, except either third row at sites of branch bifurcation or three rows for short distances along branch proximal to sites of branch bifurcation; outline rounded triangular near reverse wall, rapdily becoming irregularly pentagonal throughout mid chamber, irregularly elliptical near obverse surface with ellipse elongate distal-abaxially. Chambers elongate parallel to reverse wall in proximodistal direction. Aperture at distal-abaxial end of chamber, connected to chamber by short, variable-length vestibule. Superior and inferior hemisepta both absent. Lateral-wall budding-angle slightly variable (mean of 22°); reverse-wall budding-angle highly constant (mean of 69°).

Table 31.—Summary numerical analysis of *Apertostella venusta*, n. sp. For explanation of abbreviations of characters (left column), see Table 8b (foldout inside back cover).

	number of measurements	*mean*	*standard deviation*	*coefficient of variation*	*observed range*
1. **WB**	24	0.3952	0.0673	17.03	0.298–0.556
2. **DBC**	24	0.7297	0.1884	25.82	0.375–1.081
3. **WD**	24	0.2651	0.0567	21.39	0.173–0.363
4. **LF**	24	1.3480	0.1525	11.31	1.125–1.556
5. **WF**	24	0.4292	0.0833	19.41	0.300–0.600
6. **AF**	24	5.67	0.49	8.68	5–6
7. **AL**	24	0.1211	0.0094	7.76	0.098–0.148
8. **AW**	24	0.0746	0.0072	9.65	0.058–0.088
9. **ADB**	24	0.2956	0.0312	10.55	0.250–0.356
10. **AAB**	24	0.3145	0.0346	11.00	0.253–0.375
11. **ABB**	24	0.4775	0.1010	21.15	0.325–0.650
12. **DN**	24	0.1282	0.0208	16.22	0.015–0.275
14. **SNB**	24	1.2780	0.3285	25.70	0.790–1.920
15. **WK**	24	0.0606	0.0121	19.97	0.042–0.085
16. **DSO**	24	0.0382	0.0161	42.15	0.019–0.068
17. **SSO**	24	0.0685	0.0333	48.61	0.041–0.104
18. **WP**	24	0.0231	0.0048	20.78	0.015–0.030
22. **RSS**	24	0.0138	0.0039	28.26	0.012–0.028
24. **SSS**	24	0.0310	0.0106	34.19	0.023–0.078
32. **TRW**	24	0.0204	0.0032	15.69	0.014–0.027
33. **TLW**	24	0.0152	0.0028	18.42	0.011–0.020
34. **FWT**	24	0.0528	0.0192	36.36	0.025–0.085
35. **RWT**	24	0.0688	0.0324	48.55	0.024–0.154
36. **CL**	24	0.3555	0.0127	4.97	0.338–0.371
37. **CD**	24	0.1743	0.0114	6.54	0.156–0.193
38. **MAW**	24	0.1636	0.0133	8.13	0.144–0.191
39. **MIW**	24	0.1028	0.0213	20.72	0.075–0.148
40. **VD**	24	0.0582	0.0167	28.69	0.035–0.088
41. **RA**	24	69.08	4.48	6.49	62–76
42. **LA**	24	22.42	3.34	14.91	8–29
43. **TB**	24	0.3583	0.0855	23.86	0.214–0.525

Table 31 presents statistical criteria used in delimiting this species.

Exterior description.—Zoarium delicate, expansion flat to slightly obversely curved, fan-shaped; mesh spacing upper-end intermediate; moderate astogenetic thickening of both obverse and reverse zoarial skeleton; external zoarial pattern moderately regular. Probable mature widths 30 to 40 mm, lengths up to 50 or 60 mm.

Branches robust, width lower-end wide, moderately variable; straight to broadly curved toward lateral edge of zoarium. Branch spacing intermediate, distance between adjacent branch centers irregular. Obverse branch surface texture granular, becoming increasingly so with astogeny; surface flat to slightly concave, except for presence of single, intermediate-width keel; keel moderately well-developed, continuous, straight to slightly sinuous, extending along branch midline and causing slight positive inflection in obverse surface profile. Slight astogenetic thickening of keel, with keel becoming covered by lamellar skeleton during astogenetic

thickening of obverse surface. Nodes monoserially emplaced, well-developed, size lower-end large; shape circular to ovate, elongate proximodistally; moderately constant in both size and shape; nodes develop as projections from middle of keel; most commonly one, more rarely two nodes per fenestrule length; nodes widely, unevenly spaced; moderate increase of node diameter with astogeny. Large, highly variable size stylets irregularly positioned across obverse surface; stylets exhibiting slight astogenetic thickening. Reverse surface texture granular, becoming more coarsely so with astogeny; bearing numerous rows of closely spaced longitudinal striae which become partially covered by astogenetic thickening of lamellar skeleton; rows of small, closely spaced microstylets develop as extensions of longitudinal striae; microstylets become variably spaced across entire reverse surface and exhibit slight increase in diameter with astogeny. Autozooecia in two rows across branch; except either third row at sites of branch bifurcation where middle autozooecium evidently shared by both branches or three rows for short distances along branch proximal to sites of branch bifurcation; slight thickening proximal, thinning distal to sites of branch bifurcation. Heterozooecia absent in all zoarial fragments obversed.

Dissepiments of intermediate width, approximately two-thirds that of branch, slightly variable in width; length intermediate, slightly constant; connect branches at highly regular intervals. Dissepiments moderately barlike, exhibiting slight medial thinning and slight flaring at branch–dissepiment junction; highly recessed from obverse surface, slightly recessed from reverse. Slight astogenetic thickening toward proximal end of zoarium. Obverse dissepiment surface with four to six longitudinal striae oriented perpendicular to branch length, large stylets similar in size to obverse stylets positioned across dissepiment surface not covered by striae; striae partially covered by astogenetic thickening of lamellar skeleton, stylets increase in diameter with astogeny; reverse surface bearing numerous rows of longitudinal striae oriented perpendicular to branch width, rows of closely spaced small stylets atop striae; striae become covered by secondary lamellar thickening, stylets increase in diameter and become more irregularly positioned across dissepiment surface with astogeny. Both obverse and reverse dissepiment surfaces granular in texture, becoming increasingly so with astogeny. Emplacement of dissepiments perpendicular or approximately perpendicular to branch length. Apertures commonly positioned on proximal or distal edge or in middle of dissepiment edge at branch–dissepiment contact; arranged symmetrically or asymmetrically between branches.

Fenestrules large, shape elliptical to approaching rectangular, highly elongate proximodistally; shape moderately constant, size slightly constant; opening constant in size and shape on both obverse and reverse surfaces. Mean width of fenestrule slightly greater than branch width; astogenetic thickening, primarily toward proximal end of zoarium, causing slight infilling of fenestrule opening. Ratio of mean fenestrule width to length approximately 1:3; length moderately constant, width slightly variable. Five to six apertures per fenestrule length; distance between closest aperture centers along branch and across branch approximately equal, spacing of apertures across fenestrule 1.5 times greater; spacing along and across branch slightly variable, spacing across fenestrule highly variable.

Autozooecial aperture size intermediate, shape ovate, elongate proximodistally, width to length ratio 3:5; size highly uniform, shape variable; opening at a slight angle toward fenestrule or parallel to plane of obverse surface; thin, well-developed complete peristome surrounding aperture, commonly with very small stylets irregularly projecting from peristome outer edge. Aperture margins extend into fenestrule, causing very slight inflections in fenestrule outline on obverse surface. Terminal diaphragms lacking.

Zoarial supports rare, observed at most proximal reverse side and lateral zoarial edges.

Interior description.—Branches irregularly ovate to elliptical in transverse section, frequently flattened or slightly concave on obverse surface, enlarged on obverse surface, elongate parallel to plane of zoarial surface. Branches medium in thickness, variable.

Autozooecial living chambers intermediate in size, biserially arranged in alternating rows along planar branch axial wall; axial wall zigzags, extending diagonally across entire branch near reverse chamber wall; sinuous, anastomosing toward and connecting with chamber lateral walls throughout the rest of chamber. Chamber longest dimension paralleling reverse wall in proximodistal direction. Autozooecial chamber outline rounded triangular near reverse wall; rapidly becoming irregularly pentagonal throughout all but most obverse end of chamber where chamber becomes irregularly elliptical in shape, ellipse elongate distal-abaxially relative to branch length; chamber shape moderately uniform. Apertures positioned at distal-abaxial end of chamber, connected to chamber by short, moderately well-developed, variable-length vestibule. Ratio of autozooecial chamber minimum width to maximum width approximately 5:8; chamber depth slightly less than maximum chamber width, ratio about 15:16; ratio of chamber depth to length approximately 2:3; chamber length, depth and maximum width highly constant, minimum width highly variable. Superior and inferior hemisepta both absent. Autozooecial chambers diverge laterally from middle of branch at a slightly variable angle (mean of 22°); from reverse wall

at a highly constant angle (mean of 69°).

Three-dimensionally reconstructed chamber form an irregular rectangular box; length as viewed from lateral edge of branch; depth and width approximately equidimensional, as viewed from distal end of branch and obverse surface, respectively.

Internal granular skeletal layer relatively thick, well-developed; continuous with obverse nodes, keel, stylets, and peristome; reverse longitudinal striae and stylets; across dissepiments and in the middle of zoarial supports. Moderate astogenetic thickening of lamellar skeletal layer, most pronounced toward proximal end of zoarium.

Remarks.—*Apertostella venusta*, n. sp. is distinguished from other species of the genus by a coarser mesh, much greater number of apertures per fenestrule length, obverse stylets, wider branches, and much larger autozooecial chambers. The open mesh in *A. venusta* is not typical of *Apertostella*, but the chamber shape, large aperture size relative to branch width, and lateral-wall and reverse-wall budding-angles are typical of this genus.

The relatively rare occurrence and frequent poor preservation of this species may account for its not being recognized by Ulrich in his extensive work on the Mississippian bryozoans around Keokuk, Iowa and Warsaw, Illinois.

Material studied.—Fourteen exterior fragments; four sectioned specimens; largest zoarial fragment 22×31 mm (width to length). Microstructurally most material is well-preserved, although mechanical crushing of fragments is common due to compaction of muds in shale development.

Occurrence.—*Apertostella venusta*, n. sp. is extremely rare in the Upper Keokuk and Warsaw formations in localities from Mt. Sterling to Keokuk. It is most commonly found in shale beds on the surfaces of thin limestone lenses.

Holotype.—UI X-6875 (loc. 10, sample 33).

Paratypes.—UI X-7028–7030 (loc. 10, samples 25, 28).

Genus **HEMITRYPA** Phillips, 1841

Type species.—*Hemitrypa oculata* Phillips, 1841 [Devonian of England].

Typical Warsaw species.—*H. perstriata* Ulrich, 1890, p. 564, pl. 57, figs. 6, 6a [Keokuk Group: Bentonsport and Keokuk, Iowa].

Diagnosis.—Zoarium robustness delicate to robust, mesh spacing close to intermediate; reticulate meshwork present, developed as extension of keel across obverse zoarial surface; chamber outline an irregular pentagon, rectangle to parallelogram in mid tangential section; chamber size intermediate; aperture size intermediate to large; hemisepta absent; chamber reverse-wall budding-angle varies between 60° and 70° (means).

Three-dimensionally reconstructed chamber form an irregular rectangular to cubic box.

Description.—Zoarium robustness delicate to robust, expansion flat, undulating to obversely or reversely curved, mesh spacing close to intermediate, regular to variable; reticulate meshwork present, develops as extension of keel and extends across obverse zoarial surface in middle and at proximal ends of the zoarium.

Branch width narrow to intermediate, straight to sinuous in trace with lateral branches broadly curved toward edge of zoarium; branch surface profile rounded to angular. Keel present, single, width intermediate, exhibiting pronounced astogenetic thickening, developing into reticulate meshwork with astogeny. Nodes present, emplacement monoserial, size intermediate, shape stellate, ovate to circular, located atop keel, spacing close to intermediate. Obverse stylets present, size small to intermediate, occurring across obverse surface. Microstylets present, ranging in size from intermediate to large. Macrostylets present in some species, size intermediate to large, located at branch–dissepiment junction or irregularly across reverse branch surface. Autozooecia in two rows, third row at sites of branch bifurcation or three to four rows for moderate distances proximal to branch bifurcation. Heterozooecia (ovicells?) present in some species.

Dissepiments of intermediate width, length short to intermediate, connect branches at regular to variable intervals.

Fenestrule size small to intermediate; shape elliptical, ovate to rarely circular on obverse, rectangular, square to polygonal on reverse zoarial surfaces.

Aperture size intermediate to large, shape elliptical, ovate to rarely circular, oriented parallel to plane of

Text-figure 15.—*Hemitrypa perstriata* illustrated. 1, diagrammatic longitudinal section showing changing chamber outline from deep section near middle of branch (bottom of figure) to shallow section near abaxial edge of branch (top of figure) [Observe reticulate meshwork (arrow) characteristic of this genus and composed of granular skeletal material.], ×70; 2, diagrammatic tangential section illustrating changing chamber outline from deep section near reverse-wall budding-site (bottom of figure), to shallow section of chambers (middle of figure), to view of reticulate meshwork (arrow) in the most shallow section (top of figure) [Each chamber in the meshwork corresponds to an underlying aperture opening.], ×70; 3, diagrammatic transverse section across branch illustrating typical aperture orientation to plane of obverse surface (arrow) and reticulate meshwork covering obverse surface, ×70; 4, reconstruction of typical chamber shape (three-dimensional) as viewed from abaxial edge of branch [Observe the well-developed, long vestibule.], ×140; 5, reconstruction of typical chamber shape (three-dimensional) as viewed from distal end of branch; chamber reconstructed is from the right side of branch, ×140; 6, reconstruction of typical chamber shape (three-dimensional) as viewed from obverse surface; chamber reconstructed is from the right side of branch, ×140.

obverse surface to slight angle toward fenestrule. Peristome present, complete; apertural stylets absent; terminal diaphragms present, primarily occurring toward proximal end of zoarium.

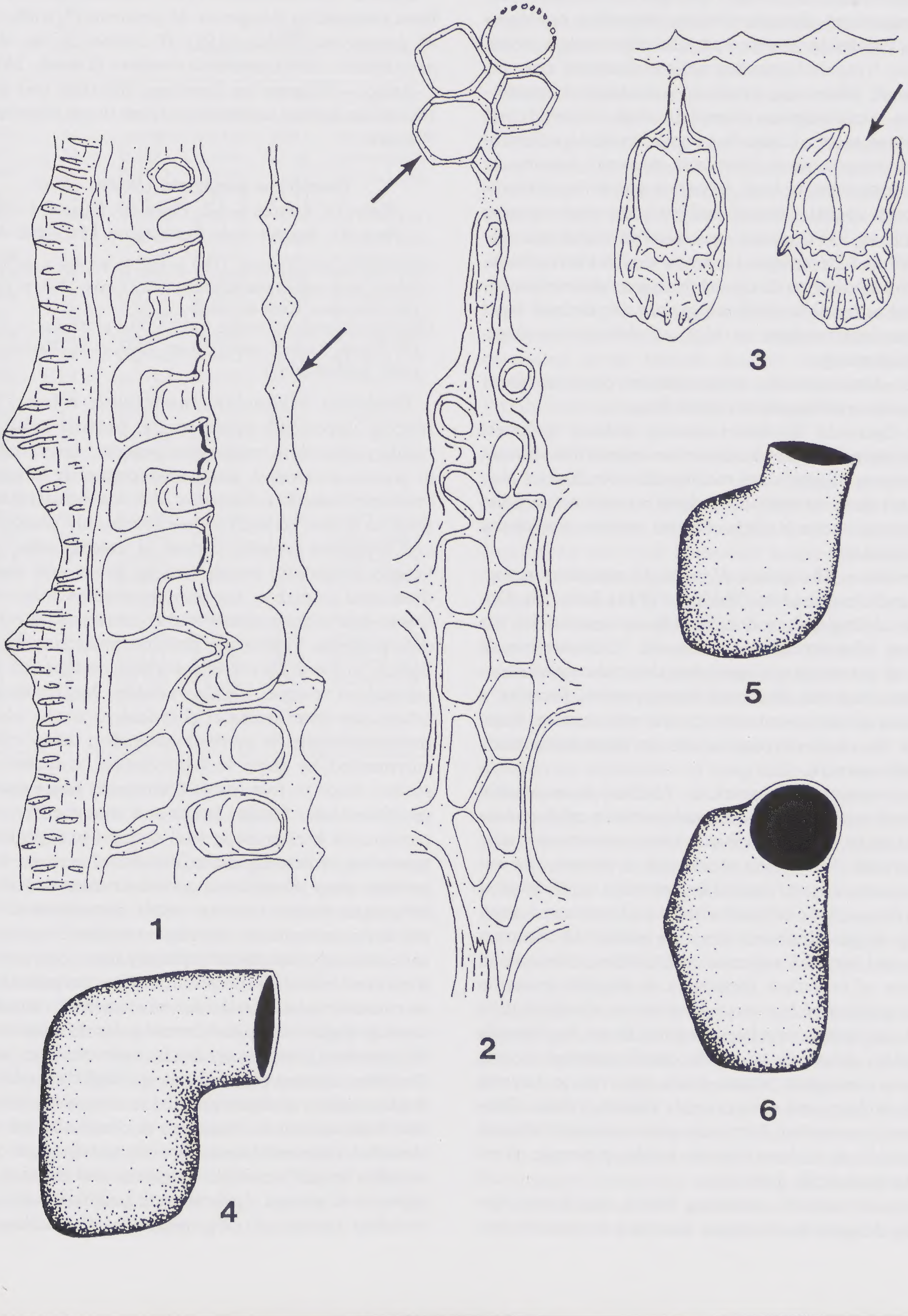

Branches ranging from circular, ovate to elliptical in cross-section, medium to very thick in depth.

Autozooecial chamber size intermediate, chambers biserially emplaced along a straight to sinuous axial wall; maximum chamber length extending proximodistally, parallel to reverse wall. Chamber outline ovate, elliptical, irregularly pentagonal to triangular near reverse wall; becoming irregularly pentagonal, rectangular to parallelogram-shaped in mid chamber and throughout most of chamber depth; ovate to elliptical near obverse surface. Vestibule present, varying in length from short to long. Superior and inferior hemisepta both absent. Lateral-wall budding-angle ranging from 17° to 23° (means); reverse-wall budding-angle from 60° to 77° (means). Lamellar skeletal layer thickness intermediate to thick, exhibiting moderate to pronounced astogenetic thickening; granular skeletal layer thickness intermediate to thick, exhibiting no astogenetic thickening.

Three-dimensionally reconstructed chamber form an irregular rectangular to cubic box.

Text-figure 15 illustrates zoarial outlines in longitudinal, tangential, and transverse orientations showing position of reticulate meshwork over zoarial surface, and three-dimensional chamber reconstructions from abaxial branch edge, obverse surface, and distal end of branch.

Remarks.—The genus *Hemitrypa* was first recognized and described by Phillips (1841) from the Devonian of England, and is readily recognized by the presence of a reticulate meshwork. This meshwork forms as extensions of granular skeletal material developing atop the keel and dissepiments, forming a honeycomb-like cover over the obverse surface. Each hole in the mesh corresponds to an underlying autozooecial aperture.

The reticulate meshwork in *Hemitrypa* is usually restricted to the more proximal portions of the zoarium, with the distalmost third of the zoarium normally not covered. Where the meshwork is absent, the exterior morphology of zoarial fragments is highly similar to and frequently confused with that of species of *Apertostella,* n. gen. Interiors are also similar in chamber shape and lack of superior and inferior hemisepta. Presence of reticulate meshwork is the best criterion for recognition of *Hemitrypa*, however, should this be absent, the genus can be separated from *Apertostella* by typical presence of more closely spaced nodes, changing fenestrule shape from obverse to reverse zoarial surface, and a more cubic chamber form. Similarities in chamber form are great enough between *Apertostella* and *Hemitrypa* to render presence of reticulate meshwork definitive.

Previous workers, including Ulrich and Keyes, frequently depended on reverse exteriors for species recognition. Reverse exteriors exhibit great change with astogeny, and their use led to species based on astogenetic stage.

Species composition.—Five Warsaw species have been assigned to this genus: *H. perstriata* Ulrich, 1890, *H. hemitrypa* (Prout, 1859), *H. aprilae*, n. sp., *H. aspera* Ulrich, 1890, and *H. vermifera* (Ulrich, 1890).

Range.—Silurian to Permian; Silurian and Lower Devonian species are distinct from those found in the Warsaw.

Hemitrypa perstriata Ulrich, 1890
Plate 39, figures 6–12, Plate 40, figures 1–10,
Plate 41, figures 1–5; Text-figure 15; Table 32

Hemitrypa perstriata Ulrich, 1890, p. 564, pl. 57, figs. 6, 6a [Keokuk Group, Bentonsport and Keokuk, Iowa]; Keyes, 1894, p. 25 [Keokuk Limestone, Keokuk, Iowa].

Hemitrypa pateriformis Ulrich, 1890, p. 564, pl. 57, figs. 7–7c [Keokuk Group, Keokuk, Iowa]; Keyes, 1894, p. 26 [Keokuk Limestone, Keokuk, Iowa].

Diagnosis.—Zoarium moderately robust, mesh spacing upper-end intermediate, pattern moderately regular; reticulate meshwork present, intermediately to poorly developed, polygonal (primarily hexagonal) in shape; branch robustness and width intermediate, thick in depth; straight to less commonly sinuous, lateral branches broadly curved at zoarial edge; transversely irregularly ovate, spacing lower-end intermediate and joined at moderately regular intervals by lower-end intermediate width, intermediate-length dissepiments. Fenestrule size intermediate; shape elliptical to ovate on obverse surface, rectangular to polygonal on reverse, highly variable. Autozooecial aperture size intermediate, elliptical to ovate, elongate proximodistally or proximoabaxially, rarely circular, surrounded by thin, well-developed, complete peristome; three to five (most commonly four) apertures per fenestrule. Single, lower-end intermediate width continuous keel present; keel straight to slightly anastomosing, extending along middle of obverse branch surface, atop which are positioned intermediate-size, irregularly stellate or ovate nodes. Autozooecial chamber size intermediate, chambers emplaced in two rows, except three rows, less frequently four rows proximal to sites of branch bifurcation; outline irregularly ovate to rounded pentagonal near reverse wall, rapidly becoming slightly irregularly rectangular throughout most of chamber, irregularly ovate near obverse surface. Chamber longest dimension very slightly greater than depth, slightly elongate parallel to reverse wall in proximodistal direction. Aperture at distal-abaxial end of chamber, connected to chamber by intermediate-length, variable length vestibule. Superior and inferior hemisepta both absent. Lateral-wall budding-angle highly variable (mean of 18°); reverse-wall budding-angle

Table 32.—Summary numerical analysis of *Hemitrypa perstriata* Ulrich, 1890. For explanation of abbreviations of characters (left column), see Table 8b (foldout inside back cover).

	number of mea-sure-ments	mean	standard deviation	coeffi-cient of variation	observed range
1. **WB**	24	0.3145	0.0550	17.48	0.248–0.480
2. **DBC**	24	0.5120	0.0608	11.88	0.346–0.612
3. **WD**	24	0.1600	0.0322	20.13	0.113–0.281
4. **LF**	24	0.5825	0.1576	27.06	0.369–0.803
5. **WF**	24	0.3563	0.0769	21.58	0.219–0.569
6. **AF**	24	4.15	0.52	12.62	3–5
7. **AL**	24	0.1320	0.0073	5.53	0.112–0.154
8. **AW**	24	0.0920	0.0065	7.07	0.058–0.108
9. **ADB**	24	0.2400	0.0167	6.96	0.222–0.302
10. **AAB**	24	0.2320	0.0238	10.26	0.152–0.292
11. **ABB**	24	0.3217	0.0435	13.52	0.226–0.434
12. **DN**	24	0.0990	0.0126	12.73	0.072–0.160
14. **SNB**	24	0.4580	0.0965	20.96	0.316–0.800
15. **WK**	24	0.0592	0.0123	20.78	0.028–0.114
16. **DSO**	24	0.0120	0.0029	23.97	0.008–0.018
17. **SSO**	24	0.0386	0.0123	31.86	0.022–0.096
18. **WP**	24	0.0135	0.0027	20.00	0.006–0.025
22. **RSS**	24	0.0220	0.0034	15.45	0.013–0.031
24. **SSS**	24	0.0456	0.0138	30.26	0.020–0.085
25. **LRM**	24	0.2380	0.0220	9.24	0.156–0.292
26. **WRM**	24	0.2240	0.0271	12.10	0.180–0.388
32. **TRW**	24	0.0128	0.0018	14.06	0.007–0.017
33. **TLW**	24	0.0094	0.0012	12.77	0.006–0.014
34. **FWT**	24	0.0741	0.0255	34.41	0.040–0.175
35. **RWT**	24	0.1884	0.0604	32.06	0.121–0.295
36. **CL**	24	0.2286	0.0162	7.09	0.195–0.245
37. **CD**	24	0.2250	0.0118	5.24	0.205–0.265
38. **MAW**	24	0.1325	0.0214	16.15	0.092–0.163
39. **MIW**	24	0.1117	0.0170	15.22	0.079–0.141
40. **VD**	24	0.0720	0.0173	24.03	0.050–0.106
41. **RA**	24	70.70	5.61	7.94	58–82
42. **LA**	24	18.00	3.38	18.78	13–25
43. **TB**	24	0.4250	0.0887	20.88	0.325–0.571

highly constant (mean of 71°).

Table 32 presents statistical criteria used in delimiting this species.

Exterior description.—Zoarium moderately robust, expansion flat to undulating, fan-shaped; mesh spacing upper-end intermediate; pronounced astogenetic thickening of both obverse and reverse zoarial skeleton; external zoarial pattern moderately regular. Intermediately to poorly developed reticulate meshwork covering primarily proximal and medial obverse zoarial surfaces, absent at lateral and distal edges of zoarium; reticulate meshwork thickened along branch midline, with mesh forming as secondary extension of keel, nodes, and dissepiments; meshwork develops toward fenestrule from branch midline and dissepiment surface to form polygonal, primarily hexagonal feature covering obverse zoarial surface, each facet of polygon (hexagon) developing around single apertural opening; width and length of meshwork dimensions approximately same as aperture spacings along and across obverse branch; width five-sevenths that of branch, meshwork opening width to length ratio approximately 1:1; variable number, four to seven, nodular extensions into meshwork opening from mesh skeletal edge. Probable mature zoarial widths and lengths of half a meter or more attained in large colonies.

Branch robustness intermediate, width intermediate, slightly variable; typically straight, less commonly exhibiting inflection toward sites of dissepiment emplacement, lateral branches broadly curved toward edge of zoarium. Branch spacing lower-end intermediate, distance between adjacent branch centers highly regular. Obverse surface texture moderately granular, becoming increasingly so with astogeny; surface rounded to moderately angular, except for presence of single keel; keel width lower-end intermediate, well-developed, continuous, straight to slightly anastomosing, extending along branch midline and causing pronounced positive inflection in obverse surface profile. Pronounced astogenetic thickening of keel; most pronounced toward proximal end of zoarium. Nodes monoserially emplaced, well-developed, intermediate-size, irregularly stellate to ovate, elongate proximodistally; nodes regular in size, variable in shape; develop as projection from middle of keel; one to three (most commonly two) per fenestrule length; spacing intermediate, moderately even; pronounced increase of node diameter with astogeny. Intermediate-size stylets, variably sized and positioned, occurring across obverse branch surface. Reverse surface texture granular, coarsening with astogeny, bearing relatively few rows of intermediately spaced longitudinal striae, which become covered by lamellar skeleton during astogeny; rows of intermediate-size microstylets, closely spaced, develop as extensions of longitudinal striae along reverse branch surface, microstylet diameters increase with astogeny and microstylets become more variably positioned across reverse branch surface. Autozooecia in two rows across branch, except three rows, less frequently four rows for moderate to pronounced distances proximal to sites of branch bifurcation; pronounced thickening proximal, moderate thinning distal to sites of branch bifurcation. Heterozooecia absent in all zoarial fragments examined.

Dissepiments of lower-end intermediate width, slightly greater than half branch width, slightly variable; length intermediate, variable; connect branches at moderately regular intervals. Dissepiments exhibit pronounced medial thinning, pronounced flaring at branch–dissepiment junction; highly recessed from obverse, approximately even with reverse branch surface. Pronounced astogenetic thickening of dissepiments toward proximal end of zoarium. Obverse dissepiment surface with two to four longitudinal ridges emplaced

perpendicular to branch length, intermediate-size stylets, similar in size to obverse branch stylets, develop atop these ridges; stylets become irregularly positioned across dissepiments with astogeny; reverse dissepiment surface with single medially thickened ridge bearing intermediate-size microstylets. Obverse dissepiment surface texture moderately granular, reverse surface texture granular, both coarsening with astogeny. Dissepiments emplaced perpendicular to branch length. Apertures commonly positioned on proximal or distal edge, or in middle of dissepiment edge at branch–dissepiment contact; arranged symmetrically or asymmetrically between branches.

Fenestrule size intermediate; shape varying from elliptical to ovate on obverse surface, becoming rectangular to polygonal with highly angular appearance on reverse, elongate proximodistally; highly irregular in size and shape; greatly expanding in width and length in obverse–reverse direction. Width of fenestrule slightly less than that of branch on obverse surface, appreciably greater than branch width on reverse; fenestrule opening size reduced toward proximal end of zoarium due to astogenetic thickening of lamellar skeleton. Width to length ratio of fenestrule variable, ranging from 1:2 to approximately 1:4; ratio of fenestrule mean width to length approximately 3:5; width more constant than length, both variable. Three to five (most commonly four) apertures per fenestrule length; distance between closest aperture centers along branch and across branch approximately equal, spacing of apertures across fenestrule approximately 1.3 times greater; spacing along and across branch moderately constant, spacing across fenestrule variable.

Autozooecial aperture size intermediate, large relative to branch, shape elliptical to ovate, rarely circular; elongate proximodistally or proximoabaxially; width to length ratio approximately 7:10; size uniform, shape variable; opening typically oriented primarily parallel to plane of obverse surface, less frequently at slight angle toward fenestrule; surrounded by thin, well-developed complete peristome. Aperture margins extend into fenestrule, causing slight to moderate inflections in fenestrule outline on obverse surface. Terminal diaphragms, in places centrally thickened, occurring at proximal end of zoarium beneath reticulate meshwork.

Zoarial supports common, well-developed, form primarily as extensions of reverse zoarial surface, less frequently from lateral edges of zoarium.

Interior description.—Branches irregularly ovate in transverse section, enlarged on obverse surface, elongate in obverse–reverse direction, becoming increasingly elongate with addition of secondary lamellar skeleton during astogeny. Branches thick, moderately variable in depth.

Autozooecial living chamber size intermediate, chambers biserially arranged in alternating rows along planar branch axial wall; axial wall highly sinuous, exhibiting inflections toward and connecting with chamber lateral walls near reverse wall, axial wall becoming straight in mid chamber and toward obverse surface. Chamber longest dimension very slightly greater than depth, elongate parallel to reverse walls in proximodistal direction. Autozooecial chamber outline irregularly ovate to rounded pentagonal near reverse wall; rapidly becoming slightly irregularly rectangular throughout mid chamber and most of chamber depth; irregularly ovate near obverse surface, longest dimension of ovoid oriented distal-abaxially; chamber shape highly uniform. Aperture positioned at distal-abaxial end of chamber, connected to chamber by well-developed vestibule of intermediate length, length variable. Ratio of autozooecial chamber minimum width to maximum width approximately 4:7; maximum width to depth ratio about 7:12; chamber depth and length essentially equal; chamber length and depth highly constant, maximum and minimum widths highly variable. Superior and inferior hemisepta both absent. Autozooecial chambers diverge laterally from middle of branch at highly variable angle (mean of 18°); from reverse wall at highly constant angle (mean of 71°).

Three-dimensionally reconstructed chamber form a slightly irregular square box; length as viewed from lateral edge of branch, and depth as viewed from distal end of branch approximately equal; width as viewed from obverse surface substantially shorter.

Internal granular skeletal layer thickness intermediate; granular skeletal layer well-developed, continuous with obverse nodes, stylets, keel, peristome, and reticulate meshwork, which is entirely formed of granular skeletal material; reverse longitudinal striae and stylets; across dissepiments and in the middle of zoarial supports. Outer lamellar layer extremely thick, exhibiting pronounced astogenetic thickening, most prominent toward proximal end of zoarium.

Remarks.—*Hemitrypa perstriata* was based on materials from the Keokuk Group in Bentonsport and Keokuk, Iowa, that emphasized the reverse zoarial surface and fenestrule dimensions, characters both highly dependent on zoarial astogeny. The "very narrow fenestrules and strongly striate branches" used by Ulrich (1890, p. 565) to differentiate *H. perstriata* from *H. pateriformis* Ulrich, 1890 are characters which are applicable toward the distal, but not proximal, end of the zoarium. As best I can determine from Ulrich's illustrations (the holotype of *H. pateriformis* was not found), *H. pateriformis* represents the most proximal end, and *H. perstriata* the most distal end, of zoarial fragments from the same species; therefore I am placing *H. pateriformis* in synonymy with *H. perstriata*.

Within the hemitrypids, *H. perstriata* most closely resembles *H. hemitrypa* (Prout, 1859), with pronounced similarity in autozooecial chamber shape and size. Although *H. hemitrypa* exhibits a characteristically greater chamber width than *H. perstriata*, the length and depth of the chambers in the two species are essentially the same. *H. perstriata* is further differentiated by thicker, deeper branches, coarser mesh with larger fenestrule openings, greater number of apertures per fenestrule length, and larger aperture openings.

The approximately equal length and depth of the autozooecial chambers in these two species group them together, separating them from other hemitrypids which characteristically have lengths substantially greater than widths. Reticulate meshwork in these two species is also not typically as well-developed as in other hemitrypids.

Those similarities in chamber shape and size observed in *H. perstriata* and *H. hemitrypa* suggest close phylogenetic affinity.

Material studied.—Fourty exterior fragments, 17 sectioned specimens; largest zoarial fragment 62×44 mm (width to length). The preservation of zoarial fragments is excellent as a result of the robust nature of zoarium. The relatively delicate character of the reticulate meshwork results in its common compaction onto the obverse zoarial surface.

Occurrence.—*Hemitypa perstriata* is most abundant in the northern half of the study area, although it is also found in lesser numbers in the southern portion. As its *in situ* occurrences are primarily in lower energy depositional environments, it is commonly found in argillaceous micrites and biomicrites.

Syntypes.—ISGS (ISM) 2717 and USNM 43766 were apparently both figured by Ulrich (1890).

Figured and/or measured specimens.—UI X-6934, 6886, 6887, 6859–6862 (loc. 10, samples 28, 29), 6730, 6731 (loc. 47A, samples 32, 35), 6924–6927, 6847–6850 (loc. 11, samples 52, 57).

Hemitrypa hemitrypa (Prout, 1859)
Plate 41, figures 6, 7, Plate 42, figures 1–12,
Plate 43, figures 1–9; Table 33

Fenestella hemitrypa Prout, 1859, p. 444, pl. 17, figs. 4, 4a [Second Archimedes Limestone, Barrett's Station, St. Louis County, Missouri].

Hemitrypa proutana Ulrich, 1890, p. 560, pl. 57, figs. 1–1c [Keokuk Group, Warsaw, Illinois, Keokuk, Iowa. Warsaw Beds, Monroe County and Warsaw, Illinois, Barrett's Station, Missouri]; Trizna, 1958, p. 25, pl. 43, figs. 3–6, pl. 44, figs. 1–3.

Hemitrypa hemitrypa Prout. Keyes, 1894, p. 25.

Diagnosis.—Zoarium moderately robust, mesh spacing intermediate, pattern regular; reticulate meshwork present, intermediately to poorly developed, polygonal in shape; branch robustness lower-end intermediate, narrow in width, medium in depth; branches straight to slightly sinuous, broadly curved at lateral zoarial edge; branches transversely circular to rarely ovate, spacing lower-end intermediate, joined at regular intervals by intermediate width and length dissepiments. Fenestrule size lower-end intermediate; shape elliptical to ovate on obverse surface, approaching rectangular to square on reverse, slightly regular. Autozooecial aperture size intermediate, elliptical to ovate, elongate proximodistally or proximoabaxially, rarely approaching circular; surrounded by thin, well-developed, complete peristome; two to three apertures per fenestrule. Single intermediate-width keel present; keel slightly anastomosing, extending along middle of obverse branch surface, atop which are upper-end intermediate size, ovate to rarely irregularly stellate nodes. Autozooecial chamber size lower-end intermediate,

Table 33.—Summary numerical analysis of *Hemitrypa hemitrypa* (Prout, 1859). For explanation of abbreviations of characters (left column), see Table 8b (foldout inside back cover).

	number of measurements	mean	standard deviation	coefficient of variation	observed range
1. **WB**	24	0.2550	0.0460	18.08	0.145–0.356
2. **DBC**	24	0.4800	0.0580	12.08	0.352–0.572
3. **WD**	24	0.1663	0.0345	20.72	0.106–0.231
4. **LF**	24	0.4513	0.0821	18.20	0.252–0.575
5. **WF**	24	0.2625	0.0518	19.72	0.156–0.425
6. **AF**	24	2.50	0.51	20.43	2–3
7. **AL**	24	0.1220	0.0083	6.80	0.096–0.146
8. **AW**	24	0.0880	0.0066	7.47	0.066–0.114
9. **ADB**	24	0.2215	0.0208	9.40	0.170–0.288
10. **AAB**	24	0.2320	0.0274	11.82	0.156–0.282
11. **ABB**	24	0.2925	0.0503	17.20	0.208–0.394
12. **DN**	24	0.1128	0.0099	8.82	0.072–0.170
14. **SNB**	24	0.4620	0.0558	12.08	0.360–0.612
15. **WK**	24	0.0920	0.0206	22.40	0.046–0.163
16. **DSO**	24	0.0114	0.0032	38.07	0.006–0.023
17. **SSO**	24	0.0286	0.0010	34.96	0.014–0.071
18. **WP**	24	0.0155	0.0343	22.18	0.007–0.032
21. **RSL**	24	0.1160	0.0279	24.05	0.074–0.146
22. **RSS**	24	0.0143	0.0023	16.15	0.008–0.020
23. **SSL**	24	0.5800	0.2197	37.88	0.240–0.784
24. **SSS**	24	0.0286	0.0076	26.40	0.013–0.052
25. **LRM**	24	0.2260	0.0188	8.33	0.160–0.310
26. **WRM**	24	0.2180	0.0228	10.47	0.160–0.322
30. **OL**	24	0.2400	0.0265	11.06	0.200–0.298
31. **OW**	24	0.2320	0.0228	9.85	0.192–0.300
32. **TRW**	24	0.0105	0.0015	15.05	0.009–0.019
33. **TLW**	24	0.0092	0.0013	13.83	0.008–0.016
34. **FWT**	24	0.0828	0.0341	41.20	0.014–0.161
35. **RWT**	24	0.0675	0.0262	38.85	0.016–0.171
36. **CL**	24	0.2244	0.0135	6.02	0.205–0.264
37. **CD**	24	0.2185	0.0094	4.28	0.198–0.250
38. **MAW**	24	0.1625	0.0240	14.75	0.135–0.230
39. **MIW**	24	0.1250	0.0208	16.62	0.075–0.171
40. **VD**	24	0.0907	0.0262	28.85	0.043–0.176
41. **RA**	24	77.00	6.58	8.55	62–85
42. **LA**	24	18.00	3.10	17.24	12–26
43. **TB**	24	0.3571	0.0759	21.25	0.257–0.593

chambers emplaced in two rows, except either third row at sites of branch bifurcation or three rows for moderate to pronounced distances proximal to sites of branch bifurcation; outline irregularly ovate to rounded pentagonal near reverse wall, irregularly pentagonal to approaching rectangular throughout most of chamber depth; irregularly ovate near obverse surface. Chamber longest dimension very slightly greater than depth, slightly elongate parallel to reverse wall in proximodistal direction. Aperture at proximodistal or distal-abaxial end of chamber, connected to chamber by intermediate and variable length vestibule. Superior and inferior hemisepta both absent. Lateral-wall budding-angle highly variable (mean of 18°); reverse-wall budding-angle constant (mean of 77°). Heterozooecia (ovicells?) occurring as intermediate size enlargements of some apertures. Table 33 presents statistical criteria used in delimiting this species.

Exterior description.—Zoarium moderately robust, expansion flat, obversely or reversely curved or undulating, fan-shaped; mesh spacing intermediate; pronounced astogenetic thickening of both obverse and reverse zoarial skeleton; external zoarial pattern regular. Intermediately to poorly developed reticulate meshwork covering primarily proximal and medial obverse zoarial surface, absent at lateral and distal edges of zoarium; reticulate meshwork slightly thickened along branch midline, with mesh forming as secondary extension of keel, nodes, and dissepiments; meshwork develops toward fenestrule from branch midline and dissepiment surface to form polygonal features covering obverse zoarial surface, each facet of polygon developing around single apertural opening; width and length of meshwork dimensions approximately same as aperture spacing along and across obverse branch surface; width six-sevenths that of branch, meshwork opening width to length ratio approximately 1:1; variable number, three to seven, nodular extensions into meshwork opening from mesh skeletal edge. Probable mature zoarial widths 30 to 40 mm, lengths 35 to 50 mm.

Branch robustness lower-end intermediate; branches narrow, slightly variable in width; straight to exhibiting slight inflections toward sites of dissepiment emplacement, lateralmost branches frequently broadly curved toward edge of zoarium. Branch spacing lower-end intermediate, distance between adjacent branch centers highly regular. Obverse surface texture granular, coarsening with astogeny; surface rounded, except for presence of single keel; keel width intermediate, well-developed, continuous, slightly anastomosing, positioned along branch midline and causing pronounced positive inflection in obverse surface profile. Pronounced astogenetic thickening of keel; most pronounced toward proximal end of zoarium. Nodes monoserially emplaced, well-developed, size upper-end intermediate, irregularly ovate to more rarely irregularly stellate, elongate proximodistally; nodes highly regular in size, moderately variable in shape; develop as projections from middle of keel; one to two (most commonly one) per fenestrule length; spacing intermediate, even; pronounced increase of node diameter with astogeny. Lower-end intermediate stylets, variably sized and positioned, occurring across obverse branch surface. Reverse surface texture granular, coarsening with astogeny, bearing relatively few rows of intermediately spaced longitudinal striae, which become covered by lamellar skeleton during astogeny; rows of small, closely spaced microstylets develop as extensions of longitudinal striae along reverse branch surface; microstylet diameters increase with astogeny, microstylets become more variably positioned across reverse branch surface. Large macrostylets present along reverse branch midline; shape circular to ovate, elongate proximodistally, with size and shape barely regular; one to two macrostylets per fenestrule length, most common placement at branch–dissepiment junction; macrostylet spacing highly irregular, with size of macrostylets greatly increasing during astogeny. Autozooecia in two rows across branch, except either third row at sites of branch bifurcation where middle autozooecium evidently shared by both branches, or three rows for moderate to pronounced distances proximal to sites of branch bifurcation; moderate thickening proximal, slight thinning distal to sites of branch bifurcation. Heterozooecia (ovicells?) occurring as intermdiate-size enlargements of some apertures; mean width and length of polymorphs approximately twice autozooecial aperture length; connection between polymorph and autozooecial chamber probable; polymorphs most commonly situated toward proximal end of zoarium.

Dissepiments of intermediate width, approximately two-thirds of branch width, variable; length intermediate, constant; connect branches at regular intervals. Dissepiments exhibit moderate medial thinning, slight flaring at branch–dissepiment junction; slightly recessed from obverse, approximately even with reverse branch surface. Pronounced astogenetic thickening of dissepiments toward proximal end of zoarium. Obverse dissepiment surface with two to four longitudinal ridges emplaced perpendicular to branch length, small stylets similar in size to obverse branch stylets develop atop these ridges; stylets become irregularly positioned across dissepiments with astogeny; reverse dissepiment surface with medially thickened ridge bearing rows of intermediate-size microstylets. Obverse and reverse surface textures granular, coarsening with astogeny. Dissepiments emplaced perpendicular to branch length. Apertures commonly positioned on proximal or distal edge, or in middle of dissepiment

edge at branch–dissepiment contact, arranged symmetrically or asymmetrically between branches.

Fenestrule size lower-end intermediate; shape varying from elliptical to ovate on obverse zoarial surface, approaching rectangular to square on reverse, elongate proximodistally; slightly regular in size, moderately regular in shape; greatly expanding in width and length in obverse–reverse direction. Width of fenestrule less than that of branch on obverse surface, appreciably greater than branch width on reverse; fenestrule opening size reduced toward proximal end of zoarium due to astogenetic thickening of lamellar skeleton. Width to length ratio of fenestrule variable, ranging from approximately 1:1 to 1:3; ratio of fenestrule mean width to length approximately 7:12; both width and length barely constant. Two to three apertures per fenestrule length (mean of 2.5); distance between closest aperture centers along branch and across branch approximately equal, spacing across fenestrule approximately 1.3 times greater; spacing along and across branch moderately constant, spacing across fenestrule variable.

Autozooecial aperture size intermediate, moderately large relative to branch, shape elliptical to ovate, rarely approaching circular; elongate proximodistally or proximoabaxially; width to length ratio approximately 7:11; size uniform, shape variable; opening orientation ranging from parallel to plane of obverse surface to slight angle toward fenestrule; surrounded by thin, well-developed, complete peristome. Aperture margins extend into fenestrule, causing moderate inflections in fenestrule outline on obverse surface. Centrally thickened terminal diaphragms persent, occurring most commonly at proximal end of zoarium beneath overlying reticulate meshwork.

Zoarial supports develop as extensions of reverse zoarial surface and lateral edges of zoarium.

Interior description.—Branches most commonly circular, rarely ovate, in transverse section, slightly enlarged on obverse surface; elongate in obverse–reverse direction when ovate, becoming increasingly elongate with addition of secondary lamellar skeleton during astogeny. Branches medium, moderately variable in depth.

Autozooecial living chamber size lower-end intermediate, chambers biserially arranged in alternating rows along planar branch axial wall; axial wall zigzagging near reverse wall, extending diagonally across entire branch; axial wall becoming less sinuous in mid chamber, inflected toward and connecting with chamber lateral walls, only slightly sinuous near obverse surface. Chamber longest dimension very slightly greater than depth, elongate parallel to reverse wall in proximodistal direction. Autozooecial chamber outline irregularly ovate to rounded pentagonal near reverse wall, rapidly becoming irregularly pentagonal to approaching rectangular throughout mid chamber and most of chamber depth; irregularly ovate near obverse surface, longest dimension of ovoid oriented proximodistally or slightly distal-abaxially; chamber shape moderately uniform. Aperture positioned at proximodistal or distal-abaxial end of chamber, connected to chamber by well-developed, intermediate-length vestibule; vestibule length highly variable. Ratio of autozooecial chamber minimum width to maximum width approximately 3:4; maximum width to depth ratio approximately 5:7; chamber depth and length essentially equal; chamber depth and length highly constant, minimum and maximum widths highly variable. Superior and inferior hemisepta both absent. Autozooecial chambers diverge laterally from middle of branch at highly variable angle (mean of 18°); from reverse wall at constant angle (mean of 77°).

Three-dimensionally reconstructed chamber form a slightly irregular cubic box; length as viewed from lateral edge of branch, and depth as viewed from distal end of branch approximately equal; width as viewed from obverse surface moderately shorter.

Internal granular skeletal layer thickness intermediate; granular skeletal layer well-developed, continuous with obverse nodes, stylets, keel, peristome, and reticulate meshwork (completely composed of granular skeletal material); reverse longitudinal striae, microstylets and macrostylets; across dissepiments and in middle of zoarial supports. Outer lamellar layer thickness intermediate to thick, exhibiting pronounced astogenetic thickening most prominent toward proximal end of zoarium.

Remarks.—*Fenestella hemitrypa* was described by Prout (1859) from the Second Archimedes Limestone (Keokuk Limestone) at Barrett's Station in St. Louis County, Missouri. The specimen reported by Prout lacked reticulate meshwork, and therefore he placed the species in *Fenestella* Lonsdale, 1839. Ulrich (1890) found zoaria having the same exterior appearance which contained reticulate meshwork locally across the obverse surface, and for this reason, Ulrich renamed the species *Hemitrypa proutana* for Prout, who originally described it. The original name *H. hemitrypa* is herein reapplied, as it has priority.

Ulrich noted similarities between *H. hemitrypa* and *H. plumosa* (*Fenestella plumosa* Prout, 1860); the two species were distinguished by the latter's coarser mesh spacing and restriction to the Keokuk Formation.

H. hemitrypa closely resembles *H. perstriata* in autozooecial chamber shape and size, although the former characteristically exhibits greater chamber width than the latter. *H. hemitrypa* also has narrower, thinner branches, finer mesh with smaller fenestrule openings, fewer apertures per fenestrule length, and smaller aperture openings.

I consider *H. hemitrypa* var. *nodulosa* Ulrich, 1890 to represent a different astogenetic stage of *H. hemitrypa*, as well as a possible response to different depositional environments.

Material studied.—Fourty-eight exterior fragments, 12 sectioned specimens; largest zoarial fragment 22 × 32 mm (width to length). The zoarial fragments are well preserved, but the reticulate meshwork commonly is compacted onto obverse zoarial surfaces.

Occurrence.—*Hemitrypa hemitrypa* is common throughout the Warsaw in the study area, primarily occurring in argillaceous micrites, biomicrites, and facies thought to have had moderate- to low-energy depositional environments.

Syntypes.—ISGS(ISM) 2818–1/2; USNM 43371.

Figured and/or measured specimens.—UI X-6844 (loc. 11, sample 55), 6845, 6928–6933 (loc. 10, samples 28, 33), 6846, 6853, 6858, 6943 (loc. 49B, samples 12, 14).

Hemitrypa aprilae, new species

Plates 44, figures 1–10, Plate 45, figures 1–8; Table 34

Etymology of name.—Named for the month of April, without doubt the finest time to do field work along the Mississippi.

Diagnosis.—Zoarium moderately robust, mesh spacing close, pattern regular; reticulate meshwork present, extremely well-developed, polygonal (primarily hexagonal) in shape; branch robustness and width intermediate, deep in thickness; branches straight, broadly curved at lateral zoarial edge; transversely approximately circular, becoming ovate to elliptical with astogeny, closely spaced and joined at moderately variable intervals by intermediate-width, short dissepiments. Fenestrules small; shape elliptical to ovate on obverse surface, approaching rectangular on reverse, moderately irregular. Autozooecial aperture size intermediate, irregularly ovate, elongate proximo-abaxially, more rarely proximodistally to rarely circular, surrounded by lower-end intermediate width, well-developed, complete peristome; two to three apertures per fenestrule (mean of 2.5). Single intermediate-width keel present; keel anastomosing, extending along middle of obverse branch surface, atop which develop upper-end intermediate size, irregularly stellate to more rarely ovate nodes. Autozooecial chamber size lower-end intermediate, chambers emplaced in two rows, except either third row at sites of branch bifurcation or three rows for moderate to pronounced distances proximal to sites of branch bifurcation; outline irregularly ovate to rounded triangular near reverse wall; irregularly pentagonal throughout most of chamber depth, approaching rectangular nearer obverse surface; irregularly ovate to elliptical nearest obverse surface. Chamber longest dimension parallel to reverse wall in proximodistal direction. Aperture at distal-abaxial end of chamber, connected to chamber by moderately long, variable-length vestibule. Superior and inferior hemisepta both absent. Lateral-wall budding-angle highly variable (mean of 20°); reverse-wall budding-angle highly constant (mean of 66°). Heterozooecia (ovicells?) occurring as intermediate to pronounced enlargements of some apertures.

Table 34.—Summary numerical analysis of *Hemitrypa aprilae*, n. sp. For explanation of abbreviations of characters (left column), see Table 8b (foldout inside back cover).

	number of measurements	mean	standard deviation	coefficient of variation	observed range
1. WB	24	0.3627	0.0470	12.96	0.320–0.431
2. DBC	24	0.4465	0.0625	14.00	0.375–0.520
3. WD	24	0.2205	0.0485	21.97	0.156–0.325
4. LF	24	0.3958	0.0835	21.10	0.225–0.475
5. WF	24	0.1901	0.0351	18.46	0.125–0.320
6. AF	24	2.50	0.52	20.89	2–3
7. AL	24	0.1238	0.0104	8.40	0.098–0.150
8. AW	24	0.0847	0.0108	12.00	0.062–0.106
9. ADB	24	0.2435	0.0230	9.45	0.210–0.280
10. AAB	24	0.2355	0.0233	9.89	0.208–0.272
11. ABB	24	0.2567	0.0511	19.91	0.160–0.352
12. DN	24	0.1138	0.0269	23.64	0.082–0.160
14. SNB	24	0.2598	0.0072	29.72	0.160–0.440
15. WK	24	0.0761	0.126	16.56	0.061–0.105
16. DSO	24	0.0156	0.0035	22.44	0.011–0.021
17. SSO	24	0.0497	0.0203	40.85	0.019–0.084
18. WP	24	0.0269	0.0068	25.28	0.016–0.043
22. RSS	24	0.0192	0.0037	19.27	0.013–0.030
24. SSS	24	0.0316	0.0093	29.43	0.020–0.055
25. LRM	24	0.2460	0.0238	9.67	0.151–0.320
26. WRM	24	0.2208	0.0297	13.45	0.141–0.309
30. OL	12	0.2242	0.0244	10.88	0.195–0.284
31. OW	12	0.1955	0.0241	12.33	0.167–0.264
32. TRW	24	0.0133	0.0029	21.80	0.008–0.022
33. TLW	24	0.0111	0.0018	16.22	0.009–0.015
34. FWT	24	0.1178	0.0339	28.78	0.065–0.186
35. RWT	24	0.1805	0.0759	42.05	0.096–0.375
36. CL	24	0.2240	0.0148	6.61	0.205–0.249
37. CD	24	0.1769	0.0091	5.14	0.161–0.195
38. MAW	24	0.1595	0.0247	15.49	0.125–0.200
39. MIW	24	0.1030	0.0205	19.90	0.068–0.133
40. VD	24	0.1361	0.0413	30.35	0.088–0.225
41. RA	24	66.00	4.36	6.61	58–76
42. LA	24	20.00	4.21	21.54	16½–24
43. TB	24	0.4851	0.0843	17.38	0.388–0.612

Table 34 presents statistical criteria used in delimiting this species.

Exterior description.—Zoarium moderately robust, expansion most commonly flat, more rarely obversely or reversely curved, or undulating, fan-shaped; mesh spacing close; pronounced astogenetic thickening of both obverse and reverse zoarial skeleton; external zoarial pattern regular. Extremely well-developed reticulate meshwork covering obverse zoarial surface with

astogeny, absent only at lateral and distal edges of zoarium; reticulate meshwork exhibiting pronounced thickening along branch midline, with mesh forming as secondary extension of keel, nodes, and dissepiments; meshwork develops toward fenestrule from branch midline and dissepiment surface to form polygonal (primarily hexagonal) features covering obverse zoarial surface, each facet of polygon (hexagon) developing around single apertural opening; width and length of meshwork dimensions approximately same as aperture spacings along and across obverse branch surface; width approximately three-fifths that of branch, mesh opening width to length ratio approximately 9:10; variable number, three to six (most commonly four) nodular extensions into meshwork opening from mesh skeletal edge. Probable mature zoarial widths 20 to 60 mm, lengths 30 to 55 mm.

Branch robustness intermediate, width intermediate, moderately constant; straight, except lateral branches broadly curved toward edge of zoarium. Branches closely spaced, distance between adjacent branch centers regular. Obverse surface texture moderately granular, coarsening with astogeny, surface rounded to slightly angular, except for presence of single keel; keel width intermediate, extremely well-developed, continuous, anastomosing, extending along branch midline and causing pronounced positive inflection in obverse surface profile. Pronounced astogenetic thickening of keel; most pronounced toward proximal end of zoarium. Nodes monoserially emplaced, well-developed, size upper-end intermediate, shape typically irregularly stellate, more rarely ovate, elongate proximodistally; nodes moderately regular in size, variable in shape; one to three (most commonly two) per fenestrule length; spacing lower-end intermediate, uneven; pronounced increase of node diameter with astogeny. Intermediate-size stylets, variably sized and highly variably positioned, occurring across obverse surface. Reverse surface texture granular, coarsening with astogeny, bearing an intermediate number of rows of closely spaced longitudinal striae, which become completely covered by lamellar skeleton during astogeny; rows of intermediate size microstylets, closely spaced, develop as extensions of longitudinal striae along reverse branch surface, microstylets slightly regular in size; microstylet diameters increase with astogeny, microstylets become more variably positioned across reverse branch surface. Autozooecia in two rows, except third row at sites of branch bifurcation where middle autozooecium evidently shared by both branches, or three rows for moderate to pronounced distances proximal to sites of branch bifurcation; moderate thickening proximal, slight thinning distal to sites of branch bifurcation. Heterozooecia (ovicells?) occurring as intermediate to pronounced enlargements of some apertures; mean widths and lengths of polymorphs slightly less than twice autozooecial aperture length; connection evident between polymorph and autozooecial chamber; polymorphs most commonly situated toward proximal end of zoarium.

Dissepiments of intermediate width, approximately three-fifths branch width, moderately variable; short, moderately constant in length; connect branches at moderately variable intervals. Dissepiments barlike at distal end of zoarium, exhibiting only slight flaring at branch–dissepiment junction; exhibiting greater medial thinning and less barlike nature toward proximal end of zoarium; highly recessed from obverse, approximately even with reverse branch surface. Pronounced astogenetic thickening of dissepiments toward proximal end of zoarium; highly recessed from obverse, approximately even with reverse branch surface. Obverse dissepiment surface with two to four longitudinal ridges emplaced perpendicular to branch length, intermediate stylets similar in size to obverse branch stylets develop atop these ridges; stylets become irregularly positioned across dissepiment surface and striae become covered by lamellar skeleton with astogeny; reverse dissepiment surface with medially thickened ridge bearing intermediate-size microstylets. Obverse and reverse dissepiment surface texture granular, coarsening with astogeny. Dissepiment emplacement typically perpendicular to branch length, more rarely at a slight angle from perpendicular. Apertures commonly positioned on proximal or distal edge, or in middle of dissepiment edge at branch–dissepiment contact, arranged symmetrically or asymmetrically between branches.

Fenestrules small; shape varying from elliptical to ovate on obverse surface, to approaching rectangular on reverse, elongate proximodistally; moderately irregular in size and shape; expanding in width and length in obverse–reverse direction. Width of fenestrule slightly less than half branch width on obverse surface, slightly greater than half branch width on reverse; fenestrule opening size greatly reduced toward proximal end of zoarium due to astogenetic thickening of lamellar skeleton. Width to length ratio of fenestrule ranging from approximately 1:2 to nearly 1:4; ratio of fenestrule mean width to length approximately 1:2, length slightly more variable than width, both variable; two to three apertures per fenestrule length (mean of 2.5); distance between closest aperture centers along branch, across branch, and across fenestrule approximately equal; spacing along and across branch moderately constant, spacing across fenestrule variable.

Autozooecial aperture size intermediate, moderately large relative to branch, shape irregularly ovate to rarely circular, enlarged at distal end, typically elongate proximoabaxially, more rarely proximodistally; width

to length ratio approximately 2:3; size moderately uniform, shape moderately variable; opening oriented typically parallel to plane of obverse surface, less commonly at slight angle toward fenestrule; surrounded by lower-end intermediate width, well-developed complete peristome. Moderate projections of apertures into fenestrule, causing inflections in fenestrule outline on obverse surface. Centrally thickened terminal diaphragm present, occurring most commonly at proximal end of zoarium beneath overlying reticulate meshwork.

Zoarial supports common, develop as extensions of reverse zoarial surfaces.

Interior description.—Branches approximately circular in transverse section; becoming irregularly ovate to elliptical, elongate in obverse–reverse direction with addition of secondary lamellar skeleton during astogeny. Branches thick, moderately variable in depth.

Autozooecial living chamber size lower-end intermediate, chambers biserially arranged in alternating rows along planar branch axial wall; axial wall zigzagging near reverse wall, extending diagonally across entire branch; axial wall becoming less sinuous in mid chamber, inflected toward and connecting with chamber lateral walls, only slightly sinuous near obverse surface. Chamber longest dimension parallel to reverse wall in proximodistal direction. Autozooecial chamber outline irregularly ovate to rounded triangular near reverse wall, rapidly becoming irregularly pentagonal throughout mid chamber and most of chamber depth, approaching rectangular nearer obverse surface; becoming irregularly ovate to elliptical nearest obverse surface, longest dimension oriented distal-abaxially; chamber shape moderately uniform. Aperture located at distal-abaxial end of chamber, connected to chamber by well-developed, moderately long, variable-length vestibule. Ratio of autozooecial chamber minimum width to maximum width approximately 2:3; maximum width to depth ratio approximately 9:10; ratio of chamber depth to length about 4:5; chamber depth and length highly constant, minimum and maximum widths highly variable. Superior and inferior hemisepta both absent. Autozooecial chambers diverge laterally from middle of branch at highly variable angle (mean of 20°); from reverse wall at highly constant angle (mean of 66°).

Three-dimensionally reconstructed chamber form an irregular rectangular box; length as viewed from lateral edge of branch; depth, viewed from distal end of branch, slightly greater than width, viewed from obverse surface.

Internal granular skeletal layer moderately thick, well-developed, continuous with obverse nodes, stylets, keel, peristome, and reticulate meshwork, which is completely composed of granular skeletal material; reverse longitudinal striae and microstylets; across dissepiments and in the middle of zoarial supports. Outer lamellar layer extremely thick, exhibiting pronounced astogenetic thickening, most prominent toward proximal end of zoarium.

Remarks.—Pronounced astogenetic thickening, which gives a highly varied appearance to the exterior reverse and to a lesser degree the obverse surface, characterizes *H. aprilae*. This species most closely resembles *H. aspera* Ulrich, 1890 among the species of *Hemitrypa*, but the two species are differentiated by the appreciably wider and deeper branches, slightly shorter and wider autozooecial chambers, moderately larger and narrower fenestrule openings, and lack of reverse macrostylets in *H. aprilae*. Similarities between *H. aprilae* and *H. aspera* do, however, suggest close phylogenetic affinities.

Material studied.—Twenty-two exterior fragments, eight sectioned specimens; largest zoarial fragment 24×32 mm (width to length). The excellent preservation, including that of the reticulate meshwork, observed in this species probably is a result of pronounced astogenetic thickening of lamellar skeleton.

Occurrence.—*Hemitrypa aprilae* is rare at the Valmeyer and St. Louis localities, and occurs primarily in the Lower and Middle Warsaw at these localities. It is present in both calcarenites and shales.

Holotype.—UI X-6867 (loc. 49B, sample 15).

Paratypes.—UI X-6865, 6866, 6935–6939 (loc. 49B, samples 12, 13).

Hemitrypa aspera Ulrich, 1890

Plate 46, figures 1–13, Plate 47, figures 1–6; Table 35

Hemitrypa aspera Ulrich, 1890, p. 563, pl. 57, figs. 3a, 4–4f [Keokuk Group, Nauvoo, Illinois, Keokuk and Bentonsport, Iowa]; Keyes, 1894, p. 25 [Keokuk Limestone, Keokuk, Iowa].

Diagnosis.—Zoarium moderately delicate, mesh spacing lower-end intermediate, pattern moderately regular; reticulate meshwork present, well-developed, polygonal in shape; branches delicate, width narrow, intermediate in depth, branches straight to broadly sinuous, lateral branches broadly curved at zoarial edge; transversely approximately circular, becoming elliptical to ovate with astogeny, closely spaced and joined at moderately regular intervals by lower-end intermediate width, short dissepiments. Fenestrules small; shape elliptical to ovate on obverse surface, approaching rectangular to square on reverse, irregular. Autozooecial aperture size intermediate, ovate, elongate proximodistally or proximoabaxially, to rarely circular; surrounded by thin, well-developed, complete peristome; one to three (most commonly two) apertures per fenestrule. Single intermediate width keel present; keel straight to anastomosing, extending along middle of obverse branch surface, atop which are intermediate

Table 35.—Summary numerical analysis of *Hemitrypa aspera* Ulrich, 1890. For explanation of abbreviations of characters (left column), see Table 8b (foldout inside back cover).

	number of measurements	mean	standard deviation	coefficient of variation	observed range
1. WB	24	0.2750	0.0447	16.25	0.156–0.388
2. DBC	24	0.4250	0.0734	17.27	0.273–0.584
3. WD	24	0.1385	0.0294	21.23	0.108–0.294
4. LF	24	0.3540	0.1128	31.86	0.200–0.488
5. WF	24	0.2400	0.0531	22.13	0.138–0.356
6. AF	24	2.25	0.45	20.10	1–3
7. AL	24	0.1300	0.0087	6.69	0.104–0.156
8. AW	24	0.0880	0.0065	7.39	0.072–0.126
9. ADB	24	0.2400	0.0173	7.21	0.204–0.270
10. AAB	24	0.2580	0.0279	10.81	0.186–0.276
11. ABB	24	0.2670	0.0388	14.53	0.214–0.385
12. DN	24	0.1060	0.0119	11.23	0.072–0.200
14. SNB	24	0.2880	0.0467	16.23	0.194–0.388
15. WK	24	0.0888	0.0159	17.91	0.038–0.139
16. DSO	24	0.0165	0.0043	36.06	0.008–0.028
17. SSO	24	0.0465	0.0181	38.92	0.024–0.120
18. WP	24	0.0212	0.0035	16.51	0.020–0.038
21. RSL	24	0.0740	0.0187	25.27	0.046–0.126
22. RSS	24	0.0320	0.0043	13.44	0.018–0.058
23. SSL	24	0.1120	0.0360	32.14	0.068–0.248
24. SSS	24	0.0425	0.0089	20.94	0.034–0.088
25. LRM	24	0.2450	0.0227	9.27	0.132–0.320
26. WRM	24	0.2240	0.0296	13.21	0.120–0.336
30. OL	24	0.2420	0.0514	21.24	0.160–0.360
31. OW	24	0.2400	0.0450	18.75	0.174–0.392
32. TRW	24	0.0114	0.0020	17.54	0.009–0.026
33. TLW	24	0.0104	0.0014	13.46	0.008–0.019
34. FWT	24	0.0428	0.0172	40.19	0.013–0.126
35. RWT	24	0.0721	0.0231	32.04	0.021–0.135
36. CL	24	0.2385	0.0115	4.84	0.225–0.295
37. CD	24	0.1620	0.0111	6.85	0.146–0.220
38. MAW	24	0.1325	0.0228	17.21	0.102–0.200
39. MIW	24	0.0750	0.0142	18.93	0.033–0.128
40. VD	24	0.0450	0.0101	22.44	0.020–0.091
41. RA	24	68.50	5.77	8.42	60–84
42. LA	24	16.65	3.35	20.12	12–31
43. TB	24	0.4550	0.0684	19.27	0.368–0.627

size, circular, ovate to iregularly stellate nodes. Autozooecial chamber size lower-end intermediate, chambers emplaced in two rows, except either third row at sites of branch bifurcation or three rows for moderate to pronounced distances proximal to sites of branch bifurcation; outline irregularly ovate to rounded triangular near reverse wall; irregularly pentagonal throughout most of chamber depth; irregularly ovate to elliptical near obverse surface. Chamber longest dimension parallel to reverse wall in proximodistal direction. Aperture at distal-abaxial end of chamber, connected to chamber by short, variable-length vestibule. Superior and inferior hemisepta both absent. Lateral-wall budding-angle highly variable (mean of approximately 17°); reverse-wall budding-angle constant (mean of 69°). Heterozooecia (ovicells?) occurring as intermediate size enlargements of some apertures.

Table 35 presents statistical criteria used in delimiting this species.

Exterior description.—Zoarium moderately delicate, expansion flat to undulating, fan-shaped; mesh spacing lower-end intermediate; moderate to pronounced astogenetic thickening of both obverse and reverse zoarial skeleton; external zoarial pattern moderately irregular. Well-developed reticulate meshwork present throughout obverse surface of zoarium best developed typically covering proximal and medial zoarium surface, less common at lateral and distal edges of zoarium; reticulate meshwork slightly thickened along branch midline, with mesh forming as secondary extensions of keel, nodes, and dissepiments; meshwork develops toward fenestrule from branch midline and dissepiment surface to form irregularly polygonal (ranging from square to hexagonal in shape) features covering obverse zoarial surface, each facet of polygon developing around single apertural opening; width and length of meshwork dimensions approximately same as aperture spacings along and across obverse branch surface; width approximately same as aperture spacings along and across obverse branch surface; width approximately four-fifths that of branch, meshwork opening width to length ratio approximately 11:12; three to seven (most commonly four) nodular extensions into meshwork opening from mesh skeletal edge. Probable mature zoarial widths 25 to 40 mm, lengths 30 to 50 mm.

Branches delicate, narrow, moderately variable in width; straight to broadly sinuous, lateral branches broadly curved toward edge of zoarium. Branches closely spaced, distance between adjacent branch centers moderately regular. Obverse surface texture moderately granular, becoming increasingly so with astogeny, surface rounded to slightly angular, except for presence of single keel; keel width intermediate, extremely well-developed, continuous, straight to anastomosing, extending along branch midline and causing pronounced positive inflection in obverse surface profile. Pronounced astogenetic thickening of keel; most pronounced toward proximal end of zoarium. Nodes monoserially emplaced, well-developed, intermediate-size, shape circular, ovate to irregularly stellate, elongate proximodistally; nodes highly regular in size, variable in shape; develop as projections from middle of keel; one to three (most commonly two) per fenestrule length; spacing intermediate, moderately even; pronounced increase of node diameter with astogeny. Intermediate-size stylets, highly variably sized and positioned, occurring across obverse surface. Reverse surface texture granular, becoming increasingly so with astogeny, bearing few rows of widely spaced longtudinal striae which become partially to completely cov-

ered by lamellar skeleton during astogeny; rows of large microstylets, closely spaced, develop as extensions of longitudinal striae along reverse branch surface; during astogeny bimodal development of reverse microstylets occurs, with some microstylets remaining relatively unchanged, others joining to form aggregates that become intermediate-size macrostylets; shape circular to ovate, slightly elongate proximodistally, with size and shape both variable; irregularly positioned across branch surface; spacing close to intermediate, variable, with size of macrostylet greatly increasing during astogeny. Autozooecia in two rows, except either third row at sites of branch bifurcation where middle autozooecium evidently shared by both branches, or three rows for moderate to pronounced distances proximal to sites of branch bifurcation; slight thickening proximal, thinning distal to sites of branch bifurcation. Heterozooecia (ovicells?) occurring as intermediate to pronounced enlargements of some apertures; mean widths and lengths of polymorphs approximately twice autozooecial aperture length; polymorph widths and lengths approximately equal; connection evident between polymorph and autozooecial chamber; polymorphs most commonly situated toward proximal end of zoarium.

Dissepiments of lower-end intermediate width, slightly greater than half branch width, variable; short, variable in length; connect branches at moderately regular intervals. Dissepiments barlike, exhibiting slight medial thinning, slight flaring at branch–dissepiment junction; highly recessed from obverse, approximately even with reverse branch surface. Moderate astogenetic thickening of dissepiments toward proximal end of zoarium. Obverse dissepiment surface with two to four longitudinal ridges emplaced perpendicular to branch length, intermediate stylets similar in size to obverse branch stylets develop atop these ridges; stylets become irregularly positioned across dissepiment surface and striae become covered by lamellar skeleton with astogeny; reverse dissepiment surface with medially thickened ridge bearing large microstylets and intermediate-size macrostylets. Obverse and reverse dissepiment surface texture granular, coarsening with astogeny. Dissepiment emplacement variable, ranging from perpendicular to branch length to angles up to 20° from perpendicular. Apertures commonly positioned on proximal or distal edge, or in middle of dissepiment edge at branch–dissepiment contact, arranged symmetrically or asymmetrically between branches.

Fenestrules small; shape varying from elliptical to ovate on obverse surface, approaching rectangular to square on reverse, elongate proximodistally; irregular in size and shape; moderately expanding in width and length in obverse–reverse direction. Width of fenestrule slightly less than branch width on obverse surface, slightly greater than branch width on reverse; fenestrule opening size greatly reduced toward proximal end of zoarium due to astogenetic thickening of lamellar skeleton. Width to length ratio of fenestrule ranging from approximately 4:5 to 1:5; ratio of fenestrule mean width to length approximately 2:3, both width and length variable, with length more so than width. One to three (most commonly two) apertures per fenestrule length; distance between closest aperture centers along branch, across branch and across fenestrule approximately equal; spacing along and across branch moderately constant to slightly variable, spacing across fenestrule variable.

Autozooecial aperture size intermediate, moderately large relative to branch, shape ovate to rarely circular; elongate proximodistally or proximoabaxially; width to length ratio approximately 2:3; size uniform, shape moderately variable; opening orientation typically at slight angle toward fenestrule, less commonly parallel to plane of obverse surface; surrounded by thin, well-developed, complete peristome. Moderate projection of apertures into fenestrule, causing inflections in fenestrule outline on obverse surface. Centrally thickened terminal diaphragms present, occurring most commonly at proximal end of zoarium beneath overlying reticulate meshwork.

Zoarial supports moderately rare, develop as extensions of reverse zoarial surface and lateral edges of zoarium.

Interior description.—Branches approximately circular in transverse section; becoming irregularly ovate to elliptical, elongate either obverse–reversely or parallel to plane of obverse surface, with addition of secondary lamellar skeleton during astogeny. Branch depth medium, moderately variable.

Autozooecial living chamber size lower-end intermediate, chambers biserially arranged in alternating rows along planar branch axial wall; axial wall zigzagging near reverse wall, extending diagonally across entire branch; axial wall becoming less sinuous in mid chamber, inflected toward and connecting with chamber lateral walls, only slightly sinuous near obverse surface. Chamber longest dimension parallel to reverse wall in proximodistal direction. Autozooecial chamber outline irregularly ovate to rounded triangular near reverse wall, rapidly becoming irregularly pentagonal throughout mid chamber and most of chamber depth; irregularly ovate to elliptical near obverse surface, longest dimension oriented distal-abaxially; chamber shape moderately to highly uniform. Aperture located at distal-abaxial end of chamber, connected to chamber by well-developed, short, variable-length vestibule. Ratio of autozooecial chamber minimum width to maximum width approximately 5:9; maximum width to depth ratio approximately 4:5; ratio of chamber

depth to length approximately 2:3; chamber depth and length highly constant, minimum and maximum widths highly variable. Superior and inferior hemisepta both absent. Autozooecial chambers diverge laterally from middle of branch at highly variable angle (mean of approximately 17°); from reverse wall at constant angle (mean of 69°).

Three-dimensionally reconstructed chamber form an irregular rectangular box; length as viewed from lateral edge of branch; depth, viewed from distal end of branch, moderately greater than width, viewed from obverse surface.

Internal granular skeletal layer relatively thick, well-developed, continuous with obverse nodes, stylets, keel, peristome, and reticulate meshwork, which is completely composed of granular skeletal material; reverse longitudinal striae, microstylets and macrostylets; across dissepiments and in middle of zoarial supports. Outer lamellar layer thickness intermediate to thick, exhibiting moderate to pronounced astogenetic thickening, most prominent toward proximal end of zoarium.

Remarks.—*Hemitrypa aspera* was first identified by Ulrich from "Keokuk Group" materials collected near Nauvoo, Illinois and Keokuk and Bentonsport, Iowa. Ulrich included what is currently considered the Lower Warsaw in his "Keokuk Group". *H. aspera* was recognized by Ulrich on the basis of nodes on the reverse dissepiment surface and strong spines extending from the reticulate meshwork. The presence of both reverse microstylets and macrostylets characterizes this species, although spinal development associated with the obverse reticulate meshwork is typical of certain astogenetic stages in all species of *Hemitrypa* Phillips, 1841.

H. aspera is distinguished from other species of *Hemitrypa* by having the smallest autozooecial chamber size of all such species analyzed, the closest spaced branches, finest mesh spacing, and presence of macrostylets on reverse branch and dissepiment surfaces. *H. aspera* is the only Warsaw species which contains these macrostylets, thus allowing species recognition from the reverse surface. It is, however, desirable to have interior analyses as well.

Material studied.—Thirty-four exterior fragments, 10 sectioned specimens; largest zoarial fragment 27 × 20 mm (width to length). The preservation of zoarial fragments, including reticulate meshwork, is excellent in this species.

Occurrence.—*Hemitrypa aspera* is common throughout the study area, most commonly occurring in facies deposited in moderately to extremely low energy depositional environments.

Syntypes.—ISGS (ISM) 2823–1/2; USNM 43764, 43765.

Figured and/or measured specimens.—UI X-6855, 6940 (loc. 10, sample 28), 6852 (loc. 11, sample 57), 6851, 6854, 6856, 6857 (loc. 49B, samples 12, 14, 17).

Hemitrypa vermifera (Ulrich, 1890)
Plate 47, figure 7, Plate 48, figures 1–10,
Plate 49, figures 1–6; Table 36

Hemitrypa proutana var. *vermifera* Ulrich, 1890, p. 562, pl. 57, figs. 5, 5a [Warsaw Beds, Warsaw, Illinois].

Diagnosis.—Zoarium robust, mesh spacing close, pattern regular; reticulate meshwork present, well-developed, polygonal (square to hexagonal) in shape; branches robust, width intermediate, very thick in depth; branches straight to less commonly sinuous, broadly curved at lateral zoarial edge; transversely circular to irregularly elliptical, spacing close and joined at moderately regular intervals by intermediate-width, short dissepiments. Fenestrule size lower-end intermediate; shape typically elliptical, less commonly ovate, rarely circular, moderately irregular. Autozooecial apertures large, irregularly ovate to elliptical, rarely circular, typically elongate proximoabaxially or proximodistally; surrounded by upper-end thin, well-developed, complete peristome; two to three apertures per fenestrule (mean of 2.5). Single, intermediate-width, continuous keel present; keel straight to slightly anastomosing, extending along middle of obverse branch surface, atop which are positioned upper-end intermediate size, irregularly stellate to ovate nodes. Autozooecial chamber size intermediate, chambers emplaced in two rows, except either third row at sites of branch bifurcation or more rarely three rows for moderate distances proximal to sites of branch bifurcation; outline irregularly ovate, elliptical to rounded triangular near reverse wall, irregularly pentagonal immediately toward mid chamber, outline irregular parallelogram to rectangle throughout most of chamber, irregularly ovate near obverse surface. Chamber longest dimension parallel to reverse wall proximodistally. Aperture at distal-abaxial end of chamber, connected to chamber by intermediate, highly variable length vestibule. Superior and inferior hemisepta both absent. Lateral-wall budding-angle highly variable (mean of 23°); reverse-wall budding-angle highly constant (mean of 60°). Heterozooecia (ovicells?) occurring as pronounced enlargements of some apertures.

Table 36 presents statistical criteria used in delimiting this species.

Exterior description.—Zoarium robust, expansion flat to rarely slightly undulating, fan-shaped; mesh spacing close; extremely pronounced astogenetic thickening of both obverse and reverse zoarial skeleton; external zoarial pattern regular. Well-developed reticulate meshwork covering obverse zoarial surface, absent only at lateral and distal edges of zoarium; retic-

ulate meshwork exhibiting pronounced thickening along branch midline, with mesh forming as secondary extension of keel, nodes, and dissepiments; mesh develops toward fenestrule from branch midline and dissepiment surface to form polygonal (ranging from square to hexagonal) feature covering obverse zoarial surface, each facet of polygon developing around single apertural opening; width and length of meshwork dimensions slightly greater than aperture spacings along and across obverse branch; width approximately seven-eighths that of branch, meshwork width to length ratio approximately 1:1, width slightly greater than length; variable number, three to seven, nodular extensions into meshwork opening from mesh skeletal edge. Probable mature zoarial widths and lengths of half a meter or more attained in large zoaria.

Branches robust, width intermediate, slightly variable; typically straight, less commonly sinuous, exhibiting minor inflections toward sites of dissepiment emplacement, lateral branches broadly curved toward edge of zoarium. Branch spacing close, distance between adjacent branch centers highly regular. Obverse surface texture slightly granular, becoming moderately granular with astogeny; surface angular to slightly rounded, containing single keel; keel width intermediate, well-developed, continuous, straight or slightly anastomosing, extending along branch midline and causing pronounced positive inflection in obverse surface profile. Pronounced astogenetic thickening of keel; most pronounced toward proximal end and middle of zoarium. Node monoserially emplaced, well-developed, size upper-end intermediate, shape irregularly stellate to ovate, elongate proximodistally; nodes highly regular in size, variable in shape; develop as projections from middle of keel; one to three (most commonly two) per fenestrule length; nodes intermediately highly regularly spaced; pronounced increase of node diameter with astogeny. Intermediate-size stylets, variably sized and positioned, occurring across obverse branch surface. Reverse surface texture granular, coarsening with astogeny, bearing relatively few rows of intermediately spaced longitudinal striae, which become covered by lamellar skeleton during astogeny; rows of numerous intermediate-size microstylets, closely spaced, develop as extensions of longitudinal striae along reverse branch surface; microstylets moderately constant, diameters exhibiting slight increase with astogeny and microstylets become more variably positioned across reverse branch surface. Autozooecia in two rows across branch, except either third row at sites of branch bifurcation, or more rarely three rows extending for moderate distances proximal to sites of branch bifurcation; pronounced thickening proximal, moderate thinning distal to sites of branch bifurcation. Heterozooecia (ovicells?) occurring as pronounced enlargements of some apertures; mean widths and lengths of polymorphs approximately twice autozooecial aperture length; polymorph width slightly less than length, ratio 4:5; connection evident between polymorph and autozooecial chamber; polymorphs most commonly situated toward proximal end of zoarium.

Table 36.—Summary numerical analysis of *Hemitrypa vermifera* (Ulrich, 1890). For explanation of abbreviations of characters (left column), see Table 8b (foldout inside back cover).

	number of measurements	*mean*	*standard deviation*	*coefficient of variation*	*observed range*
1. **WB**	24	0.3416	0.0580	16.98	0.225–0.500
2. **DBC**	24	0.5209	0.0679	13.04	0.400–0.640
3. **WD**	24	0.2334	0.0465	19.92	0.165–0.338
4. **LF**	24	0.4452	0.0945	21.23	0.231–0.588
5. **WF**	24	0.2457	0.0432	17.58	0.153–0.331
6. **AF**	24	2.50	0.51	20.43	2–3
7. **AL**	24	0.1655	0.0102	6.16	0.146–0.184
8. **AW**	24	0.1140	0.0081	7.11	0.100–0.130
9. **ADB**	24	0.2828	0.0210	7.43	0.240–0.320
10. **AAB**	24	0.2799	0.0347	12.40	0.206–0.348
11. **ABB**	24	0.3076	0.0399	12.97	0.250–0.400
12. **DN**	24	0.1181	0.0121	10.25	0.096–0.148
14. **SNB**	24	0.3057	0.0250	8.18	0.264–0.356
15. **WK**	24	0.0907	0.0165	18.19	0.066–0.136
16. **DSO**	24	0.0129	0.0028	21.71	0.008–0.021
17. **SSO**	24	0.0401	0.0117	29.18	0.024–0.078
18. **WP**	24	0.0198	0.0039	19.70	0.015–0.029
22. **RSS**	24	0.0198	0.0027	15.17	0.016–0.025
24. **SSS**	24	0.0343	0.0093	27.11	0.022–0.058
25. **LRM**	24	0.2817	0.0210	7.45	0.232–0.316
26. **WRM**	24	0.3093	0.0331	10.70	0.260–0.400
30. **OL**	24	0.2615	0.0367	14.03	0.206–0.344
31. **OW**	24	0.2113	0.0234	11.07	0.180–0.248
32. **TRW**	24	0.0243	0.0033	13.58	0.019–0.029
33. **TLW**	24	0.0163	0.0029	17.79	0.011–0.022
34. **FWT**	24	0.0898	0.0297	33.07	0.046–0.140
35. **RWT**	24	0.2186	0.0628	28.73	0.133–0.319
36. **CL**	24	0.2918	0.0133	4.56	0.278–0.318
37. **CD**	24	0.2146	0.0164	7.64	0.188–0.249
38. **MAW**	24	0.1667	0.0277	16.62	0.120–0.210
40. **VD**	24	0.0823	0.0198	24.06	0.050–0.121
41. **RA**	24	59.75	4.16	6.96	52–67
42. **LA**	24	23.00	4.47	19.44	14–30
43. **TB**	24	0.6672	0.1239	18.57	0.471–0.910

Dissepiments of intermediate width, approximately two-thirds that of branch, barely constant; short, moderately constant in length; connect branches at moderately regular intervals. Dissepiments exhibit moderate medial thinning, pronounced flaring at branch–dissepiment junction; highly recessed from obverse, approximately even with reverse branch surface. Pronounced astogenetic thickening of dissepiments toward proximal end of zoarium. Obverse dissepiment surface with one to three longitudinal ridges emplaced perpendicular to branch length, intermediate-size stylets, similar in size to obverse branch stylets, develop

atop these ridges; stylets become irregularly positioned across dissepiment with astogeny; reverse dissepiment surface bearing rows of intermediate-size microstylets. Obverse dissepiment surface texture slightly granular, reverse surface texture granular, both coarsening with astogeny. Dissepiments emplaced approximately perpendicular to branch length. Apertures commonly positioned on proximal or distal edge, or in middle of dissepiment edge at branch–dissepiment contact; arranged symmetrically or asymmetrically between branches.

Fenestrule size lower-end intermediate; shape typically elliptical; less commonly ovate, elongate proximodistally, rarely circular; moderately irregular in size and shape; slightly expanding in width and length in obverse–reverse direction. Width of fenestrule approximately half that of branch on obverse surface, four-fifths branch width on reverse; fenestrule opening size reduced toward proximal end of zoarium due to astogenetic thickening of lamellar skeleton. Width to length ratio of fenestrule variable, ranging from 1:1 to as much as 1:4; ratio of fenestrule mean width to length approximately 5:9; width more constant than length, width barely constant and length slightly variable. Two to three apertures per fenestrule length (mean of 2.5); distance between closest aperture centers along branch and across branch equal, slightly less than spacing across fenestrule which is approximately 1.1 times greater; spacing along branch moderately constant, spacing across branch and across fenestrule both moderately variable.

Autozooecial apertures large, shape irregularly ovate to elliptical, rarely circular, enlarged slightly at distal end; elongate proximoabaxially or proximodistally; width to length ratio approximately 2:3; size highly uniform, shape moderately variable; opening typically oriented parallel to plane of obverse surface, less frequently at slight angle toward fenestrule; surrounded by upper-end thin, well-developed complete peristome. Aperture margins extend into fenestrule, causing slight inflections in fenestrule outline on obverse surface. Centrally thickened terminal diaphragms occurring at proximal end of zoarium beneath reticulate meshwork.

Zoarial supports well-developed, forming as extensions of reverse zoarial surface or lateral edges of zoarium.

Interior description.—Branches circular to irregularly elliptical in transverse section, slightly enlarged on obverse surface, elongate in obverse–reverse direction, becoming increasingly elongate with addition of secondary lamellar skeleton during astogeny. Branches very thick, moderately variable in depth.

Autozooecial living chamber size intermediate, chambers biserially arranged along planar branch axial wall; axial wall zigzagging near reverse wall, extending diagonally across entire branch; becoming less sinuous toward mid chamber, extending toward and connecting with chamber lateral walls; axial wall approaching straight in mid chamber and near obverse surface, in some branches slightly sinuous. Chamber longest dimension parallel to reverse wall in proximodistal direction. Autozooecial chamber outline irregularly ovate, elliptical to rounded triangular near reverse wall; becoming irregularly pentagonal toward mid chamber and an irregular parallelogram to rectangle throughout mid chamber and most of chamber depth; irregularly ovate near obverse surface, slightly enlarged at distal end, longest dimension of ovoid oriented distal-abaxially; chamber shape highly uniform. Aperture positioned at distal-abaxial or distal end of chamber, connected to chamber by well-developed, intermediate-length vestibule of highly variable length. Ratio of autozooecial chamber width to depth approximately 7:9; chamber depth to length ratio approximately 3:4; chamber depth and length highly constant, width highly variable. Superior and inferior hemisepta both absent. Autozooecial chambers diverge laterally from middle of branch at highly variable angle (mean of 23°); from reverse wall at highly constant angle (mean of 60°).

Three-dimensionally reconstructed chamber form an irregular rectangular box, length as viewed from lateral edge of branch; depth, viewed from distal end of branch, moderately greater than width, viewed from obverse surface.

Internal granular skeletal layer thick; granular skeletal layer extremely well-developed, continuous with obverse nodes, stylets, keel, peristome, and reticulate meshwork, which is entirely formed of granular skeletal material; reverse longitudinal striae and microstylets; across dissepiments and in the middle of zoarial supports. Outer lamellar layer extremely thick, exhibiting pronounced astogenetic thickening, most prominent toward proximal end of zoarium.

Remarks.—*Hemitrypa vermifera* was first recognized by Ulrich in materials from Geode Glen (*Warsaw Beds* of Ulrich), where this species was considered a new variety of *H. hemitrypa*. Recognition of this variety was based on "certain peculiar, tubular, vermiform bodies, which are irregularly distributed over and form part of the reverse face of the zoarium" (Ulrich, 1890, p. 561). Interior analysis of these features reveals them to be zoarial supports, their tubular nature as seen by Ulrich a result of differential preservation of outer lamellar *versus* inner granular skeletal material. Similar supports are present toward the proximal end of the zoarium in all species of *Hemitrypa*, making the use of such criteria for species identification tenuous at best.

H. vermifera is distinguished from all other species of the genus by having the largest autozooecial chambers, largest aperture size, smallest reverse-wall budding-angle, and widest apertural spacing of all species analyzed. The highly granular nature caused by the presence of numerous intermediate-size stylets is highly diagnostic of *H. vermifera*. External mesh similarity between this species and *H. hemitrypa* is pronounced, probably accounting for inclusion of *H. vermifera* as a variety of *H. hemitrypa* by Ulrich, but once interior characters are considered, the differences between the two species are readily apparent. The variety *H. proutana vermifera* is, therefore, elevated to the species *H. vermifera* herein.

Material studied.—Thirty-six exterior fragments, four sectioned specimens; largest zoarial fragment 48 × 33 mm (width to length). The preservation of zoarial fragments is good to excellent as a result of the robust nature of zoarium. Physical compaction of branches is rare, although silicification of internal granular skeletal layer is common. The reticulate meshwork is frequently compacted onto the obverse zoarial surface.

Occurrence.—*Hemitrypa vermifera* is present in the northern half of the study area, occurring as far south as Mt. Sterling. *In situ* occurrences are primarily observed in lower energy depositional environments, such as argillaceous micrites and biomicrites. Vermiform features apparently were used as supports in these muddy environments.

Syntypes of H. proutana vermifera.—ISGS(ISM) 2815–1. A specimen is illustrated in Ulrich (1890, pl. 57, figs. 5, 5a).

Figured and/or measured specimens.—UI X-6880–6885, 6863–6865 (loc. 11, sample 57).

Genus **ARCHIMEDES** Hall, 1858

Type species.—*Fenestella* (*Archimedes*) *wortheni* Hall, 1857b [Lower Mississippian (Valmeyeran), Warsaw Formation].

Diagnosis.—Zoarium robustness delicate to robust, mesh spacing close; tightly coiled central axis present, composed of thickened lamellar skeletal layer formed around lateral spiraling branch from which all mesh originates; chamber outline irregularly pentagonal in mid tangential section, chamber size upper-end small to lower-end intermediate; aperture size intermediate; superior and inferior hemisepta absent; chamber reverse-wall budding-angle varies between 58° and 70° (means).

Three-dimensionally reconstructed chamber form a slightly irregular rectangular box.

Description.—Zoarial robustness varying from delicate to robust, expansion cupped or fan-shaped around tightly coiled central axis, mesh spacing close, regular; central axis present, forms as thickened lamellar skeletal layer which develops around lateralmost spiraling branch from which all mesh originates.

Branch width narrow to intermediate, trace straight as viewed from obverse, sinuous and irregular as viewed from reverse zoarial surface, with reverse sinuous due to secondary thickening of lamellar skeleton; branch surface flat to rounded. Keel present, single, width narrow, covered by lamellar skeleton with astogeny. Nodes present, emplacement monoserial, size small to intermediate, shape circular, ovate to slightly stellate, located atop keel, spacing close to intermediate. Obverse stylets present, size small, occurring across obverse surface. Microstylets present, small, positioned initially in rows, becoming more variably positioned across branch surface with astogeny. Macrostylets absent. Autozooecia in two rows, third row at sites of branch bifurcation or three rows for distance along branch proximal to branch bifurcation. Heterozooecia (ovicells?) present in some species.

Dissepiments of intermediate width, length short, connect branches at regular intervals.

Fenestrule size intermediate, shape elliptical on obverse surface; elliptical, ovate, circular to square on reverse depending on degree of thickening of lamellar skeleton.

Aperture size intermediate, shape varying from circular to ovate to elliptical, oriented parallel to plane of obverse surface. Peristome present, incomplete; apertural stylets present or absent, form as extensions of peristomal edge; terminal diaphragms present, occurring toward proximal end of zoarium and adjacent to central axis.

Branch shape in cross-section ranging from circular to ovate to elliptical, branches thin to thick in depth.

Autozooecial chamber size upper-end small to lower-end intermediate, chambers biserially emplaced

Text-figure 16.—*Archimedes wortheni* illustrated. 1, diagrammatic longitudinal section showing changing chamber outline from deep section near middle of branch (bottom of figure) to shallow section near abaxial edge of branch (top of figure) [Observe the thickened reverse lamellar skeletal layer (arrow) continuous with the lamellar central axis.], × 70; 2, diagrammatic tangential section illustrating changing chamber outline from deep section near reverse-wall budding-site (bottom of figure) to shallow section near obverse surface (top of figure) [Observe presence of incomplete peristome (arrow) characteristic of this genus.], × 70; 3, diagrammatic transverse section across branch showing typical aperture orientation (arrow) to plane of obverse surface, × 70; 4, reconstruction of typical chamber shape (three-dimensional) as viewed from abaxial edge of branch, × 140; 5, reconstruction of typical chamber shape (three-dimensional) as viewed from distal end of branch; chamber reconstructed is from the right side of branch, × 140; 6, reconstruction of typical chamber shape (three-dimensional) as viewed from obverse surface; chamber reconstructed is from the right side of branch [The smooth, curved outlines of chamber shapes are the result of a lack of hemisepta.], × 140; 7, reconstruction of tightly coiled central axis, illustrating mesh radiating outward from spire (arrow), × 140.

along sinuous axial wall; maximum chamber length extending proximodistally, parallel to reverse wall. Chamber outline ovate, irregularly pentagonal in mid chamber and throughout most of chamber depth; irregularly elliptical to irregularly ovate near obverse surface. Vestibule present, varying in length from short to intermediate. Superior and inferior hemisepta absent. Lateral-wall budding-angle ranging from 20° to 27° (means); reverse-wall budding-angle varying from 58° to 70° (means). Lamellar skeletal layer intermediate to thick, exhibiting moderate to pronounced astogenetic thickening; granular skeletal layer thickness intermediate to thick, exhibiting no astogenetic thickening.

Three-dimensionally reconstructed chamber form a slightly irregular rectangular box.

Text-figure 16 illustrates zoarial outlines in longitudinal, tangential, and transverse orientations, three-

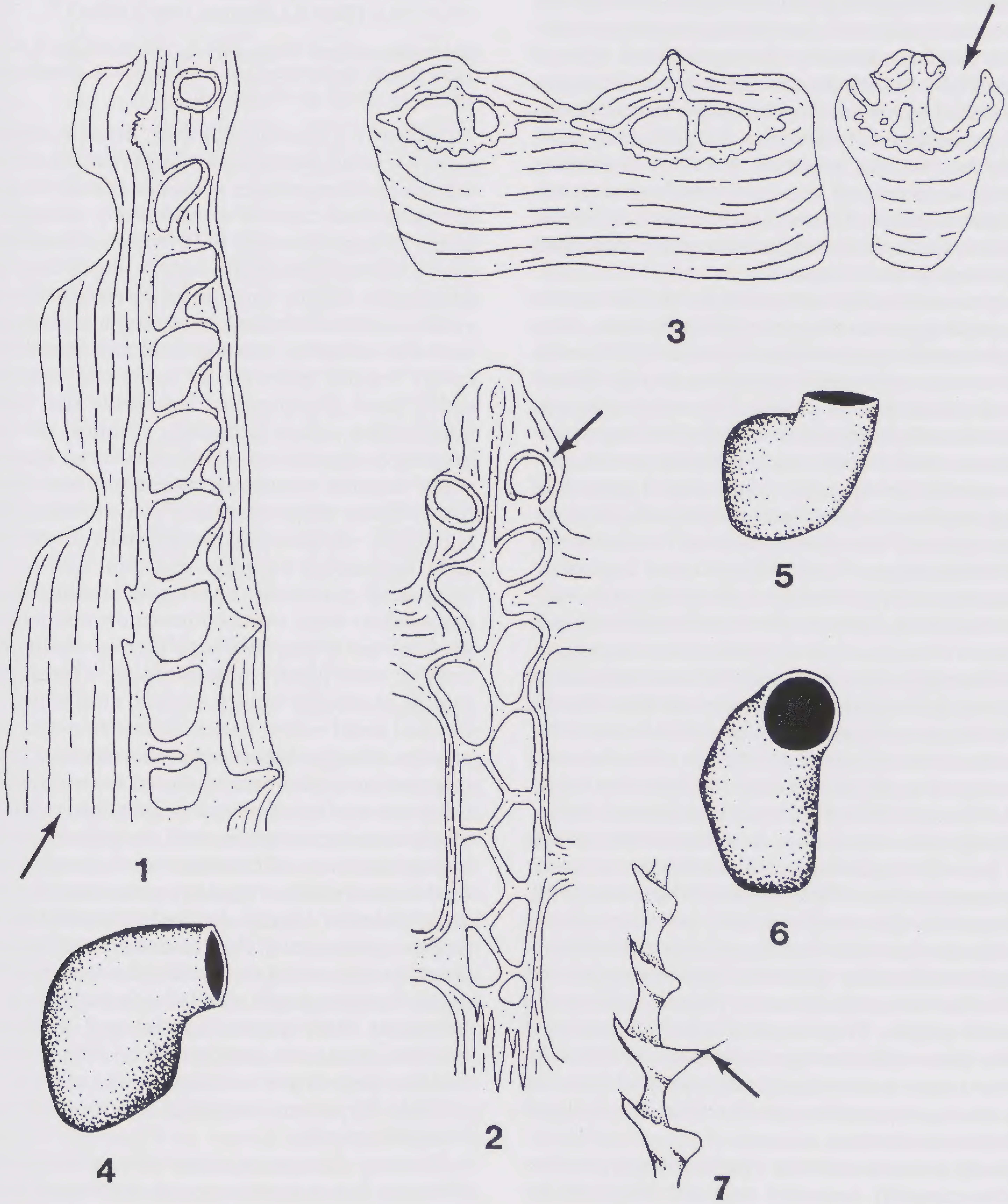

dimensional chamber reconstructions from abaxial branch edge, distal, and obverse surface views, and side view of central axis.

Remarks.—LeSueur (*fide* Owen, 1842) was apparently the first to apply the name *Archimedes* to the spiralling screw-like forms found in Mississippian rocks. Owen (1838) referred to Upper ? Mississippian rocks as "*Archimedes* limestone", recognizing the spiral axis of LeSueur but not offering a formal description. Owen (1842, p. 19) discussed and illustrated as "*Retepora Archimedes*" a fossil which was "ventricillated spirally like a continuous screw"; attributing the name *Archimedes* to this form based on the unpublished work of LeSueur. Hall (1857b) described a number of species of *Fenestella* (*Archimedes*), providing a loose description of the subgenus *Archimedes*. In 1858, Hall more formally decribed the subgenus, but when describing the species *wortheni* and *reversa* elevated the subgenus to the rank of genus. This is therefore the first formal description and species assignment to the described genus present in the literature.

The genus is readily recognized by the distinctive tightly spiraling axis at the center of the zoarium, from which the zoarial mesh radiates outward. Both loosely spiraled axes and extremely open spires are represented in several closely related genera. The axis develops as thickened lamellar skeleton around the interlateral colony branch, which rotates slightly during growth, giving the spiraled configuration of the axis. Tightness of spiraling appears to have been greatly influenced by environment and thus is not of great importance in species delimitation. Width of spiral also appears to be primarily environmentally influenced, with astogenetic thickening adding to the lamellar skeletal layer.

Accurate determination of species of *Archimedes* requires thorough examination of the axis and zoarial mesh, using both interior and exterior analyses. Species based solely on axes, such as *A. grandis* Ulrich, 1890, have little or no taxonomic validity, as environmental influence greatly affects axis diameter and whorl spacing (McKinney, 1979; McKinney and Gault, 1980).

Although the central axis is characteristic of this genus, the outer appearance of the meshwork is similar in appearance to that of *Rectifenestella* Morozova, 1974, *Laxifenestella*, *Apertostella*, n. gen., and even species of *Hemitrypa* that lack covering reticulate meshwork. Internally, *Archimedes* chambers lack hemisepta and can therefore be readily separated from *Rectifenestella* and *Laxifenestella*. Pronounced similarities in general chamber shape exist among *Archimedes*, *Apertostella*, and *Hemitrypa*; *Archimedes* can be separated from the others by its consistently smaller chamber size and incomplete peristome.

Although a central axis with attached fronds are most desirable, carefully sectioned axes are adequate for identification as all three mesh views (longitudinal, tangential, and transverse) can be obtained.

Species composition.—Four species of *Archimedes* were recognized in the Warsaw: *A. negligens* Ulrich, 1890, *A. owenanus* (Hall, 1857b), *A. wortheni* (Hall, 1857b), and *A. valmeyeri*, n. sp.

Range.—Mississippian to Permian.

Archimedes negligens Ulrich, 1890
Plate 50, figures 1–13, Plate 51, figures 1–6,
Plate 52, figures 1–4; Table 37

Archimedes negligens Ulrich, 1890, p. 569, pl. 63, figs. 6, 7–7a [Keokuk Group, Bentonsport and Keokuk, Iowa]; Condra and Elias, 1944, pp. 79–80, pl. 14, figs. 1–6.

Diagnosis.—Zoarium relatively delicate, mesh close, pattern regular; central axis well-developed, robustness delicate to intermediate; volutions dextral or sinistral, diverging from axis at a moderately constant angle (mean of approximately 66°); branch robustness delicate to intermediate, width narrow, depth thin; straight on obverse, slightly sinuous on reverse surface; transversely ovate to elliptical, becoming increasingly elliptical with astogeny, spacing close and joined at moderately regular intervals by lower-end intermediate width, short dissepiments. Fenestrule size lower-end intermediate; shape irregularly elliptical on obverse, irregularly elliptical to ovate on reverse; size regular, shape variable. Autozooecial aperture size lower-end intermediate, shape irregularly ovate to elliptical, rarely circular, elongate proximoabaxially or proximodistally; surrounded by upper-end thin, well-developed, incomplete peristome, opening at proximal to proximal-adaxial edge; two to three (most commonly two) apertures per fenestrule. Single narrow, continuous keel present; keel slightly anastomosing, extending along middle of obverse branch surface, atop which are positioned small nodes; nodes circular to ovate, elongate proximodistally. Autozooecial chamber size lower-end intermediate, chambers emplaced in two rows, except third row at sites of branch bifurcation; outline irregularly ovate near reverse wall, irregularly pentagonal throughout most of chamber depth, irregularly elliptical to more rarely irregularly ovate near obverse surface. Chamber longest dimension parallel to reverse wall proximodistally. Aperture at distal-abaxial end of chamber, connected to chamber by moderately short, highly variable length vestibule. Superior and inferior hemisepta both absent. Lateral-wall budding-angle variable (mean of approximately 26°); reverse-wall budding-angle highly constant (mean of 65°).

Table 37 presents statistical criteria used in delimiting this species.

Exterior description.—Zoarium relatively delicate; forming a flat to slightly cupped, fan-shaped expansion

Table 37.—Summary numerical analysis of *Archimedes negligens* Ulrich, 1890. For explanation of abbreviations of characters (left column), see Table 8b (foldout inside back cover).

	number of measurements	mean	standard deviation	coefficient of variation	observed range
1. WB	24	0.2484	0.0232	9.34	0.215–0.288
2. DBC	24	0.3938	0.0398	10.11	0.333–0.467
3. WD	24	0.1347	0.0249	18.49	0.105–0.182
4. LF	24	0.4353	0.0820	18.84	0.267–0.550
5. WF	24	0.2000	0.0298	14.90	0.167–0.267
6. AF	24	2.33	0.49	21.13	2–3
7. AL	24	0.1109	0.0081	7.30	0.096–0.124
8. AW	24	0.0942	0.0086	9.13	0.083–0.108
9. ADB	24	0.1984	0.0163	8.22	0.171–0.233
10. AAB	24	0.1887	0.0205	10.86	0.158–0.222
11. ABB	24	0.2434	0.0387	15.90	0.183–0.320
12. DN	24	0.0529	0.0129	24.39	0.033–0.080
14. SNB	24	0.1450	0.0383	26.41	0.067–0.204
15. WK	24	0.0192	0.0049	25.52	0.013–0.027
16. DSO	24	0.0095	0.0022	23.16	0.006–0.014
17. SSO	24	0.0237	0.0093	39.24	0.010–0.041
18. WP	24	0.0199	0.0061	30.65	0.011–0.031
22. RSS	24	0.0114	0.0026	22.81	0.009–0.018
24. SSS	24	0.0293	0.0111	37.88	0.016–0.052
27. WSC	24	5.0	1.38	27.60	2.7–7.2
28. DCA	24	5.1	1.13	21.95	3.0–7.2
29. ACA	24	65.75	11.51	17.51	48–82
30. OL	24	0.1555	0.0230	14.79	0.133–0.182
31. OW	24	0.1088	0.0122	11.21	0.092–0.120
32. TRW	24	0.0115	0.0029	25.22	0.008–0.022
33. TLW	24	0.0158	0.0029	18.35	0.011–0.020
34. FWT	24	0.1077	0.0524	48.65	0.035–0.229
35. RWT	24	0.0863	0.0626	72.54	0.025–0.257
36. CL	24	0.2092	0.0122	5.83	0.189–0.229
37. CD	24	0.1252	0.0078	6.23	0.113–0.141
38. MAW	24	0.1249	0.0135	10.81	0.109–0.160
39. MIW	24	0.0643	0.0115	17.88	0.049–0.085
40. VD	24	0.0556	0.0248	44.60	0.022–0.111
41. RA	24	65.08	3.65	5.61	59–71
42. LA	24	25.67	5.05	19.67	18–36
43. TB	24	0.2738	0.0998	36.45	0.186–0.543

radiating outward from the exterior edge of a spiraling central axis; mesh spacing close; slight to moderate astogenetic thickening of obverse and reverse zoarial skeleton; zoarial mesh pattern regular. Central axis robustness delicate to intermediate, well-developed, maximum diameter moderately variable (mean of 5.14 mm), greatly thickening immediately distal to site of initial axis development; volution spacing irregular (mean spacing 5 mm), developing into either a dextral or sinistral spiral; zoarial mesh diverging from central axis at a mean angle of approximately 66°, moderately constant. Distal end of axial flange flat to slightly concave; proximal side slightly to moderately concave; both sides of axis with slightly striated texture spiraling around and outward from central axis, resulting from thickening of lamellar skeletal material around axis with astogeny. Probable mature zoarial widths of up to 10 cm, lengths in excess of 20 cm.

Branch robustness delicate to intermediate, depending on degree of astogenetic thickening; branch narrow, highly constant in width; straight as observed on obverse surface; slightly sinuous on reverse. Branches closely spaced, distance between adjacent branch centers highly regular. Obverse surface texture moderately granular, coarsening with astogeny; surface flat to slightly rounded except for presence of single narrow, intermediately developed keel; keel continuous, slightly anastomosing, extending along branch midline, causing slight positive inflection in obverse surface profile. Keel covered by lamellar skeleton with astogeny. Nodes monoserially emplaced, well-developed, small; shape circular to ovate, elongate proximodistally; nodes slightly regular in size and shape, develop as projections from middle of keel; two to five (most commonly three) nodes per fenestrule; nodes closely and slightly unevenly spaced; node diameter moderately increasing with astogeny. Small stylets, variably sized and highly variably positioned, occurring across obverse branch surface. Reverse surface texture granular, coarsening with astogeny; bearing relatively few rows of intermediately spaced longitudinal striae which rapidly become covered by lamellar skeleton during astogeny; rows of small microstylets, closely spaced, develop as extensions of longitudinal striae along reverse branch surface; microstylet diameter moderately increasing with astogeny and microstylets become more variably positioned along reverse branch surface. Autozooecia in two rows across branch, except third row at sites of branch bifurcation; branches exhibit slight thickening proximal, slight thinning distal to sites of branch bifurcation. Heterozooecia absent in all zoarial fragments examined.

Dissepiments of lower-end intermediate width, approximately five-ninths that of branch, moderately constant; short, constant in length; connect branches at moderately regular intervals. Dissepiments exhibit slight medial thinning, slight flaring at branch–dissepiment junction; moderately recessed from obverse, approximately even with reverse branch surface. Moderate to pronounced astogenetic thickening toward proximal end of zoarium. Obverse dissepiment surface with single longitudinal ridge emplaced perpendicular to branch length; small stylets, similar in size to obverse branch stylets, develop across dissepiment surface; ridge partially to completely covered by lamellar skeleton during astogeny, stylets slightly increase in diameter; reverse dissepiment surface with relatively few rows of longitudinal striae atop which occur closely spaced rows of small microstylets; longitudinal striae become covered by lamellar skeleton, microstylets become more irregularly positioned across dissepiment surface with astogeny. Obverse dissepiment surface

texture moderately granular, reverse surface texture granular, both coarsening with astogeny. Emplacement of dissepiments perpendicular or at small angle from perpendicular to branch length. Apertures commonly positioned on proximal or distal edge, or in middle of dissepiment edge at branch–dissepiment contact; typically arranged symmetrically, less commonly asymmetrically between branches.

Fenestrule size lower-end intermediate; shape irregularly elliptical on obverse surface, irregularly elliptical to ovate, elongate proximodistally on reverse; regular in size, variable in shape; moderately expanding in width and length in obverse–reverse direction. Width of fenestrule four-fifths branch width on obverse surface, equal to or slightly greater than branch width on reverse; fenestrule opening size moderately to greatly reduced toward proximal end of zoarium and toward central axis due to astogenetic thickening of lamellar skeleton. Width to length ratio of fenestrule moderately constant, ranging from 1:1 to approximately 1:3; ratio of fenestrule mean width to length approximately 4:9; width slightly more constant than length, both moderately constant. Two to three (most commonly two) apertures per fenestrule length; distance between closest aperture centers along branch and across branch approximately equal, less than spacing across fenestrule, which is approximately 1.3 times greater; forming an overall moderately even grid of apertures across obverse zoarial surface; spacing along and across branch moderately constant, spacing across fenestrule moderately variable.

Autozooecial aperture size lower-end intermediate, shape irregularly ovate to elliptical, rarely circular, enlarged slightly at distal end; elongate proximoabaxially or proximodistally; width to length ratio approximately 6:7; size uniform, shape variable; opening oriented parallel to plane of obverse surface; aperture surrounded by upper-end thin, well-developed incomplete peristome; peristome open around one-fourth to one-third of aperture at proximal to proximal-adaxial edge of aperture. Aperture margins extend into fenestrule, causing moderate to pronounced inflections in fenestrule outline on obverse surface. Centrally thickened terminal diaphragms occurring at proximal end of zoarium and near zoarial axis.

Zoarial supports moderately well-developed, forming as extensions of reverse zoarial surface and distal edge of mesh radiating outward from central axis.

Interior description.—Branches irregularly ovate to elliptical in transverse section at distal end of zoarium, elongate parallel to plane of obverse surface, slightly enlarged on obverse surface; with astogeny branches become moderately elongate elliptical in transverse view, elongate in obverse–reverse direction due to addition of lamellar skeleton to reverse branch surface. Branches thin, highly variable in thickness.

Autozooecial chamber size lower-end intermediate, chambers biserially arranged along planar branch axial wall; axial wall moderately sinuous near reverse wall and throughout mid chamber, extending toward and connecting with chamber lateral walls; becoming less sinuous near obverse surface. Chamber longest dimension parallel to reverse wall in proximodistal direction. Autozooecial chamber outline irregularly ovate near reverse wall, rapidly becoming irregularly pentagonal in mid chamber and throughout most of chamber depth; irregularly elliptical to more rarely irregularly ovate near obverse surface, slightly enlarged at distal end, longest dimension near obverse surface oriented distal-abaxially; chamber shape highly uniform. Aperture positioned at distal-abaxial end of chamber, connected to chamber by well-developed, moderately short vestibule; vestibule highly variable in length. Ratio of autozooecial chamber minimum width to maximum width approximately 1:2; maximum width and depth equal; chamber depth to length ratio approximately 3:5; chamber depth and length highly constant, maximum width slightly variable, minimum width highly variable. Superior and inferior hemisepta both absent. Autozooecial chambers diverge laterally from middle of branch at a variable angle (mean of approximately 26°); from reverse wall at a highly constant angle (mean of 65°).

Three-dimensionally reconstructed chamber form a slightly irregular rectangular box; long dimension as viewed from lateral edge of branch, approximately twice depth; viewed from distal end of branch, and width, viewed from obverse surface, which are approximately equal.

Internal granular skeletal layer thickness intermediate; granular skeletal layer moderately well-developed, continuous with obverse nodes, stylets, keel, and peristome; reverse longitudinal striae and microstylets; across dissepiments and in the middle of zoarial supports. Outer lamellar layer thickness intermediate, exhibiting moderate astogenetic thickening; zoarial central axis formed from massively accreted lamellar skeleton which completely covers mesh surface at site of and near central axis.

Remarks.—*Archimedes negligens* was named by Ulrich (1890) from materials collected at Bentonsport and Keokuk, Iowa. Condra and Elias (1944, p. 79) observed that this species had the smallest screw or axis of any pre-Chester species; with Chester species most similar to this form being *A. distans* Condra and Elias, 1944, *A. meekanus* Condra and Elias, 1944, and *A. terebriformis* Condra and Elias, 1944. In general, Chester species are found to have smaller, finer axes than species from Osagean or Meramecian (Valmeyeran) age rocks.

Within the Warsaw fauna, *A. negligens* most closely resembles *A. owenanus* (Hall, 1857b). The characteristic smaller size and finer nature of the central axis separates the former from the latter, however. Internal chamber characteristics of these two species are similar (with the exception of one of the most constant interior characters, reverse-wall budding-angle, which is moderately greater in *A. negligens*). *A. negligens* can also be differentiated from *A. owenanus* by the former's lack of apertural stylets, narrower and thinner branches which are more closely spaced, smaller fenestrules and therefore fewer apertures per fenestrule length, and slightly larger apertures.

A. negligens and *A. owenanus* occur concurrently in the same fauna, exhibiting little or no overlap of axis form. Of all zoarial fragments observed, none were found that exhibited characteristic axes of *A. negligens* joined to an axis of *A. owenanus* or other species of *Archimedes*. Thus, retention of *A. negligens* as a separate species appears justified in spite of only slight chamber size dissimilarity from that of *A. wortheni*.

Material studied.—Twenty-four exterior fragments, five sectioned specimens; largest zoarial fragment 3.5 × 20 cm (width to length). The preservation of the central axis is good, due to its moderately robust nature, but the preservation of the mesh is intermediate. An interior analysis of the mesh was done *only* on samples in which the mesh was still attached to the central axis, to ensure no confusion in determining the source of the mesh relative to zoarial axes analyzed. The type specimen had attached meshwork and was analyzed in this way.

Occurrence.—*Archimedes negligens* is a moderately rare component of the Lower Warsaw and Upper Keokuk faunas in the northern half of the study area, having its best occurrence near Keokuk. It is found primarily in low-energy environments.

Lectotype (herein designated).—ISGS(ISM) 2785–2.

Paralectotype (herein designated).—ISGS(ISM) 2785–1.

Figured and/or measured specimens.—UI X-7009 (loc. 10, sample 33), 7010 (loc. 6, sample 36), 6975 (loc. 11, sample 52).

Archimedes owenanus (Hall, 1857b)
Plate 52, figures 5–9, Plate 53, figures 1–10, Plate 54, figures 1–7, Plate 55, figures 1–7, Plate 56, figures 1, 2; Table 38

Fenestella owenana Hall, 1857b, p. 178 [Keokuk Limestone, Keokuk, Iowa; Appanoose, Illinois].

Archimedes owenanus (Hall). Ulrich, 1890, p. 570, pl. 63, figs. 6–6c [Keokuk Group, Keokuk, Iowa; Appanoose, and 3 mi NE of Quincy, Illinois]; Keyes, 1894, p. 26, pl. 33, fig. 2 [Keokuk Limestone, St. Francisville, Missouri]; Condra and Elias, 1944, pp. 92–95, pl. 14, figs. 7–15; Burckle, 1960, pp. 1089–1090, pl. 130, fig. 7.

Archimedes grandis Ulrich, 1890, p. 569, pl. 63, fig. 10 [Keokuk Group, Jersey County, Illinois].

Archimedes halli Condra and Elias, 1944, pp. 97–98, pl. 2, fig. 3; pl. 15, fig. 4.

Table 38.—Summary numerical analysis of *Archimedes owenanus* (Hall, 1857b). For explanation of abbreviations of characters (left column), see Table 8b (foldout inside back cover).

	number of measurements	*mean*	*standard deviation*	*coefficient of variation*	*observed range*
1. **WB**	24	0.3001	0.0255	8.50	0.260–0.345
2. **DBC**	24	0.5630	0.0885	15.72	0.449–0.720
3. **WD**	24	0.2773	0.0507	18.28	0.220–0.400
4. **LF**	24	0.6215	0.1059	17.04	0.464–0.860
5. **WF**	24	0.2117	0.0435	20.53	0.157–0.285
6. **AF**	24	3.33	0.49	14.77	3–4
7. **AL**	24	0.1060	0.0059	5.57	0.096–0.113
8. **AW**	24	0.0836	0.0083	9.93	0.069–0.094
9. **ADB**	24	0.2228	0.0212	9.52	0.188–0.260
10. **AAB**	24	0.2028	0.0201	9.91	0.167–0.238
11. **ABB**	24	0.2684	0.3064	13.00	0.216–0.343
12. **DN**	24	0.0596	0.0244	40.94	0.026–0.132
14. **SNB**	24	0.7278	0.1827	25.10	0.380–1.120
15. **WK**	24	0.0184	0.0045	24.46	0.013–0.028
16. **DSO**	24	0.0090	0.0024	26.67	0.006–0.014
17. **SSO**	24	0.0259	0.0093	35.91	0.014–0.044
18. **WP**	24	0.0151	0.0035	23.18	0.011–0.025
19. **SA**	24	20.58	5.30	25.75	14–32
20. **SAD**	24	0.0087	0.0021	24.14	0.005–0.011
22. **RSS**	24	0.0158	0.0064	40.51	0.008–0.033
24. **SSS**	24	0.0373	0.0208	55.76	0.012–0.075
27. **WSC**	24	9.7	2.53	26.21	5.5–14.0
28. **DCA**	24	10.9	3.69	33.77	6.2–19.0
29. **ACA**	24	68.83	7.77	11.28	59–79
30. **OL**	24	0.3118	0.0618	19.82	0.233–0.429
31. **OW**	24	0.2240	0.0319	14.24	0.169–0.280
32. **TRW**	24	0.0178	0.0026	14.61	0.013–0.021
33. **TLW**	24	0.0131	0.0015	11.45	0.011–0.016
34. **FWT**	24	0.0682	0.0465	68.18	0.024–0.182
35. **RWT**	24	0.2958	0.1634	55.24	0.071–0.629
36. **CL**	24	0.2199	0.0118	5.37	0.200–0.240
37. **CD**	24	0.1224	0.0102	8.33	0.104–0.139
38. **MAW**	24	0.1133	0.0079	6.97	0.096–0.125
39. **MIW**	24	0.0838	0.0160	19.09	0.057–0.112
40. **VD**	24	0.0902	0.0352	39.02	0.035–0.138
41. **RA**	24	59.42	4.90	8.25	52–64
42. **LA**	24	28.08	4.55	16.20	22–35
43. **TB**	24	0.5299	0.2058	38.84	0.186–0.915

Diagnosis.—Zoarium robust, mesh close, pattern extremely regular; central axis well-developed, robust, volutions dextral or sinistral, diverging from axis at a constant angle (mean of approximately 69°), pillarlike supports between flanges of spiral; branches moderately robust, width lower-end intermediate, thick in depth; branches straight on obverse, sinuous and irregular on reverse surface; transversely circular to slightly ovate, becoming highly elliptical with astogeny, spacing close and joined at moderately regular intervals by upper-end intermediate width, short dis-

sepiments. Fenestrule size intermediate, shape irregularly elliptical on obverse, irregularly elliptical, ovate to circular on reverse; size regular, shape variable. Autozooecial aperture size lower-end intermediate, irregularly ovate to elliptical, rarely circular, elongate proximoabaxially or proximodistally; surrounded by thin, well-developed, incomplete to more rarely complete peristome, open at proximal to proximal-adaxial edge; three to four (most commonly three) apertures per fenestrule. Single narrow, continuous keel present; keel slightly anastomosing to approaching straight, extending along middle of obverse branch surface, atop which are positioned small nodes; nodes ovate, elongate proximodistally, rarely circular. Autozooecial chamber size lower-end intermediate, chambers emplaced in two rows, except either third row at sites of branch bifurcation or more rarely three rows for moderate distances proximal to sites of branch bifurcation; outline irregularly ovate to pentagonal near reverse wall, irregularly pentagonal throughout most of chamber depth; irregularly elliptical to more rarely ovate near obverse surface. Chamber longest dimension parallel to reverse wall proximodistally. Aperture at distal-abaxial end of chamber, connected to chamber by intermediate, highly variable length vestibule. Superior and inferior hemisepta both absent. Lateral-wall budding-angle moderately variable (mean of approximately 28°); reverse-wall budding-angle constant (mean of approximately 59°). Heterozooecia (ovicells?) occurring as globular expansions infilling fenestrules.

Table 38 presents statistical criteria used in delimiting this species.

Exterior description.—Zoarium robust, forming a flat to slightly cup-shaped expansion radiating outward from the exteriormost edge of a spiraling central axis; mesh spacing close; pronounced astogenetic thickening of obverse and reverse zoarial skeleton; zoarial mesh pattern extremely regular. Central axis robust, well-developed, maximum diameter moderately variable (mean of 10.93 mm), greatly thickening immediately distal to site of initial axis development; volution spacing irregular (mean spacing 9.67 mm), developing into either a dextral or sinistral spiral; zoarial mesh diverging from central axis at a mean angle of approximately 69°, constant. Distal end of axial flange flat, slightly concave, or slightly convex; proximal side slightly to moderately concave; slight striated texture to axis, with striae spiraling around and outward from central axis, resulting from thickening of zoarial skeleton around axis with astogeny. Pillarlike supports developing between flanges along axis, zoarial mesh overgrown by zoarial skeleton from axis development during astogeny. Probable mature zoarial widths half a meter or more, length greater than 1 m.

Branches moderately robust, becoming increasingly so during astogenetic thickening; lower-end intermediate in width, moderately variable; straight on obverse surface, highly sinuous and irregular on reverse surface due to astogenetic thickening of lamellar skeleton. Branch spacing upper-end close, distance between adjacent branch centers moderately regular. Obverse surface texture moderately granular, coarsening with astogeny; surface rounded, except for presence of single narrow, well-developed keel; keel continuous, slightly anastomosing to approaching straight, extending along branch midline, causing slight inflection in obverse surface profile. Keel becomes covered by lamellar skeleton during astogeny. Nodes monoserially emplaced, well-developed, small; shape ovate, elongate proximodistally, rarely circular; nodes highly variable in both size and shape; develop as projections from middle of keel; one to three (most commonly two) nodes per fenestrule; node spacing upper-end intermediate, slightly variable; node diameter greatly increasing with astogeny. Upper-end small stylets, variably sized and positioned, occurring across obverse surface. Reverse surface texture granular, coarsening with astogeny; bearing relatively few rows of closely to intermediately spaced longitudinal striae which rapidly become covered by lamellar skeleton during astogeny; rows of small microstylets, closely spaced, develop as extensions of longitudinal striae along reverse branch surface; microstylet diameters highly variable, slightly increase with astogeny and microstylets become variably positioned across reverse branch surface. Autozooecia in two rows across branch, except either third row at sites of branch bifurcation, or more rarely three rows extending for moderate distances proximal to sites of branch bifurcation. Heterozooecia (ovicells?) occurring as pronounced globular expansions infilling fenestrules; mean widths and lengths of polymorphs slightly less than three times autozooecial aperture lengths and widths; polymorph length appreciably greater than width, ratio approximately 5:7; connection between polymorph and autozooecial chamber lacking; polymorphs most commonly situated immediately distal from central axis along branch.

Dissepiments of upper-end intermediate width, approximately nine-tenths that of branch, moderately constant; short, slightly variable in length; connect branches at moderately regular intervals. Dissepiments exhibit slight medial thinning, slight flaring at branch–dissepiment junction; slightly recessed from obverse, approximately even with reverse branch surface. Pronounced astogenetic thickening of dissepiments toward proximal end of zoarium. Obverse dissepiment surface with single longitudinal ridge emplaced perpendicular to branch length; small stylets, similar in size to obverse branch stylets, develop across dissepiment surface; ridge partially covered by lamellar skel-

eton during astogeny, stylets increase in diameter; reverse dissepiment surface with an intermediate number of rows of longitudinal striae atop which occur closely spaced rows of small microstylets; longitudinal striae become covered by lamellar skeleton, microstylets become more irregularly positioned across dissepiment surface with astogeny. Obverse and reverse dissepiment surfaces granular, coarsening with astogeny. Emplacement of dissepiments perpendicular or at small angle from perpendicular to branch length. Apertures commonly positioned on proximal or distal edge, or in middle of dissepiment edge at branch–dissepiment contact; arranged symmetrically or asymmetrically between branches.

Fenestrule size intermediate; shape irregularly elliptical on obverse surface, irregularly elliptical to ovate, elongate proximodistally to more rarely circular on reverse; moderately regular in size, irregular in shape; moderately to highly expanding in width and length in obverse–reverse direction. Width of fenestrule approximately one-half branch width on obverse surface, equal to or slightly greater than branch width on reverse; fenestrule opening size greatly reduced toward proximal end of zoarium and toward central axis due to astogenetic thickening of lamellar skeleton. Width to length ratio of fenestrule moderately constant, ranging from 1:1 to approximately 1:4; ratio of fenestrule mean width to length approximately 1:3; length moderately constant, width lower-end variable. Three to four (most commonly three) apertures per fenestrule length; distance between closest aperture centers along branch and across branch approximately equal, less than spacing across fenestrule which is approximately 1.25 times greater; forming a moderately even grid of apertures across zoarium obverse surface; spacing along and across branch moderately constant, spacing across fenestrule moderately variable.

Autozooecial aperture size lower-end intermediate, shape irregularly ovate to elliptical, rarely circular, enlarged slightly at distal end; elongate proximoabaxially or proximodistally; width to length ratio approximately 7:9; size uniform, shape variable; opening oriented parallel to plane of obverse surface; aperture surrounded by thin, well-developed, typically incomplete peristome; peristome open up to one-fourth of aperture at proximal or proximal-adaxial edge of aperture; more rarely peristome complete. Aperture margins extend into fenestrule, causing pronounced inflections in fenestrule outline on obverse surface. Centrally thickened terminal diaphragms occurring at proximal end of zoarium and near zoarial axis.

Zoarial supports extremely well-developed, forming as extensions of reverse zoarial surface and distal edge of mesh radiating outward from central axis.

Interior description.—Branches approaching circular to slightly ovate in transverse section at distal end of zoarium, slightly elongate parallel to plane of obverse surface and enlarged on obverse surface; with astogeny branches become moderately to highly elongate elliptical in shape in transverse view, elongate in obverse–reverse direction due to addition of lamellar skeleton to reverse branch surface. Branches thick, highly variable in depth.

Autozooecial chamber size lower-end intermediate, chambers biserially arranged along planar branch axial wall; axial wall moderately to highly sinuous near reverse wall and throughout mid chamber, extending toward and connecting with chamber lateral walls; becoming slightly sinuous near obverse surface. Chamber longest dimension parallel to reverse wall in proximodistal direction. Autozooecial chamber outline irregularly ovate to pentagonal near reverse wall; irregularly pentagonal in mid chamber and throughout most of chamber depth; irregularly elliptical to more rarely irregularly ovate near obverse surface, slightly to moderately enlarged at distal end, longest dimension near obverse surface oriented distal-abaxially; chamber shape highly uniform. Aperture positioned at distal-abaxial end of chamber, connected to chamber by extremely well-developed, intermediate-length vestibule; vestibule highly variable in length. Ratio of autozooecial chamber minimum width to maximum width approximately 3:5; maximum width to depth ratio approximately 9:10; chamber depth to length ratio approximately 3:4; chamber maximum width, depth and length highly constant, minimum width highly variable. Superior and inferior hemisepta both absent. Autozooecial chambers diverge laterally from middle of branch at a moderately variable angle (mean of approximately 28°); from reverse wall at constant angle (mean of approximately 59°).

Three-dimensionally reconstructed chamber form a slightly irregular rectangular box; length, viewed from lateral edge of branch, greater than depth; viewed from distal end of branch, greater than width, viewed from obverse surface.

Internal granular skeletal layer thick; granular skeletal layer extremely well-developed, continuous with obverse nodes, stylets, keel, and peristome; reverse longitudinal striae and microstylets; across dissepiments and in the middle of zoarial supports. Outer lamellar layer extremely thick, exhibiting pronounced astogenetic thickening; zoarial central axis formed of massively accreted lamellar skeleton which completely covers mesh surface at site of and near central axis.

Remarks.—Although originally described by Hall, this species was never illustrated by him. For this reason, the lectotype [ISGS (ISM) 2782–1] is here designated from specimens illustrated by Ulrich and by Condra and Elias. ISGS (ISM) 2728– 2/3 are assigned

the status of paralectotypes.

A. grandis Ulrich, 1890 and *A. halli* Condra and Elias, 1944 are herein placed in synonymy under *A. owenanus*, which has priority. Condra and Elias noted the possibility that *A. grandis* should be grouped under *A. owenanus*, but did not do so. Although *A. grandis* has a slightly wider flaring flange and higher volutions than *A. owenanus*, interior analysis indicates the two to be essentially identical. Interiors of *A. halli* were also found to be essentially identical to those of *A. owenanus*, although *A. halli* has a smaller axis, probably due to environmental responses. Meshwork formulas, as given in Condra and Elias (1944), are also almost identical for *A. halli* and *A. owenanus*. This, in conjunction with interior analysis, resulted in placing the two species in synonymy in this study.

A. owenanus is extremely similar in both exterior and interior characters to *A. wortheni* (Hall, 1857b), as noted by Ulrich (1890). The former is differentiated by more numerous apertural stylets (mean of 21 as opposed to 11 in the latter), much lower reverse-wall budding-angle, slightly wider branches, more open mesh, and slightly wider spacing of apertures along, across, and between branches. The overlap in variation of axial characters makes the use of the central axis for species differentiation of little value, although the angle between the distal end of the axis and the axial whorl seems to have some taxonomic significance. This angle is slightly greater in *A. owenanus* (69°) than in *A. wortheni* (61°).

Material studied.—Seventy-three exterior fragments, 15 sectioned specimens; largest zoarial fragment 21×68 cm (width to length). The preservation of the central axis is good, even though the granular skeleton is susceptible to silicification. Interior analysis of zoarial axis and mesh was undertaken *only* on samples with mesh still attached to the central axis, ensuring there could be no confusion in determining the source of mesh relative to the zoarial axes analyzed. Type material of this species is deposited at the Illinois State Geological Survey.

Occurrence.—*Archimedes owenanus* is abundant in the Upper Keokuk and Lower Warsaw, with best occurrence at the Warsaw–Keokuk contact, and is found as far south as Jersey County, Illinois. It occurs primarily in low-energy environments, less frequently in inferred higher energy environments where zoarial fragments were probably washed in with other clastic particles.

Lectotype and *paralectotypes.*—ISGS(ISM)2782–1, and ISGS(ISM) 2782–2/3, 2790.

Figured and/or measured specimens.—UI X-6972, 6973, 7008, 6986, 6983, 7006, 6971, 7011 (loc. 6, samples 26, 27, 30, 32, 47), 6985, 6984, 7003, 6993, 7013, 7001 (loc. 10, samples 32, 42).

Archimedes wortheni (Hall, 1857b)
Plate 56, figures 3–9, Plate 57, figures 1–9, Plate 58, figures 1–9, Plate 59, figures 1–5, Plate 60, figures 1, 2; Table 39

Fenestella wortheni Hall, 1857b, p. 178 [Warsaw Limestone, Warsaw, Illinois].

Archimedes wortheni (Hall). Hall, 1858, p. 651, pl. 22, figs. 3, 4a–b, 5a–b [Warsaw Limestone, Warsaw, Illinois]; Miller, 1889, p. 292, fig. 452; Ulrich, 1890, p. 571, pl. 63, figs. 8, 8a. [Warsaw Beds, Warsaw, Illinois]; Keyes, 1894, p. 26, pl. 33, fig. 1. [Keokuk Limestone, Wayland and La Grange, Missouri]; Van Tuyl, 1925, pl. 6, fig. 6.

Archimedes reversa Hall, 1858, p. 652, pl. 22, fig. 2 [Warsaw Limestone, Warsaw, Illinois].

Archimedes welleri Condra and Elias, 1944, pp. 85–88, pl. 18, figs. 4a–b; pl. 19, figs. 1, 2; pl. 20, fig. 5 [Warsaw Formation, Warsaw, Illinois].

Diagnosis.—Zoarium robust, mesh close, pattern extremely regular; central axis well-developed, robust, volutions dextral or sinistral, diverging from axis at moderately constant angle (mean of 61°), pillarlike supports between flanges of spiral; branch robustness intermediate to pronounced; branch width narrow, depth thick; branches straight on obverse and sinuous on reverse surface; transversely ovate to circular, becoming highly elliptical with astogeny, spacing close and joined at highly regular intervals by intermediate-width, short dissepiments. Fenestrule size lower-end intermediate; shape irregularly elliptical on obverse, irregularly elliptical, ovate to circular on reverse; size regular, shape variable. Autozooecial aperture size lower-end intermediate, shape irregularly ovate to elliptical, rarely circular, elongate proximoabaxially or proximodistally; surrounded by thin, well-developed, incomplete peristome, open at proximal to proximal-adaxial edge; intermediate size apertural stylets, seven to 14 per aperture (mean of 10.5), positioned atop peristome; two to four (most commonly three) apertures per fenestrule. Single narrow, continuous keel present; keel slightly anastomosing to approaching straight, extending along middle of obverse branch surface, atop which are positioned small nodes; nodes ovate, highly elongate proximodistally, rarely circular. Autozooecial chamber size upper-end small to lower-end intermediate, chambers emplaced in two rows, except either third row at sites of branch bifurcation or more rarely three rows for moderate distances proximal to sites of branch bifurcation; outline irregularly ovate near reverse wall, irregularly pentagonal throughout most of chamber depth, irregularly elliptical to ovate near obverse surface. Chamber longest dimension parallel to reverse wall proximodistally. Aperture at distal-abaxial end of chamber, connected to chamber by intermediate, highly variable length vestibule. Superior and inferior hemisepta both absent. Lateral-wall budding-angle highly variable (mean of 23°); reverse-wall bud-

Table 39.—Summary numerical analysis of *Archimedes wortheni* (Hall, 1857b). For explanation of abbreviations of characters (left column), see Table 8b (foldout inside back cover).

	number of mea-sure-ments	mean	standard deviation	coeffi-cient of variation	observed range
1. **WB**	24	0.2620	0.3048	13.28	0.220–0.300
2. **DBC**	24	0.4140	0.0677	16.35	0.357–0.580
3. **WD**	24	0.1834	0.0277	15.10	0.144–0.255
4. **LF**	24	0.4353	0.0472	10.84	0.343–0.540
5. **WF**	24	0.2024	0.0269	13.29	0.167–0.247
6. **AF**	24	3.08	0.50	16.33	2–4
7. **AL**	24	0.1019	0.0085	8.34	0.088–0.120
8. **AW**	24	0.0844	0.0081	9.60	0.071–0.100
9. **ADB**	24	0.1909	0.0164	8.59	0.169–0.221
10. **AAB**	24	0.1878	0.0123	6.71	0.166–0.214
11. **ABB**	24	0.2133	0.0218	10.22	0.180–0.250
12. **DN**	24	0.0513	0.0170	33.14	0.031–0.088
14. **SNB**	24	0.3060	0.0624	20.39	0.225–0.393
15. **WK**	24	0.0163	0.0070	42.94	0.009–0.026
16. **DSO**	24	0.0081	0.0022	27.16	0.005–0.012
17. **SSO**	24	0.0169	0.0064	37.87	0.009–0.029
18. **WP**	24	0.0221	0.0094	42.53	0.012–0.040
19. **SA**	24	10.50	2.07	19.68	7–14
20. **SAD**	24	0.0224	0.0088	39.29	0.009–0.043
22. **RSS**	24	0.0089	0.0024	26.97	0.006–0.014
24. **SSS**	24	0.0165	0.0045	27.27	0.011–0.026
27. **WSC**	24	8.2	3.35	41.04	2.9–14.2
28. **DCA**	24	19.2	11.85	61.75	1.8–48.5
29. **ACA**	24	60.92	9.15	15.02	48–78
30. **OL**	24	0.2368	0.0245	10.35	0.205–0.286
31. **OW**	24	0.1999	0.0188	9.40	0.168–0.235
32. **TRW**	24	0.0338	0.0074	21.89	0.021–0.044
33. **TLW**	24	0.0145	0.0024	16.55	0.011–0.019
34. **FWT**	24	0.0923	0.0407	44.10	0.040–0.165
35. **RWT**	24	0.2155	0.1686	78.24	0.025–0.550
36. **CL**	24	0.1746	0.0084	4.81	0.160–0.190
37. **CD**	24	0.1278	0.0080	6.26	0.115–0.145
38. **MAW**	24	0.1151	0.0099	8.60	0.098–0.137
39. **MIW**	24	0.0680	0.0149	21.91	0.049–0.095
40. **VD**	24	0.0918	0.0444	48.37	0.028–0.140
41. **RA**	24	70.08	3.78	5.39	63–76
42. **LA**	24	23.17	4.63	19.98	7–32
43. **TB**	24	0.5123	0.1944	37.95	0.257–0.880

ding-angle highly constant (mean of 70°). Heterozooecia (ovicells?) occurring as pronounced expansions along branch midline and globular expansions infilling fenestrules.

Table 39 presents statistical criteria used in delimiting this species.

Exterior description.—Zoarium robust; forming a slightly cupped, fan-shaped expansion radiating outward from the exteriormost edge of a spiraling central axis; mesh spacing close; pronounced thickening of obverse, extremely pronounced astogenetic thickening of reverse zoarial skeleton; zoarial mesh pattern extremely regular. Central axis robust, well-developed, maximum diameter highly variable (mean of 19.19 mm), greatly thickening immediately distal to site of initial axis development; volution spacing irregular (mean spacing 8.16 mm), developing into either a dextral or sinistral spiral; zoarial mesh diverging from central axis at a mean angle of approximately 61°, moderately constant. Distal end of axial flange flat to slightly concave; proximal side slightly to moderately convex; both sides of axis with striated texture spiraling around and outward from central axis, resulting from thickening of lamellar skeletal material around axis with astogeny. Pillarlike supports developing between flanges along axis; zoarial mesh overgrown by zoarial skeleton from axis development during astogeny. Probable mature zoarial widths half a meter or more, lengths in excess of 1 m.

Branch robustness intermediate to pronounced, depending on degree of astogenetic thickening; branches narrow, moderately constant in width; straight as observed on obverse surface; highly sinuous and irregular on reverse surface due to astogenetic thickening of lamellar skeleton. Branches closely spaced, distance between adjacent branch centers moderately regular. Obverse surface texture smooth to slightly granular, coarsening with astogeny; surface irregularly rounded except for presence of single narrow, well-developed keel; keel continuous, slightly anastomosing to approaching straight, extending along branch midline, causing slight to moderate positive inflection in obverse surface profile. Keel becomes covered by lamellar skeleton with astogeny. Nodes monoserially emplaced, well-developed, small; shape ovate, highly elongate proximodistally, rarely circular; nodes variable in size and shape; develop as projections from middle of keel; one to three (most commonly two) nodes per fenestrule; node spacing intermediate, moderately evenly spaced; node diameter increasing with astogeny. Small stylets, variably sized and positioned, occurring across obverse branch surface. Reverse surface texture granular, coarsening with astogeny; bearing relatively few rows of closely to intermediately spaced longitudinal striae which rapidly become covered by lamellar skeleton during astogeny; rows of small microstylets, closely spaced, develop as extensions of longitudinal striae along reverse branch surface; microstylet diameters increase slightly with astogeny and microstylets become highly variably positioned across reverse branch surface. Autozooecia in two rows across branch, except either third row at sites of branch bifurcation, or more rarely three rows extending for moderate distances proximal to sites of branch bifurcation. Heterozooecia (ovicells?) occurring as pronounced expansions along branch midline and globular expansions infilling fenestrules; mean widths and lengths of polymorphs slightly greater than twice autozooecial aperture widths and lengths; polymorph length slightly greater than width, ratio approximately 5:6; connection between

polymorph and autozooecial chamber lacking; polymorphs most commonly situated immediately distal from central axis along branch.

Dissepiments of intermediate width, approximately seven-tenths that of branch, moderately constant; short, constant in length; connect branches at highly regular intervals. Dissepiments exhibit slight medial thinning, slight flaring at branch–dissepiment junction; slightly recessed from obverse, approximately even with reverse branch surface. Pronounced astogenetic thickening of dissepiments toward proximal end of zoarium. Obverse dissepiment surface with single longitudinal ridge emplaced perpendicular to branch length; small stylets, similar in size to obverse branch stylets, develop across dissepiment surface; ridge covered by lamellar skeleton during astogeny, stylets slightly increase in diameter; reverse dissepiment surface with an intermediate number of rows of longitudinal striae atop which occur closely spaced rows of small microstylets; longitudinal striae rapidly become covered by lamellar skeleton, microstylets become more irregularly positioned across dissepiment surface with astogeny. Obverse dissepiment surface texture smooth to slightly granular, reverse surface texture granular, both coarsening with astogeny. Emplacement of dissepiments perpendicular or at small angle from perpendicular to branch length. Apertures commonly positioned on proximal or distal edge, or in middle of dissepiment edge at branch–dissepiment contact; typically arranged symmetrically, less commonly asymmetrically between branches.

Fenestrule size lower-end intermediate; shape irregularly elliptical on obverse surface, irregularly elliptical to ovate, elongate proximodistally, to more rarely circular on reverse; regular in size, variable in shape; moderately to highly expanding in width and length in obverse–reverse direction. Width of fenestrule two-thirds branch width on obverse surface, appreciably greater than branch width on reverse; fenestrule opening size greatly reduced toward proximal end of zoarium and toward central axis due to astogenetic thickening of lamellar skeleton. Width to length ratio of fenestrule moderately constant, ranging from 1:1 to approximately 1:3; ratio of fenestrule mean width to length approximately 7:9; length slightly more constant than width, both highly constant. Two to four (most commonly three) apertures per fenestrule length; distance between closest aperture centers along branch and across branch approximately equal, slightly less than spacing across fenestrule which is approximately 1.1 times greater; forming an overall even grid of apertures across zoarium obverse surface; spacing along and across branch and across fenestrule all moderately constant.

Autozooecial aperture size lower-end intermediate, shape irregularly ovate to elliptical, rarely circular, enlarged slightly at distal end; elongate proximoabaxially or proximodistally; width to length ratio approximately 5:6; size moderately uniform, shape variable; opening oriented parallel to plane of obverse surface; aperture surrounded by thin, well-developed incomplete peristome; peristome open around one-fourth to one-third of aperture at proximal to proximal-adaxial edge of aperture. Intermediate-size apertural stylets develop as projections from peristome, seven to 14 per aperture (mean of 10.5); apertural stylets highly variable in size and number. Aperture margins extend into fenestrule, causing pronounced inflections in fenestrule outline on obverse surface. Centrally thickened terminal diaphragms occurring at proximal end of zoarium and near zoarial axis.

Zoarial supports extremely well-developed, forming as extensions of reverse zoarial surface and distal edge of mesh radiating outward from central axis.

Interior description.—Branches ovate to circular in transverse section at distal end of zoarium, elongate parallel to plane of obverse surface, slightly enlarged on obverse surface; with astogeny branches become moderately to highly elongate-elliptical in shape in transverse view, elongate in obverse–reverse direction, due to pronounced addition of lamellar skeleton to reverse branch surface. Branches thick, variable in depth.

Autozooecial chamber size upper-end small to lower-end intermediate, chambers biserially arranged along planar branch axial wall; axial wall moderately sinuous near reverse wall and throughout mid chamber, extending toward and connecting with chamber lateral walls; becoming very slightly sinuous near obverse surface. chamber longest dimension parallel to reverse wall in proximodistal direction. Autozooecial chamber outline irregularly ovate near reverse wall, rapdily becoming irregularly pentagonal in mid chamber and throughout most of chamber depth; irregularly elliptical to more rarely irregularly ovate near obverse surface, slightly enlarged at distal end, longest dimension near obverse surface oriented distal-abaxially; chamber shape highly uniform. Aperture positioned at distal-abaxial end of chamber, connected to chamber by extremely well-developed, intermediate-length vestibule; vestibule highly variable in length. Ratio of autozooecial chamber minimum width to maximum width approximately 3:5; maximum width and depth about equal, ratio of 9:10; chamber depth to length ratio approximately 3:4; chamber maximum width, depth and length highly constant, minimum width highly variable. Superior and inferior hemisepta both absent. Autozooecial chambers diverge laterally from middle of branch at a highly variable angle (mean of 23°); from reverse wall at highly constant angle (mean

of 70°).

Three-dimensionally reconstructed chamber form a slightly irregular rectangular box; length, viewed from lateral edge of branch, greater than depth, viewed from distal end of branch; which in turn is slightly greater than width, viewed from obverse surface.

Internal granular skeletal layer thick; granular skeletal layer extremely well-developed, continuous with obverse nodes, stylets, keel, peristome, and apertural stylets; reverse longitudinal striae and microstylets; across dissepiments and in the middle of zoarial supports. Outer lamellar layer extremely thick, exhibiting pronounced astogenetic thickening; zoarial central axis formed of massively accreted lamellar skeleton which completely covers mesh surface at site of and near central axis.

Remarks.—*A. wortheni* was described by Hall from the Warsaw beds near Warsaw, Illinois. *A. reversa* Hall, 1858 was later differentiated by Hall as a species having a sinistral, rather than dextral spiraling axis, as in *A. wortheni*. The direction of the axis spiral was considered an invalid criterion for species differentiation by Ulrich (1890), and he placed the two species in synonymy under *A. wortheni*, which had priority. Dextral and sinistral spiraling axes can both be observed in the same zoarium, therefore I am in agreement with Ulrich in placing these two species in synonymy with *A. wortheni*.

Ulrich (1890, pp. 571–572) criticized Hall for describing *A. wortheni* as having "three rows of apertures below a bifurcation, and sometimes with zooecia on the dissepiments", saying both assertions were based on "defective observation". In my work with over 80 axes having meshwork attached, I found numerous examples of branches having three rows present proximal to sites of branch bifurcation as well as occurrence of aperture opening on the edges of dissepiments. Ulrich's apparent overreliance on the central axis for species assignment in *Archimedes* Hall, 1858 probably led to his not observing these characters, and thus his criticism of Hall is doubly unjustified.

Archimedes welleri Condra and Elias, 1944 was based on Keyes' largest specimen and Van Tuyl's described materials. Condra and Elias' criteria for establishing this species are greater length and larger size of axial flange, and development of prominent nodes in *A. welleri*. These criteria all represent axis and branch characters that greatly increase during zoarial astogeny; the mesh spacing and other criteria listed for species differentiation are essentially identical between *A. welleri* and *A. wortheni*. For these reasons, *A. welleri* is herein placed in synonymy with *A. wortheni*, which has priority.

A. wortheni is distinguished from *A. owenanus* (Hall, 1857b), the most similar Warsaw species of *Archimedes* analyzed, by substantially smaller autozooecial chamber size, fewer apertural stylets, higher reverse-wall budding-angle, narrower branches, more tightly closed mesh, closer aperture spacing along, across and between branches, and slightly smaller angle between the distal end of the axis and axial whorl. Other taxonomic criteria are similar between these two species, suggesting close phylogenetic affinities.

Material studied.—Eighty-four exterior fragments, 20 sectioned specimens; largest zoarial fragment 30×108 cm (width to length). The preservation of the central axis is excellent due to its highly robust nature; the preservation of the mesh is moderately good. Interior analyses of the zoarial axis and mesh were undertaken only on samples in which the mesh was still attached to the central axis, thus assuring no confusion in determining the source of mesh relative to zoarial axes.

Occurrence.—*Archimedes wortheni* is an abundant component of the Upper Warsaw fauna in the northern half of the study area, having its most abundant occurrence in Geode Glen (Warsaw Beds) at Warsaw. It is found primarily in rocks deposited in lower-energy environments, such as argillaceous biocalcilutites and shales; it rarely occurs in biocalcarenites.

Holotype.—AMNH 7525/1 (Hall Coll. 5058/1).

Topotypes.—ISGS(ISM) 10636, ISGS(ISM) 2780-1/2, UI X-28–1/3.

Figured and/or measured specimens.—UI X-7005, 7012, 7004, 7014, 6995–7000, 6874, 6991, 6992, 7002 (loc. 11, samples 48, 50, 51, 58, 61, 63), 6990, 6994, 7007, 7008 (loc. 29, sample 5).

Archimedes valmeyeri, new species
Plate 60, figures 3–9, Plate 61, figures 1–8,
Plate 62, figures 1–6; Table 40

Etymology of name.—Named for the species' prime area of occurrence: Valmeyer, Illinois.

Diagnosis.—Zoarium moderately robust, mesh close, pattern extremely regular; central axis well-developed, moderately robust, volutions dextral or sinistral, diverging from axis at moderately constant angle (mean of approximately 43°), pillarlike supports between flanges of spiral; branch robustness pronounced, width intermediate, thick in depth; branches straight on obverse and sinuous on reverse surface; transversely circular to ovate, becoming highly elliptical with astogeny, spacing close and joined at highly regular intervals by intermediate-width, short dissepiments. Fenestrule size lower-end intermediate; shape irregularly elliptical on obverse, irregularly elliptical to ovate, to more rarely circular to square on reverse; size and shape both variable. Autozooecial aperture size lower-end intermediate, shape symmetrically circular, irregularly circular to slightly ovate, elongate slightly proximodis-

tally, proximoabaxially, or perpendicular to direction of branch growth; surrounded by thin, well-developed complete or incomplete peristome, open at proximal to proximal-adaxial edge; small apertural stylets, seven to 16 per aperture (mean of 11.5), positioned atop peristome; two to three (most commonly three) apertures per fenestrule. Single narrow, continuous keel present; keel slightly anastomosing to approaching straight, extending along middle of obverse branch surface, atop which are positioned intermediate-size nodes; nodes circular, ovate to slightly stellate, slightly elongate proximodistally. Autozooecial chamber size lower-end intermediate, chambers emplaced in two rows, except either third row at sites of branch bifurcation or more rarely three rows for moderate distances proximal to sites of branch bifurcation; outline irregularly ovate to rounded triangle near reverse wall, irregularly pentagonal throughout most of chamber depth, irregularly elliptical to more rarely irregularly ovate near obverse surface. Chamber longest dimension parallel to reverse wall proximodistally. Aperture at distal-abaxial end of chamber, connected to chamber by intermediate, highly variable length vestibule. Superior and inferior hemisepta both absent. Lateral-wall budding-angle highly variable (mean of approximately 20°); reverse-wall budding-angle highly constant (mean of 58°). Heterozooecia (ovicells?) occurring as pronounced globular expansions infilling fenestrules.

Table 40 presents statistical criteria used in delimiting this species.

Exterior description.—Zoarium moderately robust; forming a slightly cupped, fan-shaped expansion radiating outward from the exteriormost edge of a spiraling central axis; mesh spacing close; pronounced astogenetic thickening of obverse, extremely pronounced astogenetic thickening of reverse zoarial skeleton; zoarial mesh pattern extremely regular. Central axis moderately robust, well-developed, maximum diameter highly variable (mean of 14.48 mm), exhibiting pronounced thickening immediately distal to site of initial axis development; volution spacing irregular (mean spacing 3.77 mm), developing into either a dextral or sinistral spiral; zoarial mesh diverging from central axis at a mean angle of approximately 43°, moderately constant. Distal end of axial flange flat or slightly concave; proximal side flat to slightly concave; both sides of axis exhibiting striated texture spiraling around and outward from central axis, resulting from thickening of lamellar skeletal material around axis with astogeny. Pillarlike supports rare, develop between flanges along axis; zoarial mesh overgrown by zoarial skeleton from axis development during astogeny. Probable mature zoarial width up to 20 cm, length of 50 cm.

Branch robustness pronounced; width intermediate, variable, depending on degree of astogenetic thickening of lamellar skeleton; straight as observed on obverse surface, highly sinuous and irregular on reverse surface due to astogenetic thickening of lamellar skeleton. Branch spacing close, distance between adjacent branch centers highly regular. Obverse surface texture slightly granular, coarsening with astogeny; surface rounded, except for presence of single narrow, well-developed keel; keel continuous, straight to slightly anastomosing, extending along branch midline, causing slight to moderate positive inflection in obverse surface profile. Keel covered by lamellar skeleton with astogeny. Nodes monoserially emplaced, well-developed, size intermediate; shape circular, ovate to slightly stellate, elon-

Table 40.—Summary numerical analysis of *Archimedes valmeyeri*, n. sp. For explanation of abbreviations of characters (left column), see Table 8b (foldout inside back cover).

	number of mea-sure-ments	*mean*	*standard deviation*	*coeffi-cient of variation*	*observed range*
1. **WB**	24	0.3716	0.0769	20.69	0.225–0.505
2. **DBC**	24	0.4818	0.0553	11.48	0.431–0.575
3. **WD**	24	0.2317	0.0390	16.83	0.194–0.306
4. **LF**	24	0.4786	0.1204	25.16	0.350–0.675
5. **WF**	24	0.2425	0.0801	33.03	0.105–0.363
6. **AF**	24	2.67	0.49	18.46	2–3
7. **AL**	24	0.1112	0.0086	7.73	0.096–0.127
8. **AW**	24	0.0872	0.0126	14.45	0.069–0.105
9. **ADB**	24	0.2198	0.0154	7.01	0.196–0.246
10. **AAB**	24	0.2407	0.0252	10.47	0.208–0.293
11. **ABB**	24	0.2687	0.0521	19.39	0.169–0.365
12. **DN**	24	0.0923	0.0243	26.33	0.055–0.140
13. **DND**	24	0.0860	0.0241	28.02	0.055–0.132
14. **SNB**	24	0.1652	0.0437	26.45	0.090–0.224
15. **WK**	24	0.0187	0.0028	14.97	0.015–0.023
16. **DSO**	24	0.0081	0.0019	23.46	0.005–0.012
17. **SSO**	24	0.0218	0.0092	42.20	0.011–0.039
18. **WP**	24	0.0154	0.0052	33.77	0.011–0.027
19. **SA**	24	11.50	2.61	22.70	7–16
20. **SAD**	24	0.0140	0.0054	38.57	0.009–0.026
22. **RSS**	24	0.0099	0.0036	36.36	0.006–0.019
24. **SSS**	24	0.0158	0.0079	50.00	0.008–0.034
27. **WSC**	24	14.5	3.2	45.92	3.2–26.4
28. **DCA**	24	3.8	1.1	28.52	2.7–6.1
29. **ACA**	24	42.58	4.19	9.84	38–52
30. **OL**	16	0.2594	0.0305	11.76	0.212–0.290
31. **OW**	16	0.2096	0.0921	15.31	0.199–0.299
32. **TRW**	24	0.0129	0.0024	18.60	0.008–0.016
33. **TLW**	24	0.0135	0.0025	18.52	0.010–0.018
34. **FWT**	24	0.1396	0.0726	52.01	0.043–0.292
35. **RWT**	24	0.2926	0.1646	56.25	0.086–0.686
36. **CL**	24	0.2293	0.0110	4.80	0.214–0.251
37. **CD**	24	0.1382	0.0101	7.31	0.124–0.158
38. **MAW**	24	0.1193	0.1097	8.13	0.105–0.140
39. **MIW**	24	0.0681	0.0110	16.15	0.050–0.088
40. **VD**	24	0.1030	0.0351	34.08	0.039–0.143
41. **RA**	24	58.0	3.67	6.32	51–64
42. **LA**	24	19.67	6.39	32.47	10–30
43. **TB**	24	0.5685	0.1598	28.11	0.286–0.852

gate proximodistally; nodes variable in size, highly variable in shape; develop as projections from middle of keel; four to seven (most commonly five or six) nodes per fenestrule; node spacing close, moderately unevenly spaced; node diameter increasing with astogeny. Small stylets, variably sized and highly variably positioned, occurring across obverse branch surface. Reverse surface texture granular, coarsening with astogeny; bearing an intermediate number of closely to intermediately spaced longitudinal striae which rapidly become covered by lamellar skeleton during astogeny; rows of small microstylets, closely spaced, develop as extensions of longitudinal striae along reverse branch surface; microstylets variable in size, diameters increase with astogeny; microstylets become highly variably positioned across reverse branch surface. Autozooecia in two rows across branch, except either third row at sites of branch bifurcation, or more rarely three rows extending for short to moderate distances proximal to sites of branch bifurcation. Heterozooecia (ovicells?) occurring as pronounced globular expansions infilling fenestrules; mean widths and lengths of polymorphs slightly greater than twice autozooecial aperture widths and lengths; polymorph length moderately greater than width, ratio approximately 4:5; connection between polymorph and autozooecial chamber lacking; polymorphs most commonly located immediately distal from central axis along branch.

Dissepiments of intermediate width, approximately five-eighths that of branch, moderately constant; short, moderately constant in length; connect branches at moderately regular intervals. Dissepiments exhibit slight medial thinning, slight flaring at branch–dissepiment junction; slightly recessed from obverse, approximately even with reverse branch surface. Extremely pronounced astogenetic thickening of dissepiments toward proximal end of zoarium. Obverse dissepiment surface with single longitudinal ridge emplaced perpendicular to branch length; one to three (most commonly two) intermediate-size stylets develop as extensions of ridge; small stylets, similar in size to obverse branch stylets, develop across dissepiment surface; ridge covered by lamellar skeleton, nodes and stylets increase in diameter during astogeny; reverse dissepiment surface with an intermediate number of rows of longitudinal striae atop which occur closely spaced rows of small microstylets; longitudinal striae rapidly become covered by lamellar skeleton, microstylets become more irregularly positioned across dissepiment surface with astogeny. Obverse dissepiment surface texture slightly granular, reverse surface texture granular, both coarsening with astogeny. Emplacement of dissepiments perpendicular to moderate angle from perpendicular to branch length. Apertures commonly positioned on proximal or distal edge, or in middle of dissepiment edge at branch–dissepiment contact; arranged symmetrically or asymmetrically between branches.

Fenestrule size lower-end intermediate; shape irregularly elliptical on obverse surface, irregularly elliptical to ovate, elongate proximodistally, to more rarely circular to square on reverse; variable in both size and shape; moderately to highly expanding in width and length in obverse–reverse direction. Width of fenestrule approximately two-thirds branch width on obverse surface, appreciably greater than branch width on reverse; fenestrule size greatly reduced toward proximal end of zoarium, toward central axis, and toward distal edge of mesh where zoarial supports develop, due to pronounced astogenetic thickening of lamellar skeleton. Width to length ratio of fenestrule moderately to highly variable, ranging from approximately 1:1 to 1:6; ratio of fenestrule mean width to length approximately 1:2; length slightly more constant than width, both highly variable. Two to three (most commonly three) apertures per fenestrule length; distance between closest aperture centers along branch approximately nine-tenths distance along branch, spacing across fenestrule approximately 1.2 times greater than distance between closest apertures along branch; spacing along and across branch moderately constant, spacing across fenestrule variable.

Autozooecial aperture size lower-end intermediate, shape symmetrically circular, irregularly circular to slightly ovate, enlarged slightly at distal end; elongate slightly proximodistally, proximoabaxially, or perpendicular to direction of branch growth; where elongate, width to length ratio approximately 7:9; length moderately uniform, width moderately variable, shape variable; opening oriented parallel to plane of obverse surface; aperture surrounded by thin, well-developed complete or incomplete peristome; where incomplete, peristome open up to one-fourth of aperture at proximal to proximal-adaxial edge of aperture. Small apertural stylets develop as projections from peristome, seven to 16 per aperture (mean of 11.5); apertural stylets highly variable in size and number. Aperture margins extend into fenestrule, causing pronounced inflections in fenestrule outline on obverse surface. Centrally thickened terminal diaphragms occurring at proximal end of zoarium and near zoarial axis.

Zoarial supports extremely well-developed, forming as extensions of reverse zoarial surface and distal edge of mesh radiating outward from central axis. Lamellar skeleton on supports developing at lateral edge of mesh frequently covers apertures and fills fenestrules.

Interior description.—Branches circular to ovate in transverse section at distal end of zoarium and away from central axis, elongate parallel to plane of obverse surface, slightly enlarged on obverse surface; with as-

togeny branches become moderately to highly elongate-elliptical in shape in transverse view, elongate in obverse–reverse direction due to pronounced addition of lamellar skeleton to reverse branch surface. Branches thick, variable in depth.

Autozooecial chamber size lower-end intermediate, chambers biserially arranged along planar branch axial wall; axial wall highly sinuous near reverse wall, becoming moderately sinuous throughout mid chamber, extending toward and connecting with chamber lateral walls; becoming very slightly sinuous to approaching straight near obverse surface. Chamber longest dimension parallel to reverse wall in proximodistal direction. Autozooecial chamber outline irregularly ovate to rounded triangle near reverse wall, rapidly becoming irregularly pentagonal in mid chamber and throughout most of chamber depth; irregularly elliptical to more rarely irregularly ovate near obverse surface, slightly enlarged at distal end, longest dimension near obverse surface oriented distal-abaxially, chamber shape highly uniform. Aperture positioned at distal-abaxial end of chamber, connected to chamber by extremely well-developed, intermediate-length vestibule; vestibule highly variable in length. Ratio of autozooecial chamber minimum width to maximum width approximately 4:7; maximum width slightly less than depth, ratio about 6:7; chamber depth to length ratio approximately 3:5; chamber maximum width, depth and length highly constant, minimum width highly variable. Superior and inferior hemisepta both absent. Autozooecial chambers diverge laterally from middle of branch at a highly variable angle (mean of approximately 20°); from reverse wall at highly constant angle (mean of 58°).

Three-dimensionally reconstructed chamber form a slightly irregular rectangular box; length, viewed from lateral edge of branch substantially greater than depth, viewed from distal end of branch; which is slightly greater than width, viewed from obverse surface.

Internal granular skeletal layer thick; granular skeletal layer extremely well-developed, continuous with obverse nodes and nodes occurring on dissepiments, stylets, keel, peristome, and apertural stylets; reverse longitudinal striae and microstylets; across dissepiments and in the middle of zoarial supports. Outer lamellar layer extremely thick, exhibiting pronounced astogenetic thickening; zoarial central axis formed of massively accreted lamellar skeleton which completely covers mesh surface at site of and near central axis.

Remarks.—The chamber shape, size, and placement of *A. valmeyeri* closely resemble those of *A. owenanus*. *A. valmeyeri* is distinguished by shorter and slightly wider fenestrule openings, wider and deeper branches, slightly larger aperture openings, greater spacing of apertures along, across, and between branches, fewer apertural stylets (similar in number to *A. wortheni*), much more numerous and closely spaced nodes atop keel along obverse surface, and appreciably lower angle between the distal end of the axis and the axial whorl. Autozooecial chamber size is very similar between *A. valmeyeri* and *A. owenanus*, suggesting extremely close phylogenetic positioning of these two species.

Extremely well-developed supports at the distal end of the zoarial mesh suggest *A. valmeyeri* was highly specialized for growth in a muddy substrate or supported itself by resting on shells. Such supports are found only in this species of *Archimedes* Hall, 1858 and are useful for species recognition in the field.

Material studied.—Fourty-one exterior fragments, 11 sectioned specimens; largest zoarial fragment 16 × 34 cm (width to length). The preservation of the central axis is generally good, although frequently axes are partially silicified, probably due to the presence of moderately abundant detrital clays, which acted as a source of silica. Interior analyses of mesh were undertaken only on samples in which the mesh was still attached to the central axis, minimizing confusion in determining the source of the mesh relative to the zoarial axes analyzed.

Occurrence.—*Archimedes valmeyeri* is a moderately abundant component of the Warsaw fauna in the southern part of the study area, occurring throughout the Warsaw at the Valmeyer and St. Louis localities, and found as far north as White Hall. It occurs primarily in low-energy environments, in argillaceous biocalcilutites and shales, and more rarely in biocalcarenites.

Holotype.—UI X-6987 (loc. 49B, sample 13).

Paratypes.—UI X-6988, 6989 (loc. 47A, sample 35), 6976–6982, 6946 (loc. 49B, samples 10, 12, 15, 20).

Family **POLYPORIDAE** Vine, 1884

Zoaria robust, fan-shaped, constructed of branches bifurcating at regular to variable intervals. Dissepiments connect branches at varying distances (transverse links lacking autozooecial chambers) which may or may not have apertures opening onto the dissepiments at branch–dissepiment edge. Each individual (autozooecium) with a single apertural opening; openings occurring on one side of fan, the front or obverse surface, the back or reverse surface being without apertural openings. Three to seven rows of zooecia typically present across each branch. Exterior obverse ornamentation can consist of longitudinal keels [rarely occurring in the polyporids and referred to as carina by some authors]; nodes of various forms positioned along branch surfaces and/or on dissepiments; stylets positioned down the branch, on dissepiments and/or around apertures; peristomal structures and heterozooecial features. Reverse exterior surfaces frequently

with longitudinal striae, microstylets and macrostylets of varying sizes, zoarial supports, and exhibiting pronounced astogenetic changes. Interior features include typical autozooecial chamber shape and orientation (elongate chamber characteristically emplaced at an acute angle to reverse wall), infrequent presence of superior hemiseptum (adjacent to obverse interior wall), vestibule and terminal diaphragms.

Range.—Ordovician to Permian.

Genera included.—The Warsaw genera *Polypora* McCoy, 1844, and *Fenestralia* Prout, 1858a, are included in this family.

Genus **FENESTRALIA** Prout, 1858a

Type species.—*Fenestralia sanctiludovici* Prout, 1858a [Mississippian, Meramec, Missouri].

Diagnosis.—Zoarium robust, mesh spacing close to open; chamber outline irregularly pentagonal, rectangular or a parallelogram in mid tangential section, chamber size intermediate; chambers emplaced in two adaxial and two abaxial rows away from medial axial wall from which keel develops; aperture size intermediate; superior hemiseptum poorly developed, inferior hemiseptum absent; chamber reverse-wall budding-angle 42° (mean), adaxial zooecia bud from reverse zoarial wall, abaxial zooecia bud from two rows of abaxial axial walls.

Three-dimensionally reconstructed chamber form a slightly rectangular tube.

Description.—Zoarium robust, expansion flat to obversely curved, mesh spacing varying from close to open, irregular.

Branches wide, straight to sinuous in trace with lateral branches broadly curved toward edge of zoarium; branch surface rounded. Keel present, single, width intermediate, thickening with astogeny and frequently covered by lamellar skeleton. Nodes present, emplacement monoserial, large, shape ovate to elliptical, located in middle of keel, spacing intermediate. Obverse stylets present, size intermediate, occurring across obverse surface. Microstylets present, small. Macrostylets absent. Autozooecia in four rows, two rows on each side of medial keel; five to six rows of autozooecia at sites of branch bifurcation or for distance along branch proximal to site of branch bifurcation. Heterozooecia (ovicells?) present.

Dissepiments of intermediate width, length intermediate, connnect branches at regular intervals.

Fenestrule size intermediate to large, shape elliptical to ovate.

Aperture size intermediate, shape circular to ovate; adaxial two rows oriented approximately parallel to plane of obverse suface, abaxial two rows oriented approximately perpendicular to plane of obverse surface. Peristome present, complete; apertural stylets absent; terminal diaphragms present, located throughout zoarium.

Branch shape circular, ovate to polygonal in cross-section, thick in depth.

Autozooecial chamber size intermediate, chambers arranged in four rows, two adaxial and two abaxial, along three straight to slightly sinuous axial walls; mid axial wall separates adaxial rows of zooecia, lateral axial walls form reverse wall for abaxial rows of zooecia; maximum chamber length parallel to proximal and distal lateral chamber walls. Chamber outline ovate near reverse wall; becoming rectangular to parallelogram-shaped to more rarely irregularly pentagonal in mid chamber and throughout most of chamber depth; bilobate-ovate near obverse surface. Vestibule present, length intermediate. Superior hemiseptum present, poorly developed at proximal-abaxial vestibular edge; inferior hemiseptum absent. Adaxial lateral-wall budding-angle 17° (mean); abaxial lateral-wall budding-angle 51° (mean); reverse-wall budding-angle the same for both adaxial and abaxial rows of zooecia (mean of 42°). Lamellar skeletal layer thickness intermediate, exhibiting moderate astogenetic thickening; granular skeletal layer thickness intermediate, exhibiting no astogenetic thickenings.

Three-dimensionally reconstructed chamber form a slightly rectangular tube.

Text-figure 17 illustrates zoarial outlines in longitudinal, tangential, and transverse orientations, and three-dimensional chamber reconstructions from distal, abaxial edge of branch, and obverse surfaces.

Remarks.—*Fenestralia* was described by Prout (1858a) from Warsaw materials collected near Meramec, Missouri. Members of this genus are readily recognized in exterior view by the pronounced median keel from which two rows of autozooecia develop on either side.

Particular care must be taken in sectioning and orienting specimens of *Fenestralia*, as adaxial chambers are oriented parallel to the obverse surface and abaxial chambers are oriented perpendicular to the obverse surface. When taking this into consideration when sectioning, one finds adaxial and abaxial chambers to be identical in shape.

Only a single species, *F. sanctiludovici*, is known. The distinctive nature of abaxial zooecial budding from lateral rows of axial walls is not found in any other fenestrate, a feature that warrants generic recognition.

Fenestralia can be distinguished from *Polypora* McCoy, 1844, the most similar genus, by presence of a keel along the middle of the branch obverse surface, lack of apertural stylets, abaxial rows of zooecia budding from lateral rows of axial walls, and presence of a superior hemiseptum. Significant similarities in chamber shape exist.

Species composition.—*F. sanctiludovici* is the only known species.

Range.—Mississippian; restricted to the Kinderhookian and the Valmeyeran.

Fenestralia sanctiludovici Prout, 1858a
Plate 63, figures 1–10, Plate 64, figures 1–8; Table 41

Fenestralia St. Ludovici Prout, 1858a, p. 235, pl. 15, figs. 1–1a.
Fenestralia sancti-ludovici Prout. Ulrich, 1890, p. 604, pl. 55, fig. 5 [St. Louis Group and Warsaw Beds: St. Louis and Barrett's Station, Missouri; Monroe County, Alton, Columbia, and Warsaw, Illinois]; Simpson, 1895b, p. 717, fig. 62; Burckle, 1960, pp. 1090–1091, pl. 12a, figs. 6, 12.
Fenestralia? sancti-ludovici Prout. Keyes, 1894, p. 30 [St. Louis Limestone: St. Louis, Missouri].

Diagnosis.—Zoarium robust, mean mesh spacing lower-end intermediate, varying from close to open, pattern moderately to highly irregular; branches robust, width wide, extremely thick in depth; branches straight to slightly sinuous, broadly curved at lateral zoarial edge; transversely circular, irregularly circular, ovate to polygonal, spacing intermediate to close; branches joined at moderately constant intervals by intermediate-width, intermediate-length dissepiments. Fenestrule size large; shape irregularly elliptical to rarely irregularly ovate, moderately variable. Autozooecial aperture size lower-end intermediate, shape symmetrically circular, irregularly circular to irregularly ovate, slightly elongate proximodistally to proximoabaxially, surrounded by upper-end intermediate width, well-developed, complete peristome; four to seven (most commonly five) apertures per fenestrule. Single intermediate-width, continuous keel along branch midline, forming division between the four rows of autozooecia; large, ovate to elliptical nodes, elongate proximodistally, positioned atop keel. Autozooecial chamber size intermediate; chambers emplaced in four rows, adaxial chamber rows alternating, abaxial rows alternating or adjacent, either five or six rows at sites of branch bifurcation or five or six rows for moderate to pronounced distances proximal to sites of branch bifurcation; outline irregularly ovate near reverse wall, becoming irregularly pentagonal toward mid chamber; rectangular to parallelogram-shaped in mid chamber and throughout most of chamber length; biolbate ovate near obverse surface, enlarged at distal end with inflection at proximo-adaxial apertural edge; shape and symmetry of adaxial and abaxial autozooecial chambers equal. Chamber longest dimension parallel to proximal and distal lateral chamber walls. Aperture at distal-abaxial end of chamber for both adaxial and abaxial rows of autozooecia, connected to chamber by intermediate, highly variable length vestibule. Short superior hemiseptum present at proximal apertural edge, inferior hemiseptum absent. Lateral-wall budding-angle of adaxial two rows of autozooecial chambers moderately variable, mean of 17°; lateral budding angle of abaxial two rows of autozooecial chambers moderately variable (mean of 51°); reverse-wall budding-angle of adaxial and abaxial rows of chambers both highly constant (mean approximately 42°). Enlarged autozooecial chambers (ovicells?) observed in tangential section, length same as autozooecia, width 1.35 times greater. Table 41 presents statistical criteria used in delimiting this species.

Exterior description.—Zoarium robust, expansion flat to slightly obversely curved, fan-shaped; mean mesh spacing lower-end intermediate, varying from close to open; moderate astogenetic thickening of both obverse and reverse lamellar skeleton; zoarial pattern moderately to highly irregular. Probable mature widths 30 to 50 mm; lengths 20 to 60 mm.

Branches robust; wide, variable in width; straight to slightly irregularly sinuous, lateral branches commonly broadly curved toward edge of zoarium. Branch spacing intermediate to more rarely close in some zoarial fragments, distance between adjacent branch centers variable. Obverse surface texture slightly to moderately granular, coarsening with astogeny; surface well-rounded, except single intermediate-width, well-developed keel; keel continuous, straight, extending along branch midline and causing moderate to pronounced positive inflection on obverse surface. Keel thickens, becomes partially covered by lamellar skeleton and partially overgrows adaxial edge of middle aperture with astogeny. Single rows of well-developed, large, ovate to elliptical nodes, elongate proximodistally; size and shape of nodes moderately regular; nodes projecting from middle of keel; one to two per fenstrule

Text-figure 17.—*Fenestralia sanctiludovici* illustrated. 1, diagrammatic longitudinal section illustrating changing chamber outline for adaxial rows of chambers from deep section near middle of branch (bottom of figure) to shallow section (top of figure) [Abaxial rows of chambers exhibit same chamber outlines, but require a longitudinal section to be oriented at an angle from perpendicular required for adaxial rows. Observe relatively low reverse-wall budding-angle (arrow) typical of genera exhibiting more than two rows of chambers across the branch.], ×70; 2, diagrammatic tangential section showing change in chamber outline of adaxial chambers from deep section near reverse-wall budding-site (bottom of figure) to shallow section near obverse surface (top of figure) [Poorly developed superior hemisepta are illustrated in this figure (arrow).], ×70; 3, diagrammatic transverse section across branch [Observe orientation of adaxial (arrow **a**) and abaxial (arrow **b**) aperture openings relative to plane of obverse surface.], ×70; 4, reconstruction of typical chamber shape (three-dimensional) as viewed from distal end of branch; chamber reconstructed is from the right adaxial side of branch, ×140; 5, reconstruction of typical adaxial chamber shape (three-dimensional) as viewed from abaxial edge of branch, ×140; 6, reconstruction of typical adaxial chamber (three-dimensional) as viewed from obverse surface; chamber reconstructed is from right side of branch [Observe slight inflection into chamber caused by poorly developed superior hemiseptum (arrow).], ×140.

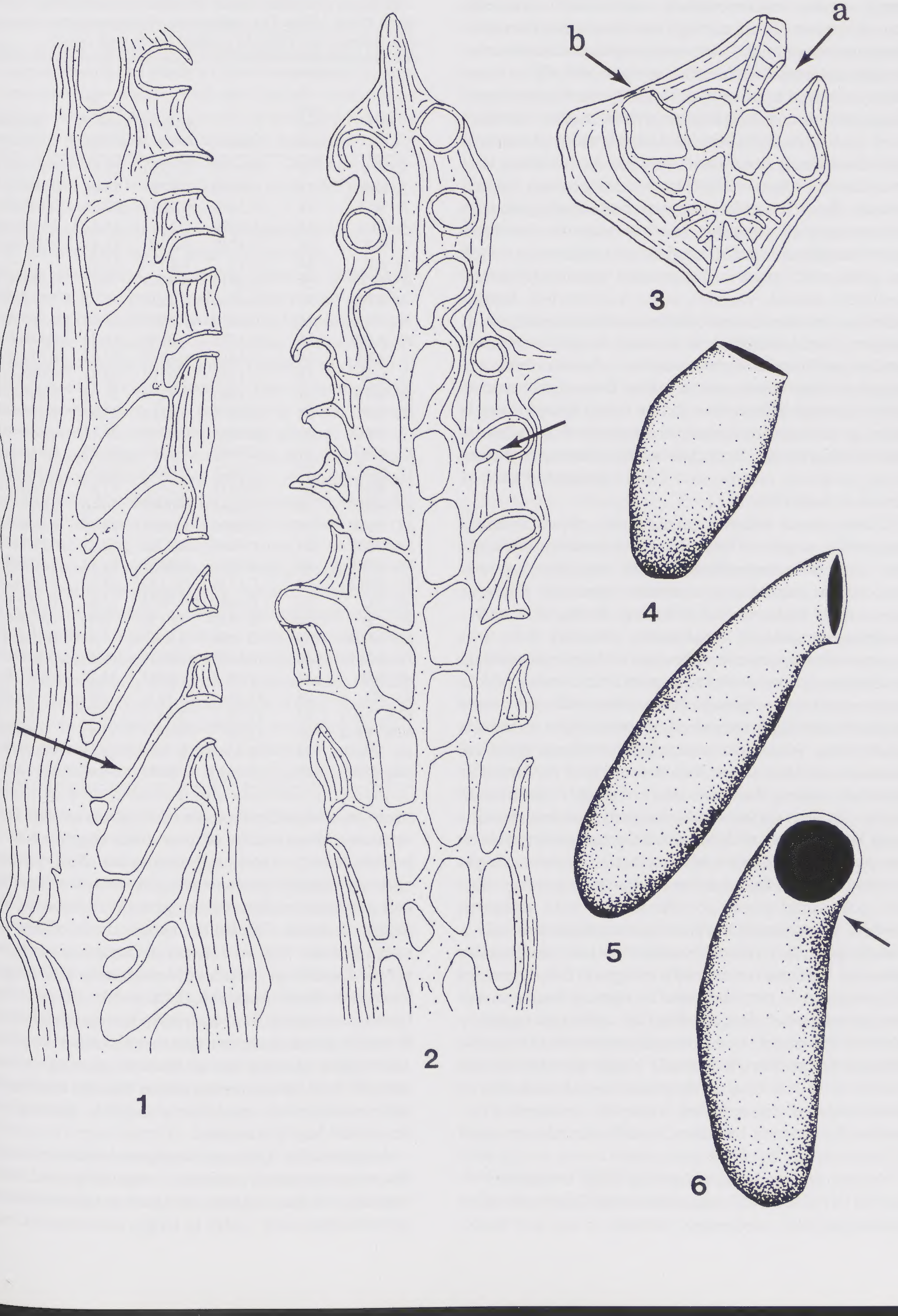
a
b
1
2
3
4
5
6

length; nodes intermediately, moderately unevenly spaced, frequently occurring at or near sites of branch–dissepiment junction; with astogeny node diameter increases and nodes frequently become partially to completely covered by secondary lamellar skeleton of keel. Lower-end intermediate-size stylets, highly variably sized and variably positioned along obverse surface; most commonly positioned between nodes along keel or at abaxial edges of keel, more rarely across branch surface. Reverse surface texture moderately granular, coarsening with astogeny; bearing relatively few rows of intermediately spaced longitudinal striae atop which are positioned rows of upper-end small-size, intermediately spaced, variably sized microstylets. Longitudinal striae become covered by lamellar skeleton with astogeny and microstylets become larger, more unevenly positioned across surface. Autozooecia arranged in four rows, except either five or six rows at sites of branch bifurcation or five or six rows for moderate to pronounced distances proximal to sites of branch bifurcation; branches with pronounced thickening proximal, pronounced thinning distal to sites of branch bifurcation.

Dissepiment width intermediate, approximately three-fifths width of branch, width moderately variable; length intermediate, highly variable; connect branches at moderately constant intervals. Dissepiments with slight medial thinning, flaring at branch–dissepiment contact; moderately recessed from obverse surface, approximately even with reverse surface. Moderate to pronounced astogenetic thickening of dissepiment. Obverse dissepiment surface with one to two longitudinal ridges emplaced perpendicular to branch length, atop which are positioned lower-end intermediate-size stylets; ridges become covered by lamellar skeleton, stylets become more variably positioned across obverse surface with astogeny; reverse dissepiment surface also with longitudinal ridges atop which are positioned upper-end small microstylets; ridges covered by lamellar skeleton, microstylets more variably positioned across obverse surface with astogeny; obverse dissepiment surface texture slightly to moderately granular, reverse surface texture moderately granular, both coarsening with astogeny. Emplacement of dissepiments perpendicular or approaching perpendicular to branch length. Abaxial apertures typically project toward and open onto dissepiment at branch–dissepiment contact, frequently highly projecting onto dissepiment, less frequently positioned at proximal or distal edge of dissepiment; typically arranged symmetrically between branches, less frequently arranged asymmetrically between branches.

Fenestrule size large; shape typically irregularly elliptical to more rarely irregularly ovate, highly elongate proximodistally; moderately variable in size and shape;

Table 41.—Summary numerical analysis of *Fenestralia sanctiludovici* Prout, 1858a. For explanation of abbreviations of characters (left column), see Table 8b (foldout inside back cover).

	number of measurements	mean	standard deviation	coefficient of variation	observed range
1. **WB**	24	0.5700	0.1250	21.93	0.414–0.833
2. **DBC**	24	0.9370	0.2160	23.05	0.500–1.200
3. **WD**	24	0.3460	0.0860	24.86	0.244–0.560
4. **LF**	24	1.2600	0.2117	17.22	1.000–1.670
5. **WF**	24	0.4720	0.1390	29.45	0.280–0.720
6. **AF**	24	5.17	0.83	16.16	4–7
7. **AL**	24	0.1030	0.0094	9.13	0.088–0.113
8. **AW**	24	0.0810	0.0091	11.23	0.063–0.092
9. **ADB**	24	0.2640	0.0400	15.15	0.203–0.358
10. **AAB**	24	0.1970	0.0320	16.24	0.120–0.269
11. **ABB**	24	0.5810	0.1570	27.02	0.356–0.890
12. **DN**	24	0.1270	0.0310	24.41	0.080–0.180
14. **SNB**	24	0.5840	0.1230	21.06	0.380–0.820
15. **WK**	24	0.0690	0.0164	23.77	0.045–0.106
16. **DSO**	24	0.0111	0.0029	26.12	0.008–0.017
17. **SSO**	24	0.0262	0.0081	30.92	0.014–0.042
18. **WP**	24	0.0423	0.0091	21.51	0.028–0.058
22. **RSS**	24	0.0174	0.0100	57.47	0.008–0.022
24. **SSS**	24	0.0462	0.0140	30.30	0.029–0.074
32. **TRW**	24	0.0098	0.0023	23.46	0.006–0.014
33. **TLW**	24	0.0088	0.0020	22.72	0.005–0.012
34. **FWT**	24	0.1133	0.0695	61.34	0.034–0.286
35. **RWT**	24	0.1718	0.1172	68.22	0.054–0.471
36. **CL**	24	0.3883	0.0204	2.67	0.370–0.410
37. **CD**	24	0.1423	0.0120	8.43	0.124–0.162
38. **MAW**	24	0.1208	0.0090	7.45	0.108–0.140
39. **MIW**	24	0.0610	0.0119	19.51	0.042–0.082
40. **VD**	24	0.0815	0.0291	35.71	0.037–0.129
41. **RA**	24	41.75	2.73	6.55	38–47
42A. **LA-1**	24	17.33	3.45	13.89	12–24
42B. **LA-2**	24	51.00	6.55	12.85	42–66
43. **TB**	24	0.6543	0.1196	18.28	0.486–0.870
44. **WOT**	10	0.1630	0.0187	11.47	0.142–0.177

equal in size and shape on both obverse and reverse surfaces. Mean width of fenestrule slightly less than branch width, ratio approximately 5:6; fenestrule opening moderately decreasing in size toward proximal end of zoarium due to astogenetic thickening of lamellar skeleton. Width to length ratio of fenestrule ranging from 7:10 to 1:6; moderately variable, mean ratio of width to length approximately 3:8; length of fenestrule more constant than width. Four to seven (most commonly five) apertures per fenestrule length; distance between closest aperture centers along branch 1.34 times spacing across branch, spacing across fenestrule 2.95 times spacing across branch; spacing along and across branch moderately variable, spacing across fenestrule highly variable.

Autozooecial aperture size lower-end intermediate, shape symmetrically circular, irregularly circular to irregularly ovate, slightly elongate proximodistally or proximoabaxially; width to length ratio approximately

7:9, size moderately uniform and shape variable; adaxial rows of apertures open parallel to plane of obverse surface, abaxial rows of apertures opening into fenestrule perpendicular to plane of obverse surface; upper-end intermediate-width, well-developed, continuous peristome present. Abaxial rows of aperture margins extend into fenestrule, causing slight inflections in fenestrule outline on obverse surface. Centrally thickened terminal diaphragms present, commonly occurring throughout the zoarium.

Zoarial supports develop as extensions of reverse zoarial surface and lateral edge of zoarium.

Interior description.—Branches circular, irregularly circular, ovate to polygonal in transverse section, slightly to moderately elongate parallel to plane of obverse surface; symmetrical on obverse or reverse surface. Branches thick, moderately variable in depth.

Autozooecial living chamber size intermediate, chambers arranged in four rows along planar branch axial walls, adaxial rows alternating, abaxial rows alternating to adjacent; mid-axial wall straight in mid chamber and toward obverse surface, extending along branch midline dividing adaxial autozooecia which are emplaced in alternating rows, highly sinuous near reverse wall, dividing adaxial two rows of chambers; abaxial two rows of chamber axial walls straight, acting as reverse walls for abaxial two rows of autozooecia, remaining moderately straight throughout branch depth. Chamber longest direction parallel to proximal and distal lateral chamber walls. Autozooecial chamber outline irregularly ovate near reverse wall, rapidly becoming irregularly pentagonal toward mid chamber; rectangular to parallelogram-shaped in outline in mid chamber and throughout most of chamber length; irregularly bilobate-ovate near obverse surface, enlarged at distal end with inflection into chamber at proximo-adaxial apertural edge; chamber shape highly uniform, same in both adaxial and abaxial rows of chambers. Aperture positioned at distal-abaxial end of chamber, connected to chamber by intermediate, highly variable length vestibule. Ratio of autozooecial chamber minimum width to maximum width 1:2; width to depth ratio approximately 6:7; depth to length ratio approximately 3:8; maximum width, depth, and length highly constant, minimum width highly variable. Short, poorly developed superior hemiseptum present at proximal-abaxial edge, inferior hemiseptum absent. Adaxial rows of autozooecial chambers diverge laterally from middle of branch at a moderately variable angle (mean approximately 17°); abaxial rows of autozooecial chambers diverge laterally from middle of branch at moderately variable angle (mean of 51°). Although orientation of apertures to chamber varies between adaxial and abaxial rows of chambers, both adaxial and abaxial chamber shapes and dimensions are the same. Autozooecial chambers diverge from respective reverse walls at a highly constant angle (mean approximately 42°). Heterozooecia (ovicells?) present, evident in tangential section, length same as autozooecia, width 1.35 times maximum chamber width; occurring most commonly toward proximal end of zoarium.

Three-dimensionally reconstructed chamber form a slightly rectangular tube; length, viewed from lateral edge for adaxial and approximately 45° from perpendicular to obverse surface, substantially greater than depth, viewed from distal end of branch; which in turn is slightly greater than width, viewed from obverse surface.

Internal granular skeletal layer thickness intermediate; granular skeletal layer well-developed, continuous with obverse nodes, stylets, keel, and peristome; reverse longitudinal striae and microstylets; across dissepiments and in the middle of zoarial supports. Outer lamellar layer thickness intermediate, exhibiting moderate astogenetic thickening; covering apertures and keel with astogeny.

Remarks.—Named by Prout (1858a) for materials found in the St. Louis Group near St. Louis, Missouri and Alton, Illinois. Ulrich (1890) recognized the species in the Warsaw Beds near Warsaw, Illinois as well as in the St. Louis near St. Louis, Missouri.

F. sanctiludovici is readily distinguished by the presence of a distinctive keel along the branch midline, dividing the four rows across the branch into two groups of two rows; inner adaxial rows oriented parallel to obverse surface and outer abaxial rows oriented at moderate angle toward the fenestrule. Lack of a keel in *Polypora* allows ready separation of *F. sanctiludovici*. Interior view allows delimitation of this species, based on the straight, well-developed mid-axial wall and adaxial two rows of autozooecia, basically identical chamber shape between adaxial and abaxial rows of autozooecia, in conjunction with distinctive lateral-wall budding-angles between adaxial and abaxial autozooecia.

This species has some similarities to species of *Banastella*, however four rows of autozooecia typically occur across the branch in *Fenestralia*, whereas typically two rows are found in *Banastella*.

Material studied.—Eighteen exterior fragments, two sectioned specimens; largest zoarial fragment 31 × 44 mm (width to length). Moderately well-preserved due to robust nature of zoarium.

Occurrence.—Common in Warsaw Beds at type section, present in Salem and St. Louis formations throughout study area.

Holotype.—ISGS (ISM) 4486-1.

Paratype.—ISGS (ISM) 4482-2.

Genus **POLYPORA** McCoy, 1844

Flabelliporella Simpson, 1895a (*fide* Bassler, 1953, p. G125).
Polyporella Simpson, 1895a (*fide* Bassler, 1953, p. G125).
Polyporina Frederiks, 1920 (*fide* Bassler, 1953, p. G125).

Type species.—Polypora dendroides McCoy, 1844 [Lower Carboniferous of Ireland].

Typical Warsaw species.—Polypora varsoviensis Prout, 1858a, p. 237 [Warsaw, Illinois].

Diagnosis.—Zoarium robust, mesh spacing varying from close to open; chamber outline variable, ranging from elliptical, rectangular, hexagonal, triangular, ovate, to circular in mid tangential section, chambers in three to five rows diagonally across branch, chamber size intermediate to large; aperture size intermediate to large; superior and inferior hemisepta absent; chamber reverse-wall budding-angle varying between 18° and 77° (means). Three-dimensionally reconstructed chamber form a polygonal or irregular tube.

Description.—Zoarium robust, expansion flat, obversely or reversely curved to cupped, mesh varying from close to open, regular to irregular.

Branches wide, straight to slightly sinuous in trace with lateral branches broadly curved toward edge of zoarium; branch surface rounded, angular to flat. Keel absent. Nodes present in most species, emplacement monoserial, size intermediate to large, shape stellate to ovate, located along middle of branch in straight to anastomosing rows, spacing intermediate to wide. Obverse stylets either present or absent, size intermediate to large, occurring in rows along or spaced across obverse surface. Microstylets present or absent, size intermediate to large. Macrostylets present or absent, size large, positioned atop longitudinal striae or at branch–dissepiment junction. Autozooecia typically in three to five rows across branch; five to seven rows at or along branch proximal to sites of branch bifurcation. Heterozooecia (ovicells?) present in some zoarial fragments reported by other workers; none observed in Warsaw specimens.

Dissepiment width thin to intermediate, length varying from short to long, connecting branches at regular to variable intervals.

Fenestrule size intermediate to large, shape highly variable, ranging from ovate, circular, rectangular, parallelogram-shaped, elliptical, to polygonal.

Aperture size intermediate to large, shape ovate, elliptical, to circular; adaxial row(s) oriented parallel to plane of obverse surface, abaxial rows parallel to plane or at slight angle toward fenestrule. Peristome present, either complete or incomplete; apertural stylets present, develop as extensions at edge of peristome; terminal diaphragms present, located at proximal end or throughout zoarium.

Branch shape elliptical, ovate, circular, to polygonal in cross-section, thick in depth.

Autozooecial chamber size intermediate to large, chambers arranged in three to five rows along straight to slightly sinuous axial wall; maximum chamber length parallel to proximal and distal lateral chamber walls. Chamber outline ovate, circular, diamond-shaped, to polygonal near reverse wall; elliptical, rectangular, hexagonal, ovate, to circular in mid chamber and throughout most of chamber depth; ovate circular, bilobate-ovate to elliptical near obverse surface. Vestibule present, length intermediate to long. Superior and inferior hemisepta absent. Adaxial lateral-wall budding-angle 7° to 12° (means); abaxial lateral-wall budding-angle 25° to 47° (means); reverse-wall budding-angles constant within species, highly variable between species, ranging from 18° to 77° (means). Lamellar skeletal layer thickness intermediate to thick, exhibiting slight to pronounced astogenetic thickening; granular skeletal layer thickness intermediate to thick, exhibiting no astogenetic thickening.

Three-dimensionally reconstructed chamber form a polygonal or irregular tube.

Text-figure 18 illustrates zoarial outlines in longitudinal, tangential, and transverse orientations, and three-dimensional chamber reconstructions from distal, abaxial edge of branch and obverse surfaces.

Remarks.—*Polypora* was described by McCoy from Lower Carboniferous specimens from Ireland. Lack of medial keel, rows of obverse nodes, and three to seven rows of autozooecia across each branch allow ready recognition.

Both adaxial and abaxial chambers, although differing in orientation relative to the branch axis, have essentially the same chamber shape. Reverse-wall budding-angle has a broad range for the genus: within species, however, this angle is highly constant.

Zoarial characters are more varied in *Polypora* than in other meshwork fenestrates. Warsaw polyporid spe-

Text-figure 18.—*Polypora varsoviensis* illustrated. 1, diagrammatic longitudinal section illustrating changing chamber outline for adaxial rows of chambers from deep section near middle of branch (bottom of figure) to shallow section (top of figure) [Low reverse-wall budding-angle (arrow) is typical of most species in this genus.], ×70; 2, diagrammatic tangential section showing changing chamber outlines from deep section near reverse-wall budding-site (bottom of figure) to shallow section near obverse surface (top of figure) [Adaxial (arrow **a**) and abaxial (arrow **b**) chamber outlines are approximately the same in mid tangential section in *Polypora*.], ×40; 3, diagrammatic transverse section across branch [Observe similar orientation of apertures to plane of obverse surface (arrows).], ×70; 4, reconstruction of typical chamber shape (three-dimensional) as viewed from distal end of branch; chamber reconstructed is from right side of branch, ×70; 5, reconstruction of typical chamber shape (three-dimensional) as viewed from abaxial edge of branch, ×70; 6, reconstruction of typical chamber shape (three-dimensional) as viewed from obverse surface; chamber reconstructed is from right side of branch [Observe how length as shown in tangential view (Text-fig. 18.2) only expresses a small amount of the total chamber length when viewed from the obverse surface.], ×70.

cies are highly distinctive, but available material does not justify generic subdivision. *Polypora spininodata* and *P. varsoviensis* are closely allied, as are *P. gracilis* and *P. simulatrix*.

Species composition.—Five Warsaw species of this genus were recognized: *P. gracilis*, *P. varsoviensis*, *P.*

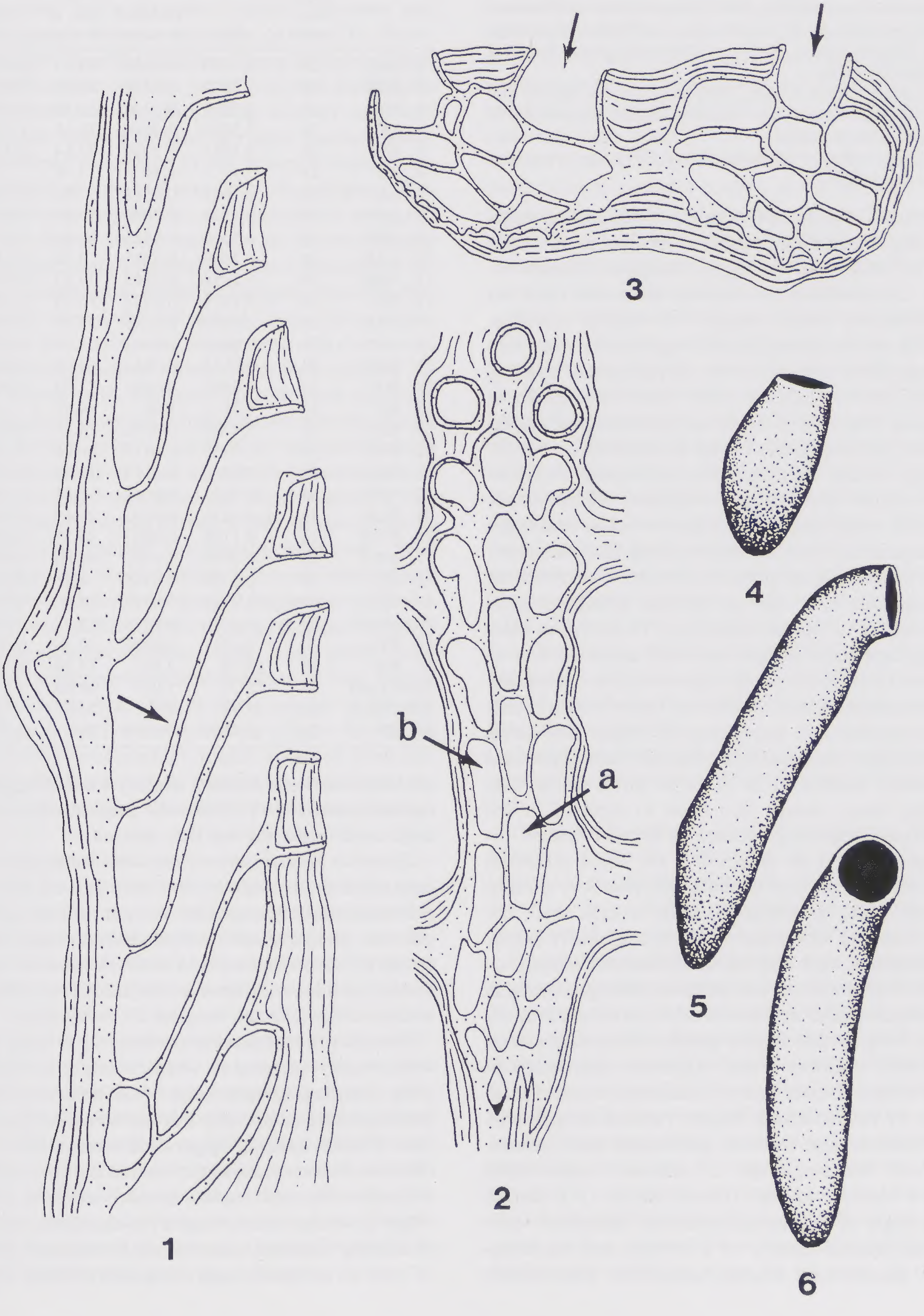

spininodata, *P. simulatrix*, and *P. retrorsa*.

Range.—Ordovician to Permian.

Polypora gracilis Prout, 1860
Plate 65, figures 1–9, Plate 66, figures 1–4; Table 42

Polypora gracilis Prout, 1860, p. 580. [Warsaw Limestone: Warsaw, Illinois]; Prout, 1866, p. 422, pl. 21., figs. 1, 1a [Keokuk Limestone: Warsaw, Illinois]; Ulrich, 1888, p. 73 [Waverly Group: Richfield and Sciotoville, Ohio].

Polypora(?) *gracilis* Prout. Ulrich, 1890, p. 590, pl. 61, figs. 10, 10a [Keokuk Group: Warsaw and Nauvoo, Illinois; Keokuk, Iowa; King's Mountain, Kentucky].

Polypora cf. *gracilis* Prout. Sakagami, 1970, p. 689 [Upper Paleozoic: Thailand and Malaya].

Diagnosis.—Zoarium moderately robust, mean mesh spacing upper-end intermediate, varying from intermediate to wide, pattern highly irregular; branch robustness intermediate to robust; branches thick in depth; branches wide, straight to slightly sinuous, broadly curved at lateral zoarial edge; transversely circular, irregularly circular, ovate to polygonal, spacing upper-end intermediate to wide; branches joined at fairly regular intervals by lower-end intermediate width, upper-end intermediate to long dissepiments. Fenestrules large; shape varying from rectangular to parallelogram-shaped to elliptical; variable. Autozooecial aperture size upper-end intermediate to lower-end large, shape irregularly ovate to approaching circular, elongate proximodistally to proximoabaxially, surrounded by intermediate size, well-developed, complete peristome; nine to 15 (most commonly 11 to 12) moderately large apertural stylets surround aperture; five to nine (most commonly seven) apertures per fenestrule. Large, irregularly lobed stellate to ovate nodes, elongate proximodistally, positioned in single row along branch midline. Autozooecial chamber size upper-end intermediate, emplaced in three or more rarely four alternating rows, except five rows at sites of or for pronounced distances proximal to sites of branch bifurcation, and two or three rows for short distances distal to sites of branch bifurcation; chamber outline irregularly ovate to polygonal near reverse wall; triangular, rounded triangular to rarely irregularly polygonal throughout mid and most of chamber length; irregularly ovate near obverse surface, enlarged at distal end; chamber shape uniform in all rows across branch. Chamber longest dimension parallel to proximal and distal lateral chamber walls. Aperture positioned at distal to distal-abaxial end of chamber, connected to chamber by intermediate, highly variable length vestibule. Superior and inferior hemisepta both absent. Lateral-wall budding-angle of adaxial autozooecial chambers highly variable (mean about 12°); lateral budding angle of abaxial autozooecial chambers variable (mean approximately 47°); reverse-wall budding-angle of adaxial and abaxial chambers individually uniform, each exhibiting a slightly variable angle (mean approximately 54°). Table 42 presents statistical criteria used in delimiting this species.

Table 42.—Summary numerical analysis of *Polypora gracilis* Prout, 1860. For explanation of abbreviations of characters (left column), see Table 8b (foldout inside back cover).

	number of measurements	*mean*	*standard deviation*	*coefficient of variation*	*observed range*
1. **WB**	24	0.5770	0.1660	28.77	0.375–0.900
2. **DBC**	24	1.3270	0.3496	26.34	0.875–1.875
3. **WD**	24	0.3000	0.0633	21.10	0.205–0.431
4. **LF**	24	2.3030	0.4646	20.17	1.750–3.380
5. **WF**	24	0.7823	0.2960	37.84	0.450–1.380
6. **AF**	24	7.17	0.94	13.08	5–9
7. **AL**	24	0.1543	0.0116	7.52	0.134–0.177
8. **AW**	24	0.1117	0.0095	8.51	0.095–0.129
9. **ADB**	24	0.4004	0.0423	10.56	0.323–0.475
10. **AAB**	24	0.2463	0.0205	8.32	0.219–0.294
11. **ABB**	24	0.8284	0.2695	32.53	0.450–1.330
12. **DN**	24	0.1976	0.0292	14.78	0.138–0.250
14. **SNB**	24	1.4990	0.5200	34.69	0.975–2.800
16. **DSO**	24	0.0147	0.0042	28.57	0.009–0.022
17. **SSO**	24	0.0623	0.0411	65.97	0.020–0.142
18. **WP**	24	0.0286	0.0061	21.33	0.018–0.039
19. **SA**	24	11.58	1.68	14.47	9–15
20. **SAD**	24	0.0360	0.0052	14.44	0.029–0.046
22. **RSS**	24	0.0330	0.0119	36.06	0.014–0.052
24. **SSS**	24	0.0528	0.0178	33.71	0.021–0.086
32. **TRW**	24	0.0103	0.0018	17.48	0.008–0.013
33. **TLW**	24	0.0155	0.0032	20.65	0.001–0.021
34. **FWT**	24	0.1108	0.0501	45.21	0.036–0.214
35. **RWT**	24	0.0786	0.0382	48.60	0.020–0.143
36. **CL**	24	0.3789	0.0161	4.25	0.354–0.402
37. **CD**	24	0.2129	0.0183	8.60	0.188–0.252
38. **MAW**	24	0.2060	0.0310	15.05	0.164–0.260
40. **VD**	24	0.1017	0.0298	29.30	0.057–0.165
41. **RA**	24	53.92	7.66	14.20	42–64
42A. **LA-1**	24	12.33	5.93	48.09	2–22
42B. **LA-2**	24	47.42	12.12	25.56	36–60
43. **TB**	24	0.5044	0.0985	19.53	0.374–0.714

Exterior description.—Zoarium moderately robust, expansion flat to slightly obversely curved, fan-shaped; mesh spacing intermediate to open, mean spacing upper-end intermediate; intermediate astogenetic thickening of both obverse and reverse lamellar skeleton; zoarial pattern moderately irregular. Probable mature widths 15 to 30 mm; lengths 20 to 40 mm.

Branch robustness intermediate to robust; branches wide, highly variable in width; straight to slightly sinuous, curving toward sites of dissepiment insertion, lateral branches broadly curved toward edge of zoarium. Branch spacing upper-end intermediate to wide, distance between adjacent branch centers moderately irregular. Obverse surface texture smooth, exhibiting slight granular coarsening with astogeny; surface flat to slightly rounded, less frequently angular. Single row of well-developed, large irregularly lobed stellate to

ovate nodes, elongate proximodistally; node size regular, shape moderately regular; nodes projecting from middle of branch in straight single row; one to two nodes per fenestrule length; widely, unevenly spaced, frequently located at or near site of branch–dissepiment junction; node diameter slightly increases and nodes frequently become partially covered by thickened secondary lamellar skeleton during astogeny. Rows of intermediate-size stylets, variable in size and highly variably positioned, anastomosing around apertures along obverse branch surface, giving a coarsely granular appearance to surface at low magnifications; stylets increasing in size and number with astogeny. Reverse surface texture granular, coarsening with astogeny; bearing an intermediate number of intermediately spaced longitudinal striae which persist throughout astogenetic thickening of lamellar skeleton; microstylets large, shape irregularly polygonal to circular, highly variable in both size and shape, microstylets positioned atop longitudinal striae, irregularly spaced, increasing in size with astogeny. Autozooecia typically arranged in four rows diagonally across branch, except as many as five rows at sites of or for pronounced distances proximal to sites of branch bifurcation and as few as two or three rows for short distances immediately distal to sites of branch bifurcation; branches exhibit pronounced thickening proximal, pronounced thinning distal to sites of branch bifurcation. Heterozooecia absent in all zoarial fragments analyzed.

Dissepiment width lower-end intermediate, slightly greater than one-half branch width, width moderately variable; length upper-end intermediate to long, highly variable; connect branches at fairly regular intervals. Dissepiments barlike, exhibiting slight flaring at branch–dissepiment contact; highly recessed from obverse, recessed from reverse branch surface. Slight astogenetic thickening of dissepiment. Obverse dissepiment surface with two to four longitudinal ridges emplaced perpendicular to branch length across dissepiment surface, rows of intermediate-size stylets atop ridges; ridges become partially covered by lamellar skeleton, stylet size increases with astogeny; reverse dissepiment surface with longitudinal striae oriented perpendicular to branch length, atop which occur rows of large microstylets; striae persist throughout astogenetic thickening, macrostylets increase slightly in diameter; obverse dissepiment texture smooth, reverse surface texture granular, both coarsening slightly with astogeny. Emplacement of dissepiment varying from perpendicular to as much as 20° from perpendicular to branch length. Apertures open on proximal or distal edge, or in middle of dissepiment edge at branch–dissepiment contact, commonly extending onto dissepiment for pronounced distances; arranged symmetrically or asymmetrically between branches.

Fenestrules large; shape varying from rectanglar to parallelogram-shaped to elliptical, moderately to highly elongate proximodistally; variable in size, moderately variable in shape; slightly expanding in width and length in obverse–reverse direction. Mean width of fenestrule 1.36 times branch width; fenestrule opening exhibiting little or no decrease in size during astogeny. Width to length ratio of fenestrule ranging from 4:5 to approximately 1:7, highly variable; mean ratio of width to length approximately 1:3, length of fenestrule more constant than width. Five to nine (most commonly seven) apertures per fenestrule length; distance between closest aperture centers along branch 1.63 times spacing diagonally across branch, spacing across fenestrule 3.63 times spacing diagonally across branch; spacing along and across branch moderately constant, spacing across fenestrule highly variable.

Autozooecial aperture size upper-end intermediate to lower-end large, shape irregularly ovate, slightly enlarged on distal end, to rarely approaching circular, elongate proximodistally to proximoabaxially; width to length ratio approximately 5:7, size and shape moderately uniform; mid-branch apertures opening parallel to plane of obverse surface, adaxial apertures opening at slight angle toward fenestrule; intermediate-size, well-developed complete peristome present. Nine to 15 (most commonly 11 to 12) moderately large, relatively constant size, well-developed and regularly positioned stylets surround aperture; stylets develop from lateral edge of peristome. Abaxial aperture margins extend into fenestrule, causing slight inflections in fenestrule outline on obverse surface. Centrally thickened terminal diaphragms present, commonly occurring throughout zoarium.

Zoarial supports well-developed, occurring as extensions of reverse zoarial surface and lateral edge of zoarium.

Interior description.—Branches circular, irregularly circular, ovate to polygonal in transverse section, slightly to moderately elongate parallel to plane of obverse surface; slightly enlarged on obverse surface. Branches thick, moderately variable in depth.

Autozooecial living chamber size upper-end intermediate, chambers arranged in three or more rarely four alternating rows along planar branch axial walls; axial walls zigzag diagonally across branch, forming chamber lateral walls throughout entire branch depth. Chamber longest dimension parallel to proximal and distal lateral chamber walls. Autozooecial chamber outline irregularly ovate to polygonal near reverse wall; becoming triangular to rounded triangular to rarely irregularly polygonal throughout mid and most of chamber length; irregularly to regularly ovate near obverse surface, enlarged at distal end; chamber shape moderately uniform, same in all rows of chambers

across branch. Aperture positioned at distal to distal-abaxial end of chamber, connected to chamber by intermediate, highly variable length vestibule. Autozooecial chamber maximum width and depth approximately equal, maximum width slightly smaller; depth to length ratio approximately 5:9; chamber depth and length highly constant, maximum width moderately variable. Superior and inferior hemisepta both absent. Adaxial rows of autozooecial chambers diverge laterally from middle of branch at a highly variable angle (mean approximately 12°); abaxial rows of autozooecial chambers diverge laterally from middle of branch at variable angle (mean approximately 47°). Orientation of apertures to chamber varies slightly between adaxial and abaxial rows of chambers, internal chamber shapes and dimensions of adaxial and abaxial rows of chambers are the same. Autozooecial chambers diverge from reverse walls at a slightly variable angle (mean approximately 54°).

Three-dimensionally reconstructed chamber form a slightly polygonal tube; length, as viewed from lateral edge of branch, slightly less than half chamber depth and width, as viewed from distal end of branch and obverse surface; which are approximately equidimensional.

Internal granular skeletal layer thickness intermediate; granular skeletal layer well-developed, continuous with obverse nodes, stylets, peristome and apertural stylets; reverse longitudinal striae and macrostylets; across dissepiment and in the middle of zoarial supports. Outer lamellar layer thickness intermediate, exhibiting slight astogenetic thickening.

Remarks.—Named by Prout (1860) for materials found in the Warsaw Limestone at Warsaw, Illinois and later recognized by Ulrich (1890) in materials from Nauvoo, Illinois; Keokuk, Iowa; and King's Mountain, Kentucky. Ulrich recongized similarity in minute characters between this species and *P. maccoyana* Ulrich, 1890 and *P. halliana* Prout, 1860; the much more open mesh, however, allows ready recognition of *P. gracilis*.

Although left in *Polypora*, Ulrich (1890) thought a new genus might be based on *P. gracilis*. A new genus was not, however, proposed by him. *P. gracilis* is distinguished from other Warsaw polyporids by rows of stylets along the obverse surface, extremely long, large fenestrules, large protruding apertural stylets, small autozooecial chambers, and relatively high reverse-wall budding-angle. Internal chamber characters are adequately similar to those of other polyporids to justify retention in this genus.

Material studied.—Eight exterior fragments, four sectioned specimens; largest zoarial fragment 22 × 41 mm (width to length). Well-preserved due to moderately robust nature of zoarium.

Occurrence.—Present throughout Warsaw study area, forming an extemely minor component of Warsaw fauna.

Topotype.—ISGS(ISM) 2816-1/2.

Figured and/or measured specimens.—UI X-6919, 6920 (location 49B, sample 12), USNM 43789.

Polypora varsoviensis Prout, 1858a
Plate 66, figures 5–12, Plate 67, figures 1–6;
Table 43; Text-figure 18

Polypora Varsoviensis Prout, 1858a, p. 237 [Warsaw, Illinois]; Ulrich, 1890, p. 593, pl. 60, figs. 2–2b [Warsaw Beds: Monroe County and Warsaw, Illinois]; Keyes, 1894, p. 29 [St. Louis Limestone: Barrett's Station, Missouri]; Trizna, 1958, p. 176, pl. 48, figs. 3–4.

Polypora Varsouviensis [*sic*] Prout. Prout, 1859, p. 451, pl. 15, figs. 3–3d.

Polypora Varsouviensis? [*sic*] Prout. Whitfield, 1891, p. 578 [Maxville Limestone: Newtonville, Ohio]; Whitfield, 1895, p. 467 [Maxville Limestone: Newtonville, Ohio].

Diagnosis.—Zoarium robust, mesh spacing close, pattern highly regular; branches robust, width extremely wide, thick in depth; branches straight, broadly curved at lateral zoarial edge; transversely irregularly circular to irregularly ovate, spacing close; branches joined at highly regular intervals by upper-end thin width, short dissepiments. Fenestrules large; shape elliptical to approaching ovate on obverse, rectangular to elliptical on reverse surface, shape moderately regular. Autozooecial apertures very large, shape irregularly ovate, enlarged at distal end, to approaching circular, elongate proximodistally to proximoabaxially, surrounded by upper-end intermediate size, well-developed complete peristome; 17 to 26 (most commonly 20 to 21) extremely small stylets surround aperture; three to six (most commonly four) apertures per fenestrule length. Upper-end intermediate size, stellate, irregularly lobed nodes positioned in single row along branch midline. Autozooecial chamber size large, emplaced in three or more rarely four alternating rows, except as many as six rows at sites of or for moderate distances proximal to sites of branch bifurcation, and two to three rows for short to moderate distances distal to sites of branch bifurcation; chamber outline irregularly ovate to rounded diamond near reverse wall; irregularly hexagonal to approaching irregularly rectangular in mid chamber and throughout most of chamber length; irregularly bilobate-ovate to elliptical near obverse surface, enlarged at distal end; chamber shape moderately uniform in all rows across branch. Chamber longest dimension parallel to proximal and distal lateral chamber walls. Aperture positioned at distal to distal-abaxial end of chamber, connected to chamber by upper-end intermediate, highly variable length vestibule. Superior and inferior hemisepta both absent. Lateral-wall budding-angle of adaxial autozooecial

Table 43.—Summary numerical analysis of *Polypora varsoviensis* Prout, 1858a. For explanation of abbreviations of characters (left column), see Table 8b (foldout inside back cover).

	number of measurements	mean	standard deviation	coefficient of variation	observed range
1. **WB**	24	0.7590	0.2176	28.67	0.375–1.100
2. **DBC**	24	1.0550	0.2678	25.38	0.625–1.438
3. **WD**	24	0.3470	0.1171	33.75	0.238–0.650
4. **LF**	24	1.1900	0.1620	13.61	0.900–1.500
5. **WF**	24	0.4730	0.1390	29.39	0.238–0.713
6. **AF**	24	4.33	0.78	17.97	3–6
7. **AL**	24	0.1976	0.0115	5.82	0.180–0.220
8. **AW**	24	0.1676	0.0150	8.95	0.143–0.193
9. **ADB**	24	0.3757	0.0644	17.14	0.290–0.470
10. **AAB**	24	0.2743	0.0408	14.87	0.218–0.350
11. **ABB**	24	0.5163	0.1542	29.87	0.219–0.720
12. **DN**	24	0.1144	0.0341	29.81	0.070–0.140
14. **SNB**	24	1.0490	0.3017	28.76	0.680–1.630
18. **WP**	24	0.0458	0.0129	28.17	0.032–0.075
19. **SA**	24	20.67	2.64	12.77	17–26
20. **SAD**	24	0.0112	0.0021	18.75	0.008–0.015
21. **RSL**	24	0.2265	0.0754	33.29	0.106–0.350
22. **RSS**	24	0.0495	0.0130	26.26	0.032–0.080
23. **SSL**	24	1.3070	0.4500	34.43	0.575–2.020
24. **SSS**	24	0.1103	0.0319	28.92	0.078–0.180
32. **TRW**	24	0.0101	0.0013	12.87	0.009–0.013
33. **TLW**	24	0.0094	0.0014	14.89	0.008–0.013
34. **FWT**	24	0.0768	0.0356	46.35	0.029–0.143
35. **RWT**	24	0.0869	0.0503	58.01	0.029–0.197
36. **CL**	24	0.7788	0.0307	3.94	0.740–0.850
37. **CD**	24	0.1401	0.0141	10.06	0.118–0.168
38. **MAW**	24	0.1742	0.0229	13.15	0.140–0.215
39. **MIW**	24	0.1075	0.0268	24.93	0.082–0.160
40. **VD**	24	0.1102	0.0314	28.49	0.062–0.160
41. **RA**	24	20.92	2.27	10.86	17–25
42A. **LA-1**	24	10.42	4.62	44.38	1–20
42B. **LA-2**	24	40.58	15.14	37.31	33–50
43. **TB**	24	0.5892	0.0632	10.73	0.477–0.725

chambers highly variable (mean approximately 10°); lateral budding-angle of abaxial autozooecial chambers variable (mean about 41°); reverse-wall budding-angle of adaxial and abaxial chambers uniform, with a slightly variable angle (mean approximately 21°). Table 43 presents statistical criteria used in delimiting this species.

Exterior description.—Zoarium robust, expansion flat to rarely slightly obversely curved, fan-shaped; mesh spacing close; slight to intermediate astogenetic thickening of both obverse and reverse lamellar skeleton; zoarial pattern highly regular. Probable mature widths 30 to 40 mm; lengths 30 to 60 mm.

Branches robust; extremely wide, highly variable in width; typically straight, with lateral branches broadly curved toward edge of zoarium. Branch spacing close, distance between adjacent branch centers moderately irregular. Obverse surface texture smooth, exhibiting slight granular coarsening with astogeny; surface typically flat, less commonly slightly rounded. Single row of well-developed, upper-end intermediate size nodes; shape stellate, irregularly lobed; node size and shape variable; nodes projecting from middle of branch, one to more rarely two per fenestrule length; widely, unevenly spaced; node diameter increases slightly and nodes become less stellate due to partial covering by lamellar skeleton during astogeny. Reverse surface texture granular, coarsening with astogeny; bearing relatively few rows of widely spaced longitudinal striae which persist throughout astogenetic thickening of lamellar skeleton. Large microstylets, positioned atop longitudinal striae, spacing intermediate, variable in size, increasing slightly in diameter with astogeny. Extremely large macrostylets present, circular, irregularly circular to ovate in shape, highly variable in both size and shape; macrostylets typically located at branch–dissepiment junction, variably spaced, greatly increasing in size with astogeny. Autozooecia typically in four rows diagonally across branch, ranging from three to five rows; as many as six rows at sites of or for moderate distances proximal to sites of branch bifurcation and as few as two to three rows for short to moderate distances immediately distal to sites of branch bifurcation; branches exhibit pronounced thickening proximal, pronounced thinning distal to sites of branch bifurcation. Heterozooecia absent in all zoarial fragments analyzed.

Dissepiment width upper-end thin, slightly less than one-half branch width, width highly variable; length short, highly variable; connect branches at highly regular intervals. Dissepiments moderately barlike, exhibiting slight medial thinning and slight flaring at branch–dissepiment contact; highly recessed from obverse, approximately even with reverse surface. Slight astogenetic thickening of dissepiment. Obverse dissepiment surface with two to six longitudinal ridges emplaced perpendicular to branch length across dissepiment surface, ridges become partially to completely covered by lamellar skeleton with astogeny; reverse dissepiment surface with longitudinal striae oriented perpendicular to branch length, atop which occur rows of large microstylets; striae partially covered during astogenetic thickening of lamellar skeleton, microstylets increase slightly in diameter; obverse dissepiment surface texture smooth, reverse surface texture granular, both coarsening slightly with astogeny. Emplacement of dissepiments varying from perpendicular to as much as 20° from perpendicular to branch length. Apertures open on proximal or distal edge, or in middle of dissepiment edge at branch–dissepiment contact, commonly extending onto dissepiment for moderate to pronounced distances; arranged symmetrically or asymmetrically between branches.

Fenestrules large; shape elliptical to approaching

ovate on obverse, rectangular to elliptical on reverse surface, moderately to highly elongate proximodistally; moderately regular in size and shape; slightly expanding in width and length in obverse–reverse direction. Mean width of fenestrule five-eighths branch width; fenestrule opening exhibiting slight to moderate decrease in size during astogeny. Width to length ratio of fenestrule ranging from 1:6 to approximately 4:5, variable; mean ratio of width to length approximately 2:5, length of fenestrule much more constant than width. Three to six (most commonly four) apertures per fenestrule length; distance between closest aperture centers along branch 1.4 times spacing diagonally across branch, spacing across fenestrule 1.88 times spacing diagonally across branch; spacing along and diagonally across branch variable, spacing across fenestrule highly variable.

Autozooecial aperture size very large, shape irregularly ovate, enlarged on distal end, to approaching circular, elongate proximodistally to proximoabaxially; width to length ratio approximately 6:7, size highly uniform, shape moderately uniform; mid-branch apertures opening parallel to plane of obverse surface, adaxial apertures opening parallel to plane of obverse surface to slight angle toward fenestrule; upper-end intermediate size, well-developed complete peristome present. Seventeen to 26 (most commonly 20 to 21) extremely small stylets, moderately variable in size, poorly developed, surround aperture; stylets develop from lateral edge of peristome. Abaxial aperture margins extend into fenestrule, causing moderate inflections in fenestrule outline on obverse surface. Centrally thickened terminal diaphragms present, most frequently occurring troward proximal end of zoarium.

Zoarial supports extremely well-developed, occurring as extensions of reverse zoarial surface and lateral edge of zoarium.

Interior description.—Branches irregularly circular to irregularly ovate in transverse section, symmetrical to slightly elongate parallel to plane of zoarial surface; slightly to moderately enlarged on obverse surface. Branches thick, constant in depth.

Autozooecial living chamber size large, chambers arranged in three or more rarely four alternating rows along planar branch axial walls; axial walls zigzag diagonally across branch near reverse wall; becoming slightly sinuous to straight in mid chamber and near obverse surface; where sinuous, extending toward and connecting with chamber lateral walls. Chamber longest dimension parallel to proximal and distal lateral chamber walls. Autozooecial chamber outline irregularly ovate to rounded diamond in shape near reverse wall; becoming irregularly hexagonal to approaching irregularly rectangular in mid chamber and throughout most of chamber length; irregularly bilobate-ovate to elliptical near obverse surface, with inflection at mid abaxial chamber edge, enlarged at distal end; chamber shape moderately uniform, same in all rows of chambers across branch. Aperture positioned at distal to distal-abaxial end of chamber, connected to chamber by upper-end intermediate length, highly variable length vestibule. Ratio of autozooecial chamber minimum width to maximum width approximately 5:8; maximum width to depth ratio 5:4; depth to length ratio approximately 2:9; chamber length highly constant, depth and maximum width slightly variable, minimum width highly variable. Superior and inferior hemisepta both absent. Adaxial rows of autozooecial chambers diverge laterally from middle of branch at a highly variable angle (mean approximately 10°); abaxial rows of autozooecial chambers diverge laterally from middle of branch at variable angle (mean approximately 41°). Orientation of apertures to chamber varies between adaxial and abaxial rows of chambers; however, internal shape and dimensions of adaxial and abaxial chambers are the same. Autozooecial chambers diverge from reverse wall at a slightly variable angle (mean approximately 21°).

Three-dimensionally reconstructed chamber form a slightly polygonal tube; length, viewed from lateral edge of branch, substantially (approximately five times) greater than depth, viewed from distal end of branch; which is slightly less than width, viewed from obverse surface.

Internal granular layer thickness intermediate; granular skeletal layer well-developed, continuous with obverse nodes, peristomes, and apertural stylets; reverse longitudinal striae, macrostylets, and microstylets; across dissepiments and in the middle of zoarial supports. Outer lamellar layer thickness intermediate, exhibiting slight to intermediate astogenetic thickening.

Remarks.—*P. varsoviensis* was first described by Prout (1858a) for specimens found near Geode Glen (Warsaw Beds) near Warsaw, Illinois. Although slight variation does exist, specimens collected through the Warsaw closely resemble those described by Prout and Ulrich from the Warsaw Beds. Some similarities do exist between this species and *P. simulatrix* Ulrich, 1890 from the Keokuk Group; however, the latter has wider branches and considerably larger fenestrules.

The highly elongate chambers in *P. varsoviensis*, as observed in longitudinal view, readily distinguish it from *P. spininodata*, its closest ally in the Warsaw. Further characters which distinguish *P. varsoviensis* from *P. spininodata* are more numerous apertural stylets, smaller reverse-wall budding-angle, larger fenestrule openings, and narrower, thinner branches. Interior analyses are required for identification of this species.

Material studied.—Fourteen exterior fragments, five

Table 44.—Summary numerical analysis of *Polypora spininodata* Ulrich, 1890. For explanation of abbreviations of characters (left column), see Table 8b (foldout inside back cover).

	number of measurements	mean	standard deviation	coefficient of variation	observed range
1. WB	24	0.8522	0.1684	19.76	0.625–1.200
2. DBC	24	1.0200	0.1926	18.88	0.688–1.350
3. WD	24	0.2823	0.0569	20.16	0.213–0.388
4. LF	24	0.9150	0.1846	20.17	0.580–1.180
5. WF	24	0.4025	0.1146	28.47	0.250–0.630
6. AF	24	3.83	0.58	15.08	3–5
7. AL	24	0.2199	0.0150	6.82	0.198–0.250
8. AW	24	0.1636	0.0109	6.66	0.138–0.178
9. ADB	24	0.3769	0.0493	13.08	0.300–0.440
10. AAB	24	0.2913	0.0357	12.26	0.250–0.363
11. ABB	24	0.4788	0.0917	19.15	0.320–0.620
12. DN	24	0.1020	0.0238	23.33	0.055–0.140
14. SNB	24	0.4709	0.1378	29.26	0.313–0.730
18. WP	24	0.0263	0.0082	31.18	0.013–0.044
19. SA	24	12.67	2.06	16.26	9–15
21. RSL	24	0.2055	0.0393	19.12	0.150–0.281
22. RSS	24	0.0224	0.0048	21.43	0.015–0.030
23. SSL	24	1.0480	0.2141	20.43	0.730–1.400
24. SSS	24	0.0513	0.0137	26.71	0.036–0.075
32. TRW	24	0.0204	0.0057	27.94	0.013–0.031
33. TLW	24	0.0222	0.0027	12.16	0.018–0.026
34. FWT	24	0.1258	0.0556	44.20	0.036–0.235
35. RWT	24	0.1460	0.0480	32.88	0.075–0.250
36. CL	24	0.5358	0.0193	3.60	0.505–0.570
37. CD	24	0.1975	0.0189	9.57	0.165–0.230
38. MAW	24	0.1892	0.0180	9.51	0.155–0.210
39. MIW	24	0.1220	0.0230	16.64	0.088–0.158
40. VD	24	0.2807	0.0631	22.48	0.188–0.410
41. RA	24	41.58	4.59	11.04	34–53
42A. LA-1	24	7.25	3.31	45.66	2–12
42B. LA-2	24	30.50	4.07	16.63	22–40
43. TB	24	0.6408	0.1032	16.10	0.450–0.820

sectioned specimens; largest zoarial fragment 38 × 60 mm (width to length). Well-preserved due to robust nature of zoarium.

Occurrence.—Moderately abundant, occurring throughout the Warsaw in the study area; associated with both relatively high and low energy depositional environments.

Figured and/or measured specimens.—UI X-7022, 6907, 6918 (location 11, samples 51, 57), 6914 (location 47A, sample 32), 6910 (location 49B, samples 10, 14).

Polypora spininodata Ulrich, 1890
Plate 67, figures 7, 8, Plate 68, figures 1–12,
Plate 69, figures 1–7, 10; Table 44

Polypora spininodata Ulrich, 1890, p. 594, pl. 60, fig. 3 [Warsaw Beds: Warsaw, Illinois]; Keyes, 1894, p. 29 [Keokuk Limestone: Warsaw, Illinois]; Trizna, 1958, p. 173, pl. 48, dif. 2 [Kunwrak Vain: U. S. S. R.].

Diagnosis.—Zoarium extremely robust, mesh spacing very close, pattern moderately regular; branches robust, width extremely wide, thick in depth; branches straight, broadly curved at lateral zoarial edge; transversely irregularly elliptical, elliptical to approaching circular, spacing close; branches joined at highly regular intervals by thin, short dissepiments. Fenestrules large; shape elliptical to ovate, becoming polygonal on reverse surface with astogeny, moderately regular. Autozooecial apertures large, shape irregularly ovate, enlarged on distal end, to rarely approaching circular, elongate proximodistally to proximoabaxially, surrounded by intermediate-size, well-developed complete peristome; nine to 15 (most commonly 12 to 13) intermediate-size stylets surround aperture; three to five (most commonly four) apertures per fenestrule length. Intermediate-size, stellate, irregularly lobed nodes positioned in single row along branch midline. Autozooecial chambers large, emplaced in three or more rarely four alternating rows, except five to six rows at sites of or for moderate to pronounced distances proximal to sites of branch bifurcation, or two to three rows for short distances distal to sites of branch bifurcation; chamber outline irregularly ovate to rounded diamond near reverse wall; irregularly hexagonal to approaching irregularly rectangular in mid chamber; irregularly ovate, rarely elliptical near obverse surface, moderately enlarged at distal end; chamber shape moderately to highly uniform in all rows across branch. Chamber longest dimension parallel to proximal and distal lateral chamber walls. Aperture positioned at distal to distal-abaxial end of chamber, connected to chamber by long, moderately variable length vestibule. Superior and inferior hemisepta both absent. Lateral-wall budding-angle of adaxial autozooecial chambers highly variable (mean approximately 7°); lateral budding-angle of abaxial autozooecial chambers variable (mean about 31°); reverse-wall budding-angle of adaxial and abaxial chambers uniform, with a slightly variable angle (mean approximately 42°). Table 44 presents statistical criteria used in delimiting this species.

Exterior description.—Zoarium extremely robust, expansion typically flat, rarely slightly curved obversely or reversely, fan-shaped; mesh spacing very close; intermediate to pronounced astogenetic thickening of both obverse and reverse lamellar skeleton; zoarial pattern moderately regular. Probable mature widths 40 to 80 mm; lengths 60 to 110 mm.

Branches robust; width extremely wide, moderately variable in width; straight, lateral branches broadly curved toward edge of zoarium. Branch spacing close, distance between adjacent branch centers moderately regular. Obverse surface texture smooth, remaining smooth throughout astogeny; surface relatively flat to slightly rounded. Single row of well-developed, intermediate-size stellate nodes, irregularly lobed; node size moderately regular, shape variable; nodes projecting

from middle of branch at proximal edge of each or every other aperture forming straight to anastomosing rows, one to three nodes per fenestrule length; nodes intermediately, unevenly spaced, commonly located at or near sites of branch–dissepiment junction; node diameter slightly increasing with astogeny. Reverse surface texture slightly granular, coarsening with astogeny; bearing an intermediate number of moderately widely spaced longitudinal striae which become covered by lamellar skeleton during astogeny; macrostylets present, size large, shape irregularly ovate to diamond, moderately regular in size and shape, macrostylets positioned along reverse branch midline at or near branch–dissepiment junction, regularly spaced, increasing in size with astogeny. Autozooecia typically arranged in three or four rows diagonally across branch, except as many as five or six rows at site of or for moderate to pronounced distances proximal to sites of branch bifurcation and as few as two or three rows for short distances immediately distal to sites of branch bifurcation; branches exhibit pronounced thickening proximal, pronounced thinning distal to sites of branch bifurcation. Heterozooecia absent in all zoarial fragments analyzed.

Dissepiment width thin, approximately equal to one-third branch width, width slightly variable; length short, moderately constant; connect branches at highly regular intervals. Dissepiments moderately barlike, exhibiting slight flaring at branch–dissepiment contact and slight medial thinning; highly recessed from obverse, slightly recessed from reverse branch surface. Slight to moderate astogenetic thickening of dissepiment. Obverse dissepiment surface lacking ornamentation; reverse dissepiment surface with longitudinal striae oriented perpendicular to branch length across dissepiment surface, atop which occur rows of upper-end intermediate-size microstylets; microstylets and striae become covered by lamellar skeleton with astogeny; obverse dissepiment surface texture smooth, reverse surface texture granular, both coarsening with astogeny. Emplacement of dissepiment perpendicular to slight angle from perpendicular to branch length. Apertures open on proximal or distal edge, or in middle of dissepiment edge at branch–dissepiment contact, commonly extending onto dissepiment for pronounced distances; arranged symmetrically or asymmetrically between branches.

Fenestrules large; shape elliptical to ovate, becoming slightly polygonal on reverse surface with astogeny, moderately to highly elongate proximodistally; variable in size, moderately regular in shape; slightly to moderately expanding in width and length in obverse–reverse direction. Mean width of fenestrule slightly less than half branch width; fenestrule opening exhibiting moderate to pronounced decrease in size during astogeny. Width to length ratio of fenestrule ranging from 1: 4 to approximately 1:1, moderately regular; ratio of mean width to length approximately 4:9, length of fenestrule more constant than width. Three to five (most commonly four) apertures per fenestrule length; distance between closest aperture centers along branch 1.29 times spacing diagonally across branch, spacing across fenestrule 1.64 times spacing diagonally across branch; spacing along and across branch moderately variable, spacing across fenestrule highly variable.

Autozooecial aperture size large, shape irregularly ovate, slightly to moderately enlarged on distal end, to rarely approaching circular, elongate proximodistally to proximoabaxially; width to length ratio approximately 3:4, size and shape highly uniform; mid-branch apertures opening parallel to plane of obverse surface, adaxial apertures opening parallel to plane of obverse surface or at slight angle toward fenestrule; intermediate-size, well-developed complete peristome present. Nine to 14 (most commonly 12 to 13) intermediate and highly variably sized, well-developed, and regularly positioned stylets surround aperture; stylets develop as extensions of lateral edge of peristome. Abaxial aperture margins extend into fenestrule, causing moderate inflections in fenestrule outline on obverse surface. Centrally thickened terminal diaphragms present, commonly occurring throughout zoarium.

Zoarial supports well-developed, occurring as extensions of reverse zoarial surface and lateral edge of zoarium; most common toward proximal end of zoarium.

Interior description.—Branches irregularly elliptical, elliptical to approaching circular in transverse section, moderately to highly elongate parallel to plane of obverse surface; moderately enlarged on obverse surface. Branches thick, moderately variable in depth.

Autozooecial living chambers large, chambers arranged in three or more rarely four alternating rows along planar branch axial walls; axial walls zigzag diagonally across branch near reverse wall, forming lateral wall of chamber; becoming slightly sinuous to straight throughout mid chamber; returning to highly sinuous near obverse surface, extending toward and connecting with chamber lateral walls. Chamber longest dimension parallel to proximal and distal lateral chamber walls. Autozooecial chamber outline irregularly ovate to rounded diamond in shape near reverse wall; becoming irregularly hexagonal to approaching irregularly rectangular in mid chamber and throughout most of chamber length; irregularly ovate, rarely elliptical near obverse surface, moderately enlarged at distal end; chamber shape moderately to highly uniform, same in all rows of chambers across branch. Aperture positioned at distal to distal-abaxial end of chamber, connected to chamber by long, moderately variable length vestibule. Ratio of autozooecial chamber minimum

width to maximum width approximately 2:3; maximum width and depth approximately equal, depth slightly larger; depth to length ratio approximately 3:8; chamber length highly constant, depth and maximum width moderately constant, minimum width variable. Superior and inferior hemisepta both absent. Adaxial rows of autozooecial chambers diverge laterally from middle of branch at a highly variable angle (mean approximately 7°); abaxial rows of autozooecial chambers diverge laterally from middle of branch at variable angle (mean approximately 31°). Orientation of apertures to chamber varies slightly between adaxial and abaxial rows of chambers; however, internal chamber shape and dimensions of adaxial and abaxial chambers are the same. Adaxial and abaxial autozooecial chambers diverge from reverse wall uniformly, at a slightly variable angle (mean approximately 42°).

Three-dimensionally reconstructed chamber form a slightly polygonal tube; length, viewed from lateral edge of branch, moderately larger than depth and width, viewed from distal end of branch and obverse surface respectively, which are approximately equal.

Internal granular layer moderately thick; granular skeletal layer well-developed, continuous with obverse nodes, peristomes, and apertural stylets; reverse longitudinal striae, macrostylets, and microstylets; across dissepiments and in the middle of zoarial supports. Outer lamellar layer thick, exhibiting intermediate to pronounced astogenetic thickening.

Remarks.—Named by Ulrich (1890) from a reverse zoarial surface found in the "Warsaw Beds" near Warsaw, Illinois. Ulrich's concept was based on presence of large hollow nodes across the reverse surface. Interior analysis demonstrates the nodes are solid granular skeletal material, rather than hollow. Ulrich considered *P. spininodata* intermediate between *P. biseriata* and *P. varsoviensis*; I have assigned *P. biseriata* to *Banastella* (see comments under that genus).

Polypora spininodata is readily distinguished from *P. varsoviensis*, the most similar species, by having fewer apertural stylets, much larger reverse-wall budding-angle, much shorter but slightly deeper and wider autozooecial chambers, smaller fenestrule openings and wider, thicker branches. It is quite probable that these two species have been confused in the past, as longitudinal sections (not used as standard in earlier taxonomic analyses) are essential in differentiating them.

Material studied.—Fifteen exterior fragments, nine sectioned specimens; largest zoarial fragment 32 × 38 mm (width to length). Well-preserved due to the extremely robust nature of zoarium.

Occurrence.—Moderately common, occurring throughout the northern Warsaw study area, not observed in southern localities; associated with relatively high and low energy depositional environments.

Syntype.—ISGS(ISM) 2786.

Figured and/or measured specimens.—UI X-6921, 7017–7020 (location 11, samples 57, 59), 6911–6913, 6888 (location 10, samples 35, 43).

Polypora simulatrix Ulrich, 1890
Plate 69, figures 8, 9, Plate 70, figures 1–12,
Plate 71, figures 1–4; Table 45

Polypora simulatrix Ulrich, 1890, p. 589, pl. 59, figs. 4–4b [Keokuk Group: Henderson Country, Nauvoo and Warsaw, Illinois; Keokuk and Bentonsport, Iowa]; Keyes, 1894, p. 28 [Keokuk Limestone: Keokuk, Iowa].

Diagnosis.—Zoarium moderately robust, mesh spacing close, pattern moderately to highly irregular; branch robustness intermediate to robust; branches wide, thick in depth; branches straight, broadly curved at lateral zoarial edge; transversely irregularly ovate to approaching circular, spacing close; branches joined at moderately irregular intervals by thin, short dissepiments. Fenestrules extremely large; shape elliptical to approaching rectangular, moderately variable. Autozooecial apertures large, shape irregularly ovate to approaching circular, elongate proximodistally to proximoabaxially, surrounded by low and wide, well-developed complete peristome; 24 to 36 (most commonly 30 to 32) intermediate-size apertural stylets surround aperture; four to seven (most commonly five or six) apertures per fenestrule. Large, stellate nodes, irregularly lobed, positioned in single row along branch midline. Autozooecial chambers moderately large, emplaced in three or four alternating rows, except as many as six or seven rows at sites of or for moderate to pronounced distances proximal to sites of branch bifurcation, and two or three rows for short to moderate distances distal to sites of branch bifurcation; chamber outline irregularly ovate to irregularly polygonal near reverse wall; elliptical to irregularly rectangular in mid chamber and throughout most of chamber length; irregularly bilobate-ovate to elliptical near obverse surface, enlarged at distal end; chamber shape moderately uniform in all rows across branch. Chamber longest dimension parallel to proximal and distal lateral chamber walls. Aperture positioned at distal to distal-abaxial end of chamber, connected to chamber by upper-end intermediate, highly variable length vestibule. Superior and inferior hemisepta both absent. Lateral-wall budding-angle of adaxial autozooecial chambers highly variable (mean approximately 9°); lateral budding-angle of abaxial autozooecial chambers variable (mean about 47°); reverse-wall budding-angle of adaxial and abaxial chambers uniform, with a slightly variable angle (mean approximately 18°). Table 45 presents statistical criteria used in delimiting this species.

Exterior description.—Zoarium moderately robust, expansion flat to rarely slightly obversely curved, fan-

shaped; mesh spacing close; slight to intermediate astogenetic thickening of both obverse and reverse lamellar skeleton; zoarial pattern moderately to highly irregular. Probable mature widths 30 to 40 mm; lengths 60 to 80 mm.

Branch robustness intermediate to robust; branches wide, highly variable in width; straight, lateral branches broadly curved toward edge of zoarium. Branch spacing close, distance between adjacent branch centers highly irregular. Obverse surface texture smooth, exhibiting slight granular coarsening with astogeny; surface typically slightly rounded, less commonly flat. Single row of well-developed, large nodes present, shape stellate, irregularly lobed; node size moderately regular, shape variable; nodes projecting from middle of branch, one to three (most commonly two) per fenestrule length; widely, moderately unevenly spaced; node diameter increases slightly and nodes become less stellate due to partial covering by lamellar skeleton during astogeny. Rows of large stylets, highly variably sized and variably positioned, occurring between and anastomosing around apertures along obverse branch surface; at low magnifications stylets appear as solid rows extending along surface; stylets increase in size and number with astogeny. Reverse surface texture granular, coarsening with astogeny; bearing an intermediate number of rows of moderately closely spaced longitudinal striae which persist throughout astogenetic thickening of lamellar skeleton. Large microstylets, positioned atop longitudinal striae, closely spaced, highly variable in size, increasing in diameter with astogeny. Autozooecia typically arranged in three to five (most commonly four) rows diagonally across branch; as many as six or seven rows at sites of or for moderate to pronounced distances proximal to sites of branch bifurcation, as few as two or three rows for short to moderate distances immediately distal to sites of branch bifurcation; branches exhibit pronounced thickening proximal, pronounced thinning distal to sites of branch bifurcation. Heterozooecia absent in all zoarial fragments analyzed.

Dissepiment width thin, approximately two-fifths branch width, width highly constant; length short, highly variable; connect branches at moderately irregular intervals. Dissepiments barlike, exhibiting slight flaring at branch–dissepiment contact; highly recessed from obverse, approximately even with reverse surface. Astogenetic thickening of dissepiment slight to lacking. Obverse dissepiment surface with two to six, typically four longitudinal ridges emplaced perpendicular to branch length across dissepiment surface, ridges become partially covered by lamellar skeleton with astogeny; reverse dissepiment surface with longitudinal striae oriented perpendicular to branch length, atop which occur rows of large microstylets; striae partially

Table 45.—Summary numerical analysis of *Polypora simulatrix* Ulrich, 1890. For explanation of abbreviations of characters (left column), see Table 8b (foldout inside back cover).

	number of measurements	*mean*	*standard deviation*	*coefficient of variation*	*observed range*
1. **WB**	24	1.1930	0.2130	26.24	0.750–1.750
2. **DBC**	24	1.4970	0.4450	29.73	0.880–2.250
3. **WD**	24	0.4750	0.0510	10.74	0.425–0.575
4. **LF**	24	2.7400	0.7080	25.84	1.670–3.900
5. **WF**	24	0.6800	0.2080	30.59	0.307–1.100
6. **AF**	24	5.75	0.87	18.06	4–7
7. **AL**	24	0.2480	0.0098	3.95	0.233–0.267
8. **AW**	24	0.1740	0.0143	8.22	0.157–0.203
9. **ADB**	24	0.5490	0.0923	16.81	0.420–0.693
10. **AAB**	24	0.3510	0.0574	16.35	0.247–0.480
11. **ABB**	24	0.7760	0.2221	28.62	0.367–1.150
12. **DN**	24	0.1940	0.0374	19.28	0.110–0.250
14. **SNB**	24	1.5870	0.4172	26.29	0.975–2.400
16. **DSO**	24	0.0491	0.0154	31.36	0.032–0.087
17. **SSO**	24	0.0816	0.0192	23.53	0.050–0.108
18. **WP**	24	0.0578	0.0076	13.15	0.045–0.073
19. **SA**	24	30.50	3.40	11.14	24–36
20. **SAD**	24	0.0223	0.0066	29.60	0.013–0.037
22. **RSS**	24	0.0284	0.0117	41.20	0.014–0.055
24. **SSS**	24	0.0498	0.0194	38.96	0.020–0.087
32. **TRW**	24	0.0143	0.0027	18.88	0.011–0.020
33. **TLW**	24	0.0185	0.0048	25.95	0.012–0.028
34. **FWT**	24	0.1693	0.0597	35.26	0.085–0.285
35. **RWT**	24	0.1925	0.0992	51.53	0.042–0.528
36. **CL**	24	0.7913	0.0401	5.07	0.725–0.875
37. **CD**	24	0.1671	0.0111	6.64	0.148–0.188
38. **MAW**	24	0.1697	0.0196	11.55	0.138–0.200
40. **VD**	24	0.1153	0.0320	27.75	0.069–0.175
41. **RA**	24	18.17	1.95	10.71	15–21
42A. **LA-1**	24	9.25	3.98	43.03	3–17
42B. **LA-2**	24	47.33	10.03	21.19	36–68
43. **TB**	24	0.7340	0.1120	15.26	0.580–0.950

covered during astogenetic thickening of lamellar skeleton, microstylets increase slightly in diameter; obverse dissepiment surface texture smooth, reverse surface texture granular, both coarsening with astogeny. Emplacement of dissepiments varying from perpendicular to as much as 50° from perpendicular to branch length. Apertures open on proximal or distal edge, or in middle of dissepiment edge at branch–dissepiment contact; arranged symmetrically or asymmetrically between branches.

Fenestrules extremely large; shape elliptical to approaching rectangular on both obverse and reverse surfaces, highly elongate proximodistally; moderately variable in size and shape; very slight expansion in width and length in obverse–reverse direction. Mean width of fenestrule four-sevenths branch width; fenestrule opening exhibiting slight decrease in size during astogeny. Width to length ratio of fenestrule ranging from 1:10 to approximately 2:3, highly variable; mean

ratio of width to length approximately 1:4, length of fenestrule slightly more constant than width. Four to seven (most commonly five to six) apertures per fenestrule length; distance between closest aperture centers along branch approximately 1.6 times spacing diagonally across branch, spacing across fenestrule 2.2 times spacing diagonally across branch; spacing along and diagonally across branch variable, spacing across fenestrule highly variable.

Autozooecial aperture size large, shape irregularly ovate, enlarged on distal end, to approaching circular, elongate proximodistally to proximoabaxially; width to length ratio approximately 7:10, size highly uniform, shape moderately uniform; mid-branch apertures opening parallel to plane of obverse surface, adaxial apertures opening parallel to plane of obverse surface or at slight angle toward fenestrule; lower-end wide, well-developed, complete peristome present. Twenty-four to 36 (most commonly 30 to 32) intermediate-size stylets, regularly sized and well-developed, surround aperture; stylets develop from lateral edge of peristome. Abaxial aperture margins extend slightly into fenestrule, causing slight inflections in fenestrule outline on obverse surface. Centrally thickened terminal diaphragms present throughout zoarium.

Zoarial supports extremely well-developed, occurring as extensions of reverse zoarial surface and lateral edge of zoarium.

Interior description.—Branches irregularly ovate to approaching circular in transverse section, slightly elongate parallel to plane of obverse surface; slightly enlarged on obverse surface. Branches thick, slightly variable in depth.

Autozooecial living chamber size moderately large, chambers emplaced in three or four alternating rows along planar branch axial walls; axial walls irregularly zigzag diagonally across branch near reverse wall; becoming straight to slightly sinuous in mid chamber and near obverse surface; where sinuous, extending toward and connecting with chamber lateral walls. Chamber longest dimension parallel to proximal and distal lateral chamber walls. Autozooecial chamber outline irregularly ovate to irregularly rectangular in mid chamber and throughout most of chamber length; irregularly bilobate-ovate to elliptical near obverse surface, with inflection at mid abaxial chamber edge, enlarged at distal end; chamber shape moderately uniform, same in all rows of chambers across branch. Aperture positioned at distal to distal-abaxial end of chamber, connected to chamber by upper-end intermediate length, highly variable length vestibule. Autozooecial chamber width and depth approximately equal; ratio of chamber width to length approximately 2:9; chamber length and depth both highly constant, width slightly variable. Superior and inferior hemisepta both absent. Adaxial rows of autozooecial chambers diverge laterally from middle of branch at a highly variable angle (mean approximately 9°); abaxial rows of autozooecial chambers diverge laterally from middle of branch at variable angle (mean approximately 47°). Orientation of apertures to chamber varies between adaxial and abaxial rows of chamber; however, internal chamber shape and dimensions of adaxial and abaxial chambers are approximately the same. Autozooecial chambers diverge from reverse wall at a slightly variable angle (mean approximately 18°).

Three-dimensionally reconstructed chamber forms a slightly polygonal tube; length, viewed from lateral edge of branch, substantially greater than depth and width, viewed from distal end of branch and obverse surface respectively, both of which are essentially equal.

Internal granular layer thin to lower-end intermediate in thickness; granular skeletal layer well-developed, continuous with obverse nodes, stylets, peristomes and apertural stylets; reverse longitudinal striae and microstylets; across dissepiments and in the middle of zoarial supports. Outer lamellar layer thickness intermediate, exhibiting slight to intermediate astogenetic thickening.

Remarks.—*P. simulatrix* was described by Ulrich (1890) for "Keokuk Group" materials found at Nauvoo and Warsaw, Illinois and Keokuk and Bentonsport, Iowa. Ulrich noted close similarities between this species and *P. maccoyana*, but separated the two on the basis of the more robust nature of *P. maccoyana*.

Of the polyporids analyzed here, *P. simulatrix* most closely resembles *P. gracilis* in general chamber shape, size of fenestrule opening, branch spacing, and number and spacing of nodes. *P. simulatrix* is distinguished by having greater chamber length and smaller depth and width, much smaller reverse-wall budding-angle, wider and thicker branches, more numerous apertural stylets, substantially larger aperture openings, and wider spacing of apertures along, across, and between branches. The two species cannot be readily distinguished on external morphology.

Material studied.—Eight exterior fragments, two sectioned specimen; largest zoarial fragment 14 × 36 mm (width to length). Relatively thin nature of internal granular skeleton results in crushing of many zoarial fragments.

Occurrence.—Found throughout Warsaw study area, however forming an extremely minor component of Warsaw fauna. Most commonly associated with argillaceous and calcilutite microfacies, presumably deposited in relatively low-energy environments.

Figured and/or measured specimens.—UI X-6922, 6923 (location 11, sample 60).

Polypora retrorsa Ulrich, 1890
Plate 71, figures 5–9, Plate 72, figures 1–8; Table 46

Polypora retrorsa Ulrich, 1890, p. 591, pl. 59, figs. 6–6d [Keokuk Group: Keokuk, Iowa]; Keyes, 1894, p. 29 [Keokuk Limestone: Keokuk, Iowa].

Diagnosis.—Zoarium robust, mesh spacing close, pattern moderately to highly regular; branches robust, wide, thick in depth; straight to slightly sinuous, curved toward sites of dissepiment emplacement, broadly curved at lateral zoarial edge; transversely irregularly elliptical, ovate to approaching circular, spacing close; branches joined at highly regular intervals by intermediate-width, extremely short dissepiments. Fenestrule size intermediate; shape ovate to approaching elliptical on obverse, ovate on reverse, becoming circular with astogeny, regular. Autozooecial aperture size upper-end intermediate, shape irregularly ovate, pointed at distal end, to approaching circular, elongate proximodistally to rarely proximoabaxially, surrounded by thin, well-developed incomplete peristome open at proximal edge to rarely at proximal-abaxial edge; six to nine (most commonly seven to eight) intermediate-size stylets surround aperture; three to six (most commonly four) apertures per fenestrule length. Moderately large stylets irregularly positioned across obverse surface. Autozooecial living chambers large, emplaced in three or four alternating rows, except five or six rows at sites of branch bifurcation or for moderate distances proximal to sites of branch bifurcation, or two or three rows for short to moderate distances distal to sites of branch bifurcation; chamber outline irregularly ovate to circular near reverse wall and throughout chamber length; more symmetrically ovate to circular near obverse surface; chamber shape moderately uniform in all rows across branch. Chamber longest dimension parallel to proximal and distal lateral chamber walls. Aperture typically positioned at distal, less commonly distal-abaxial end of chamber, connected to chamber by long, highly variable length vestibule. Superior and inferior hemisepta both absent. Lateral-wall budding-angle of adaxial autozooecial chambers highly variable (mean approximately 7°); lateral budding-angle of abaxial autozooecial chambers variable (mean approximately 25°); reverse-wall budding-angle of adaxial and abaxial chambers uniform, with a constant angle (mean approximately 77°). Table 46 presents statistical criteria used in delimiting this species.

Exterior description.—Zoarium robust, expansion flat to obversely cup-shaped, fan-shaped; mesh spacing close; moderate to pronounced astogenetic thickening of both obverse and reverse lamellar skeleton; zoarial pattern moderately to highly regular. Probable mature widths 20 to 40 mm; lengths 20 to 60 mm.

Branches robust, wide, moderately variable in width; straight to slightly sinuous, curved toward sites of dissepiment emplacement, lateral branches broadly curved toward edge of zoarium. Branch spacing close, distance between adjacent branch centers moderately regular. Obverse surface texture granular, coarsening with astogeny; surface typically slightly rounded to less commonly flat. Moderately large stylets, variable in size and irregularly positioned across obverse branch surface, stylet diameter increasing slightly to moderately with astogeny. Reverse surface texture granular, coarsening with astogeny; bearing few rows of widely spaced longitudinal striae which become covered by lamellar skeleton during astogeny. Intermediate-size microstylets develop as extensions of striae; microstylets closely and irregularly spaced, variable in size, slightly to moderately increasing in diameter with astogeny. Autozooecia typically in three or four rows diagonally across branch; except as many as five or six rows at sites of branch bifurcation or for moderate distances proximal to sites of branch bifurcation and as few as two or three rows for short to moderate distances immediately distal to sites of branch bifurcation; branch-

Table 46.—Summary numerical analysis of *Polypora retrorsa* Ulrich, 1890. For explanation of abbreviations of characters (left column), see Table 8b (foldout inside back cover).

	number of measurements	*mean*	*standard deviation*	*coefficient of variation*	*observed range*
1. **WB**	24	0.5165	0.1050	20.35	0.325–0.675
2. **DBC**	24	0.7768	0.1352	17.40	0.490–0.950
3. **WD**	24	0.4178	0.0546	13.07	0.333–0.500
4. **LF**	24	0.6578	0.0826	12.56	0.505–0.820
5. **WF**	24	0.2941	0.0426	14.48	0.225–0.375
6. **AF**	24	3.67	1.43	39.10	3–6
7. **AL**	24	0.1348	0.0101	7.49	0.112–0.150
8. **AW**	24	0.1245	0.0103	8.27	0.108–0.138
9. **ADB**	24	0.2330	0.0203	8.71	0.198–0.265
10. **AAB**	24	0.1902	0.0199	10.46	0.145–0.222
11. **ABB**	24	0.3661	0.0716	19.56	0.288–0.480
16. **DSO**	24	0.0103	0.0027	26.21	0.006–0.015
17. **SSO**	24	0.0213	0.0049	23.00	0.013–0.030
18. **WP**	24	0.0178	0.0027	15.17	0.014–0.024
19. **SA**	24	7.75	0.97	12.46	6–9
20. **SAD**	24	0.0396	0.0103	26.01	0.028–0.063
22. **RSS**	24	0.0204	0.0053	25.98	0.013–0.031
24. **SSS**	24	0.0382	0.0106	27.75	0.024–0.060
32. **TRW**	24	0.0466	0.0105	22.53	0.031–0.066
33. **TLW**	24	0.0494	0.0171	34.62	0.023–0.082
34. **FWT**	24	0.1480	0.0495	33.45	0.075–0.250
35. **RWT**	24	0.2765	0.1194	43.18	0.125–0.525
36. **CL**	24	0.6953	0.0330	4.75	0.620–0.750
37. **CD**	24	0.3357	0.0334	9.95	0.285–0.400
38. **MAW**	24	0.1275	0.0107	8.39	0.108–0.145
40. **VD**	24	0.1452	0.0467	32.16	0.088–0.240
41. **RA**	24	76.75	5.33	6.94	68–87
42A. **LA-1**	24	6.67	3.17	47.56	2–12
42B. **LA-2**	24	24.75	5.59	22.60	17–34
43. **TB**	24	0.8132	0.1500	18.45	0.575–1.150

es exhibit moderate thickening proximal, moderate to pronounced thinning distal to sites of branch bifurcation. Heterozooecia absent in all zoarial fragments analyzed.

Dissepiment width intermediate, approximately four-fifths branch width, width constant; length extremely short, constant; connect branches at highly regular intervals. Dissepiments exhibit moderate medial thinning, pronounced flaring at branch–dissepiment contact; slightly recessed from obverse, even with reverse surface. Moderate to pronounced astogenetic thickening of dissepiment. Obverse dissepiment surface with moderately large stylets irregularly positioned across dissepiment surface, stylet diameter increasing slightly to moderately with astogeny; reverse dissepiment surface with longitudinal striae oriented perpendicular to branch length, atop which occur rows of large microstylets; striae covered by lamellar skeleton during astogenetic thickening, microstylets increase slightly in diameter with astogeny; obverse and reverse surface textures granular, both coarsening with astogeny. Emplacement of dissepiments varying from perpendicular to a slight angle from perpendicular to branch length. Apertures open onto dissepiment proximal or distal edge, or in middle of dissepiment edge at branch–dissepiment junction for moderate to pronounced distances frequently with two autozooecia opening onto dissepiment edge; arranged symmetrically or asymmetrically between branches.

Fenestrule size intermediate; shape ovate to approaching elliptical on obverse; initially ovate on reverse, becoming circular with astogeny; fenestrule slightly to moderately elongate proximodistally; regular in size and shape; moderately expanding in width and length in obverse–reverse direction. Mean width of fenestrule four-sevenths branch width; fenestrule opening exhibiting pronounced decrease in size during astogeny. Width to length ratio ranging from 3:4 to approximately 1:4, moderately constant; mean ratio of width to length approximately 4:9, length and width of fenestrule both constant. Three to six (most commonly four) apertures per fenestrule length; distance between closest aperture centers along branch 1.23 times spacing diagonally across branch, spacing across fenestrule 1.93 times spacing diagonally across branch; spacing along branch moderately constant, spacing diagonally across branch slightly variable, spacing across fenestrule highly variable.

Autozooecial aperture size upper-end intermediate, shape irregularly ovate, pointed at distal end and elongate proximodistally to rarely proximoabaxially, less frequently approaching circular; width to length ratio approximately 11:12, size uniform, shape moderately uniform; mid-branch apertures open parallel to plane of obverse surface, adaxial apertures typically open at slight angle toward fenestrule, less frequently parallel to plane of obverse surface; thin, well-developed incomplete peristome present, open at proximal to more rarely proximal–abaxial edge. Six to nine (most commonly seven to eight) intermediate-size stylets, variable in size and well-developed, surround aperture; stylets develop from lateral edge of peristome. Abaxial aperture margins extend slightly into fenestrule, causing slight inflections in fenestrule outline on obverse surface. Centrally thickened terminal diaphragms present, occurring throughout the zoarium.

Zoarial supports absent in all zoarial fragments analyzed.

Interior description.—Branches irregularly elliptical, ovate to approaching circular in transverse section, slightly to highly elongate parallel to plane of zoarial surface; enlarged on obverse surface. Branches thick, slightly variable in depth.

Autozooecial living chambers large, arranged in three or four alternating rows along planar branch axial walls; axial walls highly sinuous near branch reverse wall; slightly sinuous in mid and throughout most of chamber length; approaching straight near obverse surface; where sinuous, axial walls extend toward and connect with chamber lateral walls. Autozooecial chamber outline irregularly ovate to circular near reverse wall and throughout most of chamber length; becoming more symmetrically ovate to circular near obverse surface; chamber shape moderately uniform in all rows of chambers across branch. Aperture typically positioned at distal, less commonly distal–abaxial end of chamber, connected to chamber by long, highly variable length vestibule. Ratio of autozooecial chamber width to depth approximately 3:8; depth to length ratio slightly less than 1:2; chamber length highly constant, depth and width moderately constant. Superior and inferior hemisepta both absent. Adaxial rows of autozooecial chambers diverge laterally from middle of branch at a highly variable angle (mean approximately 7°); abaxial rows of autozooecial chambers diverge from middle of branch at variable angle (mean approximately 25°). Although orientation of apertures varies between adaxial and abaxial rows of chambers, internal chamber shape and dimensions of adaxial and abaxial chambers are the same. Autozooecial chambers diverge from reverse wall at a constant angle (mean approximately 77°).

Three-dimensionally reconstructed chamber form an irregular tube; length, viewed from lateral edge of branch, over twice depth, viewed from distal end of branch; which in turn is slightly less than three times width, viewed from obverse surface.

Internal granular layer thick; granular skeletal layer poorly developed, continuous with obverse stylets, peristomes and apertural stylets; reverse longitudinal

striae and microstylets; and across dissepiments. Outer lamellar layer thick, exhibiting pronounced astogenetic thickening.

Remarks.—*P. retrorsa* was described by Ulrich (1890) from the Keokuk Group at Keokuk, Iowa. Although none of Ulrich's originally described materials were available, his description of "distinct granules and rounded fenestrules of the reverse, and the unequally developed peristome" (p. 591) are quite diagnostic.

This species is readily distinguished from other polyporids by its much more granular nature, incomplete peristome, high reverse-wall budding-angle, small number of apertural stylets, and closer mesh spacing.

Material studied.—Seven exterior fragments, two sectioned specimens; largest zoarial fragment 14 × 22 mm (width to length). Extremely poorly preserved in all samples analyzed.

Occurrence.—Rare; occurrence restricted to southern half of study area. Found almost exclusively in low-energy environments.

Figured and/or measured specimens.—UI X-6908, 6909 (location 49B, sample 17).

CHANGING DISTRIBUTION OF MESHWORK FENESTRATE SPECIES THROUGHOUT THE WARSAW STUDY AREA

This narrow stratigraphic interval yielded geographic rather than stratigraphic variations in species occurrence and community composition. The twenty-three measured sections used to determine distribution of meshwork fenestrate species are shown in Text-figure 19.

Although complete Warsaw sections are rare, the lower conformable contact between the Keokuk and Warsaw is typically well-preserved, with the Warsaw consisting of 20 to 40 ft (6.1 to 12.3 m) of calcareous or argillaceous shale, typically containing either geodes or fossiliferous calcareous interbeds. Because the upper Warsaw was absent in most sections, and because abundant and diverse bryozoan assemblages are present in the lower Warsaw, the lower Warsaw was used almost exclusively in determining geographic species distribution patterns.

A total of 37 meshwork fenestrate species was found in the Warsaw (see Table 47). In each stratigraphic section, fossiliferous slabs and loose shale samples were collected and scanned for specimen exteriors using a binocular microscope. Acetate peels were prepared where exteriors were inadequate for identification. Relative occurrence was recorded for each sample, recording whether species were rare (**R**), with one to three zoarial fragments present; common (**C**), with four to 10 zoarial fragments present; or abundant (**A**), with greater than 10 zoarial fragments. One cm^2 grid overlays were used on slab surfaces, with species counted at line intersections. Between 50 and 100 counts were made for each horizon analyzed. Averaged data for all 37 species are compiled in Table 48, with most typical abundances shown for each section.

Table 47.—Occurrence of meshwork fenestrate species throughout the Warsaw study area. Areas of occurrence are shown to the left of the species name and number by the symbol ▲ for those exclusively found in the northern part of the study area, ■ for those exclusively found in the southern part of the study area, and ● for species occurring throughout the study area. Numbers assigned to species are used consistently throughout the text.

Family Fenestellidae King, 1849	
●1.	*Rectifenestella tenax* (Ulrich, 1888)
■2.	*Rectifenestella tenuissima* (Cumings, 1906)
●3.	*Rectifenestella multispinosa* (Ulrich, 1890)
●4.	*Laxifenestella coniunctistyla,* n. sp.
●5.	*Laxifenestella maculasimilis,* n. sp.
●6.	*Laxifenestella serratula* (Ulrich, 1890)
■7.	*Laxifenestella fluctuata,* n. sp.
■8.	*Minilya sivonella,* n. sp.
●9.	*Minilya paratriserialis,* n. sp.
■10.	*Exfenestella exigua* (Ulrich, 1890)
■11.	*Banastella guensburgi,* n. sp.
●12.	*Banastella cingulata* (Ulrich, 1890)
●13.	*Banastella mediocreforma,* n. sp.
▲14.	*Banastella limitaris* (Ulrich, 1890)
▲15.	*Banastella biseriata* (Ulrich, 1890)
●16.	*Banastella delicata,* n. sp.
●17.	*Cubifenestella rudis* (Ulrich, 1890)
●18.	*Cubifenestella usitata,* n. sp.
●19.	*Cubifenestella globodensata,* n. sp.
●20.	*Apertostella foramenmajor,* n. sp.
▲21.	*Apertostella crassata,* n. sp.
▲22.	*Apertostella venusta,* n. sp.
●23.	*Hemitrypa perstriata* Ulrich, 1890
●24.	*Hemitrypa hemitrypa* (Prout, 1859)
■25.	*Hemitrypa aprilae,* n. sp.
●26.	*Hemitrypa aspera* Ulrich, 1890
●27.	*Hemitrypa vermifera* (Ulrich, 1890)
▲28.	*Archimedes negligens* Ulrich, 1890
▲29.	*Archimedes owenanus* (Hall, 1857b)
▲30.	*Archimedes wortheni* (Hall, 1857b)
■31.	*Archimedes valmeyeri,* n. sp.
Family Polyporidae Vine, 1884	
▲32.	*Fenestralia sanctiludovici* Prout, 1858a
■33.	*Polypora gracilis* Prout, 1860
●34.	*Polypora varsoviensis* Prout, 1858a
●35.	*Polypora spininodata* Ulrich, 1890
●36.	*Polypora simulatrix* Ulrich, 1890
■37.	*Polypora retrorsa* Ulrich, 1890

Twenty species recognized were found to range throughout the lower Warsaw. These include *Rectifenestella tenax*, *Rectifenestella multispinosa*, *Laxifenestella coniunctistyla*, *Laxifenestella maculasimilis*, *Laxifenestella serratula*, *Minilya paratriserialis*, *Banastella cingulata*, *Banastella mediocreforma*, *Banastella delicata*, *Cubifenestella rudis*, *Cubifenestella usitata*, *Cubifenestella globodensata*, *Apertostella foramenmajor*, *Hemitrypa perstriata*, *Hemitrypa hemitrypa*, *Hemitrypa aspera*, *Hemitrypa vermifera*, *Polypora varsoviensis*, *Polypora spininodata*, and *Po-*

Text-figure 19.—The 23 measured sections used to determine species distribution.

Table 48.—Abundance of species of Warsaw Formation meshwork fenestrate bryozoans at each locality. R = rare (<2 specimens per sample horizon); C = common (2–8); A = abundant (>8); ? = questionable occurrence due to preservation; – = not present.

	(1) *Bentonsport, Iowa*	(2) *Iowa Terminal, Iowa*	(3) *Keokuk Industrial, Iowa*	(4) *White Hollow, Iowa*	(5) *Grays Quarry, Illinois*	(6) *Hamilton-Warsaw Roadcut, Illinois*	(7) *Geode Glen, Illinois*	(8) *Soap Factory Hollow, Illinois*	(9) *Buel Branch, Illinois*	(10) *Sand Branch, Illinois*	(11) *La Grange, Missouri*	(12) *Mount Sterling, Illinois*	(13) *McKee Creek, Illinois*	(14) *Versailles West, Illinois*	(15) *Little Whitaker Creek, Illinois*	(16) *White Hall-C, Illinois*	(17) *White Hall-D, Illinois*	(18) *White Hall-F, Illinois*	(19) *Otter Branch, Illinois*	(20) *Troy Roadcut, Missouri*	(21) *Cragwold Road, Missouri*	(22) *Columbia Roadcut, Illinois*	(23) *Dennis Hollow, (Valmeyer), Illinois*
14. *Banastella limitaris*	–	R	C	C	–	R	C	C	R	–	–	–	–	–	–	–	–	–	–	–	–	–	–
22. *Apertostella venusta*	–	C	R	C	–	C	C	–	R	–	–	–	–	–	–	–	–	–	–	–	–	–	–
28. *Archimedes negligens*	R	–	R	R	–	A	–	C	R	–	–	–	–	–	–	–	–	–	–	–	–	–	–
15. *Banastella biseriata*	–	R	C	C	–	C	R	C	R	–	R	–	–	–	–	–	–	–	–	–	–	–	–
29. *Archimedes owenanus*	C	R	C	C	R	A	–	C	C	–	–	R	C	R	–	–	–	–	–	–	–	–	–
32. *Fenestralia sanctiludovici*	–	–	–	–	–	–	C	–	R	–	R	A	–	–	–	–	R	–	–	–	–	–	–
30. *Archimedes wortheni*	–	–	–	–	–	–	A	–	–	C	–	C	R	–	–	C	–	R	–	–	–	–	–
21. *Apertostella crassata*	C	–	C	C	R	A	–	C	C	R	–	A	R	–	–	–	C	R	R	C	–	–	–
35. *Polypora spininodata*	C	–	–	R	–	C	A	C	–	–	C	C	R	–	–	–	–	C	–	R	–	R	C
26. *Hemitrypa aspera*	–	R	R	C	–	C	–	R	C	R	–	–	–	R?	–	–	–	C	–	–	C	R	R
3. *Rectifenestella multispinosa*	C	C	A	C	–	A	A	A	A	R	C	A	C	R	R	–	C	–	C	C	C	C	A
4. *Laxifenestella coniunctistyla*	C	C	R	C	–	A	C	A	C	C	R	A	–	C	–	C	C	C	C	R	C	–	C
6. *Laxifenestella serratula*	C	C	C	R	–	C	C	C	C	A	–	C	C	C	C	C	C	C	A	R	C	C	C
19. *Cubifenestella globodensata*	R	–	C	R	–	–	–	–	–	–	–	R	–	R	–	R	C	R	C	R	R	C	C
23. *Hemitrypa perstriata*	C	C	C	C	C	A	C	A	A	C	C	A	C	C	C	C	C	C	C	A	C	–	A
24. *Hemitrypa hemitrypa*	R	C	A	C	R	A	C	C	R	A	C	C	C	C	R	C	C	A	C	C	C	–	C
27. *Hemitrypa vermifera*	R	–	C	R	R	C	C	C	C	R	R	C	–	–	–	–	C	C	C	R	R	–	C
1. *Rectifenestella tenax*	–	R	C	C	R	A	C	A	C	R	C	A	C	C	C	C	–	C	C	C	A	C	C
5. *Laxifenestella maculasimilis*	–	R	C	C	–	–	C	C	–	C	R	A	C	–	R	–	–	–	R	C	C	R	A
9. *Minilya paratriserialis*	–	C	C	–	R	C	–	R	–	R	C	–	R	–	–	–	C	R	–	–	C	–	R
13. *Banastella mediocreforma*	–	R	–	C	–	C	C	C	R	–	–	C	R	–	–	–	–	R	–	–	C	R	C
17. *Cubifenestella rudis*	–	C	C	C	C	A	C	C	–	A	C	A	C	C	R	C	C	C	C	C	C	R	A
20. *Apertostella foramenmajor*	C	C	C	–	C	A	R	R	–	–	R	–	–	–	–	R	–	C	–	C	C	R	–
12. *Banastella cingulata*	–	–	R	–	–	A	C	–	R	–	–	C	–	–	R	–	C	C	–	–	C	C	A
16. *Banastella delicata*	–	–	R	R	–	R	–	C	–	C	–	C	R	–	–	R	R	–	C	C	C	C	C
18. *Cubifenestella usitata*	–	–	C	R	–	C	C	A	–	–	R	C	–	–	C	–	C	C	C	R	C	C	C
36. *Polypora simulatrix*	–	R	–	–	–	C	C	C	–	–	R	–	–	–	–	–	R	–	C	–	C	R	R
34. *Polypora varsoviensis*	–	–	C	–	–	A	A	C	R	–	–	C	R	–	R	R	C	C	–	C	C	C	A
37. *Polypora retrorsa*	–	–	–	–	–	–	C	R	–	–	R	–	–	–	–	–	–	–	R	–	R	–	C
2. *Rectifenestella tenuissima*	–	–	–	–	–	–	–	–	–	–	–	C	–	–	–	C	–	R	R	C	R	R	C
11. *Banastella guensburgi*	–	–	–	–	–	–	–	–	–	–	–	C	–	–	–	–	–	–	R	–	A	C	A
33. *Polypora gracilis*	–	–	–	–	–	–	C	–	–	–	–	R	–	–	–	A	–	–	–	–	C	–	A
8. *Minilya sivonella*	–	–	–	–	–	–	C	–	–	–	–	–	–	–	C	–	R	R	C	R	C	C	A
31. *Archimedes valmeyeri*	–	–	–	–	–	–	–	–	–	–	–	–	–	–	–	C	C	C	C	R	R	R	C
10. *Exfenestella exigua*	–	–	–	–	–	–	C	–	–	–	–	–	–	–	–	–	–	–	C	–	C	–	C
7. *Laxifenestella fluctuata*	–	–	–	–	–	–	C	–	–	–	–	–	–	–	–	–	–	–	–	–	C	C	C
25. *Hemitrypa aprilae*	–	–	–	–	–	–	–	–	–	–	–	–	–	–	–	–	–	–	–	–	C	–	C

lypora simulatrix. Certain of the remaining 17 species were present throughout individual measured sections, but were restricted geographically along a north-south trend; changing composition for these 17 species is shown in Text-figure 20.

The depositional sequence present at the Keokuk–Warsaw contact is that of a carbonate shelf (the Keokuk) overlain by calcareous and argillaceous shales (the Warsaw). Sediment source for these sediments is probably from the east-northeast (Atherton and Palmer, 1979) and the northwest (see pp. 10, 11 for details). Similar facies relationships, faunal succession, and trophic structuring observed throughout the Warsaw suggest that depositional environments were probably broadly comparable. Changes in the lower Warsaw fauna probably reflect evolution rather than shifts in environment.

Unfortunately, because of little resistance to weath-

ering, the upper Warsaw frequently is poorly exposed, limiting the possibilities for detailed biostratigraphic analysis. Further work with underlying (Keokuk) and overlying (Salem, Sonora, Spergen, and St. Louis) units is required to establish definitively whether geographically changing composition of Warsaw species assemblages is biostratigraphically (evolutionarily) or environmentally (ecologically) controlled. Based on the

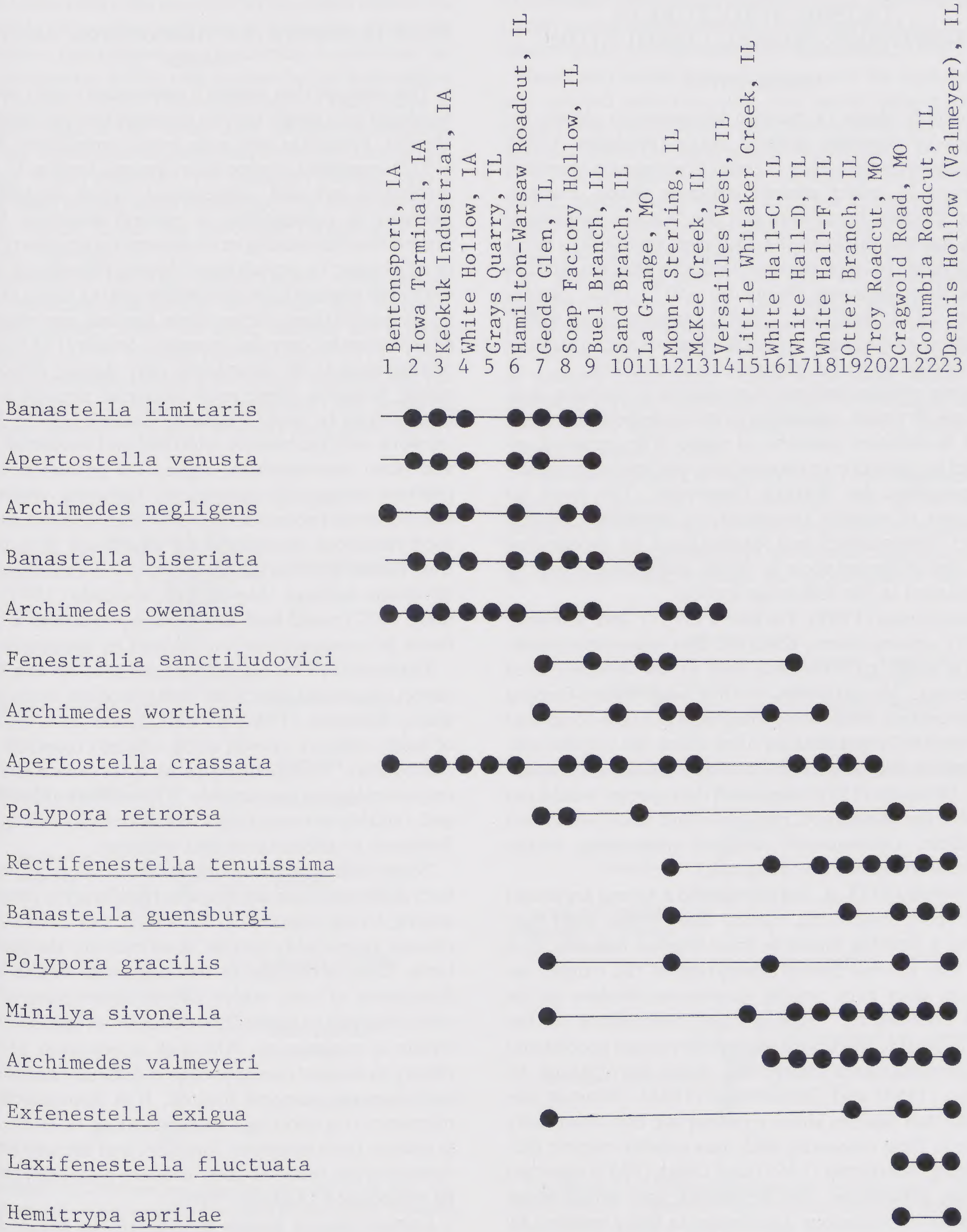

Text-figure 20.—Changing species composition of localities in the Warsaw study area.

general trend of infilling of the Illinois Basin from north to south, which would indicate the boundary between the Keokuk and Warsaw is not time equivalent throughout the basin, it appears evolutionary control is the most probable explanation.

TROPHIC STRUCTURE IN SUSPENSION-FEEDING COMMUNITIES

INTRODUCTION

Polypide shape in modern bryozoans is closely reflected by chamber skeletal shape (Winston, 1977). Chamber skeletal shape in fossil bryozoans is therefore assumed to reflect ancient polypide shape. Further, many modern bryozoans and the Warsaw fenestrates have limited intraspecific chamber variability, but a broad range of interspecific chamber variation. Studies of modern Bryozoa (Winston, 1977, 1982; Strathmann, 1973; Bullivant, 1968b) indicate niche differentiation as the most probable cause of such intraspecific consistency and interspecific variability.

Using criteria derived from studies of modern cheilostome Bryozoa, analagous in many respects to meshwork fenestrates, patterns of niche differentiation reflected by variation in zooecial size and species diversity are proposed for Warsaw fenestrates. The basis for concepts of trophic structuring in seemingly similar recent communities and implications for recognition of niche differentiation in fossil assemblages will be established in the following section.

Hutchinson (1959), Turpaeva (1957), and Schoener (1974), among others, observed that organisms inhabiting a single environment tend to use different food resources. Nevertheless, within suspension-feeding communities, the general consensus (Knight-Jones and Moyse, 1961) was that no need exists for trophic specialization because suitable and abundant food is available. Levinton (1972) suggested that species would not exploit the same food resources and thus would not complete; consequently trophic structuring within communities does not develop.

Winston (1977, p. 263) presented a strong argument for trophic structuring, stating that "While food may not be a limiting factor in most marine habitats, it is true that at least partial separation of the trophic resources does exist among suspension feeders in the same community." Basing these conclusions on her own extensive work with modern bryozoan species and on previous work concerning niche partitioning by Mullin (1963) and Edmondson (1965), Winston observed that species share overlapping but observably separate food resources, and thus exhibit trophic partitioning. Marischal (1965) and Dales (1957) reported feeding preferences for bryozoans and polychaetes; Winston's conclusions are similar to those reached by these earlier workers.

Three means by which bryozoans might achieve some degree of trophic separation are through selection based on physical, chemical, or biological factors (Winston, 1977), all primarily concerned with either food characteristics or feeding behavior.

NICHE DIFFERENTIATION AMONG LIVING AND FOSSIL SPECIES

The concept that within a community each niche is occupied by a single species (competitive exclusion *per* Hardin, 1960) has met with recent opposition. Wiens (1977) suggested competition among species is intermittent to rare and, subsequently, gave minimal importance to competition in natural selection. Wiens argued that fluctuating environments are primary causes of change in populations during periods of stress, with little competitive interaction during times of plenty, as populations during these periods are below the environmental carrying capacity. Smith (1981) found competition to be detectable only during periods of stress; however, these environmental periods are interpreted to be quite frequent. Connell (1975), based on work with the marine intertidal and terrestrial pond and plant communities, argued for predation as the primary interspecific interaction. However, when population levels become adequately high, competition for food resources becomes more significant than predation. Lesser levels of predator activity in Paleozoic than Holocene settings (Meyer and Macurda, 1977; Vermeij, 1977) could lead also to competition as a major factor in communities not thinned by predators.

Diamond (1978) argued for competition as a major aspect of natural selection, using modern birds in his study. Schoener (1982, p. 594), based on a synthesis of many authors as well as on original research, concluded that "Competition must still be considered of major ecological importance." The effects of predation and variable environments were also acknowledged by Schoener as affecting natural selection.

Niche differentiation and the constraints governing such differentiation are frequently difficult to recognize among living organisms. In fossils this difficulty increases appreciably as one must rely on skeletal features. One advantage in working with fossils is the dimension of time, which allows observation of possible progressive niche differentiation as species evolve within a community. Although application of niche theory to ancient communities is difficult conceptually and in many respects limited, it is appropriate and necessary if a thorough understanding of these communities, their structure, function, and the way ancient communities relate to their modern counterparts is to be established (Ausich, 1980).

Competition is herein considered the major factor leading to niche differentiation within Warsaw mesh-

work fenestrates; predation and variability of environment are considered to have played a minor role relative to competition.

BRYOZOAN FEEDING MECHANISM AND BEHAVIOR

The lophophore is a food gathering organ consisting of a circle of varying numbers of tentacles. Tentacles are hollow protruberances containing a coelomic lumen continuous with a ring coelom in the lophophore base (Hyman, 1959). They attached to a basal ridge at the outer edge of the mouth and, unlike the brachiopods, the lophophore is extended from the skeleton for feeding. When extended, the tentacles expand into a broad, open funnel; when contracted, the tentacles form a tight bundle inside the zooecium (Winston, 1977; also see Text-figs. 21, 22).

Retraction of the lophophore occurs when the retractor muscles, attached to the cardia, and funicular muscles contract while the atrial dilators are relaxed (Boardman, 1975; Neilsen and Pedersen, 1979). Once the tentacle sheath encloses the entire lophophore, the atrial sphincter contracts. Retraction of the tentacles is a rapid process typically, whereas protrusion occurs much more slowly (Boardman, 1975). For protrusion, the retractor and all other muscles first relax, then annular muscles of the membranous sac contract sequentially, proximally to distally in the zooid, thus forcing out the polypide (Nielsen and Pedersen, 1979). Hydrostatic pressure of coelomic fluid increases proximally as the atrium contracts, forcing fluid in the coelomic lumen in this direction (Boardman, 1975).

Inner and lateral tentacle surfaces of the lophophore are covered with fine cilia; the lateral cilia move in such a way that metachronal waves move up the left side and down the right side of each tentacle (Winston, 1977). Reversals of ciliary action can occur (Bullivant, 1968a; Strathmann, 1973), and cilia at one point may stop beating without affecting other cilia along the tentacle. Median cilia apparently lack mobility; however, they and specific lateral cilia may act as sensory organelles (Hyman, 1959; Bullivant, 1968a). Gordon (1974) observed elongate solitary and short tufts of cilia on the abfrontal tentacle surface which act apparently as sensory organelles. When stimulated, these cilia probably initiate retraction or flick of tentacles, or reverse ciliary motion (Lutaud, 1955, 1973; Bullivant, 1968a; Gordon, 1974).

Two mechanisms of feeding have been suggested for bryozoans and other lophophorates. The first of these, proposed by Bullivant (1968a), is termed impingement feeding. Outward beating of the lateral cilia causes water to flow inward through the aboral side of the ten-

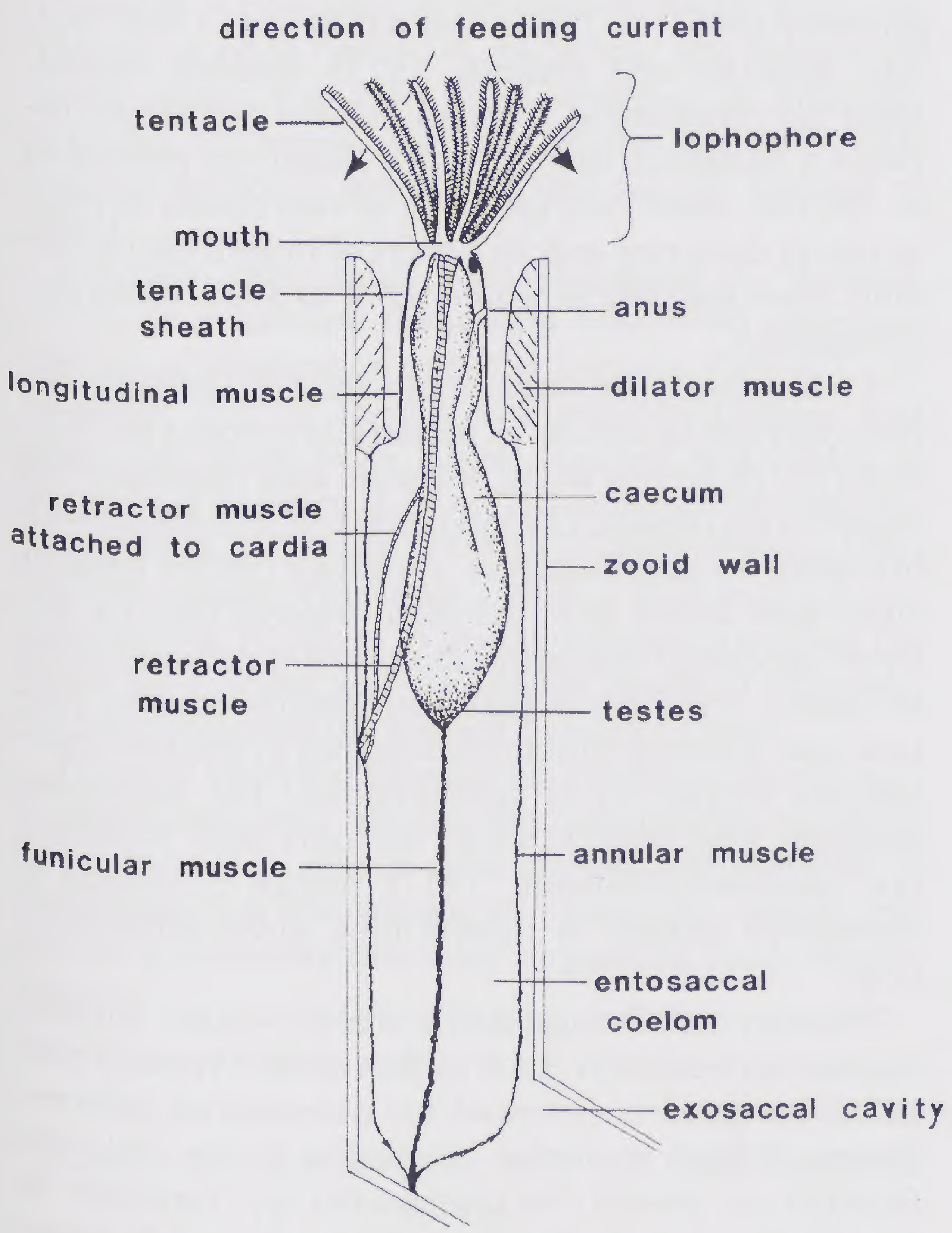

Text-figure 21.—Modern stenolaemate showing zooid with tentacles extended. Observe direction of current flow across tentacles, characteristic of all members of the Bryozoa. (adapted from Boardman, 1975; Winston, 1977; Nielsen, 1970)

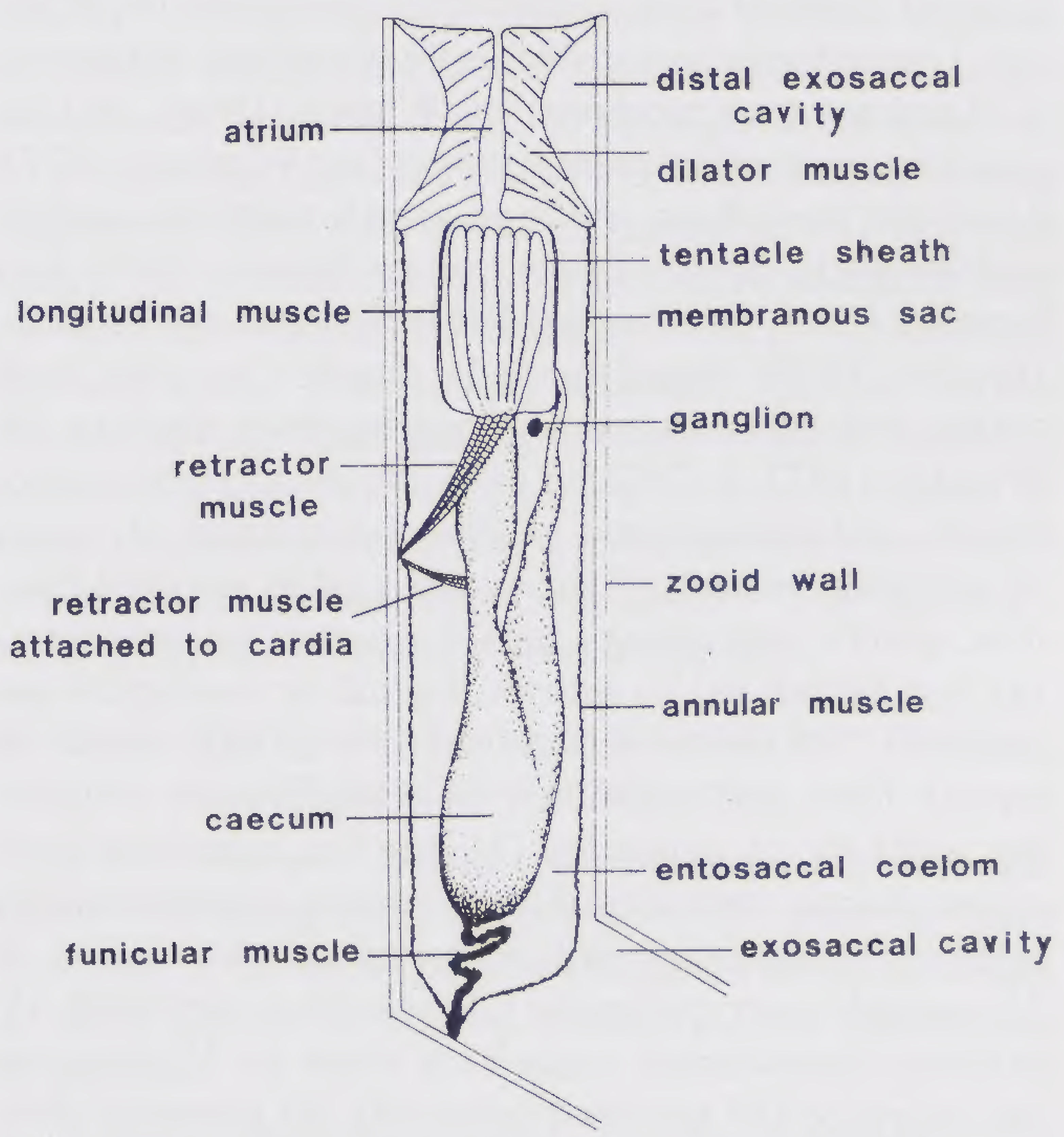

Text-figure 22.—Modern stenolaemate showing zooid with tentacles retracted. Observe how zooid almost completely fills chamber when in the retracted position. (after Boardman, 1975; Winston, 1977; Nielsen, 1970)

tacular funnel. Water carrying food particles is directed into the mouth, which lies in the middle of the tentacles. Upon reaching the mouth, the current of water is deflected upward and outward between the tentacles, and food particles are deposited in the mouth. The latter is accomplished, as suggested by Bullivant, by eddying of the current immediately over the mouth due to sharp inflection of the current at the mouth's outer edge. Carrying capacity of the current is thus reduced and food accumulates in the still water over the mouth. From here, the food is sucked into the digestive tract by muscular dilation of the pharynx. Although in general agreement with Bullivant's model, Winston (1977) modified it, reporting that rather than forcing water to flow into the tentacular funnel, the lateral cilia cause current movement up the left side and down the right side of each tentacle.

A second feeding mechanism was presented by Strathmann (1971, 1973), who suggested the impingement model could not work because of the similar density between food particles and that of water. In this second model, brief reversals of the cilia were thought by Strathmann to bounce food particles into the mouth because of the presence of strongest current in the center of the lophophore. Neither model has yet been proven.

Length and number of tentacles should cause a pronounced effect on efficiency of feeding in bryozoans, as more and longer tentacles should increase volume of food brought to the mouth, yet only recently has tentacle number been considered in studies on Bryozoa. Use of tentacle number as an important taxonomic character was proposed by Waters (1904), but ignored by most subsequent workers (*per* Winston, 1977). Attempts have been made to attach tentacle number and length to depth of occurrence (Braem, 1940; Bullivant, 1968a), but conclusions lack broad application. Hyman (1959) found tentacle number to vary both within and between species, ranging from eight to 34. Winston (1977, p. 242), in over 200 cyclostome, ctenostome, and cheilostome species determined "1) range of variation in each of the orders and in selected families, genera, and species, and 2) whether tentacle number can be related to morphological or ecological parameters." Winston recognized five groups based on growth form and taxonomy: (1) cyclostomes containing eight to 16 tentacles [31 species examined]; (2) stoloniferous ctenostomes containing predominantly eight to 10 tentacles with a few species having up to 25 tentacles per polypide [29 species examined]; (3) carnose ctenostomes containing eight to 35 tentacles per polypide [39 species examined]; (4) amascan cheilostomes, with a bimodal distribution of tentacles with peaks between 11 and 16 and between 20 and 28 tentacles per polypide [60 species examined]; and (5) ascophoran cheilostome species containing predominantly 11 to 19 tentacles per polypide, with few species having 20 to 28 tentacles per polypide [53 species examined]. In general, groupings possessing the greatest zoarial regularity in pattern (carnose ctenostomes and both amascan and ascophoran cheilostomes) show the greatest variation in tentacle count.

Bullivant (1968b) and Winston (1976, 1977) determined food passage rates (*i.e.,* from mouth to anus) depend on animal condition, food quality and concentration, and species differences, ranging from a minimum of 21 minutes in *Bugula turrita* to a maximum of 60 minutes of *Zoobotryon verticillatum*. Consistent differences between species and orders were also observed by Winston. She observed that non-nutritive particles pass through the bryozoan digestive system more rapidly than food particles.

Food Particle Size

Although based on somewhat limited data, physical size of food particles is the primary means by which niche differentiation in modern bryozoans is thought to occur (Parsons and Le Brasseur, 1970; Winston, 1977). Size of modern phytoplankton particles ranges generally from 1 to 120 microns (Dussart, 1964; Sheldon, Sutcliffe, and Prakash, 1973). Sheldon emphasized the pronounced size and volume differences between a bacterium at 1 μm and a diatom or protozoan at 100 μm, observing variation of two orders of magnitude in diameter and six orders of magnitude in volume. Such differences would seem to allow niche differentiation.

A relationship between mouth and food particle size was observed in a study of modern bryozoans by Winston (1977). In this study, Winston also illustrated the apparent correlation of phytoplankton abundance with bryozoan mouth diameters. Although certain types of algae were found to be selected preferentially by different species of bryozoan, the primary differentiation of trophic resources is based apparently on food particle size. Because mouth dimensions in modern cheilostome species equal approximately the maximum diameter food particle which an individual zooecium can assimilate (Winston, 1977), mouth dimension is considered critical in determining niche differentiation.

Winston (1977) suggested a shallow-water, tropical marine environment (such as that of the Warsaw) provided the greatest potential for pronounced differentiation of food resources. According to her, this differentiation should be represented by variation in tentacle number, lophophore diameter, mouth diameter, and apertural and zooecial characters.

Morphological Features Governing Feeding Rates in Modern Bryozoan Species

Winston (1977), in a study of shallow water marine bryozoans from Woods Hole, Massachusetts, compared ten species in terms of tentacle number, tentacle length, lophophore diameter, length of zooecium, width of zooecium, length of orifice (aperture), width of orifice (aperture), diameter of mouth, and size of fecal pellet. Moderate to pronounced variation of the above features is observed between species: tentacle numbers range from eight to 30, tentacle length from 0.2 to 1.0 mm, expanded lophophore diameters from 0.2 to 1.4 mm, and mouth diameters from 0.019 to 0.009 mm. In contrast, Winston observed pronounced regularity of these features within species.

Clearance rate, defined as the rate at which a suspension feeder clears a suspension, can be studied by placing colonies in containers with fixed amounts of suspended algae. Bullivant (1968b) observed clearance rates of between 0.152 and 1.050 ml/zooid/hr in different species of *Zoobotryon* Ehrenberg, 1831. An attempt to measure clearance rate indirectly was presented by Strathmann (1973). He proposed (for fluid flowing at a velocity of 1 cm/sec) that clearance rate is equal to the product of the tentacle length times the tentacle number times 1.4 ml/hr/cm. His theoretical results equate well with those observed by Bullivant in living *Zoobotryon* colonies (Winston, 1977). This formula indirectly provides a tool for the analysis of fossils.

Polypide dimensions were calculated by Winston (1977) to determine theoretical maximum clearance rate using Strathmann's (1973) formula. Difference in clearance rate for species with smallest number and length and those with largest number and length of tentacles is between 0.21 ml/hr/zooid (*Crisia eburnea* Lamouroux, 1812) and 3.78 to 4.20 ml/hr/zooid (*Flustrellidra hispida* Fabricius, 1780), a difference in rate approaching 20 times. Winston demonstrated that the larger the number and greater the length of tentacles, the more efficient the feeding cone developed.

Winston observed substantially greater polypide sizes associated with species having greatest clearance rates. Increased size of both mouth and polypide is associated with increased tentacle number, length, and greater lophophore diameter, suggesting food specialization.

WARSAW ENVIRONMENTAL AND PALEOECOLOGICAL SETTING

The abundant fenestrate-dominated assemblages in the Warsaw provide an opportunity to evaluate possible niche differentiation in a Paleozoic shallow-water marine community. Sequential stages of faunal succession have been recognized (Snyder, 1987) which indicate both physical and biological factors contributed to Warsaw community development.

Facies interrelationships and thus broad depositional environments appear comparable throughout the sample area (see pp. 11–14) for both the Warsaw and underlying Keokuk Formations.

Fenestrate species within Warsaw communities change between the northernmost and southernmost ends of the sample area (see p. 156). Such changes can result from evolutionary or environmental variability; however, causes for these differences are beyond the scope of this study. Warsaw communities and their trophic structuring, however, will be dealt with in terms of species confined to the northernmost area, species confined to the southernmost area, species occurring throughout the area, and all three combined. Both northern and southern communities developed in similar facies and thus in similar inferred depositional environments, with community development following highly similar stages of succession.

Materials and Approach.—Data employed for evaluating Warsaw niche differentiation are derived from the section on taxonomy (pp. 40–156). Such data sets not only establish a sound base for taxonomy but also provide the opportunity for paleoecologic studies such as that of possible trophic structuring in the meshwork fenestrates.

Table 47 lists species employed in the trophic analysis of Warsaw Bryozoa, assigning a number to each for future identification and records area(s) of occurrence (such as north, south, or throughout) in the area. The following nine characters are used in determining meshwork fenestrate niche assignment: (1) zooecial length; (2) zooecial depth; (3) maximum zooecial width; (4) aperture length; (5) aperture width; (6) aperture spacing along branch; (7) aperture spacing across branch; (8) aperture spacing between branches; and (9) number of apertural stylets. The arithmetic mean of these measurements, using 24 measurements of each character per species, was used. Table 49 lists the character dimensions from species analyzed.

ZOARIAL EMPLACEMENT AND FEEDING IN WARSAW MESHWORK FENESTRATES

In the Warsaw, zoarial emplacement and mechanisms of feeding are assumed to be the same as those observed in modern species; analagous features as well as those specific to fossils themselves are considered as follows:

A. Colony positioning within the environment.
   1. Colony growth was perpendicular or at a slight angle from perpendicular to the substrate, extending the zoarium upward into the water col-

Table 49.—Fenestrate characters used in niche differentiation. Explanations of species numbers are shown in Table 47.

	mean zooecial length (mm)	*mean zooecial depth* (mm)	*mean zooecial width* (mm)	*aper-ture length* (mm)	*aper-ture width* (mm)	*aper-ture spacing along branch* (mm)	*aper-ture spacing across branch* (mm)	*aper-ture spacing between branches* (mm)	*tentacle number (stylet number)*	*loph. dia. ≈ interp. tentacle length* (mm)	*1.5 × closest aper. space = interp. lopho-phore diameter* (mm)	*0.4 × aperture mini-mum = interp. diameter of mouth* (mm)	*0.1 × lophoph. diam-eter = interp. diameter of mouth* (mm)	*(l×d×w) zooecial volume* (mm³)
1.	0.184	0.100	0.104	0.064	—	0.231	0.282	0.301	6.42	0.347	0.347	0.026	0.035	0.0019
2.	0.215	0.105	0.106	0.101	0.090	0.230	0.230	0.297	4.33	0.345	0.345	0.036	0.035	0.0024
3.	0.261	0.151	0.146	0.117	0.096	0.234	0.225	0.214	—	0.338	0.338	0.039	0.034	0.0058
4.	0.263	0.171	0.148	0.104	—	0.300	0.289	0.378	—	0.434	0.434	0.042	0.043	0.0067
5.	0.230	0.154	0.140	0.076	—	0.255	0.301	0.257	—	0.383	0.383	0.030	0.038	0.0050
6.	0.219	0.139	0.143	0.100	0.084	0.235	0.242	0.249	—	0.353	0.353	0.034	0.035	0.0044
7.	0.281	0.147	0.162	0.091	0.074	0.262	0.295	0.399	—	0.393	0.393	0.030	0.039	0.0067
8.	0.269	0.158	0.139	0.106	—	0.394	0.370	0.391	10.42*	0.569	0.569	0.042	0.057	0.0081
9.	0.210	0.152	0.127	0.071	—	0.227	0.312	0.321	2.00	0.341	0.341	0.028	0.034	0.0041
10.	0.287	0.140	0.138	0.089	—	0.239	0.301	0.296	9.00	0.359	0.359	0.036	0.036	0.0055
11.	0.589	0.224	0.174	0.196	0.165	0.437	0.419	0.452	18.29	0.629	0.629	0.066	0.063	0.0230
12.	0.489	0.212	0.148	0.170	0.148	0.314	0.276	0.323	21.08	0.414	0.414	0.059	0.041	0.0153
13.	0.557	0.230	0.208	0.224	0.171	0.383	0.376	0.441	12.96	0.564	0.564	0.068	0.056	0.0267
14.	0.692	0.195	0.206	0.204	0.162	0.398	0.365	0.491	20.25	0.548	0.548	0.065	0.055	0.0278
15.	0.329	0.210	0.160	0.161	0.134	0.324	0.292	0.387	—	0.438	0.438	0.054	0.044	0.0111
16.	0.639	0.170	0.154	0.198	0.158	0.436	0.347	0.581	15.21	0.521	0.521	0.063	0.052	0.0167
17.	0.282	0.270	0.187	0.176	0.144	0.306	0.326	0.439	—	0.459	0.459	0.058	0.046	0.0142
18.	0.245	0.183	0.145	0.143	0.104	0.272	0.262	0.418	8.58	0.393	0.393	0.042	0.039	0.0065
19.	0.213	0.155	0.129	0.084	0.067	0.280	0.295	0.533	16.28	0.420	0.420	0.027	0.042	0.0043
20.	0.198	0.159	0.134	0.125	0.072	0.246	0.238	0.298	—	0.357	0.357	0.029	0.036	0.0042
21.	0.202	0.177	0.136	0.140	0.096	0.216	0.222	0.297	—	0.324	0.324	0.038	0.032	0.0049
22.	0.356	0.174	0.164	0.121	0.075	0.296	0.215	0.478	—	0.323	0.323	0.030	0.032	0.0102
23.	0.229	0.225	0.133	0.132	0.092	0.240	0.232	0.322	—	0.348	0.348	0.037	0.035	0.0069
24.	0.224	0.219	0.163	0.122	0.088	0.222	0.232	0.293	—	0.333	0.333	0.035	0.033	0.0080
25.	0.224	0.177	0.160	0.124	0.085	0.244	0.236	0.257	—	0.354	0.354	0.034	0.035	0.0063
26.	0.238	0.162	0.133	0.130	0.088	0.240	0.258	0.267	—	0.360	0.360	0.035	0.036	0.0051
27.	0.292	0.215	0.167	0.166	0.114	0.283	0.280	0.308	—	0.420	0.420	0.046	0.042	0.0105
28.	0.209	0.125	0.125	0.111	0.094	0.198	0.189	0.243	—	0.284	0.284	0.038	0.028	0.0033
29.	0.220	0.122	0.113	0.106	0.084	0.223	0.203	0.268	20.58	0.305	0.305	0.034	0.031	0.0030
30.	0.175	0.128	0.115	0.102	0.084	0.191	0.188	0.213	10.50	0.282	0.282	0.034	0.028	0.0026
31.	0.229	0.138	0.119	0.111	0.087	0.220	0.241	0.269	11.50	0.330	0.330	0.035	0.033	0.0038
32.	0.388	0.142	0.121	0.103	0.081	0.264	0.197	0.581	—	0.296	0.296	0.032	0.030	0.0067
33.	0.379	0.213	0.206	0.154	0.112	0.400	0.246	0.829	11.58	0.369	0.369	0.045	0.037	0.0166
34.	0.779	0.140	0.174	0.198	0.168	0.376	0.274	0.516	20.67	0.411	0.411	0.067	0.041	0.0190
35.	0.536	0.198	0.189	0.220	0.164	0.377	0.291	0.479	12.67	0.437	0.437	0.066	0.044	0.0201
36.	0.791	0.167	0.170	0.248	0.174	0.549	0.351	0.776	30.50	0.527	0.527	0.070	0.053	0.0225
37.	0.695	0.336	0.128	0.135	0.125	0.233	0.190	0.366	7.75	0.285	0.285	0.050	0.029	0.0299

* In *Minilya sivonella,* there are also two *large* stylets per aperture.

umn. Upright orientations are observed in numerous zoaria preserved *in situ.*

2. Inferred dominant colony orientation extended perpendicular (across colony width) to primary current direction, thus allowing the entire colony equal feeding opportunity. Colonies formed straight, anastomosing, obversely or reversely curved or cupped expansions.
3. Obverse colony surface was typically oriented down-current (away from direction of primary current), inferred from the significantly greater occurrence of preserved zoaria with obverse surface facing downward onto bed surfaces in areas where a single depositional event apparently resulted in colony dislocation.
4. Colony height above the sea floor was varied, ranging in mature colonies from tens of mm to in excess of 1 m in some species, with most common development from 2 to 20 cm in height.
5. Colony spacing across the sea floor appears to minimize sheltering of colonies behind one another relative to current direction, as observed on Warsaw slab surfaces.

B. Polypide feeding characteristics.

1. Lophophores are considered to be symmetrical cones, opening upward (Winston, 1977).
2. The lophophore gathers food selectively through combined tentacle and cilia activity (Bullivant, 1968a; Strathmann, 1971, 1973)

PARAMETERS USED FOR DETERMINING NICHE DIFFERENTIATION IN WARSAW FENESTRATES

In modifying Winston's (1977) work to apply to Paleozoic fenestrates, autozooecial chamber dimensions are treated as being equal approximately to those of the polypide, as is the case in many modern bryozoan species (Winston, 1977, 1982). Length and width of the aperture can be determined in both living bryozoans and fossil fenestrates. Although number of tentacles per zooid can not be determined directly in fossils, apertural stylets, where present, are taken as indicators of tentacle number because they are typically greatly consistent intraspecifically in number and size just as tentacles themselves are constant in modern bryozoans.

Interpretation of niche or trophic differentiation among Warsaw fenestrates (or any other bryozoans) requires estimating approximate tentacle length, lophophore diameter, and mouth diameter. Lacking soft parts, an indirect means of approximating these dimensions must be found in fossil bryozoans. Modern ascophoran cheilostomes offer a suitable analogue for the fenestrates. In both groups, there is a larger degree of intraspecific consistency in size and shape of both autozooecial chambers and apertures and a general regularity of pattern to the zoaria (Winston, 1977). In my work, I observed that like the fenestrates, many ascophoran cheilostome species exhibit equal aperture spacing over the zoarium surface, with apertures forming an even gridwork across the colony. This pattern suggests partitioning of the surface into individual zooecial feeding zones. Aperture spacing can vary appreciably between species, but does not vary substantially within most species of fenestrates and ascophoran cheilostomes.

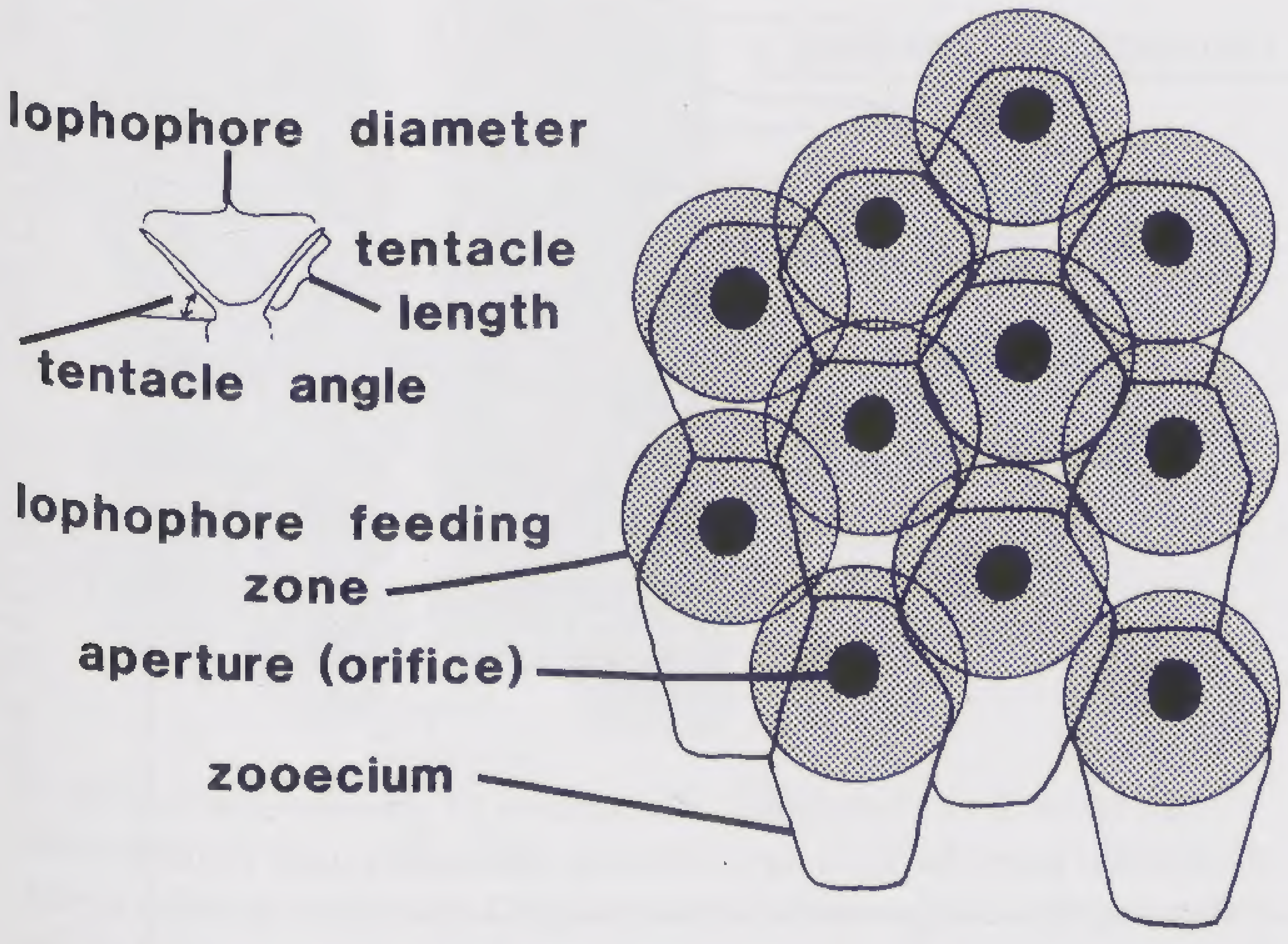

Text-figure 23.—Schematic illustration of the obverse zoarial surface of *Cryptosula pallasiana* (Moll, 1803), showing characters used for niche differentiation and lophophore feeding zones. Observe the almost complete coverage of the obverse surface by these feeding zones. Tentacle number = 16; tentacle length = 0.749 mm; lophophore diameter = 0.796 mm; zooecium length = 0.742 mm; zooecium width = 0.479 mm; orifice width = 0.188 mm; mouth diameter = 0.069–0.047 mm; fecal pellet size = 0.080–0.127 mm; mean diagonal aperture spacing = 0.531 mm (most dimensions from Winston, 1977).

Winston (1977) reported a size correlation between tentacle length, lophophore diameter, and diameter of the mouth. Tentacle length and lophophore diameter means were found to be approximately equal within any species, most lying within 10% to 20% of each other, with a maximum of ±40%. The angle between tentacles and plane of obverse surface when the lophophore was extruded was not presented by Winston. Reapplying data from Winston's study, mouth diameters are consistently found to measure approximately 10% of the lophophore diameter.

In an interpretation of Winston's data, the regular ascophoran cheilostome species *Cryptosula pallasiana* is used herein to determine the relationship between aperture spacing across the zoarial surface, tentacle number, and lophophore diameter (Text-fig. 23). Spacing between aperture centers along and diagonally across the zoarial surface yields a range of from 0.395 mm to 0.585 mm, with a mean value of 0.531 mm and a coefficient of variation of 10.48. This mean measurement corresponds closely to two-thirds of the mean lophophore diameter of 0.796 mm. Spacing of lophophores in a regular pattern over the obverse surface would seem most advantageous to the colony, as it would allow uniform tentacle coverage of the major portion of the zoarial obverse surface, resulting in efficient use of food resources. Partitioning of the obverse surface into evenly divided, uniformly positioned feeding areas for each lophophore of *C. pallasiana* is illustrated in Text-figure 23.

Based on the analysis of *C. pallasiana* and other data from Winston's works, the following conclusions concerning soft part dimensions and their relationship to preservable skeletal features are drawn:

1. Tentacle length and lophophore diameter typically approximate each other (within ± 10% to 20%). Following Winston, the lophophore is a symmetrical, conically shaped feeding organ with the mouth positioned at the tip of the cone.
2. Mean spacing of closest aperture centers across the obverse zoarial surface is approximately two-thirds the mean lophophore diameters, or lophophore diameter equals 1.5 times closest aperture spacing (based on analysis of *C. pallasiana*).
3. Diameter of the mouth can be determined two ways: (a) ±10% of the measure of the lophophore diameter; and (b) approximately 40% of the width of the orifice (aperture).
4. A direct relationship is observed between lophophore and mouth diameter in modern Bryozoa (Win-

ston, 1977, p. 247, fig. 4). Chamber volume (calculated from Winston, 1977, table 1) is found also to increase proportionally to lophophore and mouth diameter.

The above relationships provide a means by which the probable soft part dimensions can be calculated (*i.e.,* tentacle length and lophophore and mouth diameter) for fossils from skeletal dimensions. Once mean spacing of closest apertures is found, this is multiplied by 1.5 to determine lophophore diameter, which in turn approximates (± 10% to 20%) the tentacle length. Mouth diameter can next be determined as approximately ±10% of the lophophore diameter and checked by comparing this measurement with 40% of that of the orifice (aperture) width. These two measurements should be equal approximately.

Interpreted lophophore feeding zones for *Banastella guensburgi*, a Warsaw fenestrate species exhibiting moderately uniform aperture spacing are illustrated in Text-figure 24. Spacing of aperture centers along, across, and between branches gives a range of 0.320 to 0.660 mm, with mean values quite similar, ranging from 0.419 to 0.452 mm, and standard deviations of 11.98 to 18.83. If lophophore diameter in *B. guensburgi* were 1.5 × mean aperture spacing (as in *C. pallasiana*), then coverage of the obverse surface would have been relatively complete (Text-fig. 24).

Text-figure 25 shows mean ranges of aperture spacing along, across, and between branches across the fenestrule in Warsaw fenestrate species. The pronounced similarities in all three dimensions for most species of meshwork fenestrates are considered important to my hypothesis: they are considered to reflect colony integration for feeding purposes. Such integration is not a new idea, but has been developed in works of numerous authors for both recent and fossil Bryozoa (Banta, McKinney, and Zimmer, 1974; McKinney, 1977; Cook, 1977; Winston, 1978). More open meshwork in some species produces anomalously large spacings between branches across the fenestrule relative to spacings along and across the branch, due to wider branch spacings. This might reflect response to currents or even lack thereof, although this is a tenuous hypothesis.

POSSIBLE NICHE DIFFERENTIATION IN WARSAW FENESTRATE BRYOZOA

Interspecific variation in tentacle number, lophophore size, and mouth size are criteria used to indicate, probably, the separation of trophic resources in modern cheilostomes. Such criteria can be also applied to meshwork fenestrates for recognition of niche partitioning.

In modern bryozoans a direct relationship has been observed between orifice (aperture) diameter and mouth diameter, as has a relationship between mouth and lophophore diameters. Text-figure 26 illustrates inferred mouth diameter (based on 40% minimum aperture dimension) plotted against lophophore diameter (calculated from 1.5 × the closest aperture spacing across the zoarial surface) for Warsaw meshwork fenestrates. Arithmetic means of characters are used for interpreting soft-part dimensions; use of character ranges in these interpretations is deemed unnecessary due to their extremely low coefficients of variation and consequently low ranges. (Character ranges and coefficients of variation are given for all respective species in section on systematics.) From Text-figure 26D, a grouping of species occur in the range of the range of 0.025 to 0.040 mm mouth diameter and 0.259 to 0.400 mm lophophore diameter. The remaining species, with the exception of a few anomalies, plot in a linear manner, showing that species with inferred larger mouth sizes typically have inferred larger lophophores. Winston (1977) observed similar distribution of mouth size *versus* lophophore diameter in modern species, and suggested larger mouth and lophophore sizes for species indicates the ability to exploit larger size food particles.

Text-figure 26A–C shows plots of species restricted to the northern, occurring throughout, and restricted to the southern parts of the study area, respectively. Similarities in values observed in Text-figures 26A and 26C suggest species replacement between the northern and southern areas, thus suggesting similar niches. Spe-

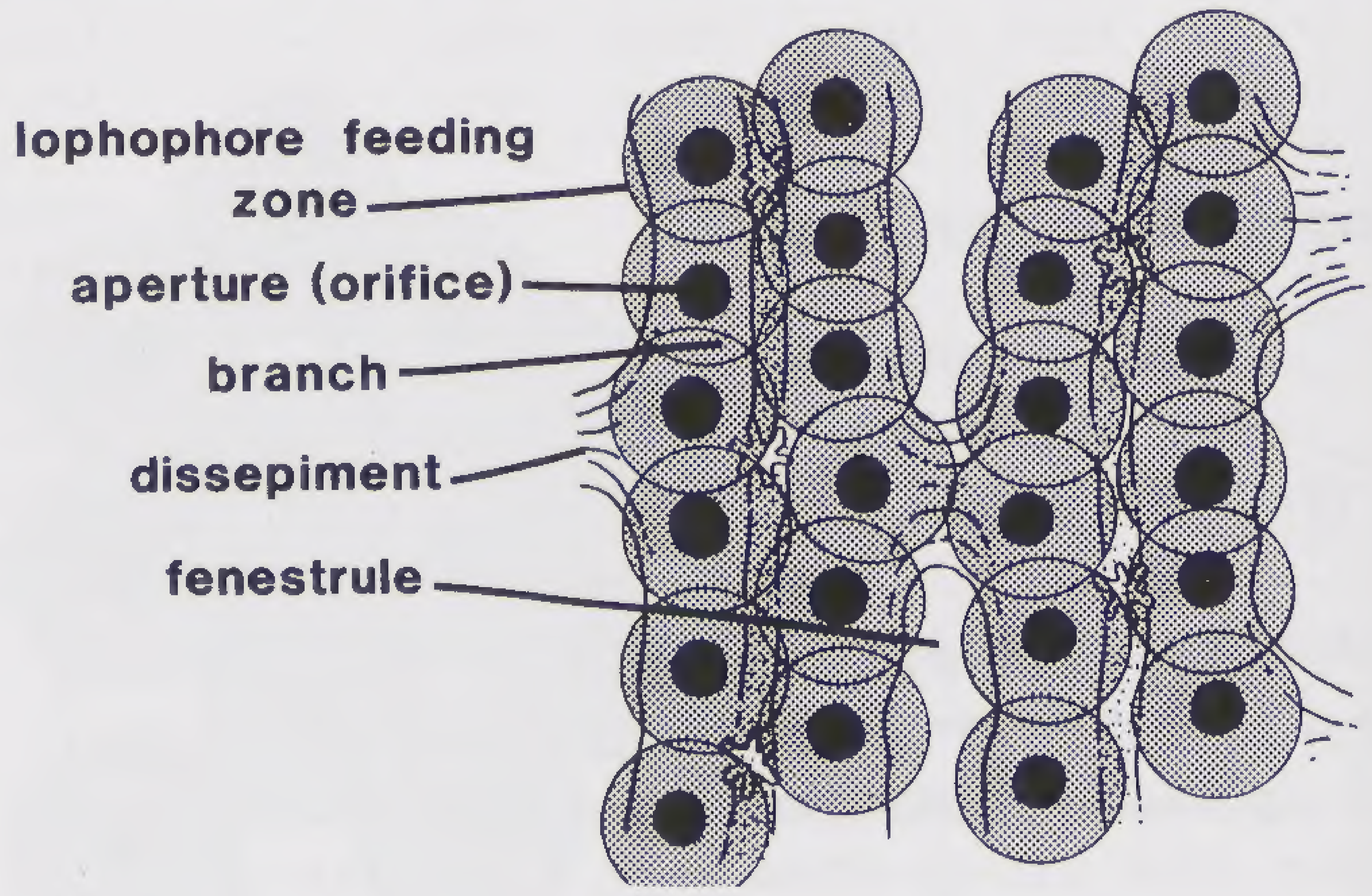

Text-figure 24.—Schematic illustration of the obverse surface of *Banastella guensburgi*, n. sp., showing characters used to infer niche differentiation and possible positioning of lophophore feeding zones. Such zones form a moderately even, overlapping covering of the obverse zoarial surface in most meshwork fenestrate species. Tentacle number = 18; tentacle length = 0.629 mm; lophophore diameter = 0.629 mm; zooecium length = 0.589 mm; zooecium depth = 0.224 mm; zooecium width = 0.174 mm; zooecial volume = 0.023 mm^3; aperture (orifice) length = 0.196 mm; aperture (orifice) width = 0.165 mm; mouth diameter (10% of lophophore diameter) = 0.063 mm; mouth diameter (40% of aperture width) = 0.066 mm; aperture spacing along branch = 0.437 mm; aperture spacing across branch = 0.419 mm; aperture spacing between branches = 0.452 mm.

cies might possess slightly larger lophophore diameters relative to mouth size in the southern area.

In some species of fenestrates, stylets surround the autozooecial aperture. Based on their largely consistent interspecific number, size, and positioning, these stylets are interpreted as tentacle guides, with their number equal to or closely approximating the number of tentacles. Text-figure 27 illustrates calculated tentacle number plotted against inferred tentacle length, herein considered approximately equal to the lophophore diameter (see above). As inferred tentacle count increases, so does inferred tentacle length in many extant species, although this relationship is not as clear as that between mouth and lophophore diameters.

A general similarity between Text-figures 27A and 27C again suggests species replacement between the northern and southern areas, although data points are relatively few.

Table 50 and Text-figure 28 show clearance rate calculated for all Warsaw meshwork fenestrates (*per* Strathmann, 1973; see above), along with parameters used in clearance rate determination and calculated chamber volume.

If chamber volume indeed approximates polypide dimensions, assuming similar interspecific metabolic rates, an increase in calculated clearance rate should be proportional to increased chamber volume. Although an anomalous reading is given by species number 37, a general increase in chamber volume is associated with increased calculated rates, and presumably ability of polypide to gather food.

Twenty of the 37 Warsaw species do not possess apertural stylets and thus do not lend themselves to calculation of inferred clearance rates. The relationship of increased clearance rates to increases in chamber volume allows additional interpretations to be made

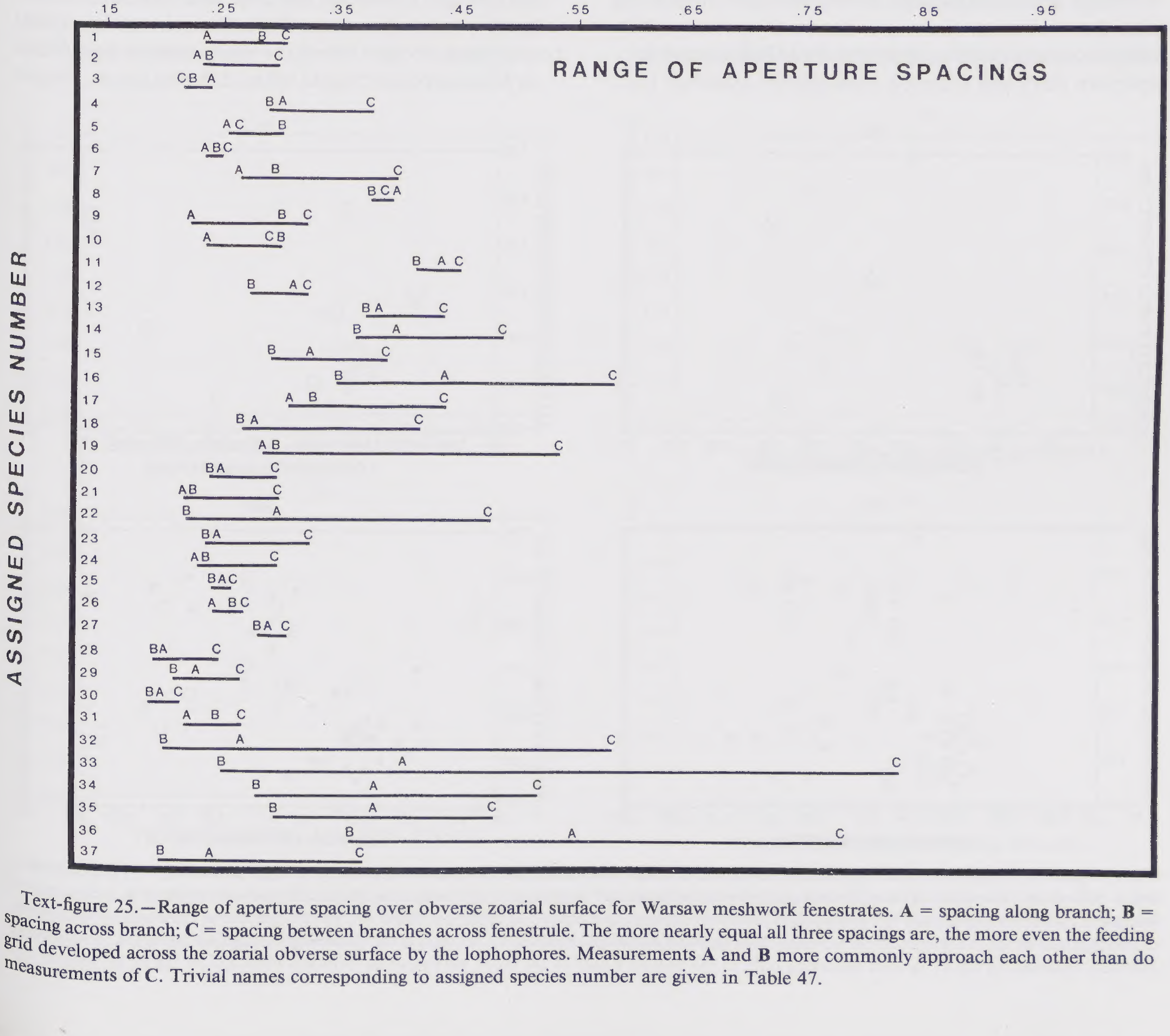

Text-figure 25.—Range of aperture spacing over obverse zoarial surface for Warsaw meshwork fenestrates. **A** = spacing along branch; **B** = spacing across branch; **C** = spacing between branches across fenestrule. The more nearly equal all three spacings are, the more even the feeding grid developed across the zoarial obverse surface by the lophophores. Measurements **A** and **B** more commonly approach each other than do measurements of **C**. Trivial names corresponding to assigned species number are given in Table 47.

on species both with stylets and without. Following the observations presented in previous paragraphs, as chamber volume increases and therefore a larger polypide occupies the chamber, an increase in mouth and lophophore diameter is expected.

Text-figures 29 and 30 plot calculated mouth diameter (based on 0.4 × aperture minimum dimension) and calculated lophophore diameter (based on 1.5 × closest aperture spacing), respectively, against autozooecial chamber volume. In Text-figure 29, a grouping of inferred mouth diameters between 0.025 and 0.040 mm is found at chamber volumes of between 0.0025 and 0.0080 mm^3, with the remainder exhibiting steady increase of inferred mouth diameter (0.4 × aperture minimum dimension) and corresponding chamber volumes. Text-figure 30 exhibits a grouping of inferred lophophore diameters in the lower chamber-volume ranges, between 0.0025 and 0.0080 mm^3, with a steady increase in inferred lophophore diameter (1.5 × closest aperture spacing) corresponding to increasing chamber volumes. Correspondence of species exhibiting increases in both apparent mouth diameter (*i.e.*, aperture size) and inferred lophophore diameter (*i.e.*, aperture spacing) with increase in chamber volume is extremely good, fitting the observation in modern species that increase in lophophore and mouth diameter occur together. Text-figures 29A and 29C exhibit similar patterns resulting from similar niche placement of different species between the northern and southern areas, as do Text-figures 30A and 30C. Trends in species character of this type suggest niche replacement by species in essentially the same community between the northern and southern parts of the study area. Although species composition of the community has changed, niche positioning within the community does not appear to have changed appreciably.

Within the Warsaw's meshwork fenestrate dominated communities, niche differentiation could have occurred on two levels:

1. Position within the physical environment, including both height above the sea floor and location relative to direction of current flow. Ausich (1978, 1980) considered height above the sea floor to be significant in Mississippian crinoid niche differentiation. Height

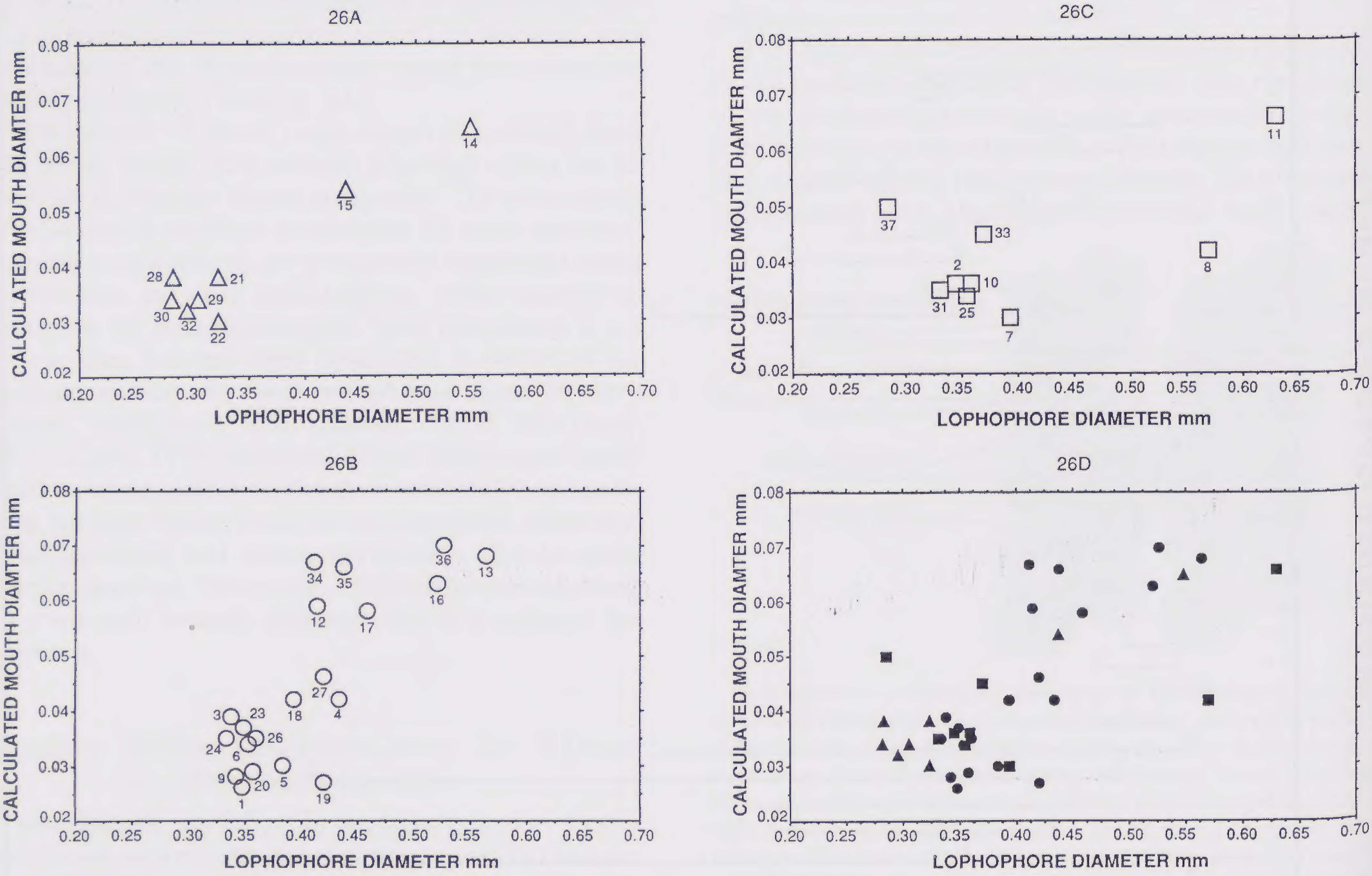

Text-figure 26.—Relationship of mouth diameter (calculated as 40% of minimum aperture diameter) to lophophore diameter (calculated as 1.5 × closest aperture spacing) for Warsaw meshwork fenestrates. The general trend of increased mouth diameter appears as a function of increased lophophore diameter in most species. Species numbers correspond to those on Table 47, which also shows their names. **A**, species occurring only in the northern half of the study area (species numbers enclosed by △); **B**, species occurring throughout the study area (species numbers enclosed by ○); **C**, species occurring only in the southern half of the study area (species numbers enclosed by □); **D**, all species.

is of more minor significance among the Warsaw fenestrates as zooecia are of uniform size throughout the zoarium, and thus do not exhibit the vertical stratification suggested by Ausich for the crinoids.

2. Competition for available food resources. Food size selection, considered secondary by Ausich in crinoid communities, is herein considered the dominant means of trophic structuring in Warsaw fenestrate communities.

Among modern suspension-feeding assemblages, trophic structuring is suggested by broad interspecific variation among organisms dependent on a common food supply (Winston, 1977), consisting of phytoplankton varying in size but generally under 50 μm in diameter. Further, increased food-gathering capabilities and ability to assimilate larger size food particles in modern species are associated with larger individual polypides and their enclosing zooecium.

Zoaria of different Warsaw species exhibiting similarity in some physical characteristics (*i.e.*, height, width, robustness, and — as can best be determined — orientation to each other and to current direction) express pronounced differences in zooecial skeletal dimensions and shapes, which suggests different polypide sizes and/or shapes. Zooecia with larger chamber dimensions are associated with characters interpreted to allow the individual greater food gathering capability; such increased capability is directly related to the ability of the individual polypide to assimilate larger size food particles in modern species. Consequently, partitioning of resources based on food particle size appears to have occurred in Warsaw meshwork fenestrates.

Where taxa of similar zooecial morphologies are sympatric, differences such as behavior with regard to suspended particles, feeding height, and positioning across the sea floor relative to current direction could have been significant. Understanding what effects these differences could produce on niche differentiation in modern bryozoans might allow their use as an analogue for fossils; however, such studies have not been undertaken.

Schoener (1974) observed that although species sim-

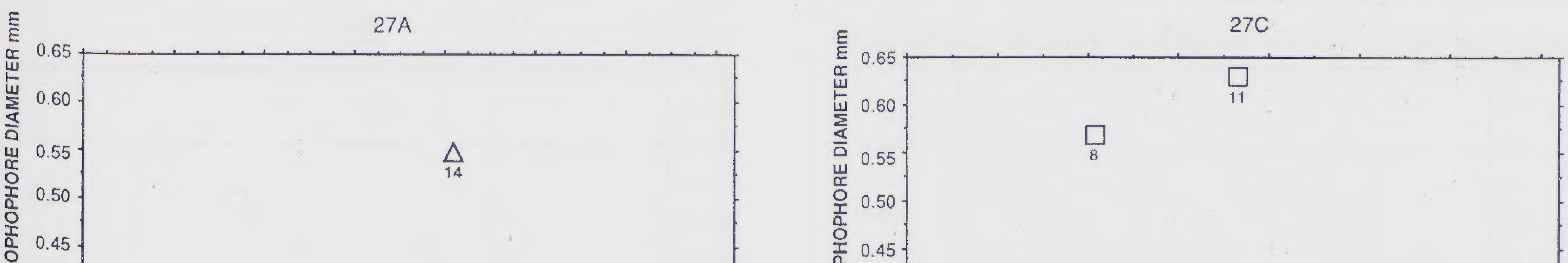

Text-figure 27.—Relationship between tentacle length (= lophophore diameter) and tentacle number (= number of apertural stylets) for the 17 species of Warsaw meshwork fenestrates that bear apertural stylets. Species numbers correspond to those in Table 47, which also shows their names. **A**, species occurring only in the northern half of the study area (species numbers enclosed by △); **B**, species occurring throughout the study area (species numbers enclosed by ○); **C**, species occurring only in the southern half of the study area (species numbers enclosed by □); **D**, all 17 species.

ilarities exist in one of several dimensions, dissimilarities can and frequently do exist in others. Although height above the sea floor and orientation to direction of currents are observed in some individuals and appear significant to niche differentiation, the difficulty in gathering precise data which yield significant confidence in their application to a species population prohibits use of this in any but a broad sense.

CONCLUSIONS

Winston (1977) demonstrated that bryozoan species within a fauna specialize in food based on particle size, with a correlation between particle size and mouth size. Mouth dimension is considered critical by Winston in determining niche differentiation. Clearance rate (based on tentacle length and tentacle number), when considered in conjunction with lophophore diameter and zooecial character (predominantly dimensions), were proposed to be factors in partitioning of resources by different modern species. From Winston's work, increased clearance rate is associated with increased mouth and lophophore diameters, which in turn occur in conjunction with increased chamber volume in modern species. Intraspecific consistency of the above features is great; however, great interspecific variability commonly exists, suggesting trophic structuring. Further, consistent trends of increased polypide size and clearance rate associated with increased mouth size and thus increased size of food particle assimilable indicate that polypide size and clearance rate are parameters also worth considering when determining possible niche differentiation between modern species.

Parameters applied to modern species can be interpreted for Paleozoic meshwork fenestrates in the following manner, based on analysis of and comparison to modern cheilostomes:

1. mouth diameter = 0.4 × minimum aperture dimensions or 0.1 × lophophore diameter.
2. lophophore diameter = 1.5 × closest aperture spacing across the zoarial surface.
3. tentacle length ≈ lophophore diameter.
4. polypide size ≈ autozooecial chamber volume.
5. tentacle number = number apertural stylets (where present).

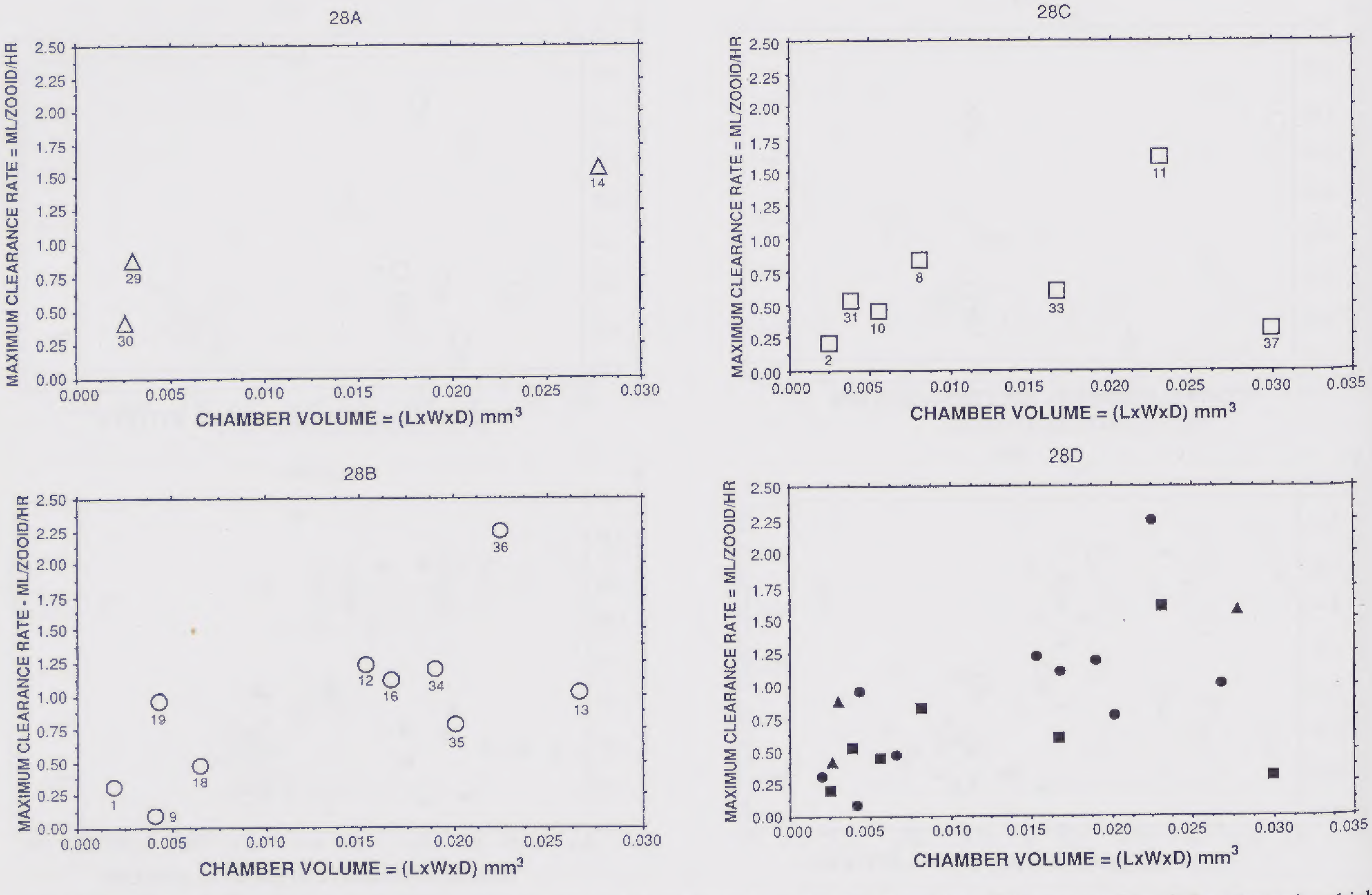

Text-figure 28.—Relationship of maximum clearance rate and chamber volume for the 17 species of Warsaw meshwork fenestrates in which number of tentacles can be indirectly determined. Observe the moderately good correlation between chamber volume and clearance rate in the species analyzed. Species numbers correspond to those shown in Table 47, which also shows their names. **A**, species occurring only in the northern half of the study area (species numbers enclosed by △); **B**, species occurring throughout the study area (species numbers enclosed by ○); **C**, species occurring only in the southern half of the study area (species numbers enclosed by □); **D**, all 17 species.

Table 50.—Calculated tentacle lengths, clearance rates, and chamber volumes for species with determinable tentacle numbers, in order of increasing chamber volume. Explanations of species numbers are shown in Table 47.

species number	*tentacle number*	*tentacle length* (cm)	*maximum clearance rate* (ml/ hr/zooid)	*chamber volume* (mm^3)
1	6.42	0.0347	0.31	0.0019
2	4.33	0.0345	0.21	0.0024
30	10.50	0.0282	0.41	0.0026
29	20.58	0.0305	0.88	0.0030
31	11.50	0.0330	0.53	0.0038
9	2.00	0.0341	0.10	0.0041
19	16.28	0.0420	0.96	0.0043
10	9.00	0.0359	0.45	0.0055
18	8.58	0.0393	0.47	0.0065
8	10.42	0.0569	0.83	0.0081
12	21.08	0.0414	1.22	0.0153
33	11.58	0.0369	0.60	0.0166
16	15.21	0.0521	1.11	0.0167
34	20.67	0.0411	1.19	0.0190
35	12.67	0.0437	0.78	0.0201
36	30.50	0.0527	2.25	0.0225
11	18.29	0.0629	1.61	0.0230
13	12.96	0.0564	1.02	0.0267
14	20.25	0.0548	1.55	0.0278
37	7.75	0.0285	0.31	0.0299

The same proportional size increases present in modern species are observed in Warsaw meshwork fenestrates, and thus based on these calculations, trophic structuring appears to have existed among these fossils. Predominance of a single group of organisms, in this case meshwork fenestrates, using similar food sizes at a time when predation levels were presumed small, sugests interspecific competition for food resources leading to niche differentiation.

The difficulties biologists experience in defining interspecific competition and niche differentiation in modern organisms are numerous and varied (Schoener, 1974), contain many unresolved areas, and thus suggest even greater problems and pitfalls for the paleontologist. However, exceptionally well-preserved materials, such as those found in the Warsaw, can provide unexpected insight into the history of ecologic dynamics.

APPENDIX A

DESCRIPTIONS OF WARSAW FORMATION SAMPLED OUTCROPS AND LOCALITIES

Columnar sections for some localities are included

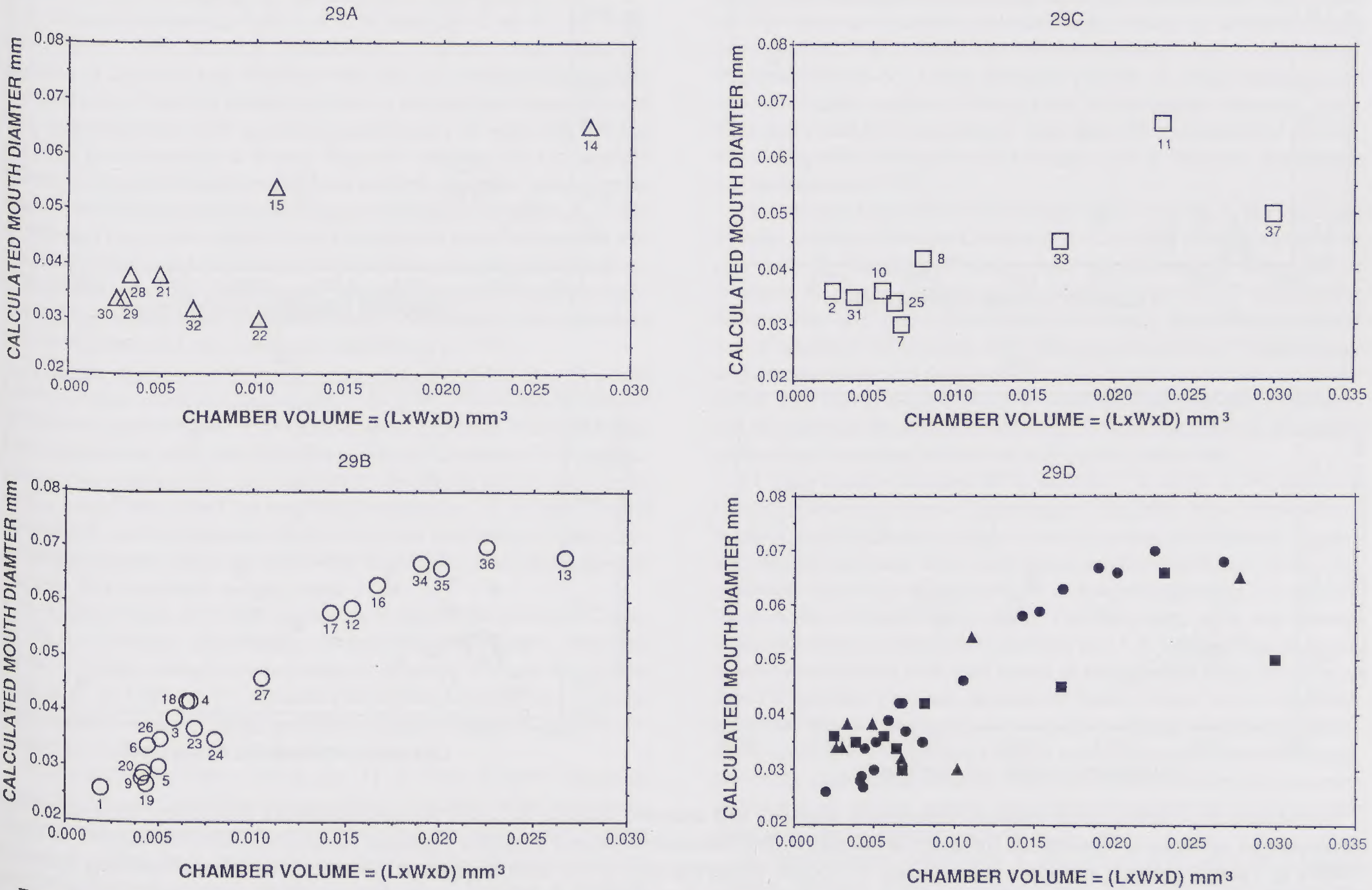

Text-figure 29.—Relationship between inferred mouth diameter and calculated chamber volume for some Warsaw meshwork fenestrates. Species numbers correspond to those shown in Table 47, which also gives their names. **A**, species occurring only in the northern half of the study area (species numbers enclosed by △); **B**, species occurring throughout the study area (species numbers enclosed by ○); **C**, species occurring only in the southern half of the study area (species numbers enclosed by □); **D**, all species.

as Appendix B; these sections were used for analysis of faunal occurrence. Brief lithologic descriptions are provided here for sections not so illustrated.

1. Augusta Northwest. W ½ NE ¼, sec. 8, T. 69 N., R. 4 W., Des Moines County, Iowa (no quadrangle map available at time of study). Section described by Harris and Parker (1964), exposed on north side of dirt road approximately 4 mi west of Augusta, Iowa. Measured from stream base and correlated with road cut following resistant bed connecting the two. Exposure consists of 7′ Keokuk (cherty, crinoidal, and bryozoan biocalcarenite interbedded with thin shale) conformably overlain by 24′ Warsaw (fossiliferous argillaceous shale and thin calcarenitic beds containing abundant bryozoan skeletal debris). Keokuk–Warsaw contact picked on change in lithology from moderately massive calcarenite to predominantly argillaceous shale with calcarenite interbeds. Exposure moderately overgrown and fossils leached. Possibly 14″ overgrown and very poorly preserved Sonora (Spergen) unconformably overlying Warsaw. Sonora a cross-bedded calcareous sandstone.

2. Bentonsport, Iowa. SE ¼ SE ¼, sec. 35, T. 69 N., R. 9 W., Van Buren County, Iowa. Bonaparte Quadrangle, 1:24,000; 1968. From downtown Bentonsport, proceed two blocks northwest, then right and proceed four blocks northeast. Section measured exposed in ditch along east side of road cut toward top of hill. Exposure consists of 14′ Keokuk (fairly massive, crinoidal calcarenite) conformably overlain by approximately 6′ of Warsaw (interbedded lenticular bryozoan calcarenite with argillaceous shale). Keokuk–Warsaw contact picked on lithologic change from crinoidal calcarenite to lenticular bryozoan calcarenite interbedded with argillaceous shale. Exposure fresh, fossils well-preserved and moderately abundant. See columnar section on p. 177.

3. Lacy Keosauqua. N ½ SW ¼, sec. 1, T. 68 N., R. 10 W., Van Buren County, Iowa. Keosauqua Quadrangle, 1:24,000; 1968. Two large, and numerous smaller exposures along main road leading into Lacy Keosauqua Park. Exposures measured: (1) 0.7 mi in from park entrance along small stream valley on north side of road. Exposed is 5′2″ calcareous, unfossiliferous shale (Warsaw) unconformably overlain by 16′ cross-bedded calcareous sandstone (Sonora); (2) 150 yards downstream from first exposure is found 11′8″ of unfossiliferous calcareous shale (Warsaw) containing small amounts of chert unconformably overlain by 2′4″ of cross-bedded calcareous sandstone (Sonora). Relative thicknesses of both formations vary considerably laterally due to the unconformable boundary between them. Warsaw–Sonora contact picked on abrupt lithologic change from unfossiliferous calcareous shale to cross-bedded calcareous sandstone. Exposure well-weathered and partly overgrown in stream cut.

4. Niota, Illinois. E. ½ NW ¼, sec. 17, T. 7 N., R. 8 W., Hancock County, Illinois. Niota Quadrangle, 1:24,000, 1964. Section exposed along west bank of stream valley on road southeast of Niota, Illinois. Measured section starts 50′ upstream from power lines crossing road

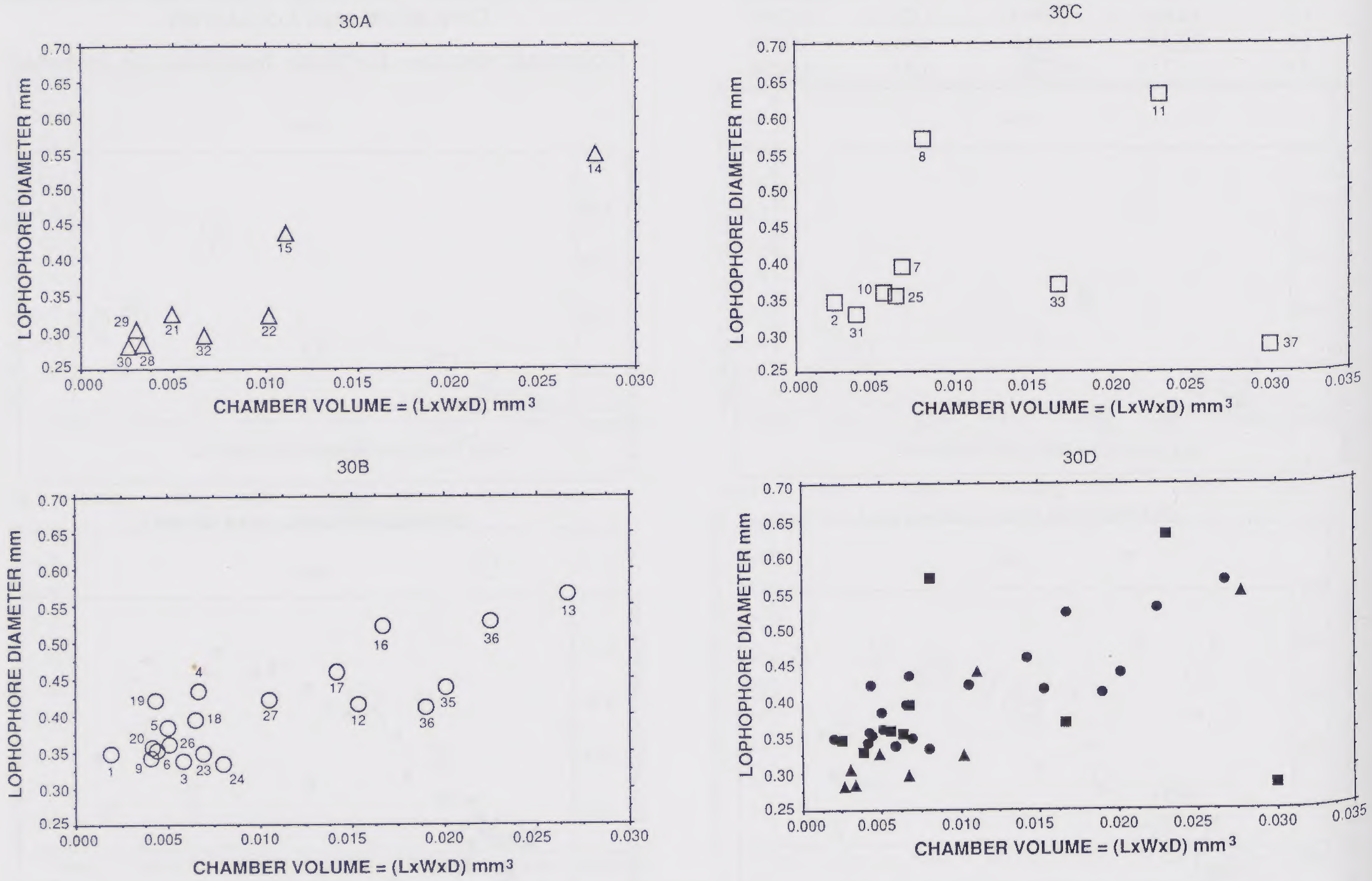

Text-figure 30.—Relationship between lophophore diameter and chamber volume for some Warsaw meshwork fenestrates. As with mouth diameter, an increase in lophophore diameter is normally observed with increased chamber volumes. Species numbers correspond to those shown in Table 47, which also gives their names. **A**, species occurring only in the northern half of the study area (species numbers enclosed by ; △); **B**, species occurring throughout the study area (species numbers enclosed by ○); **C**, species occurring only in the southern half of the study area (species numbers enclosed by □); **D**, all species.

and extending up stream valley for approximately ½ mi. Exposure consists of 42′ Warsaw (unfossiliferous to locally fossiliferous calcareous and argillaceous shale interbedded and locally containing abundant small geodes) conformably overlain by 6′ Spergen (massive laminated and cross-bedded silty dolostone probably representing channel deposits and silty calcareous shale) unconformably overlain by thin conglomeratic zone consisting of Spergen and St. Louis lithic clasts, topped by approximately 2′ of bedded St. Louis Limestone. Contacts picked on the lithic changes described above. Although exposure moderately fresh where cut by stream, fossils are highly leached and poorly preserved.

5. Iowa Terminal. NW ¼ SW ¼, sec. 19, T. 66 N., R. 5 W., Lee County, Iowa. Keokuk Quadrangle, 1:24,000; 1964. Section exposure along railroad tracks and roadway cut in cliff along Mississippi River for grain terminal. Section measurement starting 150 yards south of road crossing railroad tracks; measurements carried to excellent exposure in cliff along roadcut to the south side of the road. Exposure consists of 15¾′ of Keokuk (cherty, crinoidal biocalcarenite) conformably overlain by 52½′ of Warsaw (bryozoan biocalcarenite interbedded with argillaceous shale and thick accumulations of argillaceous shale locally containing dolomitic and geodiferous zones) conformably overlain by 8′ of Sonora (massive lamellar and cross-bedded calcareous sandstone with thin shale interbeds), which is in turn overlain unconformably by highly weathered St. Louis Limestone (calcilutite varying in thickness from 2′ to 23′). Keokuk–Warsaw contact picked on pronounced increase in argillaceous shale (dominant over calcarenites, which characterize the Keokuk). Warsaw–Sonora and Sonora–St. Louis contacts picked on abrupt lithologic changes and unconformable nature of the contacts. Exposure very fresh, highly fossiliferous, with skeletal debris generally well-preserved; excellent outcrop. See columnar section on p. 177.

6. Keokuk Industrial. SW ¼ NW ¼, sec. 35, T. 65 N., R. 5 W., Lee County, Iowa. Keokuk Quadrangle, 1:24,000; 1964. Good exposures of Keokuk and Warsaw west of river road along Keokuk industrial area. Section measured directly across from Foote Mineral Co., approximately 100′ north of transformers on west side of road south of main entrance to Foote. Exposure consists of 21½′ Keokuk (cherty, crinoidal biocalcarenite interbedded with thin beds of bryozoan fossiliferous argillaceous shale) conformably overlain by 29.3′ of Warsaw (bryozoan fossiliferous argillaceous shale, calcareous fossiliferous shale, and thin beds of fossiliferous biocalcarenite). Keokuk–Warsaw contact picked where argillaceous shale becomes dominant lithic component. Exposure fresh, with fossils both abundant and well-preserved. See columnar section on p. 177.

7. White Hollow. NW ¼ SE ¼, sec. 26, T. 65 N., R. 5 W., Lee County, Iowa. Keokuk Quadrangle, 1:24,000; 1964. Good exposure of Warsaw on north side of streamcut approximately ½ mi upstream from its joining with the Mississippi River. Consists of 32′ argillaceous shale, calcarenite, and calcilutite containing geodes and cherty lenses on the bottom of the exposure overlain by 11′ of fossiliferous calcarenite and argillaceous shale. Exposure moderately fresh, containing abundant, although frequently slightly leached, fauna toward the top. See columnar section on p. 178.

8. Keokuk West. SE ¼ NE ¼, sec. 33, T. 65 N., R. 5 W., Lee County, Iowa. Keokuk Quadrangle, Illinois–Iowa–Missouri, 1:24,000; 1964. Partially overgrown exposure of Warsaw in roadcut on west side of U. S. Highway 61 at north end of Des Moines River bridge. Exposure consists of 24′ of geodiferous shale interbedded with argillaceous dolomite and calcarenite.

9. Grays Quarry. SW ¼ NE ¼, sec. 31, T. 5 N., R. 8 W., Hancock County, Illinois. Hamilton Quadrangle, 1:24,000; 1964. Measured section taken in northeastmost corner of quarry along road leading up north quarry face; measurement started approximately 5′ below Keokuk–Warsaw contact, however, over 80′ of Keokuk is exposed in the quarry. Warsaw consists of 39¾′ of predominantly unfossiliferous, geodiferous argillaceous dolomicrite, micrite, calcarenite, and shale. A small number of bryozoan fragments are observed in thinly bedded calcarenite present toward the top of the measured section. Keokuk–Warsaw contact picked where massive calcarenite is conformably overlain by argillaceous geodiferous dolomicrite. Exposure is very fresh, but fossil fragments are frequently leached and poorly preserved. See columnar section on p. 178.

10. Hamilton–Warsaw Roadcut. S ½ NE ¼, sec. 2, T. 4 N., R. 9 W., Hancock County, Illinois. Warsaw Quadrangle, 1:24,000; 1964. Excellent exposure of Keokuk and Warsaw on east side of Hamilton–Warsaw road, extending along road uphill from stream valley to entrance to Kibbe Station. Exposure consists of over 80′ of Keokuk conformably overlain by Warsaw. Measured section includes upper 18′ of Keokuk (massive cherty biocalcarenite) overlain by approximately 38′ Warsaw (argillaceous fossiliferous and unfossiliferous shale with thin beds and lenses of highly bryozoaniferous biocalcarenite). Keokuk–Warsaw contact picked where change in dominant lithic type from cherty biocalcarenite to argillaceous shale occurs. Exposure moderately fresh along roadcut, with fossils well-preserved and abundant, but large spalled slabs atop shale starting to cover lower shale. See columnar section on p. 179.

11. Geode Glen (type section of the Warsaw). SE ¼, sec. 4, NE ¼ NE ¼, sec. 9, and NW ¼, sec. 10, T. 4 N., R. 9 W., Hancock County, Illinois. Warsaw Quadrangle, 1:24,000; 1964. Warsaw, Sonora, and St. Louis formations exposed in stream valley (Geode Glen) at north edge of Warsaw, extending upstream to south side of highway. Warsaw at this locality informally divided into lower and upper members by Ulrich (1890); such a division does not appear appropriate and is not followed herein. Exposure consists of 74′ Warsaw (bottom 40′ argillaceous geodiferous dolomicrite occurring in moderately thick beds interbedded with dolomitic argillaceous shale; upper 34′ consists of fossiliferous argillaceous shale with beds of fossiliferous biocalcarenite and argillaceous biocalcarenite), unconformably overlain by 5.3′ Sonora (massive biocalcarenite) which is unconformably overlain by 3.3′ St. Louis (massive cherty micrite, locally brecciated). Warsaw–Sonora–St. Louis contacts picked on lithic changes and unconformable surfaces. Moderately well-exposed outcrop; however, beds had to be correlated upstream for continuity of section. Fossil fragments well-preserved in upper 34′ of Warsaw. See columnar section on p. 179.

12. Warsaw East. SW ¼ NW ¼, sec. 4, T. 4 N., R. 9 W., Hancock County, Illinois. Warsaw Quadrangle, 1:24,000; 1964. Exposure on east side of Hamilton–Warsaw road approximately ½ mi east of Warsaw. Exposure consists of 40′ Warsaw; bottom 20′ argillaceous dolomicrite and shale, becoming increasingly fossiliferous toward top of upper 20′ of section, with lithology consisting of fossiliferous argillaceous shale and thin fossiliferous biocalcarenitic beds and lenses. At very top of section occur several beds that appear to be channel-fill deposits. Exposure moderately fresh along roadcut, but much of the fossil material is leached and poorly preserved.

13. Soap Factory Hollow. SE ¼, sec. 16, T. 4 N., R. 9 W., Hancock County, Illinois. Warsaw Quadrangle, 1:24,000; 1964. Exposure of Keokuk and Warsaw in stream valley ½ mi south of Warsaw. Section started just upstream from farm house at end of dirt road, measured upstream. Exposure consists of 31′ of Keokuk (massive to medium-thick beds of fossiliferous cherty biocalcarenite with argillaceous shale interbeds) conformably overlain by 19.3′ Warsaw (fossiliferous biocalcarenitic thin beds and lenses in argillaceous shale; number of fossil fragments reduced, geodes in shale toward top of section). Keokuk–Warsaw contact picked where overlying shale becomes the dominant lithic component relative to the cherty biocalcarenite typical of the underlying Keokuk. Exposure highly weathered, occurring in bottom of stream valley; hand-level required to correlate beds upstream. See columnar section on p. 180.

14. Buel Branch. NE ¼ SW ¼, sec. 13, T. 2 N., R. 9 W., Adams County, Illinois. Mendon Quadrangle, 1:62,500; 1946. Good exposure on north side of road following Buel Branch to the Mississippi flood plain. Exposure consists of 7.7′ of Keokuk (massive cherty biocalcarenite) conformably overlain by 14.9′ of Warsaw (argilla-

ceous and calcareous shale with fossiliferous biocalcarenitic beds). Keokuk–Warsaw contact picked on break in lithic type from massive cherty biocalcarenite to predominantly shale. Moderately fresh exposure in roadcut, fossil fragments fairly well-preserved. See columnar section on p. 180.

15. Sand Branch. SW ¼ NW ¼, sec. 28, T. 1 N., R. 8 W., Adams County, Illinois. Mendon Quadrangle, 1:62,500; 1946. Exposure of Salem and Warsaw in abandoned quarry along Sand Branch Creek. Section measured in middle of south quarry face. Exposure consists of 17.9′ of typical Salem (massive laminated and cross-bedded biocalcarenite) conformably overlain by and interbedded with 5′ of typical Warsaw (fossiliferous argillaceous shale with thin lenses of biocalcarenite). This section gives no appearance of being overturned, and is an example of contemporaneous nature of Salem (Sonora) and Warsaw deposition in the northern part of the study area. Salem–Warsaw contact is picked on break in lithic type from massive biocalcarenite to fossiliferous shale. Exposure partially overgrown; however, fossils found in the Warsaw are complete with excellent preservation of fine detail. See columnar section on p. 180.

16. La Grange. E ½ SW ¼, sec. 35, T. 61 N., R. 6 W., Lewis County, Missouri. La Grange Quadrangle, 1:24,000; 1950. Good exposure of Keokuk, Warsaw, and Salem in roadcut ½ mi west of U. S. Highway 61; section measured on east side of highway. Exposure consists of 15¾′ Keokuk (moderately massive fossiliferous cherty biocalcarenite with thin argillaceous shale interbeds) conformably overlain by 22¾′ of Warsaw (locally fossiliferous argillaceous shale and calcareous shale, both with thin dolomicritic lenses), which is unconformably overlain by 6.9′ of Salem (massive lamellar and cross-bedded cherty and silty dolocalcarenite). Keokuk–Warsaw contact is picked on change in lithic type from cherty biocalcarenite to predominantly argillaceous shale. Warsaw–Salem contact is based on lithic change from argillaceous shale to dolocalcarenite. Roadcut probably 20 years old, moderately weathered. Fossil debris frequently highly leached and poorly preserved. See columnar section on p. 181.

17. Canton, Missouri – A. SE ¼ NE ¼, sec. 36, T. 62 N., R. 6 W., Lewis County, Missouri. La Grange Quadrangle, 1:24,000; 1950. Section measured in roadcut 1 mi south of Canton exit on U. S. Highway 61, exposed on east side of road. Exposure consists of 12.2′ of Keokuk (cherty fossiliferous biocalcarenite) conformably overlain by 3.2′ of Warsaw (argillaceous shale and dolocalcarenite). Keokuk–Warsaw contact picked on lithic change from biocalcarenite to predominantly shale and dolocalcarenite. Best exposed of Canton outcrops, containing moderately well-preserved fossil fragments.

18. Canton, Missouri – B. NW ¼ NE ¼, sec. 33, T. 62 N., R. 6 W., Lewis County, Missouri. La Grange Quadrangle, 1:24,000; 1950. Section measured in roadcut 1 mi south of Canton exit on U. S. Highway 61, exposed on east side of road. Exposure consists of 7.8′ of Keokuk (cherty fossiliferous biocalcarenite) conformably overlain by 2.4′ of Warsaw (argillaceous shale and dolocalcarenite). Keokuk–Warsaw contact picked on lithic change from biocalcarenite to predominantly shale. Although a partially overgrown and moderately old exposure, fossil fragments are well-preserved.

19. Canton, Missouri – C. NW ¼ SE ¼, sec. 33, T. 62 N., R. 4 W., Lewis County, Missouri. La Grange Quadrangle, 1:24,000; 1950. Section measured in roadcut on east side of U. S. Highway 61, 1.4 mi south of Canton exit. Exposure consists of 3.3′ of Keokuk (cherty biocalcarenite with thin shale interbeds) conformably overlain by 23.7′ of Warsaw (geodiferous unfossiliferous argillaceous and calcareous shales), which is unconformably overlain by 3′ of Salem (massive fossiliferous cross-bedded biocalcarenite). Keokuk–Warsaw contact based on lithic change from cherty biocalcarenite to geodiferous argillaceous and calcareous shale. Warsaw–Salem contact picked on unconformable break between the shale and massive cross-bedded biocalcarenite. Exposure moderately well-weathered and overgrown, with some Warsaw shale covered.

20. Mount Sterling. NE ¼ SE ¼, sec. 24, T. 2 S., R. 4 W., Brown County, Illinois. Mount Sterling Quadrangle, 1:62,5000; 1926. Excellent section of Warsaw 200 yards upstream from bridge crossing McKee Creek. Exposure consists of 23.6′ of Warsaw (fossiliferous argillaceous shale with biocalcarenitic beds toward bottom and lenses toward top of section). Shale and biocalcarenitic beds and lenses contain abundant and extremely well-preserved bryozoan fossils. Exposure in cut bank of stream and although fresh, the upper shale is covering the lower calcarenitic beds in many places. See columnar section on p. 181.

21. McKee Creek. Middle SE ¼, sec. 19, T. 2 S., R. 3 W., Brown County, Illinois. Mount Sterling Quadrangle, 1:62,500; 1926. Exposure in bank of small stream south of and emptying into McKee Creek, section measured upstream. Warsaw and Salem interdigitating at this locality (all grouped under Warsaw in section). Exposure consists of 9.9′ of Warsaw (calcareous argillaceous shale) unconformably overlain by 8.7′ of Salem (fossiliferous cross-bedded biocalcarenite) conformably overlain by 7.7′ of Warsaw (as below), which is in turn unconformably overlain by 10.7′ of Salem (as below). No faulting or folding is evident, so the above relationships appear depositional in origin. Contacts are based on lithic changes from shale for the Warsaw to biocalcarenite for the Salem. Exposure highly weathered and although fossil debris is abundant, much of it is leached. See columnar section on p. 181.

22. Versailles West. SW ¼ NE ¼. sec. 24, T. 2 S., R. 3 W., Brown County, Illinois. Meredosia Quadrangle, 1:62,500; 1928. Measured section in roadcut on north side of dirt road going west from Versailles. Section consists of 25.3′ of Warsaw (argillaceous and calcareous shale containing moderately thick interbeds of biocalcarenite and dolocalcarenite, many of which are geodiferous). Collinson *et al.* (1962) refer to the section as Sonora, due to the presence of biocalcarenite and dolocalcarenite beds, but it appears these beds are channels developed in the Warsaw. Section moderately to highly overgrown, with many fossil fragments leached and poorly preserved. See columnar section on p. 182.

23. Little Whitaker Creek. NE ¼ SE ¼, sec. 25, T. 11 N., R. 12 W., Greene County, Illinois. Roodhouse Quadrangle, 1:62,500; 1924. Exposure along north bank of Little Whitaker Creek, 50′ upstream from blacktop road over stream. Outcrop consists of 10.6′ of typical Warsaw (fossiliferous argillaceous and calcareous shale interbedded with fossiliferous biocalcarenitic beds, many of which are laterally discontinuous). Exposure moderately overgrown, with many fossil fragments partially leached. See columnar section on p. 182.

24. White Hall – A. NW ¼ NE ¼, sec. 25, T. 11 N., R. 12 W., Greene County, Illinois. Roodhouse Quadrangle, 1:62,500; 1924. Exposure in Whitaker Creek stream bottom. Outcrop consists of approximately 4′ of Warsaw (argillaceous biocalcarenite with fine interbeds of argillaceous shale). Highly weathered exposure with a few fossils present; however, most are leached and poorly preserved.

25. White Hall – B. NE ¼ SE ¼, sec. 25, T. 11 N., R. 12 W., Greene County, Illinois. Roodhouse Quadrangle, 1:62,500; 1924. Exposure in stream bed of Whitaker Creek. Outcrop consists of 3.5′ of typical lower Warsaw (fossiliferous biocalcarenite with thin argillaceous interbeds). Moderately weathered exposure, although the abundant bryozoan fossils are well-preserved.

26. White Hall – C. Middle SE ¼, sec. 25, T. 11 N., R. 12 W., Greene County, Illinois. Roodhouse Quadrangle, 1:62,500; 1924. Exposure in stream bed of Whitaker Creek. Outcrop consists of 8.2′ of typical Warsaw (medium- to thin-bedded bryozoan biocalcarenite interbedded with argillaceous shale). Good, although moderately weathered, exposure; well-preserved abundant bryozoan fossils. See columnar section on p. 182.

27. White Hall – D. SE ¼ SW ¼, sec. 31, T. 11 N., R. 11 W., Greene County, Illinois. Roodhouse Quadrangle, 1:62,500; 1924. Exposure in stream bed of Whitaker Creek approximately ¼ mi south of county road bridge crossing stream. Outcrop consists of 19.3′ of

typical lower Warsaw (slightly geodiferous medium- to thin-bedded biocalcarenite turning to geodiferous argillaceous shale upsection). Exposure moderately overgrown; fossils rare, frequently poorly preserved due to freshwater leaching of calcite. See columnar section on p. 182.

28. White Hall – E. SE ¼ NW ¼, sec. 31, T. 11 N., R. 11 W., Greene County, Illinois. Roodhouse Quadrangle, 1:62,500; 1924. Exposure 100 yards south of small bridge across Whitaker Creek. Outcrop consists of 2.5′ of typical lower Warsaw in stream valley (fossiliferous biocalcarenite with thin argillaceous interbeds, small amount of geode float in stream). Moderately weathering exposure in bottom of stream valley containing well-preserved fossil debris.

29. White Hall – F. SE ¼ NE ¼, sec. 25, T. 11 N., R. 12 W., Greene County, Illinois. Roodhouse Quadrangle, 1:62,500; 1924. Good exposure in stream bed of Whitaker Creek. Outcrop consists of 12.1′ of lower Warsaw (predominantly geodiferous argillaceous shale interbedded with medium beds and lenses of bryozoaniferous biocalcarenite). Fresh exposure containing both bryozoan fossils and geodes in the lower biocalcarenite and shale, a combination of occurrences rare in the Warsaw. See columnar section on p. 182.

30. White Hall – G. NW ¼ SE ¼, sec. 2, T. 11 N., R. 12 W., Greene County, Illinois. Roodhouse Quadrangle, 1:62,500; 1924. Exposed on north bank of Seminary Creek, section measured 50 yards east of Highway 167 bridge. Outcrop consists of 9.9′ of lower Warsaw (fossiliferous cherty biocalcarenite containing moderately abundant chert nodules and interbeds; thin argillaceous shale interbeds also present). Highly weathered exposure, fossils leached and poorly preserved.

31. White Hall – H. W ½, sec. 11, T. 11 N., R. 12 W., Greene County, Illinois. Roodhouse Quadrangle, 1:62,500; 1924. Exposure in stream bed of Seminary Creek 200 yards east of Highway 167; outcrop on both sides of stream. Outcrop consists of 3.4′ of Keokuk (massive crinoidal biocalcarenite) conformably overlain by 11.8′ of lower Warsaw (bryozoaniferous cherty biocalcarenite interbedded with thin bands of fossiliferous argillaceous shale). Exposure moderately fresh. Although some fossils are slightly leached, many others are extremely well-preserved.

32. Carrollton, Illinois. NE ¼ SW ¼, sec. 35, T. 9 N., R. 12 W., Greene County, Illinois. Roodhouse Quadrangle, 1:62,500; 1924. Outcrop consists of 3.8′ of Warsaw (unfossiliferous calcareous argillaceous shale) unconformably overlain by 10.4′ of typical Salem (massive biocalcarenite with few fine shale interbeds). Exposure moderately weathered.

33. Benchmark on State Highway 369. NW ¼, sec. 26, T. 14 N., R. 13 W., Scott County, Illinois. Brighton Quadrangle, 1:62,500; 1925. Exposure in roadcut on north side of State Highway 369, extending approximately 100 yards along highway. Exposure consists of 2.4′ of Warsaw (unfossiliferous argillaceous shale) unconformably overlain by 8.1′ of Salem (massive cross-bedded biocalcarenite). Moderately weathered exposure with bioclasts highly leached.

34. Otter Branch. W ½ SE ¼, sec. 12, T. 7 N., R. 11 W., Jersey County, Illinois. Jerseyville Quadrangle, 1:62,500; 1930. Exposure in stream bottom of small stream emptying into Otter Creek; section measured from north to south, upstream in stream bottom. Outcrop consists of 11.8′ of Keokuk (cherty crinoidal biocalcarenite with thin argillaceous shale interbeds) conformably overlain by 21½′ of Warsaw (fossiliferous argillaceous shale interbedded with medium thickness to lenses of cherty bryozoan biocalcarenite). Although moderately weathered and poorly exposed, bryozoan fossils are moderately well-preserved, particularly in the upper shale. See columnar section on p. 183.

35. McClusky West. NE ¼ SW ¼, sec. 18, T. 7 N., R. 11 W., Jersey County, Illinois. Jerseyville Quadrangle, 1:62,500; 1930. Exposure along north fork of Otter Creek, north–south trending on west side of stream immediately south of road crossing stream. Outcrop consists of 2.4′ of Warsaw (argillaceous shale) unconformably overlain by 4′ of Salem (massive cross-bedded biocalcarenite). Outcrop moderately highly weathered and overgrown in stream valley.

36. South Fork Otter Creek. NE ¼ NW ¼, sec. 17, T. 7 N., R. 11 W., Jersey County, Illinois. Jerseyville Quadrangle, 1:62,500; 1930. Exposure along south fork of Otter Creek, along east–west running section of stream in stream bottom. Outcrop consists of 1.8′ of Warsaw (argillaceous shale) unconformably overlain by 2.9′ of Salem (fossiliferous biocalcarenite). Exposure highly weathered.

37. Briggs Branch. SW ¼ NW ¼, sec. 10, T. 6 N., R. 11 W., Jersey County, Illinois. Jerseyville Quadrangle, 1:62,500; 1954. Exposure in small stream bed along dirt road, much of section covered. Outcrop consists of approximately 24′ of Keokuk (cherty fossiliferous biocalcarenite) conformably overlain by 6.2′ of Warsaw (fossiliferous argillaceous shale interbedded with bryozoan biocalcarenite). Exposure highly weathered and partially covered, with fossil debris frequently leached.

38. Piasa Creek. N ½ SW ¼, sec. 13, T. 6 N., R. 11 W., Jersey County, Illinois. St. Charles Quadrangle, 1:62,500; 1954. Exposure in roadcut along cutbank of bend in Piasa Creek, extended to quarry ¼ mi east of road outcrop. Outcrop consists of 31.7′ of Warsaw (geodiferous argillaceous and calcareous shale interbedded with medium to thick beds of dolocalcarenite and dolocalcilutite) unconformably overlain by 43′ of Salem (extremely massive fossiliferous biocalcarenite with thin shale interbeds). Warsaw–Salem contact picked on change in lithology from predominantly shale to biocalcarenite. Exposure moderately weathered, with fossil debris leached and poorly preserved.

39. Cuiver River. NE ¼ NW ¼, sec. 30, T. 49 N., R. 1 E., Lincoln County, Missouri. Mary Knott Quadrangle, 1:24,000; 1972. Exposure ½ mi west of Cuiver River bridge on Highway 47, on north side of highway. Section consists of 24.2′ of Warsaw (geodiferous and nongeodiferous argillaceous and calcareous shale) apparently conformably overlain and interdigitating with 18.8′ of Salem (extremely massive cross-bedded biocalcarenite with thin shale and geodiferous dolocalcilutitic interbeds). Contact between Warsaw and Salem picked on lithic break from predominantly shale to biocalcarenite. Exposure fresh, good, although some of the Warsaw shale beds are covered.

40. Troy Roadcut. NE ¼ NE ¼, sec.25, T. 49 N., R. 1 E., Lincoln County, Missouri. Troy Quadrangle, 1:24,000; 1972. Exposure in roadcut on Highway 61 1 mi south of northern Troy exits, section measured on east side of road. Measured section consists of 3.8′ of Keokuk (fossiliferous cherty biocalcarenite) conformably overlain by 13.1′ of typical lower Warsaw (interbedded bryozoan biocalcarenite with fossiliferous argillaceous shale; local cherty areas are also present). Keokuk–Warsaw contact picked on lithic change from predominantly cherty biocalcarenite to interbedded biocalcarenite and shale. Exposure moderately fresh along roadcut, with fossil debris well-preserved. See columnar section on p. 183.

41. Moscow Mills. SW ¼ NW ¼, sec. 4, T. 48 N., R. 1 E., Lincoln County, Missouri. Troy Quadrangle, 1:24,000; 1972. Exposure ¼ mi east of Moscow Mills on main blacktop road leading to town from Highway 61, section measured along south side of road. Exposure consists of 26.2′ of Warsaw (biocalcarenite interbedded with argillaceous geodiferous shale, both of which are moderately fossiliferous). Section moderately overgrown, with fossil debris frequently poorly preserved because of leaching.

42. County Road U. SW ¼ SW ¼, sec. 31, T. 48 N., R. 1 E., Lincoln County, Missouri. Troy Quadrangle, 1:24,000; 1972. Exposure on both sides of intersection of county road U with Highway 61, section measured on west side of highway. Exposure consists of 23′ of upper Warsaw (interbedded massive biocalcarenite with argillaceous shale and dolocalcarenite). Outcrop fresh, containing an extremely well-preserved diverse bryozoan assemblage.

43. Lisbon, Missouri. NE ¼, sec. 26, T. 50 N., R. 18 W., Howard County, Missouri. Arrow Rock Quadrangle, 1:24,000; 1971. Exposure along cutbank of Missouri River ¾ mi south of Lisbon, Missouri and in an old quarry 1½ mi south of Lisbon. Outcrop consists of 18.8′ of Keokuk (cherty biocalcarenite with thin shale partings) conformably overlain by 16.7′ of lower Warsaw (fossiliferous argillaceous shale interbedded with medium beds to lenses of fossiliferous, sometimes cherty biocalcarenite). Keokuk–Warsaw contact picked on lithic change from predominantly biocalcarenite to predominantly argillaceous shale. Exposure moderately highly weathered, fossil debris fairly well-preserved.

44. Dupo Quarry. NW ¼ SW ¼, sec. 27, T. 1 N., R. 10 W., St. Clair County, Illinois. Cahokia Quadrangle, 1:24,000; 1954. Exposure on northwest face of quarry along east bluff of the Mississippi River. Exposure consists of a total of 112.8′ of Warsaw–Salem–St. Louis, with Warsaw and Salem exhibiting a gradational contact, as do the Salem and overlying St. Louis. This exposure environmentally probably represents a high-energy bank deposit which existed throughout Warsaw, Salem and St. Louis deposition. Exposure is excellent, but access is restricted and only cursorily analyzed.

45. Meramec River Bend. NW ¼ NE ¼, sec. 15, T. 44 N., R. 5 E., St. Louis County, Missouri. Kirkwood Quadrangle, 1:24,000; 1954. Exposure at sharp bend in the Meramec River, at what was once cutbank of river. Outcrop consists of 21.2′ of Keokuk (cherty crinoidal biocalcarenite with thin shale interbeds) conformably overlain by 12′ of Warsaw (fossiliferous argillaceous shale interbedded with thin biocalcarenitic lenses). Contact picked on lithic change from predominantly biocalcarenite to dominantly argillaceous shale. Outcrop highly weathered, overgrown and leached.

46. Marshall Road. SE ¼, sec. 10, T. 44 N., R. 5 E., St. Louis County, Missouri. Kirkwood Quadrangle, 1:24,000; 1954. Exposure along roadcut on Marshall Road. Outcrop consists of 28′ of Keokuk (cherty crinoidal biocalcarenite with thin argillaceous interbeds) conformably overlain by 22.4′ of Warsaw (fossiliferous argillaceous and dolomitic shale interbedded with fossiliferous biocalcarenite) unconformably overlain by 6.2′ of Salem (massive cross-bedded biocalcarenite). Keokuk–Warsaw contact picked on lithic change from predominantly biocalcarenite to argillaceous and dolomitic shale. Warsaw–Salem contact picked on distinctive lithic change from shale to massive biocalcarenite. Outcrop highly weathered, overgrown and poorly exposed.

47. Cragwold Road (A and B). SE ¼ NW ¼, sec. 14, T. 44 N., R. 5 E., St. Louis County, Missouri. Kirkwood Quadrangle, 1:24,000; 1954. Exposure is a composite of two outcrops in the northeast quadrant of the intersection of Interstate 270 and Interstate 44; lower part of section east of bridge crossing the Missouri River on I-44, upper section at northeast onramp to I-270 from I-44. Outcrop consists of 22.1′ of Keokuk (cherty biocalcarenite with argillaceous shale interbeds) conformably overlain by 35′ of Warsaw (fossiliferous argillaceous shale interbedded with cherty biocalcarenitic beds and lenses) apparently conformably overlain by 61.3′ of Salem (massive geodiferous argillaceous calcilutite and dolocalcilutite, massive cross-bedded cherty biocalcarenite, and argillaceous shale). Keokuk–Warsaw contact picked on lithic break from predominantly biocalcarenite to dominantly argillaceous shale. Warsaw–Salem contact established on lithic break from argillaceous shale to massive geodiferous argillaceous dolocalcilutite. This section is particularly well-exposed and well-preserved, having fresh surfaces and good, whole fossil debris. It is also part of the Meramecian Series stratotype. See columnar sections on p. 184.

48. Columbia Roadcut. NE ¼ SE ¼ and SE ¼ SE ¼, sec. 22; and NW ¼ SW ¼ and SW ¼ SW¼, sec. 23, T. 1 S., R. 10 W., Monroe County, Illinois. Waterloo Quadrangle, 1:62,500; 1955. Exposure in a long roadcut along Illinois Highway 3, about 1 mi south of Columbia, Illinois; measured on west side of road from north to south. Outcrop consists of 23.6′ of Warsaw (locally fossiliferous argillaceous shale with cherty and geodiferous biocalcarenitic interbeds and lenses) apparently conformably overlain by 40.2′ of Salem (massive, cross-bedded, locally cherty and geodiferous biocalcarenite with fossiliferous argillaceous and calcareous shale interbeds). Valmeyeran rocks in this section are not typical of either the Warsaw or Salem in the Illinois Basin. Warsaw–Salem contact picked on lithic change from predominantly argillaceous shale to massive biocalcarenite. Section well-exposed and fossil debris well-preserved. See columnar section on p. 183.

49. Dennis Hollow (Valmeyer). S ½, sec. 2, T. 35 N., R. 11 W., Monroe County, Illinois. Valmeyer Quadrangle, 1:24,000; 1954. Exposure on north side of Illinois Highway 156, 1.5 mi east of Valmeyer, Illinois; outcrops at two sites (A and B) along road approximately 200 yards apart. Outcrop consists of 50.8′ of Keokuk (cherty crinoidal biocalcarenite with thin argillaceous shale interbeds) conformably overlain by 18.8′ of Warsaw (fossiliferous argillaceous shale with thin biocalcarenitic beds and lenses). Keokuk–Warsaw contact picked on lithic change from crinoidal biocalcarenite to predominantly argillaceous shale. Exposure moderately fresh, containing excellent bryozoan fauna which is both diverse and extremely well-preserved. This section was studied extensively because of the excellent bryozoan fauna. See columnar sections on p. 185.

APPENDIX B

COLUMNAR SECTIONS FOR LOCALITIES INCLUDED IN THE SPECIES DISTRIBUTION STUDY

Arrows mark horizons of samples used for faunal analysis.

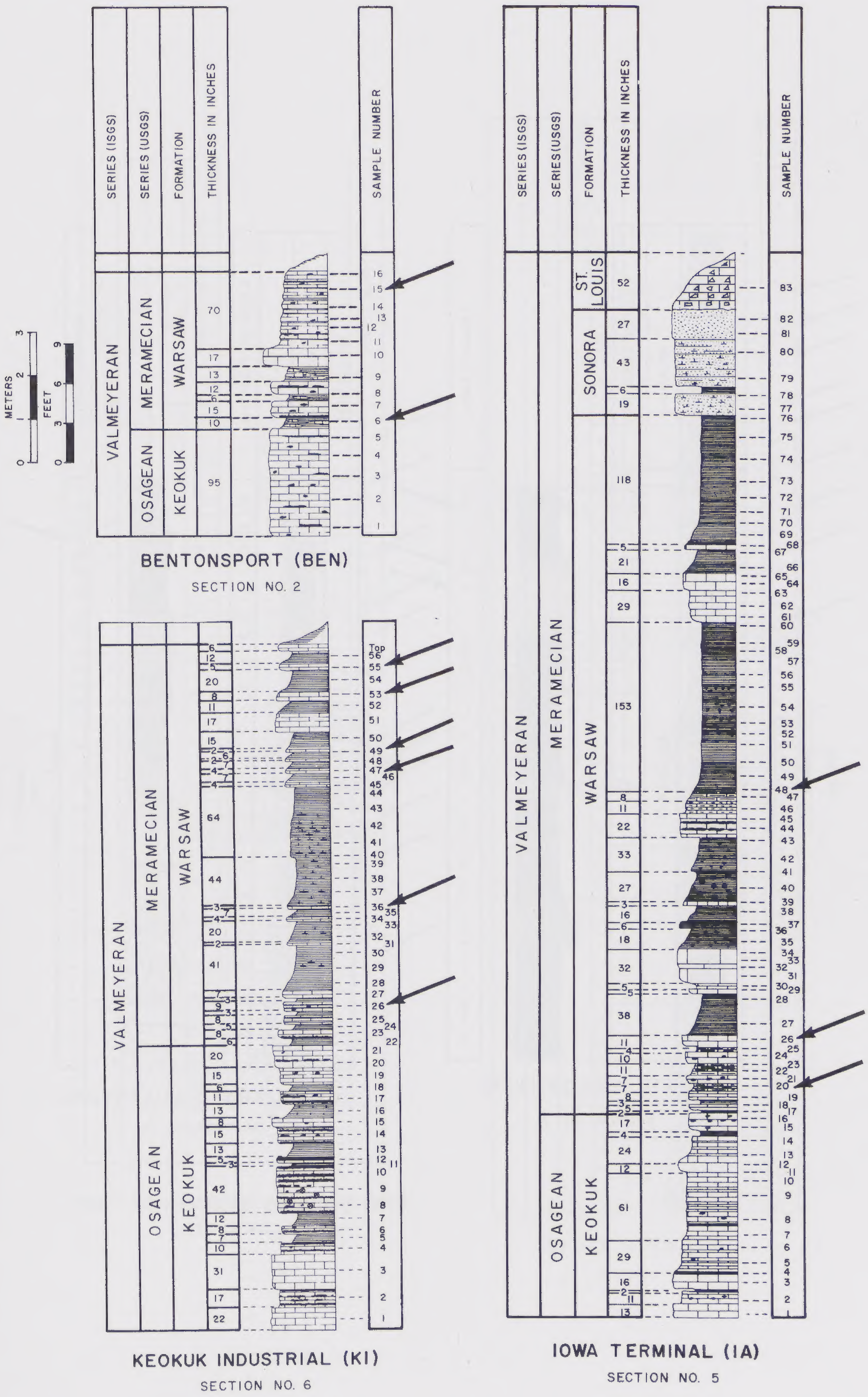
SERIES (ISGS)
SERIES (USGS)
FORMATION
THICKNESS IN INCHES
SAMPLE NUMBER
VALMEYERAN
MERAMECIAN
OSAGEAN
WARSAW
KEOKUK
METERS
FEET
BENTONSPORT (BEN)
SECTION NO. 2
ST. LOUIS
SONORA
KEOKUK INDUSTRIAL (KI)
SECTION NO. 6
IOWA TERMINAL (IA)
SECTION NO. 5

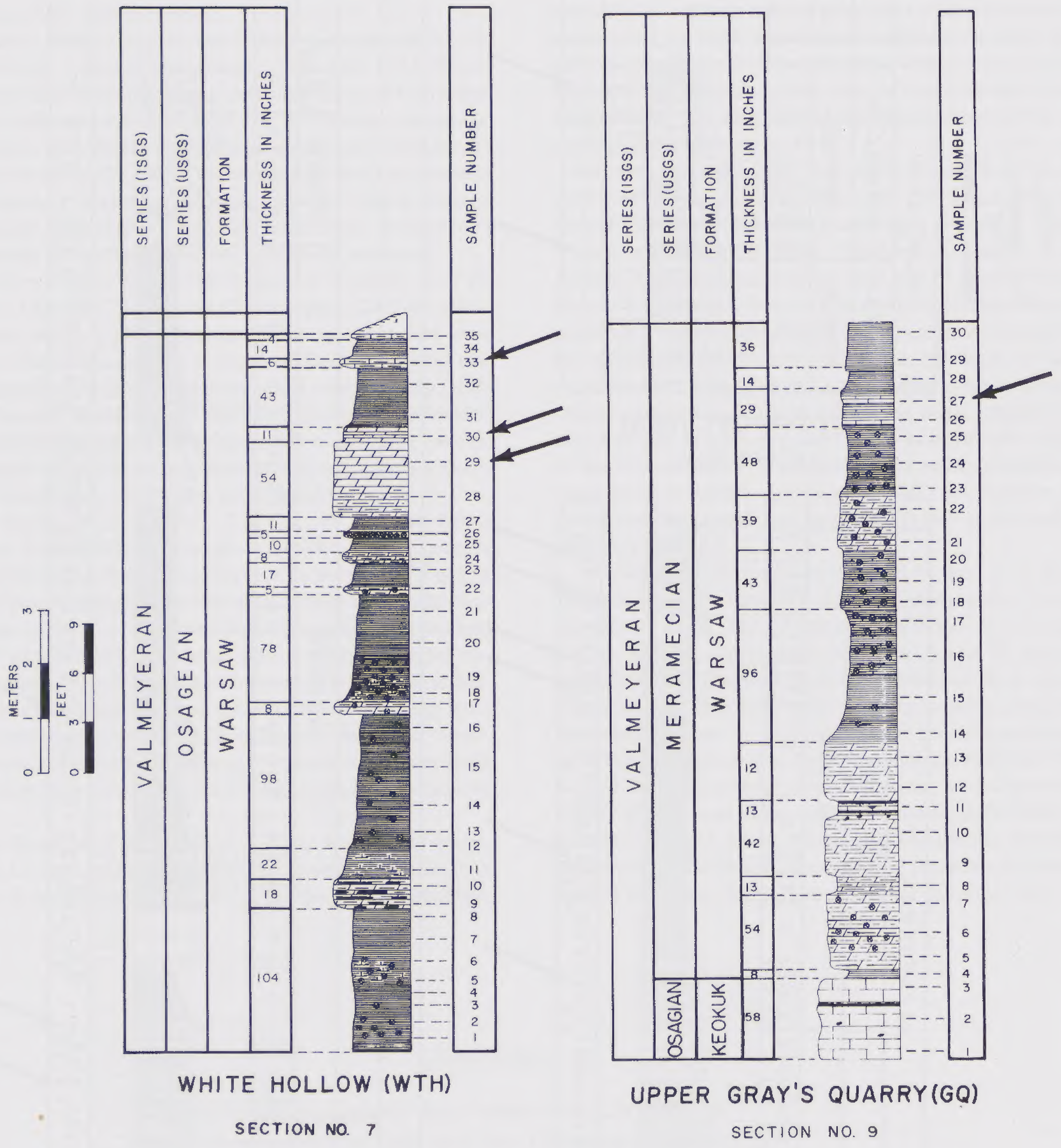
SERIES (ISGS)
SERIES (USGS)
FORMATION
THICKNESS IN INCHES
SAMPLE NUMBER
VALMEYERAN
OSAGEAN
WARSAW
METERS
FEET
WHITE HOLLOW (WTH)
SECTION NO. 7
VALMEYERAN
MERAMECIAN
WARSAW
OSAGIAN
KEOKUK
UPPER GRAY'S QUARRY (GQ)
SECTION NO. 9

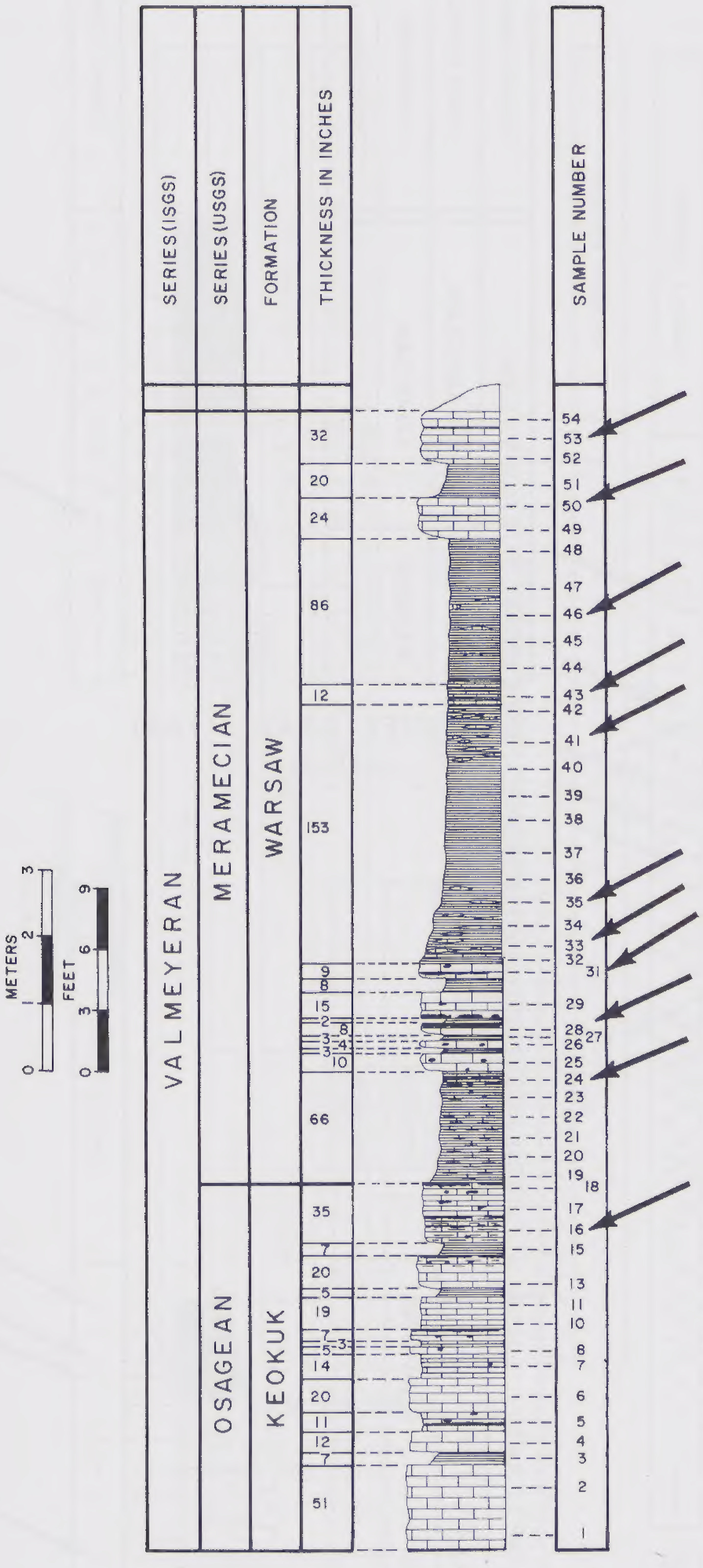

HAMILTON-WARSAW ROADCUT (WR)

SECTION NO. 10

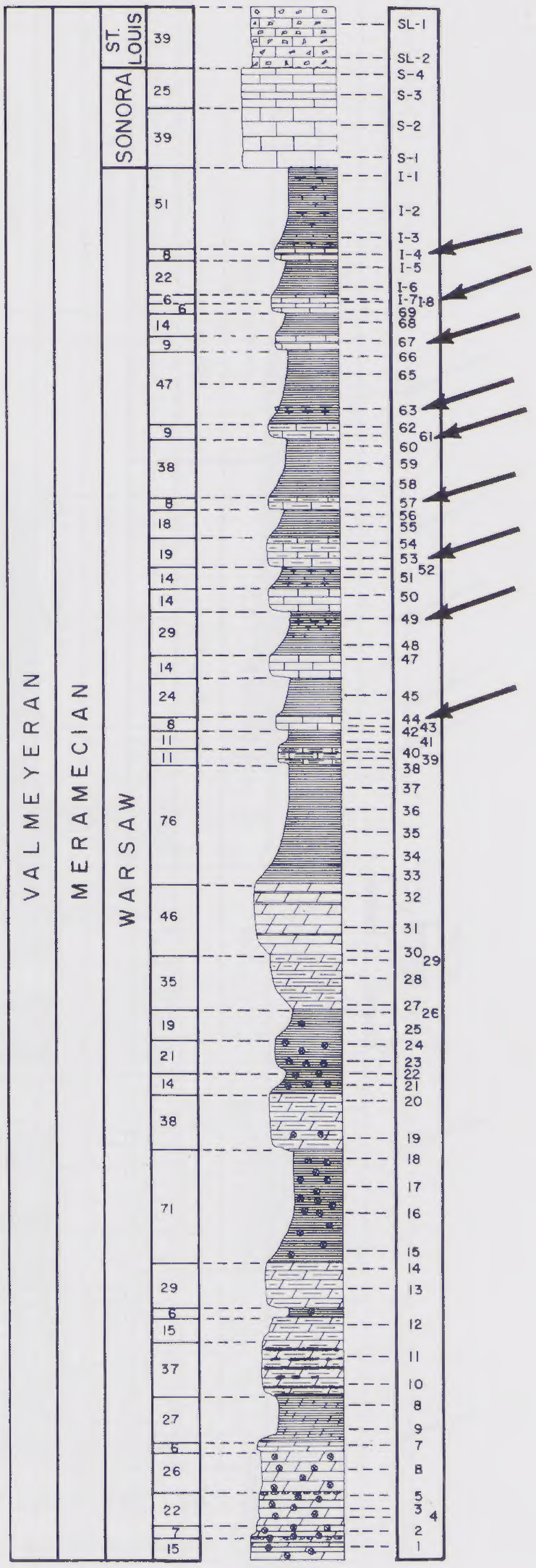

GEODE GLEN (GG)

SECTION NO. 11

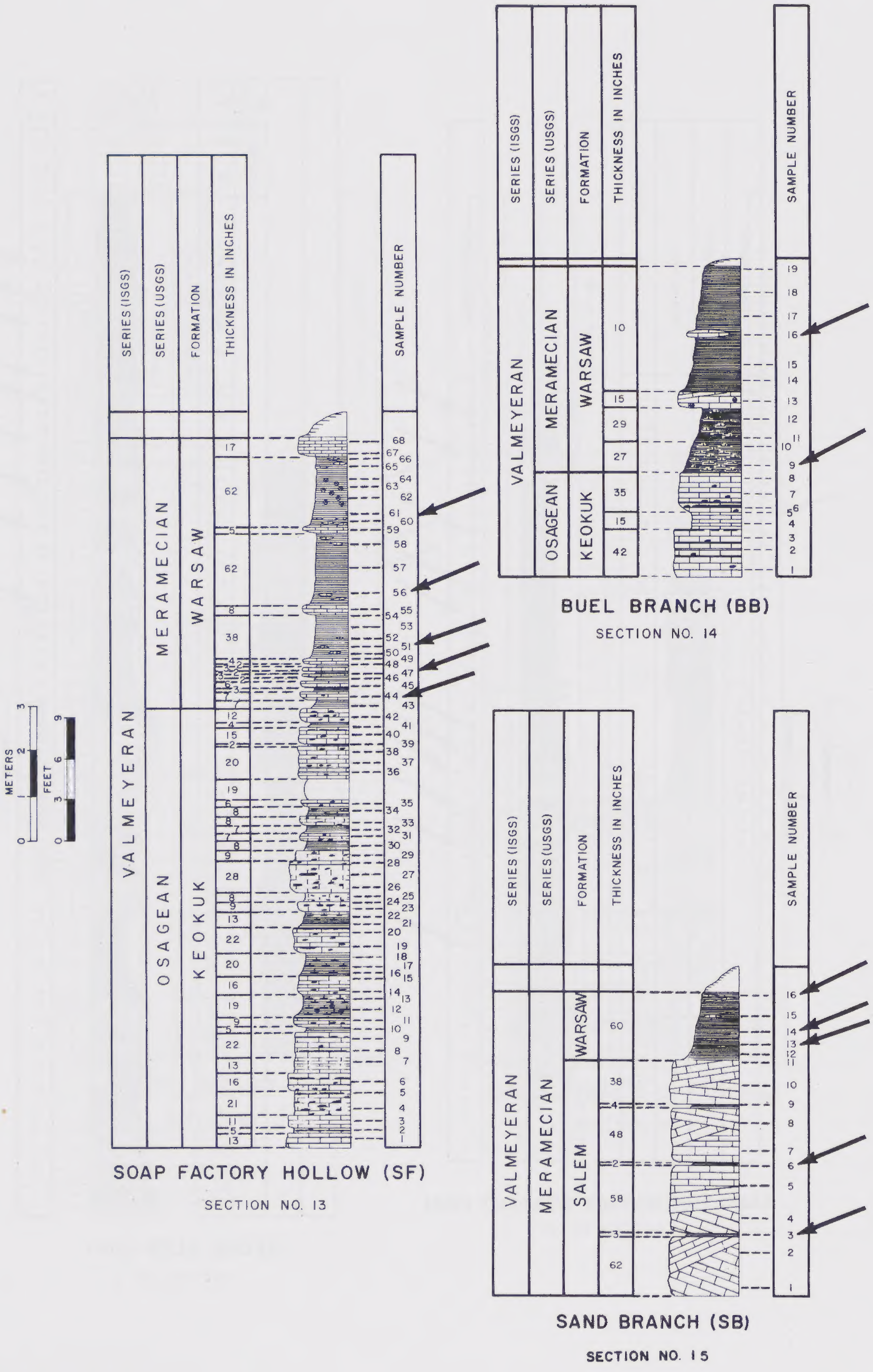
SERIES (ISGS)
SERIES (USGS)
FORMATION
THICKNESS IN INCHES
SAMPLE NUMBER
VALMEYERAN
MERAMECIAN
OSAGEAN
WARSAW
KEOKUK
SALEM
METERS
FEET
BUEL BRANCH (BB)
SECTION NO. 14
SOAP FACTORY HOLLOW (SF)
SECTION NO. 13
SAND BRANCH (SB)
SECTION NO. 15

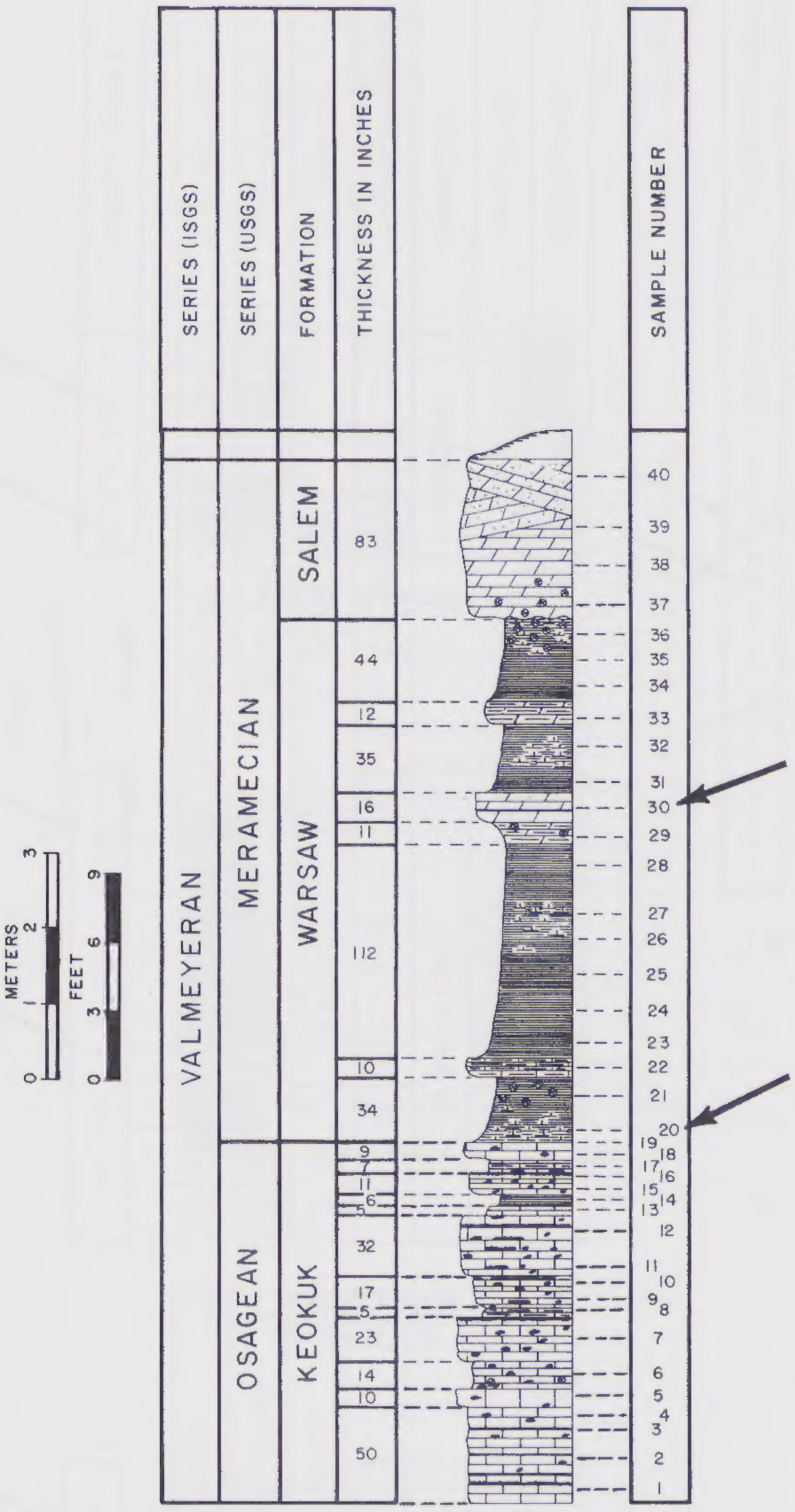

LA GRANGE (LG)
SECTION NO. 16

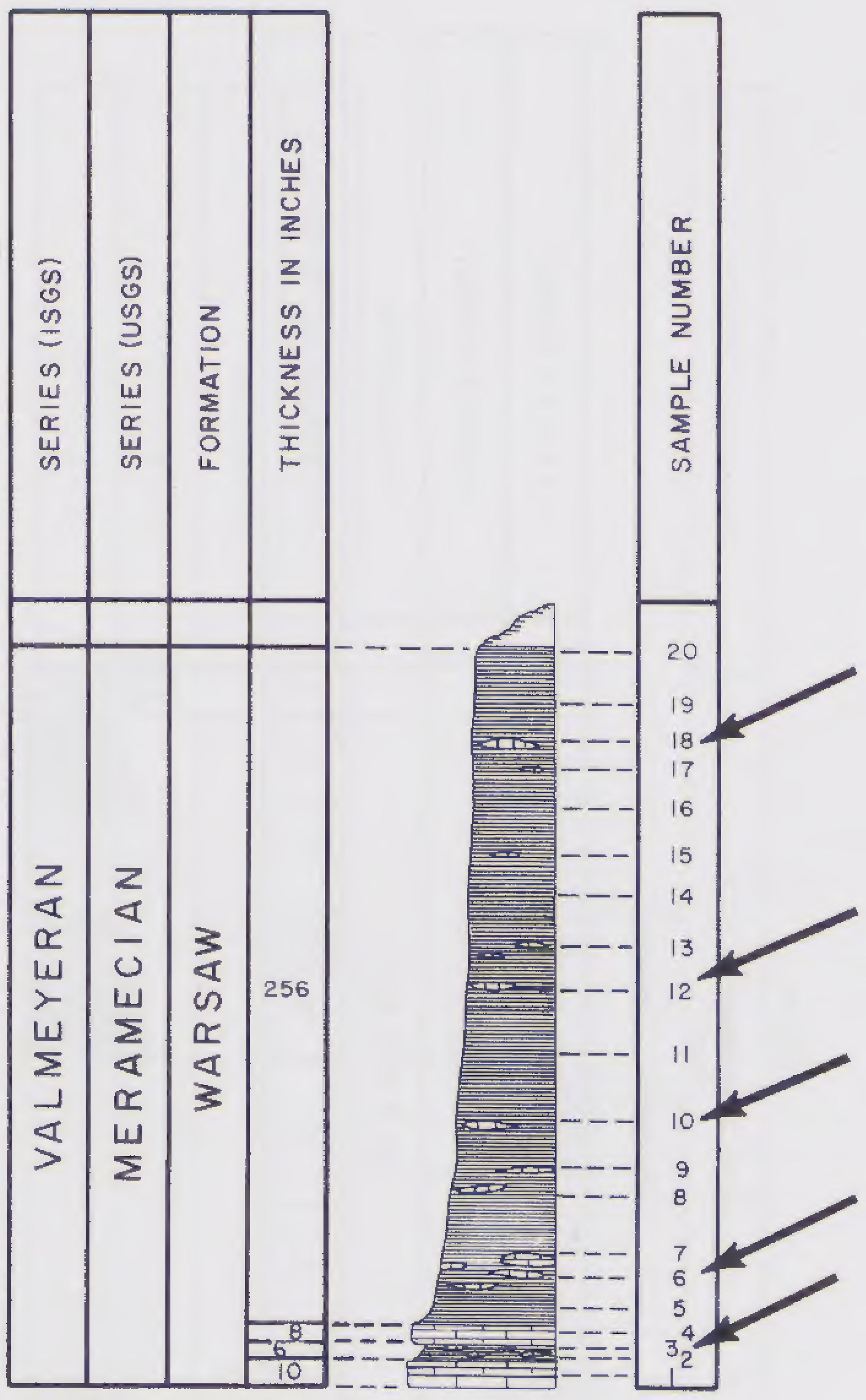

MOUNT STERLING (MST)
SECTION NO. 20

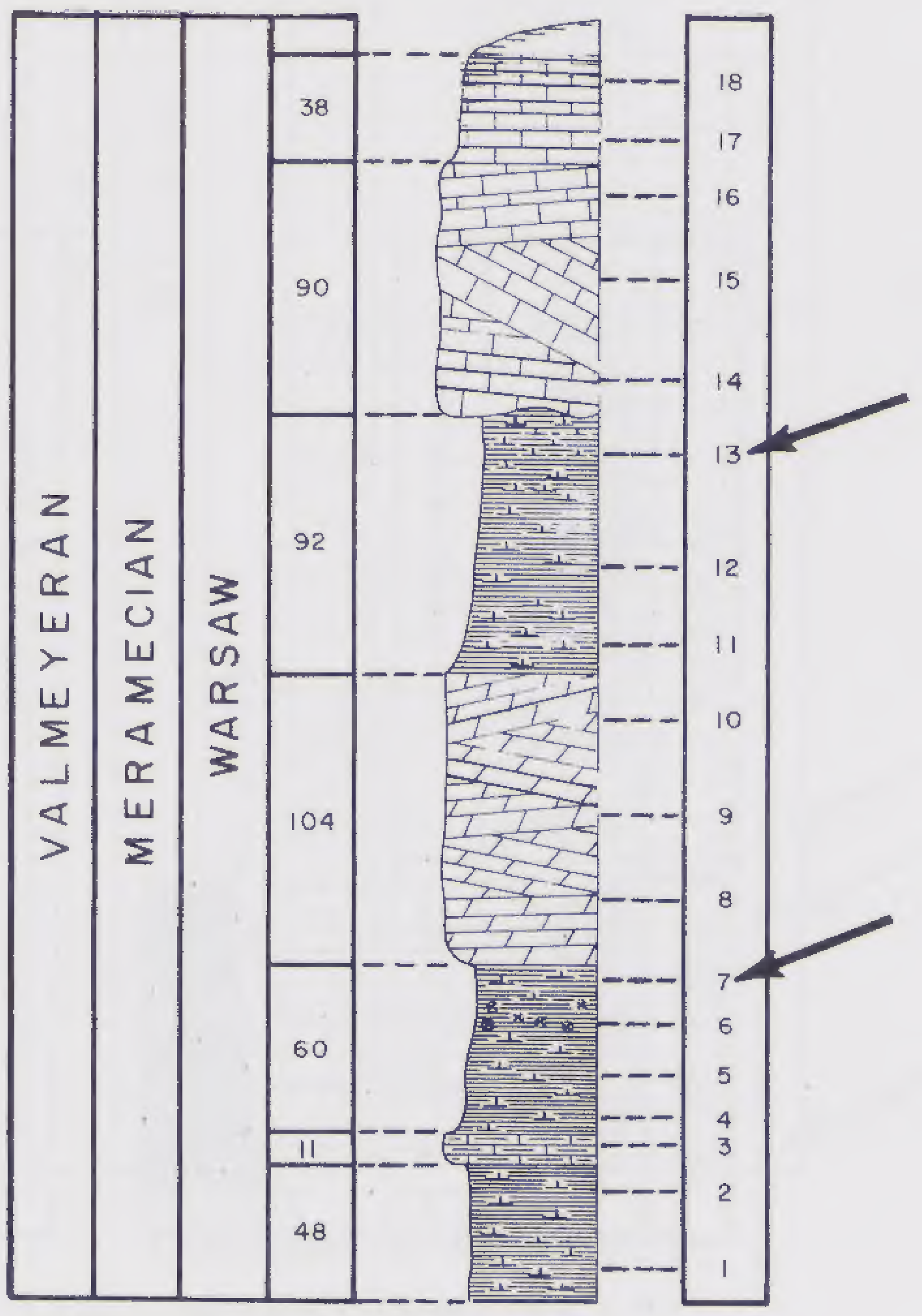

McKEE CREEK (MK)
SECTION NO. 21

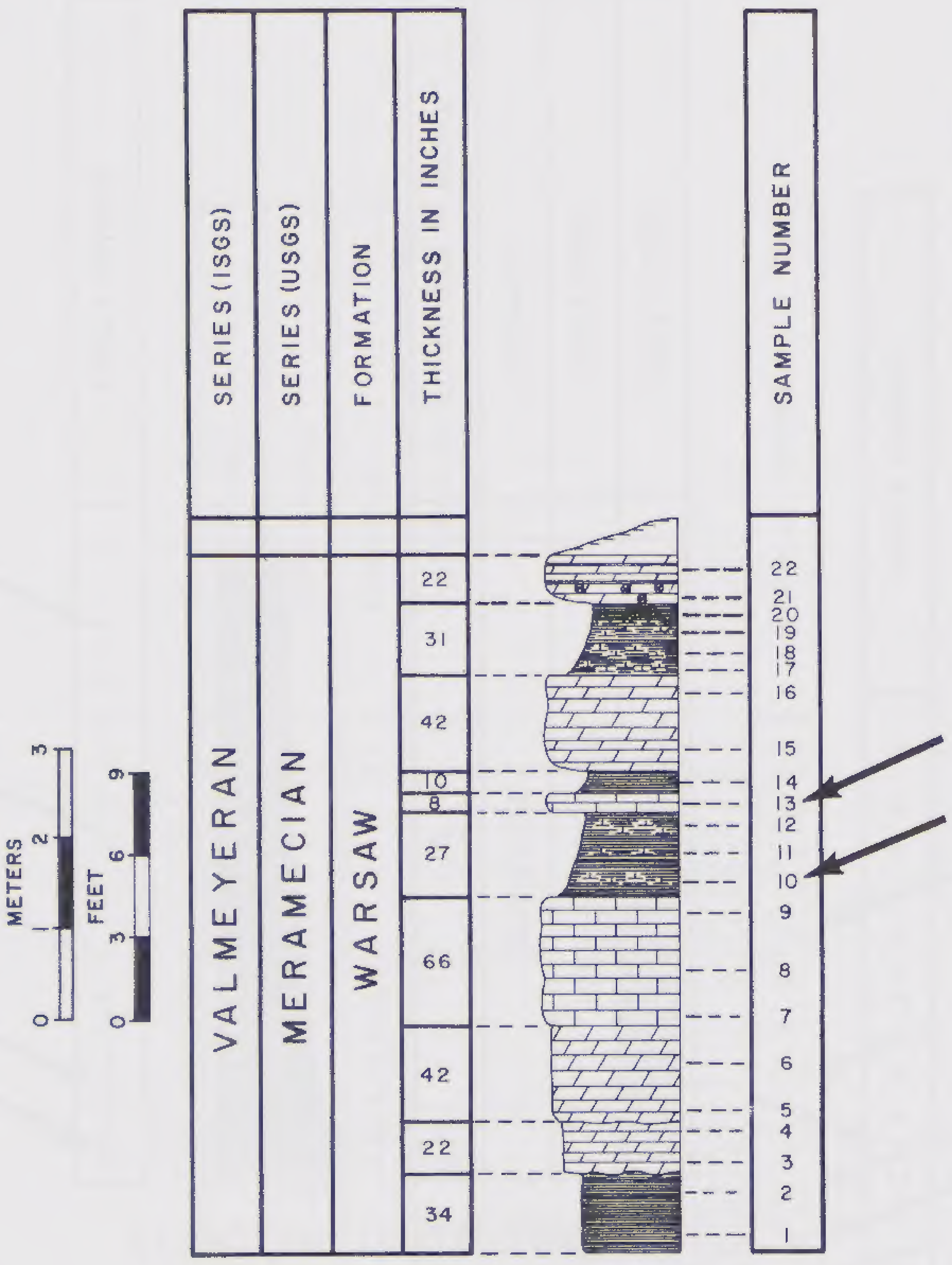

VERSAILLES WEST (VW)

SECTION 22

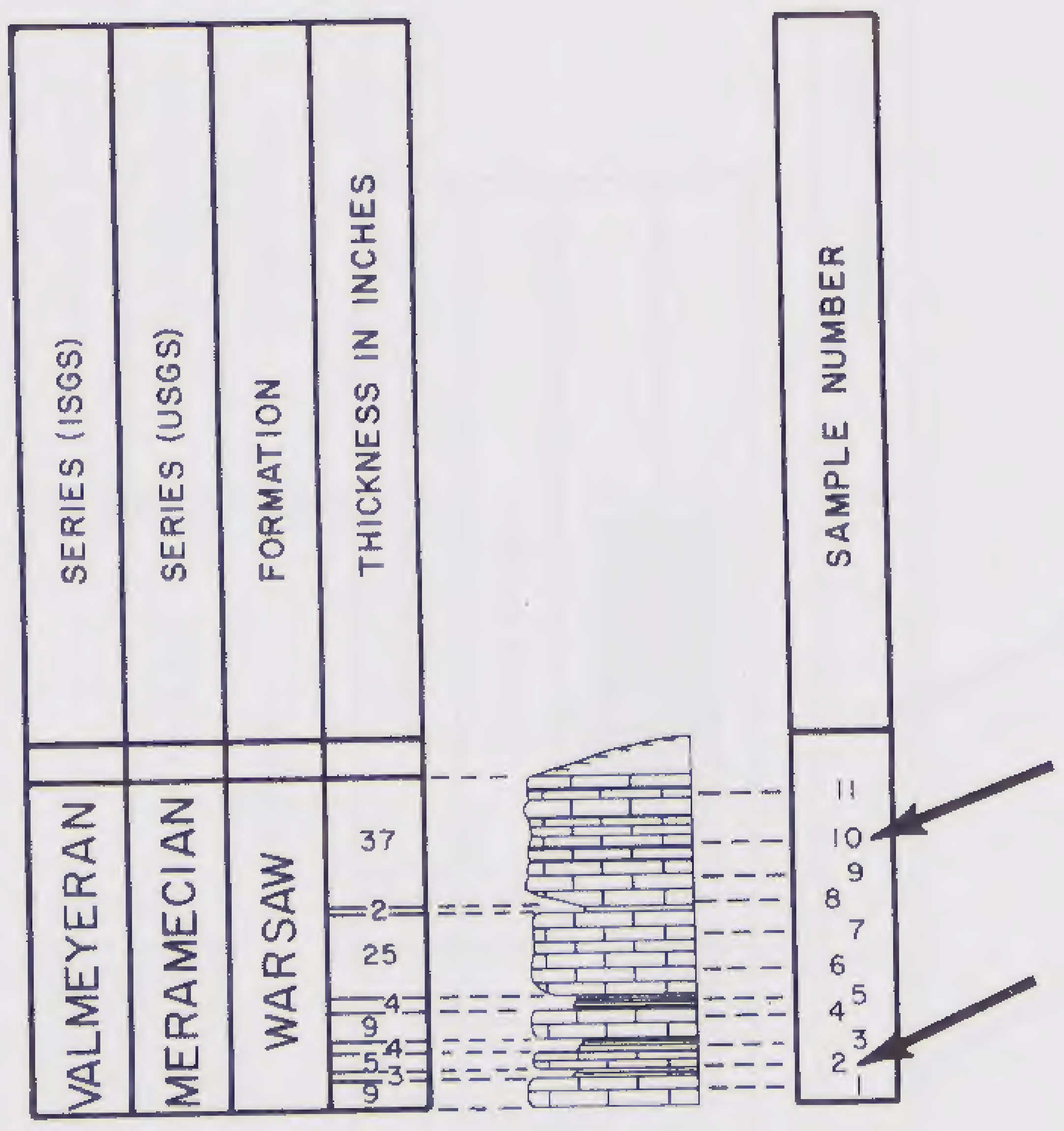

WHITE HALL-C

SECTION 26

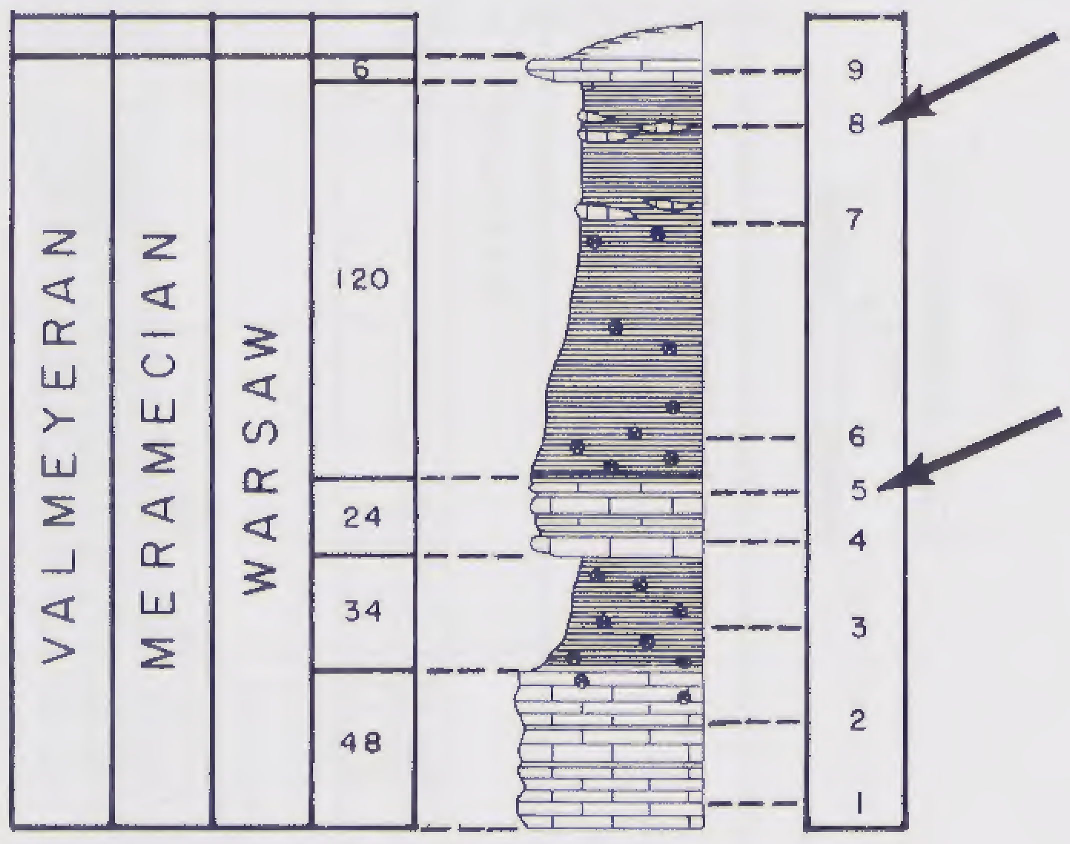

WHITE HALL-D

SECTION NO. 27

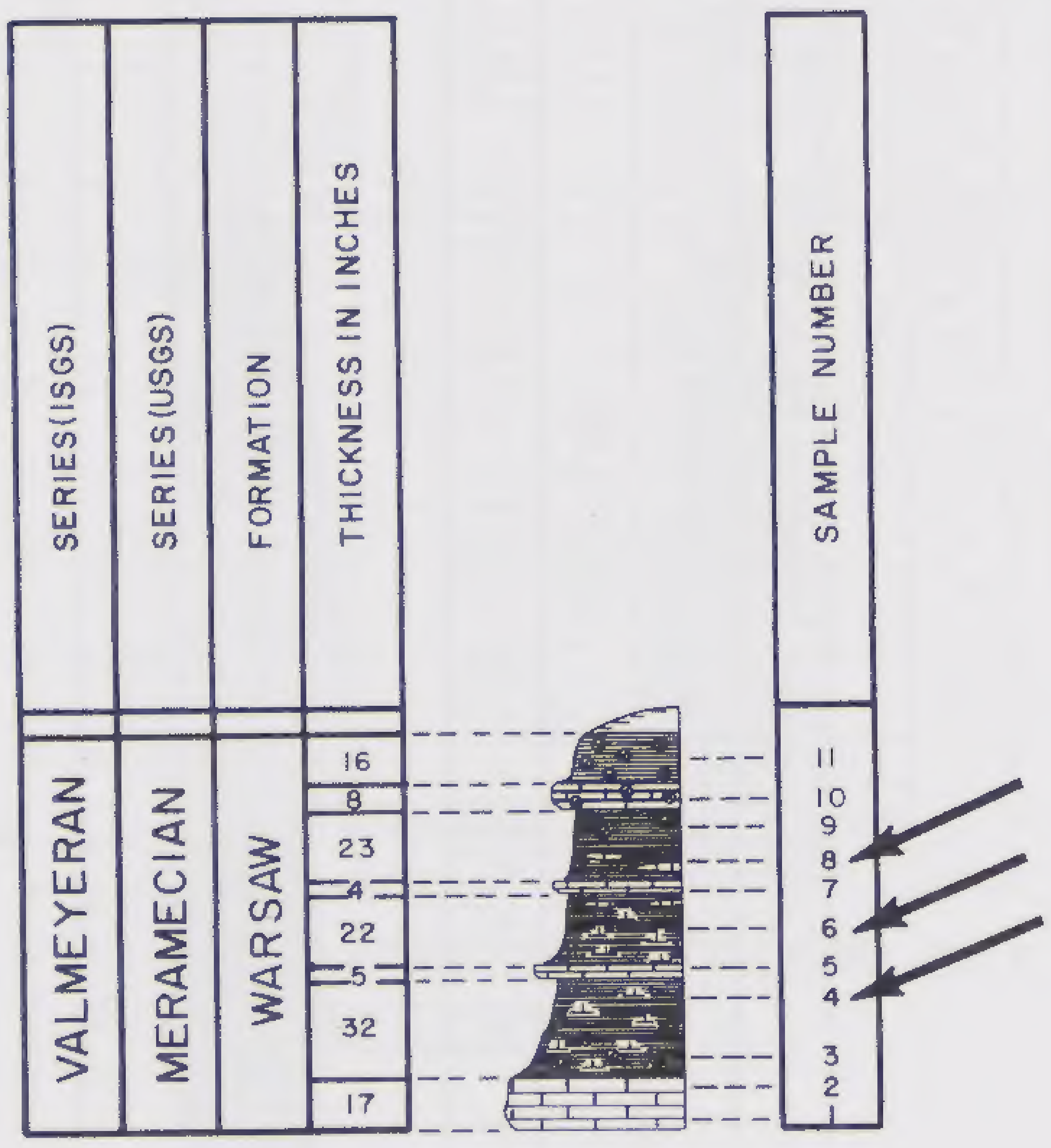

LITTLE WHITAKER CREEK

SECTION NO. 23

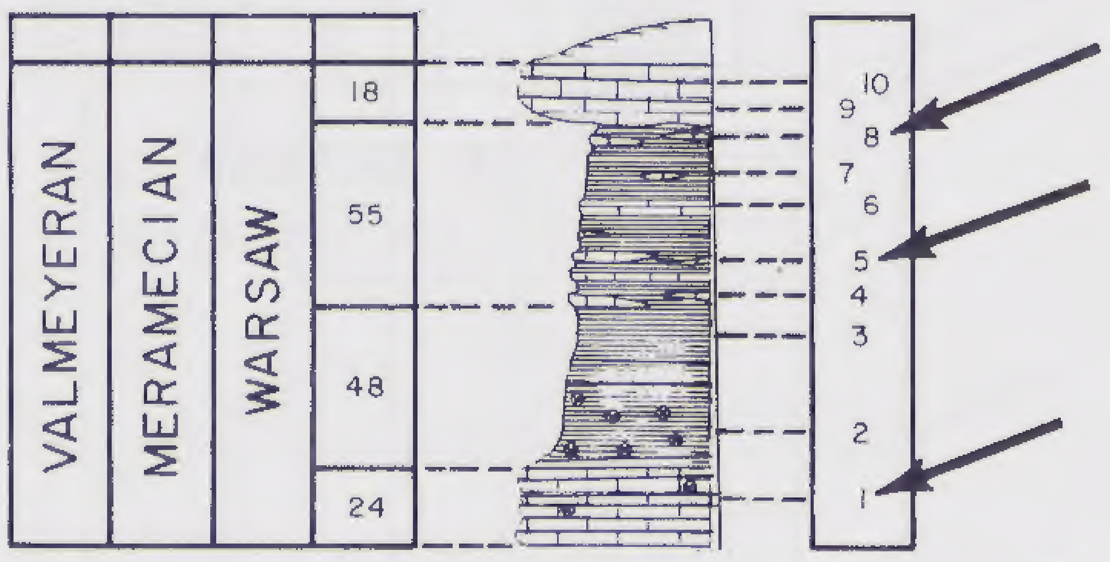

WHITE HALL-F

SECTION NO. 29

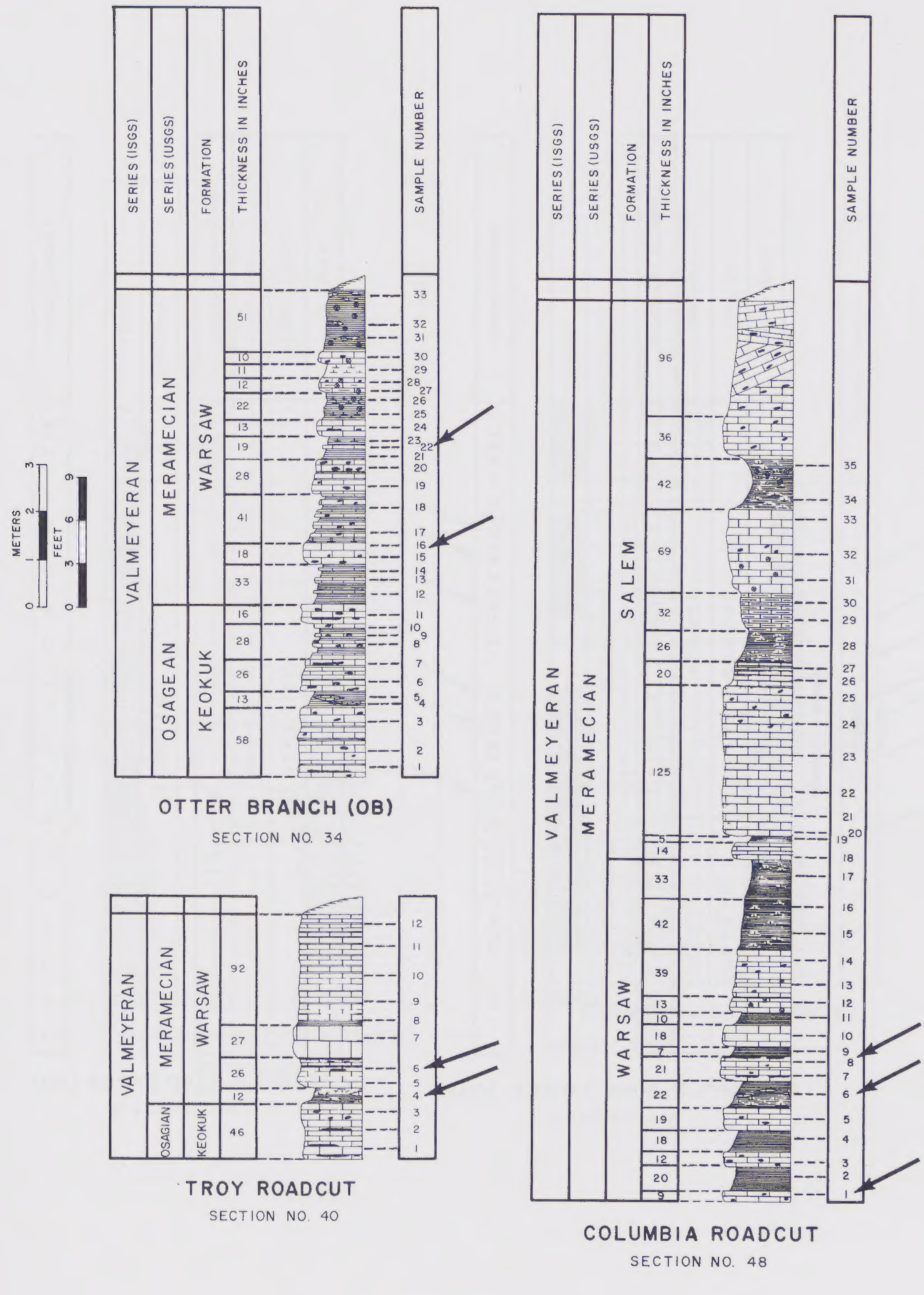
SERIES (ISGS)
SERIES (USGS)
FORMATION
THICKNESS IN INCHES
SAMPLE NUMBER
VALMEYERAN
MERAMECIAN
WARSAW
OSAGEAN
KEOKUK
METERS
FEET
OTTER BRANCH (OB)
SECTION NO. 34
VALMEYERAN
MERAMECIAN
WARSAW
OSAGIAN
KEOKUK
TROY ROADCUT
SECTION NO. 40
VALMEYERAN
MERAMECIAN
SALEM
WARSAW
COLUMBIA ROADCUT
SECTION NO. 48

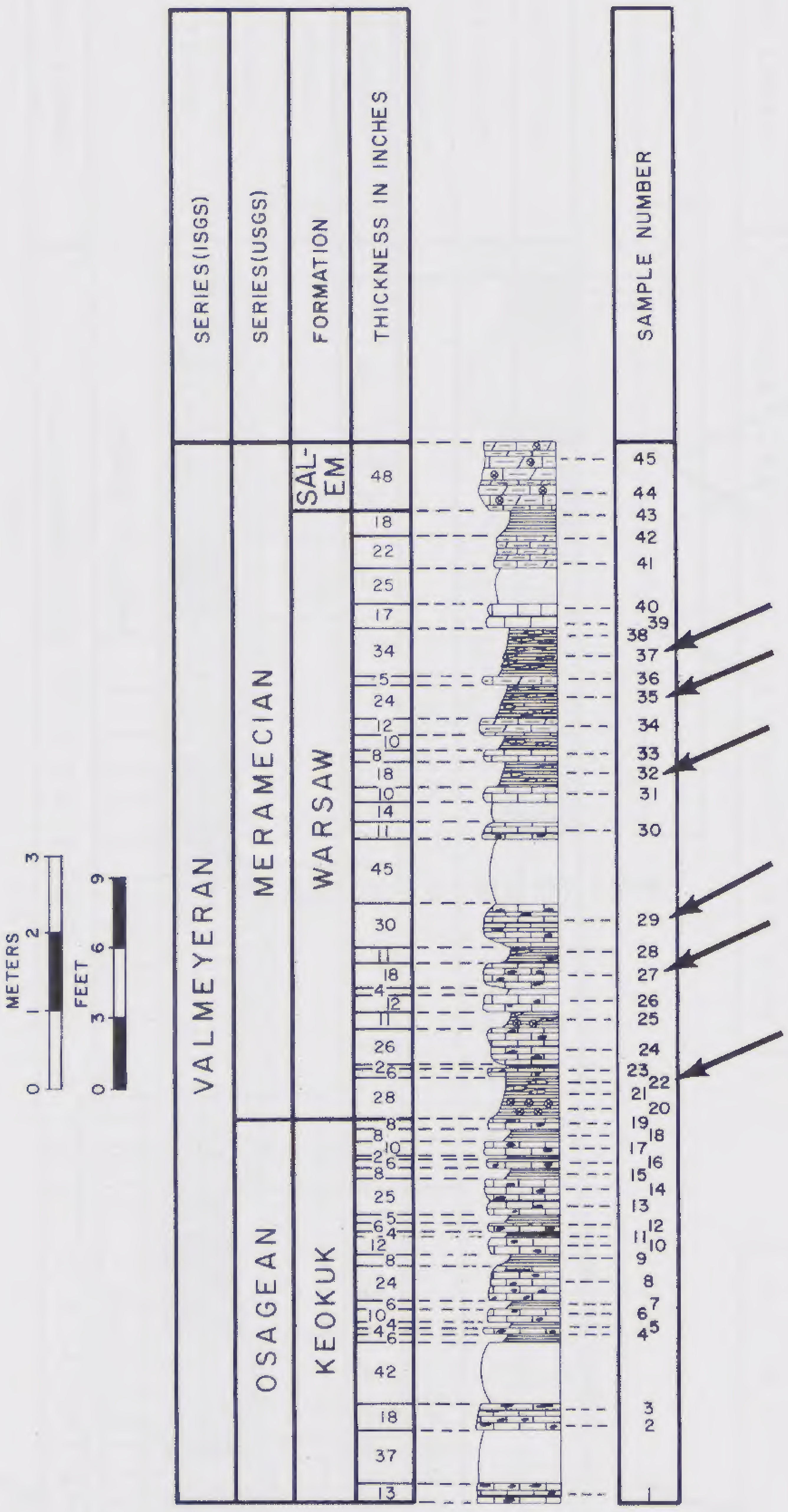

CRAGWOLD ROAD LOWER (CA)

SECTION NO. 47A

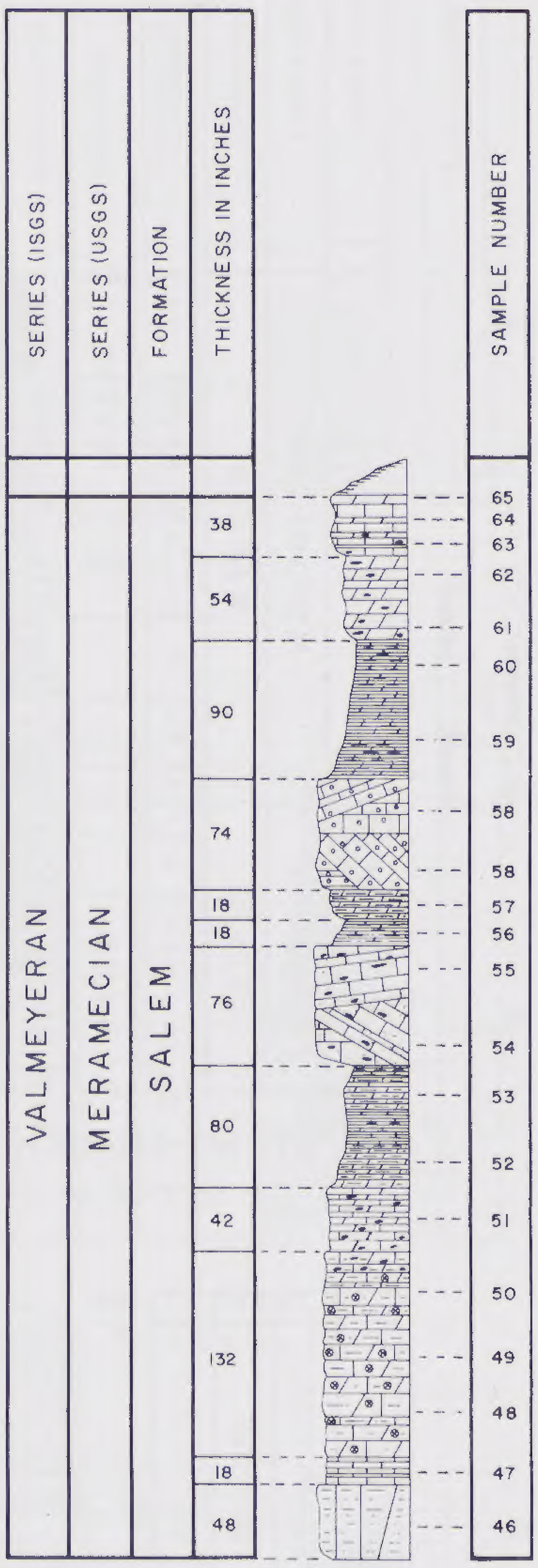

CRAGWOLD ROAD UPPER (CB)

SECTION NO. 47 B

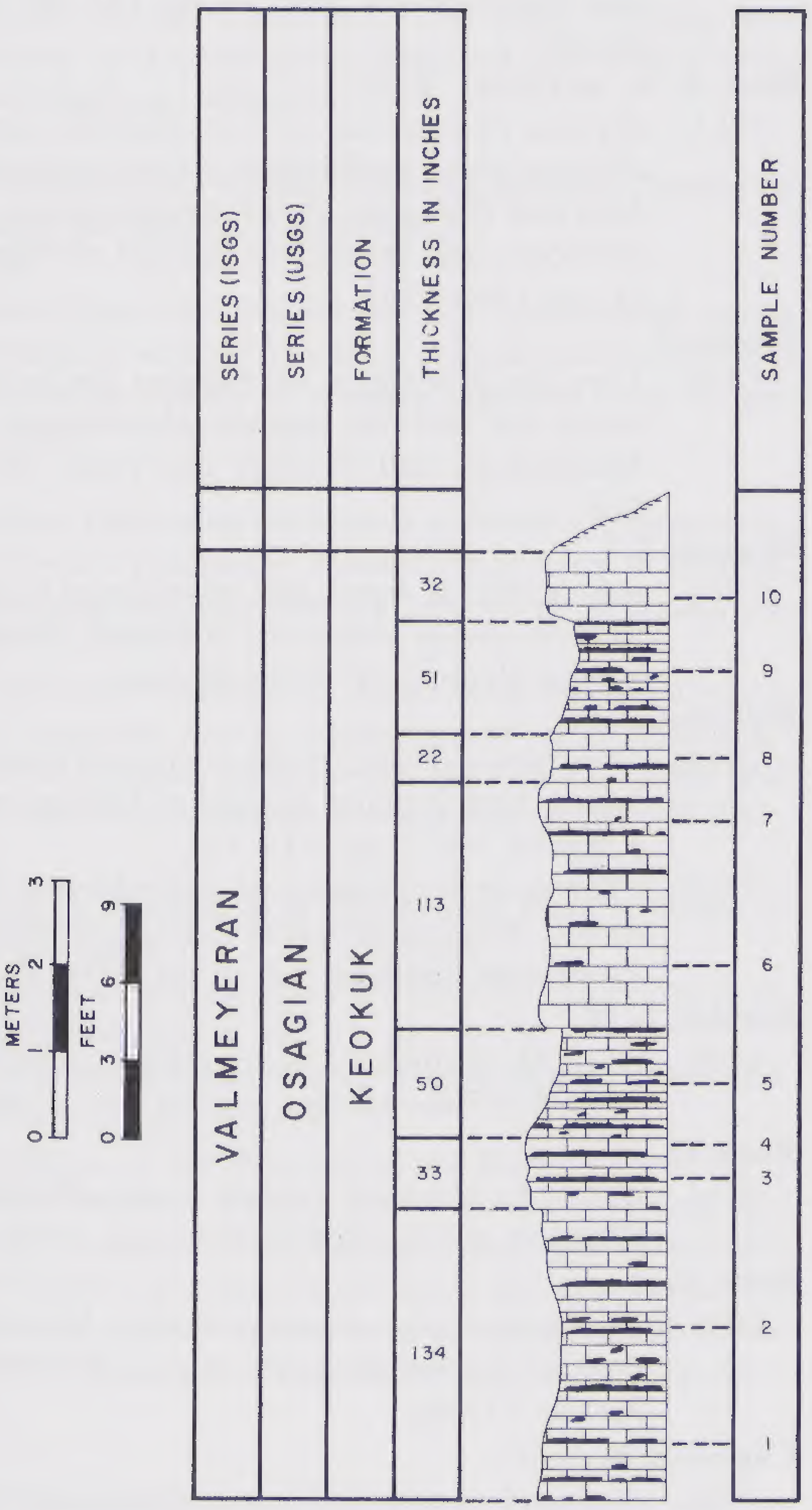

DENNIS HOLLOW (LOWER)
SECTION NO. 49A

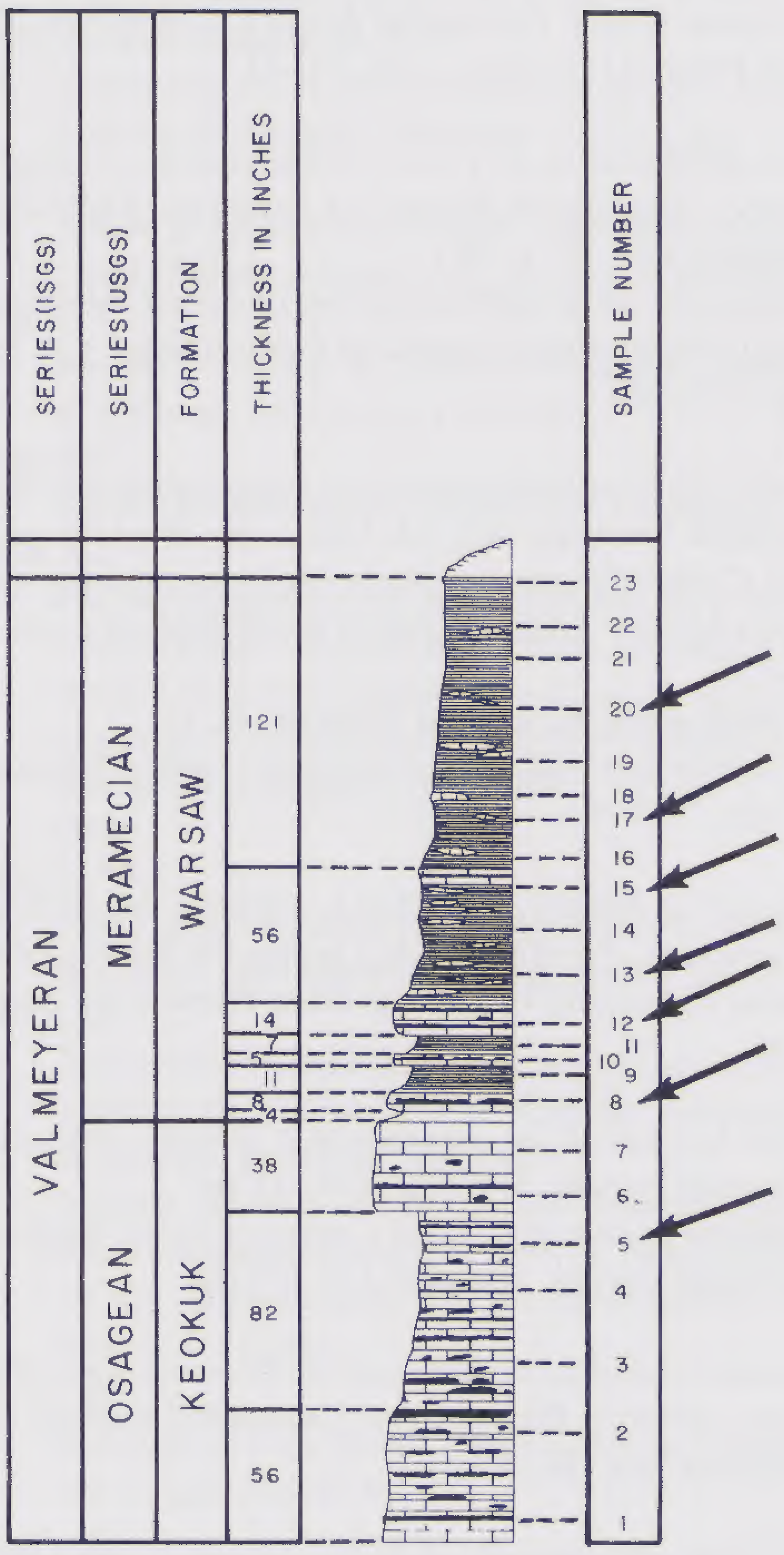

DENNIS HOLLOW (UPPER)
SECTION NO. 49B

REFERENCES CITED

Anstey, R. L., and Perry, T. G.

1970. *Biometric procedures in taxonomic studies of Paleozoic bryozoans.* Journal of Paleontology, vol. 44, pp. 383–398.

1973. *Eden Shale bryozoans; a numerical study (Ordovician, Ohio Valley.* Michigan State University, Publications of the Museum, Paleontological Series, vol. 1, No. 1, pp. 1–80.

Astrova, G. G., and Morozova, I. P.

1956. *Systematics of Bryozoa of the order Cryptostomata.* Doklady Akademiya Nauk S. S. S. R, new ser., vol. 110, pp. 661–664.

Atherton, E., and Palmer, J.

1979. *The Mississippian and Pennsylvanian (Carboniferous) in the United States*: Geological Society of America, Professional Paper 1110, vol. 1, pp. 11–41.

Ausich, W. I.

1978. *Niche partitioning in Lower Mississippian crinoid communities.* Geological Society of America, Abstracts with Programs, vol. 10, p. 361.

1980. *A model for niche differentiation in Lower Mississippian crinoid communities.* Journal of Paleontology, vol. 54, No. 2, pp. 273–288.

Bancroft, A. J.

1986a. *A new Carboniferous fenestrate bryozoan genus.* Scottish Journal of Geology, vol. 22, No. 1, pp. 96–108.

1986b. *The Carboniferous fenestrate bryozoan* Hemitrypa hibernacia *McCoy.* Irish Journal of Earth Sciences, vol. 7, pp. 111–124.

Banta, W. C., McKinney, F. K., and Zimmer, R. L.

1974. *Bryozoan monticules; excurrent water outlets?* Science, vol. 185, pp. 783–784.

Bassler, R. S.

1953. *Bryozoa,* in Moore, R.C. [ed.], *Treatise on Invertebrate Paleontology, Part G,* 253 pp. Geological Society of America and University of Kansas Press (New York and Lawrence).

Baxter, J. W.

1960. *Salem Limestone in southwestern Illinois.* Illinois State Geological Survey, Circular 284, 32 pp.

1972. *Limestone resources of Scott County, Illinois.* Illinois State Geological Survey, Circular 472, 24 pp.

Bell, A. H.

1932. *Structure and oil possibilities of the Warsaw area, Hancock County, Illinois.* Illinois State Geological Survey, Illinois Petroleum, vol. 24, 17 pp.

Blake, D. B.

1975. *The Cryptostomata resurrected,* in Poutet, S. [ed.], *Bryozoa 1974,* Documents des Laboratorie de Géologie, Faculté des Sciences de Lyon, France, hors-serie 3, fasc. 1, pp. 211–223.

1980. *Homemorphy in Paleozoic bryozoans; a search for explanations.* Paleobiology, vol. 6, pp. 451–465.

1983. *Introduction to the suborder Rhabdomesina,* in Boardman, R. S. *et al.* [eds.], *Treatise on Invertebrate Paleontology, Part G [revised],* vol. 1, pp. 530–592.

Boardman, R. S.

1975. *Taxonomic characters for phylogenetic classifications of cyclostome Bryozoa,* in Poutet, S. [ed.], *Bryozoa 1974,* Documents des Laboratoire de Géologie, Faculté des Sciences de Lyon, France, hors-serie 3, fasc. 2, pp. 595–606.

Boardman, R. S., and Cheetham, A. H.

1969. *Skeletal growth, intracolony variation, and evolution in Bryozoa; a review.* Journal of Paleontology, vol. 43, pp. 205–233.

1983. *Glossary of morphological terms,* pp. 304–320 in Robinson, R. A. [ed.], *Treatise on Invertebrate Paleontology, Part G, Bryozoa (Revised).* Geological Society of America and University of Kansas Press; Boulder, Colorado, and Lawrence, Kansas.

Boardman, R. S., and Utgaard, J.

1964. *Modifications of study methods for Paleozoic Bryozoa.* Journal of Paleontology, vol. 38, pp. 768–770.

Borg, F.

1926. *Studies on recent cyclostomatous Bryozoa.* Zoologiska Bidrag Från Uppsala, Band 10, pp. 181–507, pls. 1–14, 109 text-figs.

Bork, K. B., and Perry, T. G.

1967. *Bryozoa (Ectoprocta) of Champlainian age (Middle Ordovician) from northwestern Illinois and adjacent parts of Iowa and Wisconsin, Part I;* Amplexopora, Monotrypella, Hallopora *and* Batostoma. Journal of Paleontology, vol. 41, pp. 1365–1392.

Braem, F.

1940. *Über die Querstrefun im Pharynx der gymnolämen Bryozoen und über den Bau des Munddarms.* Zeitschrift für Morphologie und Ökologie der Tiere, vol. 36, pp. 668–676.

Branner, J. C.

1888. *Administrative report and introduction to the report upon western central Arkansas.* Arkansas Geological Survey, Annual Report, vol. 1, pp. xv–xxxi.

Bullivant, J. S.

1968a. *The rate of feeding of the bryozoan* Zoobotryon verticillatum. New Zealand Journal of Marine and Freshwater Research, vol. 2, pp. 111–134.

1968b. *The method of feeding of lophophorates (Bryozoa, Phoronida, Brachiopoda).* New Zealand Journal of Marine and Freshwater Research, vol. 2, pp. 135–146.

Burckle, L. H.

1960. *Some Mississippian fenestrate Bryozoa from central Utah.* Journal of Paleontology, vol. 34, No. 6, pp. 1077–1098.

Busk, G.

1852. *Catalogue of marine Polyzoa in the collection of the British Museum, vol. 1, Cheilostomata.* pp. 1–54, pls. 1–68.

Butts, C.

1915. *Descriptions and correlations of the Mississippian formations of western Kentucky; Part I.* Kentucky Geological Survey, 119 pp.

Campbell, K. S. W.

1961. *Carboniferous fossils from the Kutting Rocks of New South Wales.* Palaeontology, pt. 3, No. 4, pp. 428–474.

Carozzi, A. V.

1972. *Microscopic Sedimentary Petrology.* Krieger Publishing Co. (Huntington), 485 pp.

Chronic, J.

1949. *The Upper Paleozoic of Peru,* in Newell, N. D., Chronic, J., and Roberts, T. G. [eds.], Geolological Society of America, Memoirs, vol. 58, pp. 1–241.

Cole, V. B.

1961. *The Cap au Gres fault in northeastern Missouri and west-central Illinois.* Kansas Geological Society, Guidebook, 20th Annual Field Conference, pp. 86–88.

Collinson, C.

1964. *Western Illinois.* Illinois Geological Survey, Guidebook, ser. 6, 28th Tri-State Field Conference, Quincy, Illinois, 30 pp.

Collinson, C., Scott, A. J., and Rexroad, C. B.
1962. *Six charts showing biostratigraphic zones and correlations based on conodonts from the Devonian and Mississippian rocks of the Upper Mississippi Valley.* Illinois State Geological Survey, Circular 328, 32 pp.

Condra, G. E., and Elias, M. K.
1944. *Study and revision of* Archimedes *(Hall).* Geological Society of America Special Paper No. 53, viii + 243 pp., 41 pls., 6 figs., 83 tables.

Connell, J. H.
1975. *Some mechanisms producing structure in natural communities; a model and evidence from field experiments,* in Cody, M. L., and Diamond, J. M. [eds.], *Ecology and Evolution of Communities.* Harvard University Press (Cambridge), pp. 460–490.

Cook, P. L.
1977. *Colony-wide water currents in living Bryozoa.* Cahiers de Biologie Marine, vol. 8, pp. 31–47.

Crockford, J. M.
1944. *Bryozoa from the Wandagee and Noonkanbah series (Permian) of western Australia.* Journal and Proceedings of the Royal Society of Western Australia, vol. 28, pp. 165–185.

Cuffey, R. J.
1967. *Bryozoan* Tabulipora carbonaria *in Wreford Megacyclothem (Lower Permian) of Kansas.* University of Kansas, Paleontological Contributions, Art. 43 (I, Bryozoa), pp. 1–96.
1973. *An improved classification, based upon numerical–taxonomic analyses, for the higher taxa of entoproct and ectoproct bryozoans,* in Larwood, G. P. [ed.], *Living and Fossil Bryozoa.* Academic Press (London), pp. 549–564.

Cumings, E. R.
1901. *The use of Bedford as a formational name.* Journal of Geology, vol. 9, No. 3, pp. 232–333.
1904. *Development of some Paleozoic Bryozoa.* American Journal of Science, ser. 4, vol. 17, pp. 49–78.
1905. *Development of* Fenestella. American Journal of Science, ser. 4, vol. 20, pp. 169–177.
1906. *Descriptions of the Bryozoa of the Salem Limestone of southern Indiana.* Indiana Department of Geology and Natural Resources, 30th Annual Report, pp. 1274–1296.
1922. *Nomenclature and description of the geologic formations of Indiana.* Indiana Department of Conservation, Publication 21, *Handbook of Indiana Geology,* part IV, pp. 403–570.

Dales, R. P.
1957. *Some quantitative aspects of feeding in sabellid and serpulid fan worms.* Journal of the Marine Biologists Association, U. K., vol. 36, pp. 309–316.

Diamond, J. M.
1978. *Niche shifts and the rediscovery of interspecific competition.* American Scientist, vol. 66, pp. 322–331.

Dunaeva, N. H., and Morozova, I. P.
1974. *Revision of the suborder Fenestelloidea,* in Pouyet, S. [ed.], *Bryozoa 1974.* Documents des Laboratoire de Géologie, Faculté des Sciences de Lyon, France, hors-serie 3, fasc. 1, pp. 225–233.

Dussart, B. M.
1964. *Les differentes categories de plancton.* Hydrobiology, vol. 26, pp. 72–74.

Edmondson, W. T.
1965. *Reproductive rate of planktonic rotifers as related to food and temperature in nature.* Ecological Monographs, vol. 35, pp. 61–111.

Ehrenberg, C. G.
1831. *Invertebrata other than Insecta,* in *Symbolae Physicae, seu Icones et descriptiones Corporum Naturalium novorum aut minus cognitorum, quae ex itineribus per Libyam, Aegyptum, Nubiam, Dongalam, Syriam, Arabiam et Habessiniam . . . P. C. Hemprich et C. G. Ehrenberg . . . studio annis 1820–25 redierunt . . . .* Pars Zoologica, 4 vols. (Berlin)

Elias, M. K.
1964. *Stratigraphy and paleoecology of some Carboniferous bryozoans (with discussion).* Cinquième Congrés Internationale de Stratigraphie et de Geologie du Carbonifère, Paris, Compte Rendu, 1963, vol. 1, pp. 375–381.

Elias, M. K., and Condra, G. E.
1957. Fenestella *from the Permian of West Texas.* Geological Society of America, Memoir 70, 158 pp.

Engel, B. A.
1975. *A new (?) bryozoan from the Carboniferous of eastern Australia.* Palaeontology, vol. 18, pp. 571–605.

Engelmann, G.
1847. *Remarks on the St. Louis Limestone.* American Journal of Science, vol. 3, pp. 119–120.

Fabricius, O.
1780. *Fauna Groenlandica.* Hafniae et Lepsiae, 452 pp.

Frederiks, G.
1915. *La faune paleozoïque superieure des environs de la ville de Krasnoufinsk.* Comite de Géologie, Mémoire 109 [not seen].
1920. *Études Paléontologiques. 1 – Essai de la Classification de la familie Fenestellidae King* [in Russian]. Bulletin of the Russian Geological Committee, xxxvii + pp. 545–560, table.

Ganesan, T. M.
1972. *Fenestellid Bryozoa from the Boulder Slate sequence of Garhwal.* Himalayan Geology, vol. 2, pp. 431–451.

Gautier, T. G.
1970. *Interpretive morphology and taxonomy of bryozoan genus* Tabulipora. University of Kansas, Paleontological Contributions, Paper 48, pp. 1–21.
1972. *Growth, form, and functional morphology of Permian acanthocladiid Bryozoa from the Glass Mountains, West Texas.* unpublished. Ph. D. dissertation, University of Kansas, 187 pp.

Gordon, C. H.
1895. *Geology of Van Buren County.* Iowa Geological Survey, vol. 4, pp. 197–254.

Gordon, D. P.
1974. *Microarchitecture and function of the lophophore in the bryozoan* Cryptosula pallasiana. Marine Biology, vol. 27, pp. 147–163.

Hageman, S. J.
1987. *Concepts and methods for taxonomic analysis of fenestrate Bryozoa.* unpublished M. S. Thesis, University of Illinois, Champaign–Urbana, Illinois, 189 pp.

Hall, J.
1847. *Organic remains of the lower division of the New York system.* Natural History of New York, Pt. 6, Paleontology of New York, vol. 1, pp. 1–338.
1852. *Organic remains of the lower middle divisions of the New York system.* Natural History of New York, Pt. 6, Paleontology of New York, vol. 2, pp. 40–52, 144–173.
1857a. *Observations upon the Carboniferous limestones of the Mississippi Valley [abstract].* American Journal of Science, vol. 23, pp. 187–203.

Hall, J.
1857b. *Observations on the genus* Archimedes, *or* Fenestella, *with descriptions of species, etc.* American Association for the Advancement of Science, Proceedings, vol. 10, pt. 2, pp. 176–180.
1858. *Geology of Iowa, Paleontology.* vol. 1, pt. 2, 652 pp.
1864. *Description of new species of fossils from the Carboniferous limestone of Indiana and Illinois.* Transactions of the Albany Institute, vol. 4, pp. 2–36.
1883. *Bryozoans of the Upper Helderberg and Hamilton groups.* Transactions of the Albany Institute, vol. 10, pp. 145–197.
1885. *On the mode of growth and relation of the Fenestellidae.* New Jersey State Geologists Report, [Albany], pp. 35–46.

Hardin, G.
1960. *The competitive exclusion principle.* Science, vol. 131, pp. 1292–1297.

Harris, S. E., Jr., and Parker, M. C.
1964. *Stratigraphy of the Osage Series in southeastern Iowa.* Iowa Geological Survey, Report of Investigations, No. 1, 52 pp.

Hopkins, T. C., and Siebenthal, C. E.
1897. *Bedford oolitic limestone of Indiana.* Indiana Department of Geology and Natural Resources, Annual Report, vol. 21, pp. 291–427.

Horowitz, A. B.
1968. *The ectoproct (bryozoan) genus* Actinotrypa *Ulrich.* Journal of Paleontology, vol. 42, pp. 356–373.

Hutchinson, G. E.
1959. *Homage to Santa Rosalia or why are there so many different kinds of animals.* American Naturalist, vol. 93, pp. 145–149.

Hyman, L. H.
1959. *The Invertebrates, Smaller Coelomate Groups.* McGraw-Hill Book Co. (New York), vol. 5, 783 pp.,

Jackson, J. B. C., and Cheetham, A. H.
1990. *Evolutionary significance of morphospecies: a test with cheilostome Bryozoa.* Science, vol. 248, pp. 579–583.

Kaisin, F.
1942. *Les Bryozoaires Fenestrellinides et Acanthocladiides du Tournaisien de la Belgique.* Mémoires de l'Institut de Geologie de Louvain, vol. 13, pp. 92–141.

Keyes, C. R.
1894. *Paleontology of Missouri, Pt. 2*: Missouri Geological Survey, vol. 5, pp. 13–37.
1895. *Geology of Lee County.* Iowa Geological Survey, vol. 3, pp. 305–407.

King, W.
1849. *On some families and genera of corals.* Annals and Magazine of Natural History, 2nd ser., vol. 3, pp. 388–390.
1850. *The Permian Fossils of England.* Palaeontographical Society (London), pp. i–xxxvii, 1–258.

Knight-Jones, E. W., and Moyse, J.
1961. *Intraspecific competition in sedentary marine animals.* Symposium of the Society of Exploration Biology, vol. 15, pp. 72–95.

Koenig, J. W.
1958. *Fenestrate Bryozoa in the Chouteau group of central Missouri.* Journal of Paleontology, vol. 32, pp. 126–143.

Lamouroux, J. V.
1812. *Extrait d'un mémoire sur la Classification des Polypiers coralligènes non entierement pierreux.* Noveau Bulletin des Sciences, publié par la Société Philomatique de Paris, vol. 3, pp. 181–188.

Laudon, L. R.
1948. *Osage–Meramec contact.* Journal of Geology, vol. 56, No. 4, pp. 288–302.

Levinsen, G. M. R.
1925. *Undersogelser over Bryozoerne i den danske Dridt formation.* Kongelige Danske Videnskapelige Selskaps Skrifter, nat.-mat. Afd., vol. 7, pp. 283–445.

Levinton, J.
1972. *Stability and trophic structure in deposit-feeding and suspension-feeding communities.* American Naturalist, vol. 106, pp. 472–486.

Lineback, J. A.
1966. *Deep-water sediments adjacent to the Borden Siltstone (Mississippian) delta in southern Illinois.* Illinois State Geological Survey, Circular 401, 48 pp.

Lonsdale, W.
1839. *Corals,* in Murchison, R. I. *The Silurian System, Part II — organic remains*, John Murray (London), pp. 675–694.

Lutaud, G.
1955. *Sur la ciliature du tentacule chéz les Bryozoaires cheilostomes.* Archives de Zoologie Expérimentale et génerale, vol. 92, pp. 13–19.
1973. *L'innervation du lophophore chéz le Bryozoaire cheilostome* Electra pilosa *(L.).* Zeitschrift für Zellforschung und mikroskopische Anatomie. vol. 140, pp. 217–234.

Marcus, E.
1924. *Zur vergleichenden Embryologie der Bryozoen.* Mitteilungen aus dem Zoologischen Museum in Berlin, vol. 11, pp. 155–166.

Marischal, R. N.
1965. *The adult and larval morphology and life history of the entoproct* Barentsia gracilis *(M. Sars, 1835).* Journal of Morphology, vol. 116, pp. 311–338.

McCoy, F.
1844. *A synopsis of the characters of the Carboniferous limestone fossils of Ireland.* Fossilum Catalogus (Dublin), pp. 194–207.

McFarlan, A. C.
1942. *Chester Bryozoa of Illinois and western Kentucky.* Journal of Paleontology, vol. 16, pp. 437–458.

McKee, E. D., and Weir, G. W.
1953. *Terminology for stratification and cross-stratification in sedimentary rocks.* Geological Society of America, Bulletin 64, pp. 381–390.

McKinney, F. K.
1977. *Functional interpretation of lyre-shaped Bryozoa.* Paleobiology, vol. 3, pp. 90–97.
1979. *Some paleoenvironments of the coiled fenestrate bryozoan* Archimedes, in Larwood, G. P., and Abbott, M. B., [eds.], Proceedings of the Fourth International Bryozoology Association Symposium on Advances in Bryozoology, Systematics Association, Special Volume 3, No. 13, pp. 321–334, Academic Press (London).
1980. *The Devonian fenestrate bryozoan* Utropora *Počta.* Journal of Paleontology, vol. 54, No. 1, pp. 241–252.

McKinney F. K., and Gault, H. W.
1980. *Paleoenvironment of Late Mississippian fenestrate bryozoans, eastern United States.* Lethaia, vol. 13, pp. 127–146.

McNair, A. H.
1937. *Cryptostomatous Bryozoa from the Middle Devonian Traverse group of Michigan.* University of Michigan Museum of Paleontology, Contributions, vol. 5, No. 9, pp. 103–170.

McQueen, H. S., Hinchey, N. S., and Aid, K.

1941. *The Lincoln fold in Lincoln, Pike, and Ralls Counties, northeast Missouri.* Kansas Geological Society, 15th Annual Field Conference, Guidebook, pp. 99–110.

Meek, F. B., and Worthen, A. H.

1860. *Description of new Carboniferous fossils from Illinois and other western states.* Philadelphia Academy of Sciences, Proceedings for 1860, pp. 447–472.

Meyer, D. L., and Macurda, D. B.

1977. *Adaptive radiation of the comatulid crinoids.* Paleobiology, vol. 3, pp. 74–82.

Miller, S. A.

1889. *North American Geology and Paleontology for the Use of Amateurs, Students, and Scientists.* Western Methodist Book Concern (Cincinnati), 664 pp.

Miller, T. G.

1961a. *New Irish Tournasian fenestellids.* Geological Magazine, vol. 98, No. 6, pp. 493–500.

1961b. *Type specimens of the genus* Fenestella *from the Lower Carboniferous of Great Britain.* Palaeontology, vol. 4, pt. 2, pp. 221–242.

1962. *Some Wenlockian fenestrate Bryozoa.* Palaeontology, vol. 5, pt. 3, pp. 540–549.

Moll, J. P. C.

1803. *Eschara, ex Zoophytorum, seu, Phytozoorum ordine pulcherrimum ac notatu dignissimum genus novis speciebus auctum, methodice descriptum, et iconibus ad naturam delineatis illustratum.* viii + 70 pp., 4 pls. (Vindobonae).

Moore, R. C.

1933. *Historical Geology.* McGraw-Hill (New York), 673 pp.

Morozova, I. P.

1962. *On the systematics and phylogeny of the Fenestelloidea.* Paleontologiceskij Zhurnal, No. 4, pp. 104–115.

1970a. *Late Permian bryozoans.* Trudy Geologičeskogo Museja Akademii Nauk SSSR, Paleontol. Inst., vol. 122, 314 pp.

1970b. *Some Late Permian Bryozoa from northeast U. S. S. R.* Paleontological Journal, vol. 4, No. 3, pp. 361–370.

1973. *New and little-known structures of Fenestelloidea,* in Larwood, G. P. [ed.], *Living and Fossil Bryozoa,* pp. 327–333, Academic Press (London).

1974. *Revision of the bryozoan genus* Fenestella. Paleontological Journal, vol. 8, No. 2, pp. 167–180.

Mullin, M.

1963. *Some factors affecting the feeding of marine copepods of the genus* Calanus. Limnology and Oceanography, vol. 8, pp. 239–250.

Nekhoroshev, V. P.

1926. *Lower Carboniferous Bryozoa from the Kuznetzk Basin.* Geologičeskogo Komiteta (ou Kommissii) Léningrad, Bulletin., vol. 43, pp. 1237–1290.

1928. *Istoriya razvitiya Paleozoisikh msakok semeistva Fenestellidae [Developmental history of Paleozoic bryozoans of the family Fenestellidae].* Izvestiya Geologičeskogo Kommissii, vol. 47, No. 5, pp. 479–518.

1932. *A microscopic method for investigation of Paleozoic bryozoans of the family Fenestellidae.* Izvestiya Vsesojuznogo Geologičeskii Ob'yedin, vol. 51, No. 17, pp. 279–303.

1949. Fenestella *from the Devonian of Kazakhstan with unusual structure of the zooecia.* Ežegodnik vsesojuznogo obshchestva, vol. 8, pp. 31–39.

1953. *Lower Carboniferous Bryozoa of Kazakhstan.* Izdanie Akademii Nauk (SSSR), pp. 1–182, 25 pls.

1956. *Lower Carboniferous Bryozoa of the Altai and Siberia.* Izdanie Akademii Nauk (SSSR), new series, vol. 13, pp. 1–148, 57 pls.

1960. *Fenestellidae,* in Sarycheva, T. G. [ed.], *Principles of Paleontology; Bryozoa, Brachiopoda.* Izdanie Akademii Nauk (SSSR), pp. 77–81.

Nicholson, H. A., and Lydekker, R.

1889. *Manual of paleontology,* [third ed.], pp. 889–1624, William Blackwood (Edinburgh and London).

Nickles, J. M., and Bassler, R. S.

1900. *A synopsis of American fossil Bryozoa including bibliography and synonymy.* United States Geological Survey, Bulletin 173, 663 pp.

Nielsen, C.

1970. *On metamorphosis and ancestrula formation in cyclostomatous bryozoans.* Ophelia, vol. 7, pp. 217–256.

Nielsen, C., and Pedersen, J. P.

1979. *Cystid structure and protrusion of the polypide in* Crisia *(Bryozoa, Cyclostomata).* Acta Zoologica Stockholm, vol. 60, pp. 65–88.

Nikiforova, A. I.

1927. *Materials for the understanding of Lower Carboniferous Bryozoa of the Donets Basin.* Izvestiya Geologičeskogo Komiteta (ou Kommissii) Léningrad, vol. 46, pp. 245–268, pls. 12–14.

1933. *Middle Carboniferous Bryozoa of the Donets Basin.* Transactions of the United Geological and Prospecting Service of USSR [Tr VGRO], fasc. 237, 46 pp.

1935. *On the finding of the genus* Hemitrypa *in the Lower Carboniferous of the Urals.* Ežegodnik Vserossijskogo paleontologičeskogo obshchestva, vol. 10, pp. 80–82.

1938. *Types of Carboniferous Bryozoa of the European part of the USSR.* Akademeii Nauk SSSR Paleontologičeskogo Instituta, Paleontologija SSSR, vol. 4, ch. 5, vyp. 1, 290 pp.

Nye, O. B., Jr., Dean, D. A., and Hinds, R. S.

1972. *Improved thin section techniques for fossil and recent organisms.* Journal of Paleontology, vol. 46, pp. 271–275.

d'Orbigny, A. D.

1839. *Zoophytes,* in *Voyage dans l'Amérique méridionale (le Brézil . . . l'Uruguay, la République Argentine, la Patagonie . . . Chili . . . Bolivia . . . Pérou), exécuté pendant . . . 1826–33.* vol. 5, pt. 4, 28 pp., 13 pls.

1848–1852. *Prodrome de paleontologie stratigraphique.* Paleozoic–Triassic–Jurassic (1849), pp. 1–394; Jurassic–Cretaceous–Tertiary (1852), pp. 1–427; Tertiary (1852), pp. 1–196.

Owen, D. D.

1838. *Report of a geological reconnaissance of the state of Indiana made in the year 1837,* 34 pp. (reissued with the Second Report in 1839).

1842. *Regarding human footprints in solid limestone.* American Journal of Science, first series, vol. 43, pp. 14–32, 1 pl.

1852. *Report of a geological survey of Wisconsin, Iowa, and Minnesota and incidentally of a portion of Nebraska Territory.* 638 pp., (Philadelphia).

Parsons, R. R., and Le Brasseur, R. J.

1970. *The availability of food to different trophic levels in the marine food chain,* in Steele, J. H. [ed.], *Marine Food Chains,* pp. 325–343, University of California Press (Berkeley).

Phillips, J.

1836. *Illustrations of the geology of Yorkshire, or, a description of the strata and organic remains of the Yorkshire coast, etc. Part II.—The Mountain Limestone district.* xx + 253 pp., 24 pls., map (London).

1841. *Figures and Descriptions of the Paleozoic Fossils of Cornwall, Devon, and West Somerset.* 231 pp., Longmans, Brown, Green, and Longmans (London).

Počta, P.
1894. *Bryzoaires, Hydrozoaires, et partie des anthozoaires,* in Barrande, J. [ed.], *Système Silurien du centre de la Bohême.* (Prague), vol. 8, x + 230 pp., 21 pls.

Potter, P. E., and Pryor, W. A.
1961. *Dispersal centers of Paleozoic and later clastics of the Upper Mississippi Valley and adjacent areas*: Geological Society of America, Bulletin, vol. 72, No. 8, pp. 1195–1249 [reissued as Illinois State Geological Survey, Reprint 1961-T, 55 pp.]

Prout, H. A.
1858a. *First of a series of descriptions of Carboniferous Bryozoa.* Transactions of the St. Louis Acaddemy of Science, vol. 1, No. 2, pp. 235–237.
1858b. *Second series of descriptions of Bryozoa from the Palaeozoic rocks of the western states and territories.* Transactions of the St. Louis Academy of Science, vol. 1, pp. 266–273.
1859. *Third series of descriptions of Bryozoa from the Palaeozoic rocks of the western states and territories.* Transactions of the St. Louis Academy of Science, vol. 1, pp. 443–452. [issued in 1859 and 1860]
1860. *Fourth series of descriptions of Bryozoa from the Palaeozoic rocks of the western states and territories.* Transactions of the St. Louis Academy of Science, vol. 1, pp. 571–581 [issued in 1859 and 1860]
1866. *Descriptions of Polyzoa from the Paleozoic rocks.* Illinois State Geological Survey, vol. 2, pp. 412–423.

Pryor, W. A., and Sable, E. G.
1974. *Carboniferous of the eastern interior basin.* Geological Society of America, Special Paper 148, pp. 281–313.

Rexroad, C. B., and Collinson, C.
1965. *Conodonts from the Keokuk, Warsaw, and Salem formations (Mississippian) of Illinois.* Illinois State Geological Survey, Circular 388, 26 pp.

Rhodes, F. H. T., Austin, R. L., and Druce, E. C.
1969. *British Avonian (Carboniferous) conodont faunas, and their value in local and intercontinental correlation.* British Museum (Natural History), Bulletin of Geology, Supplement 5, pp. 1–313.

Ross, J. R. P.
1964. *Early Paleozoic Stenolaemata.* Geological Society of America, Bulletin, vol. 75, pp. 927–948.

Rubey, W. W.
1952. *Geology and mineral resources of the Hardin and Brussels Quadrangle.* United States Geological Survey, Professional Paper 218, 179 pp.

Sakagami, S.
1970. *On the Paleozoic Bryozoa of Japan and Thai-Malayan districts.* Journal of Paleontology, vol. 44, No. 4, pp. 680–692.

Schoener, T. W.
1974. *Resource partitioning in ecological communities.* Science, vol. 185, p. 27–39.
1982. *The controversy over interspecific competition.* American Scientist, vol. 70, pp. 586–595.

Sheldon, R. W., Sutcliffe, W. H., Jr., and Prakash, A.
1973. *The production of particles in the surface waters of the ocean with particular reference to the Sargasso Sea.* Limnology and Oceanography, vol. 18, pp. 719–733.

Shishova, N. A.
1968. *New Order of Paleozoic bryozoans.* Paleontological Journal, vol. 2, No. 1, pp. 117–121.

Shulga-Nesterenko, M. I.
1936. Fenestella *and* Archimedes *from the middle Pechora region of the North Ural.* Trudy Paleontologyčeskogo Instituta, Komiteta Poliarnaia, vol. 38, pp. 233–385.
1941. *Lower Permian Bryozoa of the Urals,* in *Paleontology of the USSR.* Trudy Paleontologyčeskogo Instituta, SSSR, vol. 5, pt. 5, No. 1, pp. 1–276.
1949. *An attempt of phylogenetic analysis of bryozoans of the family Fenestellidae.* Trudy Paleontologyčeskogo Instituta, SSSR, vol. 20, pp. 293–316.
1951. *Carboniferous fenestellids of the Russian Platform.* Trudy Akademiya Nauk SSSR, Paleontologyčeskogo Instituta, vol. 32, pp. 3–156, 34 pls..
1952. *New Lower Permian bryozoans of Cisuralia.* Trudy Paleontologyčeskogo Instituta, SSSR, vol. 37, pp. 3–83.
1955. *Carboniferous bryozoans of the Russian Platform.* Trudy Paleontologyčeskogo Instituta, SSSR, vol. 57, 204 pp. 32 pls.
1960. *Family Phylloporinidae Ulrich, 1890,* in *Principles of Paleontology.* Bryozoa, Brachiopoda, pp. 76–77.

Silen, L., and Harmelin, J. G.
1974. *Observations on living Diastoporidae (Bryozoa Cyclostomata), with special regard to polymorphism.* Acta Zoologica, Stockholm, vol. 55, pp. 81–96.

Simpson, G. G.
1895a. *A handbook of the genera of the North American Paleozoic Bryozoa.* Report of the State Geologist (New York) for 1894, pp. 407–608.
1895b. *Thirteenth Annual Report of the State Geologist of New York for 1893,* 717 pp.

Smith, D. C.
1981. *Competitive interactions of the striped plateau lizard* (Sceloporus virgatus) *and the tree lizard* (Urosaurus oratus). Ecology, vol. 62, pp. 679–687.

Snyder, E. M.
1987. *Ecologic succession observed in the Warsaw Formation (Valmeyeran, Mississippian) of the Mississippi valley,* pp. 245– 252 in Ross, J.P. [ed.], *Bryozoa: Present and Past,* Proceedings of the Seventh International Bryozoological Association meeting, Bellingham, Washington (1986).

Snyder, E. M., and Kepler, K.
1987. *Numerical test of species assignment for fenestrate Bryozoa af the Warsaw Formation: An application of DISK.* Proceedings for the Association for Media and Technology in Education in Canada, Saskatoon, Saskatchewan, p. 72.

Stockdale, P. B.
1929. *Stratigraphic units of the Harrodsburg Limestone.* Indiana Academy of Sciences, Proceedings for 1928, vol. 38, pp. 233–242.
1939. *Lower Mississippian rocks of the east-central interior.* Geological Society of America, Special Paper 22, pp. 1–248.

Strathmann, R. R.
1971. *The feeding behavior of planktotrophic echinoderm larvae; mechanisms, regulation and rates of suspension feeding.* Journal of Marine Biology and Ecology, vol. 6, pp. 109–160.
1973. *Function of lateral cilia in suspension feeding of lophophorates (Brachiopoda, Phronida, Ectoprocta).* Marine Biology, vol. 23, pp. 129–136.

Swann, D. W.
1963. *Classification of Genevievian and Chesterian (Late Mississippian) rocks of Illinois.* Illinois State Geological Survey, Circular 216, 91 pp.

Tavener-Smith, R.
1965. *A new fenestrate bryozoan from the Lower Carboniferous of County Fermanagh.* Palaeontology, vol. 8, pp. 478–491.
1966. *The micrometric formula and the classification of fenestrate cryptostomes.* Palaeontology, vol. 9, pp. 413–425.
1973. *Fenestrate Bryozoa from the Visean of County Fermanagh, Ireland.* British Museum (Natural History), Geological Bulletin, vol. 23, No. 7, pp. 392–483.

Tavener-Smith, R., and Williams, A.
1972. *The secretion and structure of the skeleton of living and fossil Bryozoa.* Philosophical Transactions of the Royal Society of London, ser. B, vol. 264, pp. 97–159.

Termier, H., and Termier, G.
1971. *Bryozoaires du Paleozoique superieur de l'Afghanistan.* Documents de la Laboratoire de Geologie, Faculte des Sciences, Lyon, No. 47, 52 pp.

Treworgy, J.
1981. *Structural features in Illinois — a compendium.* Illinois State Geological Survey, Circular 519, 22 pp.

Trizna, V. B.
1939. *New bryozoan species of the families Fenestellidae and Acanthocladiidae in the piedmont belt of Bashkiria.* Trans. naučno-issledovatel'skyj geologo-razvedočnyj Instituta [Tr NIGRI], ser. A, vol. 11, pp. 102–144.
1950. *Characterization of reef and bedded facies of the central region of the Ufimsk plateau.* Trudy Vsesojuznyj naučno-issledotel'skyj geologořazvedočnyj instituta [Tr VNIGRI], n. ser., vol. 50, pp. 47–144, pl. 1–16.
1958. *Early Carboniferous Bryozoa of the Kuznetsk Basin.* Trudy Vsesojuznyj naučno-issledotel'skyj geologořazvedočnyj instituta [Tr VNIGRI], vol. 122, 436 pp.

Trizna, V. B., and Kautsan, R. A.
1951. *Bryozoa of the Artinskian stage of the Ufa Plateau and their role in the stratigraphy of this stage in Cisuralia.* Trudy Vsesojuznyj naučno-issledotel'skyj geologořazvedočnyj instituta [Tr VNIGRI], vol. 170, pp. 332–453.

Turpaeva, E. P.
1957. *[Food interrelationships of dominant species in marine benthic biocoenoses].* Trudy Instituta okeanologii, vol. 22, pp. 171–185, Moskva [in Russian].

Ulrich, E. O.
1882. *American Paleozoic Bryozoa.* Journal of the Cincinnati Society of Natural History, vol. 5, pp. 121–175, 232–257.
1888. *A list of the Bryozoa of the Waverly Group in Ohio, with descriptions of new species.* Denison University Scientific Laboratories, Bulletin, vol. 4, pp. 62–96.
1890. *Palaeozoic Bryozoa.* Illinois State Geological Survey, vol. 8, pp. 283–688.
1893. *On Lower Silurian Bryozoa of Minnesota.* Minnesota Geological and Natural History Survey, Final Report, vol. 3, pt. 1, pp. 96–332. [published in 1895]
1904. *Determination and correlation of formations (of northern Arkansas).* United States Geolological Survey, Professsional Paper 24, pp. 90–113.

Utgaard, J., and Perry, T. G.
1960. *Fenestrate bryozoans from the Glen Dean Limestone (Middle Chester) of southern Indiana.* Geological Society of America, Bulletin, vol. 70, No. 12, pt. 2, pp. 1–32.

Van Tuyl, F. M.
1925. *Stratigraphy of the Mississippian formations of Iowa.* Iowa Geological Survey, vol. 30, pp. 33–349.

Vermeij, F. J.
1977. *The Mesozoic marine revolution; evidence from snails, predators and grazers.* Paleobiology, vol. 3, pp. 245–258.

Vine, R. G.
1880. *Report of the Committee, consisting of Professor P. M. Duncan and Mr. G. R. Vine, appointed for the purpose of reporting on the Carboniferous Polyzoa, drawn up by Mr. Vine (Secretary).* Report of the Fiftieth Meeting of the British Association for the Advancement of Science, Swansea, August and September, 1850, pp. 76–87.
1884. *Fourth report of the committee consisting of Dr. H. C. Sorby and Mr. G. R. Vine, appointed for the purpose of reporting on fossil Bryozoa.* Report to the Director of the Association for the Advancement of Science, 53rd Meeting (Southport, 1883), pp. 161–209.
1886. *Notes on Yorkdale Polyzoa of north Lancashire and Yorkshire.* Proceedings of the Yorkshire Geological Society, vol. 9, pp. 70–98.

Waagen, W., and Pichl, J.
1885. *Salt Range fossils; Productus-limestone fossils.* Memoirs of the Geological Survey of India (Palaeontologia Indica), ser. 13, vol. 1, pt. 5, pp. 771–834.

Walker, K. R.
1962. *Lithofacies map of Lower Mississippian clastics of eastern and east-central United States.* American Association of Petroleum Geologists, Bulletin, vol. 46, pp. 105–111.

Wanless, H. R.
1957. *Geology and mineral resources of the Beardstown, Glasford, Havana, and Vermont quadrangles.* Illinois State Geological Survey, Bulletin 82, 233 pp.

Wass, R.
1966. *On the species* Fenestella horoogia *Bretnall and* Minilya duplaris *Crockford.* University of Sydney, Department of Geology and Geophysics, Publication, pp. 90–95.

Waters, A. W.
1891. *On cheilostomatous characters in Meliceratidae and other fossil Bryozoa.* Annals and Magazine of Natural History, ser. 6, vol. 8, pp. 48–58.
1904. *Bryozoa.* Expedition Antarctique Belgique, Resulte Voyage, Belgique Rappord de Science et Zoologie, vol. 2, pp. 1- 114.

Weller, J. M.
1934. *The Warsaw Formation.* Transactions of the Illinois Academy of Sciences, vol. 26, No. 3, pp. 106.

Weller, J. M., Williams, J. S., Bell, W. A., Dunbar, C. O., Laudon, L. R., Moore, R. C., Stockdale, P. B., Warren, P. S., Caster, K. E., Cooper, C. L., Willard, B., Croneis, C., Malott, C. A., Price, P. H., and Sutton, A. H.
1948. *Correlation of the Mississippian Formations of North America.* Geological Society of America, Bulletin, vol. 59, No. 2, pp. 91–196.

Weller, J. M., and Sutton, A. H.
1940. *Mississippian border of Eastern Interior Basin.* American Association of Petroleum Geologists, Bulletin, vol. 24, pp. 765–858; Illinois Geological Survey, Report of Investigations 62.

Weller, S.
1908. *The Salem Limestone.* Illinois State Geological Survey, Extract B8, pp. 81–102.
1914. *The Mississippian Brachiopoda of the Mississippi Valley Basin.* Illinois State Geological Survey, Monograph 1, pt. 1, 508 pp.; pt. 2, 187 pp.
1926. *Faunal zones in the standard Mississippian section.* Journal of Geology, vol. 34, No. 4, pp. 320–335.

Whitfield, R. P.
1891. *Contributions to invertebrate palaeontology.* Annals of the New York Academy of Sciences, vol. 5, pp. 505–620.

Whitfield, R. P.
1895. *Contributions to the paleontology of Ohio.* Report of the Ohio Geological Survey, vol. 7, pp. 407–494. [published in 1895]

Whiting, L. L., and Stevenson, D. L.
1965. *Sangamon Arch.* Illinois Geological Survey, Circular 383, 20 pp.

Wiens, J. A.
1977. *On competition and variable environments.* American Scientist, vol. 65, pp. 590–597.

Willman, H. B., Atherton, E., Bushbach, T. C., Collinson, C., Frye, J. C., Hopkins, M. E., Lineback, J. A., and Simon, J. A.
1975. *Handbook of Illinois stratigraphy.* Illinois Geological Survey, Bulletin 95, 261 pp.

Wills, D. L.
1971. *Sonora Sandstone stratigraphy, Illinois and Iowa outcrop belt.* unpublished Ph. D. dissertation, University of Iowa.

Winston, J. E.
1976. *Experimental culture of the estuarine ectoproct* Conopeum tenuissimum *from Chesapeake Bay.* Biological Bulletin, Woods Hole, Mass., vol. 150, pp. 318–335.
1977. *Feeding in marine bryozoans*, in Woollacott, R. M., and Zimmer, R. L. [eds.], *The Biology of Bryozoans.* pp. 233–271, Academic Press (New York).
1978. *Polypide morphology and feeding behavior in marine ectoprocts.* Bulletin of Marine Science, vol. 28, pp. 1–31.
1982. *Marine bryozoans (Ectoprocta) of the Indian River area (Florida).* Bulletin of Marine Science, vol. 28, pp. 1–31.

Worthen, A. H.
1866. *Geology.* Illinois State Geological Survey, vol. 1, 504 pp.
1870. *Geology and paleontology.* Illinois State Geological Survey, vol. 5, 619 pp.

Worthen, A. H., Shaw, J., and Meek, F. B.
1873. *Geology and paleontology.* Illinois State Geological Survey, vol. 5, 632 pp.

Young, J.
1881. *Remarks on the genus* Synocladia *and other allied forms, with description of a new species.* Proceedings of the Natural History Society of Glasgow, vol. 5, pp. 30–35.

Zittel, K. A.
1880. *Handbuch der Paläontologie, Abt. 1. Paläozoologie.* d. 1, 765 pp., R. Oldenbourg (München).

EXPLANATION OF PLATE 1

Figure		Page
1–12.	***Rectifenestella tenax*** (Ulrich, 1888)	41

1. Figured specimen, UI X-6803. Obverse exterior surface of zoarial fragment exhibiting pronounced secondary ontogenetic thickening. Illustrated are typical inflections of apertures into fenestrules (arrow **a**), shared aperture at branch bifurcation (arrow **b**), longitudinal striae across dissepiment surfaces (arrow **c**), and typical meshwork pattern, ×30.

2. Figured specimen, UI X-6798. Reverse exterior surface of highly ontogenetically thickened zoarial fragment showing enlarged macrostylets (arrow) as well as branch and dissepiment diameters greater than those in non-thickened zoaria, ×30.

3, 4. Figured specimen, UI X-6801. zoarial fragment exhibiting slight to moderate ontogenetic thickening. 3. Obverse exterior surface showing peristomal gaps at proximal end of aperture (arrow **a**), slightly centrally thickened terminal diaphragm (arrow **b**), and keel not covered by thickened lamellar skeleton, ×30; 4. Reverse exterior surface showing longitudinal striae (arrow **a**), macrostylet development (arrow **b**), and reverse zoarial support (arrow **c**), ×30.

5, 12. Figured specimen, UI X-6799. 5. FF69, longitudinal section through mid chamber, obverse to right, showing typical chamber outline in this view, ×70; 12. FF70, oblique longitudinal section, obverse to right, from mid chamber at top to shallowest branch edge, and cross-section of dissepiment (arrow **a**) at bottom. Shallowest chamber views (arrow **b**) show extension of aperture into fenestrule, ×70.

6, 8, 11. Figured specimen, UI X-6896. Zoarial fragment exhibiting moderate ontogenetic thickening; 6. EF46, mid to shallow longitudinal section, obverse to right, illustrating zoarial support development (arrow **a**) and ontogenetic thickening of lamellar skeleton (arrow **b**) of zoarial fragment from proximal end of zoarium, ×70; 8. EF48, transverse section showing continuity of granular skeleton across dissepiment (arrow **a**), connecting with nodes (arrow **b**) and completely surrounding autozooecial chambers (arrow **c**), ×70; 11. EF47, oblique longitudinal section, obverse to left, ranging from mid chamber at top to branch edge at bottom. Shown is change in autozooecial chamber outline form from deep to shallow section. Arrow illustrates continuity of granular skeletal material with obverse surface nodes, ×70.

7. Figured specimen, UI X-6806. FF30, transverse section of highly ontogenetically thickened zoarial fragment; note consistency of aperture openings parallel to plane of obverse surface. Superior hemiseptum (arrow **a**) causes restriction between aperture and chamber proper. Thickened lamellar skeleton (arrow **b**) and thickened branch axial wall (arrow **b**) characterize ontogenetic thickening in this species, ×70.

9, 10. Figured specimen, UI X-6889. Serial tangential sections; 9. EF28, mid section with short superior hemisepta (arrow **a**) and typical bilobate-elliptical chamber outline (arrow **b**), ×70; 10. shallow section illustrating aperture positioning at abaxial edge of autozooecial chamber (arrow **a**) and stylets along obverse surface (arrow **b**), ×70.

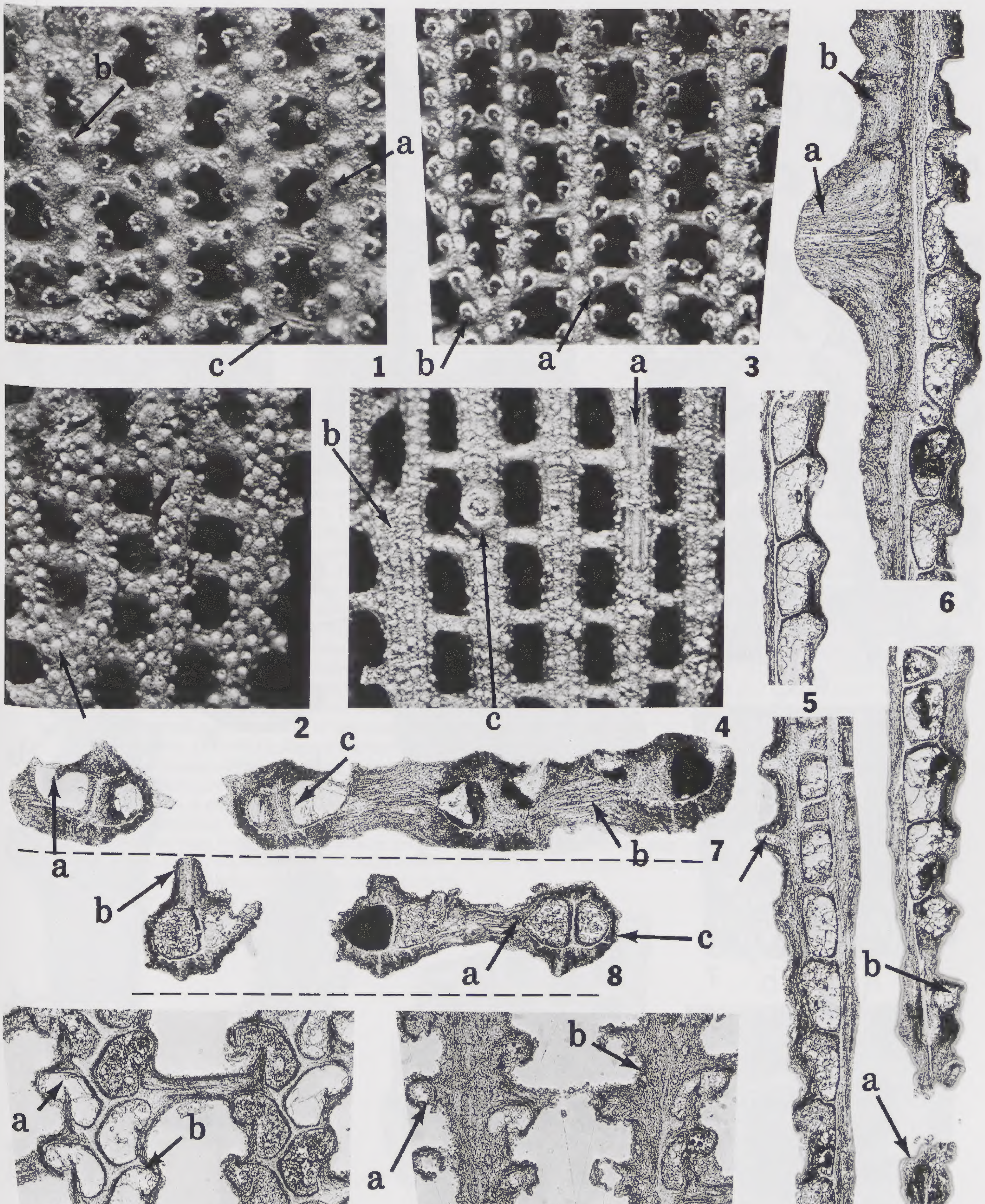
1
2
3
4
5
6
7
8
9
10
11
12

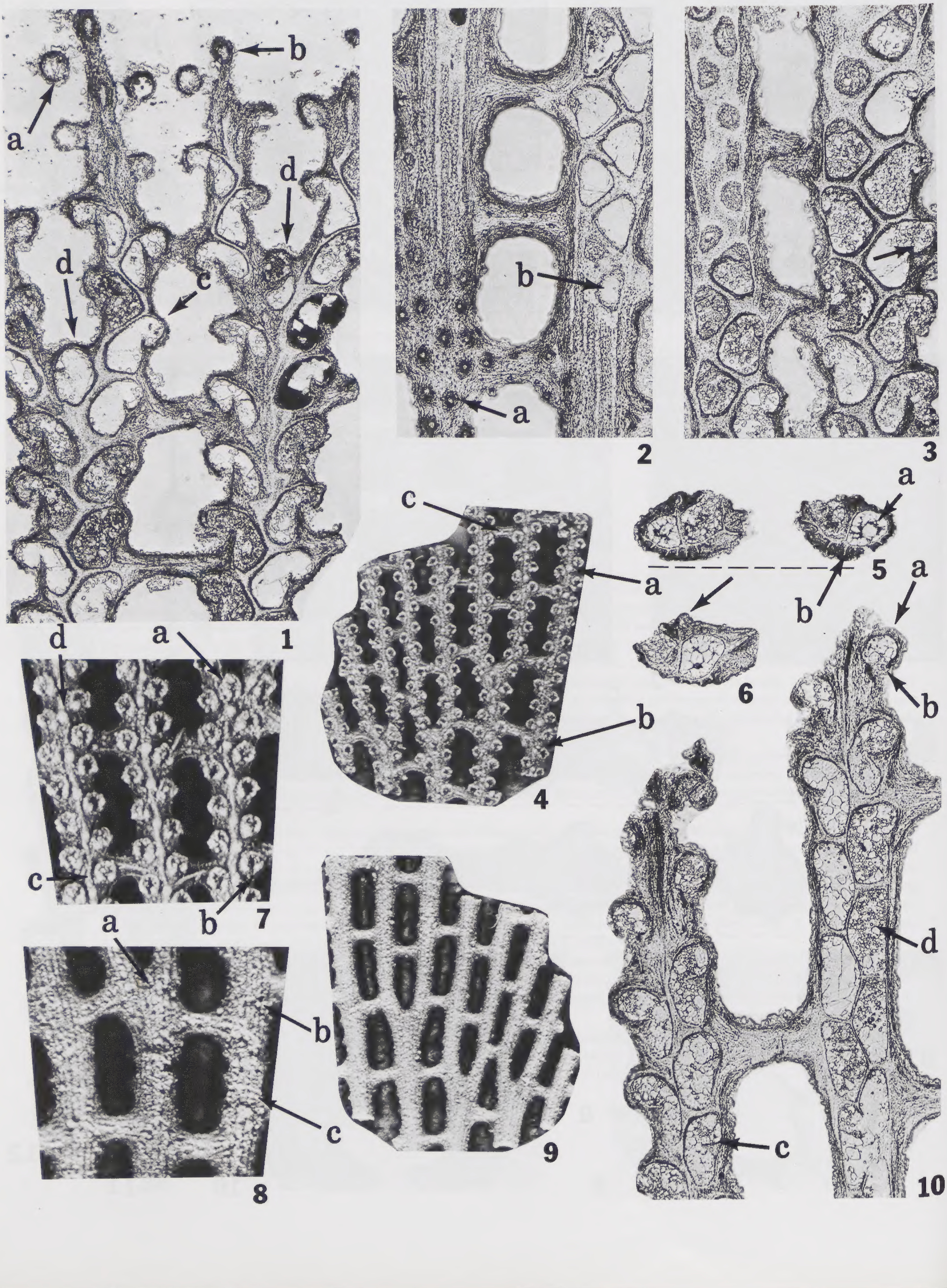
1
2
3
4
5
6
7
8
9
10

EXPLANATION OF PLATE 2

Figure Page

1–3. ***Rectifenestella tenax*** (Ulrich, 1888) 41

1. Figured specimen, UI X-6889. EF28, shallow to mid tangential section illustrating peristomal development surrounding the aperture (arrow **a**), nodal development (arrow **b**), typical chamber outline in mid tangential view (arrow **c**), and chamber placement at site of branch bifurcation (arrow **d**), ×70.
2. Figured specimen, UI X-6801. FF85, deep to mid tangential section, fragment exhibits slight to moderate ontogenetic thickening of the lamellar skeleton. Shown is development of reverse wall macrostylets (arrow **a**) with their rim of lamellar calcite and center of granular calcite, and typical chamber outline near reverse-wall budding-site (arrow **b**), ×70.
3. Figured specimen, UI X-6805. FF95, deep to mid tangential section, with zoarial fragment exhibiting moderate to pronounced ontogenetic thickening; arrow shows short superior hemiseptum at proximal–abaxial edge of vestibule, ×70.

4–10. ***Rectifenestella tenuissima*** (Cumings, 1906) 45

4, 9, 10. Hypotype, UI X-6833. Zoarial fragment exhibiting moderate secondary overgrowth by lamellar skeleton; 4. Obverse exterior surface showing lamellar skeleton causing enlargement of nodes (arrow **a**), obscuring keel (arrow **b**), and increasing size of striae across the dissepiment (arrow **c**), ×8; 9. reverse exterior zoarial surface, ×8; 10. FD63, mid to shallow tangential section illustrating well-developed peristome (arrow **a**) with typical opening at proximal end of aperture (arrow **b**), superior hemiseptum at vestibule proximal-abaxial edge (arrow **c**) resulting in bilobate-elliptical chamber shape near obverse surface, and typical chamber outline in mid tangential section (arrow **d**), ×70.

5–8. Hypotype, UI X-6834. Zoarial fragment exhibiting slight ontogenetic thickening; 5. FD66, transverse section showing typical branch outline, transverse chamber shape in mid chamber view (arrow **a**) and continuity of granular skeletal layer around the autozooecial chamber and with reverse-wall striae (arrow **b**), ×70; 6. FD66, transverse section illustrating continuity of granular skeletal layer surrounding autozooecial chamber with obverse surface nodes (arrow), ×70; 7. Obverse exterior surface, showing aperture placement at site of branch bifurcation (arrow **a**), typical orientation of aperture openings into fenestrule (arrow **b**), anastomosing keel (arrow **c**) and nodes positioned atop keel (arrow **d**), ×20; 8. Reverse exterior zoarial surface illustrating site of branch bifurcation (arrow **a**), and longitudinal striae (arrow **b**) atop which are positioned rows of intermediate microstylets (arrow **c**), ×20.

EXPLANATION OF PLATE 3

Figure Page

1–8. ***Rectifenestella tenuissima*** (Cumings, 1906) 45

1, 3, 5, 8. Hypotype, UI X-6832. 1. FD51, oblique longitudinal section, obverse to right, ranging from very shallow at top of figure to moderately deep at bottom. Shown is dissepiment development (arrow **a**), chamber profile in mid longitudinal section (arrow **b**), nodal development on obverse surface (arrow **c**), and microstylet originating from granular skeleton on reverse wall (arrow **d**), ×70; 3. FD55, mid to deep tangential section illustrating chamber outline near reverse-wall budding-site (arrow **a**), longitudinal striae developed along reverse wall (arrow **b**) and continuity of striae with granular skeletal layer, and microstylet development on the reverse-wall surface (arrow **c**) as a rearward extension of the longitudinal striae, ×40; 5. FD56, transverse section at proximal end of zoarium. Illustrated is continuity of granular skeleton across dissepiment (arrow **a**) and around autozooecial chambers (arrow **b**), and attitudinal relationship of aperture to plane of obverse surface (arrow **c**), ×70; 8. FD53, shallow to mid tangential section of fragment exhibiting moderate ontogenetic thickening. Observe widened keel (arrow **a**) and increased nodal diameter (arrow **b**) resulting from thickening of outer lamellar skeleton, ×40.

2, 4. Hypotype, UI X-6833. 2. FD57, moderately to very shallow longitudinal section, obverse to right, illustrating short superior hemiseptum (arrow **a**), aperture opening positioned at distal end of chamber (arrow **b**) and aperture (arrow **c**) opening onto dissepiment (arrow **d**), ×70; 4. FD63, mid to shallow tangential section showing short superior hemiseptum positioned at proximal end of aperture (arrow **a**) in shallow view of autozooecial chamber resulting in bilobate-elliptical chamber shape near obverse surface and extension of aperture laterally into fenestrule (arrow **b**), ×70.

6, 7. Hypotype, UI X-6834. FD70. 6. Shallow to mid tangential section showing typical chamber outline in mid (arrow **a**), mid shallow (arrow **b**) and shallow (arrow **c**) chamber views. Note enlargement of distal end and closing of proximal end of chamber. Granular skeletal material is continuous around autozooecial chambers (arrow **c**), across dissepiment (arrow **d**), and along medial keel (arrow **e**), ×70; 7. Shallow to mid tangential section illustrating small stylets across obverse branch surface (arrow **a**) and apertural stylets (arrow **b**) observed only in the most shallow views, ×70.

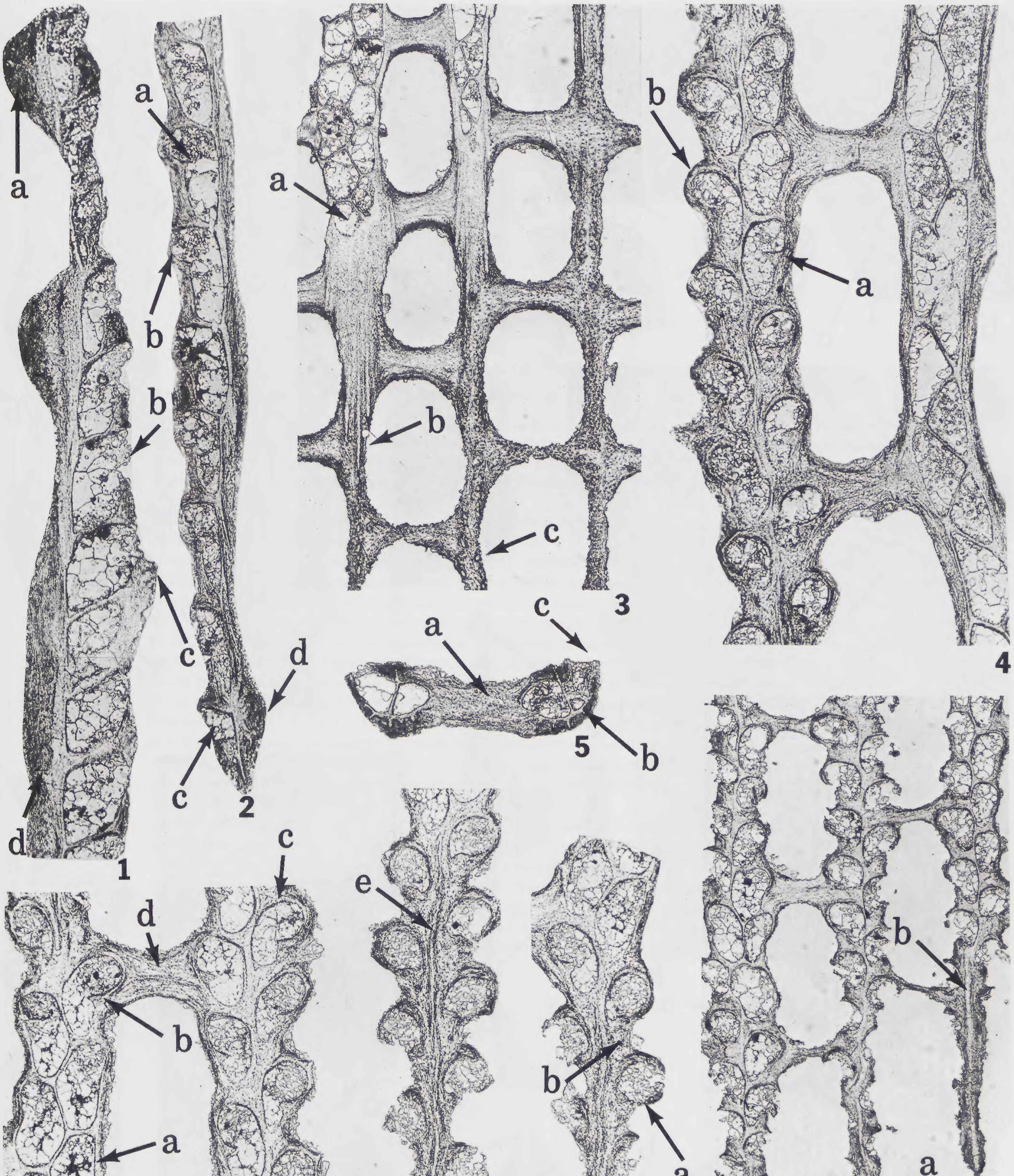
a
a
b
b
c
d
c
d
1
2
a
b
c
3
b
a
4
a
c
5
b
c
d
b
a
6
e
b
a
7
b
a
8

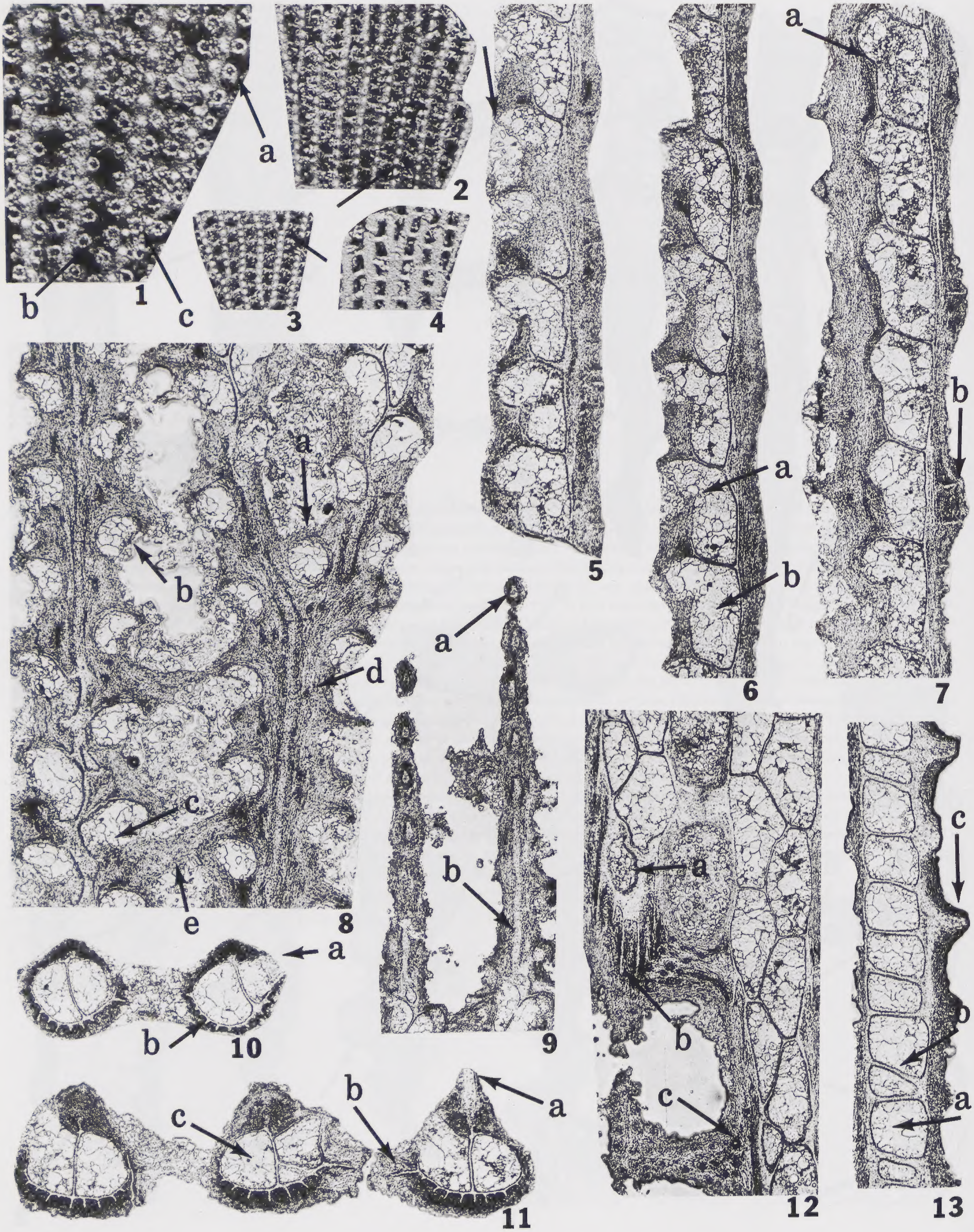
1 a b c
2
3
4
5
6 a b
7 a b
8 a b c d e
9 a b
10 a b
11 a b c
12 a b c
13 a b c

EXPLANATION OF PLATE 4

Figure Page
1–13. ***Rectifenestella multispinosa*** (Ulrich, 1890) 47

1. Figured specimen, UI X-6870. Obverse exterior surface of moderately secondarily thickened zoarial fragment illustrating aperture opening (arrow **a**) and its attitudinal relationship to plane of obverse surface, aperture extension into fenestrule and onto dissepiment (arrow **b**), and stylet development on obverse surface (arrow **c**) near site of branch bifurcation, ×25.

2, 4–8, 11, 12. Figured specimen, UI X-6874. Zoarial fragment exhibiting pronounced secondary thickening; 2. Obverse exterior surface. Note nodal placement (arrow) atop keel, ×8; 4. Reverse exterior surface illustrating rounded, thickened branches and barlike dissepiments, ×8; 5. FH44, shallow to mid longitudinal section, obverse to left, showing terminal diaphragm development (arrow), ×70; 6. FH44, mid longitudinal section, obverse to left, illustrating short hemiseptum at proximal end of aperture (arrow **a**) and typical chamber outline in mid longitudinal view (arrow **b**). Note thin terminal diaphragms over most aperture openings, ×70; 7. FH43, deep mid longitudinal section, obverse to left, illustrating autozooecial chamber at maximum length (arrow **a**) and microstylet development (arrow **b**) continuous with internal granular skeleton, ×70; 8. FH47, shallow tangential section showing aperture position at site of branch bifurcation (arrow **a**), terminal diaphragm across aperture opening (arrow **b**), superior hemiseptum at proximal end of aperture (arrow **c**), small stylets along obverse surface (arrow **d**), and rodlike dissepiment between branches (arrow **e**), ×70; 11. FH43, transverse section. Note continuity of granular skeletal layer with obverse node (arrow **a**) and across dissepiment (arrow **b**); typical chamber outline in mid transverse section (arrow **c**) is also shown, ×70; 12. FH49, deep to mid tangential section showing chamber outline near reverse-wall budding-site (arrow **a**), continuity of granular skeleton with reverse longitudinal striae (arrow **b**) and presence of reverse microstylets (arrow **c**) forming as extensions of longitudinal striae, ×70.

3, 9, 10, 13. Figured specimen, UI X-6872. Zoarial fragment exhibiting slight to moderate ontogenetic thickening. 3. Obverse exterior surface showing site of branch bifurcation (arrow), ×8; 9. FH35, very shallow tangential section illustrating nodal development and placement (arrow **a**) and keel (arrow **b**) from which nodes arise, ×40; 10. FH31, transverse section. Note attitudinal relationship of aperture opening to plane of obverse surface (arrow **a**) and continuity of granular skeleton with longitudinal striae (arrow **b**), ×70; 13. FH33, deep longitudinal section, obverse to right, showing typical chamber outline in this view (arrow **a**), and inner granular skeletal layer (arrow **b**) continuous around autozooecial chambers and with obverse nodes (arrow **c**), ×70.

EXPLANATION OF PLATE 5

Figure Page

1–3. ***Rectifenestella multispinosa*** (Ulrich, 1890) 47

Figured specimen, UI X-6874. 1. FH47, shallow to mid tangential section showing prominent keel and attitudinal relationship of aperture to fenestrule opening (arrow), ×40; 2. FH49, deep to moderately shallow tangential section illustrating typical chamber outline in mid chamber (arrow **a**), chamber outline at site of branch bifurcation (arrow **b**) and fenestrule in mid chamber view (arrow **c**), ×40; 3. FH96, mid to shallow tangential section showing bilobate-elliptical chamber outline near obverse surface (arrow **a**) due to presence of superior hemiseptum (arrow **b**) positioned proximal to the vestibular edge, ×40.

4–12. ***Laxifenestella coniunctistyla,*** new species........ 50

4. Paratype, UI X-6801. Obverse exterior surface of highly ontogenetically thickened zoarial fragment with zoarial support developed at lateral zoarial edge (arrow **a**), highly thickened keel, atop which are positioned large nodes (arrow **b**) and centrally thickened terminal diaphragms capping apertures (arrow **c**), ×15.

5, 6. Paratype, UI X-6791. Zoarial fragment exhibiting little ontogenetic thickening; 5. Reverse exterior surface illustrating site of branch bifurcation (arrow **a**) and microstylets (arrow **b**) positioned along reverse branch surface, ×8; 6. Obverse exterior surface. Note lack of terminal diaphragms (arrow) characteristic of apertures at most distal end of the zoarium, ×8.

7, 9–11. Holotype, UI X-6790. Extremely well-preserved zoarial fragment exhibiting slight secondary thickening; 7. FK53, transverse section. Note granular skeletal material surrounding autozooecial chambers and continuous with nodes (arrow **a**) and longitudinal striae (arrow **b**), ×70; 9. Obverse exterior surface illustrating aperture attitudinal relationship relative to plane of obverse surface (arrow **a**), aperture placement at site of branch bifurcation (arrow **b**), distinctive nodal development atop dissepiment (arrow **c**), small stylets atop surface (arrow **d**), and characteristic extension of apertures into the fenestrule opening (arrow **e**), ×30; 10. FK53, transverse section showing typical chamber outline in this view, inferior hemiseptal development from reverse wall (arrow **a**) and short superior hemiseptum at proximal edge of vestibule (arrow **b**), ×70; 11. FK52, extremely shallow longitudinal section section across dissepiment and lateral edge of branch, obverse to left, illustrating nodal development atop dissepiment (arrow **a**) and continuous with granular skeleton across middle of dissepiment (arrow **b**), ×70.

8. Paratype, UI X-6784. Reverse exterior surface illustrating the pronounced differences in meshwork symmetry within a zoarial fragment. Note branch thickening proximal and thinning distal to sites of branch bifurcation (arrow) and longitudinal striae apparent on reverse branch surface, ×8.

12. Paratype, UI X-6788. FK37, transverse section of zoarial fragment exhibiting pronounced thickening of lamellar skeleton with ontogeny. Shown is centrally thickened terminal diaphragm (arrow **a**), node atop dissepiment (arrow **b**), continuity of granular skeleton across dissepiment (arrow **c**) and connecting with granular layer surrounding chambers, and thickened lamellar skeleton (arrow **d**), ×70.

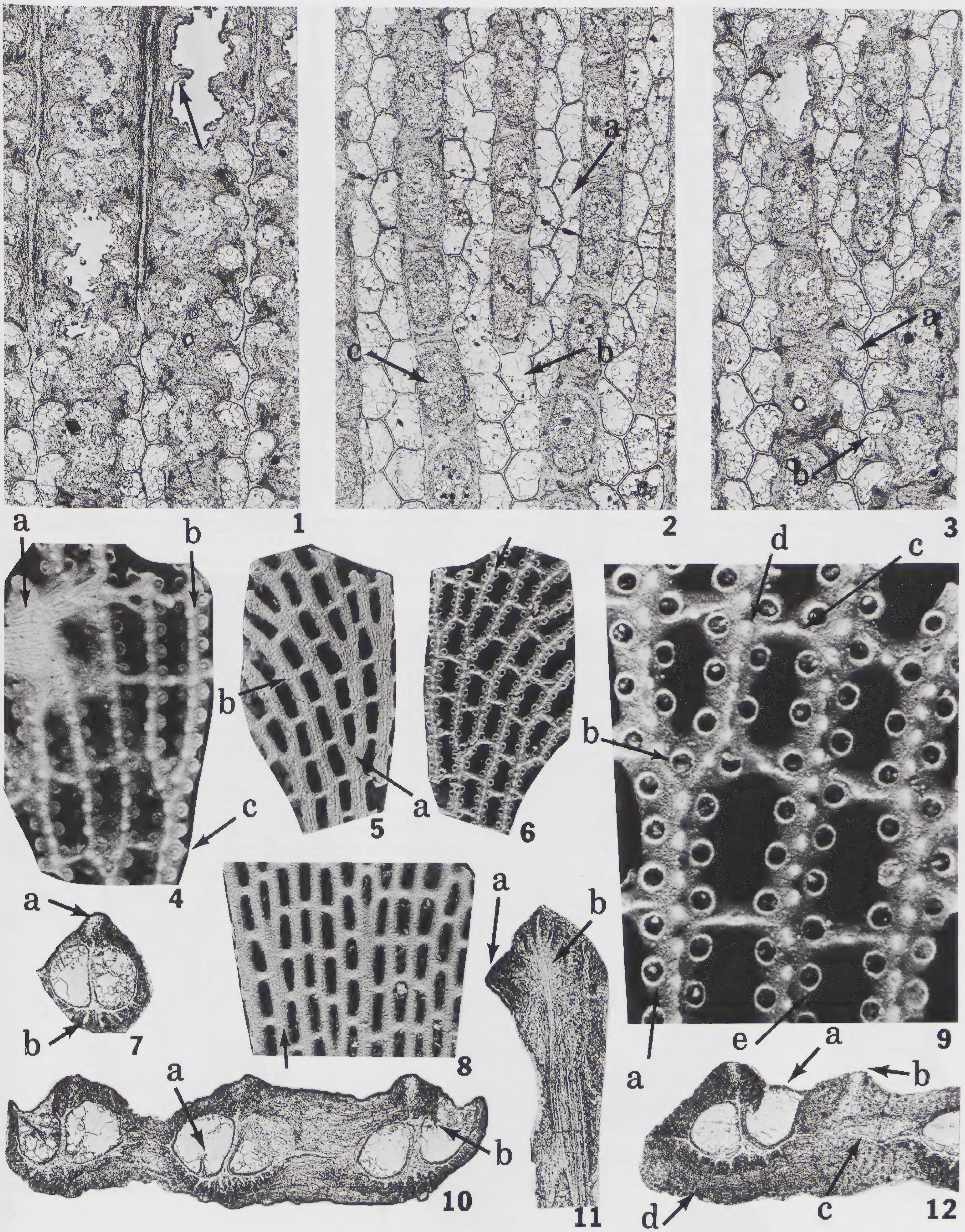
1
2
a
c
b
3
a
b
4
a
b
c
5
b
a
6
9
d
c
b
a
e
7
a
b
8
10
a
b
11
a
b
12
a
b
c
d

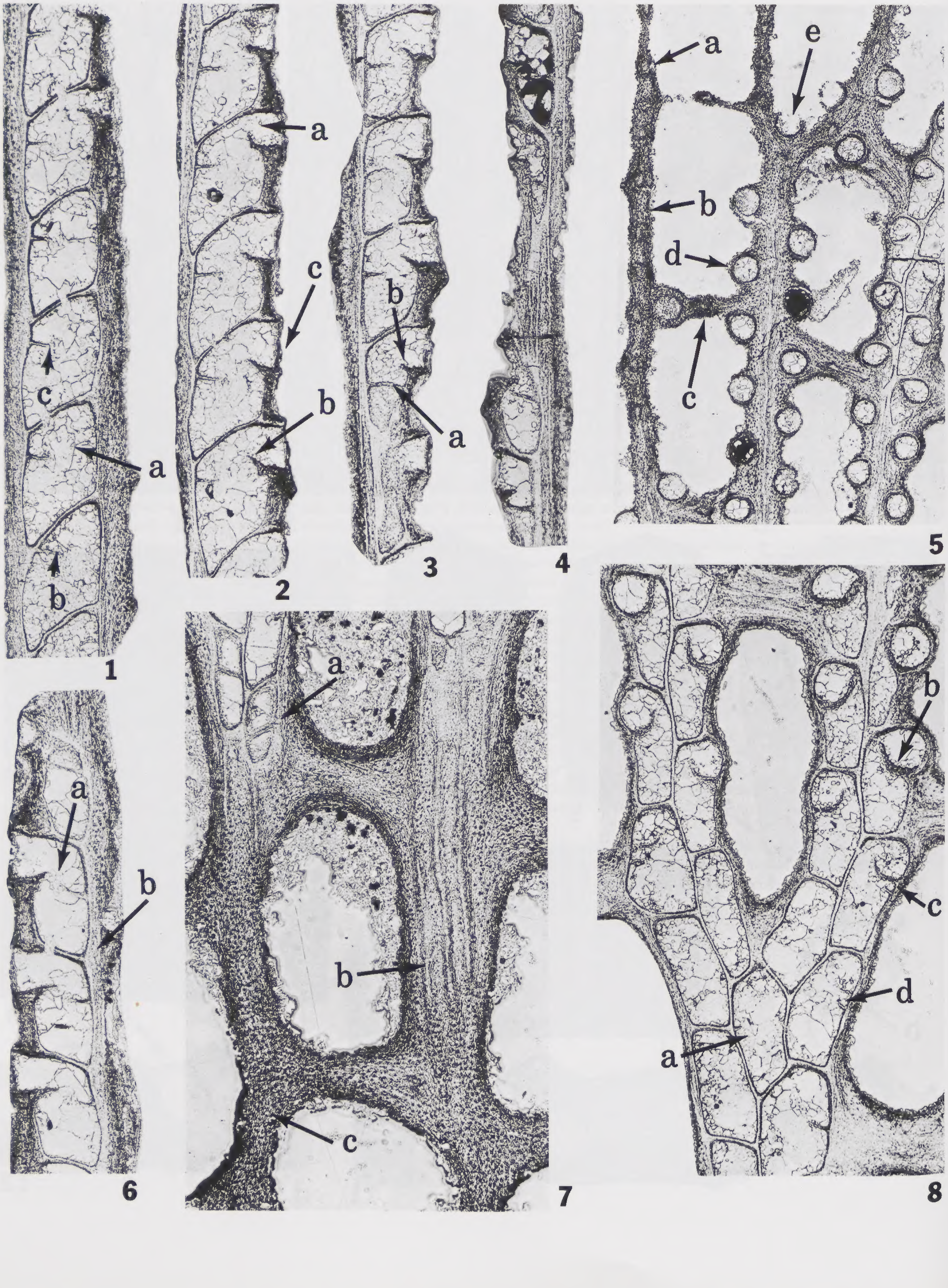
a
c
b
1
a
c
b
2
b
a
3
4
a
e
b
d
c
5
a
b
6
a
b
c
7
b
c
d
a
8

EXPLANATION OF PLATE 6

Figure Page

1–8. ***Laxifenestella coniunctistyla,*** new species 50

1–3. Paratype, UI X-6791. 1. FK63, deep to mid longitudinal section, obverse to right, illustrating chamber outline in deep section (arrow **a**) and migration of inferior hemiseptum from lateral–reverse wall junction in deep section (arrow **b**) toward a more proximal location in mid sectional view (arrow **c**), ×70; 2. FK61, mid longitudinal section, obverse to right, showing well-developed vestibule (arrow **a**) with restriction at chamber–vestibule edge caused by development of the superior hemiseptum (arrow **b**); also ilustrated is centrally thickened terminal diaphragm (arrow **c**) capping apertures, ×70; 3. FK60, shallow longitudinal section, obverse to right, illustrating inferior hemiseptum continuous across chamber (arrow **a**) yet not joined with superior hemiseptum (arrow **b**), ×70.

4, 6. Holotype, UI X-6790. FK53. 4. Very shallow longitudinal section, obverse to left, at lateral branch edge, ×70; 6. Mid shallow longitudinal section, obverse to left, showing close proximity of superior and inferior hemisepta (arrow **a**) without their joining, and continuity of granular skeleton (arrow **b**) along reverse wall, and surrounding autozooecial chambers, ×70.

5, 8. Paratype, UI X-6792. 5. FK68, very shallow to mid tangential section illustrating obverse zoarial surface characters, including nodes (arrow **a**), keel along middle of obverse branch surface (arrow **b**), nodal development in middle of dissepiment (arrow **c**), aperture placement relative to fenestrule opening (arrow **d**), and aperture development at site of branch bifurcation (arrow **e**), ×40; 8. FK69, shallow to mid tangential section illustrating change in chamber outline from mid (bottom of figure) to shallow (top of figure) tangential section. Note the distinctive chamber shape at site of branch bifurcation (arrow **a**), curved superior hemiseptum development at vestibular proximal edge (arrow **b**), spacing between superior (distal) and inferior (proximal) hemisepta (arrow **c**), and wider spacing of hemisepta with increased depth of tangential section (arrow **d**), ×70.

7. Paratype, UI X-6787. FK28, deep tangential section illustrating bridging of autozooecial chambers by inferior hemiseptum near reverse wall (arrow **a**) in deep section, longitudinal striae (arrow **b**) of granular skeletal material, and microstylet development (arrow **c**) along reverse wall as extensions of longitudinal striae, ×70.

EXPLANATION OF PLATE 7

Figure	Page

1, 2. ***Laxifenestella coniunctistyla,*** new species 50

1. Paratype, UI X-6792. FK69, mid to shallow tangential section showing typical autozooecial chamber outline in these views, ×40.
2. Paratype, UI X-6787. FK27, mid to shallow tangential section illustrating nodal development atop dissepiment (arrow **a**), complete peristome surrounding aperture (arrow **b**), and position of aperture at site of branch bifurcation (arrow **c**), ×70.

3–9. ***Laxifenestella maculasimilis,*** new species 54

3, 6. Paratype, UI X-6815. Large zoarial fragment exhibiting slight secondary thickening. 3. Obverse exterior surface illustrating typical zoarial symmetry and appearance. Note presence of shared aperture immediately distal to site of branch bifurcation (arrow), ×8; 6. FI92, shallow longitudinal section, obverse to right, illustrating typical chamber outline in this view, and terminal diaphragm (arrow), ×70.

4. Paratype, UI X-6813. Reverse exterior surface, showing slight to no visible extension of aperture into fenestrule (arrow **a**), site of branch bifurcation (arrow **b**), and longitudinal striae extending along reverse branch surface (arrow **c**). Note branch thickening proximal and thinning distal to sites of branch bifurcation, ×8.

5, 7. Holotype, UI X-6811. Large, well-preserved, moderately secondarily thickened zoarial fragment. 5. Greatly enlarged reverse exterior zoarial surface showing microstylet (arrow **a**) and macrostylet (arrow **b**) development. Note macrostylet placement typically at or near site of branch bifurcation, ×30; 7. Greatly enlarged obverse exterior zoarial surface illustrating centrally thickened terminal diaphragm (arrow **a**), slight aperture extension into fenestrule (arrow **b**), well-developed obverse node (arrow **c**), striae developed across the dissepiment surface (arrow **d**), heterozooecia (ovicell?) development (arrow **e**) between apertures (arrow **f**) along branches, ×30.

8, 9. Paratype, UI X-6767. 8. Obverse exterior zoarial surface showing aperture position at site of branch bifurcation (arrow **a**) and small obverse stylets (arrow **b**), ×30; 9. FG36, transverse section illustrating continuity of granular skeletal layer with reverse macrostylets (arrow **a**), obverse nodes (arrow **b**), and typical chamber outline in mid transverse view (arrow **c**), ×70.

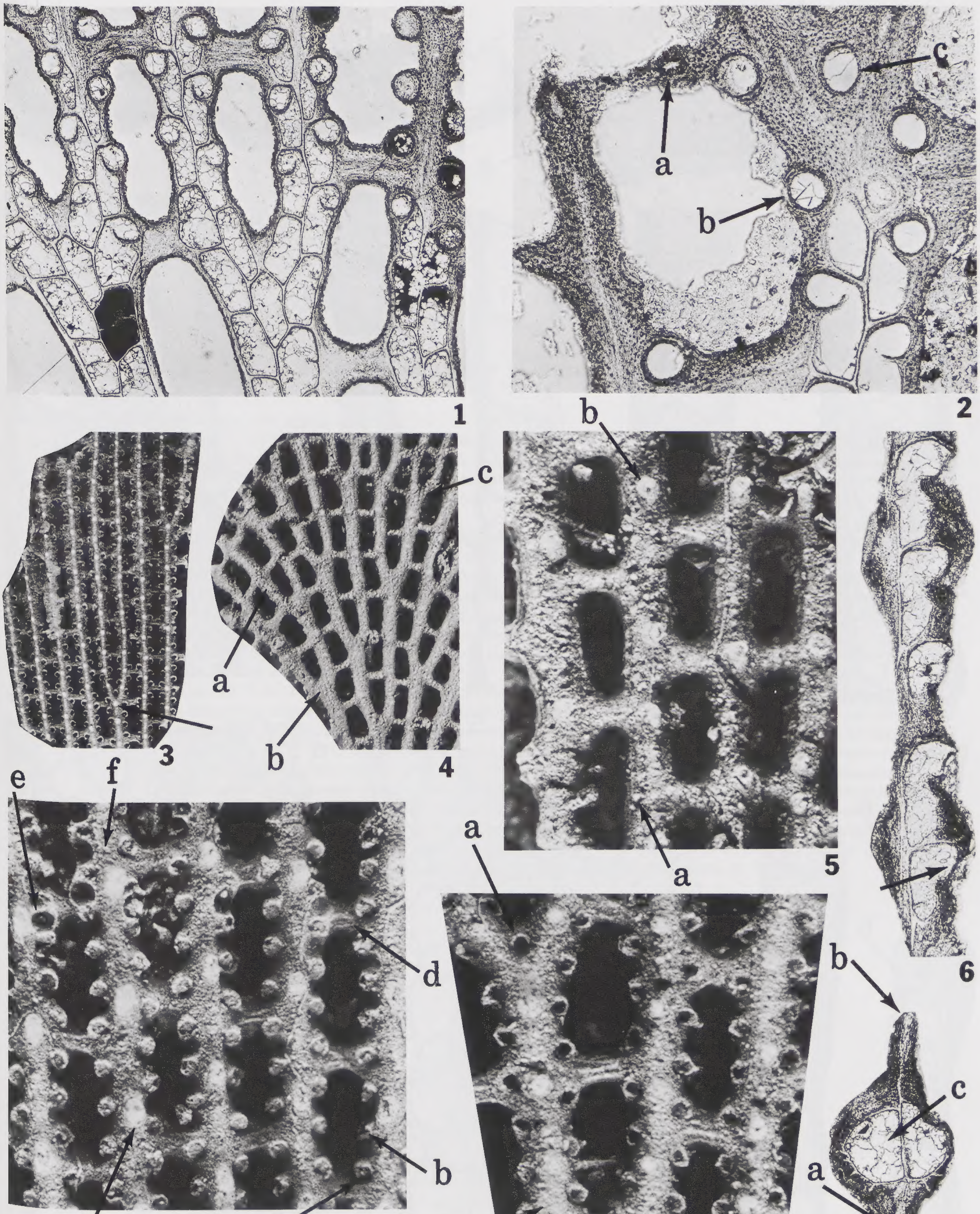
1
a
b
c
2
b
c
a
b
3
4
b
a
5
6
e
f
d
c
b
a
7
a
b
8
b
c
a
9

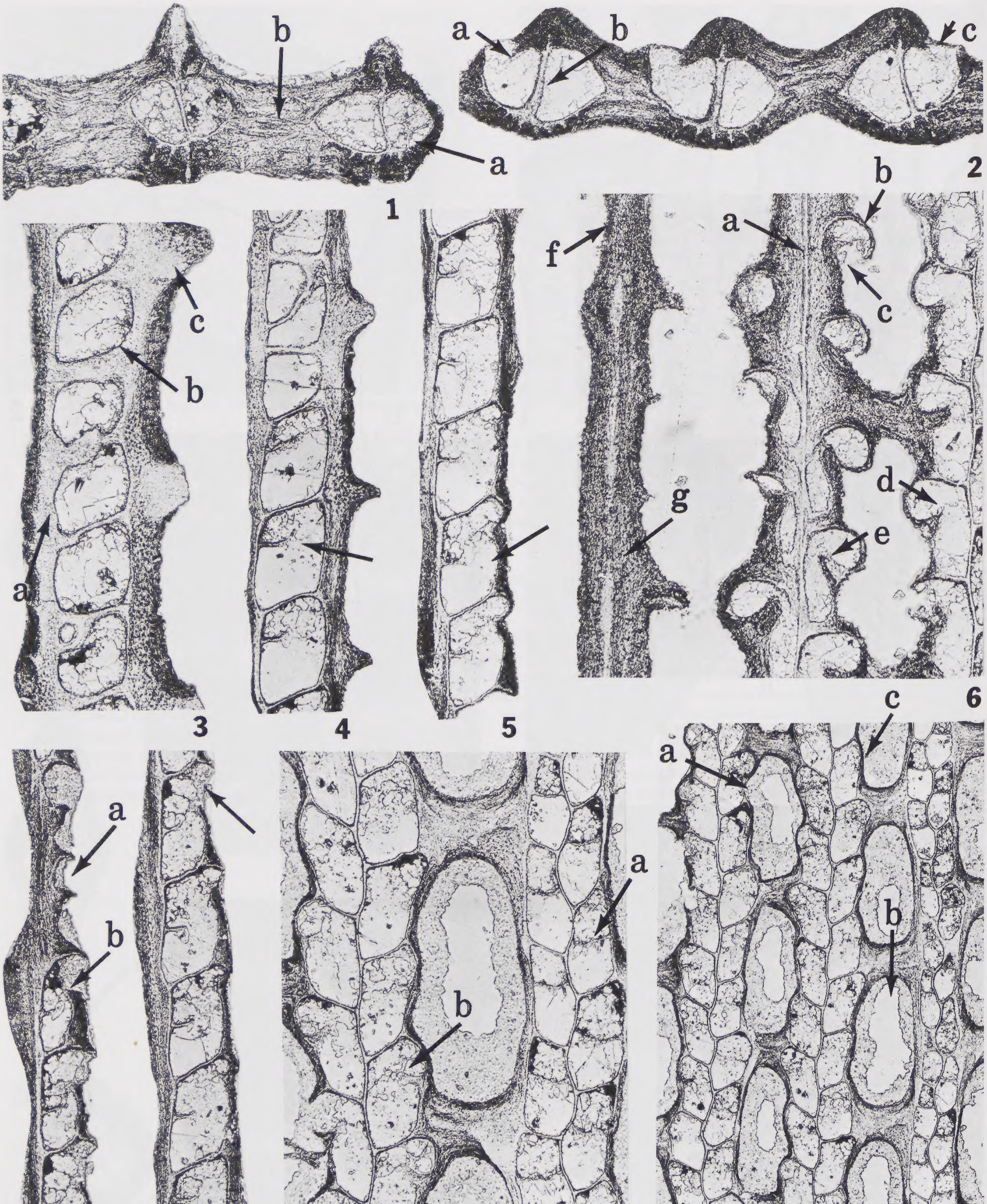
1
2
3
4
5
6
7
8
9
10

EXPLANATION OF PLATE 8

Figure	Page

1–10. ***Laxifenestella maculasimilis,*** new species 54

1, 3. Paratype, UI X-6767. Moderately ontogenetically thickened zoarial fragment. 1. FG36, transverse section showing inferior hemiseptum extending from reverse wall (arrow **a**) continuous with granular skeletal layer surrounding autozooecial chamber and across dissepiment (arrow **b**) connecting chambers, ×70; 3. FG38, deep longitudinal section, obverse to right. Note granular skeletal layer (arrow **a**) continuous around autozooecial chambers (arrow **b**) and with obverse nodes (arrow **c**), ×70.

2, 6. Paratype, UI X-6815. FI94. Large moderately astogenetically thickened zoarial fragment, with thickening occurring primarily in lamellar skeleton although slight thickening is also observed in the granular skeletal layer. 2. Transverse section illustrating superior hemiseptum developed at proximal vestibular adaxial edge (arrow **a**), thickened chamber granular wall (arrow **b**), and terminal diaphragm (arrow **c**), ×70; 6. Shallow to mid tangential section showing upper axial wall development of granular skeleton (arrow **a**), incomplete peristome (arrow **b**) surrounding aperture, and open at proximal–adaxial edge (arrow **c**), and bilobate chamber outline (arrow **d**) near obverse surface caused by development of the superior hemiseptum (arrow **e**). Note thick median keel (arrow **f**), large nodes atop keel, and small stylets (arrow **g**) across obverse surface, ×70.

4, 5, 7–9, 10. Holotype, UI X-6811. Large, well-preserved zoarial fragment. 4. FI3, mid to deep longitudinal section, obverse to right, illustrating chamber outline and well-developed inferior hemiseptum (arrow), ×70; 5. FI3, mid longitudinal section, obverse to right, showing typical autozooecial chamber outline with aperture development at distal end of chamber (arrow), ×70; 7. FI1, shallow to mid longitudinal section, obverse to right, at abaxial edge of branch illustrating aperture opening orientation (arrow **a**) and superior hemiseptum (arrow **b**) at proximal edge of peristome, ×70; 8. FI4, mid longitudinal section, obverse to right, illustrating attitude of aperture opening (arrow) relative to plane of obverse surface, ×70; 9. FI7, mid to deep tangential section illustrating inferior hemiseptum near reverse wall (arrow **a**) and superior hemiseptum at proximal edge of peristome (arrow **b**), ×70; 10. FI41, mid to deep tangential section showing inflection of apertures into fenestrule outline near obverse surface (arrow **a**) and lack of such inflections in deeper view (arrow **b**). Note typical chamber outline in mid tangential view (arrow **c**), ×40.

EXPLANATION OF PLATE 9

Figure	Page

1, 2. ***Laxifenestella maculasimilis,*** new species 54

1. Paratype, UI X-6759. FG23, deep tangential section showing macrostylets (arrow **a**) and microstylets (arrow **b**) both in continuity with granular skeletal material forming longitudinal striae (arrow **c**), ×70.
2. Paratype, UI X-6808. FI18, mid to shallow tangential section, illustrating typical chamber outlines and characteristic mid tangential outline of chamber at site of branch bifurcation (arrow), ×40.

3–11. ***Laxifenestella serratula*** (Ulrich, 1890) 56

3–5, 9, 11. Figured specimen, UI X-6838. Large, well-preserved zoarial fragment exhibiting slight ontogenetic thickening. 3. FJ28, shallow to very shallow longitudinal section, obverse to right, illustrating bridging of chamber by fused superior and inferior hemisepta (arrow **a**), centrally thickened terminal diaphragm (arrow **b**), and continuous granular skeleton extending across middle of dissepiment (arrow **c**), ×70; 4. Obverse exterior surface showing typical mesh symmetry and aperture positioning at site of branch bifurcation (arrow), ×8; 5. Reverse exterior view of same site of branch bifurcation as shown in figure 4 above (arrow), ×8; 9. FJ29, transverse section illustrating centrally thickened terminal diaphragm (arrow **a**), short superior hemiseptum (arrow **b**), and longitudinal striae (arrow **c**) continuous with granular skeletal layer surrounding autozooecial chamber, ×70; 11. FJ27, transverse section of typical branch segment, ×70.

6–8. Figured specimen, UI X-6839. Large, well-preserved zoarial fragment exhibiting moderate ontogenetic thickening. 6. Greatly enlarged obverse exterior surface illustrating typical mesh symmetry and obverse characteristics, including nodes (arrow **a**), aperture placement and peristomal development (arrow **b**), inflection of apertures into fenestrule (arrow **c**), small stylets along obverse surface (arrow **d**), and longitudinal ridges developed across dissepiment surface (arrow **e**), ×30; 7. Greatly enlarged reverse exterior surface. Observe larger fenestrule openings (arrow **a**) compared to those on obverse surface, and microstylet development (arrow **b**), ×30; 8. Obverse exterior surface showing typical meshwork pattern and well-developed, centrally thickened terminal diaphragm (arrow), ×8.

10. Figured specimen, UI X-6765. FG11, transverse section of zoarial fragment showing typical curved inferior hemiseptum (arrow **a**), nodal development atop keel (arrow **b**) and continuity of granular skeletal material across dissepiment (arrow **c**), ×70.

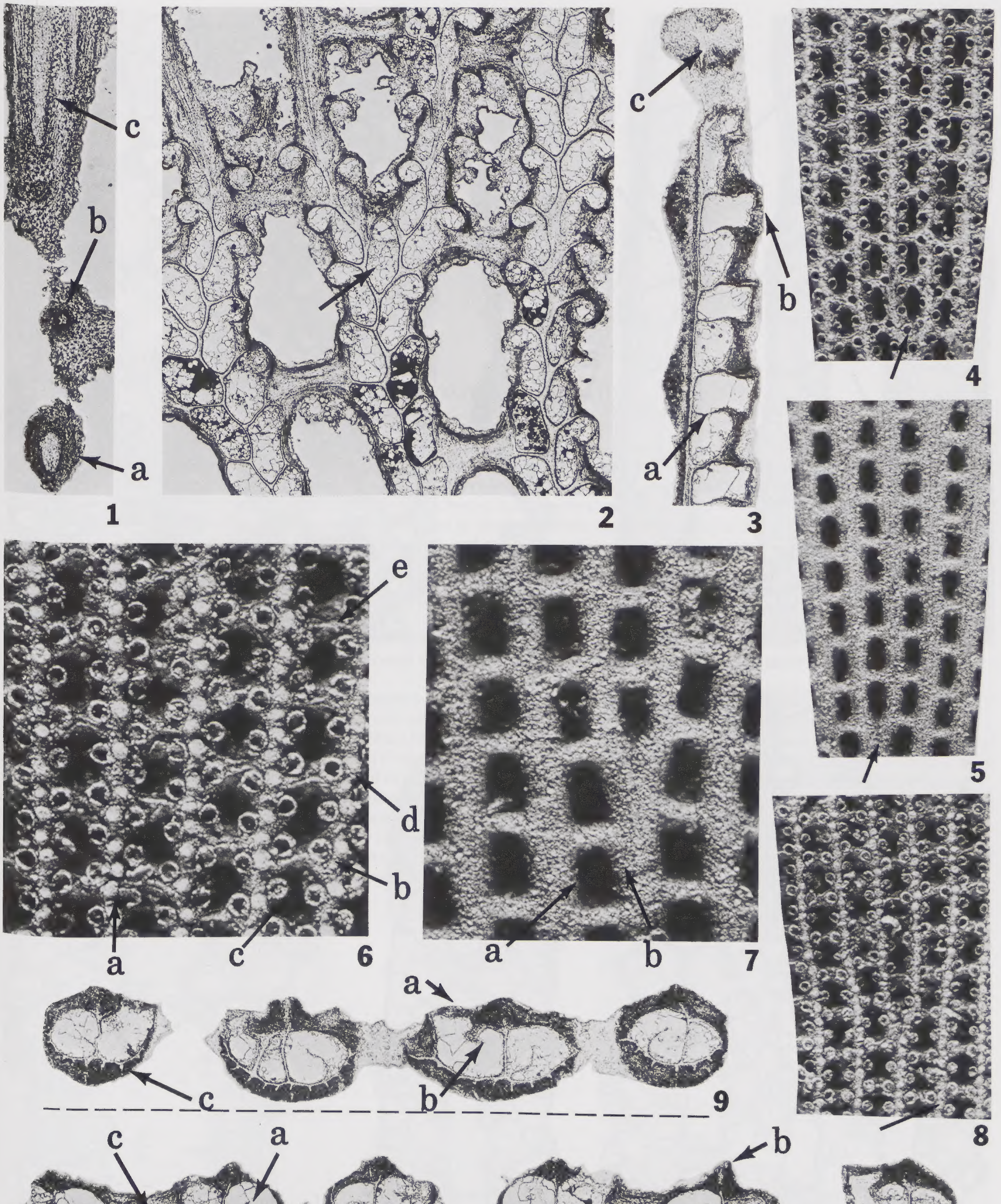
c
b
a
1
2
c
b
a
3
4
5
e
d
b
a
c
6
a
b
7
8
a
c
b
9
c
a
b
10
11

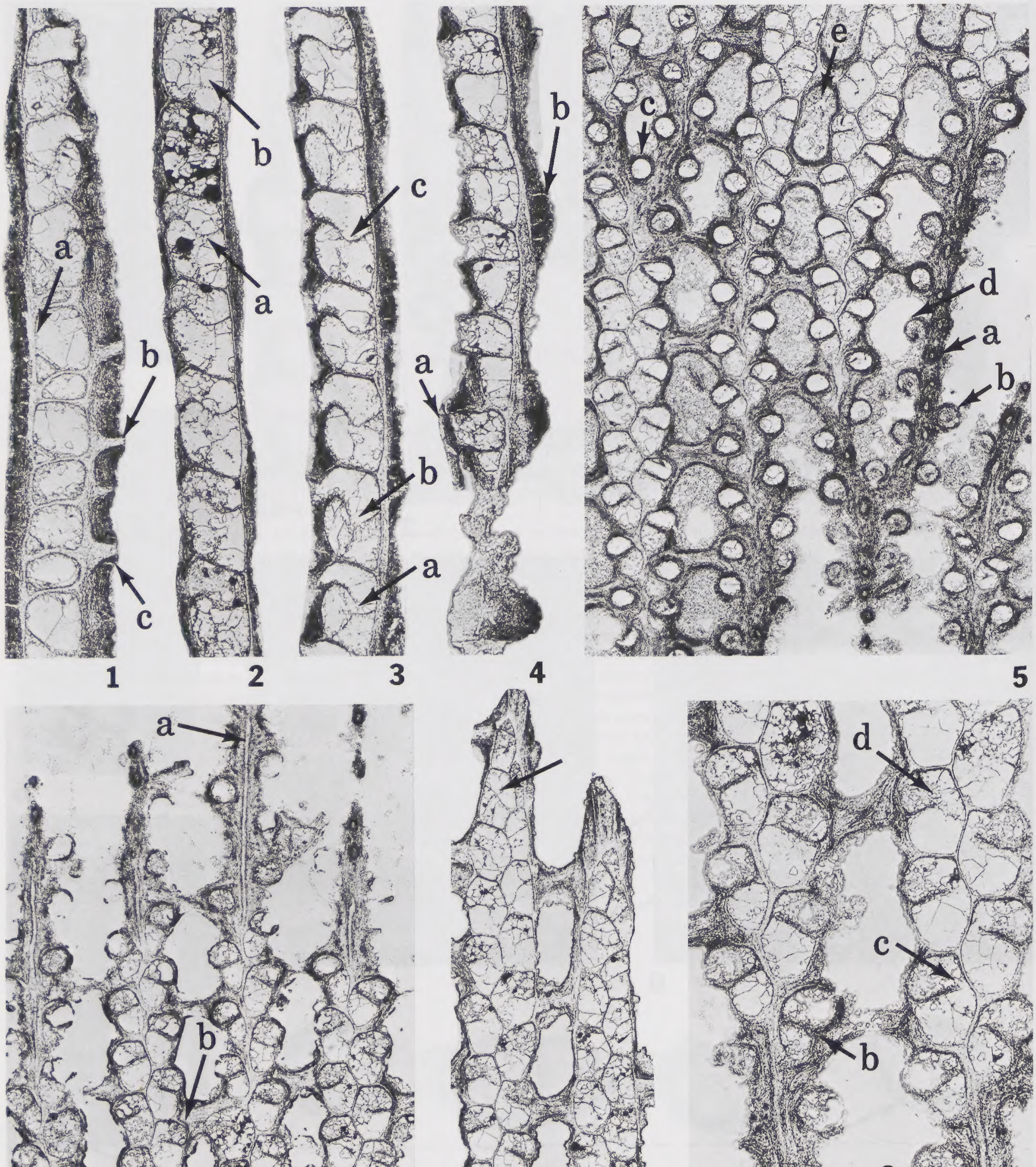
1
2
3
4
5
6
7
8

EXPLANATION OF PLATE 10

Figure Page
1–8. ***Laxifenestella serratula*** (Ulrich, 1890) 56

1, 5. Figured specimen, UI X-6838. 1. FJ29, mid to deep longitudinal section, obverse to right, illustrating continuity of granular skeleton (arrow **a**) surrounding autozooecial chambers and continuous with obverse nodes (arrow **b**) and stylets (arrow **c**), ×70; 5. FJ31, shallow to mid tangential section. Observe node (arrow **a**) positioned atop thick well-developed keel, peristome (arrow **b**) surrounding aperture positioned parallel to obverse surface, aperture position at site of branch bifurcation (arrow **c**), extension of aperture into fenestrule (arrow **d**), and fenestrule outline in mid section (arrow **e**) showing smaller size than shallow section fenestrule and lack of aperture extension into fenestrule opening, ×40.

2. Figured specimen, UI X-6837. FJ18, mid to deep longitudinal section, obverse to left, showing presence of joined superior and inferior hemiseptum (arrow **a**) disappearing as section approaches middle of branch (*i.e.*, becomes deeper) (arrow **b**), ×70.

3. Figured specimen, UI X-6839. FJ36, mid longitudinal section, obverse to left, illustrating joining of inferior and superior hemisepta as autozooecial chambers proceed from most shallow (arrow **a**) to slightly deeper (arrow **b**) to deepest (arrow **c**) longitudinal view, ×70.

4, 6–8. Figured specimen, UI X-6765. Large zoarial fragment exhibiting little ontogenetic thickening. 4. FG11, very shallow to mid longitudinal view of slightly inclined section, obverse to left. Apertures at top of figure are not capped by terminal diaphragms, bottom apertures are capped and chambers bridged by fused inferior and superior hemisepta (arrow **a**). Granular skeletal layer surrounding autozooecial chambers connects to microstylets (arrow **b**) on the reverse wall, ×70; 6. FG13, shallow to mid tangential section. Note well-defined axial ridge of granular skeletal material from which nodes arise (arrow **a**) and typical autozooecial chamber outline in mid tangential view (arrow **b**) with superior hemiseptum almost completely dividing chamber, ×40; 7. FG14, shallow to deep tangential section showing continuity of inferior hemiseptum (arrow) across autozooecial chamber width, ×40; 8. FG13, shallow to mid tangential section illustrating obverse stylets (arrow **a**), superior hemiseptum extending entirely across chamber in extremely shallow view (arrow **b**), lack of continuity of superior hemiseptum across chamber as section deepens (arrow **c**), with further reduction of superior hemiseptum (arrow **d**) as section deepens further, ×70.

EXPLANATION OF PLATE 11

Figure Page

1. ***Laxifenestella serratula*** (Ulrich, 1890) 56
Figured specimen, UI X-6837. FJ22, mid to deep tangential section illustrating typical chamber outline in mid autozooecial chamber view (arrow **a**) with inferior hemiseptum across chamber width, and microstylets (arrow **b**) which originate as extensions of granular skeletal material in reverse-wall longitudinal striae (arrow **c**), ×70.

2–11. ***Laxifenestella fluctuata,*** new species 58
2, 3, 5, 7–9. Holotype, UI X-6778. Large, well-preserved zoarial fragment exhibiting moderate ontogenetic thickening. 2. Obverse exterior surface, observe granular dissepiment surface (arrow **a**), autozooecial aperture position (arrow **b**) relative to branch and fenestrule, heterozooecia (ovicells?) developed from enlarged aperture toward middle of branch (arrow **c**), and small obverse stylets (arrow **d**), ×25; 3. Reverse surface of zoarial fragment showing typical symmetry, site of branch bifurcation (arrow), and longitudinal striae almost completely covered by secondary lamellar skeleton, ×8; 5. Obverse exterior surface illustrating general mesh symmetry and branch character at site of branch bifurcation (arrow), ×8; 7. FN3, transverse section of dissepiment, obverse to right, illustrating continuity of granular skeleton across dissepiment (arrow), ×70; 8. FN1, transverse section showing development of short superior hemiseptum (arrow **a**) and longitudinal striae along reverse chamber wall (arrow **b**), ×70; 9. FN4, transverse section of zoarial fragment showing continuity of granular skeletal layer around autozooecial chambers, across dissepiment (arrow **a**) and with nodes (arrow **b**), ×70.
4, 6. Paratype, UI X-6773. Well-preserved zoarial fragment. 4. High magnification of obverse exterior surface illustrating lack of extension of aperture into fenestrule opening (arrow **a**), heterozooecia (ovicells?) developed from enlarged lateral aperture (arrow **b**), keel (arrow **c**), and node (arrow **d**) developed atop keel, ×30; 6. Reverse exterior zoarial surface exhibiting typical granular texture (arrow) and lack of apertural inflections into fenestrule, ×30.
10. Paratype, UI X-6727. FV26, transverse section of slightly ontogenetically thickened zoarial fragment illustrating attitudinal relationship of aperture to plane of obverse surface (arrow **a**), development of short inferior hemiseptum (arrow **b**), and wall partitioning two autozooecial chambers (arrow **c**), ×70.
11. Paratype, UI X-6729. FV35, mid to deep longitudinal section, obverse to left, showing typical chamber outline (arrow **a**) and development of zoarial support from reverse wall of zoarium (arrow **b**), ×70.

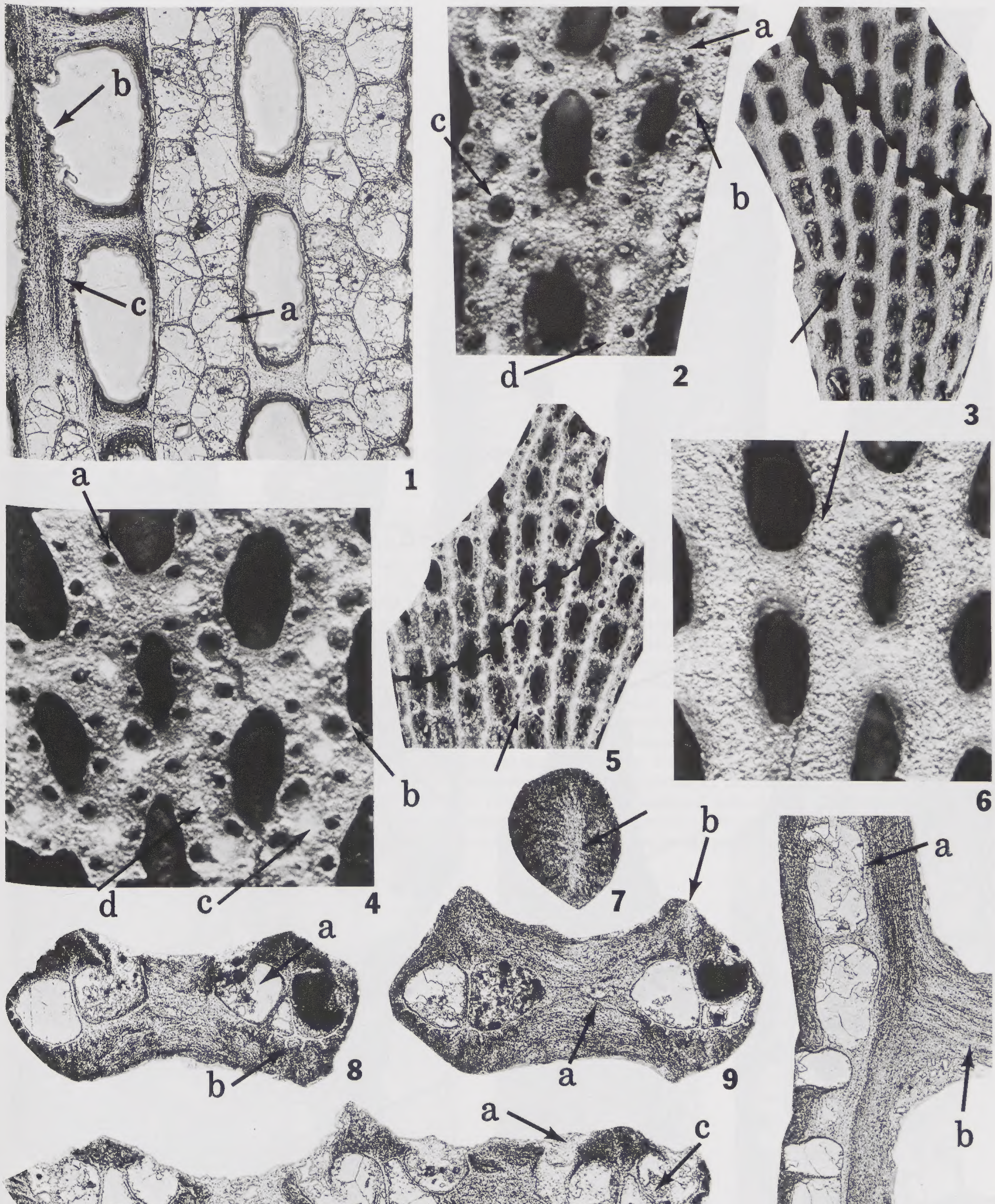

a
b
1
b
a
2
a
b
c
3
a
b
4
5
b
a
6
b
a
c
7
a
e
b
c
d
8

EXPLANATION OF PLATE 12

Figure — Page

1–8. ***Laxifenestella fluctuata,*** new species 58

1, 2. Paratype, UI X-6772. 1. FN23, very deep longitudinal section, obverse to left, illustrating chamber outline in deep longitudinal view (arrow **a**) and continuity of microstylets with internal granular skeleton (arrow **b**), ×70; 2. FN19, mid to deep longitudinal section, obverse to left, illustrating continuity of obverse stylet (arrow **a**) with granular skeleton. Note inferior hemiseptum (arrow **b**) and thickened lamellar skeleton, ×70.

3. Paratype, UI X-6729. FV34, shallow to mid longitudinal section, obverse to left, showing typical attitudinal relationship of aperture to obverse surface, and capped by terminal diaphragm (arrow **a**), superior hemiseptum (arrow **b**) not fused with inferior hemiseptum, and granular skeletal layer (arrow **c**) which, although thin, is continuous around autozooecial chambers, ×70.

4–8. Holotype, UI X-6778. 4. FN4, shallow to mid shallow longitudinal section, obverse to right, illustrating autozooecial chamber bridged by superior hemiseptum (arrow **a**) and typical aperture orientation in shallow longitudinal view (arrow **b**). Observe both granular and lamellar skeletal material associated with superior hemiseptum, with inferior hemiseptum composed solely of granular skeleton, ×70; 5. FN7, mid to mid shallow tangential section illustrating chamber outline (arrow) and moderate variation in chamber outline evident in this species, ×70; 6. FN7, mid to deep tangential section showing typical mesh symmetry, and enlargement of fenestrule proceeding from mid (arrow **a**) to deep (arrow **b**) sectional view, ×40; 7. FN7, deep tangential section with longitudinal striae (arrow **a**) atop which develop reverse microstylets (arrow **b**), and bridging of chamber by inferior hemiseptum (arrow **c**) near reverse wall, ×70; 8. FN6, very shallow to mid tangential section. Note continuity of granular skeleton across dissepiment (arrow **a**), keel (arrow **b**), node developed atop keel (arrow **c**), obverse stylet (arrow **d**), and bilobate-ovate outline (arrow **e**) of chamber near obverse surface due to inflection of superior hemiseptum into chamber, ×70.

EXPLANATION OF PLATE 13

Figure Page

1. ***Laxifenestella fluctuata,*** new species 58
 Paratype, UI X-6727. FV28, mid to deep tangential section showing typical zoarial pattern and autozooecial chamber outline at site of branch bifurcation (arrow), ×20.

2–12. ***Minilya sivonella,*** new species 62

2, 3, 5, 10, 11. Holotype, UI X-6905. Large, well-preserved zoarial fragment exhibiting moderate ontogenetic thickening of lamellar skeletal layer. 2. Reverse exterior surface. Note macrostylet development (arrow **a**) most commonly occurring at or near sites of branch–dissepiment contact, fenestrule shape with no indication of inflection by apertures on reverse surface (arrow **b**), and site of branch bifurcation (arrow **c**), ×8; 3. Obverse exterior surface illustrating typical mesh pattern and symmetry. Centrally thickened hemiseptum shown by arrow, ×8; 5. Highly enlarged obverse exterior surface view illustrating aperture position relative to branch surface, and incomplete peristome partially surrounding aperture (arrow **a**) with gap at proximal end of peristome (arrow **b**). Such gaps also develop at distal end of peristome in some zoaria of the species. Biserially alternating rows of stylets (arrow **c**) form at either proximal or distal–adaxial peristomal edge, ×25; 10. FA35, transverse section showing typical chamber shape in cross-section and attitudinal relationship of apertures to plane of obverse surface, initiation of apertural stylets (arrow **a**) as extension of peristome, and granular skeletal material surrounding autozooecial chamber (arrow **b**), ×40; 11. FA37, transverse section illustrating well-developed apertural stylet at proximal edge of aperture (arrow **a**), small stylets infilling peristomal gap (arrow **b**), reverse macrostylet (arrow **c**), microstylets (arrow **d**), and continuous granular skeletal layer across dissepiment (arrow **e**), ×40.

4. Paratype, UI X-6877. Obverse exterior surface of zoarial fragment exhibiting pronounced ontogenetic thickening. Note thickening of keel across branch surface (arrow), in places overgrowing apertures, ×8.

6, 9. Paratype, UI X-6876. Large zoarial fragment exhibiting pronounced secondary thickening of lamellar skeletal layer. 6. Obverse exterior surface showing aperture position (arrow **a**) with development of large stylet at proximal–adaxial apertural edge (arrow **b**), small obverse stylets (arrow **c**), aperture position, and orientation at site of branch bifurcation (arrow **d**), and inflection into fenestrules of apertures along obverse surface (arrow **e**), ×25; 9. Reverse exterior surface showing thickening of lamellar skeleton (arrow), ×8.

7, 8, 12. Paratype, UI X-6904. 7. FA32, mid longitudinal section, obverse to left, illustrating well-developed superior hemiseptum (arrow **a**), typical chamber outline in mid longitudinal view (arrow **b**), diaphragm plugging aperture (arrow **c**), and possible brown bodies in lower three chambers shown, ×60; 8. FA32, shallow to deep longitudinal section, obverse to left, showing granular skeleton at distal edge of autozooecial chamber bifurcating to develop into large apertural stylet (arrow **a**) and peristome (arrow **b**), well-developed apertural stylet toward middle of branch (arrow **c**), and continuity of granular skeletal layer across dissepiment (arrow **d**), ×40; 12. FA30, mid to deep longitudinal section, obverse to left. Note chamber outline in deep longitudinal view (arrow **a**) and continuity of granular skeleton with reverse macrostylets (arrow **b**), ×40.

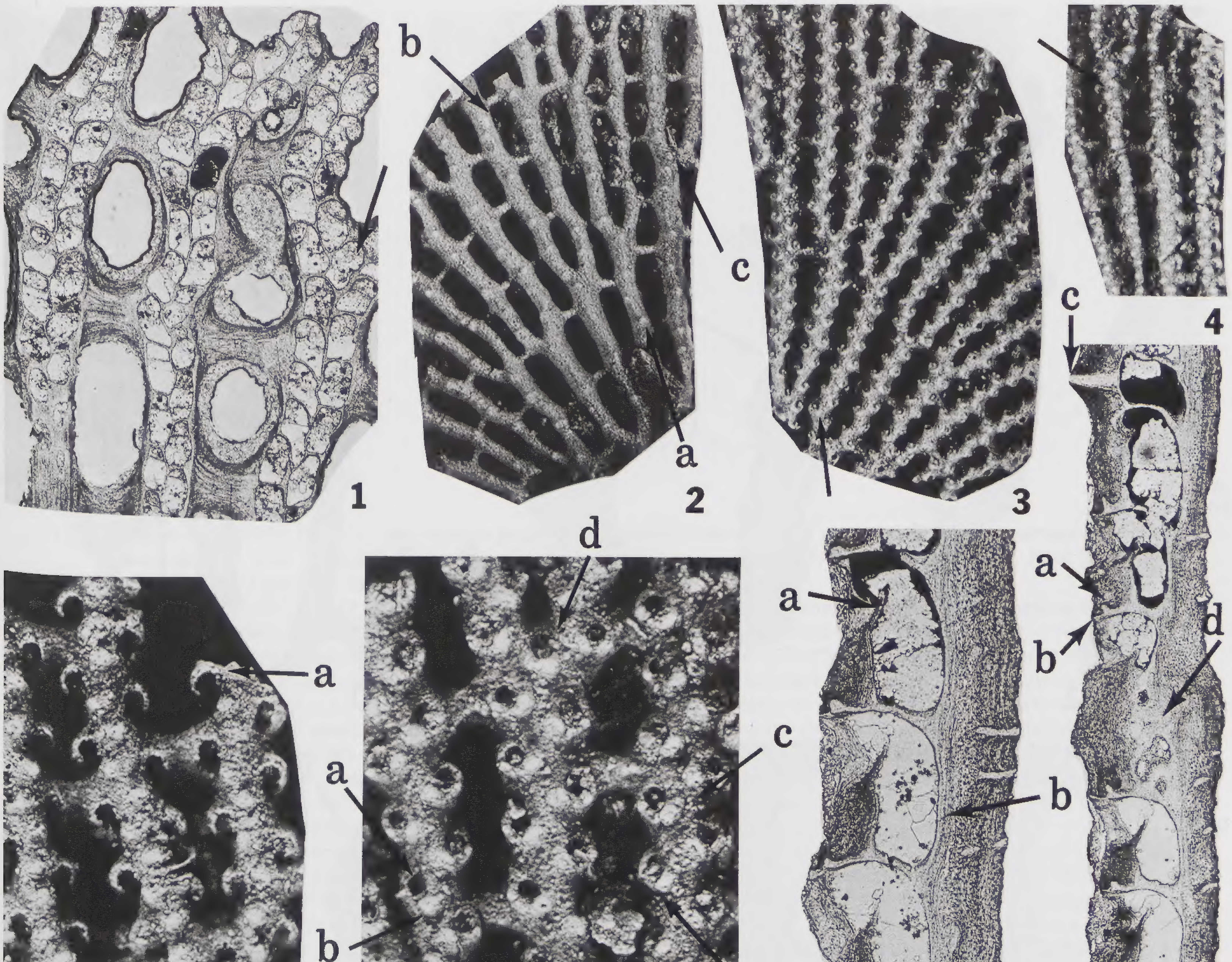
1
b
c
a
2
3
4
c
a
b
d
8
d
a
c
b
e
6
a
b
c
5
a
b
c
7
a
b
10
a
b
e
c
d
11
b
a
12
9

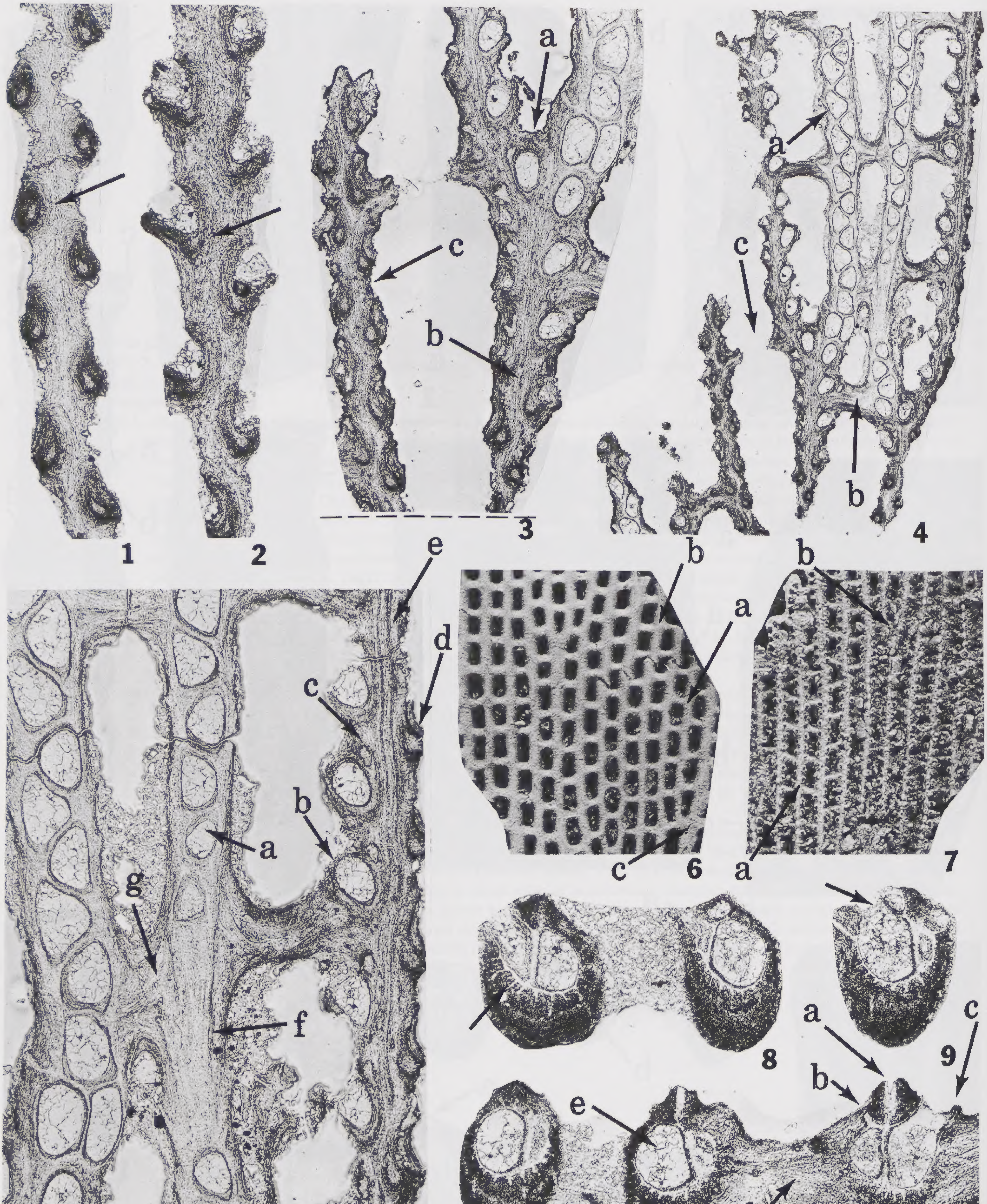
1
2
a
c
b
3
a
c
b
4
e
d
c
b
a
g
f
5
b
a
c
6
b
a
7
8
a
c
9
b
e
d
10

EXPLANATION OF PLATE 14

Figure Page

1–5. ***Minilya sivonella,*** new species 62

1, 2. Paratype, UI X-6876. FA45. 1. Very shallow tangential section illustrating biserial arrangement of large apertural stylets across branch (arrow), ×60; 2. Shallow tangential of zoarium exhibiting pronounced ontogenetic thickening. Note large stylet at proximal–adaxial apertural edge (arrow), ×60.

3–5. Holotype, UI X-6905. FA43. 3. Very shallow to shallow tangential section illustrating apertural placement at site of branch bifurcation (arrow **a**) and small obverse stylets (arrow **b**) positioned atop thickened median keel (arrow **c**), ×40; 4. Shallow to deep tangential section showing typical chamber outline in mid section (arrow **a**), continuity of granular skeleton across dissepiment (arrow **b**), and recessed dissepiment relative to obverse branch surface (arrow **c**), ×20; 5. Greatly enlarged shallow to deep tangential section. Observe chamber outline near reverse-wall budding-site (arrow **a**), attitudinal relationship of aperture to obverse surface, and small apertural stylets (arrow **b**), large single apertural stylet developed at distal–adaxial apertural edge (arrow **c**) and across branch, large single apertural stylet developed at proximal–adaxial apertural edge (arrow **d**), granular center of keel (arrow **e**), longitudinal striae along reverse surface (arrow **f**), and microstylets atop these striae and across dissepiments (arrow **g**), ×60.

6–10. ***Minilya paratriserialis,*** new species 65

Holotype, UI X-6871. 6. Reverse exterior of zoarial fragment exhibiting moderate consistency of fenestrule size and shape (arrow **a**), microstylet development atop longitudinal striae (arrow **b**), and site of branch bifurcation (arrow **c**), ×8; 7. Obverse exterior view illustrating general mesh symmetry, variability in fenestrule shape (arrow **a**) when compared with that of reverse surface, and aperture position (arrow **b**) at site of branch bifurcation, ×8; 8. FH15, transverse section of branches illustrating continuity of granular skeletal layer (arrow) around autozooecial chambers, ×60; 9. FH15, transverse section showing typical opening of aperture (arrow) relative to branch surface, ×60; 10. FH15, transverse section showing continuity of granular skeleton with obverse node (arrow **a**), large apertural stylet (arrow **b**), peristome (arrow **c**), and across dissepiment (arrow **d**), and typical autozooecial chamber shape in mid transverse view (arrow **e**), ×60.

EXPLANATION OF PLATE 15

Figure Page

1–9. ***Minilya paratriserialis,*** new species 65

1. Paratype, UI X-6947. Obverse exterior surface of zoarial fragment illustrating nodes (arrow **a**) positioned atop keel, longitudinal striae developed across fenestrule (arrow **b**), intermediate-size stylet developed at proximal–adaxial edge of aperture (arrow **c**), second stylet at proximal–abaxial edge of aperture (arrow **d**), and peristome surrounding aperture (arrow **e**), ×25.

2–9. Holotype, UI X-6871. 2. FH4, mid longitudinal section, obverse to right, showing typical chamber outline (arrow) in mid section, ×70; 3. FH3, mid to shallow longitudinal section showing cross-section of dissepiment across which granular skeleton extends (arrow **a**), most abaxial edge of aperture (arrow **b**) opening into fenestrule, adaxial intermediate-size apertural stylet (arrow **c**), and outer edge of abaxial intermediate-size apertural stylet (arrow **d**), ×70; 4. FH4, mid shallow longitudinal section, obverse to right, illustrating continuity of thick granular skeleton along reverse wall of chambers (arrow **a**) and centrally thickened terminal diaphragm (arrow **b**), ×70; 5. FH3, mid shallow to deep longitudinal section, obverse to right, showing typical mid chamber outline with vestibule development (arrow **a**), chamber outline in deep longitudinal view (arrow **b**), and continuity of granular skeleton with reverse microstylets (arrow **c**), ×70; 6. FH6, very shallow to shallow tangential section illustrating chamber outline in very shallow (arrow **a**) to shallow (arrow **b**) tangential view, ×70; 7. FH6, very shallow to mid tangential section illustrating intermediate-size apertural stylets developed from abaxial (arrow **a**) and adaxial (arrow **b**) edges of the aperture. The adaxial stylet is connected to the vestibular granular layer in some individuals, to the peristome in others; the abaxial stylet is always connected to the peristome. The keel (arrow **c**) from which nodes (arrow **d**) extend is also shown, ×40; 8. FH5, mid to mid shallow tangential section illustrating typical chamber outline in mid tangential section (arrow **a**), slight inflection of apertures into fenestrule in mid shallow tangential view (arrow **b**), and lack of such inflection as section deepens (arrow **c**), ×40; 9. FH5, deep tangential section showing chamber outline near reverse-wall budding-site (arrow **a**), and longitudinal striae (arrow **b**) continuous with inner granular skeletal layer, with reverse microstylets (arrow **c**) emerging from and continuous with granular skeleton of striae, ×70.

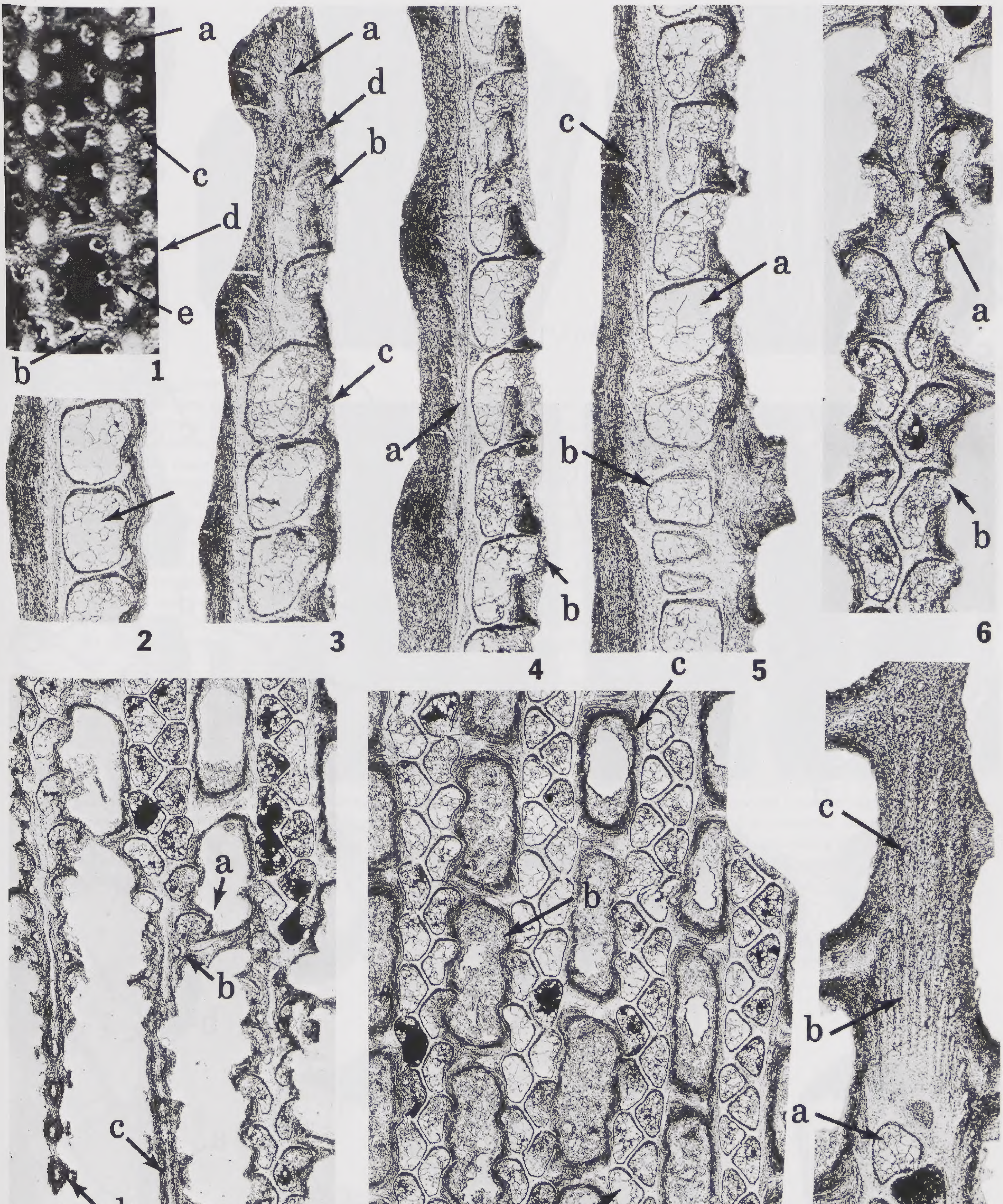

1
2
3
4
5
6
7
8
9

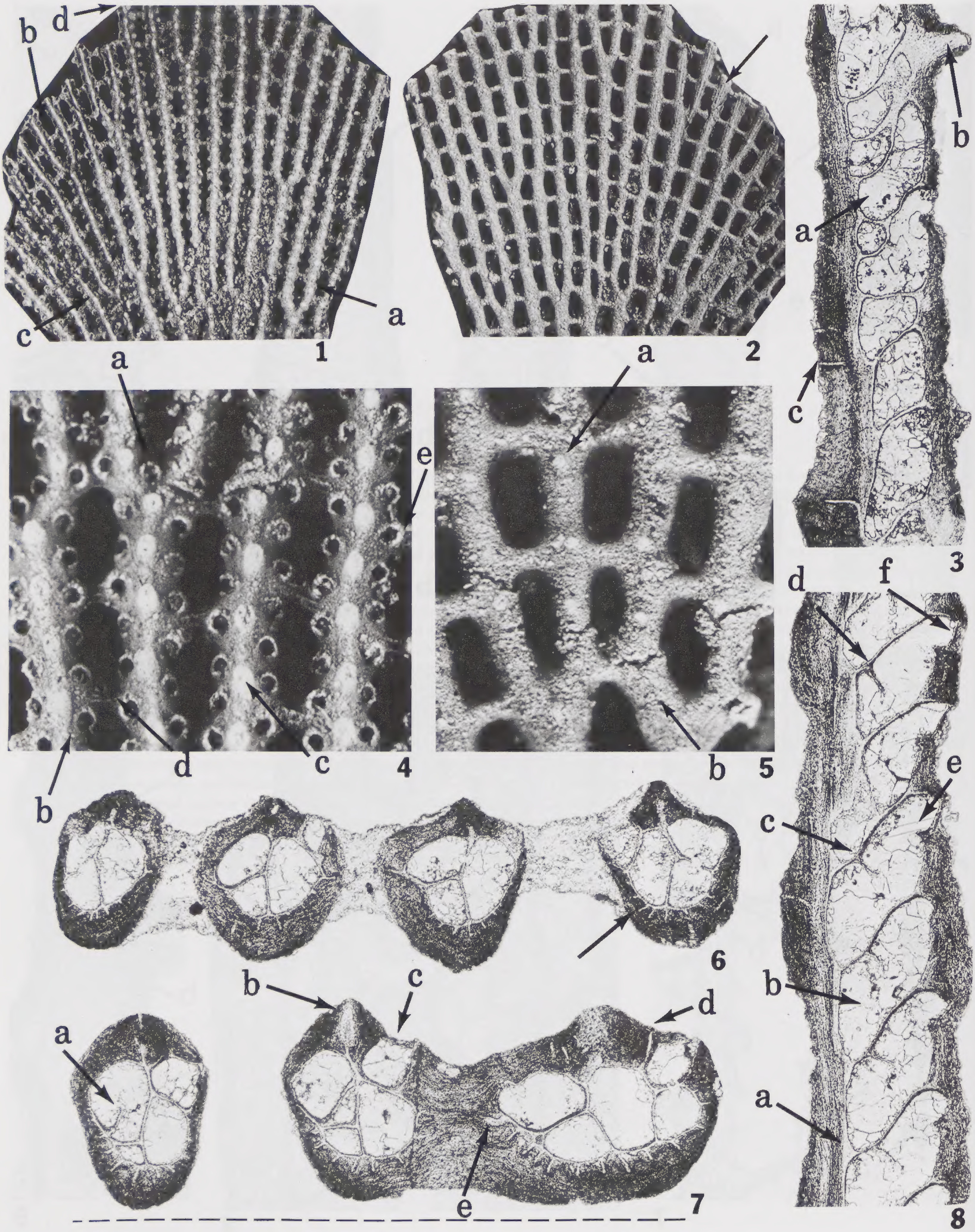
b
d
c
a
1
2
a
b
c
3
a
a
e
d
c
b
4
b
5
d
f
e
c
6
b
c
d
a
e
7
b
a
8

EXPLANATION OF PLATE 16

Figure Page
1–8. ***Exfenestella exigua*** (Ulrich, 1890) 68

1–5. Figured specimen, UI X-6816. Large, well-preserved zoarial fragment. 1. Obverse exterior surface exhibiting moderate ontogenetic thickening near proximal end of zoarium (arrow **a**) and slight ontogenetic thickening toward more distal end of zoarium (arrow **b**), Note terminal diaphragms (arrow **c**) capping apertures near proximal end of zoarium, which are absent toward more distal end of fragment (arrow **d**), ×8; 2. Reverse exterior surface illustrating similar ontogenetic thickening toward proximal end of zoarium and thinning toward more distal end. Note longitudinal striae (arrow) evident at most distal end of zoarium but covered by lamellar skeleton toward proximal end of zoarium due to ontogenetic thickening of lamellar skeleton, ×8; 3. FI33, deep longitudinal section, obverse to right, showing typical chamber shape near middle of branch (arrow **a**) and granular skeletal layer continuous with obverse nodes (arrow **b**), and microstylets (arrow **c**), ×70; 4. Obverse exterior surface showing aperture placement at site of branch bifurcation (arrow **a**), small stylet placement across obverse branch surface (arrow **b**), nodes (arrow **c**), longitudinal striae across dissepiments (arrow **d**), small stylets forming as extensions of peristome (arrow **e**), and attitudinal relationship of aperture to plane of obverse zoarial surface. Note slight inflection of apertures into fenestrule, ×30; 5. Reverse exterior surface illustrating macrostylet (arrow **a**) and microstylet (arrow **b**) development along reverse zoarial surface, and general fenestrule shape as viewed from reverse surface. Note placement of macrostylets near sites of branch bifurcation, ×30.

6. Figured specimen, UI X-6817. FI53, transverse section showing typical general branch outline and continuity of thin granular layer encompassing autozooecial chambers and continuous with reverse longitudinal striae (arrow), ×70.

7, 8. Figured specimen, UI X-6810. FI69. 7. Transverse section showing major zooecial characteristics in this view including inferior hemiseptal development (arrow **a**), nodes (arrow **b**), terminal diaphragm (arrow **c**) capping aperture that exhibits typical attitudinal relationship to plane of obverse surface, granular skeleton of peristome (arrow **d**) continuous with internal granular skeletal layer around autozooecia, and granular skeletal layer (arrow **e**) extending between branches across dissepiment, ×70; 8. Mid longitudinal section, obverse to right, showing granular skeletal layer continuous around autozooecial chamber (arrow **a**), typical autozooecial chamber shape in mid tangential view (arrow **b**), inferior hemiseptum positioned on proximal side of distal lateral chamber wall (arrow **c**) about one-third of the way toward obverse surface, with hemiseptum increasing in length as section shallows (arrow **d**), short superior hemiseptum (arrow **e**) at proximal edge of vestibule, and terminal diaphragm capping aperture (arrow **f**), ×70.

EXPLANATION OF PLATE 17

Figure — Page

1–7. ***Exfenestella exigua*** (Ulrich, 1890) 68

1, 2. Figured specimen, UI X-6810. 1. Deep tangential section illustrating microstylet (arrow **a**) and macrostylet (arrow **b**) development, ×70; 2. shallow to mid shallow longitudinal section, obverse to right, catching lateral edge of autozooecial chambers and showing terminal diaphragm capping aperture (arrow **a**), and microstylet (arrow **b**) continuous with inner granular skeleton, ×70.

3, 5, 6. Figured specimen, UI X-6749. Large, moderately ontogenetically thickened zoarial fragment. 3. TD90, deep longitudinal section, obverse to right, showing typical chamber outline in deep longitudinal view (arrow **a**), reverse macrostylet (arrow **b**), and obverse node (arrow **c**), both continuous with granular skeleton surrounding autozooecial chamber, ×40; 5. TD91, shallow longitudinal section, obverse to right, showing typical chamber outline in this view and extension of apertures onto dissepiments (arrow), ×40; 6. TD94, shallow to mid tangential section. Illustrated is chamber outline at site of branch bifurcation (arrow **a**) and continuity of granular skeleton across dissepiment (arrow **b**), ×40.

4. Figured specimen, UI X-6817. FI57, mid to very shallow tangential section illustrating nodes (arrow **a**) and small obverse stylets (arrow **b**) positioned across obverse branch surface, aperture shape and positioning relative to plane of obverse surface (arrow **c**), complete peristome (arrow **d**) and small stylets that form as extensions of peristome (arrow **e**). Although an extension of the axial wall toward the obverse surface is observed (arrow **f**), a true keel is lacking, ×70.

7. Figured specimen, UI X-6768. FG32, mid shallow to deep tangential section showing typical chamber outline in mid tangential view (arrow **a**) and inferior hemiseptum placement diagonally across autozooecial chamber (arrow **b**), also shown is superior hemiseptum placement at proximal peristomal edge (arrow **c**) giving bilobate appearance to chamber outline, and chamber outline near reverse-wall budding-site (arrow **d**), ×70.

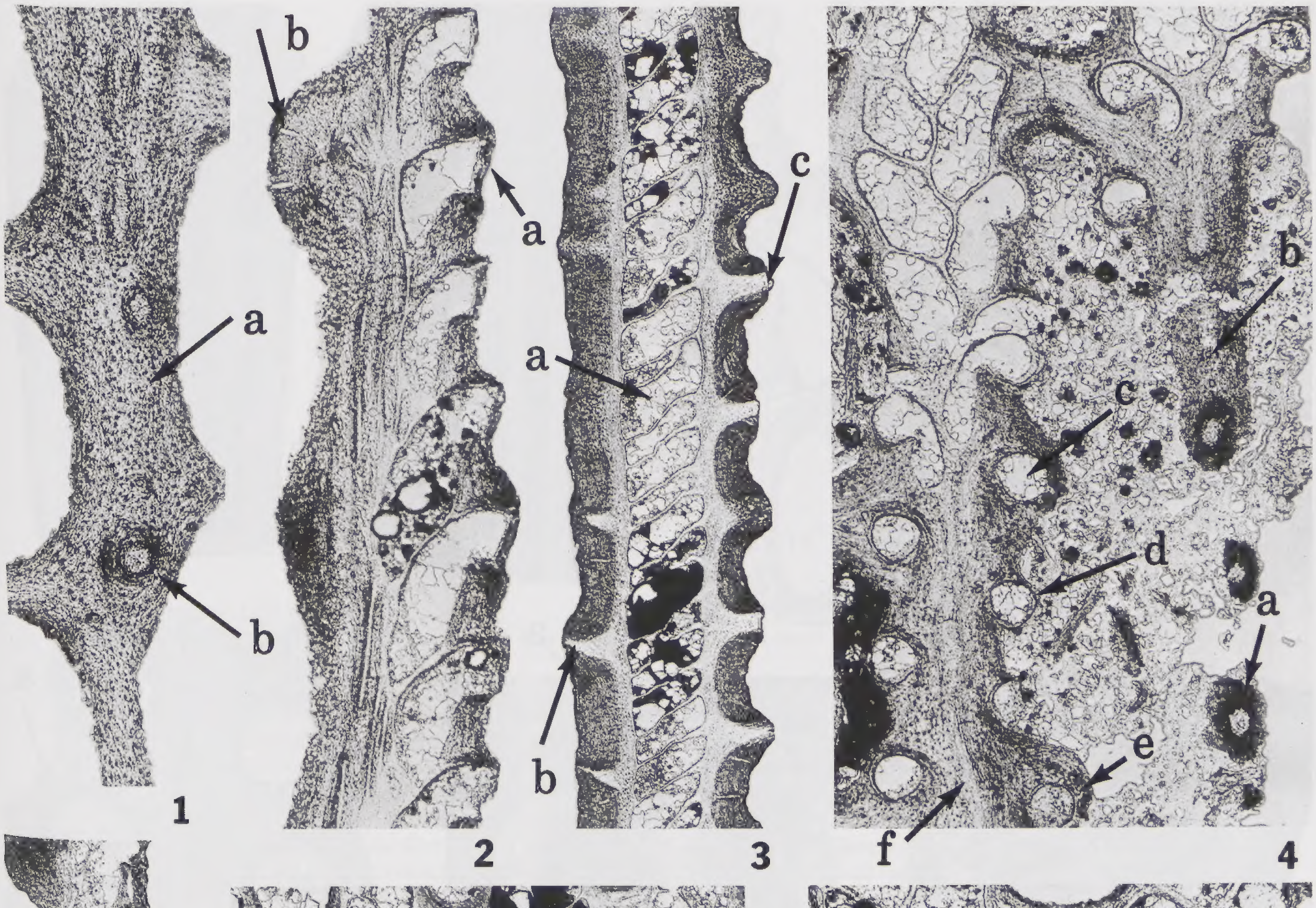
1
2
3
4
5
6
7

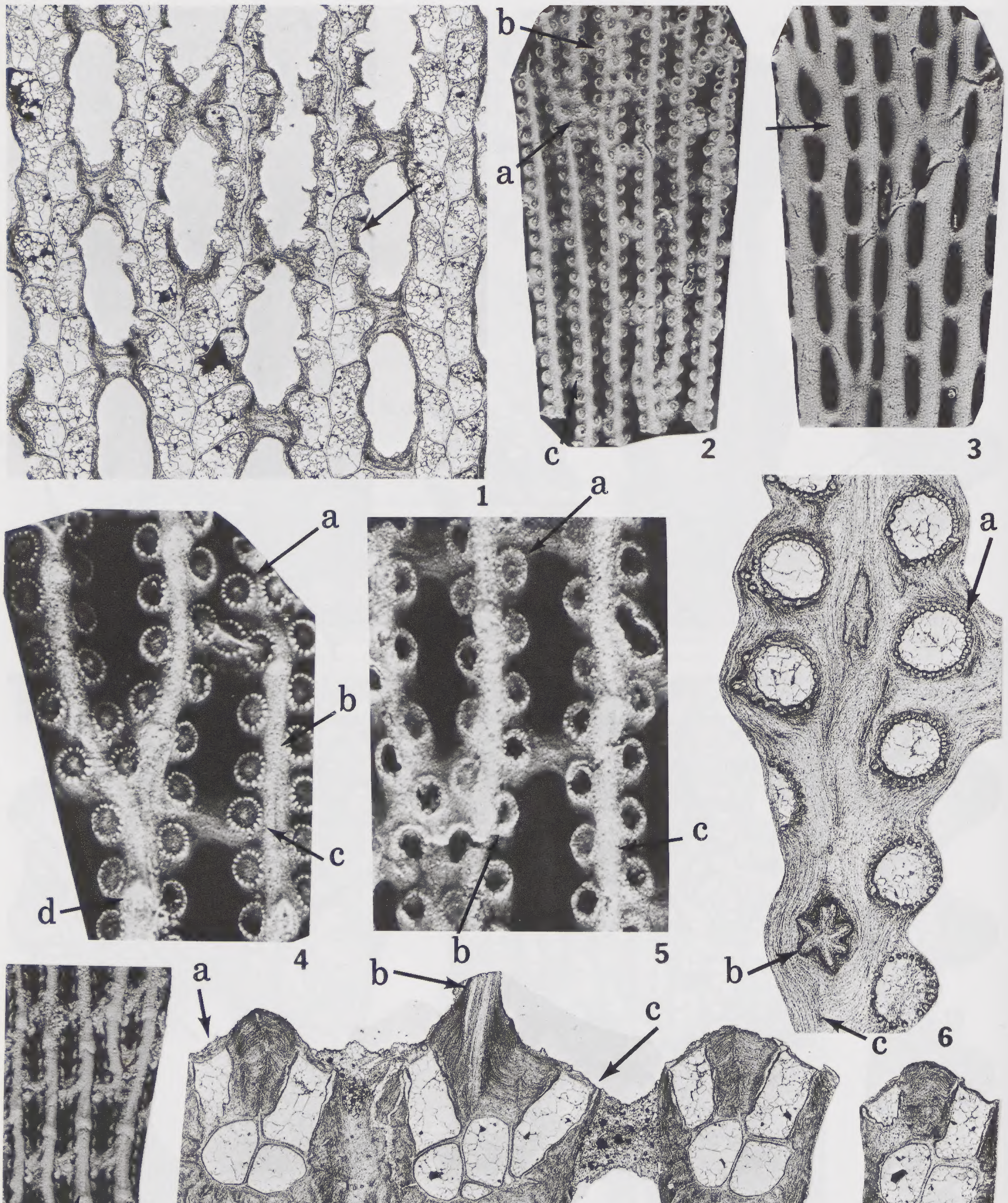
b
a
c
2
3
1
a
a
b
c
d
4
a
c
b
5
a
b
c
6
a
b
c
7
8
9

EXPLANATION OF PLATE 18

Figure Page

1. ***Exfenestella exigua*** (Ulrich, 1890) 68
Figured specimen, UI X-7021. FM22, shallow to mid tangential section of zoarial fragment exhibiting little ontogenetic thickening of lamellar skeletal layer (arrow), ×40.

2–9. ***Banastella guensburgi,*** new species 73

2–4. Paratype, UI X-7016. Large, well-preserved zoarial fragment exhibiting slight ontogenetic thickening of lamellar skeletal layer. 2. Obverse exterior surface. Observe presence of either third row of autozooecia at site of branch bifurcation (arrow **a**) or three rows for moderate to pronounced distances proximal to sites of branch bifurcation (arrow **b**) and recessed dissepiments (arrow **c**), relative to plane of obverse zoarial surface, ×8; 3. Reverse exterior surface illustrating longitudinal striae atop which are positioned rows of small, variable-size microstylets (arrow). Note pronounced thickening of branch proximal and thinning distal to sites of branch bifurcation, and variable fenestrule size and shape in this species, ×8; 4. Greatly enlarged obverse exterior surface illustrating large, well-developed and regularly positioned apertural stylets (arrow **a**) surrounding essentially circular aperture capped in this case by centrally thickened terminal diaphragm; also shown is well-developed ropy keel (arrow **b**), atop which develop small stylets (arrow **c**) positioned between large nodes (arrow **d**) and along edge of keel, ×25.

5, 6, 8, 9. Holotype, UI X-6779. Large moderately ontogenetically thickened zoarial fragment exhibiting good preservation of interior detail. 5. Obverse exterior surface illustrating fusion of apertural stylets around aperture (arrow **a**), overgrowth of aperture adaxial edge by keel (arrow **b**) and thickened keel (arrow **c**) in this zoarial fragment, ×25; 6. FA18, very shallow tangential section. Note typical attitudinal relationship of aperture to plane of obverse surface and well-developed apertural stylets (arrow **a**) surrounding apertural opening, well-developed node (arrow **b**) atop keel and small stylets along obverse surface (arrow **c**), ×60; 8. FA14, transverse section illustrating terminal diaphragm development (arrow **a**), node (arrow **b**), and apertural stylet (arrow **c**) in view exhibiting typical attitudinal relationship of aperture to obverse surface, ×40; 9. FA11, transverse section of single branch showing reverse microstylets (arrow) with core of granular skeleton, ×40.

7. Paratype, UI X-6796. Obverse exterior surface of highly ontogenetically thickened zoarial fragment. Note pronounced thickening of keel (arrow) almost completely overgrowing apertural openings, ×8.

EXPLANATION OF PLATE 19

Figure Page

1–10. ***Banastella guensburgi***, new species 73

1–5, 10. Paratype, UI X-7016. 1. PA9, very shallow longitudinal section, obverse to right, illustrating aperture opening onto edge of and continuity of granular skeleton across dissepiment (arrow **a**) and abaxial edge of aperture (arrow **b**) where it extends into fenestrule, ×40; 2. PA9, shallow to mid longitudinal section, obverse to right, showing centrally thickened terminal diaphragm (arrow **a**) and "brown bodies" (arrow **b**) often positioned behind these diaphragms, ×40; 3. PA2, mid longitudinal section, obverse to right, illustrating typical chamber outline and continuity of granular skeleton around autozooecial chambers (arrow), ×40; 4. PA1, mid longitudinal section obverse to right. Observe typical chamber outline in this view (arrow **a**) showing low reverse-wall budding-angle typical of this species; also shown are reverse microstylets (arrow **b**) continuous with granular skeleton, ×40; 5. PA1, mid to deep longitudinal section, obverse to right, showing chamber outline in deep view (arrow **a**) and continuity of large nodes (arrow **b**) with internal granular skeletal layer, ×40; 10. PA5, shallow to deep tangential section showing continuity of granular skeleton across dissepiment (arrow **a**), variation of chamber outline in mid tangential view from that of a parallelogram (arrow **b**) to that of a rectangle (arrow **c**), inflections in fenestrule outline near obverse surface due to projections of apertures into fenestrule (arrow **d**) and lack of such inflections in mid to deep tangential view (arrow **e**), ×20.

6–9. Holotype, UI X-6779. 6. FA15, transverse section showing development of apertural stylets (arrow) which, when observed in vestibule, are inflected into inner vestibular area causing a restriction in the vestibular opening, ×40; 7. FA18, very shallow tangential section illustrating keel development (arrow **a**) betwen large stellate nodes, and small stylets occurring between nodes (arrow **b**), ×60; 8. FA9, shallow tangential section showing typical node and aperture arrangement along branch and at site of branch bifurcation (arrow) where, in this case, the third aperture is shared between both diverging branches, ×20; 9. FA18, shallow to mid tangential section showing typical chamber outline in mid section view and site of branch bifurcation (arrow), ×20.

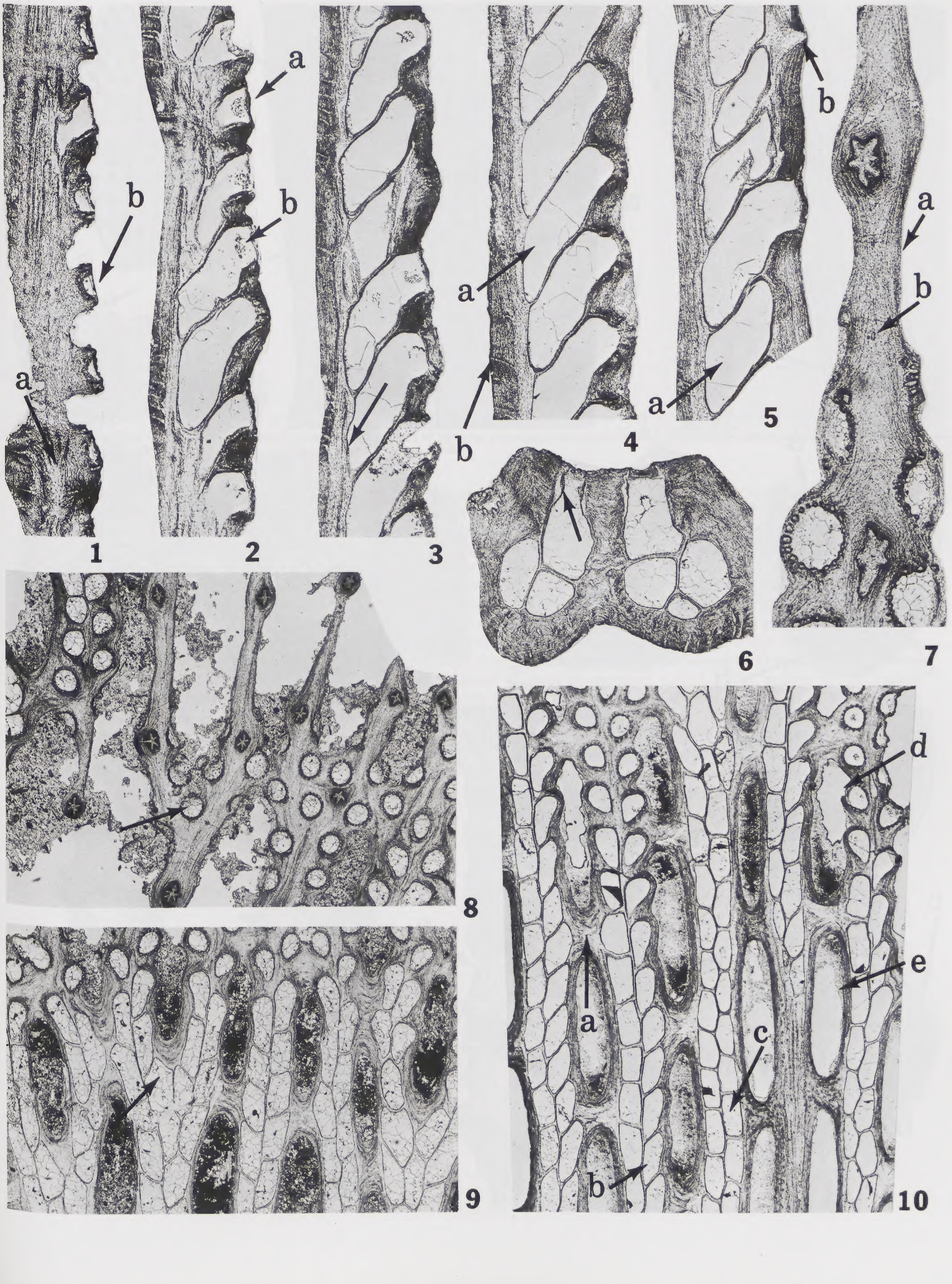
1
2
3
4
5
6
7
8
9
10
a
b
c
d
e

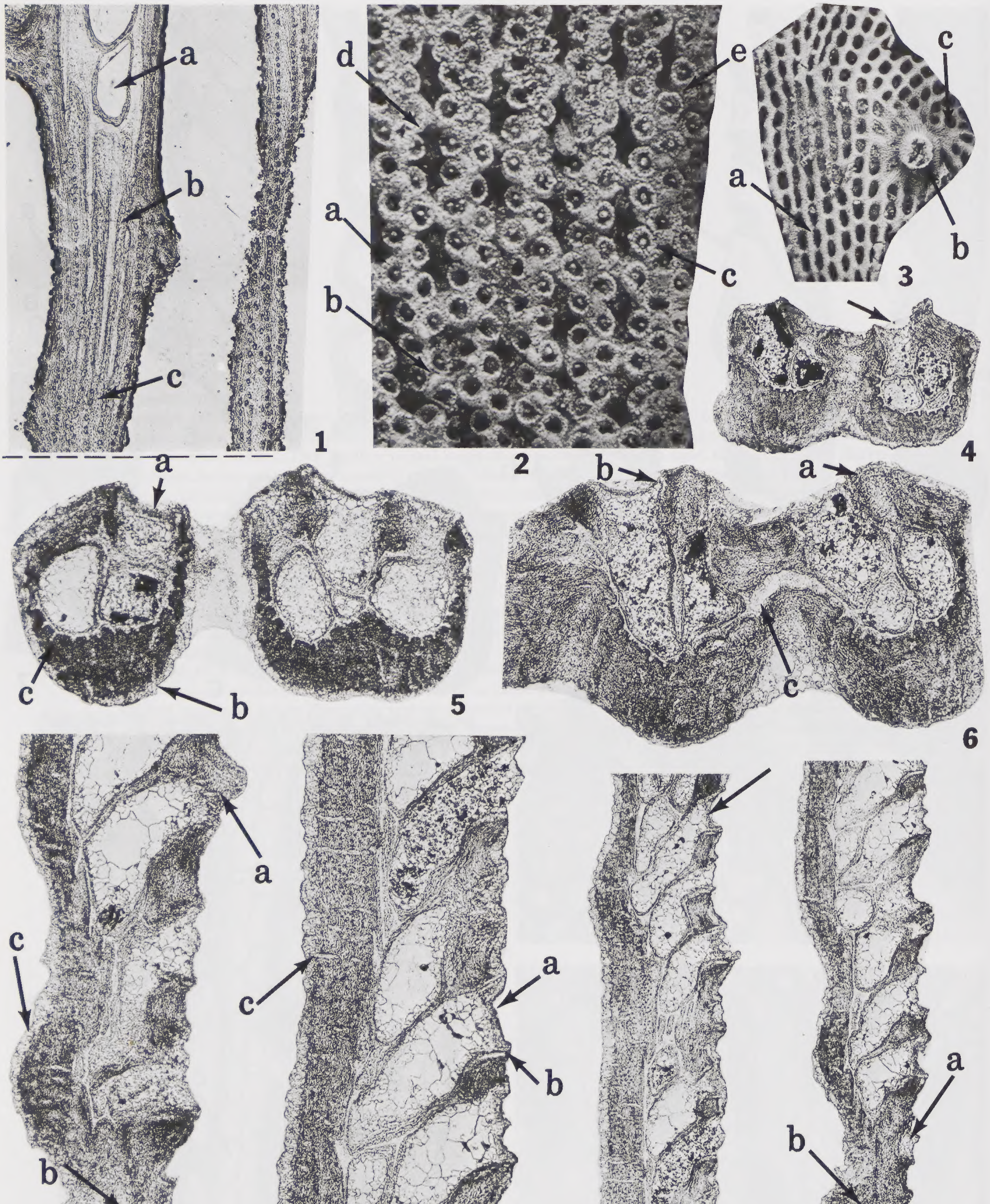
a
b
c
1
d
e
a
b
c
2
a
b
c
3
4
a
c
b
5
b
a
c
6
a
c
b
7
c
a
b
8
9
a
b
10

EXPLANATION OF PLATE 20

Figure Page

1. ***Banastella guensburgi,*** new species 73
Paratype, UI X-7016. PA5, deep tangential section illustrating autozooecial chamber outline near reverse-wall budding-site (arrow **a**), longitudinal striae (arrow **b**) developing as extensions of reverse granular autozooecial wall and small microstylets (arrow **c**) which form as projections from these striae, ×40.

2–10. ***Banastella cingulata*** (Ulrich, 1890) 77
Figured specimen, UI X-6720. Large, well-preserved zoarial fragment exhibiting moderate ontogenetic thickening. 2. Obverse exterior surface illustrating centrally thickened terminal diaphragm capping aperture (arrow **a**), intermediate-size stellate nodes (arrow **b**), peristome (arrow **c**) surrounding pronounced inflection of apertures into fenestrule opening (arrow **d**), and site of branch bifurcation (arrow **e**) showing greatly widened three rows across branch proximal and narrowed two rows distal to site, ×20; 3. Reverse exterior surface showing typical ovate shape of fenestrule in this species (arrow **a**), large zoarial support developed as extension of reverse zoarial surface (arrow **b**) and longitudinal striae (arrow **c**) atop which are positioned rows of microstylets, ×8; 4. TX40, transverse section illustrating thickening of lamellar skeletal layer and typical attitudinal relationship of aperture to plane of obverse surface (arrow), ×40; 5. TX38, transverse section. Note typical branch outline in cross-section, terminal diaphragm (arrow **a**) and attitudinal relationship of aperture to obverse surface, and microstylets (arrow **b**) which connect with granular skeleton of longitudinal striae (arrow **c**), ×70; 6. TX40, transverse section showing continuity of nodes (arrow **a**) and peristome (arrow **b**) with granular skeleton as well as continuity of granular skeleton between branches (arrow **c**) across dissepiment, ×70; 7. TX39, shallow to mid shallow longitudinal section, obverse to right, illustrating apertural stylets (arrow **a**), stylets developed along lateral edge of branch (arrow **b**) and thickened area on reverse surface (arrow **c**) corresponding to occurrence of dissepiment, ×70; 8. TX40, mid longitudinal section, obverse to right, showing typical chamber outline in this view (arrow **a**), and continuity of apertural stylets (arrow **b**) and microstylets (arrow **c**) with internal granular skeleton, ×70; 9. TX40, mid longitudinal section, obverse to right, showing variable chamber outline in this view (arrow), ×40; 10. TX40, shallow to mid longitudinal section, obverse to right, showing apertural edge extending into fenestrule (arrow **a**) and continuity of granular skeleton across dissepiment (arrow **b**), ×40.

EXPLANATION OF PLATE 21

Figure Page

1–6. ***Banastella cingulata*** (Ulrich, 1890) 77

Figured specimen, UI X-6720. 1. TX43, mid longitudinal section, obverse to right, illustrating continuity of granular skeleton along reverse wall (arrow **a**), along chamber lateral walls (arrow **b**) and in center of nodes (arrow **c**). Note typical chamber outline in mid longitudinal view (arrow **d**), ×70; 2. TX49, shallow to mid tangential section illustrating typical chamber outline in mid tangential (arrow **a**) and shallow tangential (arrow **b**) view. Observe continuity of granular skeleton across dissepiments (arrow **c**), typical fenestrule shape (arrow **d**) and overall chamber arrangement and symmetry, ×40; 3. TX45, deep tangential section showing chamber outline near reverse-wall budding-site (arrow **a**) and microstylets (arrow **b**) occurring in rows along reverse branch surface, developing as extensions of longitudinal striae (arrow **c**), ×70; 4. TX49, shallow tangential section. Observe typical attitudinal relationship of aperture to obverse zoarial surface (arrow **a**), apertural stylets (arrow **b**), aperture inflection into fenestrule opening near obverse surface (arrow **c**), and stellate node appearance (arrow **d**) as well as relatively close placement of nodes, ×70; 5. TX49, shallow to mid tangential section showing typical symmetry and site of branch bifurcation (arrow), ×40; 6. TX45, mid to deep tangential section illustrating pronounced thickening of lamellar skeleton associated with site of zoarial support development (arrow **a**). Observe partial plugging of fenestrule (arrow **b**) along reverse zoarial surface associated with lamellar skeletal thickening, ×40.

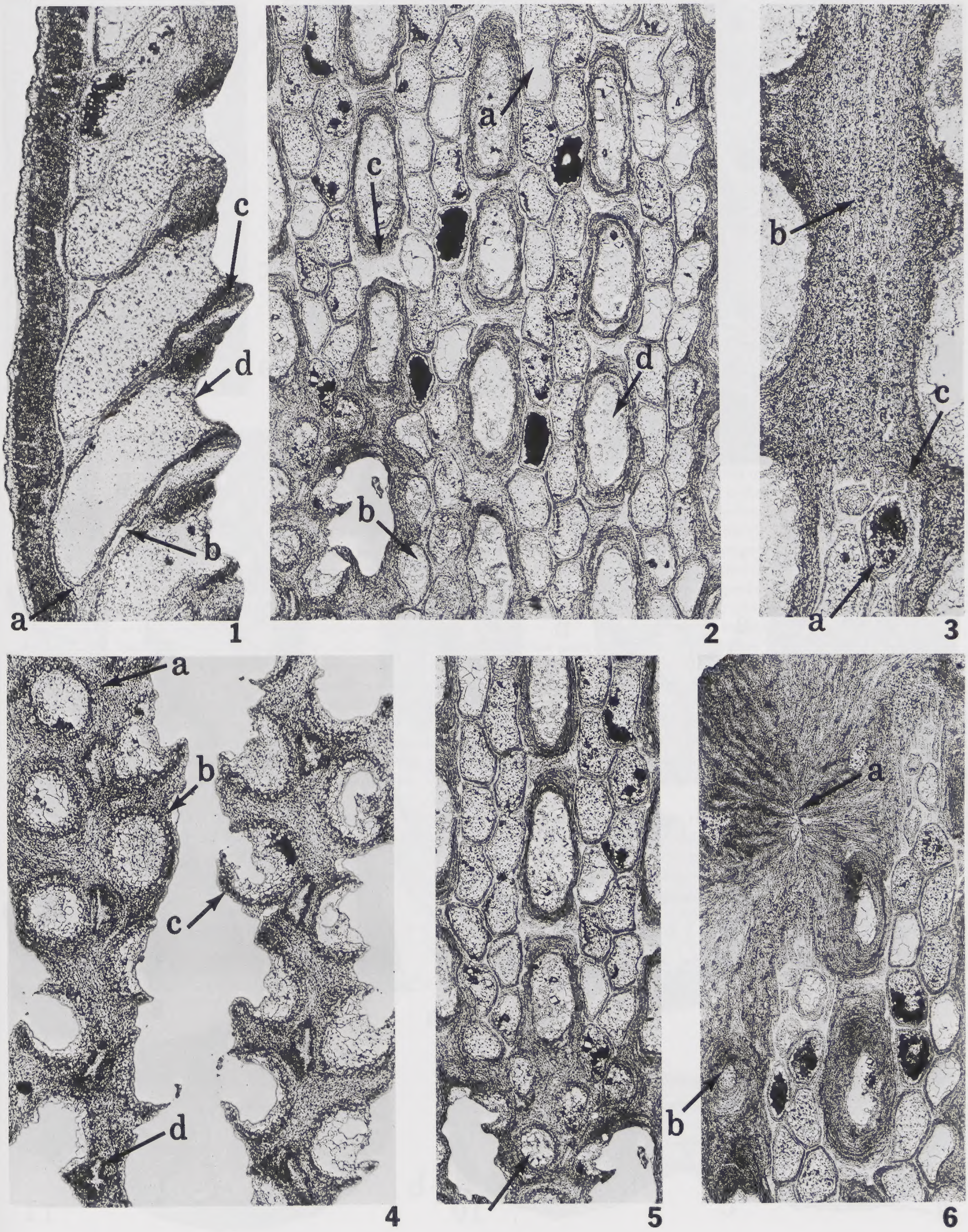
c
d
b
a
1
c
a
d
b
2
b
c
a
3
a
b
c
d
4
5
a
b
6

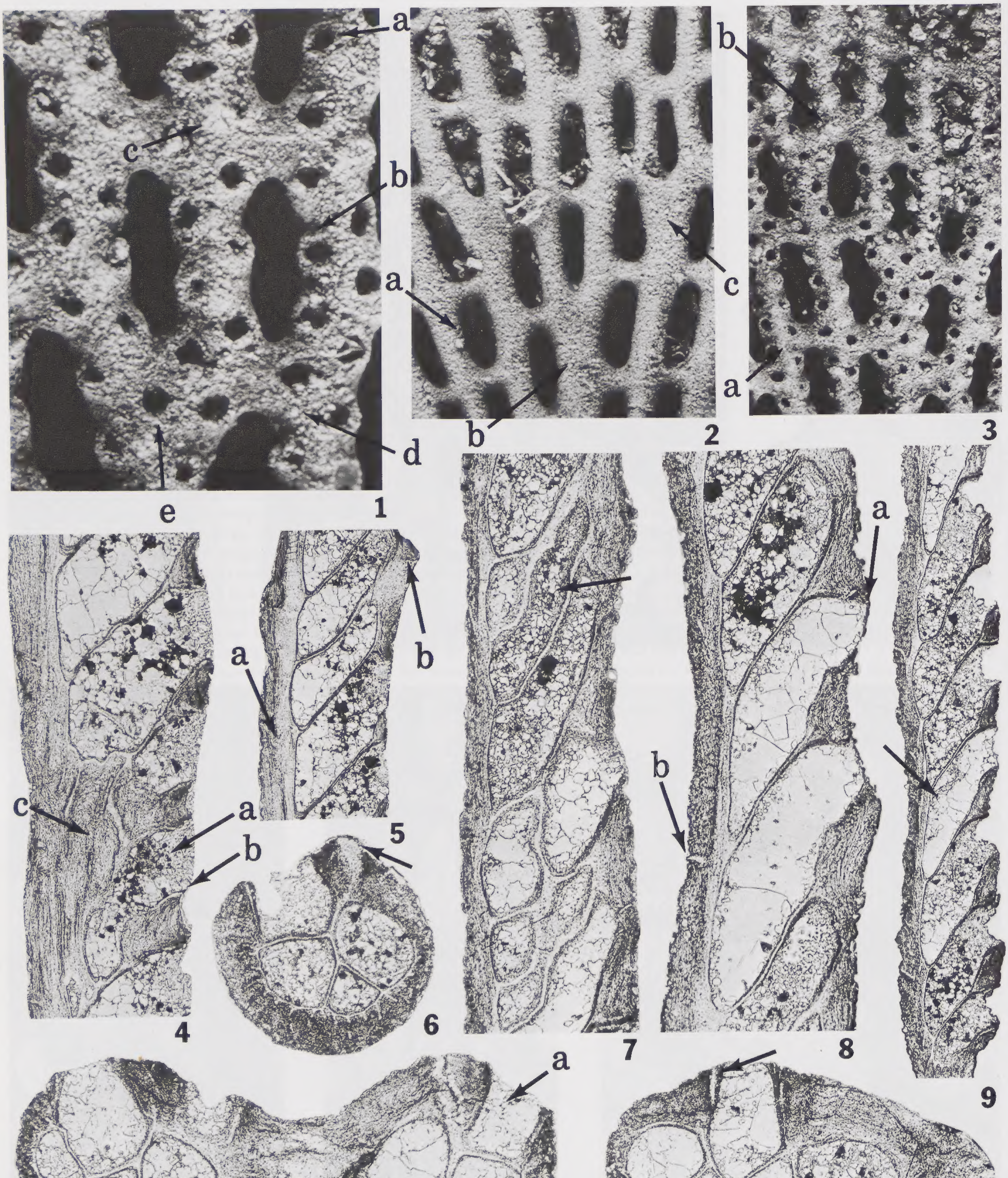
1
2
3
4
5
6
7
8
9
10
11
a
b
c
d
e

EXPLANATION OF PLATE 22

Figure Page

1–11. ***Banastella mediocreforma,*** new species 79

1–3, 6–11. Holotype, UI X-6717. Large, well-preserved zoarial fragment exhibiting moderate ontogenetic thickening. 1. Obverse exterior surface illustrating typical autozooecial aperture shape and attitudinal relationship to plane of obverse surface (arrow **a**), peristome surrounding aperture (arrow **b**) formed from fusion of apertural stylets and slight extension of aperture into fenestrule margin, nodes (arrow **c**) widely spaced along middle of obverse branch surface, small stylets (arrow **d**) across obverse surface and aperture placement at site of branch bifurcation (arrow **e**), ×30; 2. Reverse exterior surface showing fenestrules (arrow **a**) that exhibit irregularity in size and shape, small microstylets across reverse branch surface (arrow **b**), and thickening proximal and thinning distal to sites of branch bifurcation (arrow **c**), ×12; 3. Obverse exterior surface showing typically moderately irregular mesh pattern, keel (arrow **a**) and apertures partially to completely overgrown by lamellar skeleton (arrow **b**), ×12; 6. TX1, transverse section showing typical branch outline in cross-section and node (arrow) continuous with granular skeleton, ×70; 7. TX7, deep to mid longitudinal section, obverse to right, showing typical chamber outline in deep longitudinal view (arrow), ×70; 8. TX5, shallow mid longitudinal section, obverse to right, showing lamellar skeleton partially overgrowing aperture (arrow **a**) and reverse microstylets (arrow **b**) in continuity with internal granular skeletal layer, ×70; 9. TX7, mid longitudinal section, obverse to right, illustrating typical autozooecial chamber outline (arrow) associated with low reverse-wall budding-angle, ×40; 10. TX5, transverse section illustrating branch that is rounded in cross-section, typical attitudinal relationship of aperture (arrow **a**) to plane of obverse surface, granular skeleton continuous around autozooecial chambers, with reverse longitudinal striae (arrow **b**) and across dissepiments (arrow **c**). Note moderate thickening of lamellar skeletal layer (arrow **d**), ×70; 11. TX5, transverse section of widened branch near site of branch bifurcation illustrating apertural stylets (arrow) at edge of aperture, ×70.

4, 5. Paratype, UI X-6917. PI92. 4. Shallow to mid longitudinal section, obverse to right, illustrating typical attitudinal relationship of aperture to obverse surface (arrow **a**), apertural stylets (arrow **b**), and granular skeleton extending across dissepiments between branches (arrow **c**), ×70; 5. Mid longitudinal section, obverse to right, showing continuity of granular skeleton along reverse chamber wall (arrow **a**), around autozooecial chambers, and with obverse nodes (arrow **b**), ×40.

EXPLANATION OF PLATE 23

Figure	Page
1–6. ***Banastella mediocreforma,*** new species	79

1, 3–6. Holotype, UI X-6717. 1. TX13, mid to shallow tangential section showing three rows of autozooecia across branch surface proximal to site of branch bifurcation (arrow **a**) and slight inflection of apertures into fenestrule in mid shallow tangential view (arrow **b**), ×25; 3. TX13, shallow tangential section illustrating apertural stylets (arrow **a**) that fuse to become the peristome (arrow **b**), and median keel (arrow **c**) atop which are located small stylets (arrow **d**), ×70; 4. TX1, transverse section showing typical cross-section of autozooecial chamber (arrow), ×70; 5. TX13, shallow to deep tangential section showing chamber outline in mid tangential view (arrow **a**), mid shallow tangential view (arrow **b**) and near reverse-wall budding-site (arrow **c**). Note longitudinal striae (arrow **d**) from which microstylets (arrow **e**) originate, ×25; 6. TX50, shallow tangential section showing inflection of autozooecial apertures into fenestrule (arrow **a**), well-developed median keel (arrow **b**) atop which are positioned widely spaced stellate nodes (arrow **c**), ×40.

2. Paratype, UI X-6917. PI94, shallow to deep tangential section of zoarial fragment exhibiting slight ontogenetic thickening. Observe lack of inflection into fenestrule outline by apertures in mid tangential section (arrow), ×20.

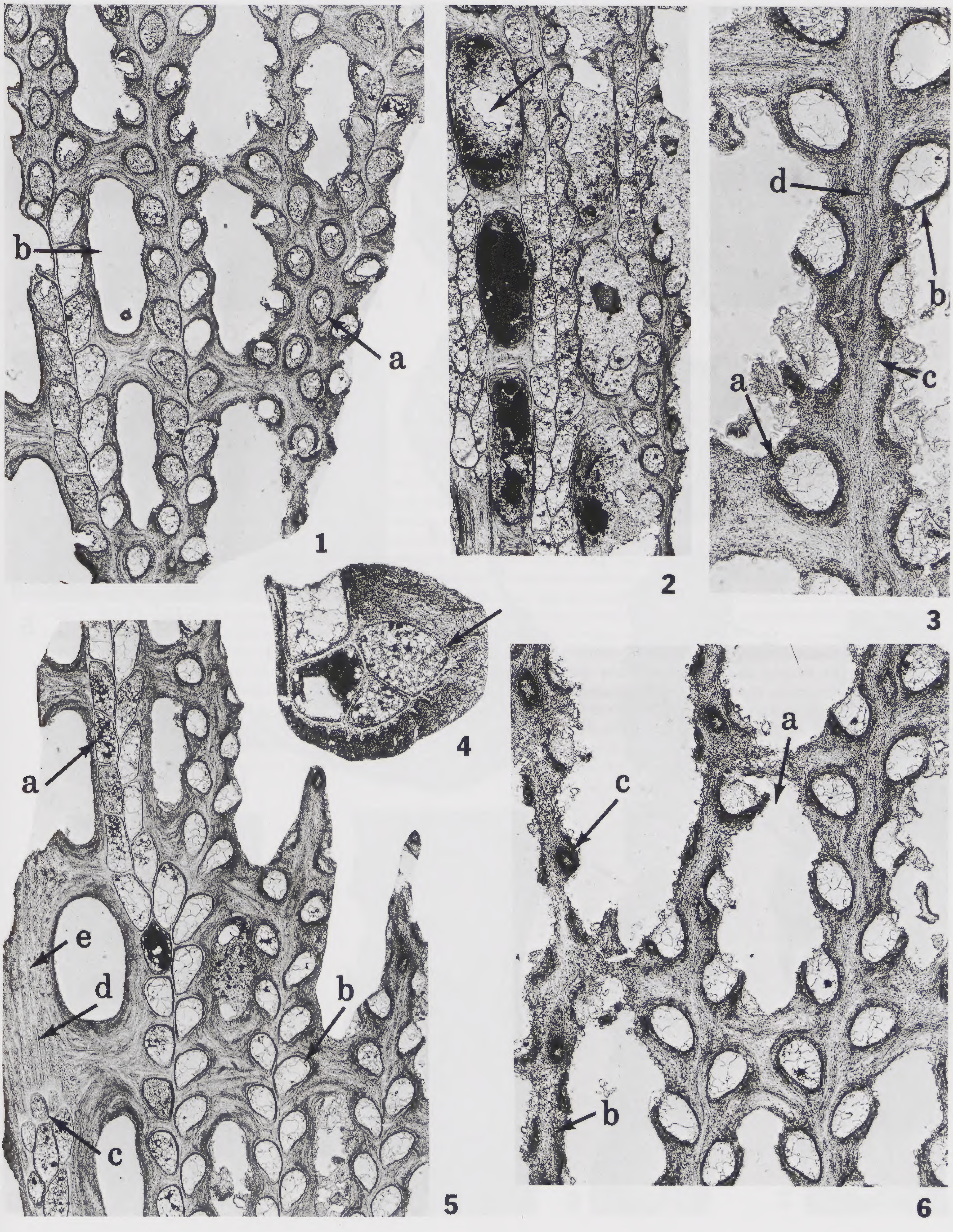

b
a
1
2
d
b
a
c
3
4
a
a
c
e
d
b
c
b
5
6

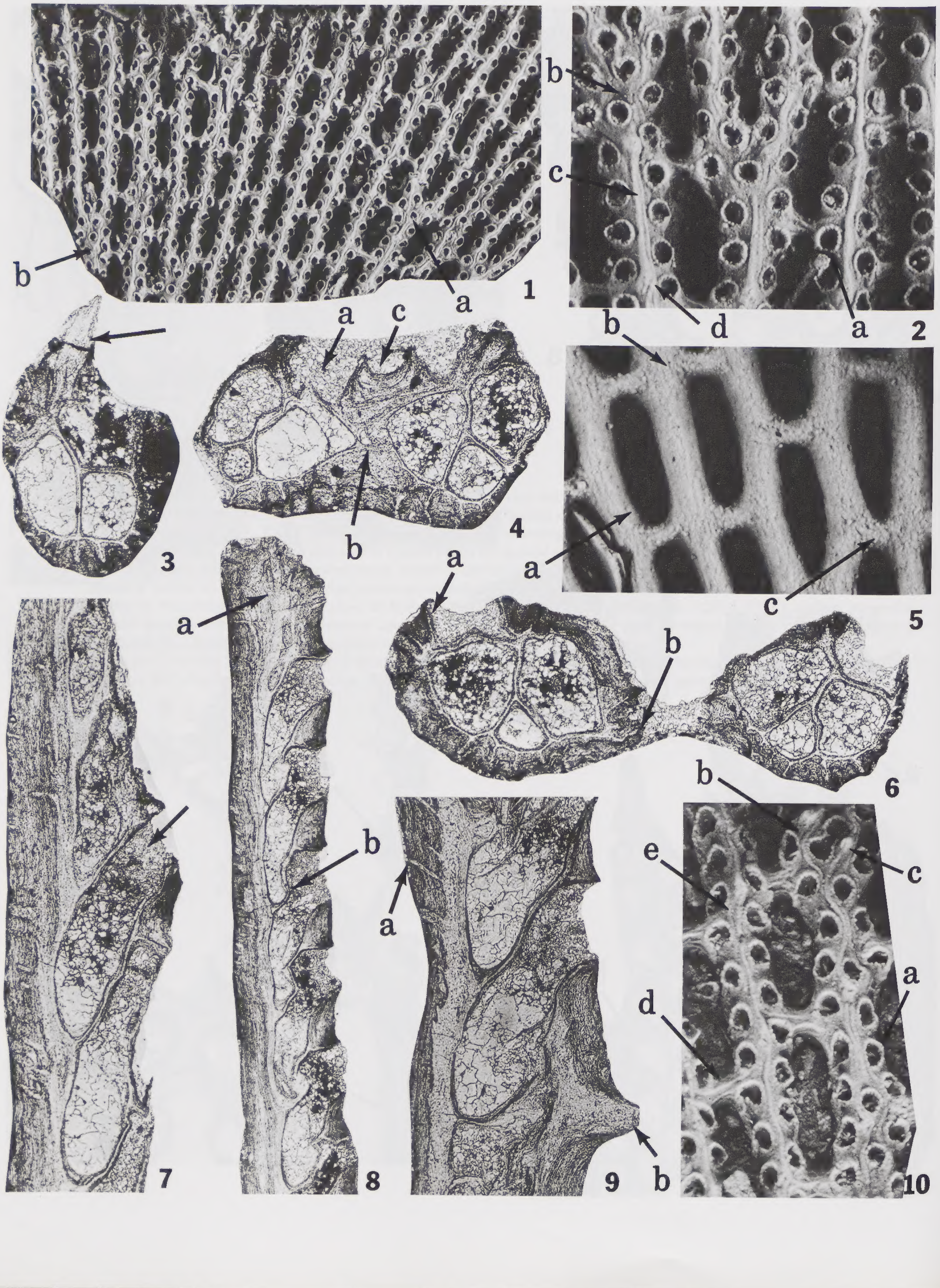
1
a
b
2
a
b
c
d
3
4
a
b
c
5
a
b
c
6
a
b
7
8
a
b
9
a
b
10
a
b
c
d
e

EXPLANATION OF PLATE 24

Figure Page

1–10. ***Banastella limitaris*** (Ulrich, 1890) 81

Hypotype, UI X-7015. Large, well-preserved zoarial fragment exhibiting slight ontogenetic thickening. 1. Obverse exterior surface illustrating typical mesh symmetry. Observe either third row at site of branch bifurcation (arrow **a**) or three rows for moderate distance proximal to site of branch bifurcation (arrow **b**), ×8; 2. Enlarged obverse exterior surface showing ring of apertural stylets partially fused to become peristome (arrow **a**), site of branch bifurcation (arrow **b**), and median keel (arrow **c**) atop which are positioned well-developed nodes (arrow **d**), ×20; 3. WR56, transverse section showing well-developed node (arrow) continuous with interior granular skeletal material, ×70; 4. WR56, transverse section illustrating typical attitudinal relationship of aperture to plane of obverse surface (arrow **a**), continuity of granular skeletal layer across dissepiment (arrow **b**) and longitudinal ridge development across dissepiment obverse surface (arrow **c**), ×70; 5. Enlarged reverse exterior surface showing variability in fenestrule shape (arrow **a**), microstylets (arrow **b**) developing as extensions of longitudinal striae, and microstylets (arrow **c**) developed across dissepiments, ×20; 6. WR53, transverse section showing continuity of granular skeleton with stylets and subsequently with peristome surrounding aperture (arrow **a**), and inception of dissepiment as extension of longitudinal striae at lateral edge of branch (arrow **b**), ×70; 7. WR51, mid shallow to shallow longitudinal section, obverse to right, showing narrow longitudinal outline of autozooecial chamber (arrow), ×70; 8. WR51, mid to shallow longitudinal section, obverse to right, showing continuity of granular skeleton across dissepiment (arrow **a**) and elongate typical autozooecial chamber in mid longitudinal section with shape altered by fracturing of chamber lateral walls (arrow **b**),x40; 9. WR57, mid longitudinal section, obverse to right, illustrating granular skeleton surrounding autozooecial chambers and continuous with reverse microstylets (arrow **a**) and obverse nodes (arrow **b**), ×70; 10. Enlarged obverse exterior view. Note slight to moderate extension of aperture into fenestrule (arrow **a**), sinuous keel (arrow **b**), nodes developing as extensions of keel (arrow **c**), barlike longitudinal ridges across dissepiments (arrow **d**), and small obverse stylets (arrow **e**), ×20.

EXPLANATION OF PLATE 25

Figure Page

1–8. ***Banastella limitaris*** (Ulrich, 1890) 81

Hypotype, UI X-7015. 1. WR64, very shallow to shallow tangential section showing keel (arrow **a**), nodes (arrow **b**) developed atop keel, small obverse stylets (arrow **c**), typical aperture shape and orientation to plane of obverse surface (arrow **d**), apertural stylets (arrow **e**), and fusion of these stylets to become the peristome (arrow **f**), ×70; 2. WR63, mid to deep tangential section showing autozooecial chamber shape near reverse-wall budding-site (arrow **a**), granular skeletal composition of longitudinal striae extending along reverse chamber surface (arrow **b**), microstylets (arrow **c**) developing atop the longitudinal striae and across disepiments (arrow **d**) along reverse zoarial surface, ×40; 3. WR53, transverse section of branch proximal to site of branch bifurcation, ×70; 4. Reverse exterior surface illustrating longitudinal striae and site of branch bifurcation (arrow), ×8; 5. WR63, mid to deep mid tangential section. Observe continuity of granular skeleton across dissepiments (arrow **a**) and lack of aperture extension into fenestrule (arrow **b**) in this view, ×40; 6. WR64, shallow tangential section showing aperture extending onto edge of dissepiment (arrow **a**) and thin axial ridge (arrow **b**) along obverse surface, ×40; 7. WR63, mid shallow tangential section showing typical autozooecial chamber outline in this view (arrow), ×40; 8. WR64, shallow to mid tangential section showing chamber outline in mid tangential view (arrow), ×40.

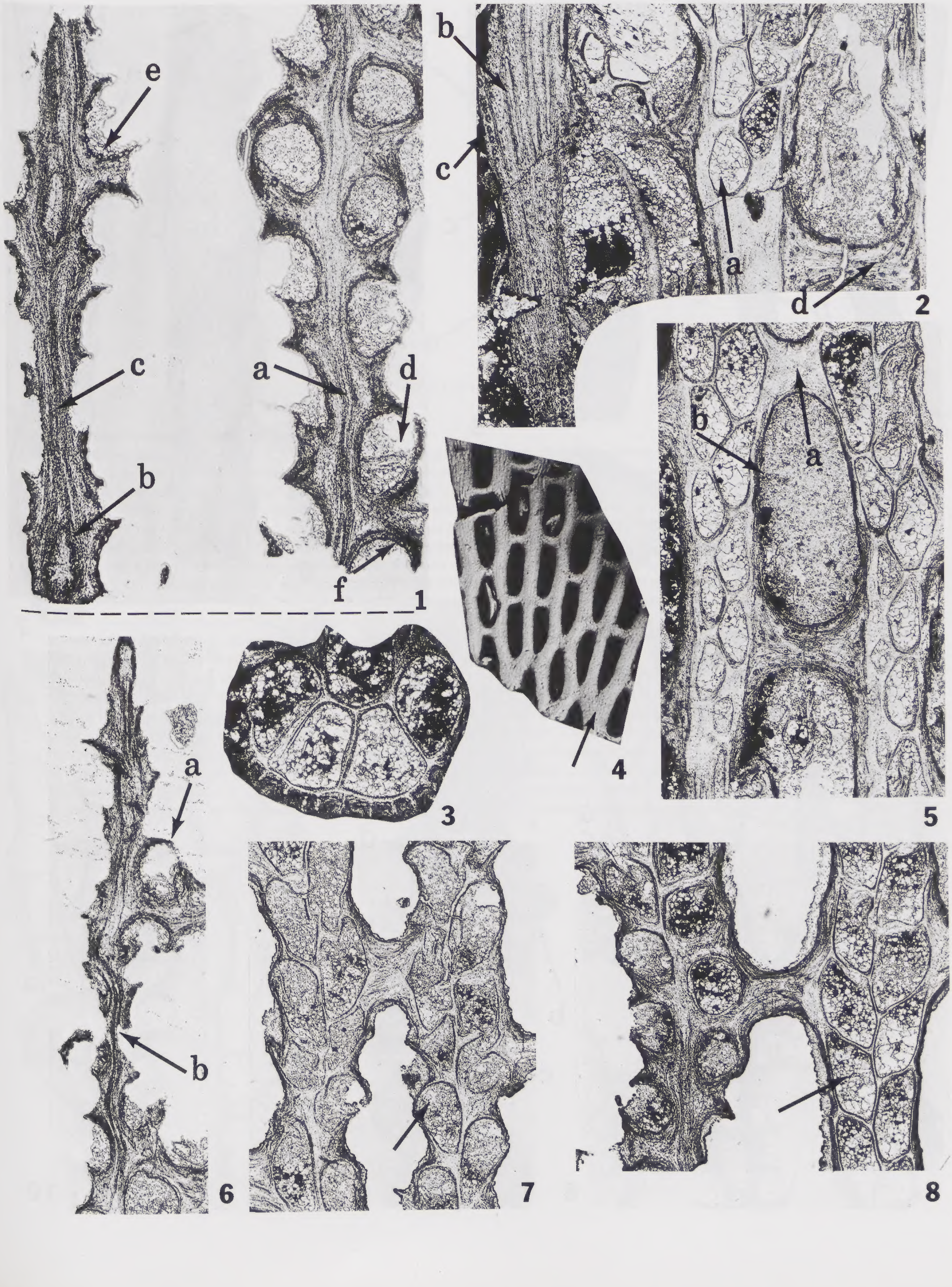
e
c
b
a
d
f
1
b
c
a
d
2
b
a
5
4
3
a
b
6
7
8

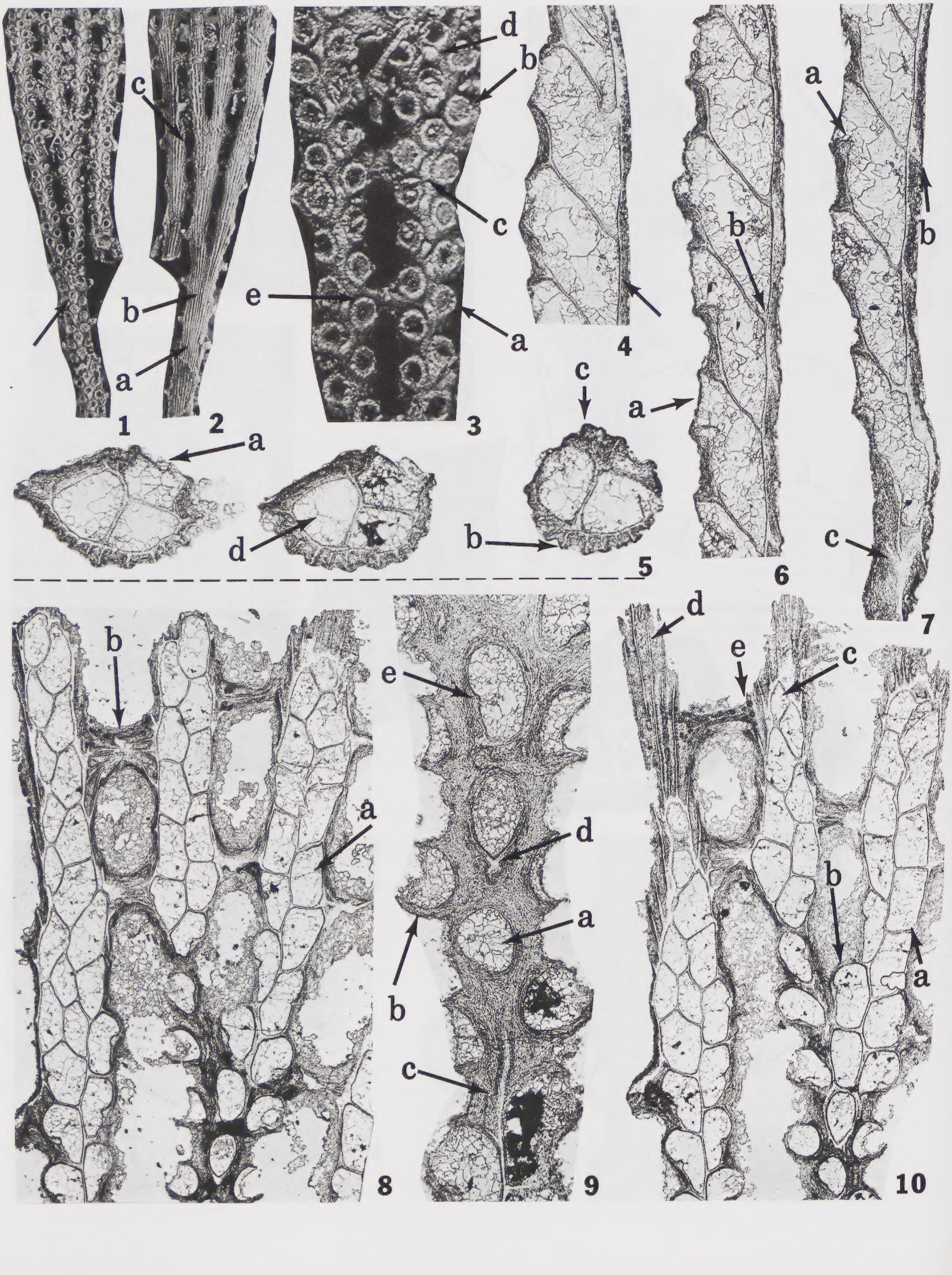
1
2
3
4
5
6
7
8
9
10

EXPLANATION OF PLATE 26

Figure Page

1–10. ***Banastella biseriata*** (Ulrich, 1890) 83

Figured specimen, UI X-6915. 1. Obverse exterior of zoarial fragment illustrating three rows of apertures across branch surface developed for pronounced distances proximal to site of branch bifurcation (arrow) and polyporid-like appearance of zoarium exterior, ×8; 2. Reverse exterior of zoarial fragment showing longitudinal striae (arrow **a**) atop which occur rows of small microstylets, site of branch bifurcation (arrow **b**) and typical fenestrule shape in reverse view (arrow **c**), ×8; 3. High magnification obverse exterior view illustrating typical attitudinal relationship of aperture (arrow **a**) to plane of obverse surface, peristome (arrow **b**), intermittent and anastomosing keel (arrow **c**), stellate node (arrow **d**), and longitudinal striae atop obverse dissepiment surface (arrow **e**), ×25; 4. PO22, mid longitudinal section, obverse to left, showing continuity of granular skeleton (arrow) around autozooecial chambers, ×70; 5. PO26, transverse section showing centrally thickened terminal diaphragm capping aperture oriented in typical fashion to plane of obverse surface (arrow **a**), and longitudinal striae (arrow **b**) continuous with internal granular skeletal layer and nodes (arrow **c**), and characteristic chamber outline in mid transverse view (arrow **d**), ×70; 6. PO20, shallow to mid longitudinal section, obverse to left, showing terminal diaphragm (arrow **a**) and typical chamber outline in mid tangential section (arrow **b**) illustrating low budding-angle of reverse wall, ×70; 7. PO22, shallow to mid longitudinal section, obverse to left, illustrating typical chamber outline in mid longitudinal view and short vestibule with superior hemiseptum (arrow **a**), continuity of granular skeletal layer with reverse microstylets (arrow **b**) and across dissepiments (arrow **c**), ×70; 8. PO27, shallow to mid tangential section showing typical chamber outline in mid section view (arrow **a**) and continuity of granular skeleton across dissepiment (arrow **b**). Note typical zoarial surficial view in tangential section, ×35; 9. PO31, very shallow tangential section. Observe typical aperture outline (arrow **a**), peristome (arrow **b**), keel (arrow **c**), and node (arrow **d**) developed at proximal edge of aperture, also very slight superior hemiseptum present at inner vestibule proximal edge (arrow **e**), ×70; 10. PO29, shallow to deep tangential section showing typical chamber outline in mid tangential view (arrow **a**), site of branch bifurcation (arrow **b**), chamber outline near reverse-wall budding-site (arrow **c**), microstylets developed as extensions of longitudinal striae (arrow **d**) and across dissepiment surface (arrow **e**), ×35.

EXPLANATION OF PLATE 27

Figure Page
1. ***Banastella biseriata*** (Ulrich, 1890) 83

Figured specimen, UI X-6915. PO29, shallow to mid tangential section. Observe short superior hemiseptum present at proximal aperture edge (arrow **a**) and typical autozooecial chamber outline near obverse surface (arrow **b**), ×70.

2–10. ***Banastella delicata,*** new species 86

2. Holotype, UI X-6793. Obverse exterior surface of large, well-preserved zoarial fragment showing apertures surrounded by peristomes (arrow **a**) which apparently develop from fusion of apertural stylets, aperture position at site of branch bifurcation (arrow **b**), keel (arrow **c**), nodes (arrow **d**) positioned atop keel, ornamentation across dissepiment surface (arrow **e**) and projection of aperture into fenestrule opening (arrow **f**), ×8.

3, 7–10. Paratype, UI X-6781. 3. Reverse exterior surface showing longitudinal striae (arrow **a**) atop which develop microstylets (arrow **b**). Note site of branch bifurcation (arrow **c**), ×8; 7. FA58, shallow longitudinal section, obverse to left, showing slight aperture extension into fenestrule at branch lateral edge (arrow **a**) and continuity of granular skeleton across dissepiment (arrow **b**), ×70; 8. FA58, shallow to mid shallow longitudinal section, obverse to left, illustrating typical chamber outline in mid shallow section (arrow) ×40; 9. FA66, mid to mid shallow longitudinal section, obverse to left, illustrating terminal diaphragm (arrow **a**) and mid longitudinal section with low reverse-wall budding-angle (arrow **b**), ×40; 10. FA66, mid deep to deep longitudinal section, obverse to left, showing typical chamber outline in deep longitudinal view (arrow **a**) and apertural stylet development at adaxial aperture edge (arrow **b**), ×70.

4, 5. Paratype, UI X-6782. 4. FA63, transverse section showing apertural stylet (arrow **a**) at edge of aperture exhibiting typical attitudinal relationship to plane of obverse surface, longitudinal striae continuous with inner granular skeleton (arrow **b**), and part of longitudinal ridge across dissepiment surface (arrow **c**), ×70; 5. FA57, transverse section showing continuity of granular skeleton with obverse nodes and keel (arrow **a**) and typical circular cross-section of branch (arrow **b**), ×70.

6. Paratype, UI X-6783. FA65, mid shallow tangential section illustrating well-developed longitudinal ridge (arrow) extending between branches atop dissepiment, ×40.

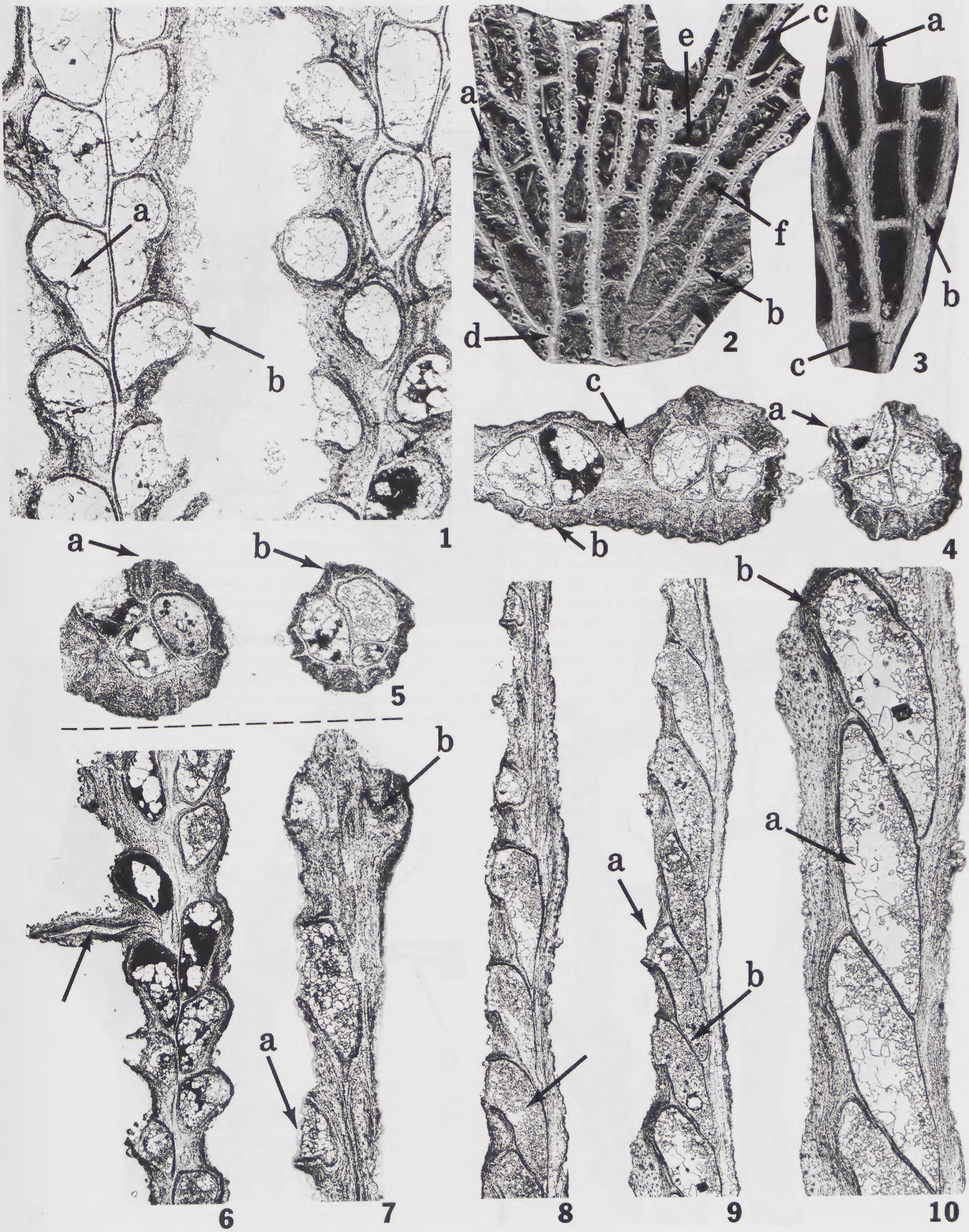
a
b
1
a
e
c
f
b
d
2
a
b
c
3
c
a
b
4
a
b
5
b
a
6
7
8
a
b
9
b
a
10

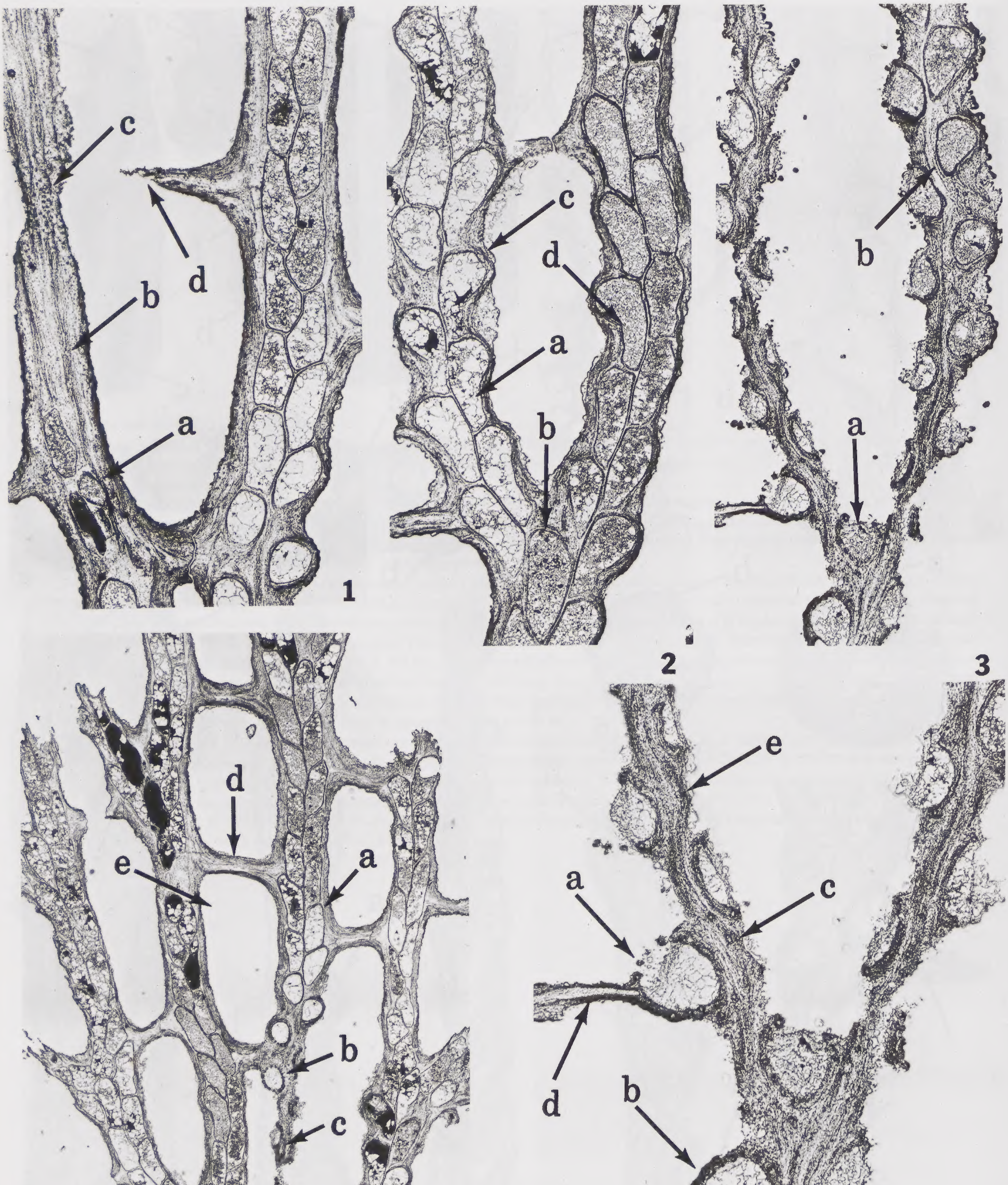
c
d
b
a
1
c
d
a
b
2
b
a
3
d
e
a
b
c
4
e
a
c
d
b
5

EXPLANATION OF PLATE 28

Figure Page

1–5. ***Banastella delicata***, new species 86

Holotype, UI X-6793. Large zoarial fragment exhibiting slight ontogenetic thickening. 1. FA73, shallow to deep tangential section illustrating chamber outline near reverse-wall budding-site (arrow **a**), reverse longitudinal striae (arrow **b**) atop which develop microstylets (arrow **c**) and recessed dissepiment relative to plane of reverse surface (arrow **d**), ×40; 2. FA51, mid shallow tangential section showing typical chamber outline (arrow **a**) in this view and at site of branch bifurcation (arrow **b**), slight inflection of apertural abaxial edge into fenestrule (arrow **c**) and short superior hemiseptum (arrow **d**) at proximal vestibular edge, ×40; 3. FA65, shallow tangential section. Note aperture location at site of branch bifurcation (arrow **a**) and autozooecial chamber outline as section slightly deepens (arrow **b**), ×40; 4. FA71, shallow to deep tangential section illustrating typical autozooecial chamber outline in mid tangential view (arrow **a**), typical aperture shape and attitudinal relationship to plane of obverse surface (arrow **b**), node (arrow **c**), continuity of granular skeleton across dissepiment (arrow **d**) and lack of apertural inflection into fenestrule (arrow **e**), ×20; 5. FA65, enlarged shallow tangential view showing aperture surrounded by stylets (arrow **a**) at edge of dissepiment, fusing of these stylets in slightly deeper section to form peristome (arrow **b**), stylets along obverse branch surface (arrow **c**), ridge atop dissepiment formed from granular skeleton (arrow **d**) and thickened keel along middle of branch (arrow **e**), ×70.

EXPLANATION OF PLATE 29

Figure Page
1–11. ***Cubifenestella rudis*** (Ulrich, 1890) 90

1–4, 9–11. Figured specimen, UI X-6752. Large, well-preserved zoarial fragment exhibiting pronounced ontogenetic thickening. 1. Reverse exterior surface. Observe fenestrules overgrown by lamellar skeleton (arrow **a**) near proximal end of zoarium and those not overgrown (arrow **b**) toward more distal end of zoarium, zoarial supports developed from reverse surface (arrow **c**), and initial site of zoarial development (arrow **d**), ×4; 2. Obverse exterior surface illustrating pronounced ontogenetic thickening of lamellar skeleton near proximal end of zoarium covering autozooecial apertures (arrow **a**) when compared to more distal end of zoarial fragment where apertures remain uncovered (arrow **b**), zoarial supports developed at lateral mesh edge (arrow **c**), and initial site of zoarial development (arrow **d**), ×4; 3. Obverse exterior surface near proximal end of zoarium showing pronounced thickening of keel (arrow **a**), most autozooecial apertures covered by lamellar skeleton (arrow **b**), and increased node diameter (arrow **c**), all resulting from ontogenetic thickening, ×8; 4. Obverse exterior toward more distal end of zoarium showing apertures not covered by lamellar skeleton (arrow **a**) and less keel and nodal thickening (arrow **b**), ×8; 9. TA94, deep to mid longitudinal section, obverse to right, showing macrostylets (arrow **a**), nodes (arrow **b**), small obverse stylets (arrow **c**), microstylets (arrow **d**) all in continuity with granular skeletal layer (arrow **e**) surrounding autozooecial chambers, ×40; 10. TA3, transverse section illustrating typical chamber shape and attitudinal relationship of aperture to plane of obverse surface (arrow **a**), characteristic chamber outline in mid transverse view (arrow **b**), and intermediate thickening of lamellar skeletal layer, ×40; 11. TA6, transverse section showing typical branch profile in cross-sectional view, branch spacing, and centrally thickened terminal diaphragm (arrow), ×40.

5–7. Figured specimen, UI X-6902. Zoarial fragment exhibiting slight to moderate ontogenetic thickening. 5. Obverse exterior illustrating slight keel and nodal development (arrow **a**) as well as apertures not covered by lamellar skeleton, and site of branch bifurcation (arrow **b**), ×8; 6. Reverse exterior surface illustrating variability in fenestrule size and shape and macrostylets (arrow) typically positioned at or near site of branch–dissepiment junction, ×8; 7. Greatly enlarged obverse exterior surface view. Note aperture shape and attitudinal relationship to plane of obverse surface (arrow **a**), centrally thickened terminal diaphragm capping aperture (arrow **b**), peristome (arrow **c**), nodes (arrow **d**) atop keel, obverse stylets (arrow **e**) and median ridge across dissepiment (arrow **f**), ×25.

8. Figured specimen, UI X-6900. EF12, transverse section of moderately ontogenetically thickened zoarial fragment showing granular skeletal layer continuous around autozooecial chambers and with longitudinal striae (arrow **a**), microstylets (arrow **b**), obverse node (arrow **c**), across dissepiment (arrow **d**) and with apertural stylets (arrow **e**), ×70.

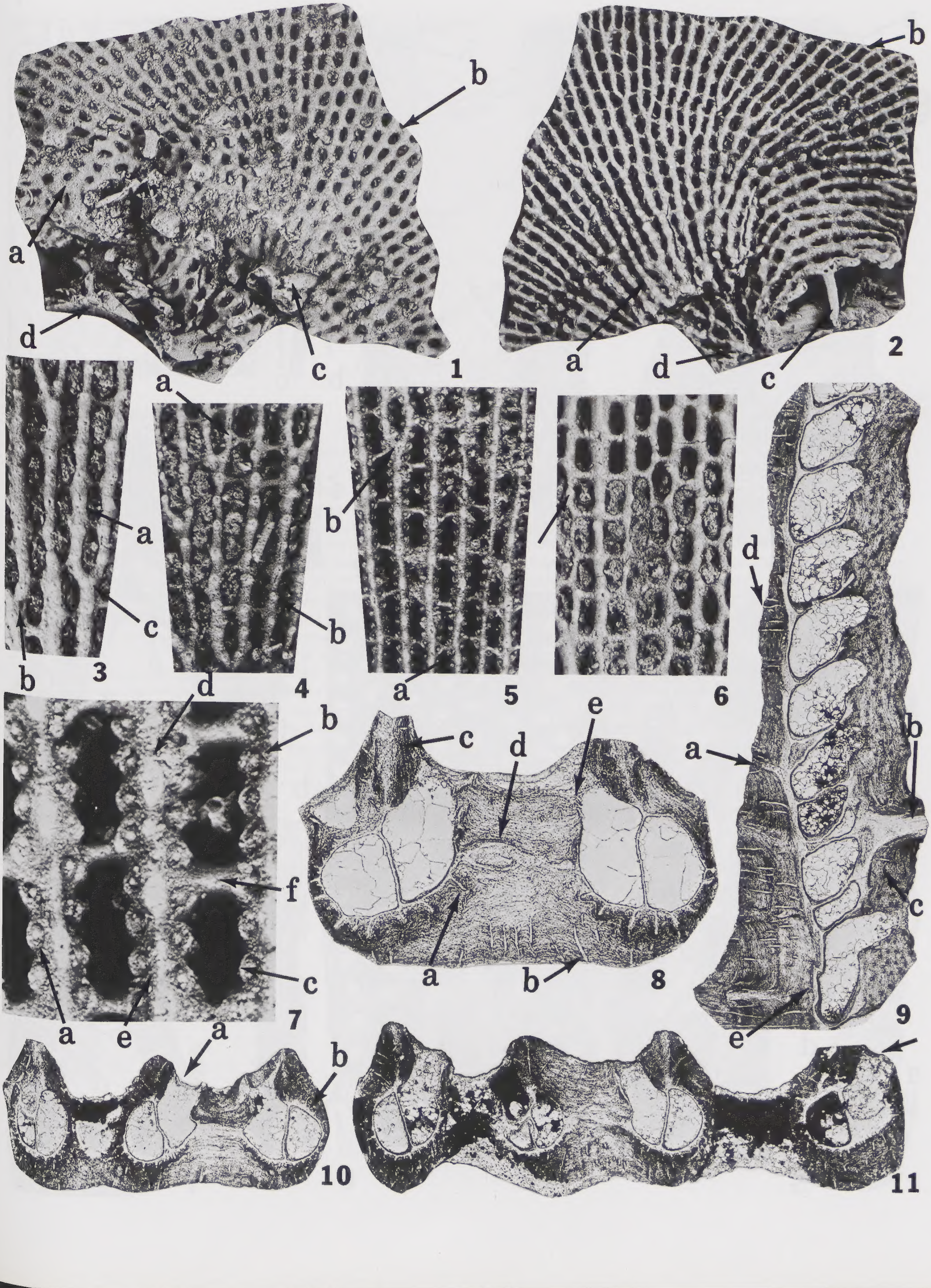

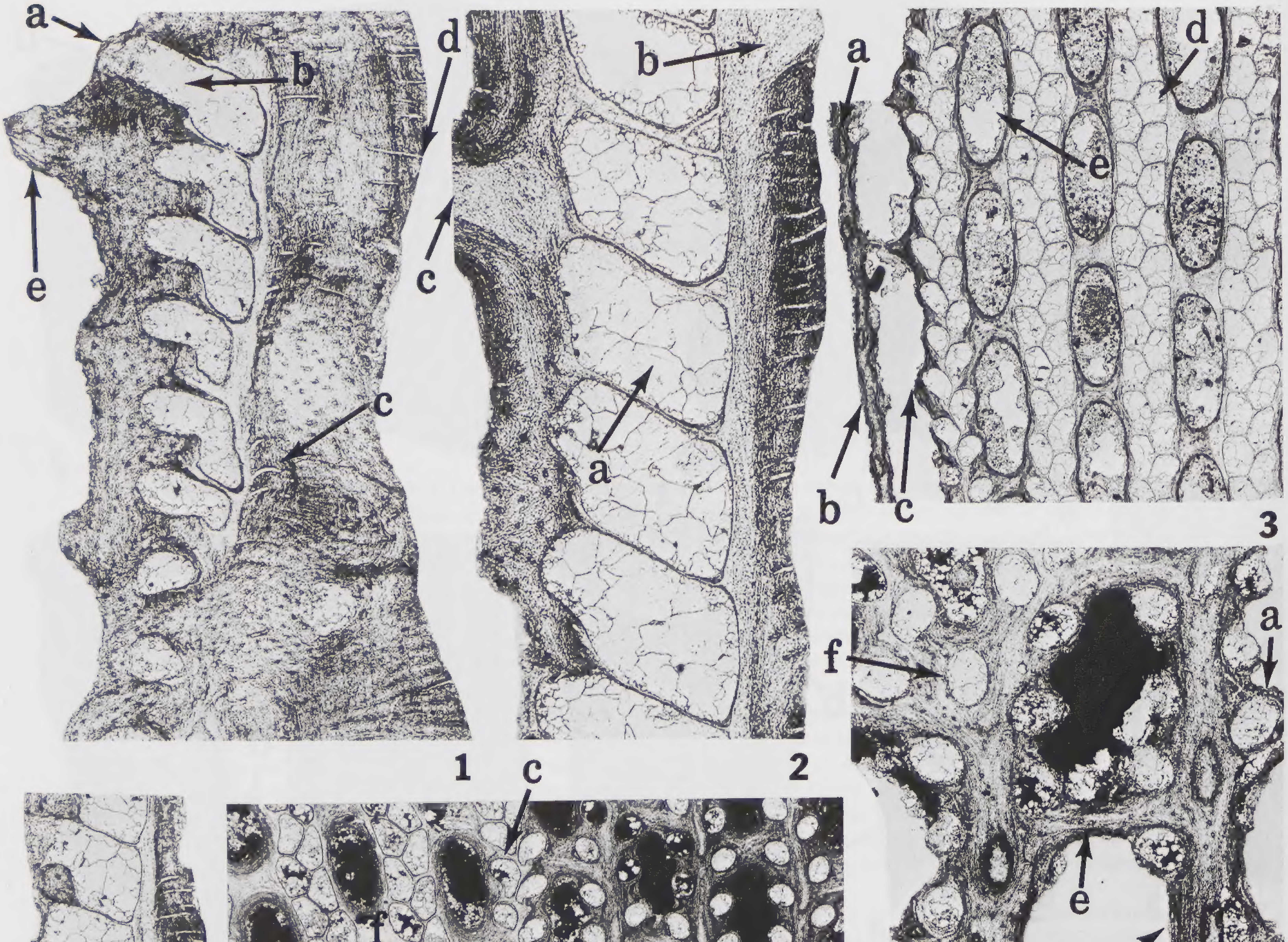
1
2
3
4
5
6
7

EXPLANATION OF PLATE 30

Figure Page

1–7. ***Cubifenestella rudis*** (Ulrich, 1890) 90

1, 4, 6. Figured specimen, UI X-6752. 1. TA4, shallow to mid longitudinal section, obverse to left, showing centrally thickened terminal diaphragm (arrow **a**) capping autozooecial chamber with extremely long vestibule (arrow **b**) developed due to thickened lamellar skeletal layer, microstylets (arrow **c**) continuous with granular skeleton extending to reverse exterior surface (arrow **d**) and obverse node (arrow **e**), ×40; 4. TA12, very shallow tangential section showing typical features including peristome surrounding aperture (arrow **a**), thick keel (arrow **b**), slightly stellate node (arrow **c**), obverse stylet (arrow **d**), and similar stylets across dissepiment (arrow **e**), and site of branch bifurcation (arrow **f**), ×40; 6. TA97, shallow to deep tangential section. Note nearly complete plugging of fenestrule by lamellar skeleton near reverse surface (arrow **a**), pronounced inflection of aperture into fenestrule on obverse surface (arrow **b**), shallow tangential chamber outline (arrow **c**) and typical aperture outline (arrow **d**), continuity of granular skeleton across dissepiment (arrow **e**) and mid tangential view at site of branch bifurcation (arrow **f**), ×20.

2, 3, 5, 7. Figured specimen, UI X-6900. 2. EF9, mid to deep longitudinal section, obverse to left, showing typical chamber outline in deep section (arrow **a**) and granular skeleton continuous with reverse macrostylets (arrow **b**) and obverse nodes (arrow **c**), ×70; 3. EF96, very shallow to mid tangential section. Observe nodes (arrow **a**) positioned atop well-developed keel (arrow **b**), autozooecial chamber outline in shallow (arrow **c**) and mid (arrow **d**) tangential view, and lack of aperture extension into fenestrule opening in mid tangential view (arrow **e**), ×20; 5. EF14, very shallow to mid longitudinal section, obverse to left. Note slight extension of aperture onto lateral edge of dissepiment (arrow **a**) and into fenestrule opening (arrow **b**), typical chamber outline in mid longitudinal view (arrow **c**), and granular skeleton continuous across dissepiment (arrow **d**), ×40; 7. EF96, deep tangential section showing autozooecial chamber outline near reverse-wall budding-site (arrow **a**), longitudinal striae (arrow **b**) from which develop microstylets (arrow **c**), and macrostylets typically associated with sites of branch–dissepiment junction (arrow **d**), ×40.

EXPLANATION OF PLATE 31

Figure | Page
1–12. ***Cubifenestella usitata,*** new species 92

1, 3, 6–8, 10–12. Paratype, UI X-6708. Large, well-preserved moderately ontogenetically thickened zoarial fragment. 1. Obverse exterior surface illustrating typical mesh symmetry, ×8; 3. Reverse exterior surface showing variation in fenestrule size and shape in this species (arrows **a** and **b**), longitudinal striae atop which rows of microstylets develop (arrow **c**), and site of branch bifurcation (arrow **d**), ×8; 6. FL36, transverse section of branch illustrating typical chamber and branch profile in cross-sectional view, ×70; 7. FL36, deep to mid longitudinal section, obverse to left, showing continuity of granular skeleton around autozooecial chambers (arrow **a**) and with reverse microstylets (arrow **b**), typical chamber outline in deep longitudinal view (arrow **c**), and adaxial apertural stylets (arrow **d**), ×70; 8. FL34, deep to mid longitudinal section, obverse to left, showing obverse nodal development (arrow **a**), obverse stylets (arrow **b**) and typical chamber outline in mid longitudinal view (arrow **c**), ×70; 10. FL36, transverse section illustrating longitudinal striae (arrow **a**) and microstylets (arrow **b**) continuous with inner granular skeleton, and terminal diaphragm over aperture (arrow **c**) exhibiting typical attitudinal relationship of aperture to plane of obverse surface, ×70; 11. FL34, transverse section showing typical branch outline with well-developed node (arrow) in continuity with interior granular skeleton, ×70; 12. FL34, shallow longitudinal section, obverse to left, showing typical chamber outline in shallow view (arrow **a**) and obverse stylet (arrow **b**), ×70.

2, 5. Paratype, UI X-6712. High magnification of obverse exterior surface showing apertures (arrow **a**) without terminal diaphragm development, thickened ridge across dissepiment (arrow **b**), aperture positioning at site of branch bifurcation (arrow **c**) and thickened keel (arrow **d**), ×30. 5. Reverse exterior surface with development of reverse zoarial support (arrow), ×8.

4, 9. Holotype, UI X-6709. Large, slightly ontogenetically thickened zoarial fragment. 4. High magnification of obverse exterior surface, illustrating aperture capped by centrally thickened terminal diaphragm (arrow **a**), nodes (arrow **b**), obverse stylets (arrow **c**), keel (arrow **d**), and site of branch bifurcation (arrow **e**), ×20; 9. FL46, shallow to mid longitudinal section, obverse to left, illustrating centrally thickened terminal diaphragm (arrow **a**) and apertural stylet (arrow **b**) continuous with interior granular skeleton, ×70.

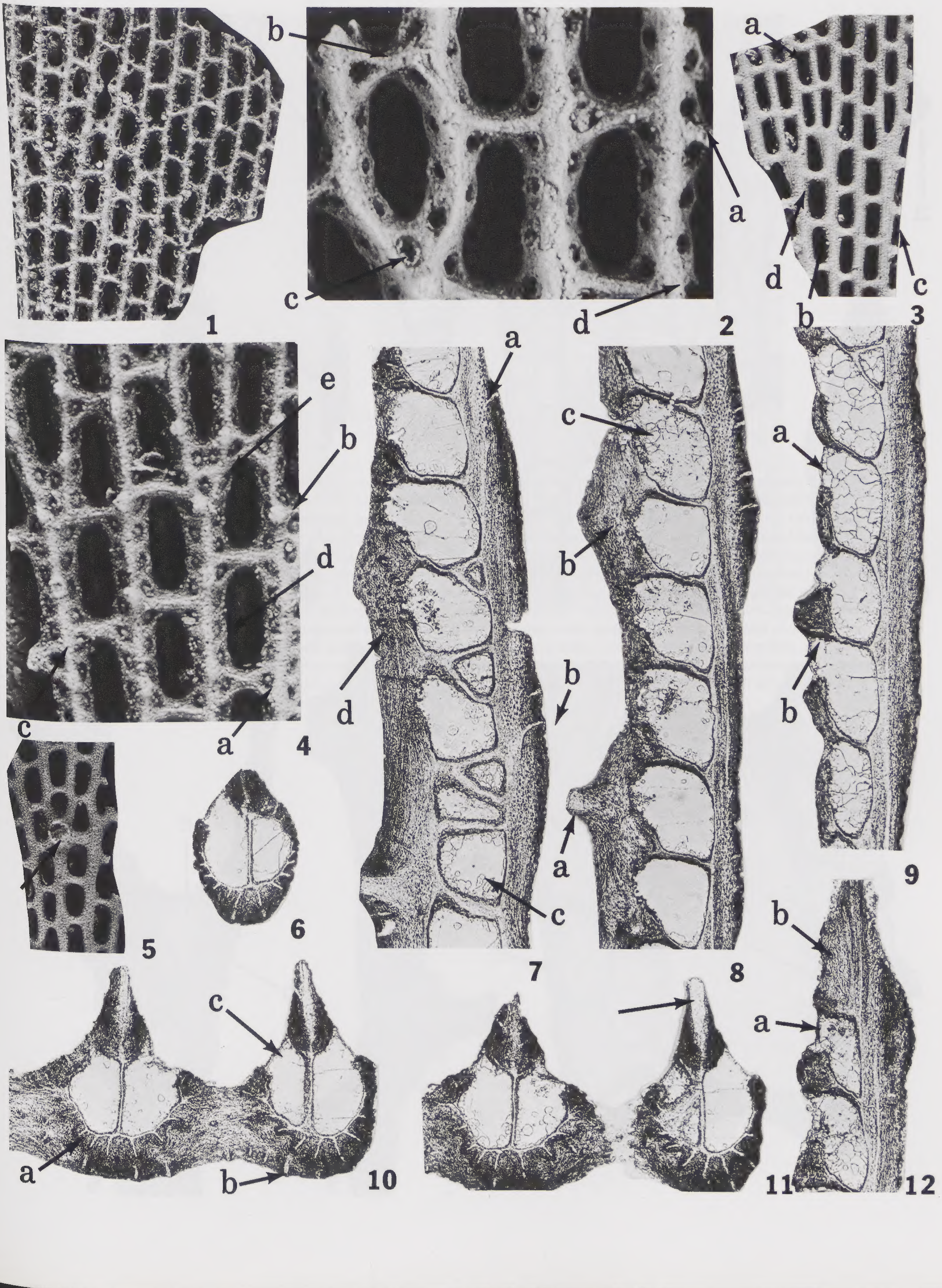
1
b
c
a
d
2
a
d
b
c
3
e
b
d
c
a
4
5
6
a
d
b
c
7
c
b
a
8
a
b
9
b
a
12
c
a
b
10
11

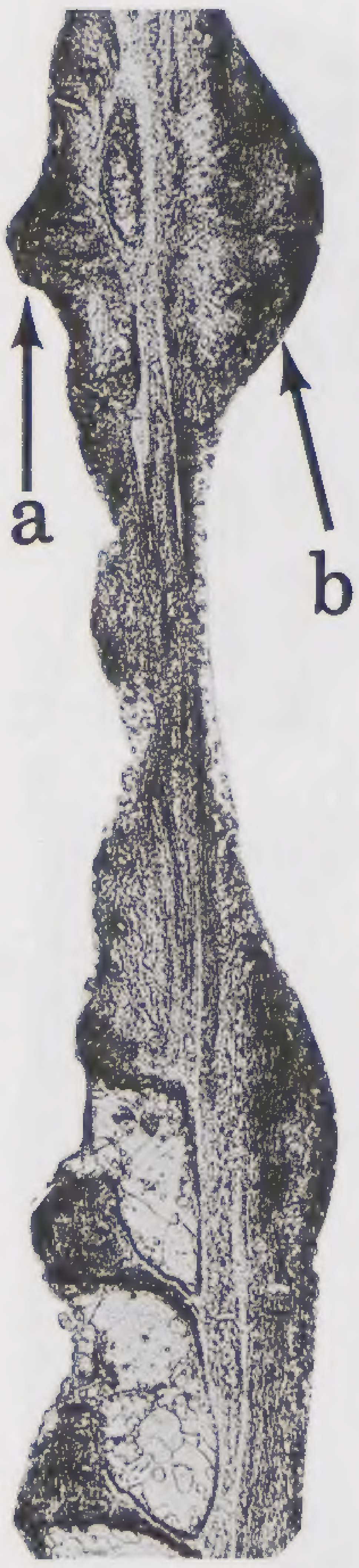

1

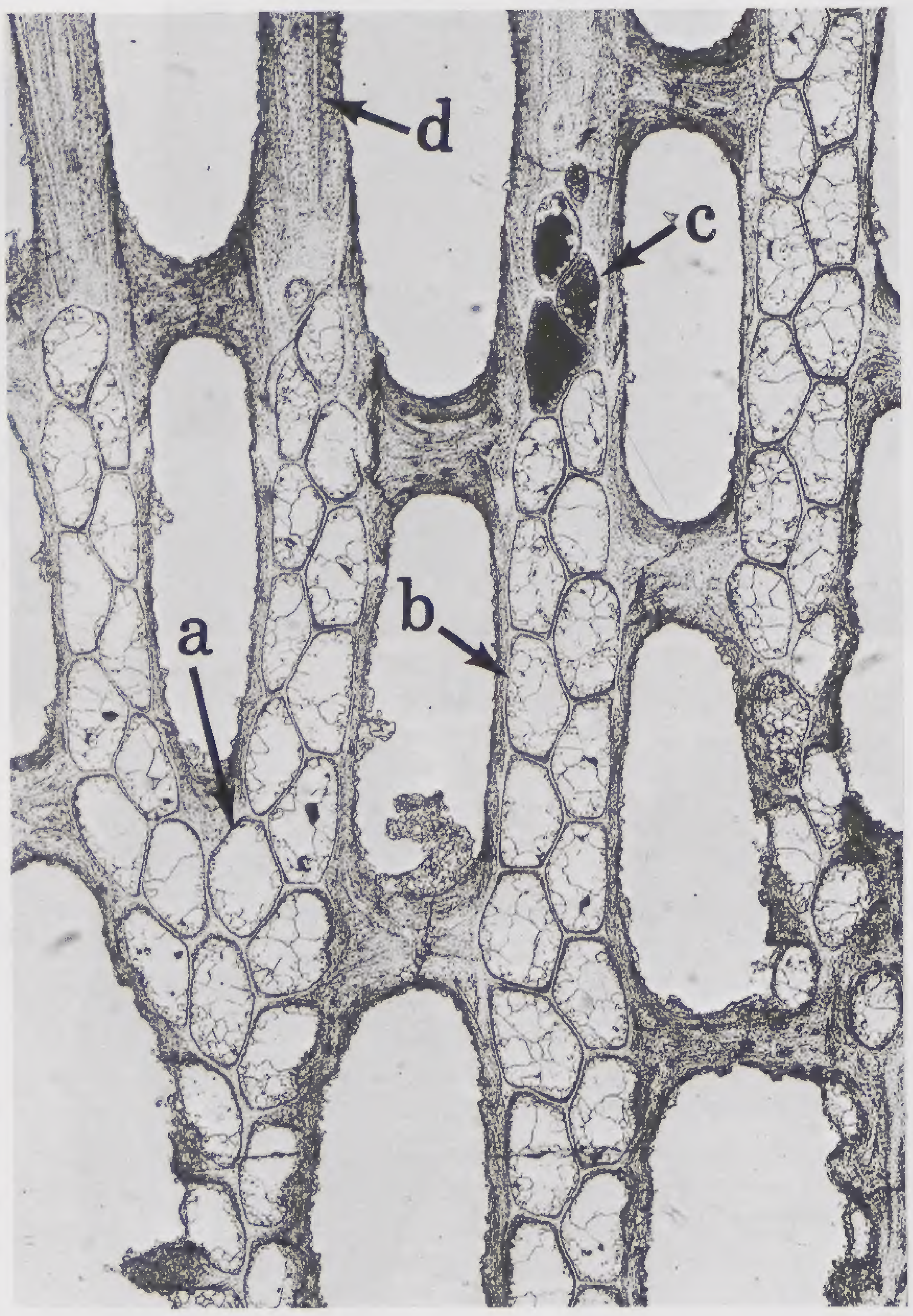

2

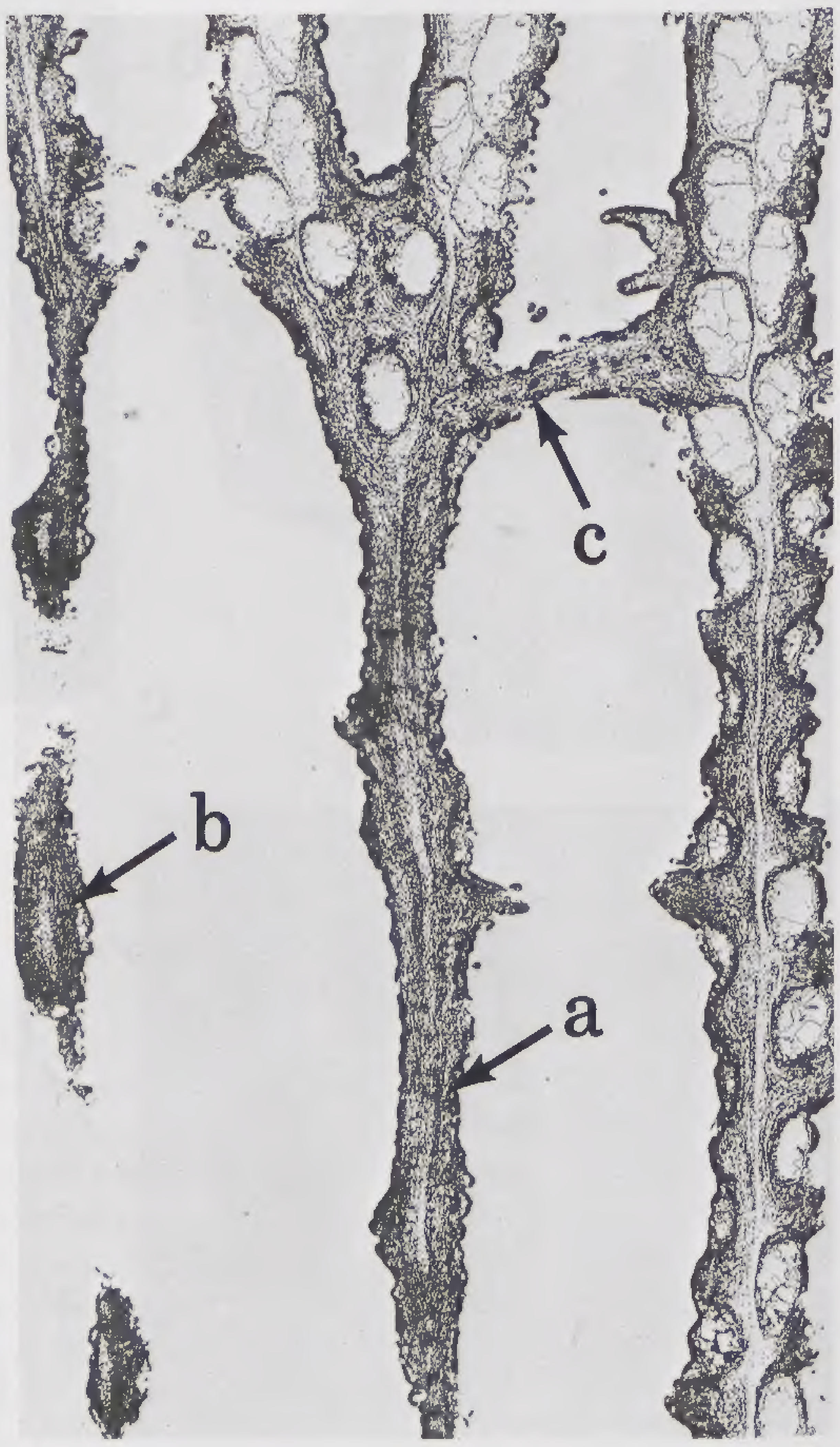

3

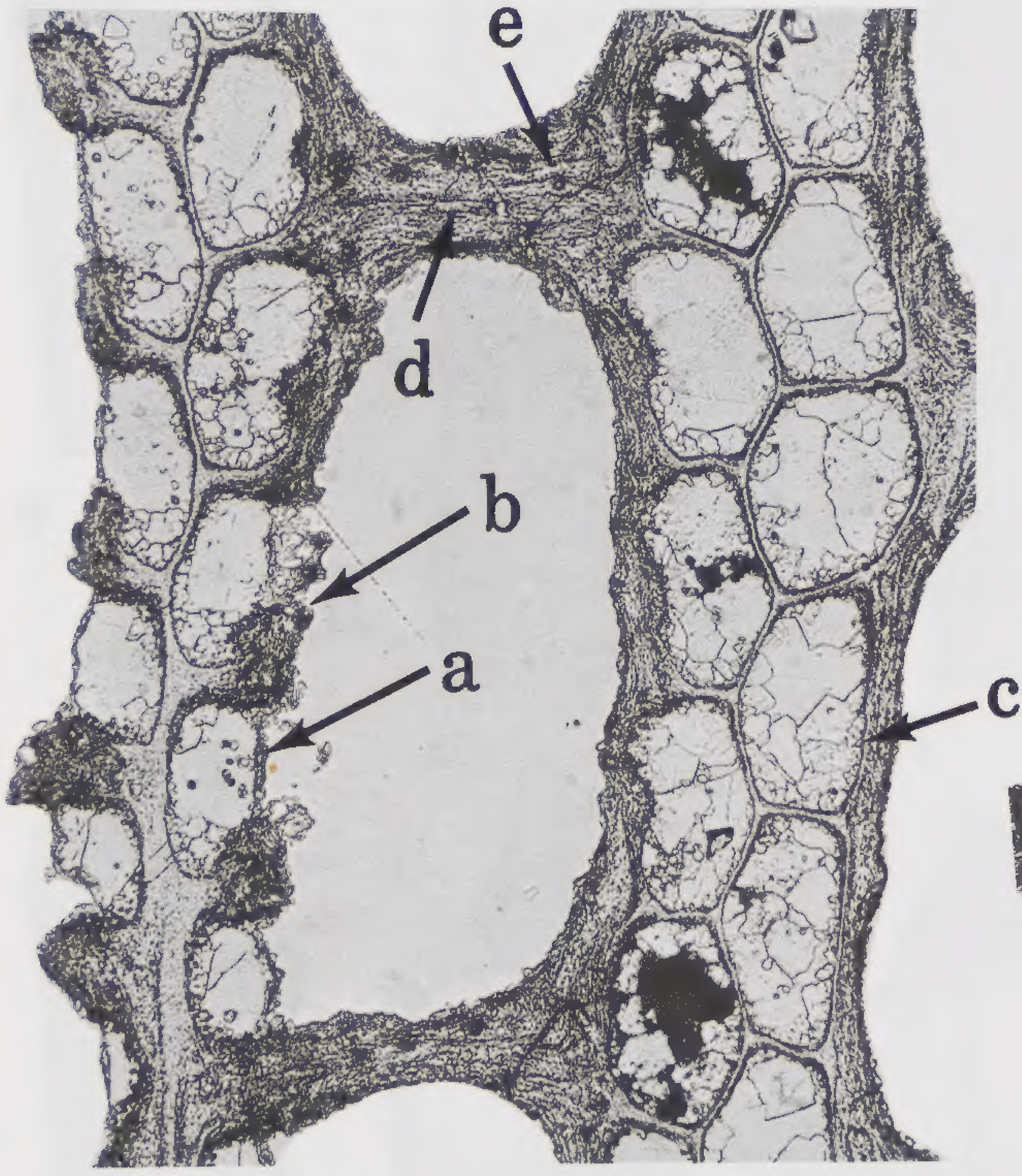

4

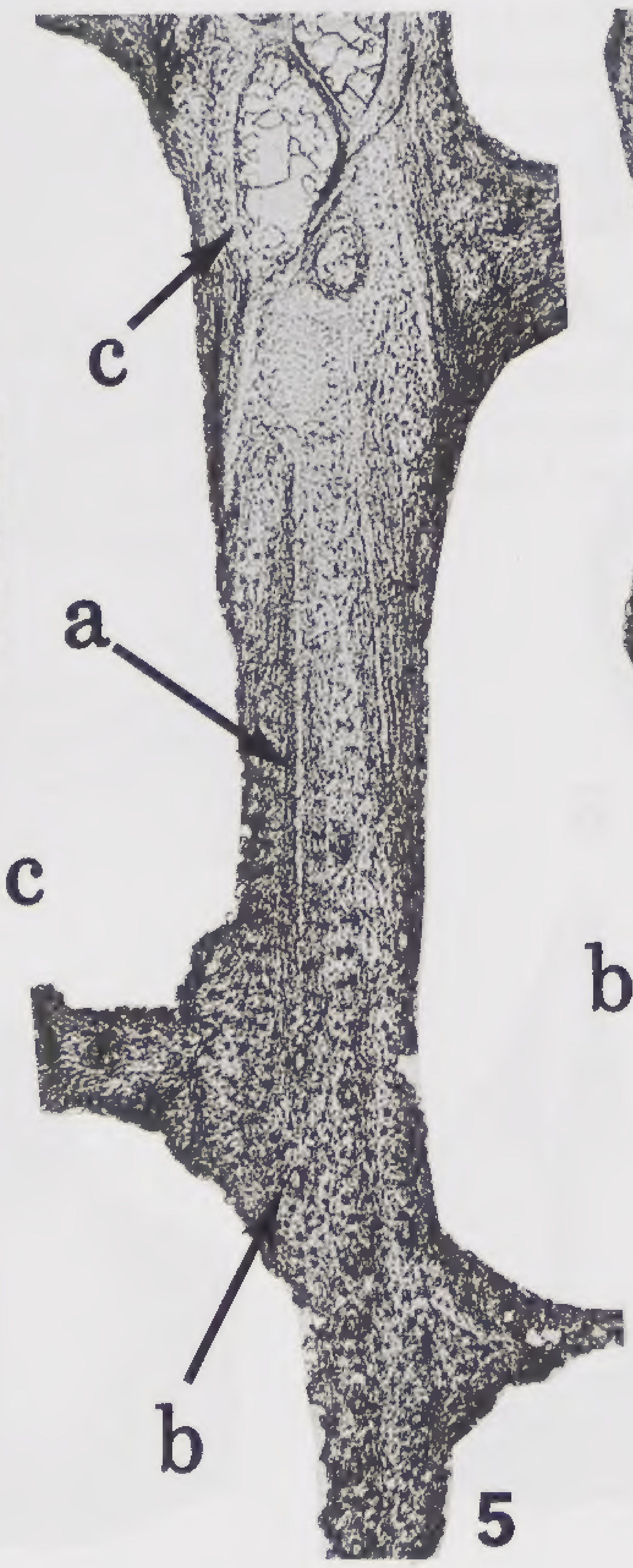

5

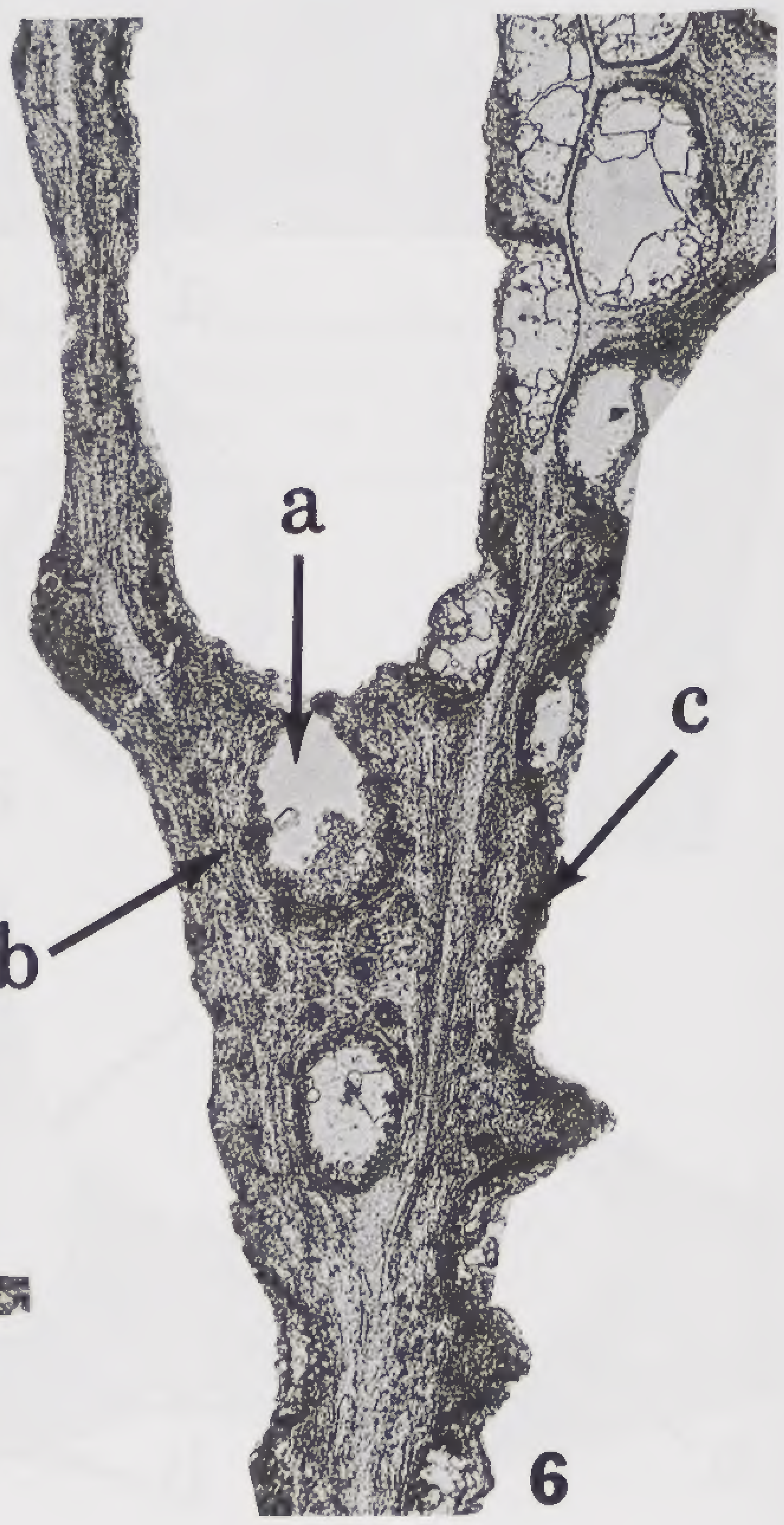

6

EXPLANATION OF PLATE 32

Figure Page

1–6. ***Cubifenestella usitata,*** new species 92

1. Paratype, UI X-6708. FL34, very shallow to shallow longitudinal section, obverse to left, illustrating transverse view of dissepiment with ridge developed on obverse surface (arrow **a**) and thickened lamellar skeleton on reverse (arrow **b**), ×70.

2–6. Holotype, UI X-6709. 2. FL48, shallow to deep tangential section. Observe variable chamber outline in mid tangential view at site of branch bifurcation (arrow **a**) when compared to typical chamber outline in mid tangential view along branch (arrow **b**), chamber outline near reverse-wall budding-site (arrow **c**) and longitudinal striae along reverse wall (arrow **d**), ×40; 3. FL47, very shallow to mid tangential section illustrating well-developed keel (arrow **a**), nodes developed atop keel (arrow **b**), and recessed dissepiment relative to plane of obverse surface (arrow **c**), ×40; 4. FL48, mid to shallow tangential section showing terminal diaphragm (arrow **a**) across aperture of chamber exhibiting typical view in shallow chamber outline, apertural stylets (arrow **b**), chamber outline in mid tangential view (arrow **c**), barlike ridge across dissepiment (arrow **d**), and obverse dissepiment stylets (arrow **e**), ×70; 5. FL48, deep tangential section illustrating longitudinal striae (arrow **a**) from which develop reverse microstylets (arrow **b**). Observe continuity of granular skeleton around autozooecial chamber near reverse-wall budding-site (arrow **c**) and with striae and microstylets, ×70; 6. FL48, shallow tangential section at site of branch bifurcation illustrating typical aperture placement (arrow **a**), apertural stylets (arrow **b**), and obverse stylets (arrow **c**), ×70.

EXPLANATION OF PLATE 33

Figure Page
1–11. ***Cubifenestella globodensata,*** new species 95

1, 3. Paratype, UI X-6710. Zoarial fragment exhibiting pronounced ontogenetic thickening. 1. Obverse exterior surface showing site of branch bifurcation (arrow **a**) and large, closely spaced nodes (arrow **b**) along obverse surface, ×15; 3. Reverse exterior surface illustrating intermediate-size microstylets covering reverse zoarial surface, site of branch bifurcation (arrow **a**) and rows of microstylets across dissepiment surface (arrow **b**), ×30.

2. Paratype, UI X-6711. Obverse exterior surface of zoarial fragment illustrating aperture opening (arrow **a**), slight extension of aperture into fenestrule (arrow **b**), aperture placement at site of branch bifurcation (arrow **c**) and well-developed keel (arrow **d**), ×30.

4, 5, 7, 8. Holotype, UI X-6702. Large, well-preserved moderately ontogenetically thickened zoarial fragment. 4. Reverse exterior surface showing variation in fenestrule size and shape, and site of branch bifurcation (arrow), ×8; 5. Obverse exterior surface. Observe terminal diaphragm capping aperture (arrow **a**), intermediate-size obverse stylets (arrow **b**), barlike expansions across dissepiment surface (arrow **c**), and loss of distinct zoarial features due to surficial covering by lamellar skeleton, ×30; 7. FL27, deep to mid longitudinal section, obverse to left, illustrating continuity of granular skeleton along reverse wall (arrow **a**), around autozooecial chambers, reverse microstylets (arrow **b**), and obverse nodes (arrow **c**). Note typical chamber outline in deep mid longitudinal view (arrow **d**), ×70; 8. FL29, shallow to mid longitudinal section, obverse to left, showing autozooecial chamber outline in shallow (arrow **a**) and longitudinal (arrow **b**) views, ×70.

6. Paratype, UI X-6750. TA65, transverse section of moderately ontogenetically thickened zoarial fragment showing continuity of granular skeleton with longitudinal striae and microstylets (arrow **a**), across dissepiment between branches (arrow **b**) and thickened in the branch axis (arrow **c**), ×70.

9. Paratype, UI X-6826. FD35, transverse section showing typical chamber shape and attitudinal relationship to plane of obverse surface (arrow **a**), obverse stylets (arrow **b**) and chamber plugged by thickened granular skeleton (arrow **c**), ×70.

10–11. Paratype, UI X-6823. 10. FD20, transverse section showing continuity of granular skeleton with keel (arrow) and initial nodal development, ×70; 11. FD21, shallow longitudinal section, obverse to right, illustrating terminal diaphragm development (arrow **a**), apertural stylets (arrow **b**), and chamber outline in very shallow longitudinal view (arrow **c**), ×70.

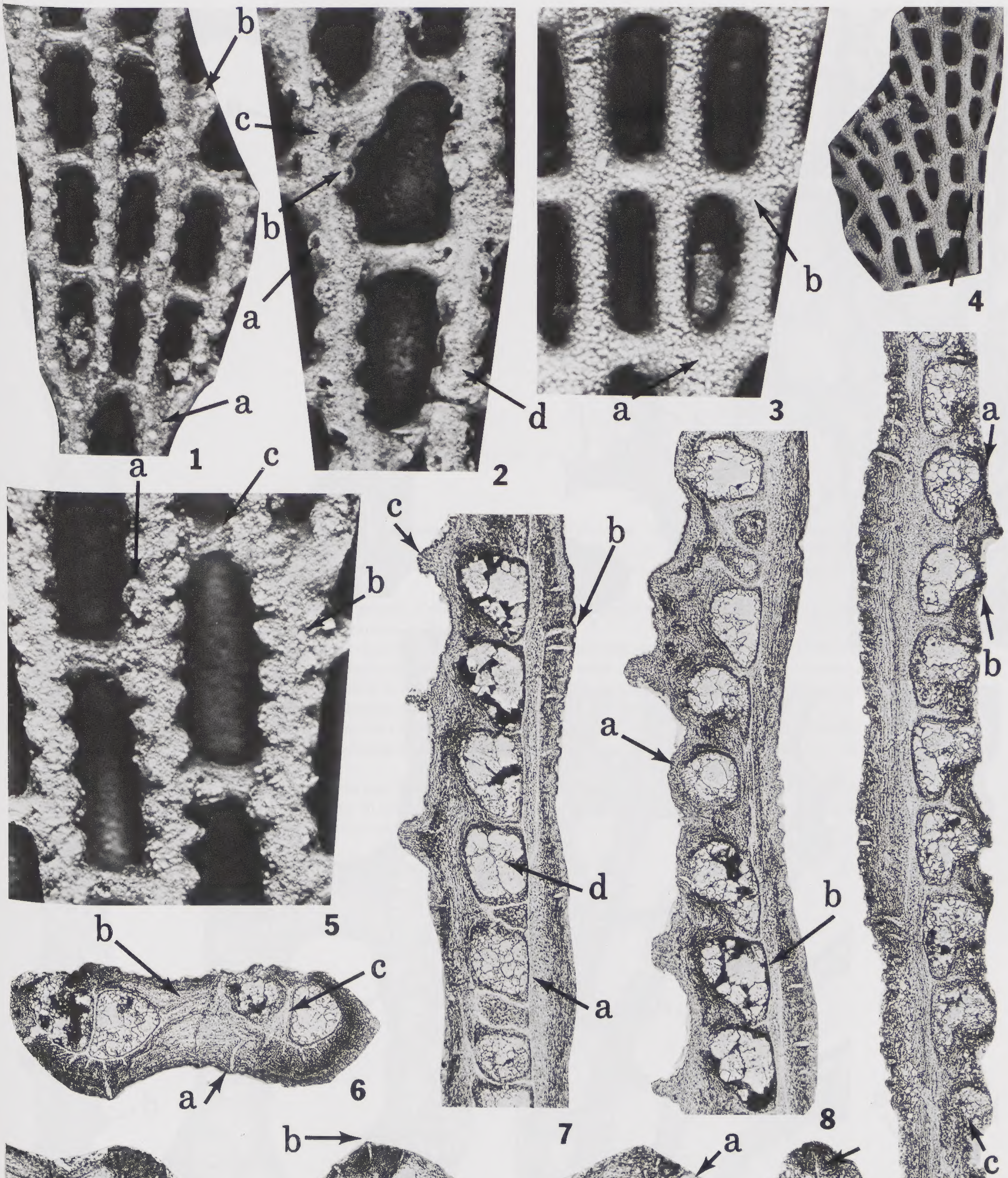
1
2
3
4
5
6
7
8
9
10
11
a
b
c
d

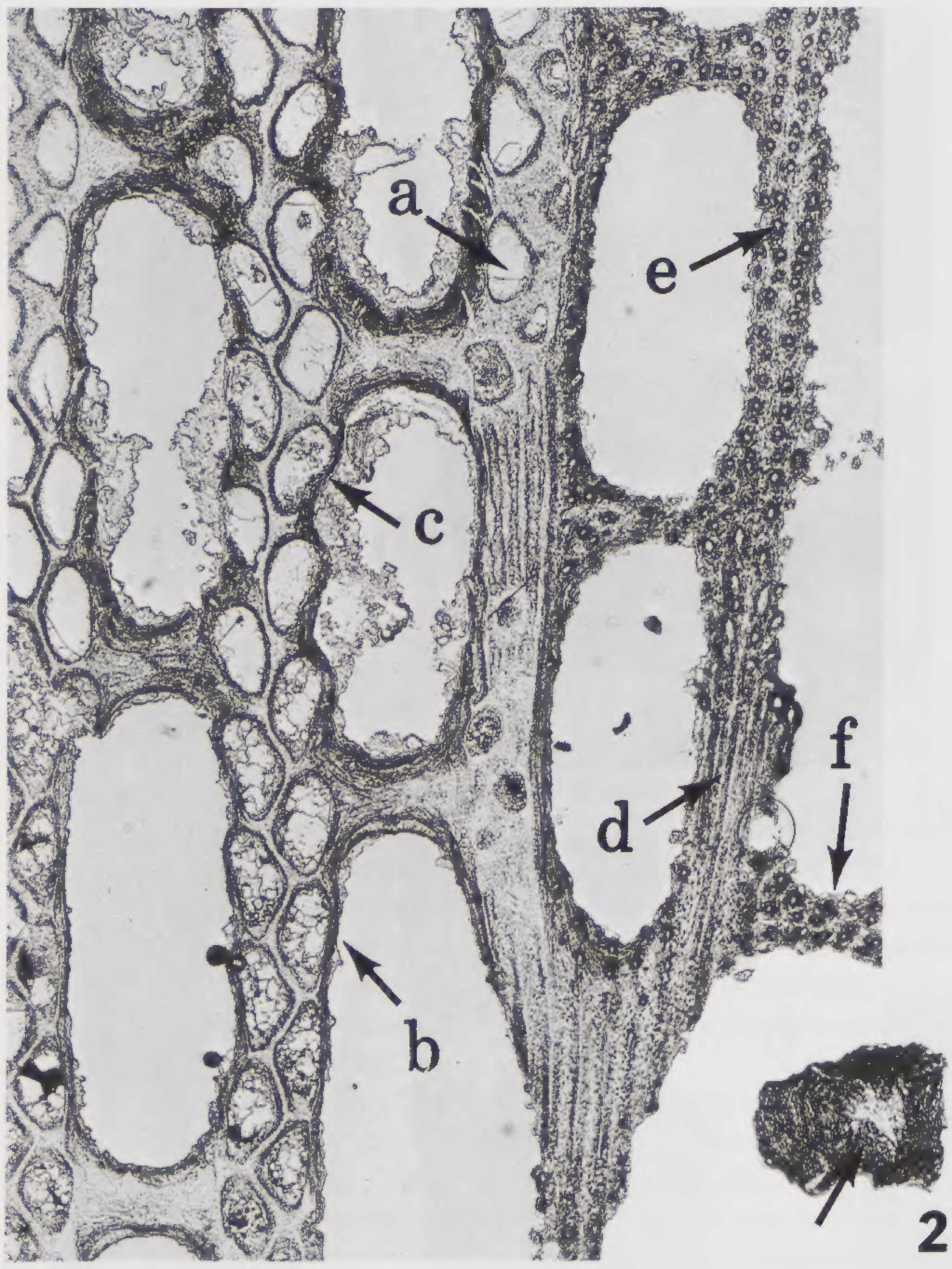

1

2

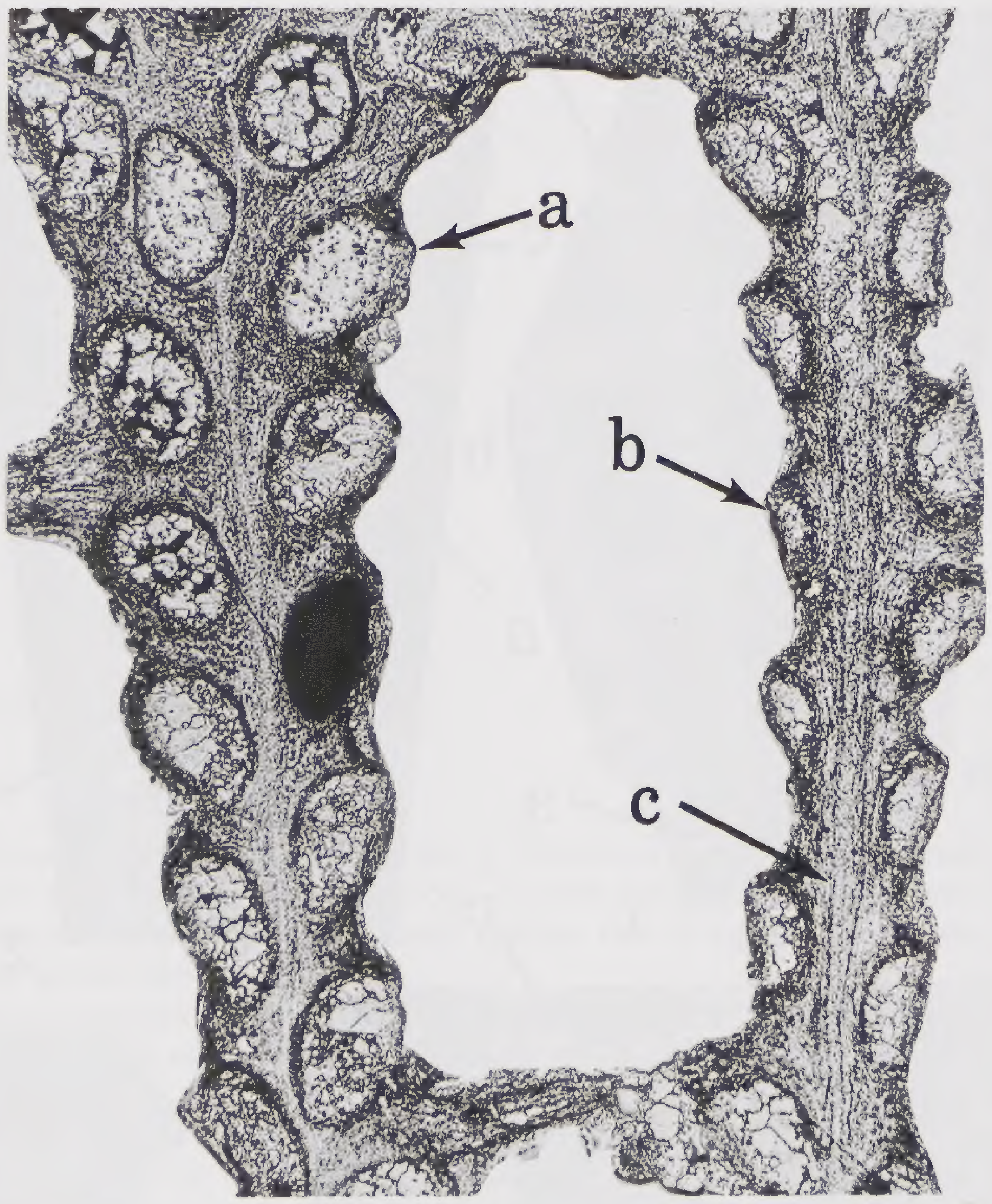

3

4

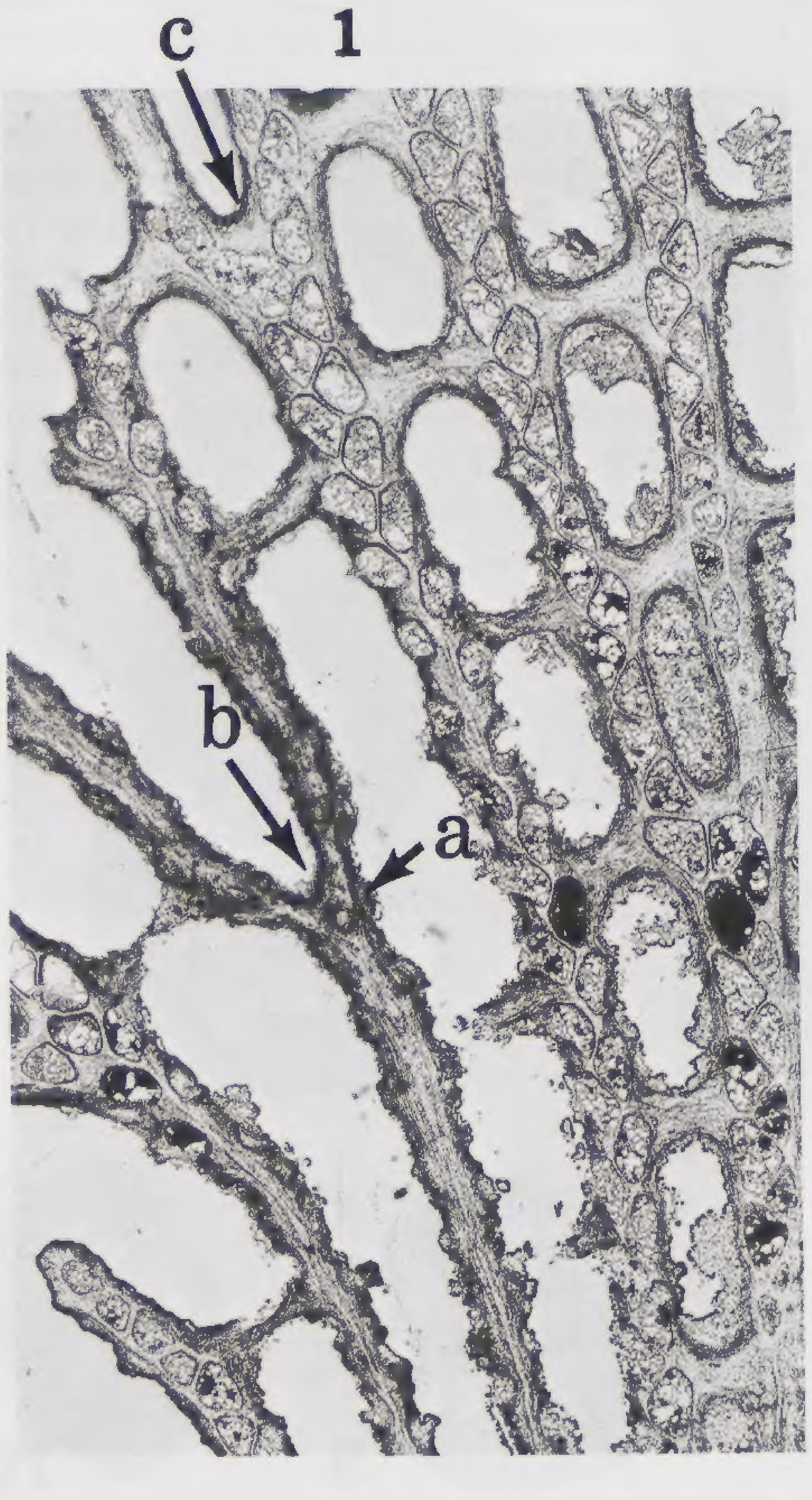

5

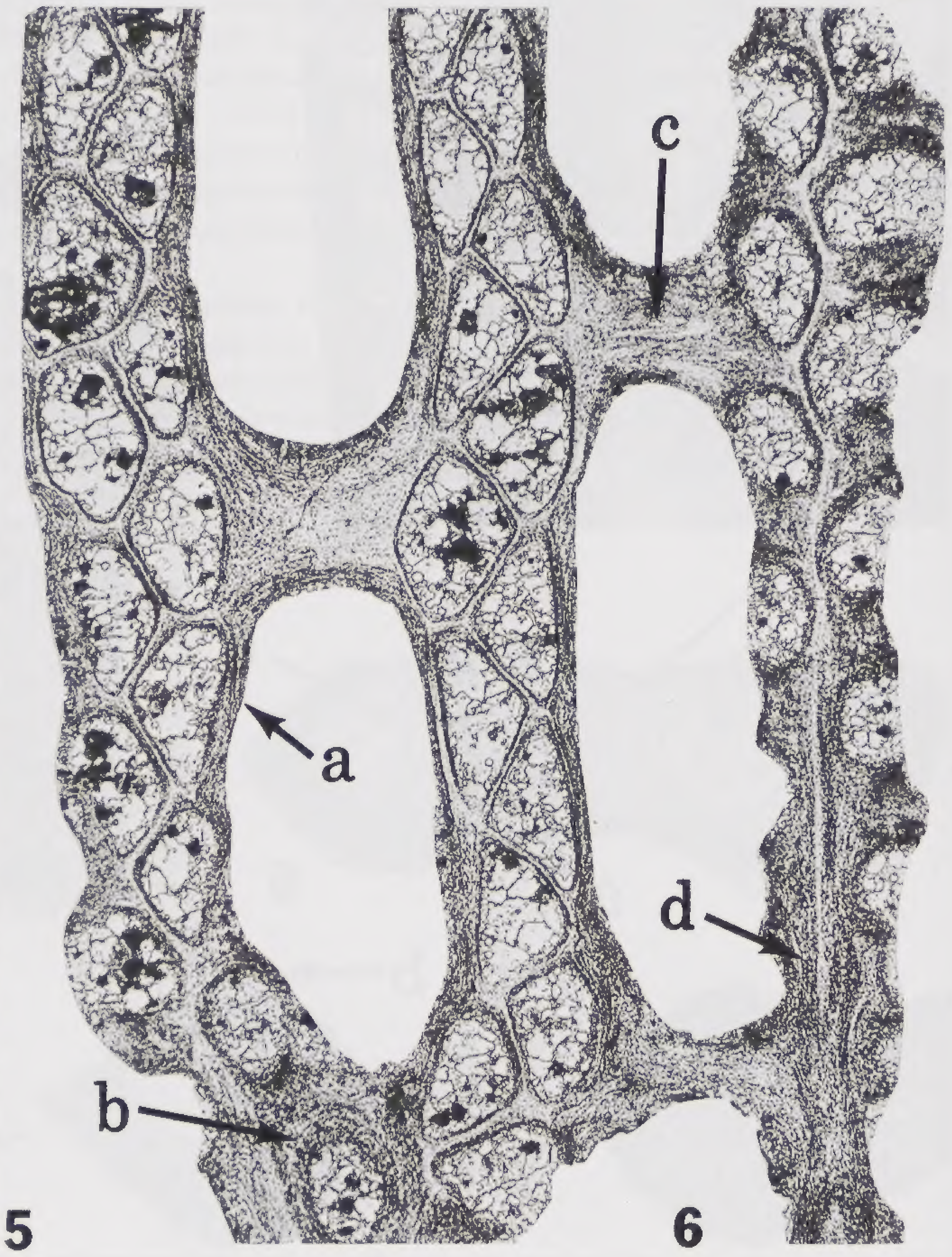

6

EXPLANATION OF PLATE 34

Figure Page

1–6. ***Cubifenestella globodensata,*** new species 95

1. Paratype, UI X-6828. FD38, shallow to deep tangential section of well-preserved zoarial fragment. Note change in chamber outline from deep tangential (arrow **a**) to mid tangential (arrow **b**) and to shallow tangential (arrow **c**) views: also, longitudinal striae (arrow **d**) continuous with inner granular skeletal layer and microstylets developing atop striae along reverse surface (arrow **e**), and dissepiments (arrow **f**), ×40.
2. Paratype, UI X-6713. FL89, transverse section of dissepiment, distal to top and obverse to right, showing continuity of granular skeleton across center of dissepiment (arrow), ×70.

3, 5. Holotype, UI X-6702. FV69. 3. Shallow tangential section showing aperture outline (arrow **a**), apertural stylet developed at abaxial aperture edge (arrow **b**) and granular skeleton along center of branch over which keel (arrow **c**) develops from thickened lamellar skeletal material, ×70; 5. Shallow to deep tangential section illustrating nodes (arrow **a**) developed atop keel, and both shallow (arrow **b**) and mid (arrow **c**) tangential views of sites of branch bifurcation, ×25.

4. Paratype, UI X-6822. FD14, shallow to very shallow longitudinal section, obverse to left, illustrating granular skeleton at edge of branch continuous with that at developing dissepiment edge (arrow **a**) and most adaxial edge of aperture (arrow **b**) extending slightly into fenestrule opening, ×70.

6. Paratype, UI X-6750. TA67, shallow to mid tangential section. Note typical chamber outline in mid tangential view (arrow **a**), apertural stylets around aperture (arrow **b**) which fuse to form the peristome, continuity of granular skeleton across dissepiment (arrow **c**), and obverse node developing atop keel (arrow **d**), ×70.

EXPLANATION OF PLATE 35

Figure — Page

1–12. ***Apertostella foramenmajor,*** new species 99

1, 3, 5–12. Holotype, UI X-6766. Large, well-preserved, moderately ontogenetically thickened zoarial fragment. 1. Reverse exterior surface showing macrostylet development (arrow), fenestrule openings, and site of branch bifurcation, ×8; 3. FG7, transverse section of dissepiment, distal to top and obverse to left, showing continuity of granular skeleton across middle of dissepiment (arrow), ×70; 5. Greatly enlarged obverse exterior surface. Note typical attitudinal relationship of aperture to plane of obverse surface (arrow **a**), peristome surrounding aperture and slight extension of aperture into fenestrule (arrow **b**), keel (arrow **c**), nodes atop keel (arrow **d**), and longitudinal ridges across dissepiment (arrow **e**), ×30; 6. Obverse exterior surface illustrating site of branch bifurcation (arrow) and typical mesh pattern, ×8; 7. FG52, shallow to shallow mid longitudinal section, obverse to left, showing continuity of granular skeletal material around chambers and with peristome at distal end of aperture (arrow), ×70; 8. FG3, transverse section showing continuity of granular skeleton with longitudinal striae (arrow **a**), obverse nodes (arrow **b**), and across dissepiments (arrow **c**). Note moderately thickened lamellar skeleton (arrow **d**) covering reverse surface, ×70; 9. FG52, mid longitudinal section, obverse to left, illustrating typical chamber outline in this view (arrow **a**). Note pronounced increase in chamber depth when compared to shallow longitudinal section, and high reverse-wall budding-angle (arrow **b**), ×70; 10. FG3, deep mid to deep longitudinal section, obverse to left, showing typical chamber outline in deep mid longitudinal view (arrow **a**), terminal diaphragm (arrow **b**), and granular skeletal layer continuous around autozooecial chambers (arrow **c**), and with reverse microstylets (arrow **d**), ×70; 11. FG7, transverse section illustrating typical attitudinal relationship of aperture to plane of obverse surface (arrow **a**) and mid cross-sectional chamber outline (arrow **b**), ×70; 12. FG7, shallow longitudinal section, obverse to left, showing chamber outline in this view (arrow). Note greatly reduced thickness of lamellar skeleton in this zoarium, ×70.

2. Paratype, UI X-6721. Reverse exterior surface of highly ontogenetically thickened zoarial fragment showing increased size of macrostylets (arrow) and reduced fenestrule opening size due to thickening of branches by lamellar skeletal layer, ×8.

4. Paratype, UI X-6770. Reverse exterior surface of zoarial fragment exhibiting slight ontogenetic thickening of lamellar skeleton. Note longitudinal striae (arrow **a**), microstylets (arrow **b**), barlike ridge extending across reverse dissepiment surface (arrow **c**), and site of branch bifurcation (arrow **d**), ×30.

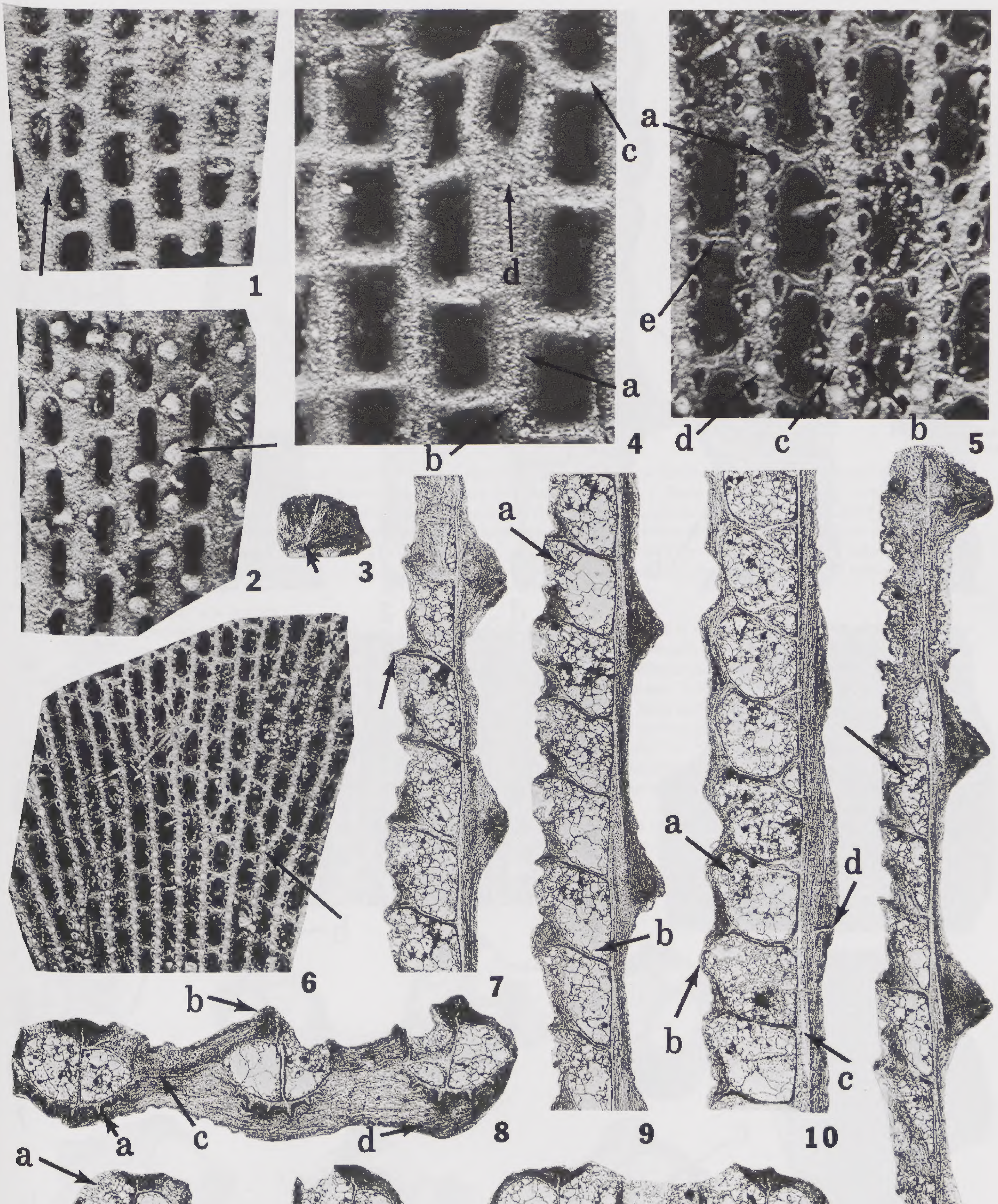
1
2
3
a
c
d
a
b
4
a
e
d
c
b
5
6
7
a
b
9
a
d
b
c
10
b
a
c
d
8
a
b
11
12

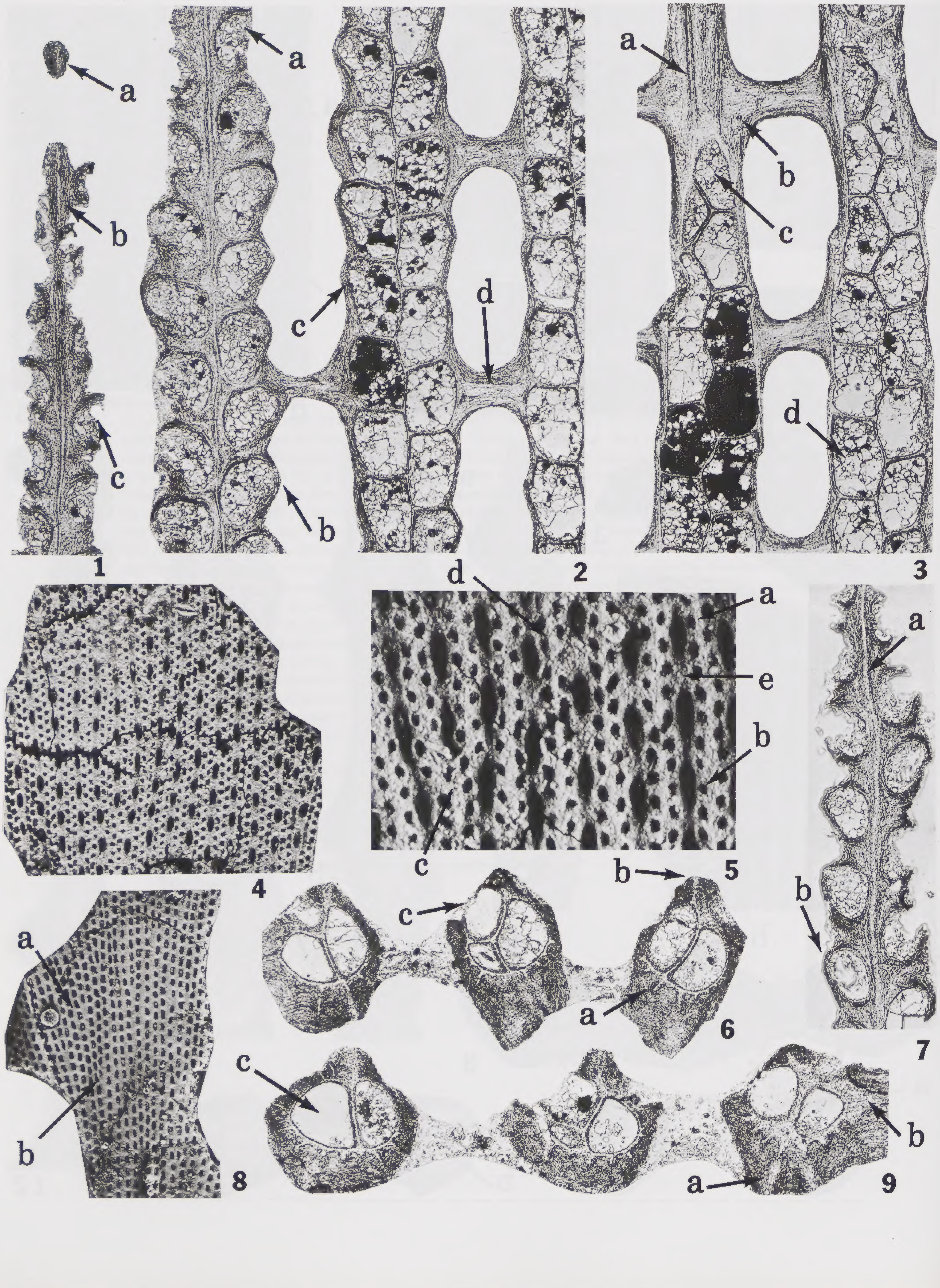
1
2
3
4
5
6
7
8
9

EXPLANATION OF PLATE 36

Figure Page

1–3. ***Apertostella foramenmajor,*** new species 99

Holotype, UI X-6766. FG53. 1. Shallow tangential section showing node (arrow **a**) positioned atop and as projection of keel (arrow **b**). Note attitudinal relationship of aperture (arrow **c**) to plane of obverse surface, ×70; 2. Shallow to mid tangential section illustrating typical mesh symmetry. Observe change in chamber outline from very shallow (arrow **a**), to shallow (arrow **b**) to shallow mid tangential section (arrow **c**), and continuity of granular skeleton across dissepiment (arrow **d**) between branches, ×70; 3. Mid to deep tangential section illustrating longitudinal striae (arrow **a**) extending along reverse chamber wall from which microstylets (arrow **b**) develop, and change in chamber outline from deep tangential (arrow **c**) near reverse-wall budding-site to mid tangential section (arrow **d**), ×70.

4–9. ***Apertostella crassata,*** new species 101

4–6, 8, 9. Holotype, UI X-6737. Large, highly ontogenetically thickened zoarial fragment. 4. Obverse exterior surface showing typical mesh symmetry and sites of branch bifurcation, ×8; 5. Greatly magnified obverse exterior surface illustrating keel (arrow **a**), aperture opening (arrow **b**) and its attitudinal relationship to plane of obverse surface, site of branch bifurcation (arrow **c**), nodes (arrow **d**), and recessed dissepiment (arrow **e**) connecting branches, ×20; 6. FR7, transverse section Observe continuity of granular skeleton with reverse longitudinal striae (arrow **a**), keels and nodes (arrow **b**), and aperture opening (arrow **c**) illustrating typical attitudinal relationship of aperture to plane of obverse surface, ×70; 8. Reverse exterior surface illustrating fenestrule shape (arrow **a**) and site of branch bifurcation (arrow **b**). Note change in fenestrule outline from obverse (ovate) to reverse (elliptical) zoarial surfaces, ×4; 9. FR7, transverse section showing continuity of granular skeleton with reverse microstylets (arrow **a**) and across dissepiment (arrow **b**). Note typical chamber outline in cross-sectional view (arrow **c**), ×70.

7. Paratype, UI X-6740. FR37, shallow tangential section illustrating keel (arrow **a**) and complete peristome (arrow **b**) surrounding aperture, also shown is typical aperture outline in this view, ×70.

EXPLANATION OF PLATE 37

Figure Page

1–9. ***Apertostella crassata,*** new species 101

1, 8, 9. Holotype, UI X-6737. 1. FR5, shallow longitudinal section, obverse to right, abaxial edge of aperture (arrow **a**), and granular skeletal layer continuous across dissepiment (arrow **b**), ×70; 8. FR11, mid tangential section illustrating continuity of granular skeleton across dissepiment (arrow), ×70; 9. FR12, deep tangential section. Observe autozooecial chamber outline near reverse-wall budding-site (arrow **a**) and continuity of lamellar skeletal layer with longitudinal striae, along branch (arrow **b**), and across dissepiment (arrow **c**), and microstylets developing as extensions of these striae (arrow **d**), ×70.

2, 3, 5, 6. Paratype, UI X-6738. 2. FR41, mid longitudinal section, obverse to left, illustrating typical chamber outline in this view (arrow **a**) and peristome developed at distal end of aperture (arrow **b**), ×70; 3. FR42, deep to mid longitudinal section, obverse to left, showing continuity of granular skeleton around autozooecial chambers (arrow **a**) and chamber outline in deep longitudinal view (arrow **b**), ×70; 5. FR41, very shallow longitudinal section, obverse to left, showing continuity of granular skeleton across dissepiment and with reverse microstylets (arrow), ×70; 6. FR42, mid longitudinal section, obverse to left, illustrating typical chamber outline in this view (arrow) and high reverse-wall budding-angle, ×70.

4, 7. Paratype, UI X-6740. 4. FR39, shallow to mid shallow tangential section showing recessed dissepiment relative to plane of obverse surface (arrow **a**) and dissepiment continuous between branches in deeper view (arrow **b**), autozooecial chamber outline in mid shallow section (arrow **c**), and peristome surrounding aperture exhibiting slight inflection into fenestrule in shallow section (arrow **d**), ×70; 7. FR37, mid tangential section illustrating typical chamber outline in this view (arrow **a**) and lack of apertural inflection into fenestrule (arrow **b**), ×70.

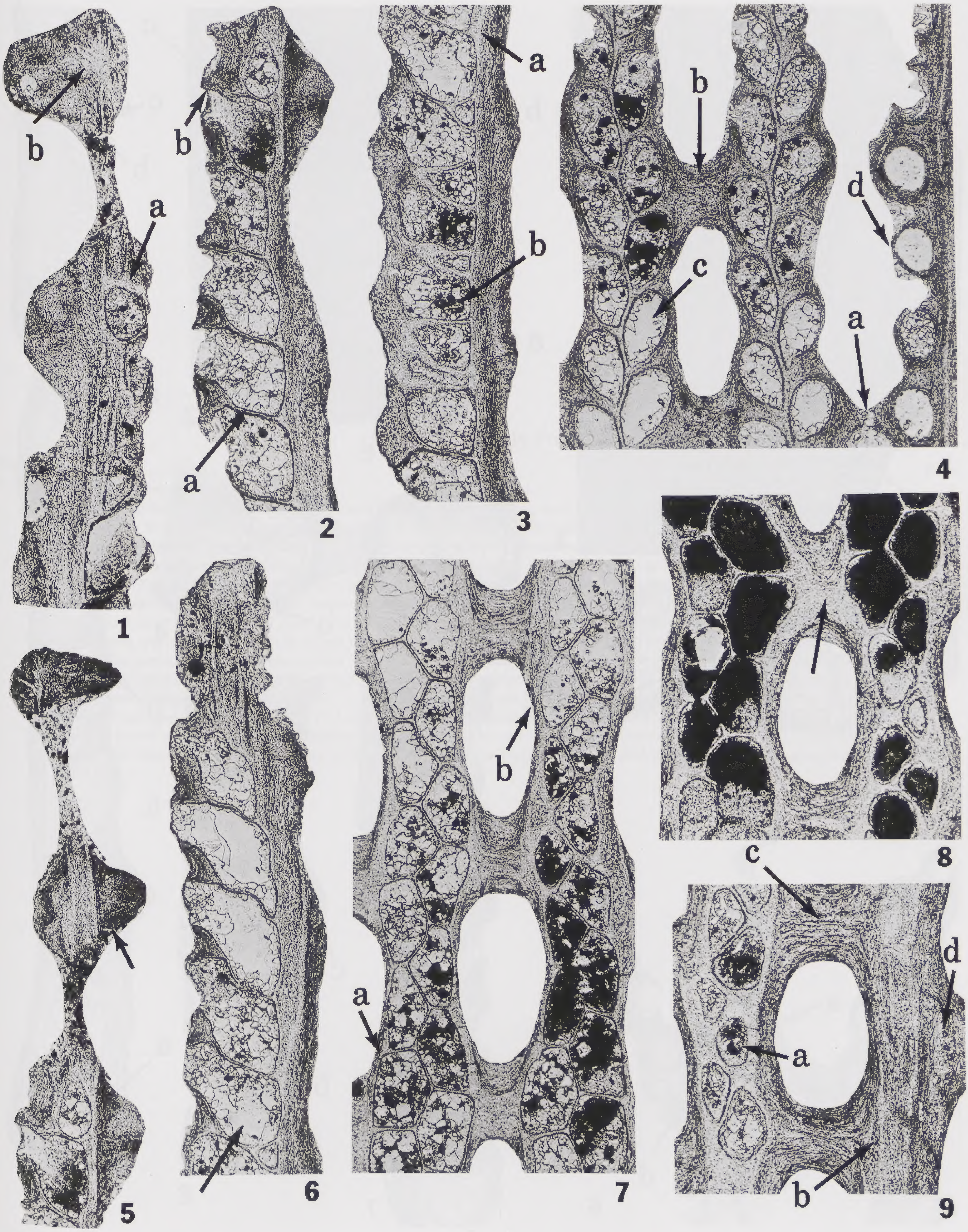
b
a
1
b
a
2
a
b
3
b
c
d
a
4
5
6
b
a
7
8
c
d
a
b
9

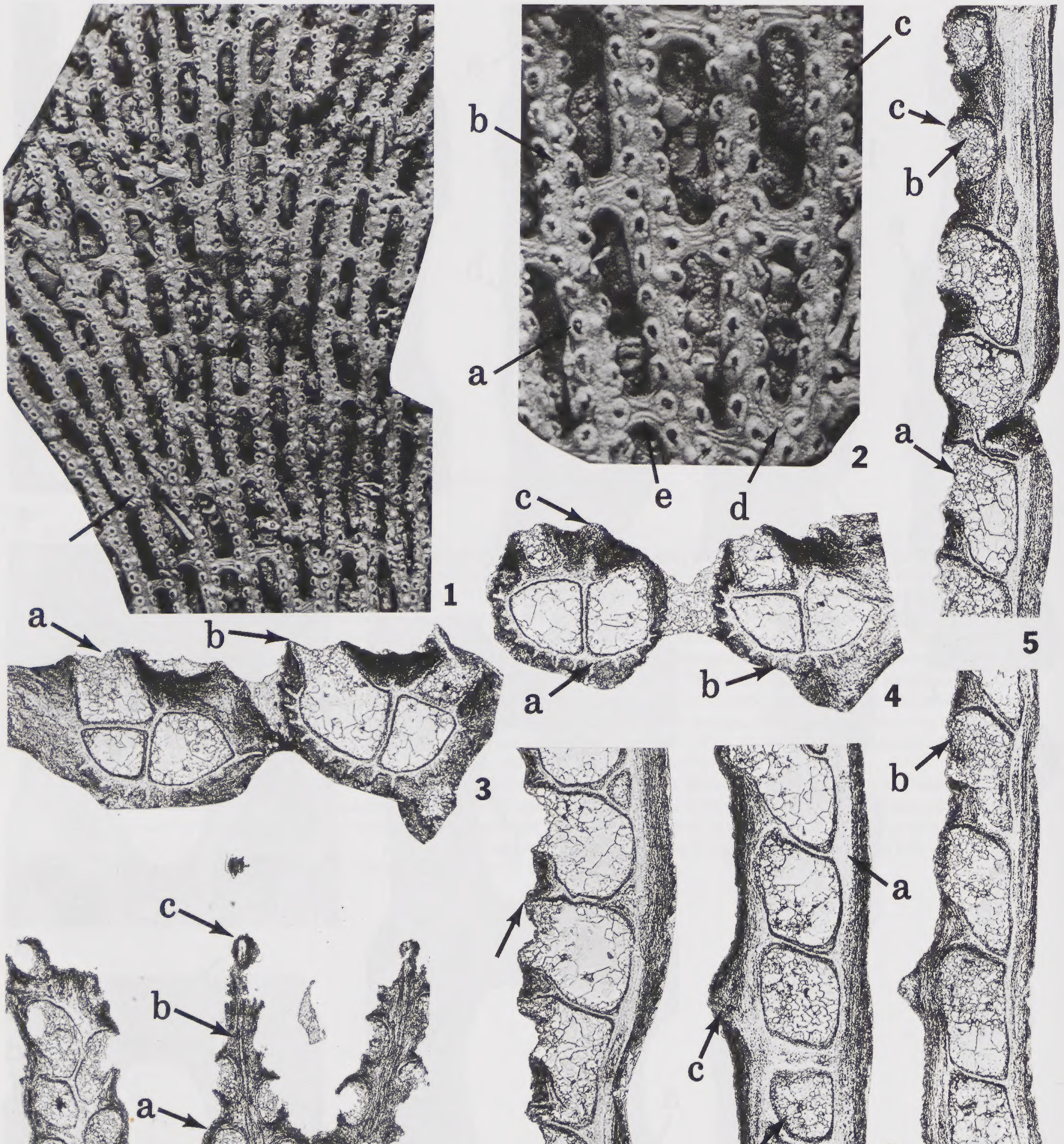
1
b
a
c
e
d
2
c
b
a
5
a
b
c
a
b
4
a
b
3
c
b
a
e
d
6
7
a
c
b
8
b
a
9

EXPLANATION OF PLATE 38

Figure Page

1–9. ***Apertostella venusta*,** new species 104

Holotype, UI X-6875. Large, well-preserved zoarial fragment exhibiting slight ontogenetic thickening. 1. Obverse exterior surface showing typical mesh symmetry and appearance, and sites of branch bifurcation (arrow), ×8; 2. Enlarged obverse exterior surface view showing typical aperture surrounded by peristome (arrow **a**) and attitudinal relationship of aperture to fenestrule opening, keel (arrow **b**) atop which develop nodes (arrow **c**), site of branch bifurcation (arrow **d**), and longitudinal ridges across dissepiment (arrow **e**), ×20; 3. WR22, transverse section showing aperture (arrow **a**) and peristome surrounding aperture (arrow **b**) continuous with inner granular skeletal layer, ×70; 4. WR14, transverse section illustrating continuity of granular skeleton around autozooecial chamber (arrow **a**), with reverse longitudinal striae (arrow **b**) and nodes (arrow **c**), ×70; 5. WR1, mid to shallow longitudinal section, obverse to left, showing typical chamber outline in mid chamber (arrow **a**) and shallow longitudinal view illustrating edge of aperture extending into fenestrule (arrow **b**) and peristome (arrow **c**), ×70; 6. WR20, shallow tangential section showing peristome surrounding aperture (arrow **a**), keel (arrow **b**) with nodes developed atop keel (arrow **c**), site of branch bifurcation (arrow **d**), and continuity of granular skeleton across dissepiment (arrow **e**), ×40; 7. WR5, mid longitudinal section, obverse to left, showing peristome continuous with granular skeletal layer (arrow), ×70; 8. WR15, deep to mid longitudinal section, obverse to left. Observe granular skeletal layer along reverse wall (arrow **a**), surrounding autozooecial chambers (arrow **b**), and obverse node (arrow **c**), ×70; 9. WR15, longitudinal section, obverse to left, showing change in chamber outline from moderately deep (arrow **a**) to mid shallow (arrow **b**) longitudinal view, ×70.

EXPLANATION OF PLATE 39

Figure | Page

1–5. ***Apertostella venusta,*** new species 104
Holotype, UI X-6875. 1. WR20, shallow tangential section showing granular skeletal layer around peristome (arrow **a**) and small obverse stylets (arrow **b**), ×40; 2. WR20, very shallow to deep tangential section. Note typical chamber outline in mid tangential (arrow **a**) and mid shallow (arrow **b**) tangential view, continuity of granular skeleton across dissepiment (arrow **c**) and site of branch bifurcation (arrow **d**), ×40; 3. WR20, deep tangential section illustrating granular skeletal composition of longitudinal striae (arrow), ×40; 4. WR22, shallow to deep tangential section showing slight inflection of aperture into fenestrule (arrow **a**), chamber outline near reverse-wall budding-site (arrow **b**) and reverse microstylets (arrow **c**), ×40; 5. WR22, mid to mid shallow tangential section, illustrating typical chamber outline in mid shallow section (arrow), ×40.

6–12. ***Hemitrypa perstriata*** Ulrich, 1890 108

6, 12. Figured specimen, UI X-6927. HB14. 6. Transverse section illustrating typical chamber profile in cross-section and terminal diaphragm (arrow) capping aperture, ×70; 12. Transverse section illustrating continuity of granular skeletal layer with longitudinal striae (arrow **a**), microstylets (arrow **b**), nodes (arrow **c**), and with peristome surrounding aperture (arrow **d**), ×70.

7–9, 11. Figured specimen, UI X-6848. 7. Obverse exterior surface of zoarial fragment showing typical poorly developed reticulate meshwork (arrow). Note widening of branch proximal and thinning distal to sites of branch bifurcation, ×8; 8. Enlarged obverse exterior surface showing typical aperture outline (arrow **a**) with aperture surrounded by well-developed complete peristome, obverse stylets (arrow **b**), and nodes (arrow **c**) positioned atop keel (arrow **d**), ×25; 9. Enlarged obverse exterior surface illustrating slight to moderate extension of aperture into fenestrule (arrow **a**) and onto dissepiment (arrow **b**). Note longitudinal ridge developed across obverse dissepiment surface (arrow **c**), ×25; 11. Reverse exterior surface showing typical angular appearance of branches and dissepiments. Note variation in fenestrule outline from approximately hexagonal (arrow **a**) to rectangular (arrow **b**), medially thickened ridge across dissepiment surface, and site of branch bifurcation (arrow **c**), ×8.

10. Figured specimen, UI X-6849. HB6, shallow longitudinal section, obverse to right, illustrating continuity of granular skeleton along reverse wall (arrow **a**), reverse microstylets (arrow **b**), and across dissepiment (arrow **c**), ×40.

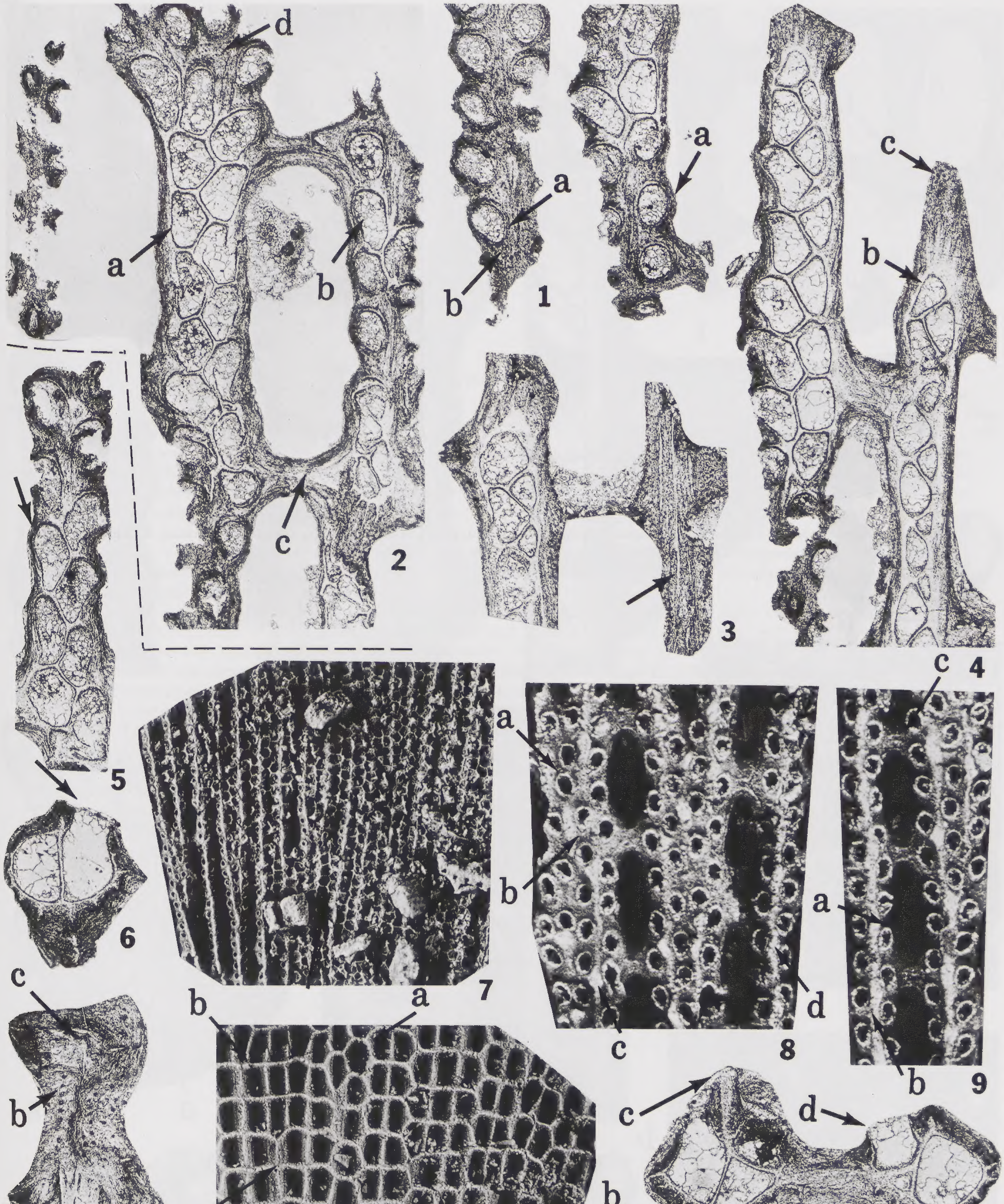
a
b
c
d
1
2
3
4
5
6
7
8
9
10
11
12

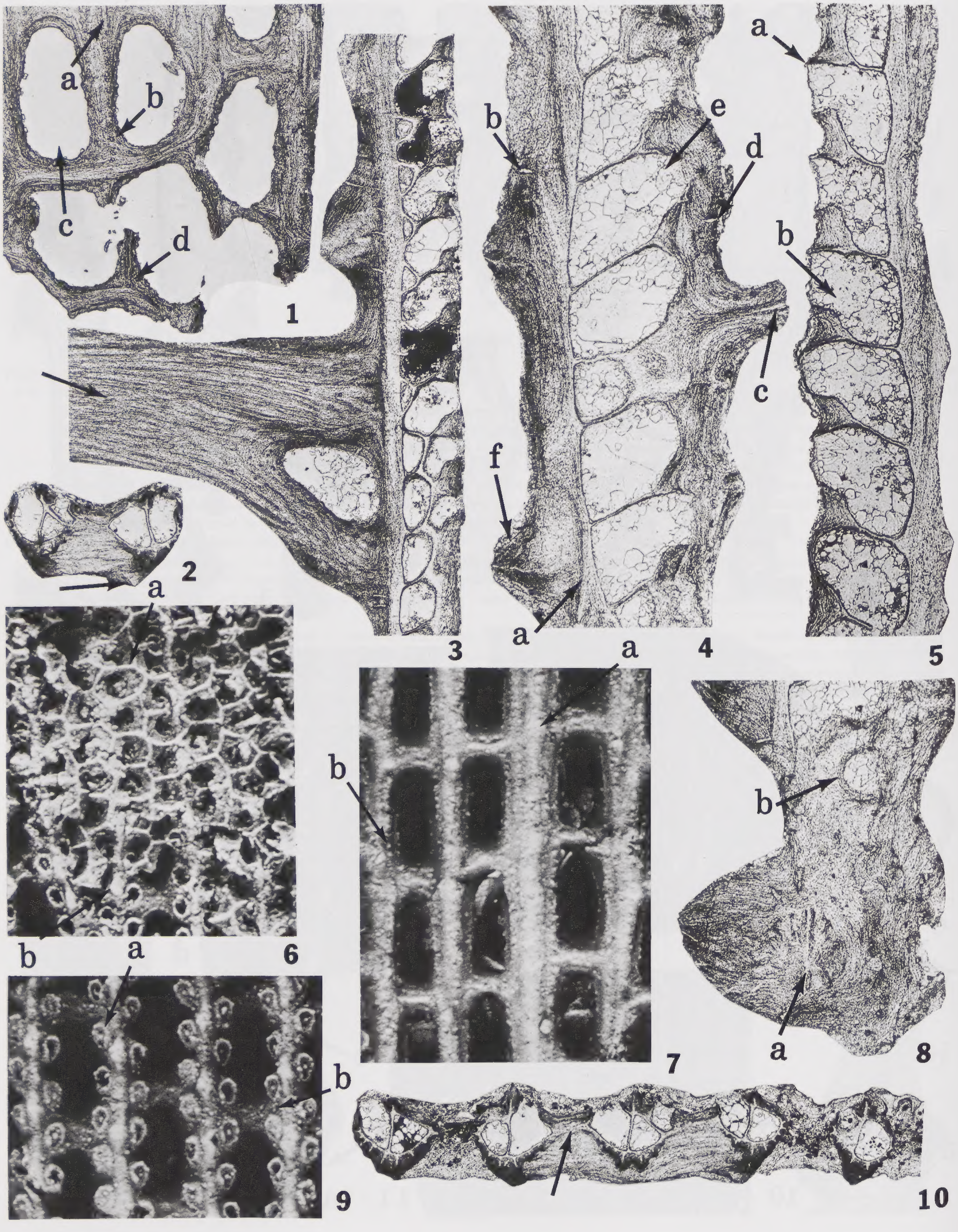
1
a
b
c
d
2
a
3
4
a
b
c
d
e
f
5
a
b
6
a
b
7
a
b
8
a
b
9
a
b
10

EXPLANATION OF PLATE 40

Figure Page

1–10. ***Hemitrypa perstriata*** Ulrich, 1890 108

1. Figured specimen, UI X-6848. HB3, deep tangential section illustrating reverse view of longitudinal striae (arrow **a**), rows of microstylets developed atop these striae (arrow **b**), rounded fenestrule outline in mid deep tangential view (arrow **c**), and much more rhombic fenestrule outline in deep tangential section associated with sharp or angular appearance to reverse branch surface (arrow **d**), ×40.

2, 10. Figured specimen, UI X-6927. HB14. 2. Transverse section showing sharp, angular appearance of reverse branch surface (arrow), ×40; 10. Transverse section showing continuity of granular skeleton between branches (arrow), ×40.

3. Figured specimen, UI X-6925. HB7, slightly tilted mid longitudinal section, obverse to right, illustrating well-developed zoarial support (arrow) extending from reverse zoarial surface, ×40.

4, 6, 8. Figured specimen, UI X-6849. 4. HB6, mid to deep longitudinal section, obverse to right, showing continuous granular skeletal layer (arrow **a**) extending along reverse wall and around autozooecial chambers, with same granular layer also continuous with microstylets (arrow **b**), nodes (arrow **c**), and obverse stylets (arrow **d**); also illustrated is typical chamber outline in mid longitudinal view (arrow **e**) and angular dissepiments (arrow **f**), ×70; 6. Enlarged obverse exterior surface illustrating reticulate meshwork (arrow **a**) developed atop zoarial surface, with meshwork developing from nodes, keel, and dissepiment ridges along obverse surface (arrow **b**) and mesh intersection in middle of branch and middle of fenestrule, ×25; 8. HB6, shallow longitudinal section, obverse to right, showing continuity of granular skeleton across dissepiment (arrow **a**) and apertural extension into fenestrule at branch abaxial edge (arrow **b**), ×70.

5. Figured specimen, UI X-6934. FA76, shallow mid longitudinal section, obverse to left, showing granular skeleton continuous with peristome at obverse edge of aperture (arrow **a**) and typical chamber outline in this view (arrow **b**), ×70.

7, 9. Figured specimen, UI X-6730. 7. Enlarged reverse exterior surface showing longitudinal ridges (arrow **a**) and reverse microstylets (arrow **b**), ×30; 9. Enlarged obverse exterior surface showing typical aperture capped by centrally thickened terminal diaphragm (arrow **a**) and obverse stylets across dissepiment (arrow **b**) and atop branches, ×30.

EXPLANATION OF PLATE 41

Figure Page
1–5. ***Hemitrypa perstriata*** Ulrich, 1890 108

1, 3, 4. Figured specimen, UI X-6849. HB57. 1. Shallow to deep tangential section showing mesh symmetry characteristic of this species. Note longitudinal striae (arrow **a**), typical chamber outline near reverse-wall budding-site (arrow **b**), and irregular outline of fenestrule near obverse surface due to inflection of apertural adaxial edges into opening (arrow **c**) as compared to smooth elliptical fenestrule outline (arrow **d**) in mid tangential section and increasingly ovate (arrow **e**) to angular outline near reverse surface, ×20; 3. Mid to shallow tangential section showing typical chamber outline in mid tangential (arrow **a**) and in shallow tangential (arrow **b**) views, keel (arrow **c**) atop which develop obverse stylets (arrow **d**) and nodes (arrow **e**), and granular skeletal layer extending across dissepiment between branches (arrow **f**), ×40; 4. Shallow to very shallow tangential section. Observe slightly anastomosing or sinuous thickened keel (arrow **a**), near complete closure of fenestrule (arrow **b**) by thickened keel, typical attitudinal relationship of aperture to plane of obverse surface (arrow **c**) and peristome surrounding aperture (arrow **d**), ×40.

2. Figured specimen, UI X-6848. HB10, very shallow to shallow tangential section illustrating elongate node (arrow **a**) developed atop keel from which reticulate meshwork develops (arrow **b**), and intermediate-size obverse stylets (arrow **c**), ×70.

5. Figured specimen, UI X-6924. HB13, shallow to deep tangential section showing site of branch bifurcation (arrow), ×20.

6, 7. ***Hemitrypa hemitrypa*** (Prout, 1859) 111

6. Figured specimen, UI X-6846. HB69, transverse section illustrating typical attitudinal relationship of aperture to plane of obverse surface (arrow **a**), longitudinal striae (arrow **b**) continuous with granular skeleton around autozooecial chambers, and thickened lamellar skeleton on reverse branch surface (arrow **c**), ×70.

7. Figured specimen, UI X-6930. Reverse exterior view of large zoarial fragment showing typically rectangular, variably sized fenestrules (arrows **a** and **b**), ×8.

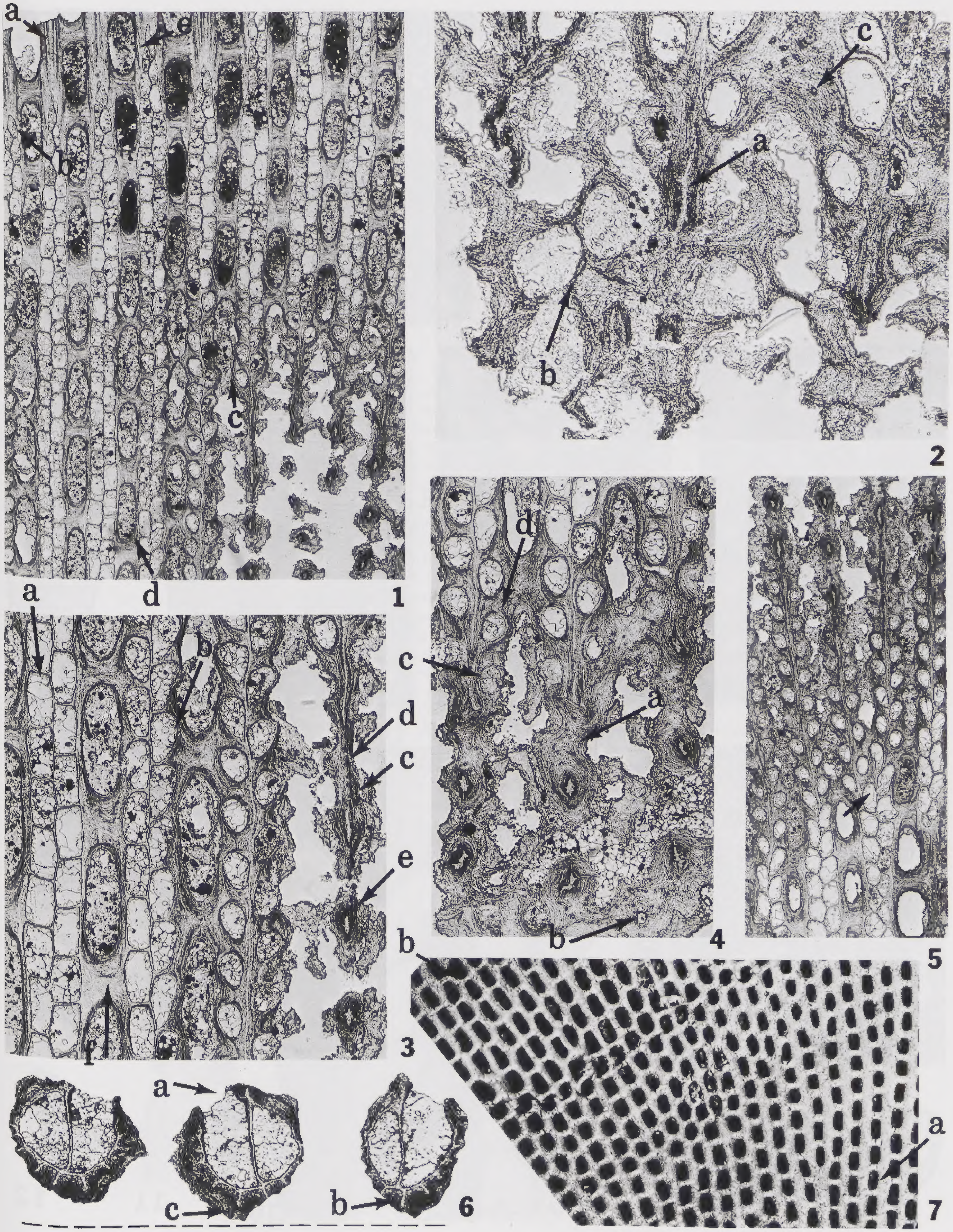
a
e
b
c
d
1
a
b
c
2
d
c
a
b
4
5
a
b
d
c
e
f
3
b
a
7
a
c
b
6

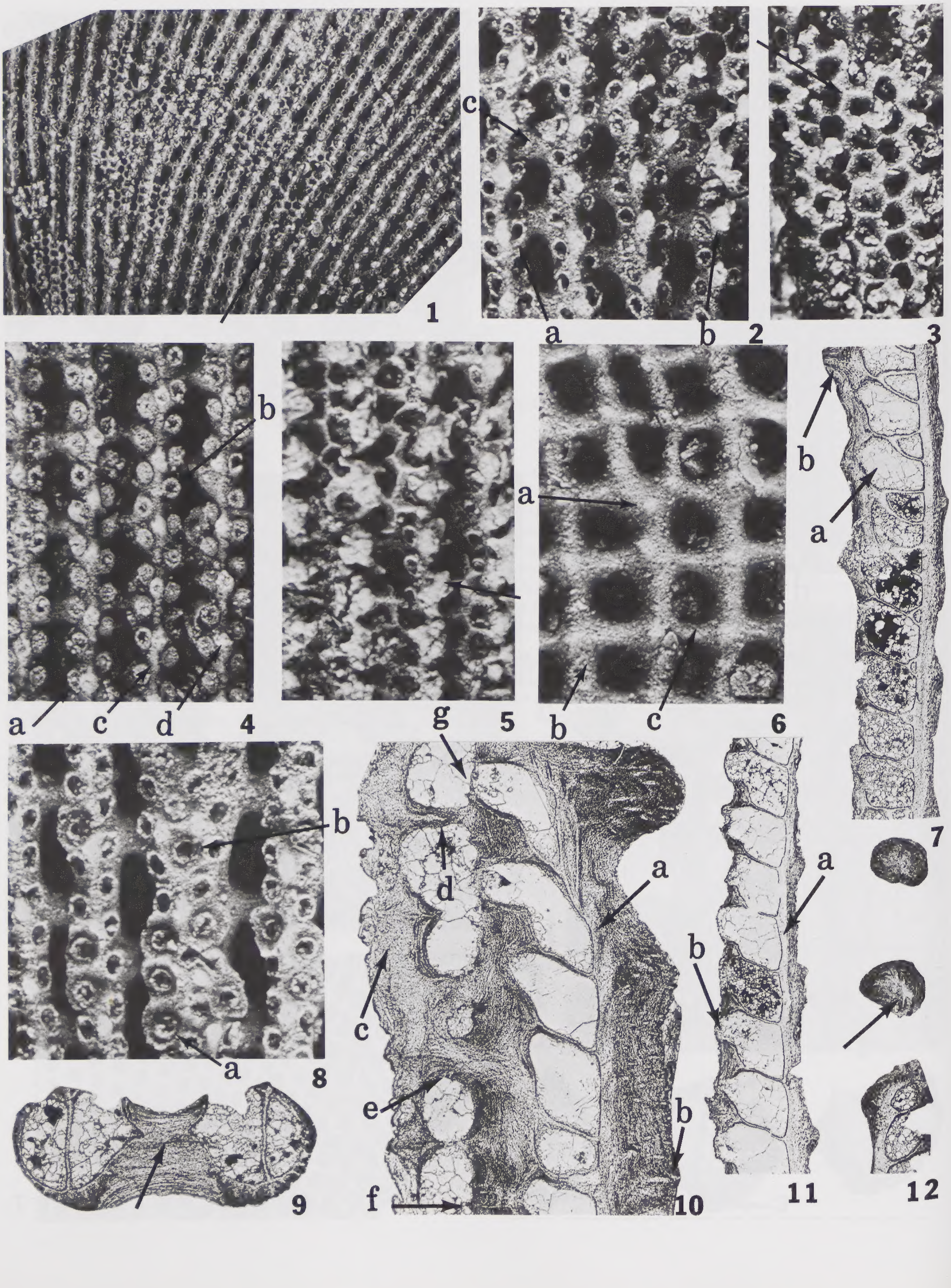
1
c
a
b
2
3
b
a
c
d
4
5
a
b
c
6
b
a
7
g
b
d
a
c
e
b
f
10
a
8
9
a
b
11
12

EXPLANATION OF PLATE 42

Figure Page

1–12. ***Hemitrypa hemitrypa*** (Prout, 1859) 111

1–3. Figured specimen, UI X-6930. 1. Obverse exterior surface of large zoarial fragment illustrating intermediate to poor development of reticulate meshwork across obverse surface that exhibits typical mesh symmetry for this species. Arrow denotes site of branch bifurcation, ×8; 2. Enlarged obverse exterior surface showing aperture (arrow **a**) exhibiting typical outline and attitudinal relationship to plane of obverse surface, peristome surrounding aperture, large nodes (arrow **b**), and poorly developed ridges across obverse dissepiment surface (arrow **c**), ×25; 3. Enlarged exterior view of obverse surface partially covered by reticulate meshwork (arrow) that is typical of this species, ×25.

4–6, 8, 9. Figured specimen, UI X-6844. 4. Enlarged obverse exterior surface showing aperture capped by centrally thickened terminal diaphragm (arrow **a**), inflection of aperture into fenestrule (arrow **b**), and intermediate-width keel (arrow **c**) atop which nodes develop (arrow **d**), ×25; 5. Enlarged obverse exterior surface illustrating highly enlarged nodes (arrow) expanded to form reticulate meshwork which has been removed (probably during transport of specimen), ×25; 6. Enlarged reverse exterior surface showing macrostylet (arrow **a**) located at site of branch bifurcation, microstylets (arrow **b**), and typical fenestrule outline (arrow **c**), ×25; 8. Enlarged obverse exterior surface showing heterozooecia (ovicells?) developing as intermediate-size enlargements of autozooecial apertures (arrows **a** and **b**), ×25; 9. FM8, transverse section showing continuity of granular skeleton (arrow) across dissepiment between branches, ×70.

7, 11. Figured specimen, UI X-6932. HB23. 7. Mid to deep longitudinal section, obverse to left, showing typical chamber outline in deep longitudinal view (arrow **a**) and obverse node (arrow **b**) connecting with inner granular skeletal material, ×40; 11. Mid longitudinal section, obverse to left, showing granular skeletal layer (arrow **a**) and typical autozooecial chamber outline (arrow **b**), and large reverse-wall budding-angle, ×40.

10. Figured specimen, UI X-6928. HB29, mid shallow to deep longitudinal section, obverse to left. Note granular skeletal layer continuous along reverse wall (arrow **a**) and surrounding autozooecial chambers; also shown are microstylets (arrow **b**), reticulate meshwork (arrow **c**), nodes (arrow **d**) of granular skeletal material connecting with reticulate meshwork, thickened nodes toward more medial section (arrow **e**), obverse stylets (arrow **f**) continuous with granular skeleton, and apertures capped by terminal diaphragms (arrow **g**) of granular skeletal material, ×70.

12. Figured specimen, UI X-6931. HB24, shallow longitudinal section, obverse to right, showing granular skeletal layer continuous across middle of dissepiment between branches (arrow), ×40.

EXPLANATION OF PLATE 43

Figure Page

1–9. ***Hemitrypa hemitrypa*** (Prout, 1859) 111

1, 2, 7. Figured specimen, UI X-6930. HB26. 1. Shallow to deep tangential section showing typical mesh symmetry and longitudinal striae (arrow **a**) continuous with reverse microstylets (arrow **b**). Note inflection of autozooecial apertures into fenestrule (arrow **c**) causing slight closing of fenestrule toward obverse surface, ×40; 2. Deep tangential section showing reverse microstylet development in rows along branch (arrow **a**) and across dissepiment (arrow **b**), ×70; 7. Shallow tangential section illustrating thickened keel (arrow **a**) atop which develop nodes (arrow **b**) and obverse stylets (arrow **c**) all composed of granular skeletal material. Note reticulate meshwork (arrow **d**) developing as lateral extension of keel and nodes, and general appearance of meshwork in shallow tangential view (arrow **e**), ×70.

3, 4. Figured specimen, UI X-6933. HB33. 3. Transverse section showing typical branch profile in cross-section and attitudinal relationship of aperture to plane of obverse surface (arrow), ×70; 4. transverse section showing granular skeletal layer (arrow **a**) continuous around autozooecial chamber, and obverse node (arrow **b**), ×70.

5, 6, 8, 9. Figured specimen, UI X-6844. 5. FM9, mid longitudinal section, obverse to left, showing typical chamber outline (arrow) in this view, ×70; 6. FM10, shallow to mid longitudinal section, obverse to left, showing typical chamber outline (arrow) in shallow longitudinal view, ×70; 8. FM56, shallow to deep tangential section illustrating typical chamber outline in mid tangential view (arrow **a**), outline of enlarged heterozooecial chamber (arrow **b**), chamber shape at site of branch bifurcation (arrow **c**), extension of autozooecial aperture into fenestrule opening (arrow **d**), recessed dissepiment (arrow **e**), and continuity of granular skeletal layer across dissepiment (arrow **f**), ×40; 9. FM57, shallow to mid tangential section showing changing autozooecial chamber outline from shallow (arrow **a**) to mid (arrow **b**) tangential view, ×40.

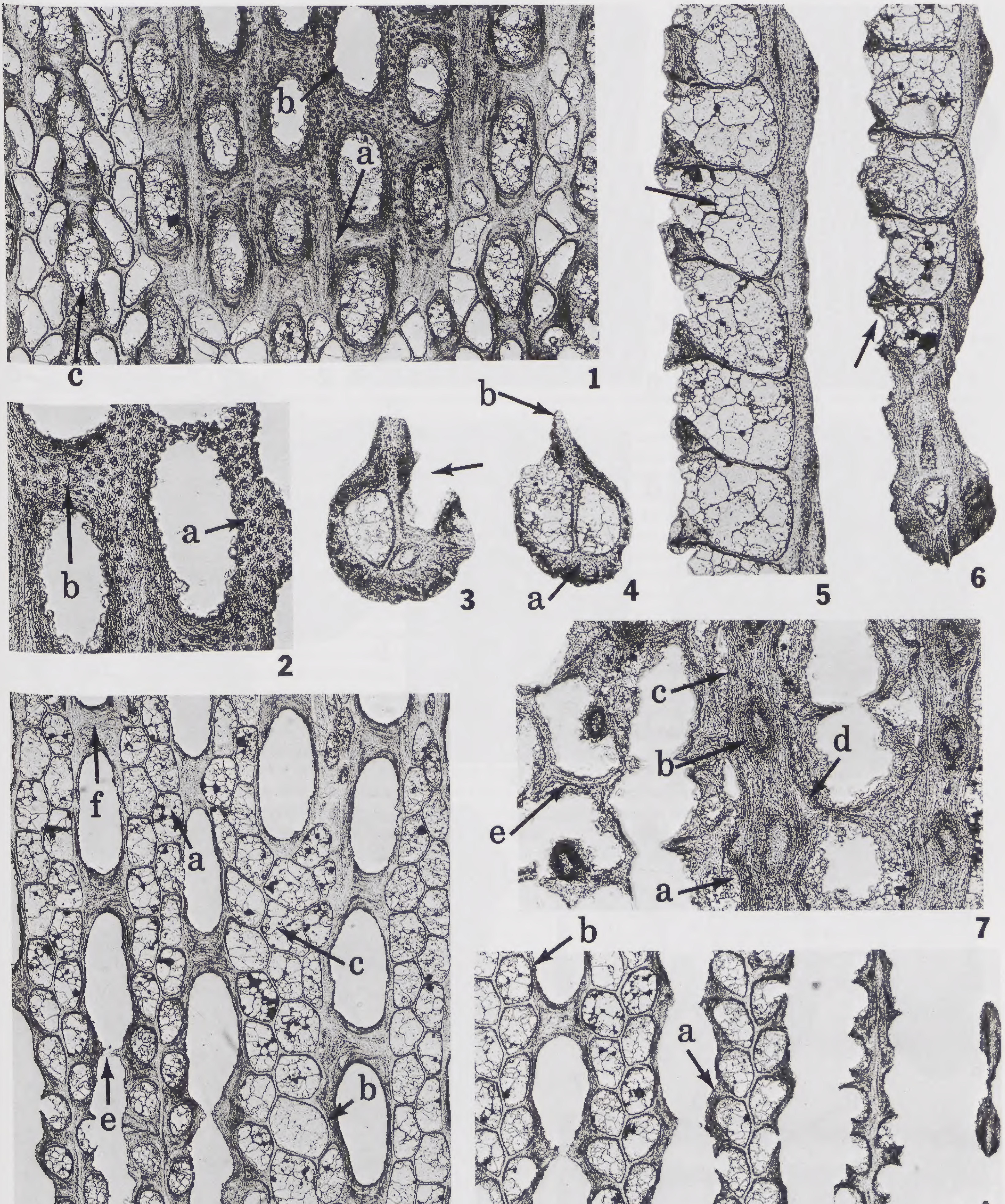
b
a
c
1
b
a
b
2
3
b
a
4
5
6
c
b
d
e
a
7
f
a
c
b
e
d
8
b
a
9

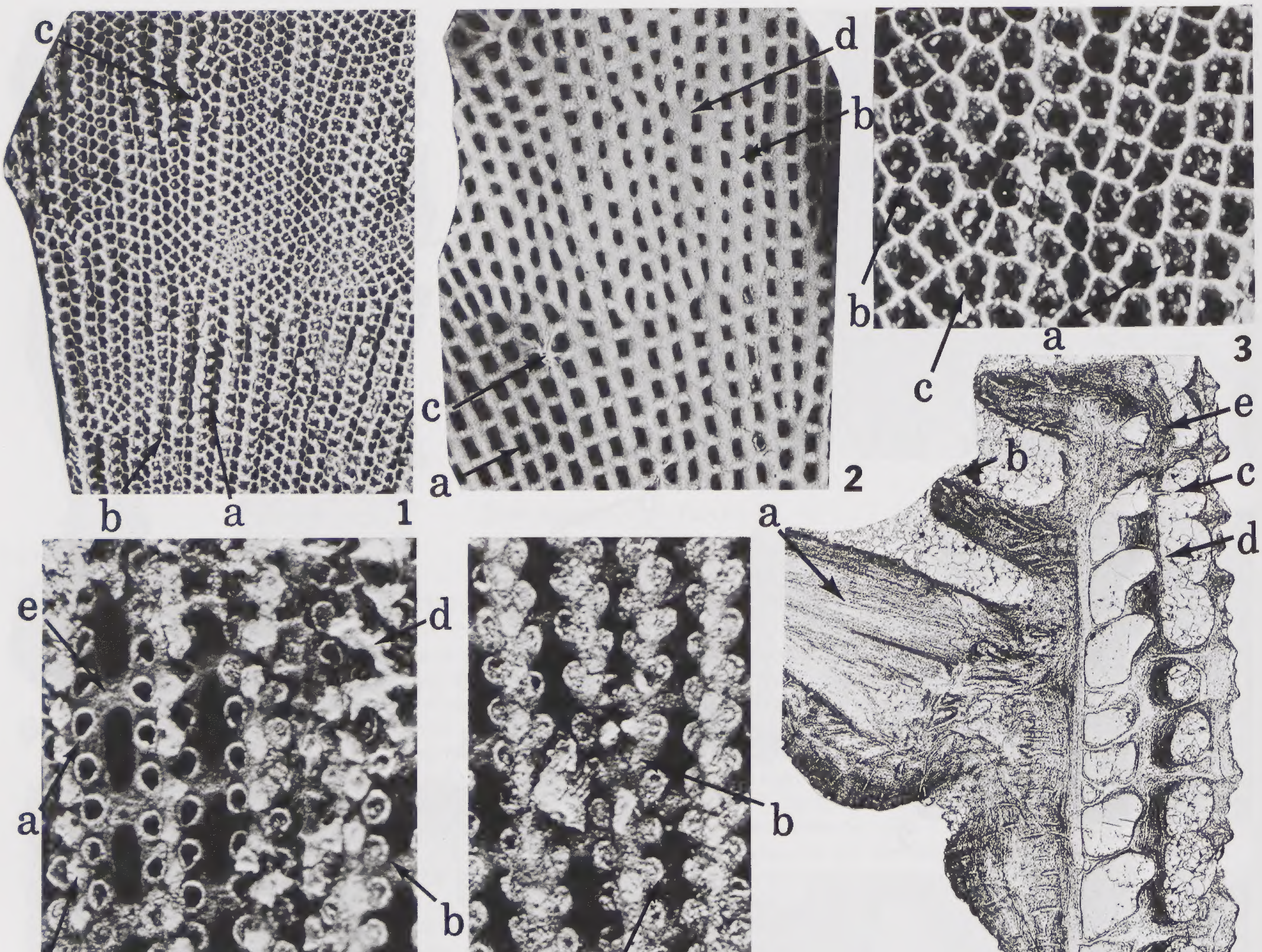
1
2
3
4
5
6
7
8
9
10

EXPLANATION OF PLATE 44

Figure Page

1–10. ***Hemitrypa aprilae,*** new species 114

1–3, 6–10. Holotype, UI X-6867. Large, well-preserved zoarial fragment exhibiting extremely well-developed reticulate meshwork characteristic of this species. 1. Obverse exterior surface illustrating thickened rows of meshwork atop branches (arrow **a**) compared to recessed, narrower rows between branches (arrow **b**), and in the middle of dissepiments and fenestrules; also note bifurcation of meshwork (arrow **c**) at site of branch bifurcation, ×8; 2. Reverse exterior surface showing variation in fenestrule size, when comparing fenestrule at arrow **a** with fenestrule at arrow **b**, due to variation in thickening of lamellar skeletal layer, well-developed zoarial supports (arrow **c**) extending from reverse zoarial surface, and site of branch bifurcation (arrow **d**), ×8; 3. Enlarged obverse exterior surface of reticulate meshwork. Observe variation in mesh outline, varying from approaching square (arrow **a**) to hexagonal (arrow **b**), and typical four small projections into mesh openings (arrow **c**), ×25; 6. HB94, deep to shallow longitudinal section, obverse to right, illustrating well-developed zoarial support (arrow **a**) projecting from reverse zoarial surface, enlarged dissepiments due to thickened lamellar skeletal layer (arrow **b**), centrally thickened terminal diaphragm with central granular skeletal spine (arrow **c**), typical chamber outline in mid longitudinal view (arrow **d**) and at abaxial edge of branch (arrow **e**), ×40; 7. HB89, transverse section illustrating typical attitudinal relationship of aperture opening (arrow **a**) to plane of obverse surface, granular skeletal material composing reticulate meshwork (arrow **b**) and continuous with granular skeleton around autozooecial chambers (arrow **c**) and with reverse microstylets (arrow **d**), ×70; 8. HB89, transverse section showing granular skeletal layer continuous with node (arrow **a**) which develops along middle of obverse surface atop keel to become centrally thickened ridge (arrow **b**) of reticulate meshwork (arrow **c**). Note typical chamber outline in mid transverse view (arrow **d**), ×40; 9. HB89, deep to mid longitudinal section, obverse to right, illustrating chamber outline in deep longitudinal view (arrow **a**), and granular skeletal layer (arrow **b**) surrounding autozooecial chambers and continuous with reverse microstylets (arrow **c**), nodes developing into initial reticulate meshwork (arrow **d**), reticulate meshwork itself (arrow **e**), and obverse stylets (arrow **f**), ×70; 10. HB89, mid to shallow longitudinal section, obverse to right, showing continuity of granular skeletal layer across dissepiment (arrow **a**) and typical chamber outline (arrow **b**) in mid longitudinal view, ×40.

4. Paratype, UI X-6865. Enlarged obverse exterior surface illustrating aperture with well-developed surrounding peristome (arrow **a**), centrally thickened terminal diaphragm (arrow **b**), nodes (arrow **c**) located atop keel along branch midline; also note initiation of reticulate meshwork atop branch (arrow **d**) and longitudinal ridges (arrow **e**) atop dissepiment surface, ×25.

5. Paratype, UI X-6866. Enlarged obverse exterior surface showing inflection of adaxial apertural edge into fenestrule opening (arrow **a**) and obverse stylet positioned near site of branch bifurcation (arrow **b**), ×25.

EXPLANATION OF PLATE 45

Figure Page
1–8. ***Hemitrypa aprilae,*** new species 114

1, 2, 5, 6, 8. Holotype, UI X-6867. 1. HB89, mid to shallow longitudinal section, obverse to right, illustrating typical autozooecial chamber outline in mid shallow longitudinal view (arrow **a**), abaxial apertural edge projecting into fenestrule (arrow **b**), centrally thickened terminal diaphragm (arrow **c**), peristome (arrow **d**) at distal edge of aperture and continuous with granular skeletal layer, and from which obverse spines (arrow **e**) project and which are connected to the reticulate meshwork (arrow **f**). Note stylets projecting into fenestrule (arrow **g**), ×70; 2. HB86, mid to very shallow tangential section. Note well-developed peristome (arrow **a**) surrounding aperture, nodes (arrow **b**) that when enlarged become part of reticulate meshwork (arrow **c**), which is composed of granular skeletal material (arrow **d**), obverse stylets (arrow **e**), recessed dissepiments (arrow **f**) and projections of apertures into fenestrule opening (arrow **g**), ×40; 5. HB86, mid to very shallow tangential section showing stylets (arrow **a**) developing as projections of peristome surrounding aperture (arrow **b**), and thick keel (arrow **c**) from which projections develop to form the reticulate meshwork (arrow **d**), ×20; 6. HB86, shallow to deep tangential section. Observe pronounced projections of apertures into fenestrules (arrow **a**) near obverse surface not evident in mid tangential view (arrow **b**), where fenestrule outline is elliptical, fenestrule approaching rectangular (arrow **c**) in deep tangential view near reverse surface; note chamber outline at site of branch bifurcation (arrow **d**), ×20; 8. HB86, mid shallow to deep tangential section showing typical chamber outline near obverse surface (arrow **a**), in mid tangential view (arrow **b**) and near reverse-wall budding-site (arrow **c**); also shown are longitudinal striae (arrow **d**) from which reverse microstylets develop, ×40.

3, 4. Paratype, UI X-6866. 3. HB39, deep tangential section showing numerous well-developed microstylets (arrow), ×40; 4. Reverse exterior surface showing typical fenestrule outline (arrow) in zooecial fragment exhibiting little secondary thickening of lamellar skeleton, ×8.

7. Paratype, UI X-6865. HF94, transverse section illustrating branch spacing and continuity of granular skeleton between branches (arrow) across dissepiment, ×40.

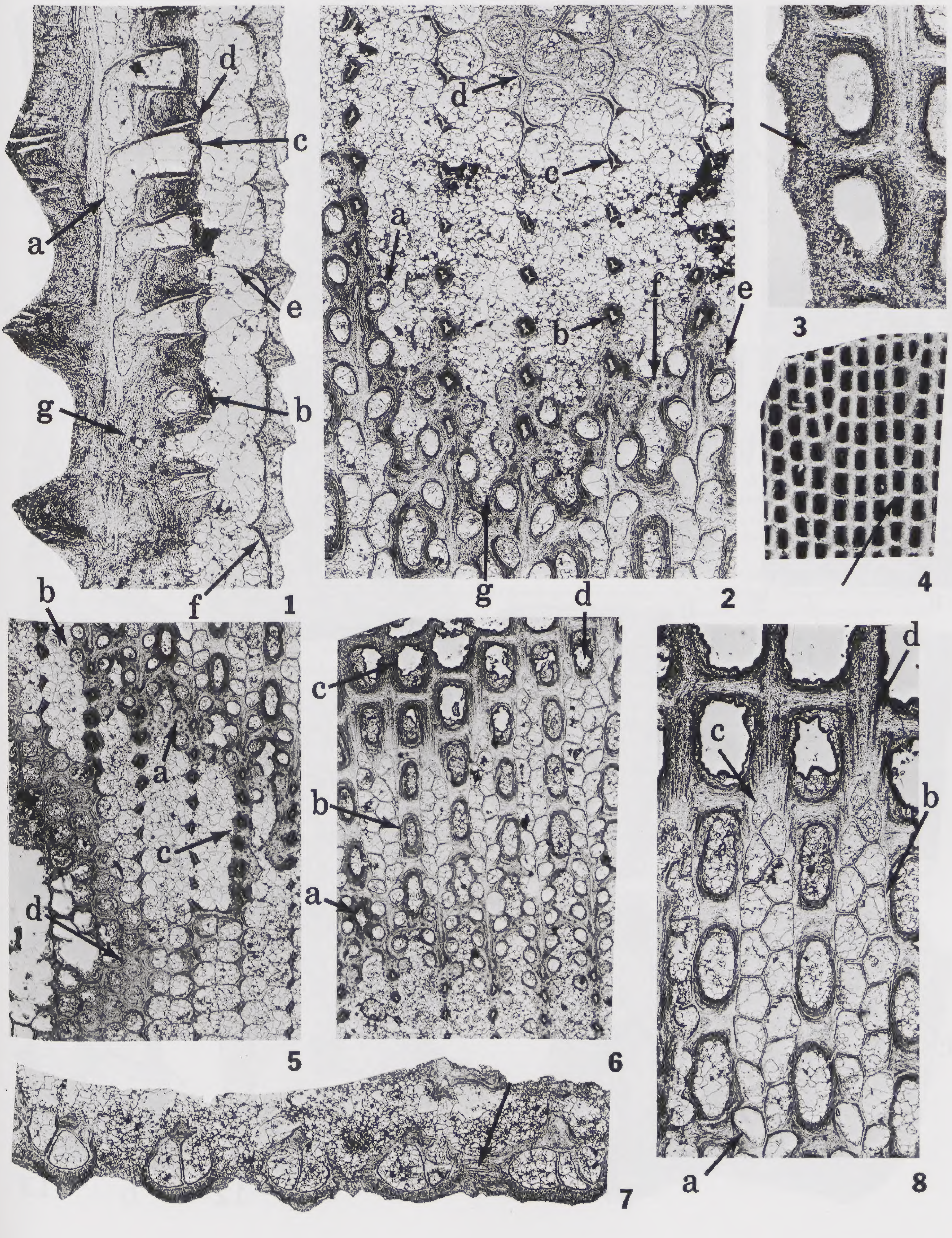
1
2
3
4
5
6
7
8

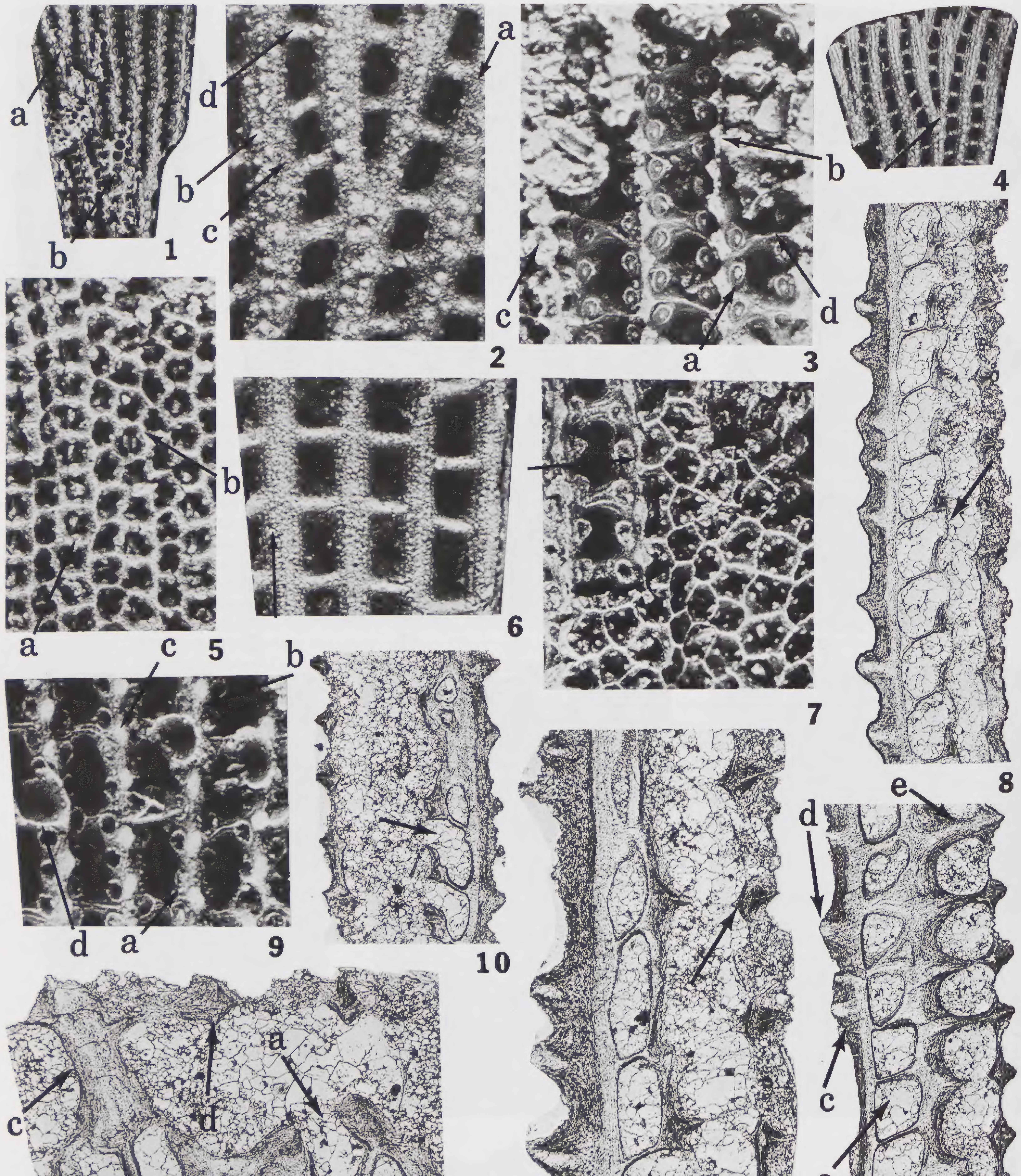
a
b
1
d
a
b
c
2
b
c
d
a
3
4
b
a
c
5
6
7
8
c
b
d
a
9
10
e
d
c
a
b
13
a
c
d
b
11
12

EXPLANATION OF PLATE 46

Figure — Page

1–13. ***Hemitrypa aspera*** Ulrich, 1890 116

1. Figured specimen, UI X-6852. Obverse exterior surface of well-preserved zoarial fragment showing site of branch bifurcation (arrow **a**) and reticulate meshwork (arrow **b**) covering obverse surface, ×8.

2–5. Figured specimen, UI X-6854. Highly ontogenetically thickened zoarial fragment. 2. Enlarged reverse exterior surface illustrating longitudinal striae (arrow **a**), macrostylets (arrow **b**), microstylets (arrow **c**) and positioning of both macrostylets and microstylets across reverse branch and dissepiment surfaces, ×25; 3. Enlarged obverse exterior surface illustrating aperture (arrow **a**) capped by centrally thickened terminal diaphragm, nodal development (arrow **b**) with nodes and keel extending outward to form reticulate meshwork (arrow **c**), and longitudinal ridge developed across obverse dissepiment surface (arrow **d**), which also extends outward to form meshwork, ×25; 4. Reverse exterior surface showing macrostylet development toward proximal end of zoarium (arrow) and lack of macrostylets at distal zoarial end, ×8; 5. Enlarged obverse exterior surface illustrating typical appearance of well-developed reticulate meshwork (arrow **a**) and inflections (arrow **b**) into mesh openings due to enlargement of nodes, ×25.

6, 7, 10, 11, 13. Figured specimen, UI X-6856. Well-preserved zoarial fragment exhibiting slight ontogenetic thickening. 6. Enlarged reverse exterior surface showing initial macrostylet development (arrow), ×25; 7. Enlarged obverse exterior surface illustrating development of reticulate meshwork (arrow) extending from atop nodes, keel, and dissepiment. Note well-developed rounded inflections into meshwork openings, ×25; 10. HF98, shallow to very shallow longitudinal section, obverse to left, showing typical chamber outline in shallow longitudinal view (arrow) and height of reticulate meshwork above branch surface, ×40; 11. HF94, transverse section illustrating aperture opening (arrow **a**) and its attitudinal relationship to plane of obverse surface, granular skeleton continuous with longitudinal striae (arrow **b**), around autozooecial chambers, and with obverse nodes (arrow **c**). Note reticulate meshwork covering obverse surface (arrow **d**), ×70; 13. HF98, deep longitudinal section, obverse to right. Observe typical chamber outline in deep longitudinal view (arrow **a**), thick granular skeletal layer (arrow **b**) continuous around autozooecial chambers, and with reverse microstylets (arrow **c**), macrostylets (arrow **d**), obverse nodes (arrow **e**), and reticulate meshwork which forms in part as an extension of these nodes, ×40.

8, 12. Figured specimen, UI X-6857. 8. HF60, mid longitudinal section, obverse to right, illustrating chamber size and outline (arrow) and spacing of reticulate meshwork above obverse surface, ×40; 12. HF64, mid to shallow longitudinal section. Note continuity of granular skeleton of stylets with reticulate meshwork (arrow) covering obverse surface, ×70.

9. Figured specimen, UI X-6940. Enlarged obverse exterior surface illustrating keel (arrow **a**), obverse stylets formed across branch surface (arrow **b**), nodes (arrow **c**) atop keel, and heterozooecia (arrow **d**) probably representing ovicells and developing as pronounced enlargements of some apertures, ×25.

EXPLANATION OF PLATE 47

Figure Page

1–6. ***Hemitrypa aspera*** Ulrich, 1890 116

1–4. Figured specimen, UI X-6857. 1. HF64, mid longitudinal section, obverse to right, illustrating typical chamber outline in this view (arrow **a**) and terminal diaphragm capping aperture (arrow **b**), relatively high reverse-wall budding-angle (arrow **c**) and well-developed reticulate meshwork (arrow **d**), ×70; 2. HF61, deep to shallow tangential section. Note extension of apertures into fenestrule (arrow **a**) causing inflections in fenestrule outline near obverse surface with lack of such inflections in mid tangential view (arrow **b**), reverse longitudinal striae (arrow **c**), macrostylets (arrow **d**), chamber arrangement at site of branch bifurcation (arrow **e**), and continuity of granular skeleton across dissepiment (arrow **f**), ×20; 3. HF67, shallow tangential section illustrating autozooecial aperture (arrow **a**) and sequence of mesh development from keel (arrow **b**) to node (arrow **c**) to layer of granular skeletal material bridging between nodes to form the base of the reticulate meshwork (arrow **d**), ×40; 4. HF67, mid to shallow tangential section showing autozooecial aperture enlarged to become heterozooecium (ovicell?) (arrow), ×40.

5, 6. Figured specimen, UI X-6856. 5. HF99, shallow to deep tangential section of zoarial fragment showing changing chamber outline from near reverse-wall budding-site (arrow **a**), to mid chamber view (arrow **b**), to near obverse surface (arrow **c**). Observe longitudinal striae (arrow **d**) from which microstylets (arrow **e**) and macrostylets (arrow **f**) develop; also shown are obverse stylets (arrow **g**), ×40; 6. HF100, very shallow tangential section of reticulate meshwork showing mesh initiation from nodes on obverse surface (arrow **a**), and thick mesh (arrow **b**) composed of granular skeletal material, ×40.

7. ***Hemitrypa vermifera*** (Ulrich, 1890) 119

Figured specimen, UI X-6884. HF25, transverse section showing typical close spacing of branches and extension of longitudinal striae (arrow) laterally, connecting to form dissepiment, ×40.

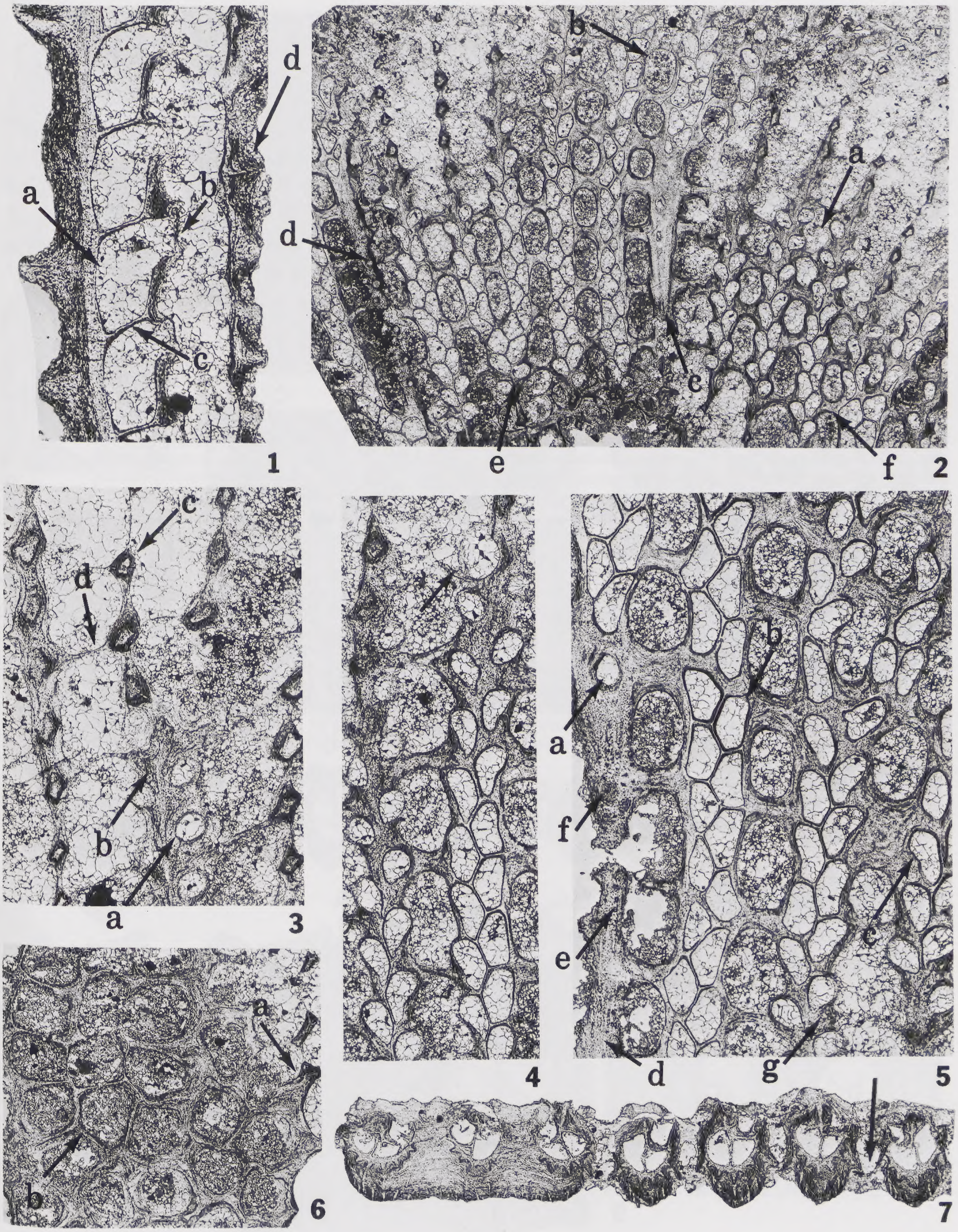
d
a
b
c
1
b
a
d
c
e
f
2
c
d
b
a
3
4
b
a
f
e
c
d
g
5
a
b
6
7

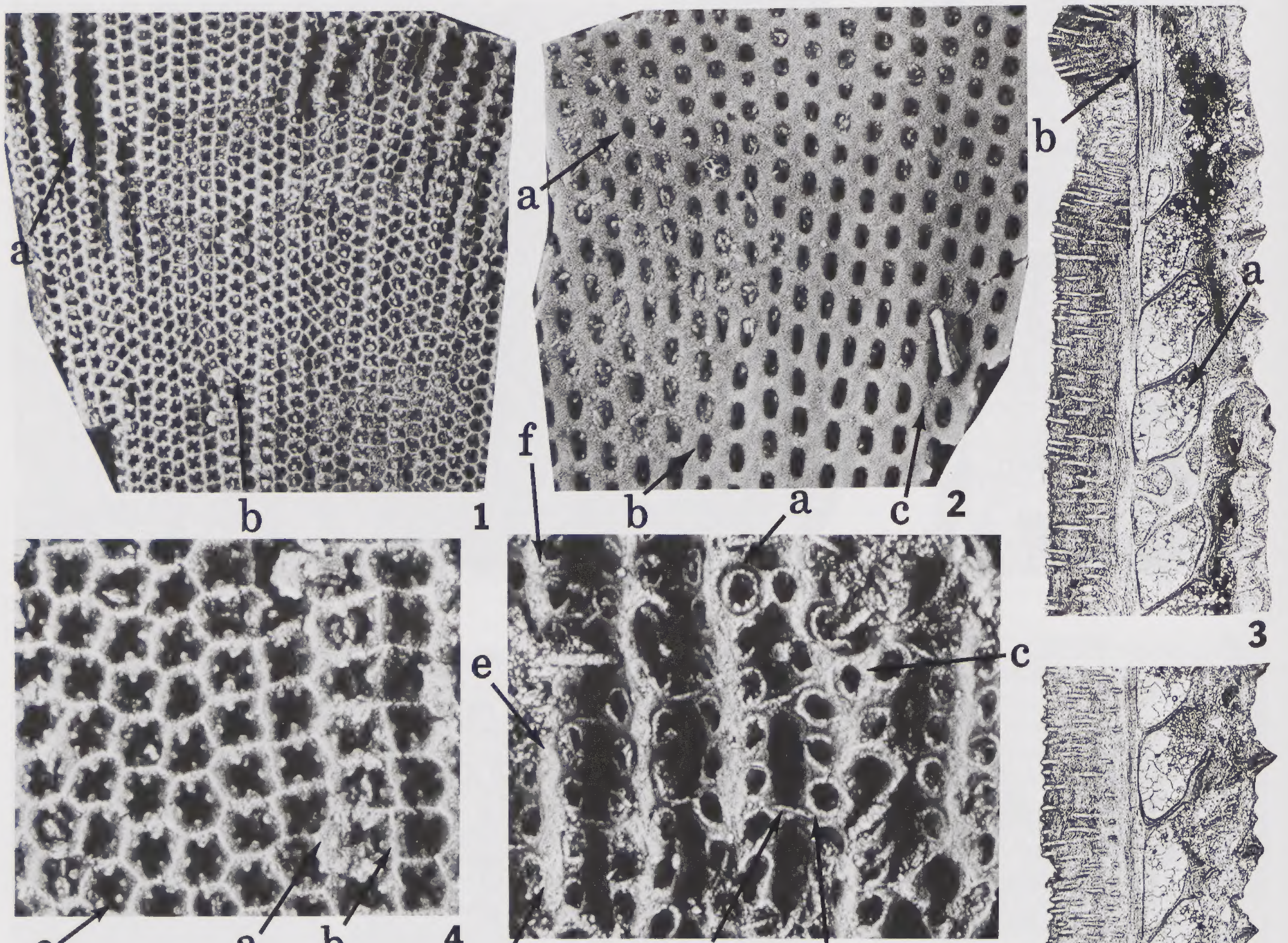
a
b
1
a
b
c
2
b
a
3
c
a
b
4
f
a
e
c
d
g
b
5
6
7
8
d
a
c
b
a
9
b
c
10

EXPLANATION OF PLATE 48

Figure Page
1–10. ***Hemitrypa vermifera*** (Ulrich, 1890) 119

1, 2, 7. Figured specimen, UI X-6864. Large, well-preserved zoarial fragment exhibiting moderate ontogenetic thickening and well-developed reticulate meshwork. 1. Obverse exterior surface showing pronounced thickening along branch midline (arrow **a**) and bifurcation of branches (arrow **b**) evident in pattern of overlying reticulate meshwork, ×8; 2. Reverse exterior surface illustrating variation in fenestrule outline from ovate (arrow **a**) to elliptical (arrow **b**), and site of branch bifurcation (arrow **c**), ×8; 7. HF25, transverse section showing typical branch spacing, ×40.

3. Figured specimen, UI X-6865. HF18, shallow to deep longitudinal section, obverse to right, illustrating typical chamber outline in deep longitudinal view (arrow **a**) and granular skeletal layer (arrow **b**) continuous across dissepiment, ×40.

4, 5. Figured specimen, UI X-6880. 4. Enlarged obverse exterior surface view of reticulate meshwork showing thickened mesh along branch midline (arrow **a**) and thinned meshwork between branches (arrow **b**); also note small inflections into mesh (arrow **c**) along the edges of mesh openings, ×25; 5. Enlarged obverse exterior surface showing heterozooecia (ovicells?) (arrow **a**) developing as enlargements of some apertures, complete peristome (arrow **b**) surrounding autozooecial aperture, aperture position at site of branch bifurcation (arrow **c**), keel (arrow **d**), and node (arrow **e**) atop keel, obverse stylet (arrow **f**), and longitudinal ridges developed atop dissepiments (arrow **g**), ×25.

6, 8. Figured specimen, UI X-6882. HF28. 6. Shallow longitudinal section, obverse to left, showing cross-section of dissepiment with continuity of granular skeleton across middle (arrow), ×40; 8. Shallow to mid longitudinal section, obverse to right, illustrating typical chamber outline in shallow longitudinal view (arrow) ×40.

9. Figured specimen, UI X-6881. HF29, deep tangential section showing longitudinal striae (arrow **a**) from which rows of microstylets (arrow **b**) develop. These become increasingly irregularly positioned (arrow **c**) in deepest section toward reverse zoarial surface, ×40.

10. Figured specimen, UI X-6883. HF34, transverse section illustrating terminal diaphragm (arrow **a**) across aperture, which exhibits typical attitudinal relationship of opening to plane of obverse surface, continuity of granular skeletal material around autozooecial chambers, with longitudinal striae (arrow **b**), microstylets (arrow **c**), and nodes (arrow **d**), ×70.

EXPLANATION OF PLATE 49

Figure Page

1–6. ***Hemitrypa vermifera*** (Ulrich, 1890) 119

1, 5. Figured specimen, UI X-6881. 1. HF17, shallow to deep tangential section illustrating typical autozooecial chamber outline in mid tangential view (arrow **a**) as compared to outline in shallow tangential view (arrow **b**), site of branch bifurcation in mid chamber view (arrow **c**), and fenestrule outline in deep (arrow **d**), mid (arrow **e**), and mid shallow (arrow **f**) tangential view, ×20. 5. HF33, mid to deep tangential section showing autozooecial chamber outline near reverse-wall budding-site (arrow **a**) and continuity of granular skeletal material between branches in middle of dissepiment (arrow **b**), ×20.

2, 3, 6. Figured specimen, UI X-6864. 2. HF35, shallow tangential section showing aperture (arrow **a**) surrounded by complete peristome, heterozooecium (arrow **b**) probably representing ovicell, obverse stylets (arrow **c**) projecting from top of recessed dissepiment, keel (arrow **d**), and nodes (arrow **e**) developing as extension of keel, ×40; 3. HF35, shallow tangential section of reticulate meshwork illustrating nodes (arrow **a**) with stylets (arrow **b**) developing atop keel between nodes, initial reticulate meshwork development as extensions of node, dissepiment, and keel (arrow **c**), increasing thickening of mesh granular skeleton (arrow **d**), with four inflections into mesh opening in most shallow view, and stylets of granular skeleton (arrow **e**) connecting with mesh. Note that each opening or hole in the meshwork corresponds to one aperture opening on the obverse surface, ×40; 6. HF27, tangential section of reticulate meshwork illustrating typical mesh pattern and inflections into mesh opening (arrow), ×20.

4. Figured specimen, UI X-6863. HF20, shallow to deep longitudinal section, obverse to left, illustrating terminal diaphragm (arrow **a**) capping autozooecial chamber that exhibits a typical outline in mid longitudinal view, aperture extension into fenestrule at abaxial branch edge (arrow **b**), granular skeletal layer surrounding autozooecial chambers (arrow **c**) continuous with reverse microstylets (arrow **d**), nodes (arrow **e**), reticulate meshwork (arrow **f**), and thinned meshwork (arrow **g**), not continuous with nodes, bridging obverse surface, ×70.

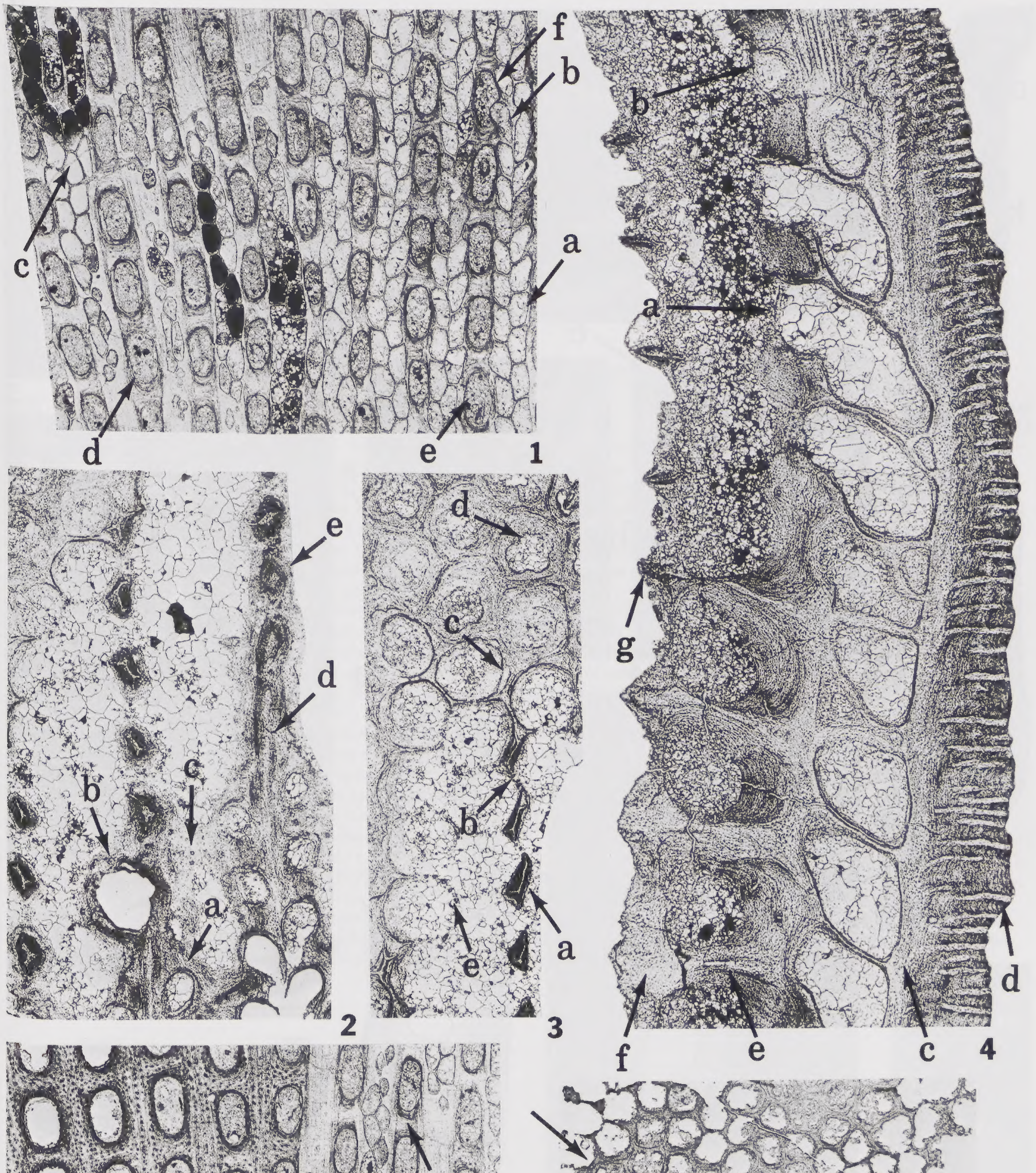
f
b
c
a
d
e
1
e
d
b
c
a
2
d
c
b
a
e
3
b
a
g
f
e
c
d
4
a
b
5
6

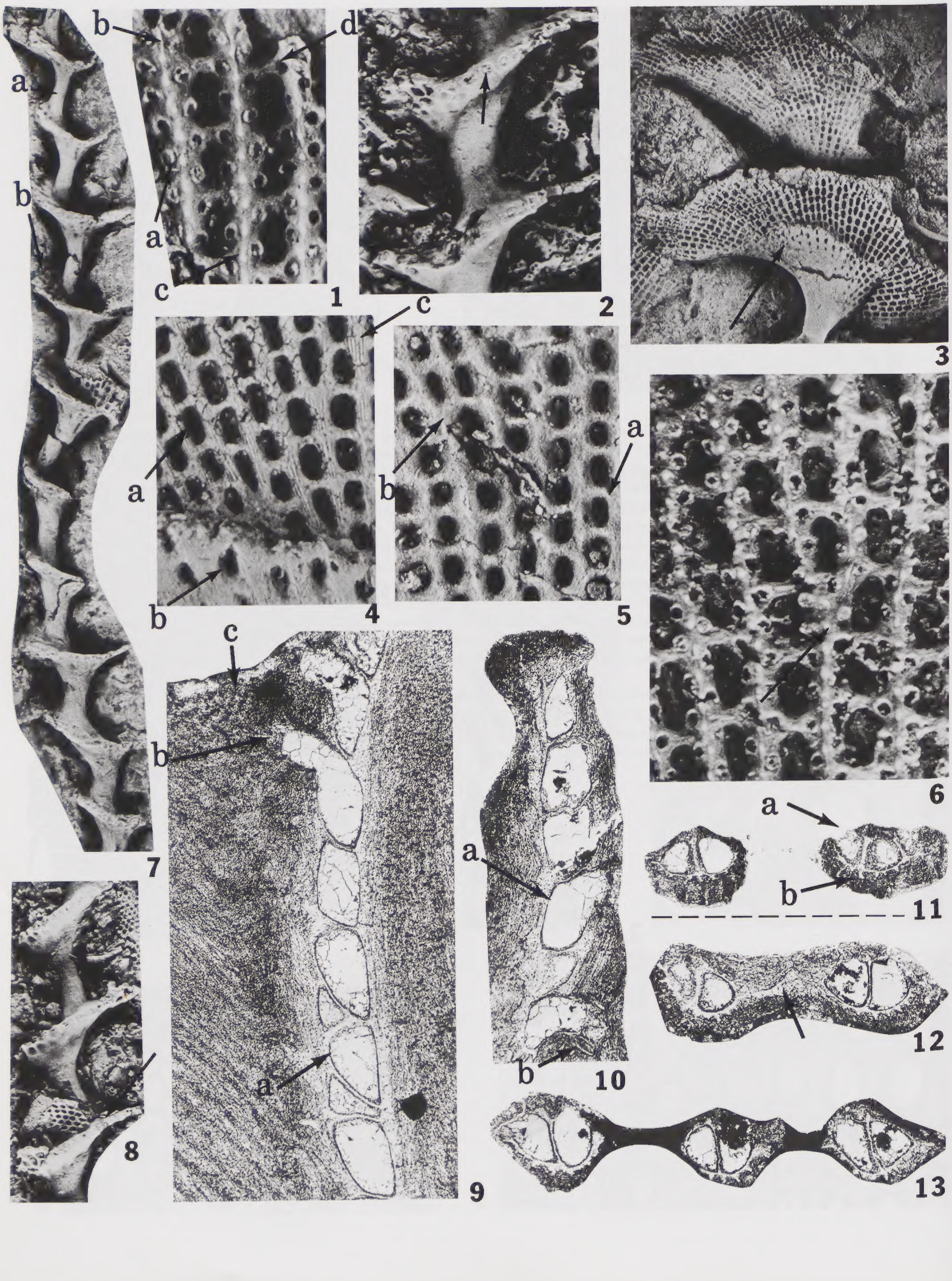
1
2
3
4
5
6
7
8
9
10
11
12
13

EXPLANATION OF PLATE 50

Figure | Page
1–13. ***Archimedes negligens*** Ulrich, 1890 124

1, 2, 5, 8, 10, 11. Figured specimen, UI X-6975. Well-preserved zoarial fragment containing central axis with attached mesh. 1. Enlarged obverse exterior surface illustrating incomplete peristome surrounding all but most proximal to proximal–adaxial edge of aperture (arrow **a**), moderate projection of aperture into fenestrule, keel (arrow **b**) atop which nodes develop (arrow **c**). Note longitudinal ridges across dissepiments (arrow **d**), ×30; 2. Exterior side view of dextrally spiraling central axis showing typical axial shape and areas at the outer edge of axial whorls (arrow) where branches have been broken from spiral, ×7.5; 5. Reverse exterior surface of mesh exhibiting moderate thickening due to addition of lamellar skeleton during ontogeny and illustrating typical fenestrule size and shape (arrow **a**), and site of branch bifurcation (arrow **b**), ×15; 8. Exterior side view of dextrally spiraling central axis showing angle at which whorls diverge from plane of axis (arrow), ×6; 10. AN88, shallow mid to mid longitudinal section, obverse to right, showing typical chamber outline in mid longitudinal section (arrow **a**) and continuity of granular skeletal material with peristome (arrow **b**), ×70; 11. AN58, transverse section showing autozooecial aperture (arrow **a**) and typical attitudinal relationship of aperture to plane of obverse surface, and granular skeletal layer continuous with longitudinal striae (arrow **b**) and around autozooecial chambers, ×70.

3, 4, 6, 12, 13. Lectotype, ISGS (ISM) 2785-2. 3. Exterior side view of sinistrally spiraling zoarial axis attached to zoarial mesh (arrow) radiating outward from branch axis, ×3; 4. Reverse exterior surface of zoarial mesh illustrating typical fenestrule shape and size (arrow **a**). Note fenestrule almost closed by thickened lamellar skeleton at edge of spiral axis (arrow **b**) and longitudinal striae (arrow **c**) along reverse branch surface, ×12; 6. Enlarged obverse exterior surface showing typical mesh symmetry and site of branch bifurcation (arrow), ×30; 12. AN42, transverse section showing two branches joined by dissepiment (arrow) across which extends granular skeletal material continuous around autozooecial chambers, ×70; 13. AN42, transverse section illustrating typical spacing of branches and chamber outline in mid transverse view, ×70.

7, 9. Paralectotype, ISGS (ISM) 2785-1. 7. Exterior side view of sinistrally spiraling central axis illustrating delicate axis in this species (arrow **a**) and mesh (arrow **b**) developing at edge of axial whorls, ×3; 9. AN9, mid shallow to deep longitudinal section, obverse to left, illustrating typical autozooecial chamber outline in deep view (arrow **a**), highly elongate vestibule (arrow **b**) in mid longitudinal autozooecial chamber view. Note plugging of aperture by thickened lamellar skeleton composing central axis (arrow **c**), ×70.

EXPLANATION OF PLATE 51

Figure Page
1–6. ***Archimedes negligens*** Ulrich, 1890 124

1. Paralectotype, ISGS (ISM) 2785-1. AN2, transverse view of zoarial axis exhibiting sinistral spiraling as viewed toward proximal end of zoarium. Observe transverse section of central axial branch (arrow **a**), flattening of mesh in tangential section at edge of whorl (arrow **b**), and fenestrule (arrow **c**) in tangential view; also shown is reorientation of mesh during spiraling from middle to lateral edge of axis, ×40.

2–5. Lectotype, ISGS (ISM) 2785-2. 2. AN47, shallow to mid tangential section illustrating extension of abaxial aperture margin into fenestrule (arrow **a**) causing inflection in fenestrule outline near obverse surface, lack of inflection in mid tangential view (arrow **b**) of fenestrule, typical chamber outline in shallow tangential view (arrow **c**) and incomplete peristome surrounding all but proximal to proximal–adaxial edge of aperture with apertural diaphragm (arrow **d**), ×70; 3. AN49, shallow to mid tangential section showing well-developed incomplete peristome (arrow **a**) and slight inflection of aperture opening onto dissepiment (arrow **b**), ×70; 4. AN44, mid shallow to mid tangential section showing typical mesh symmetry, and continuity of granular skeleton (arrow) across dissepiment, there forming single longitudinal ridge across dissepiment obverse surface, ×70; 5. AN49, shallow to deep tangential section illustrating typical chamber outline in mid tangential view (arrow **a**), chamber outline near reverse-wall budding-site (arrow **b**), and longitudinal striae (arrow **c**), connected with granular skeletal material which also connects with reverse microstylets (arrow **d**), ×70.

6. Figured specimen, UI X-7009. AN24, section cutting along central plane of sinistrally spiraling axis, illustrating change in central axial branch orientation from proximal to distal end of axial fragment. Spiraling central axial branch is well-documented in this figure, showing longitudinal section (arrow **a**) with obverse to left near proximal end of axial fragment, becoming a tangentially oriented branch (arrow **b**) in middle of axial fragment, shifting toward longitudinal (arrow **c**) toward distal end and at most distal edge of axial fragment becoming a longitudinal section (arrow **d**) with obverse now to right; fenestrule (arrow **e**) and apertures surrounded by peristome (arrow **f**) are visible in mid axis tangential view, ×35.

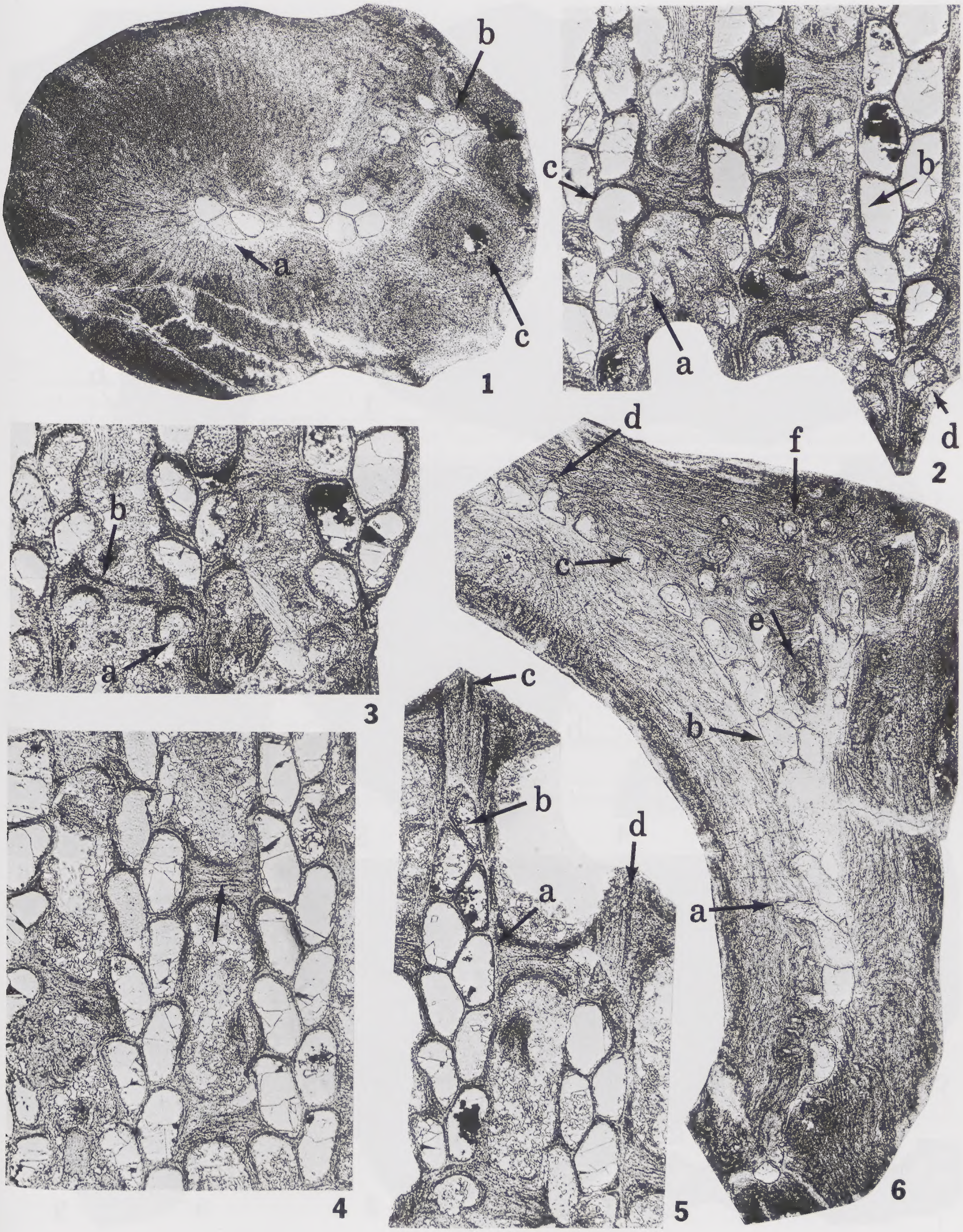
1
a
b
c
2
a
b
c
d
3
a
b
4
5
a
b
c
d
6
a
b
c
d
e
f

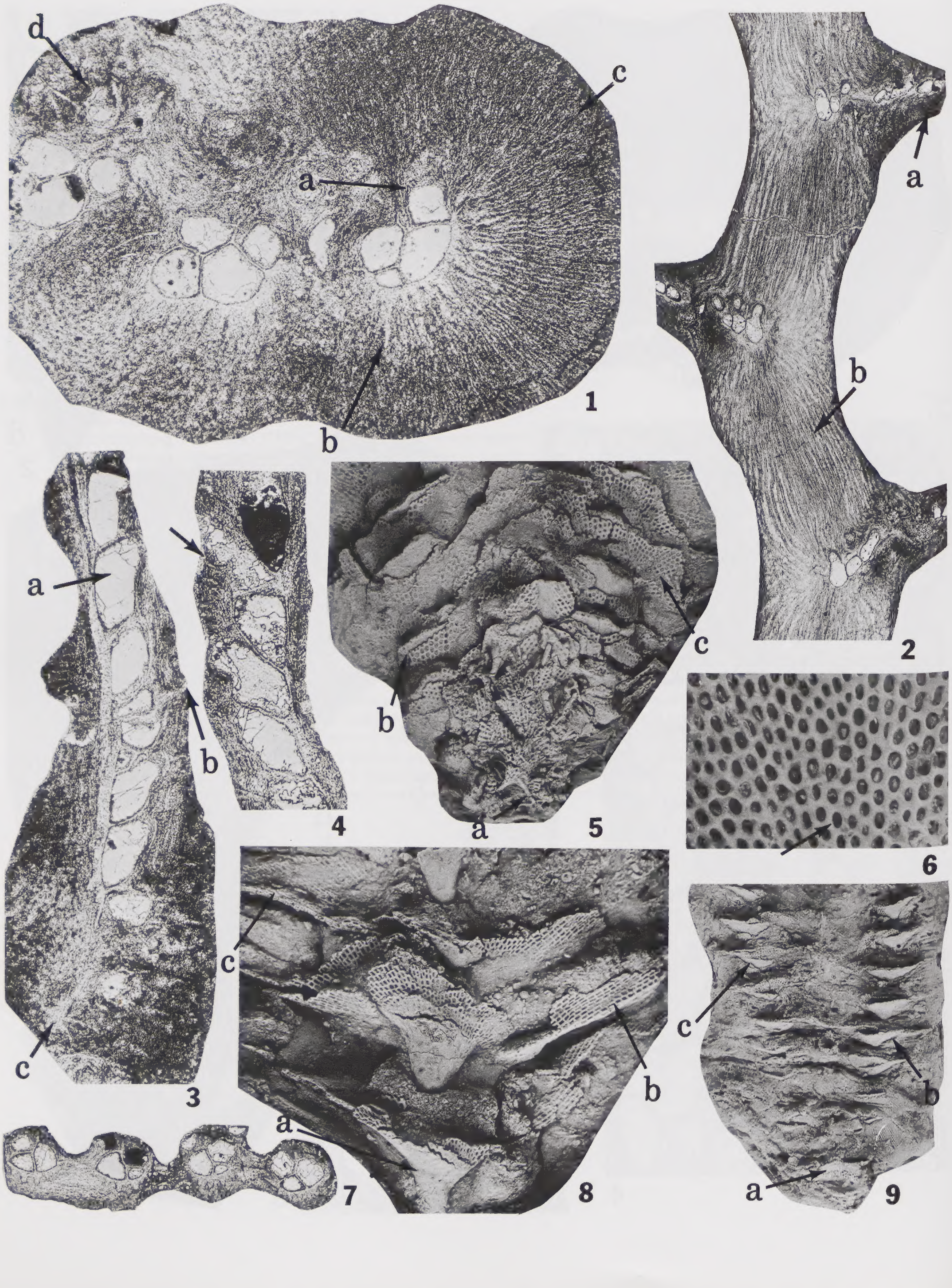
d
c
a
b
1
a
b
2
a
b
c
3
4
c
b
a
5
6
c
a
7
b
8
c
b
a
9

EXPLANATION OF PLATE 52

Figure Page

1–4. ***Archimedes negligens*** Ulrich, 1890 124

1–3. Figured specimen, UI X-6975. 1. AN73, transverse view of zoarial axis illustrating transverse section of central axial branch (arrow **a**) showing aperture plugged by lamellar skeleton of axis, granular skeletal layer continuous around autozooecial chambers and with reverse longitudinal striae (arrow **b**) and microstylets (arrow **c**), and flattening of mesh at edge of axis (arrow **d**). View is toward proximal end of axis, with lateral branches developing to the left of the axial branch in dextral spiraling, ×79; 2. AN81, longitudinal section near center of dextrally spiraling axis showing axial whorls (arrow **a**) and thickened lamellar skeletal layer forming bulk of central axis (arrow **b**), ×20; 3. AN56, shallow to deep longitudinal section, obverse to right, showing typical chamber outline in mid longitudinal view (arrow **a**), and continuity of granular skeletal layer with obverse nodes (arrow **b**) and across dissepiment (arrow **c**), ×70.

4. Paralectotype, ISGS (ISM) 2785-1. AN10, mid to shallow longitudinal section, obverse to left, showing continuity of granular skeletal material continuous with peristome (arrow), ×70.

5–9. ***Archimedes owenanus*** (Hall, 1857b) 127

5, 9. Paralectotype, ISGS (ISM) 2790. 5. Exterior side view of two central axes having a common point of origin (arrow **a**), exhibiting both dextral (arrow **b**) and sinistral (arrow **c**) spiraling within the same zoarium. Note abundant zoarial supports developed on reverse mesh surfaces, ×2; 9. Other side of zoarial fragment shown in figure 5 above, illustrating common source (arrow **a**) from which both dextral (arrow **b**) and sinistral (arrow **c**) spiraling are observed. Oppositely coiled spirals of this nature as extensions of one zoarium are commonly observed in *Archimedes*, ×1.

6. Figured specimen, UI X-6993. Reverse exterior mesh surface illustrating variation in fenestrule outline (arrow) as a result of thickening of lamellar skeletal layer during ontogeny, ×6.

7. Figured specimen, UI X-6973. AM41, transverse section showing typical branch and autozooecial chamber outline in this view, ×40.

8. Figured specimen, UI X-6983. Exterior side view of well-preserved zoarial fragment illustrating well-developed central axis (arrow **a**), reverse mesh surface extending outward from axis (arrow **b**), and obverse surface (arrow **c**) extending outward from axis showing slightly concave mesh, ×2.

EXPLANATION OF PLATE 53

Figure Page

1–10. ***Archimedes owenanus*** (Hall, 1857b) 127

1–3. Figured specimen, UI X-6993. 1. exterior side view of sinistrally spiraling central axis illustrating overgrowths of mesh by lamellar skeleton extending for moderate distances laterally from edge of axis (arrow **a**) and zoarial supports formed from reverse mesh surfaces (arrow **b**), ×2; 2. Exterior side view of sinistrally spiraling central axis illustrating pronounced thickening of lamellar skeleton along reverse mesh surface (arrow **a**), reverse mesh surface without overgrowths (arrow **b**) and zoarial support (arrow **c**) with three prongs extending toward distal end of support, ×1; 3. Obverse exterior surface of mesh exhibiting partial (arrow **a**) to complete (arrow **b**) overgrowth of obverse surface by thickened lamellar skeleton, ×6.

4, 5, 7, 8. Figured specimen, UI X-7001. 4. Enlarged obverse exterior surface of extremely well-preserved zoarial fragment illustrating incomplete peristome (arrow **a**) partially surrounding aperture with gap (arrow **b**) at proximal to proximal–adaxial apertural edge. Note extension of aperture into fenestrule opening, aperture position at site of branch bifurcation (arrow **c**) with centrally thickened terminal diaphragm capping aperture, and keel (arrow **d**) atop which are positioned nodes (arrow **e**), ×30; 5. Enlarged obverse exterior surface showing site of branch bifurcation (arrow **a**) and single ridge (arrow **b**) extending across dissepiment, ×30; 7. Obverse exterior surface illustrating typical mesh pattern in this species, ×10; 8. Enlarged reverse exterior surface of mesh illustrating variation in fenestrule shape (arrows **a** and **b**) as observed in reverse surficial view. Pronounced variation in reverse surface is a result of secondary overgrowths of lamellar skeleton on the reverse zoarial mesh surface, ×24.

6. Figured specimen, UI X-7006. Exterior side view of sinistrally spiraling zoarial fragment illustrating typical form of central axis (arrow) and axial whorls from which zoarial mesh emerges, ×2.

9, 10. Figured specimen, UI X-6985. AO7. 9. Transverse section showing aperture capped by centrally thickened terminal diaphragm (arrow **a**) and exhibiting typical attitudinal relationship to plane of obverse surface. Note granular skeletal layer continuous with longitudinal striae (arrow **b**) and around autozooecial chambers (arrow **c**) as well as thickened lamellar skeletal layer covering reverse branch surface, ×70; 10. Mid to deep longitudinal section, obverse to right, illustrating typical chamber outline in mid longitudinal section (arrow **a**), and granular skeletal layer continuous with obverse nodes (arrow **b**), around autozooecial chambers (arrow **c**) and with reverse microstylets (arrow **d**), ×70.

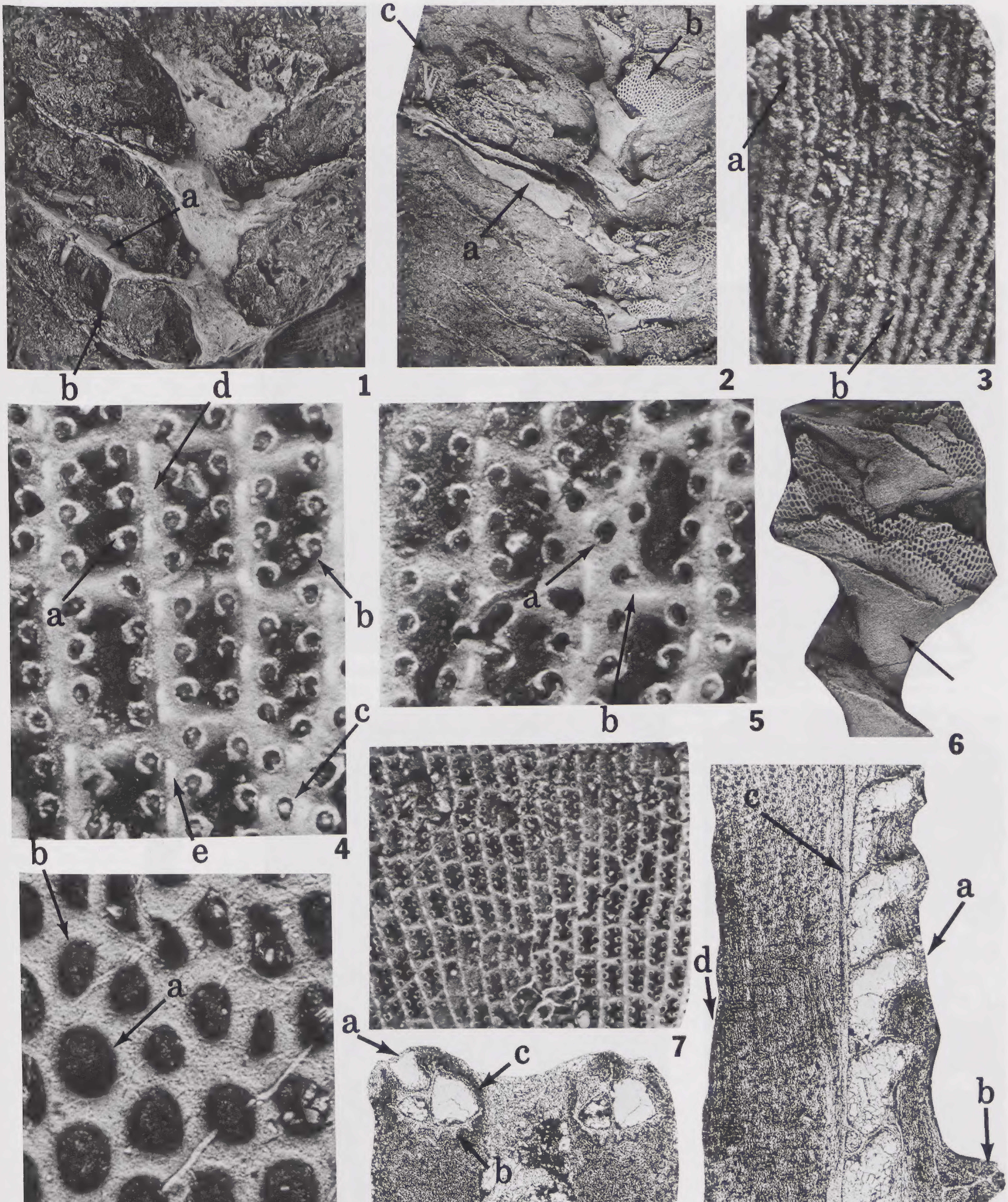
a
b
1
c
b
a
2
a
b
3
d
a
b
c
e
4
a
b
5
6
7
b
a
8
a
c
b
9
c
a
d
b
10

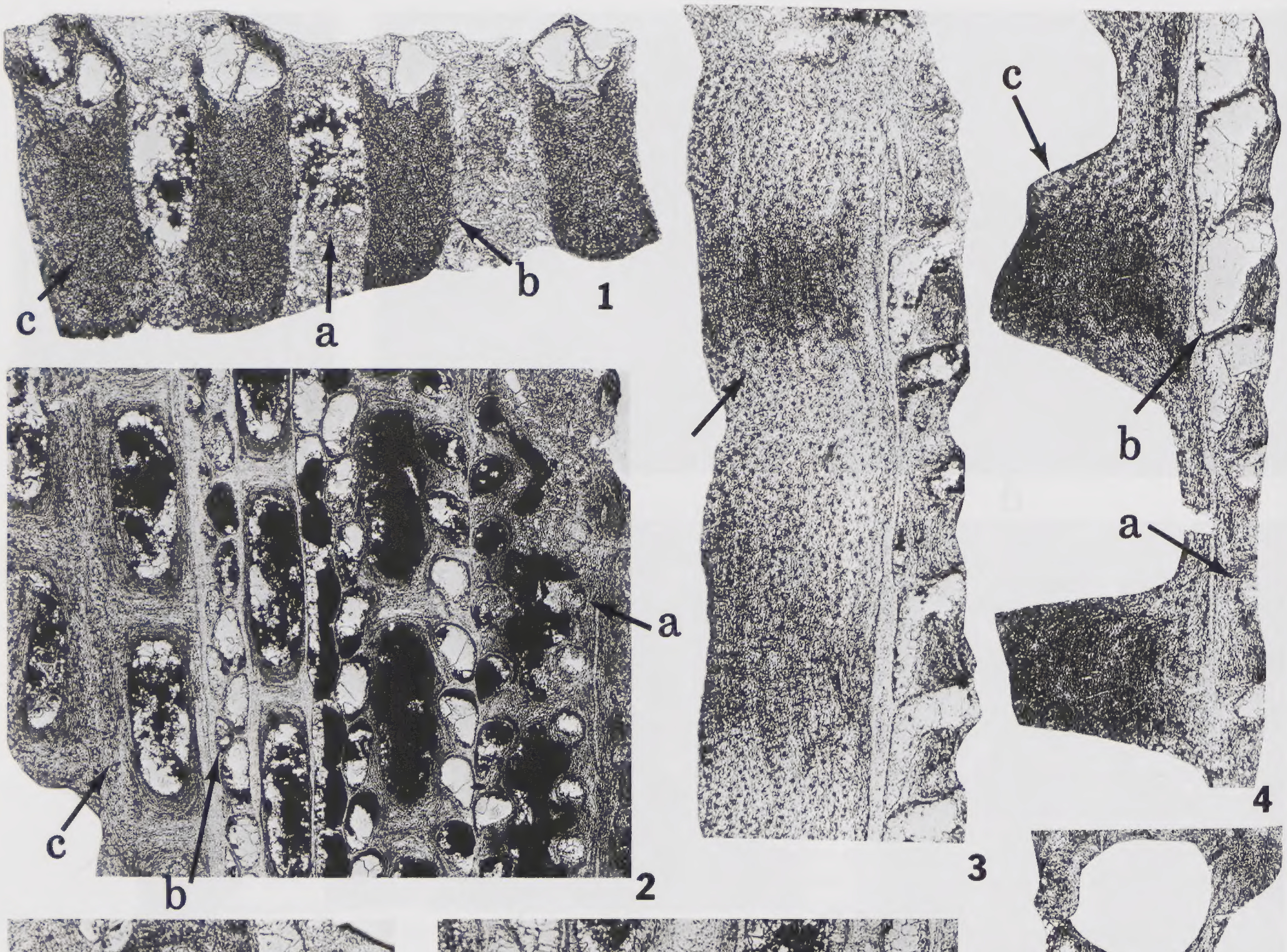
c
a
b
1
a
c
b
2
3
c
b
a
4
a
b
5
c
b
a
6
d
b
c
a
7

EXPLANATION OF PLATE 54

Figure Page

1–7. ***Archimedes owenanus*** (Hall, 1857b) 127

1–4. Figured specimen, UI X-6985. 1. AO7, transverse section illustrating spacing between branches and fenestrule opening between branches. Note great thickening of reverse lamellar skeletal layer (arrow **a**) and continuity of granular skeleton with reverse microstylets (arrows **b** and **c**), ×70; 2. AO2, shallow to deep tangential section showing aperture capped by terminal diaphragm (arrow **a**), chamber outline near reverse-wall budding-site (arrow **b**), and longitudinal striae continuous with reverse microstylets (arrow **c**), initially occurring in rows which become more randomly positioned across reverse branch surface with ontogeny, ×40; 3. AO7, mid shallow to very shallow longitudinal section, obverse to right, illustrating typical chamber outline in this view and significant ontogenetic thickening (arrow) of lamellar skeleton along reverse branch surface, ×70; 4. AO7, very shallow to mid shallow longitudinal section, obverse to right, showing aperture in most shallow tangential view (arrow **a**) extending into fenestrule opening and onto distal part of dissepiment, typical chamber outline in mid shallow longitudinal view (arrow **b**) and thickened lamellar skeletal layer across dissepiment (arrow **c**), ×70.

5, 7. Figured specimen, UI X-6986. 5. AO47, shallow to mid tangential section illustrating heterozooecia (ovicells?) with central perforation (arrow **a**) and multi-generation heterozooecial development partially plugging fenestrule (arrow **b**), ×70; 7. AO48, very shallow to deep longitudinal section, obverse to left, showing typical autozooecial chamber outline in deep (arrow **a**) and mid (arrow **b**) longitudinal views, thin lamellar skeletal layer (arrow **c**) due to positioning of this zoarial fragment a pronounced distance laterally away from central axis, and reverse zoarial support development (arrow **d**), ×40.

6. Figured specimen, UI X-6971. AG8, mid tangential section. Note typical autozooecial chamber outline in this view (arrow **a**), lack of apertural inflection into fenestrule (arrow **b**) in mid tangential view, and chamber outline at site of branch bifurcation (arrow **c**), ×70.

EXPLANATION OF PLATE 55

Figure Page

1–7. ***Archimedes owenanus*** (Hall, 1857b) 127

1. Figured specimen, UI X-6986. AO47, shallow tangential section illustrating common heterozooecia (ovicells?) (arrow) developed locally across zoarial obverse surface, ×70.

2, 6. Figured specimen, UI X-6971. 2. AG8, mid to deep tangential section illustrating heterozooecia (arrow **a**) rimmed by lamellar skeletal layer and containing a central perforation (arrow **b**) giving it a doughnut-like appearance, typical chamber outline in mid tangential view (arrow **c**), and continuity of granular skeletal layer around autozooecial chambers and across dissepiment (arrow **d**), ×70; 6. Exterior side view of central axis with mesh attached (arrow) illustrating angle of mesh with axis, ×2.

3, 7. Figured specimen, UI X-6973. 3. AM40, section cutting along central plane of sinistrally spiraling axis illustrating change in central axial branch orientation from slightly askew tangential (arrow **a**), to longitudinal with obverse to left (arrow **b**), and back to tangential section (arrow **c**) at distal end of axis, ×40; 7. AM46, section cutting along central plane of sinistrally spiraling axis with central axial branch exhibiting change of branch orientation (*i.e.*, changing direction of obverse branch surface), which results in spiraling axis. Observe longitudinal section with obverse to left (arrow **a**), branch facing outward from page and becoming a tangential section distally (arrow **b**), and finally a nearly 180° turn is completed toward most distal end of axial section shown with obverse branch now to right (arrow **c**). Thick lamellar skeletal material comprises the axis, ×20.

4, 5. Figured specimen, UI X-7001. 4. AM5, mid to deep tangential section. Note longitudinal striae (arrow **a**) continuous with granular skeletal material that also connects with reverse microstylets (arrow **b**), and fenestrule outline in mid (arrow **c**) and deep (arrow **d**) tangential view, showing increase in fenestrule dimensions, ×40; 5. AM21, very shallow to deep tangential section illustrating aperture outline in most shallow tangential view (arrow **a**), with aperture surrounded by peristome and capped by terminal diaphragm. Note change in autozooecial chamber size as aperture is connected to chamber at proximal edge (arrow **b**), autozooecial chamber outline in mid tangential view (arrow **c**) and near reverse-wall budding-site (arrow **d**), and nodes (arrow **e**) positioned atop keel, ×40.

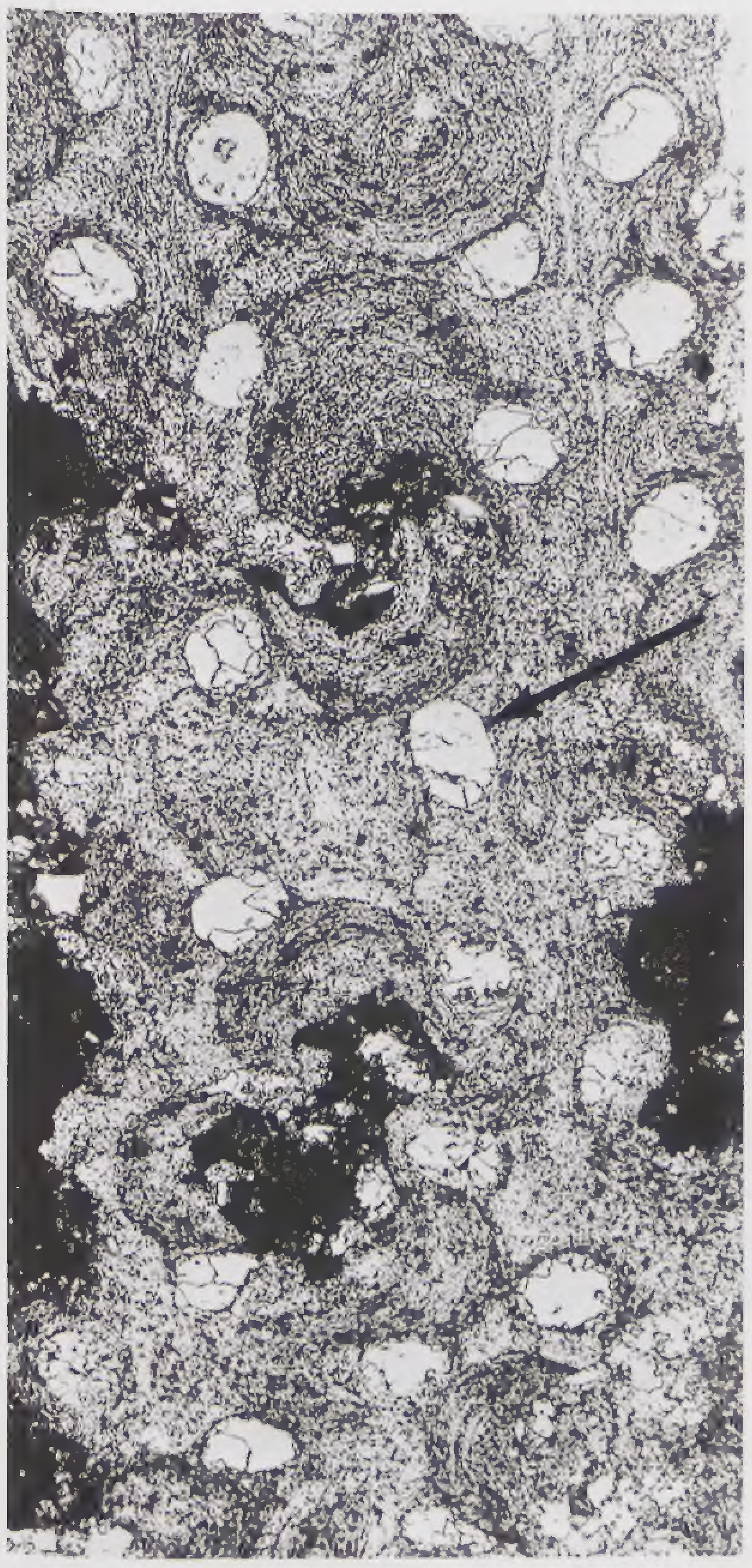

1

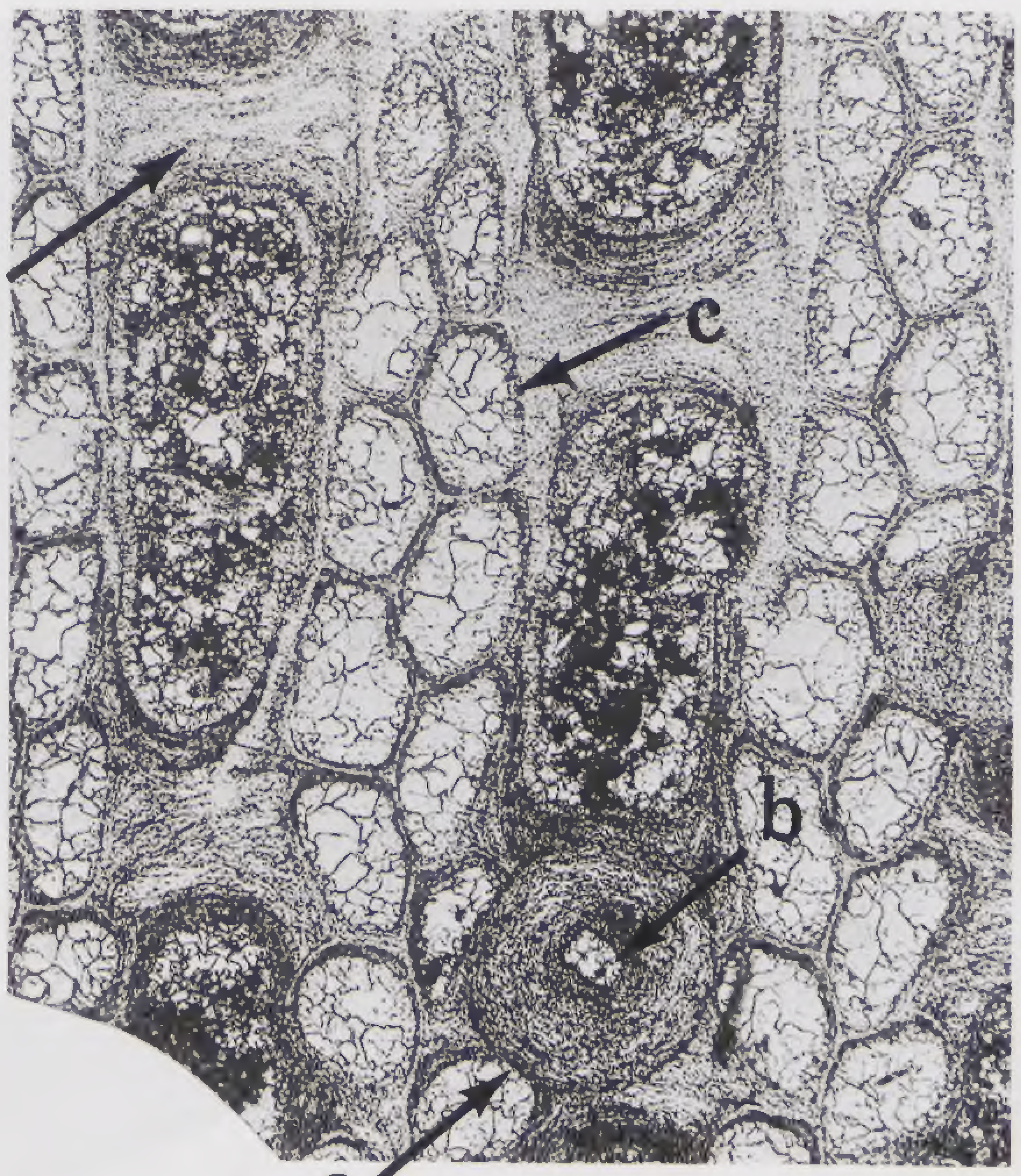

2

3

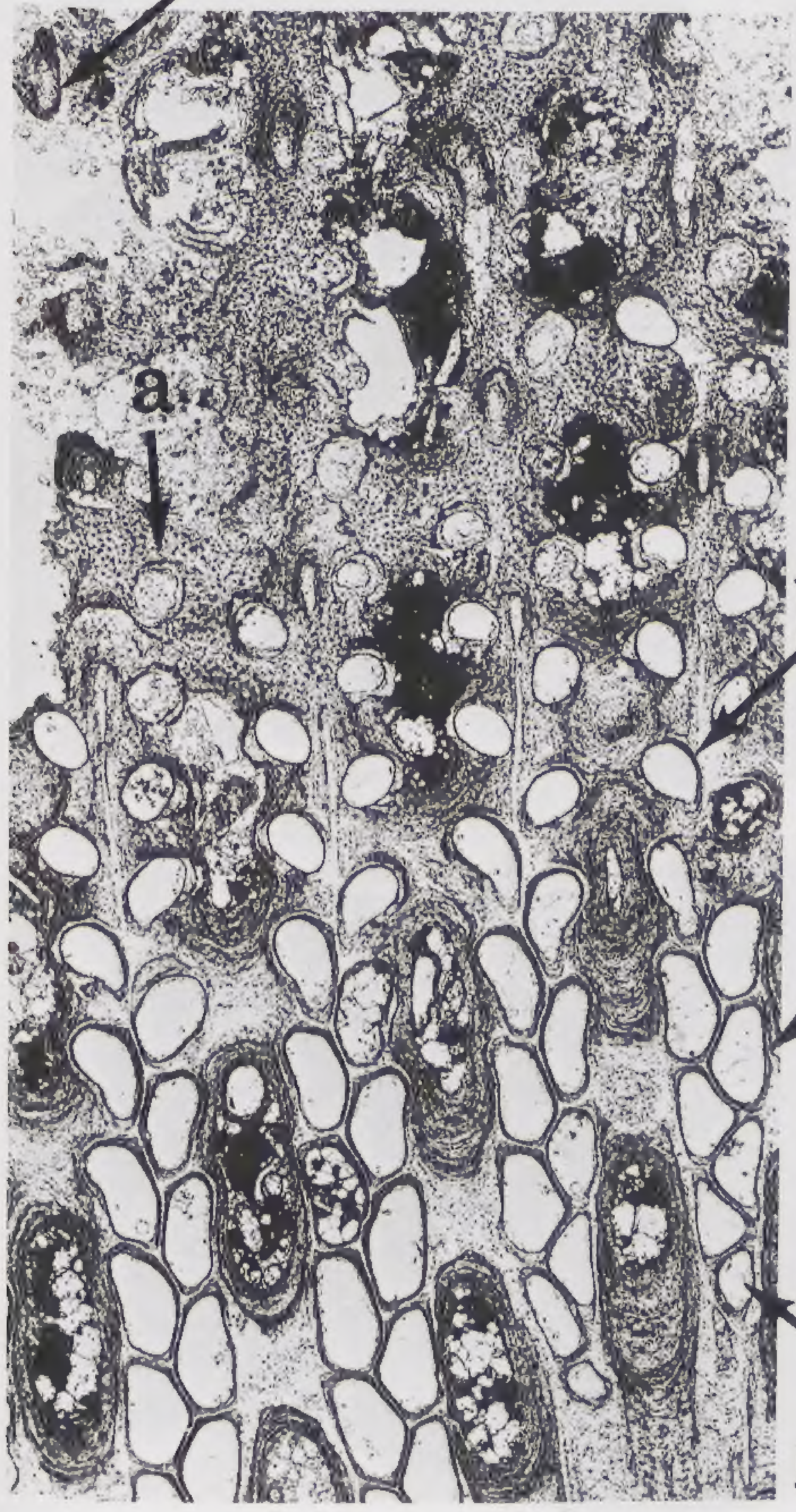

5

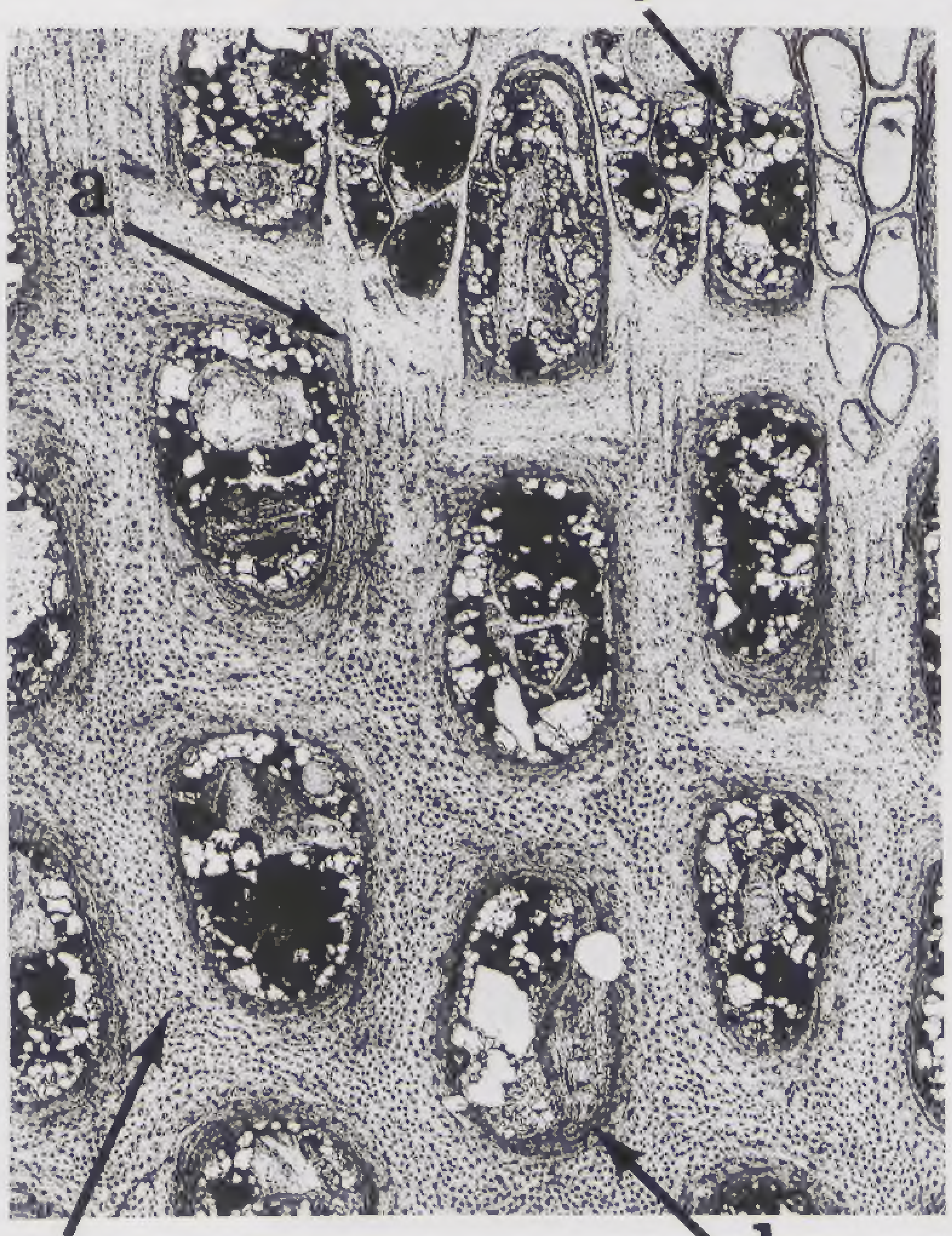

4

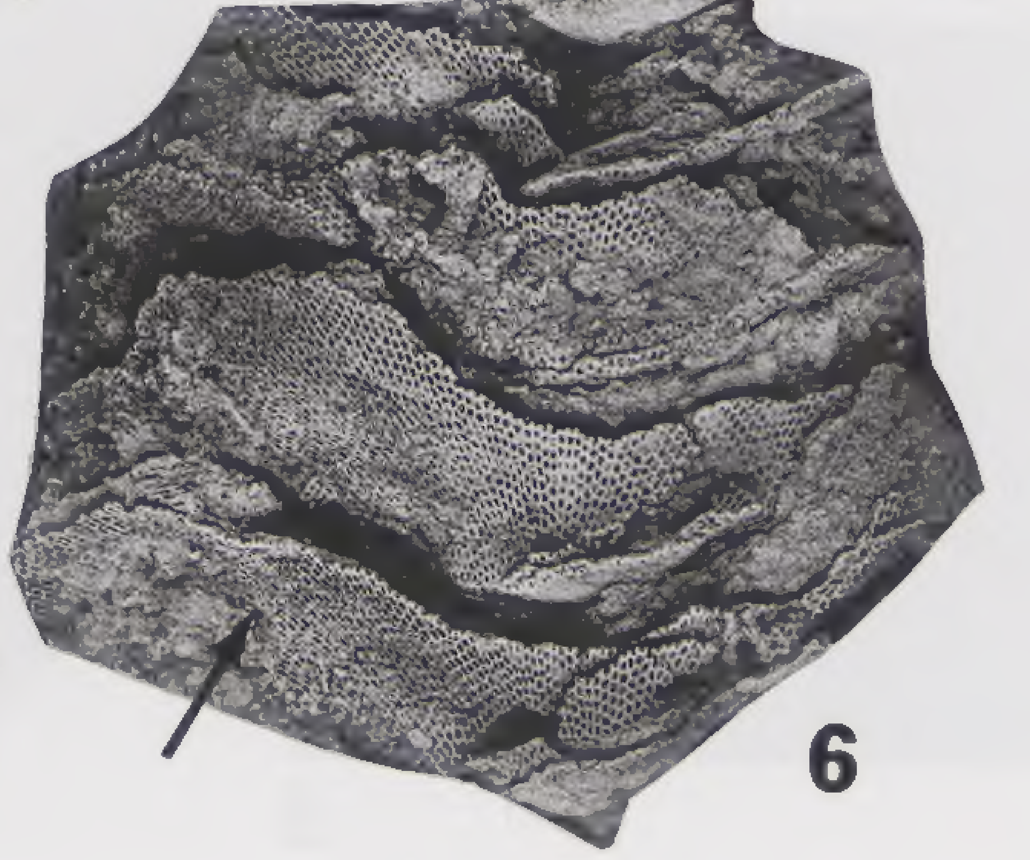

6

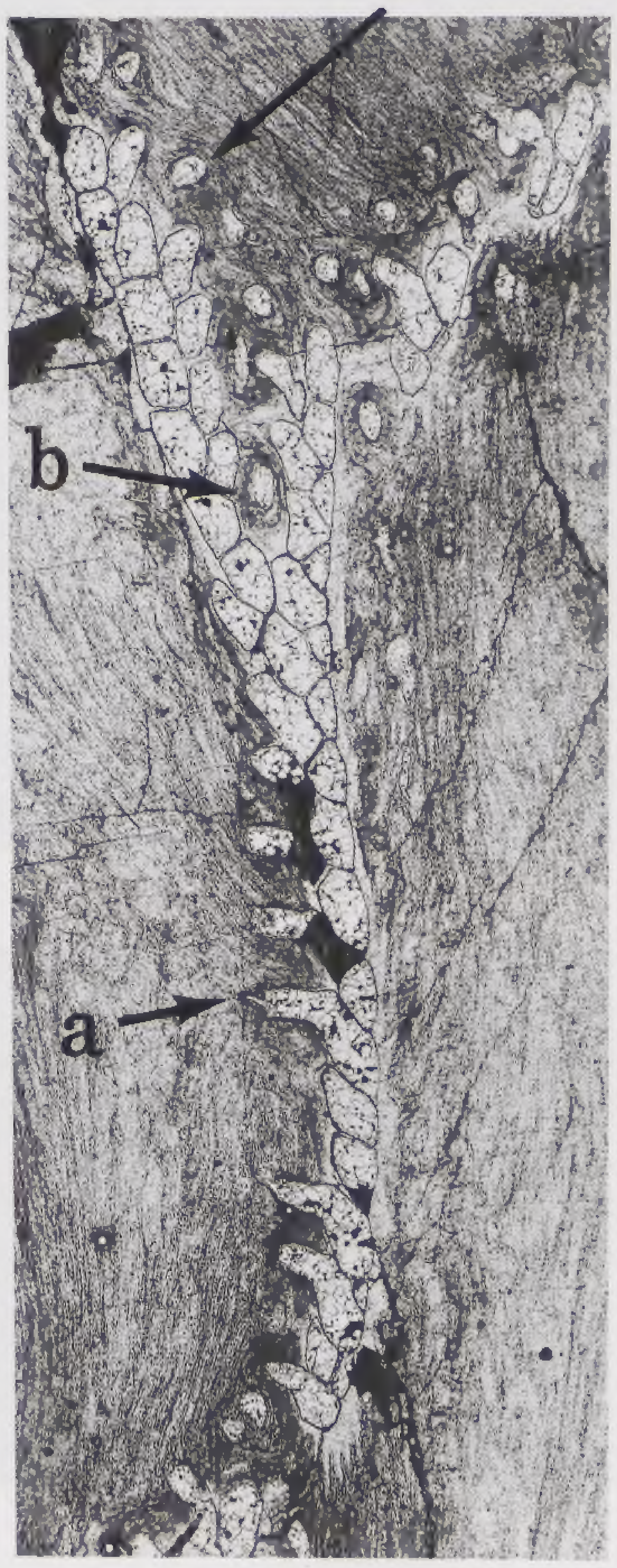

7

1
2
3
4
5
6
7
8
9

EXPLANATION OF PLATE 56

Figure | Page

1, 2. ***Archimedes owenanus*** (Hall, 1857b) 127

Figured specimen, UI X-6973. 1. AM42, section cutting plane of central axis showing whorl development (arrows **a** and **b**) as a result of thickened lamellar skeleton (arrow **c**) covering mesh surfaces laterally away from axial branch. Note obverse surface always faces upward in life position, ×12. 2. AM40, longitudinal section of spiral axis showing whorl (arrow **a**) connected to central axial branch which changes orientation with spiraling (arrow **b**), ×20.

3–9. ***Archimedes wortheni*** (Hall, 1857b) 130

3. Figured specimen, UI X-6991. Reverse exterior view of mesh showing typical mesh pattern (arrow **a**) adjacent to area overgrown by lamellar skeleton (arrow **b**). Such overgrown areas appear to represent healing of injured or broken areas of zoarial meshwork, ×2.

4, 6. Figured specimen, UI X-7014. 4. Dextrally spiraling central axis developed distal (arrow) to inferred ancestrula, ×6; 6. Site of initial axial development at apparent distal end of mesh. Observe tip of thickened branch edge possibly representing ancestrula (arrow **a**) from which single thickened branch develops (arrow **b**). Mesh extends outward from one side of branch as suggested by fenestrule development (arrow **c**), with initial spiral observed shortly in distal direction (arrow **d**), ×24.

5. Figured specimen, UI X-6992. Exterior side view of well-preserved dextrally spiraling specimen showing thick central axis (arrow **a**) with mesh still attached to axis and extending outward at angle characteristic of that in life (arrows **b** and **c**). Observe area at edge of axis (arrow **d**) where mesh is partially overgrown by thickened lamellar skeleton of axis, and typical pattern of reverse mesh (arrow **e**), which radiates outward from axis, ×2.

7. Figured specimen, UI X-6995. Exterior side view of dextrally spiraling central axis (arrow **a**) showing zoarial supports (arrow **b**) developed between whorls as extensions of reverse zoarial (axial) surface (arrow **c**). Note thickened edge of axis from which mesh projects (arrow **d**), ×2.

8. Topotype, ISGS (ISM) 2780-2, exterior view of reverse mesh surface illustrating central axis (arrow **a**) with attached mesh radiating outward (arrow **b**) from axis, ×2.

9. Figured specimen, UI X-7005. View looking distally from end of axis showing mud and broken skeletal fragments infilling spacing between mesh projecting from axial whorls (arrow). Such infilling may have occurred while colony was in life position, ×2.

EXPLANATION OF PLATE 57

Figure Page

1–9. ***Archimedes wortheni*** (Hall, 1857b) 130

1, 3. Figured specimen, UI X-6997. 1. Reverse exterior surface illustrating elliptical, ovate, or circular fenestrule shape (arrow **a**) and initial development of reverse zoarial supports (arrow **b**), ×10; 3. Exterior side axial view showing mesh still attached to central axis (arrow), ×1.

2, 7. Figured specimen, UI X-7005. 2. Exterior view of central axis from distal end of zoarium illustrating whorled appearance of thickened lamellar skeleton that forms the axis (arrow **a**), zoarial mesh overgrown by lamellar skeleton at edge of axis (arrow **b**) and mesh not overgrown (arrow **c**) toward most distal end of mesh, ×5; 7. Obverse exterior surface of zoarial mesh illustrating extension of abaxial aperture edge into fenestrule (arrow **a**), and thickening of keel and nodes along obverse branch surface (arrow **b**). Note thickening of lamellar skeleton across zoarial surface and capping of apertures by terminal diaphragms, ×30.

4–6. Figured specimen, UI X-6994. 4. Obverse exterior mesh surface of well-preserved fragment illustrating incomplete peristome (arrow **a**) surrounding aperture with opening occurring at proximal to proximal–adaxial aperture edge (arrow **b**), central keel (arrow **c**) atop which develop nodes (arrow **d**). Note site of branch bifurcation (arrow **e**) and centrally thickened terminal diaphragms capping apertures, ×30; 5. Obverse exterior surface view of meshwork overgrown by ridged lamellar skeleton (arrow) developing at edge of axis, ×12; 6. Exterior side axial view of large zoarial fragment containing large areas of mesh attached to axis (arrow), ×2.

8. Figured specimen, UI X-6999. Obverse exterior surface showing heterozooecia (ovicells?) developed along branch midline (arrow), ×40.

9. Figured specimen, UI X-7008. Reverse exterior surface of mesh illustrating pronounced variations in fenestrule outline (arrows **a** and **b**) in reverse view and appearance at site of branch bifurcation (arrow **c**), ×20.

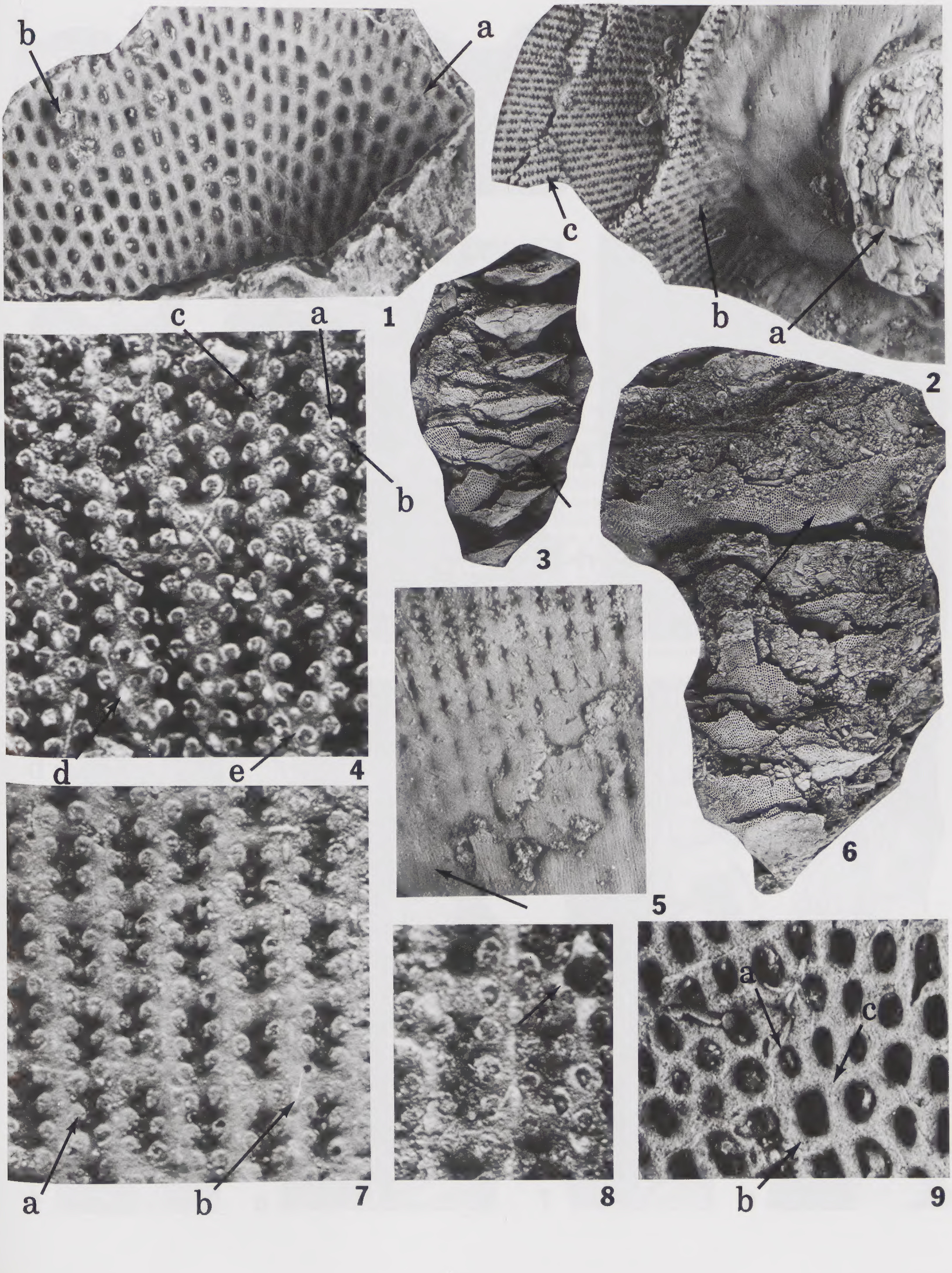
b
a
1
c
b
a
2
c
a
b
3
d
e
4
5
6
a
b
7
8
a
c
b
9

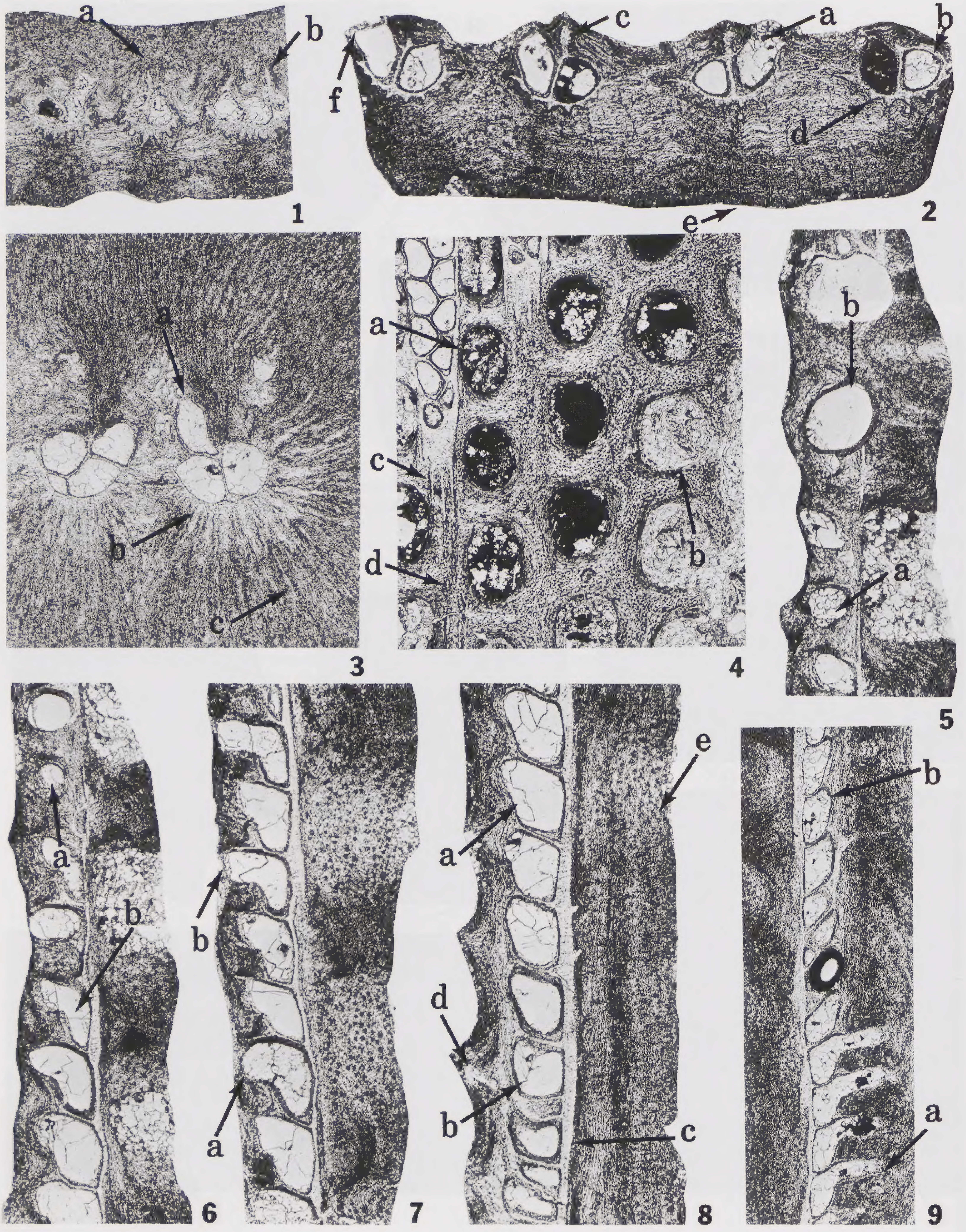
a
b
1
c
a
b
f
d
e
2
a
b
c
3
a
c
d
b
4
b
a
5
a
b
6
b
a
7
e
a
d
b
c
8
b
a
9

EXPLANATION OF PLATE 58

Figure Page
1–9. ***Archimedes wortheni*** (Hall, 1857b) 130

1, 2, 4–8. Figured specimen, UI X-6991. 1. AG72, transverse section showing secondary lamellar skeletal layer (arrow **a**) at axial edge overgrowing apertures (arrow **b**) which are capped with granular skeletal plug developed as extensions of centrally thickened diaphragm, ×40; 2. AG69, transverse section showing typical attitudinal relationship of aperture to plane of obverse surface (arrow **a**), and granular skeletal layer continuous around autozooecial chambers (arrow **b**), with nodes (arrow **c**), reverse longitudinal striae (arrow **d**) and microstylets (arrow **e**). Note terminal diaphragm (arrow **f**) capping aperture, ×70; 4. AG77, mid to deep tangential section showing change in fenestrule outline from mid (arrow **a**) to deep (arrow **b**) tangential view, and granular skeletal layer continuous with longitudinal striae (arrow **c**), and reverse microstylets developing as extensions of these striae (arrow **d**), ×40; 5. AG70, shallow to very shallow longitudinal section, obverse to left, illustrating aperture edge in very shallow longitudinal view (arrow **a**) and heterozooecia (ovicells?) as enlargements of aperture (arrow **b**) extending into fenestrule, ×70; 6. AG70, mid to shallow longitudinal section, obverse to left, showing aperture opening at edge of fenestrule (arrow **a**) and typical chamber outline in shallow longitudinal view (arrow **b**), ×70; 7. AG74, mid to mid shallow longitudinal section, obverse to left, illustrating typical autozooecial chamber outline in mid shallow longitudinal view (arrow **a**) and terminal diaphragm (arrow **b**) capping aperture, ×70; 8. AG70, mid to deep longitudinal section, obverse to left, illustrating typical chamber outline in mid (arrow **a**) to deep (arrow **b**) longitudinal view, and continuity of granular skeletal material (arrow **c**) around autozooecial chambers, and with obverse nodes (arrow **d**) and reverse microstylets (arrow **e**), ×70.

3. Figured specimen, UI X-6998. AM61, transverse section of axial branch (arrow **a**) viewed toward proximal end of zoarium with aperture plugged by lamellar skeleton of the axis, thick granular skeletal layer (arrow **b**) surrounding branch and continuous with microstylets (arrow **c**) extending through lamellar skeleton of axis. The axial branch acts as a guide determining direction and rate of of axis rotation, with adjacent lateral branches following the lead of this central, pivotal branch. The obverse surface of the axial branch "points" toward the direction of spiraling; whether the lateral branches are in the left or right side of the axial branch determines if the spiral will be dextral or sinistral, ×60.

9. Figured specimen, UI X-7000. AM79, deep to mid shallow longitudinal section, obverse to right, showing elongate vestibule (arrow **a**) developed as aperture was overgrown by lamellar skeleton in an attempt by the individual to remain connected with the outside environment, and chamber outline in deep longitudinal view (arrow **b**), ×40.

EXPLANATION OF PLATE 59

Figure | Page

1–5. ***Archimedes wortheni*** (Hall, 1857b) 130

1. Figured specimen, UI X-6990. AI71, shallow to deep tangential section of zoarial fragment exhibiting pronounced ontogenetic thickening. Note site of branch bifurcation (arrow **a**) and fenestrules partially to completely plugged by lamellar skeleton (arrow **b**), ×20.
2. Figured specimen, UI X-6997. AM84, very shallow tangential section showing incomplete peristome (arrow **a**) surrounding all but most proximal to proximal–adaxial aperture edge (arrow **b**), peristome at edge of aperture overgrown by lamellar skeleton (arrow **c**), keel (arrow **d**) atop which nodes develop (arrow **e**), and obverse stylets (arrow **f**) continuous with inner granular skeletal layer, ×70.

3–5. Figured specimen, UI X-6991. Large, well-preserved zoarial fragment. 3. AG75, mid to shallow tangential section. Observe circular heterozooecia (ovicells?) with central opening (arrow **a**) surrounded by a circular layer of lamellar skeleton (arrow **b**), and extension of abaxial edge of aperture (arrow **c**) into fenestrule causing inflections in fenestrule outline near obverse surface, ×70; 4. AG75, very deep tangential section illustrating granular appearance caused by presence of abundant microstylets (arrow) continuous with inner granular skeletal layer, ×70; 5. AG67, mid to deep tangential section showing typical autozooecial chamber outline in mid (arrow **a**) and deep (arrow **b**) tangential views. Note increased variability of chamber outline in mid tangential view at site of branch bifurcation (arrow **c**), lack of extension of aperture into fenestrule in mid tangential view (arrow **d**), and continuity of granular skeletal material between branches across dissepiment (arrow **e**), ×70.

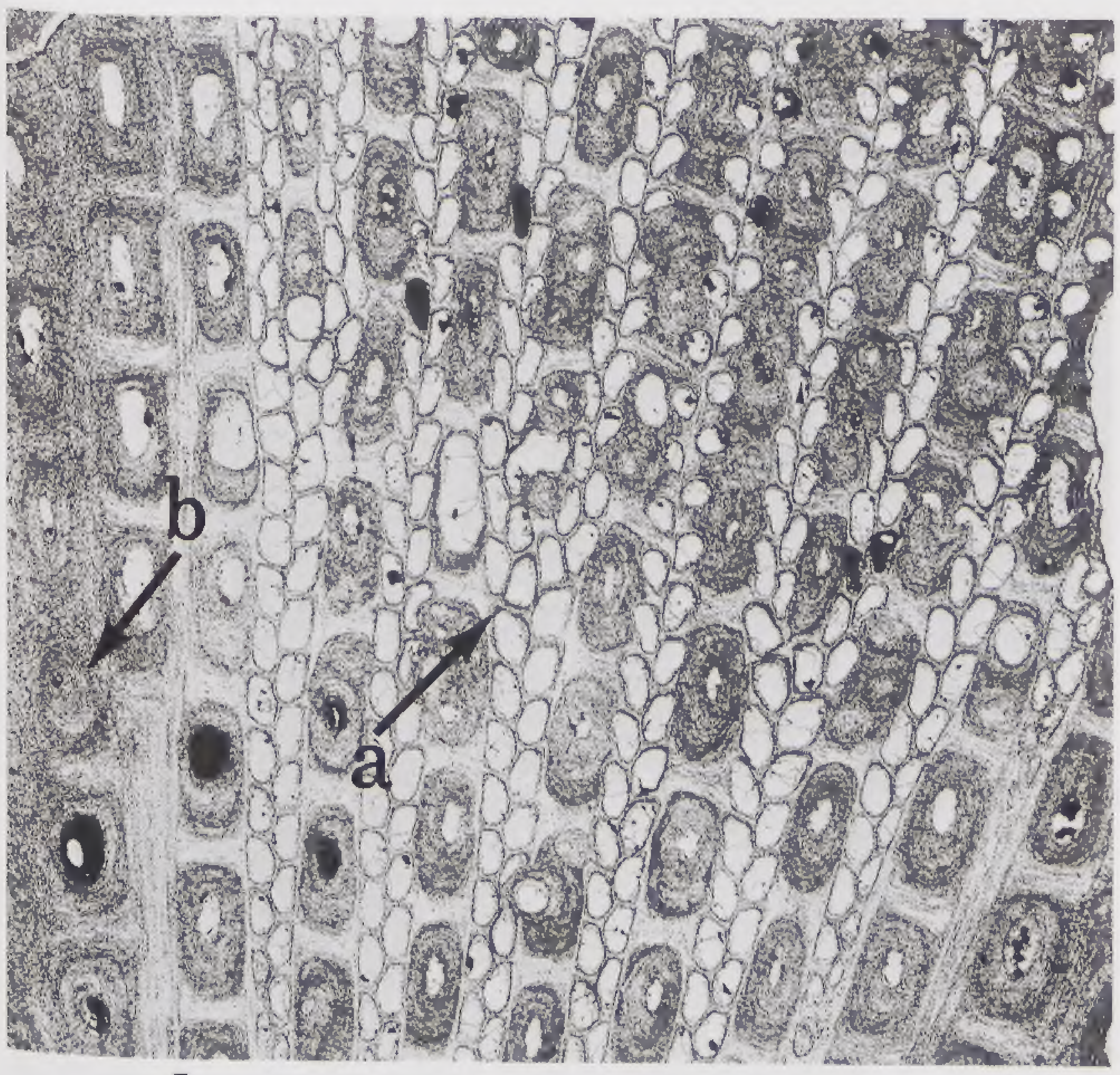

1

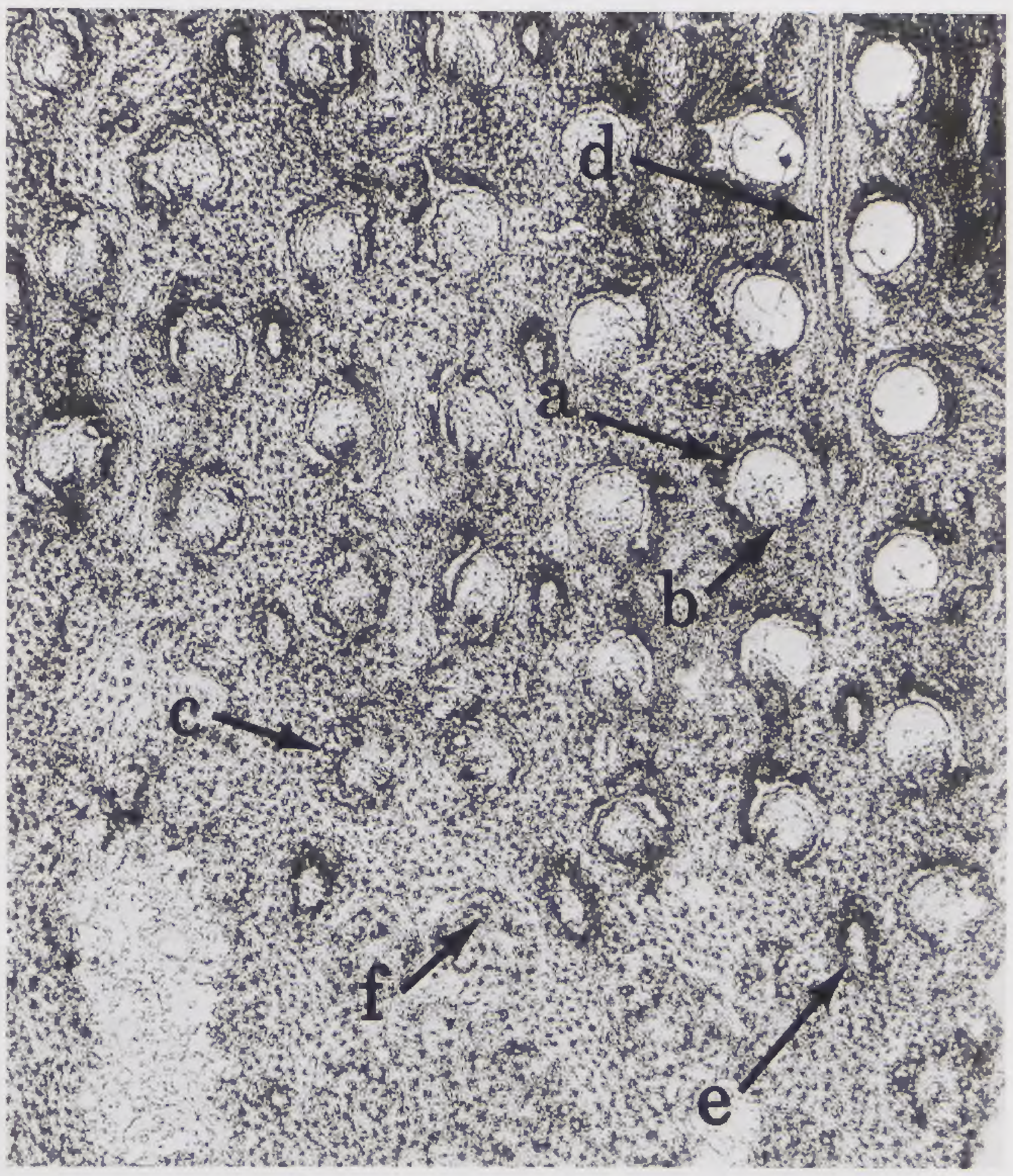

2

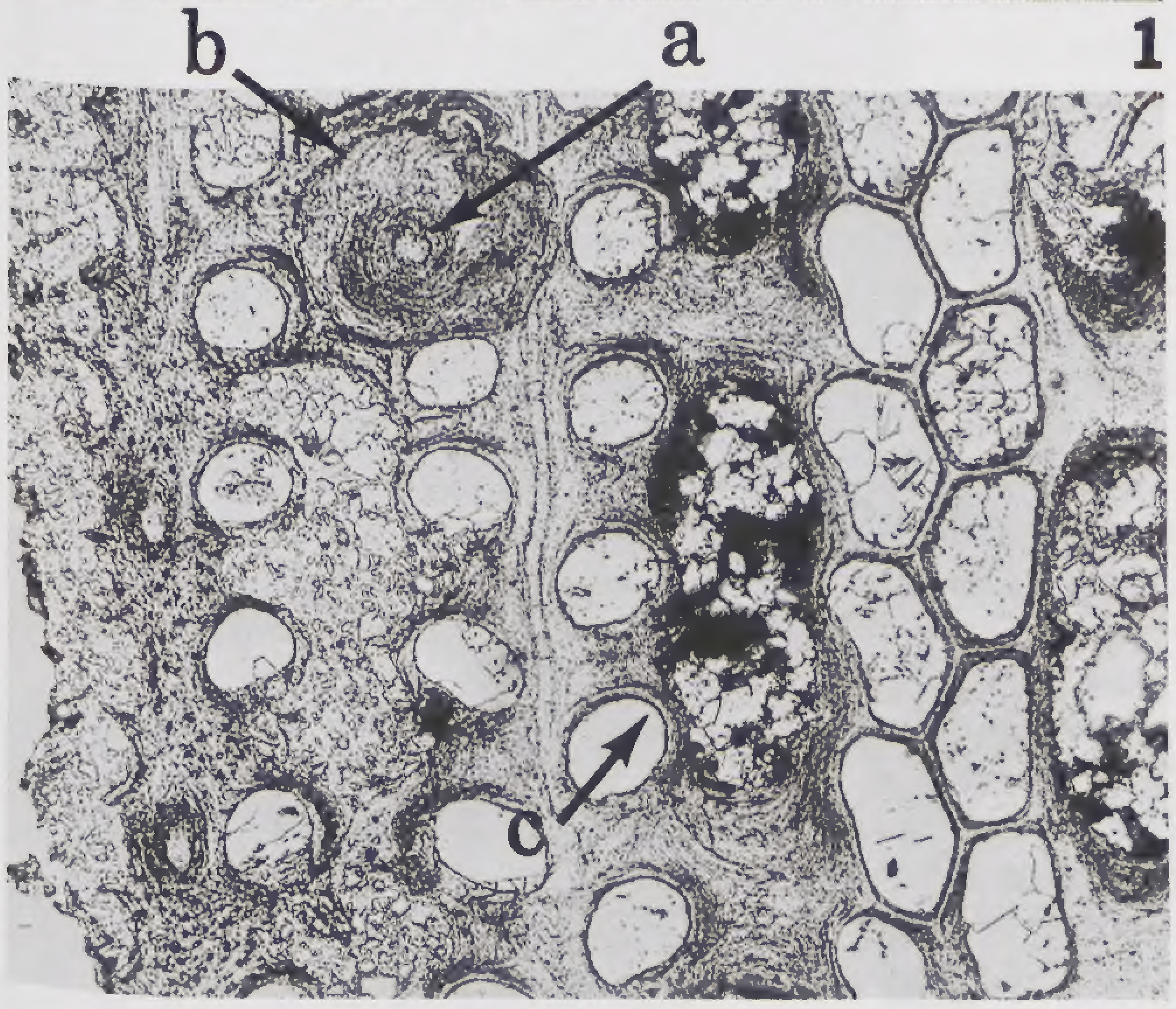

3

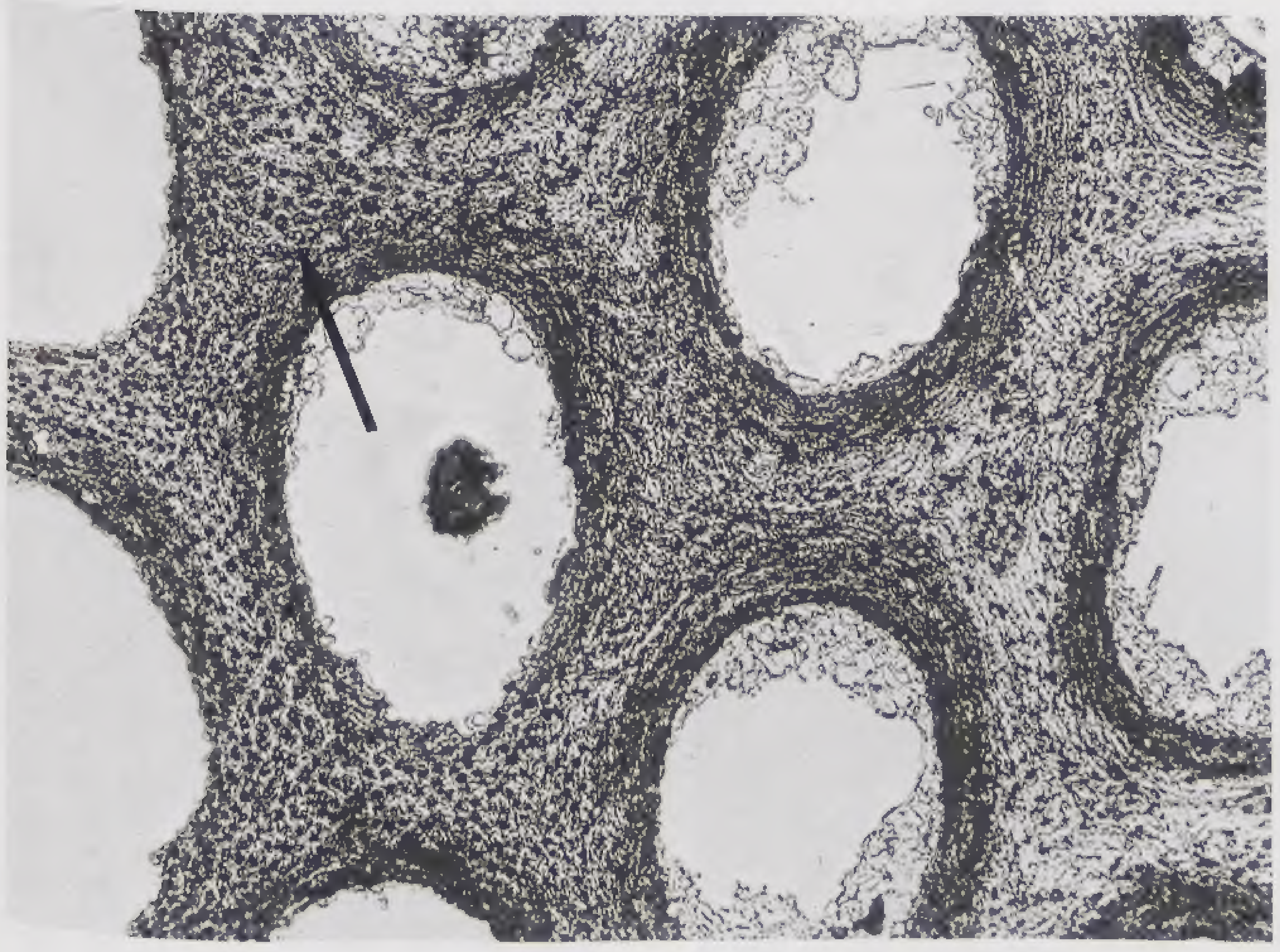

4

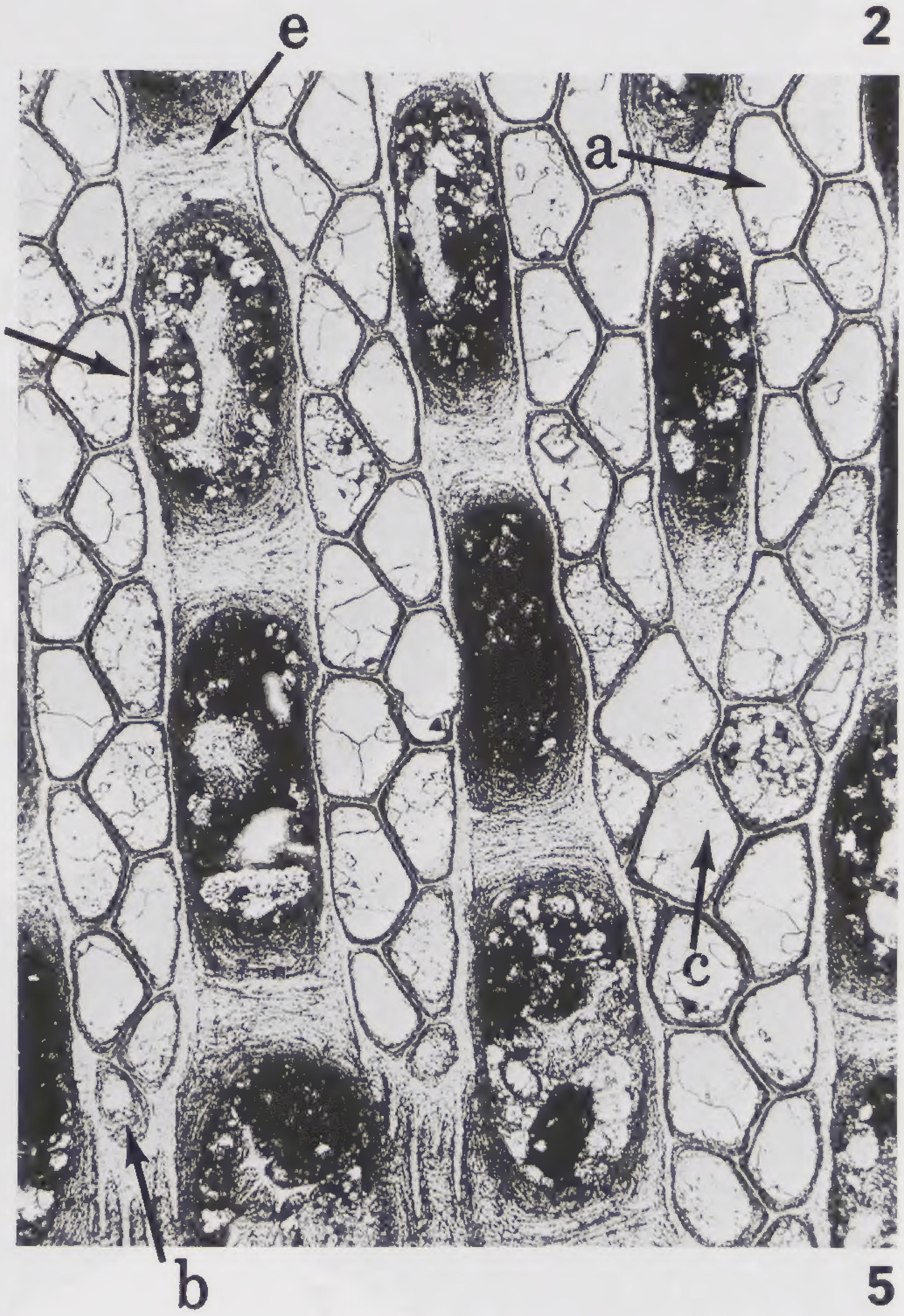

5

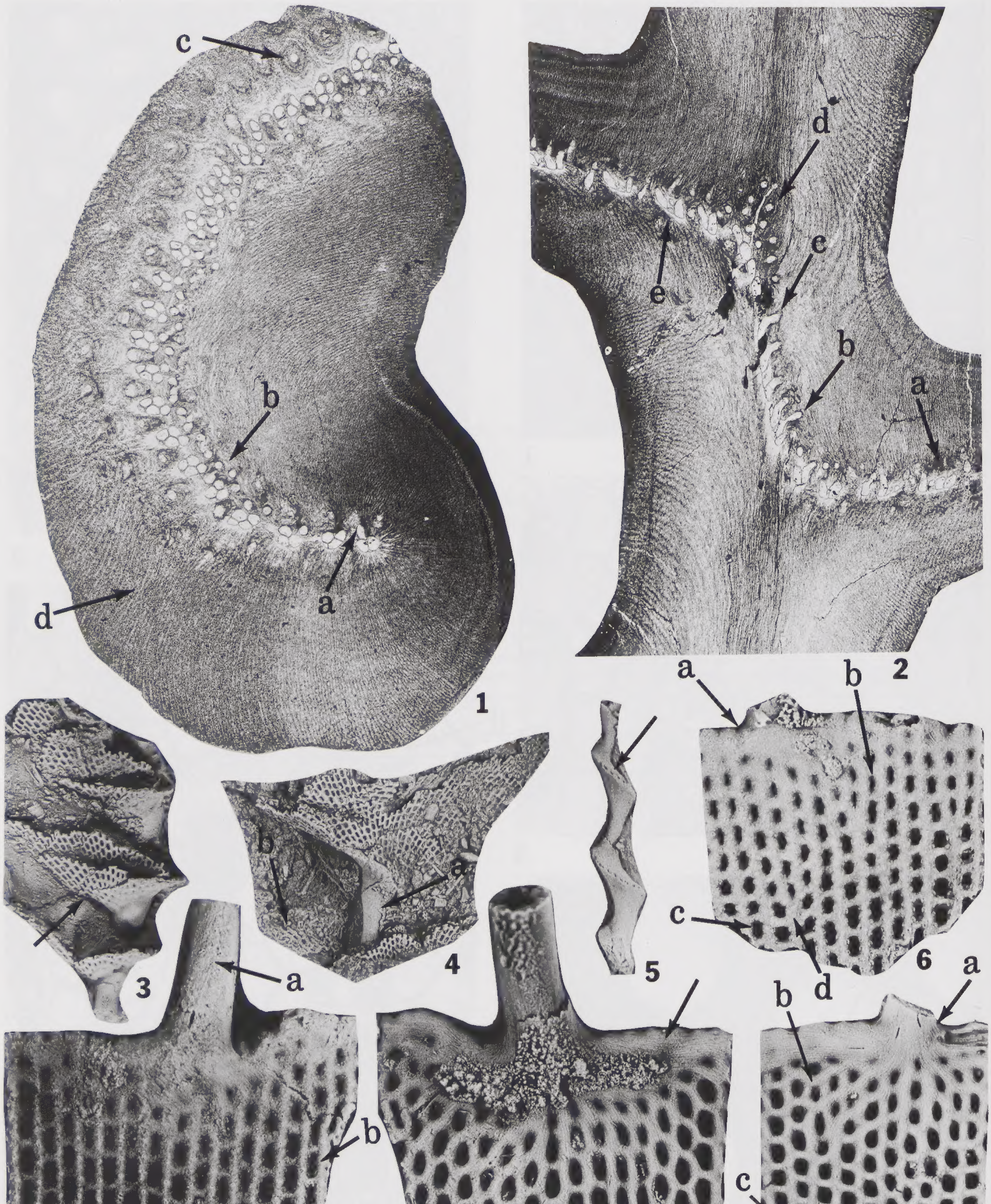

EXPLANATION OF PLATE 60

Figure Page

1, 2. ***Archimedes wortheni*** (Hall, 1857b) 130

Figured specimen, UI X-6998. 1. AM61, transverse section of large central axis showing central axial branch (arrow **a**) pointing toward direction of axial spiral (in this case dextral) as viewed from proximal end of axis looking toward distal end. When viewed toward distal end of zoarium, if lateral branches develop to the right of the axial branch, spiraling is dextral; when lateral branches develop to the left of axial branch in the same view, spiraling is sinistral. The axis spirals toward the obverse surface, resulting in concave obverse and convex reverse mesh surfaces, respectively. Observe change in mesh orientation proceeding outward from central axis, going from transverse (arrow **a**) to slightly askew, poorly oriented transverse (arrow **b**) to approaching tangential view as mesh flattens toward whorl (arrow **c**). Also note development of thick lamellar skeletal layer (arrow **d**) forming central axis surrounding axial branch, ×15; 2. AM58, longitudinal section near center of axis just shallow of central axial branch. Change in branch orientation can be observed proceeding from axial whorl (arrow **a**), to longitudinal section approximately pointing toward axial whorl (arrow **b**). Also shown is a misoriented longitudinal section exhibiting elongate vestibule (arrow **c**), tangential section (arrow **d**) associated with change of central axial branch orientation deeper in central axis than shown in section, and axial whorl (arrow **e**). Direction of axial spiral is dextral, ×12.

3–9. ***Archimedes valmeyeri***, new species 133

3. Holotype, UI X-6987. Exterior side view of dextrally spiraling specimen illustrating central axis (arrow) with zoarial mesh developed as extensions at lateral edge of axial whorls, ×2.

4. Paratype, UI X-6988. Exterior side view of sinistrally spiraling zoarium showing central axis (arrow **a**) and obverse mesh surfaces (arrow **b**) radiating outward from central axis, ×2.

5. Paratype, UI X-6989. Exterior side view of sinistrally spiraling specimen illustrating whorls (arrow) from which branches extend, ×2.

6, 9. Paratype, UI X-6981. 6. Obverse exterior surface of zoarial fragment having well-developed zoarial support (arrow **a**) at distal edge of fragment. Note fenestrules almost completely overgrown by lamellar skeleton at distal end of fragment (arrow **b**), and open with lesser overgrowths (arrow **c**) toward proximal end; also shown is site of branch bifurcation (arrow **d**), ×8; 9. Reverse exterior surface illustrating zoarial support (arrow **a**) developed at distal edge of fragment, fenestrules almost completely overgrown by lamellar skeleton at fragment distal edge (arrow **b**) and fenestrules open toward proximal end (arrow **c**), and site of branch bifurcation (arrow **d**), ×8.

7, 8. Paratype, UI X-6979. 7. Obverse exterior surface showing zoarial support (arrow **a**) and obverse mesh surface not covered by thickened lamellar skeleton (arrow **b**). Note typical mesh appearance in this species, ×8; 8. Reverse exterior surface of zoarial fragment exhibiting pronounced ontogenetic thickening, with zoarial support developed at distal mesh edge and thickened lamellar skeleton (arrow) coating distal edge of zoarial mesh, ×8.

EXPLANATION OF PLATE 61

Figure Page

1–8. ***Archimedes valmeyeri,*** new species 133

1. Paratype, UI X-6979. Obverse exterior surface showing aperture extending into fenestrule (arrow **a**) with incomplete peristome partially surrounding aperture open at proximal to proximal–adaxial edge, keel atop which develop numerous nodes (arrow **b**) which also are present atop dissepiment (arrow **c**), and small stylets (arrow **d**) atop obverse surface, ×25.

2, 3, 5–7. Paratype, UI X-6981. FY72. 2. Transverse section illustrating terminal diaphragm (arrow **a**) plugging aperture that exhibits typical attitudinal relationship to plane of obverse surface, granular skeletal layer continuous around autozooecial chambers, with reverse longitudinal striae (arrow **b**) and nodes (arrow **c**). Note fenestrule width between branches (arrow **d**) and typical chamber outline in transverse cross-sectional view (arrow **e**), ×70; 3. Very shallow longitudinal section, obverse to left, illustrating transverse section of dissepiment and continuity of granular skeleton through middle of dissepiment (arrow), ×70; 5. Mid to deep longitudinal section, obverse to left, illustrating chamber outline in mid (arrow **a**) and deep (arrow **b**) longitudinal views; also shown is obverse node (arrow **c**) continuous with granular skeletal layer surrounding autozooecial chambers, ×70; 6. Very shallow to mid longitudinal section, obverse to left, showing elongate vestibule (arrow) developing as a result of thickening of obverse lamellar skeletal layer, ×70; 7. mid to very shallow longitudinal section showing autozooecial chamber outline in mid (arrow **a**) and very shallow (arrow **b**) longitudinal views. Note extensions of aperture opening into fenestrule (arrow **c**), ×70.

4. Holotype, UI X-6987. AI30, transverse section exhibiting pronounced ontogenetic thickening of lamellar skeletal layer at edge of axis covering obverse surface. Note continuity of granular skeletal layer around autozooecial chambers, across dissepiment (arrow **a**), with terminal diaphragm (arrow **b**), small obverse stylets (arrow **c**) and reverse microstylets (arrow **d**), ×70.

8. Paratype, UI X-6989. AI90, section cutting along central plane of sinistrally spiraling axis showing change in central branch orientation as this branch spirals along center of axis, changing branch orientations include tangential at proximal fragment end (arrow **a**), longitudinal with obverse to left in middle of fragment (arrow **b**), and back to approaching deep tangential at distal end of fragment (arrow **c**), ×20.

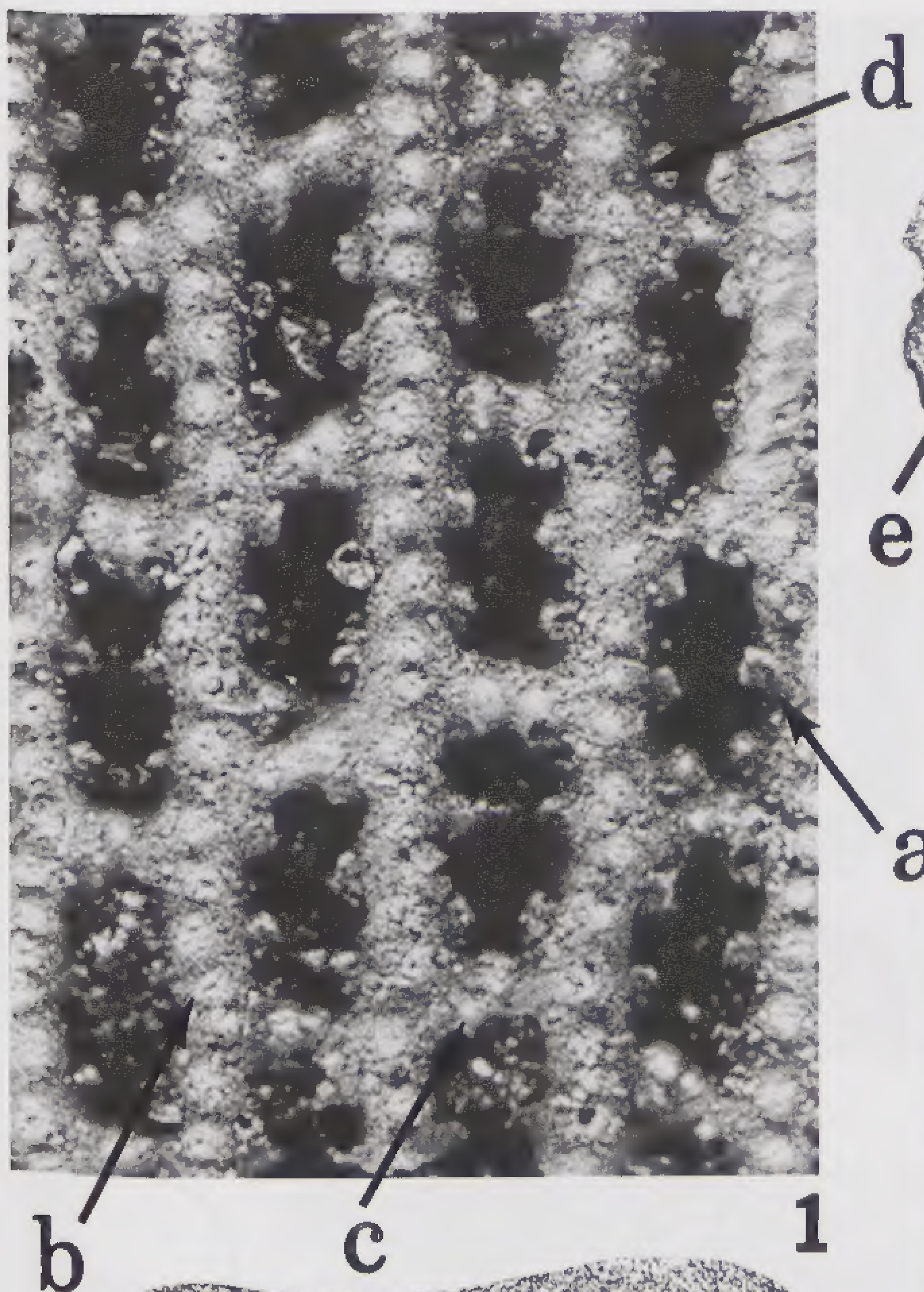

1

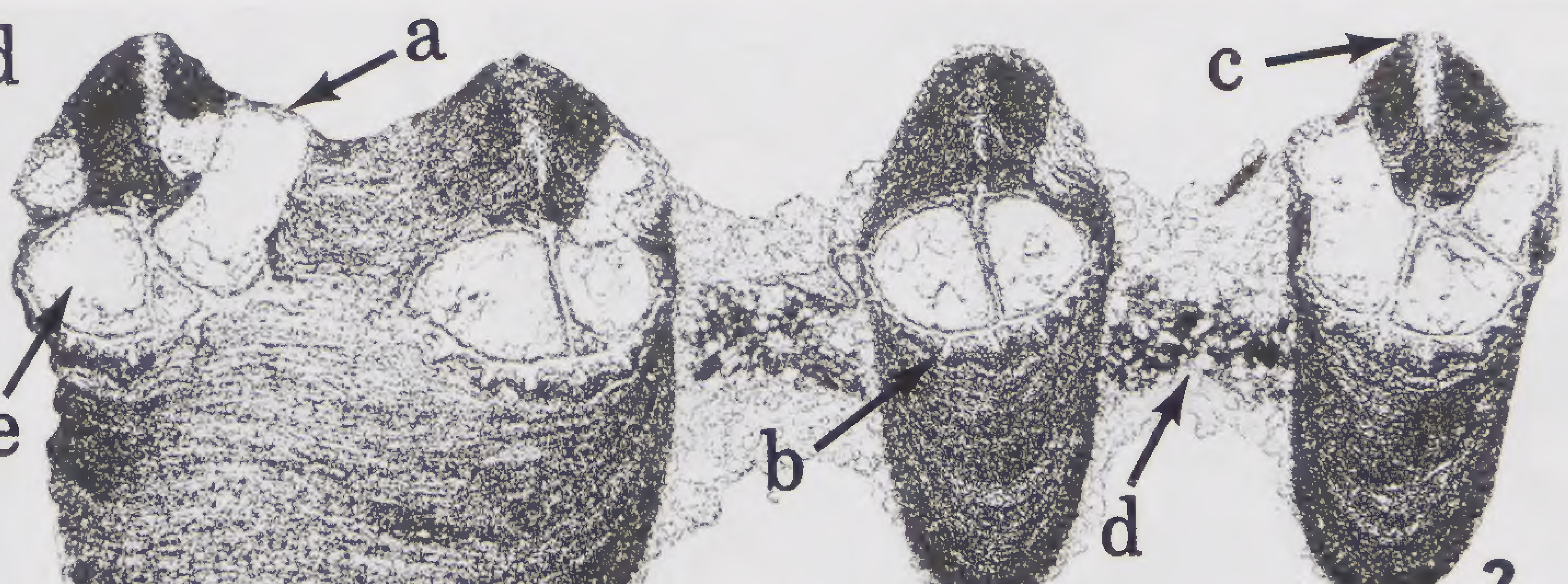

2

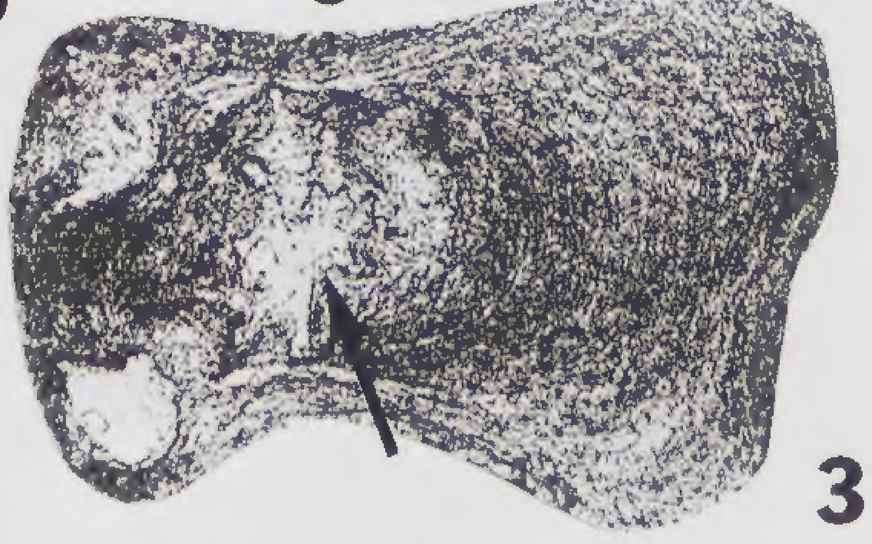
3

4

5

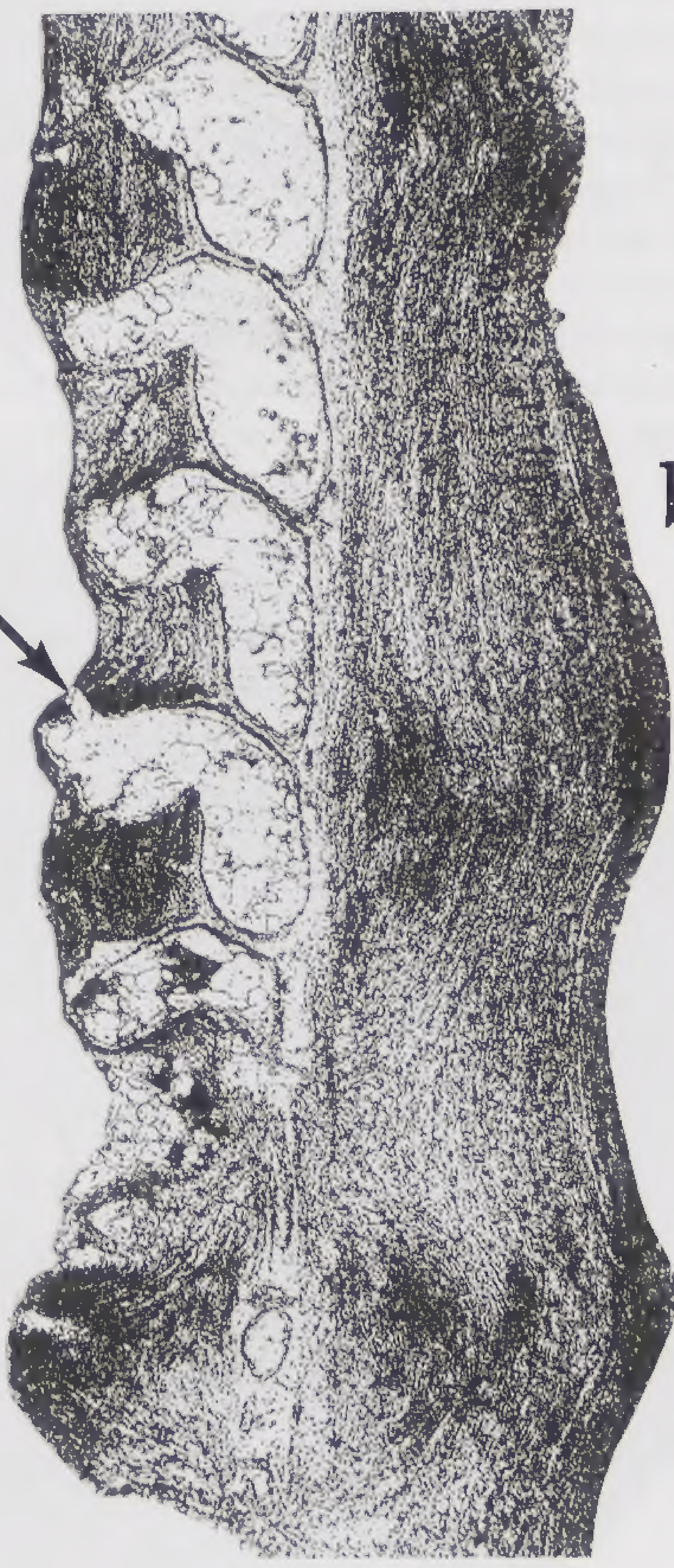
6

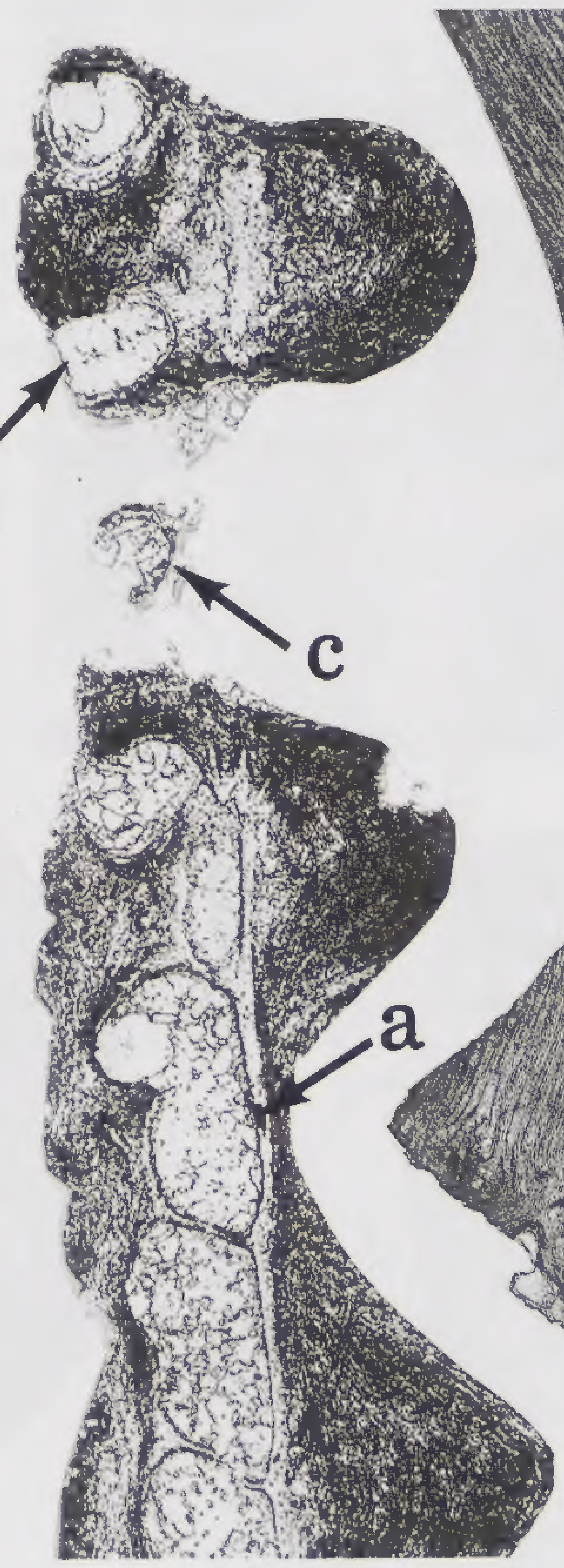

7

8

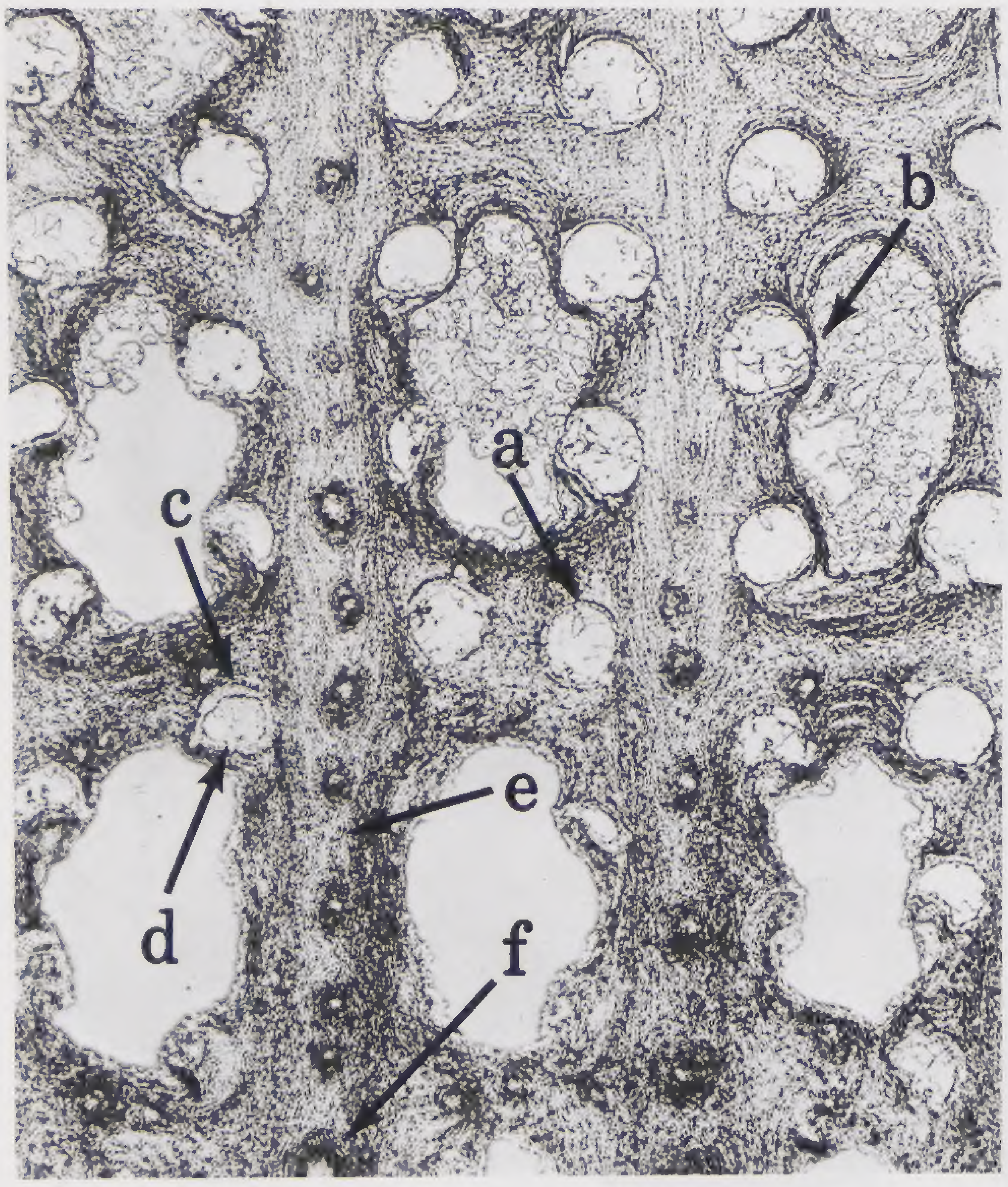

1

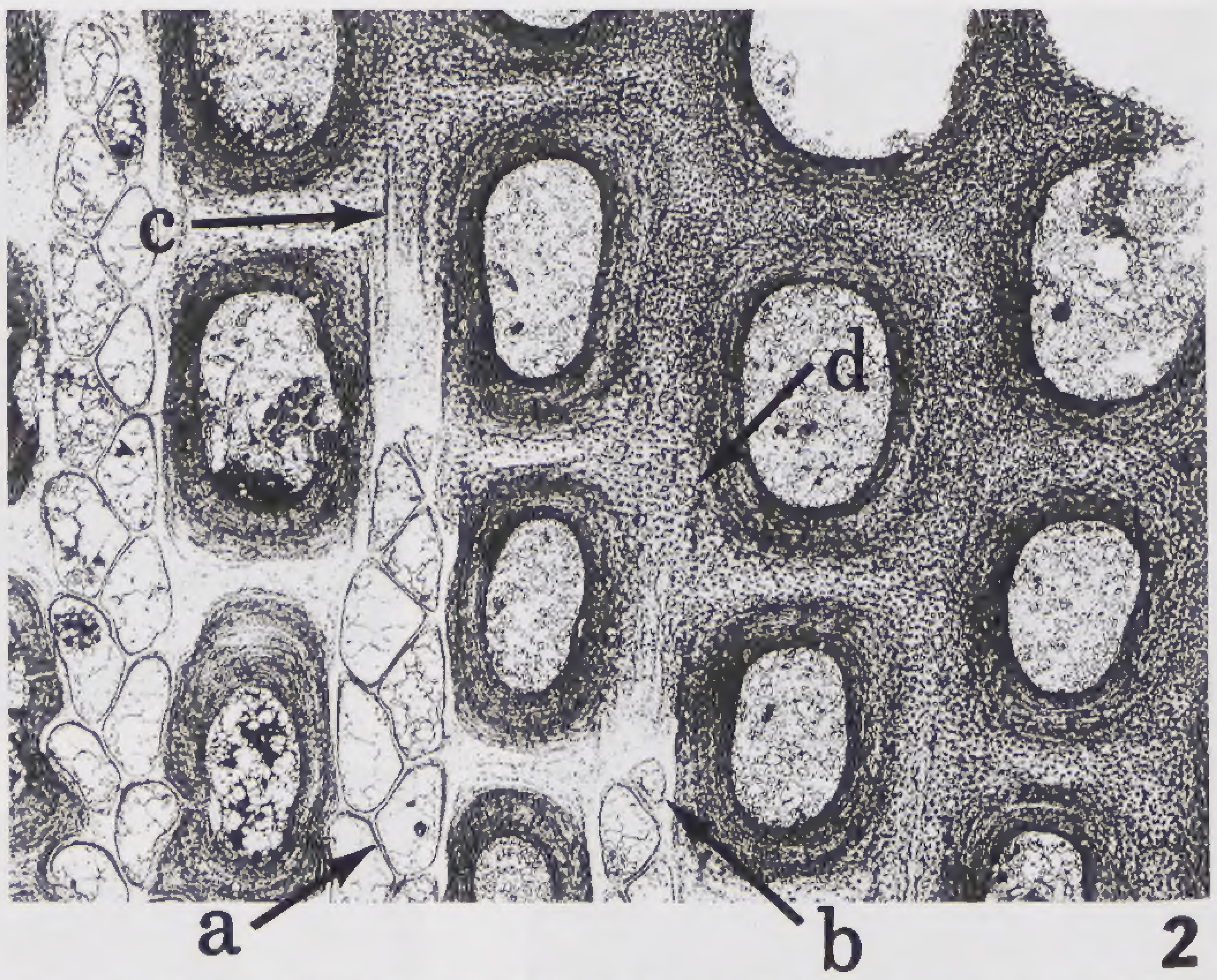

2

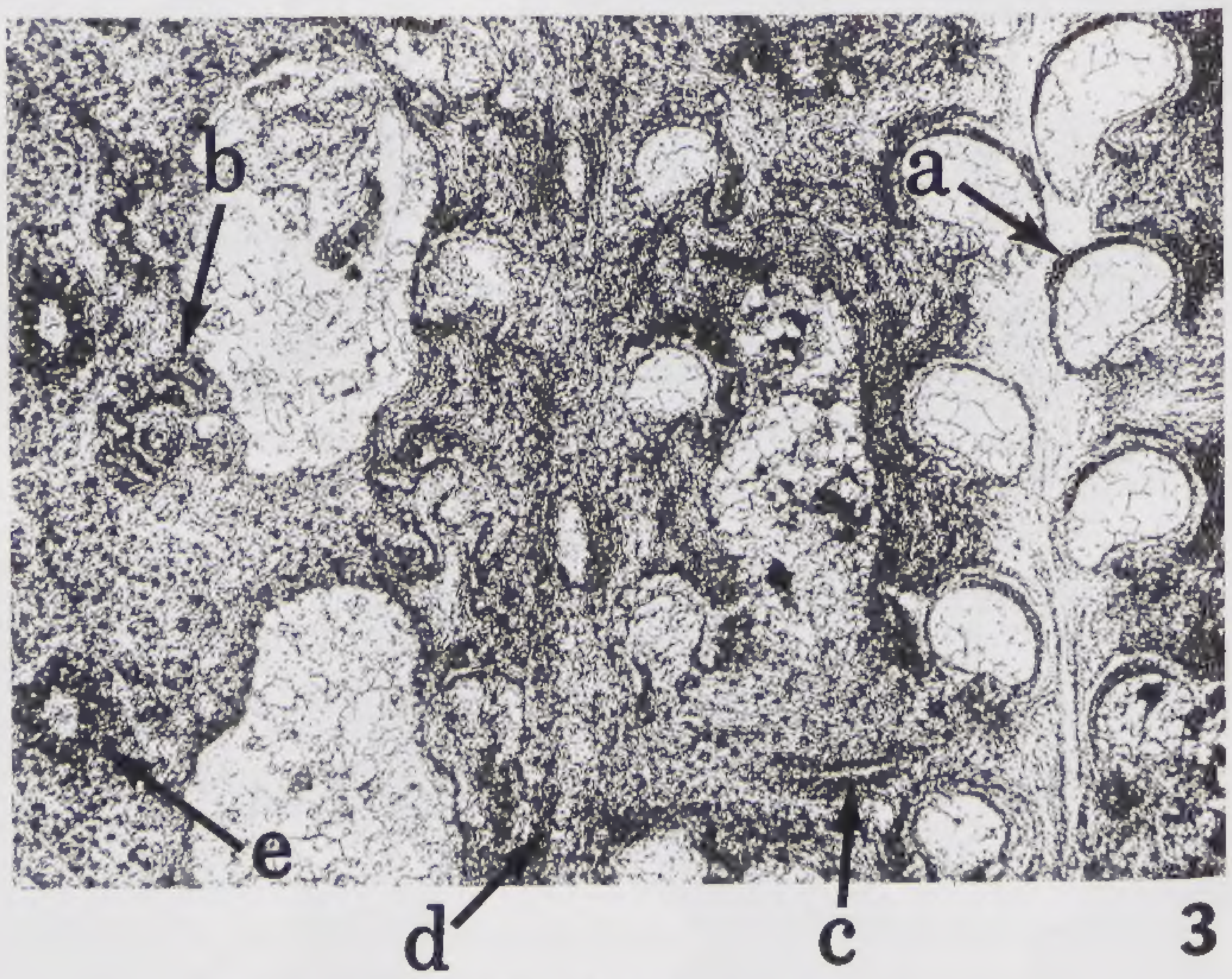

3

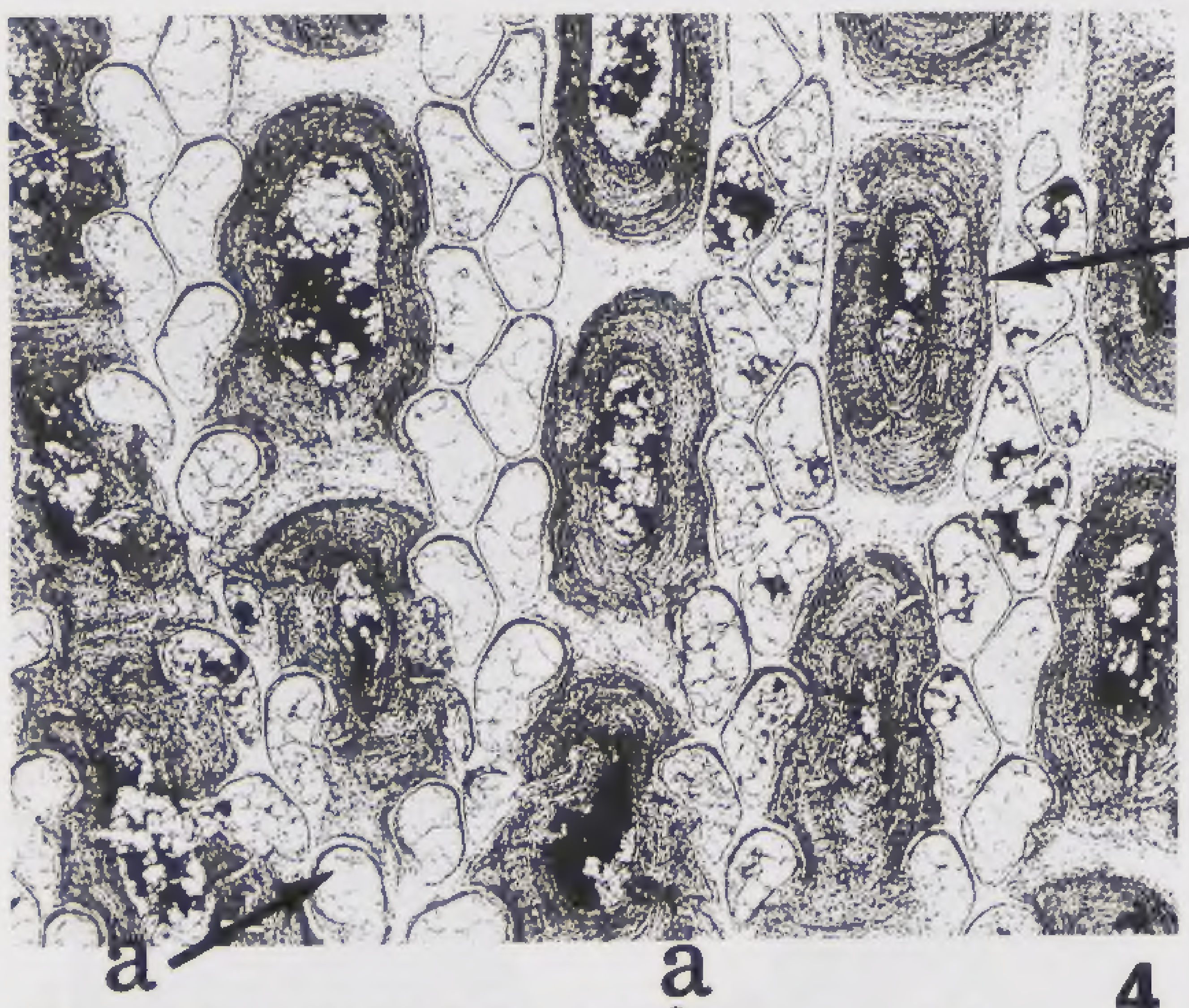

4

5

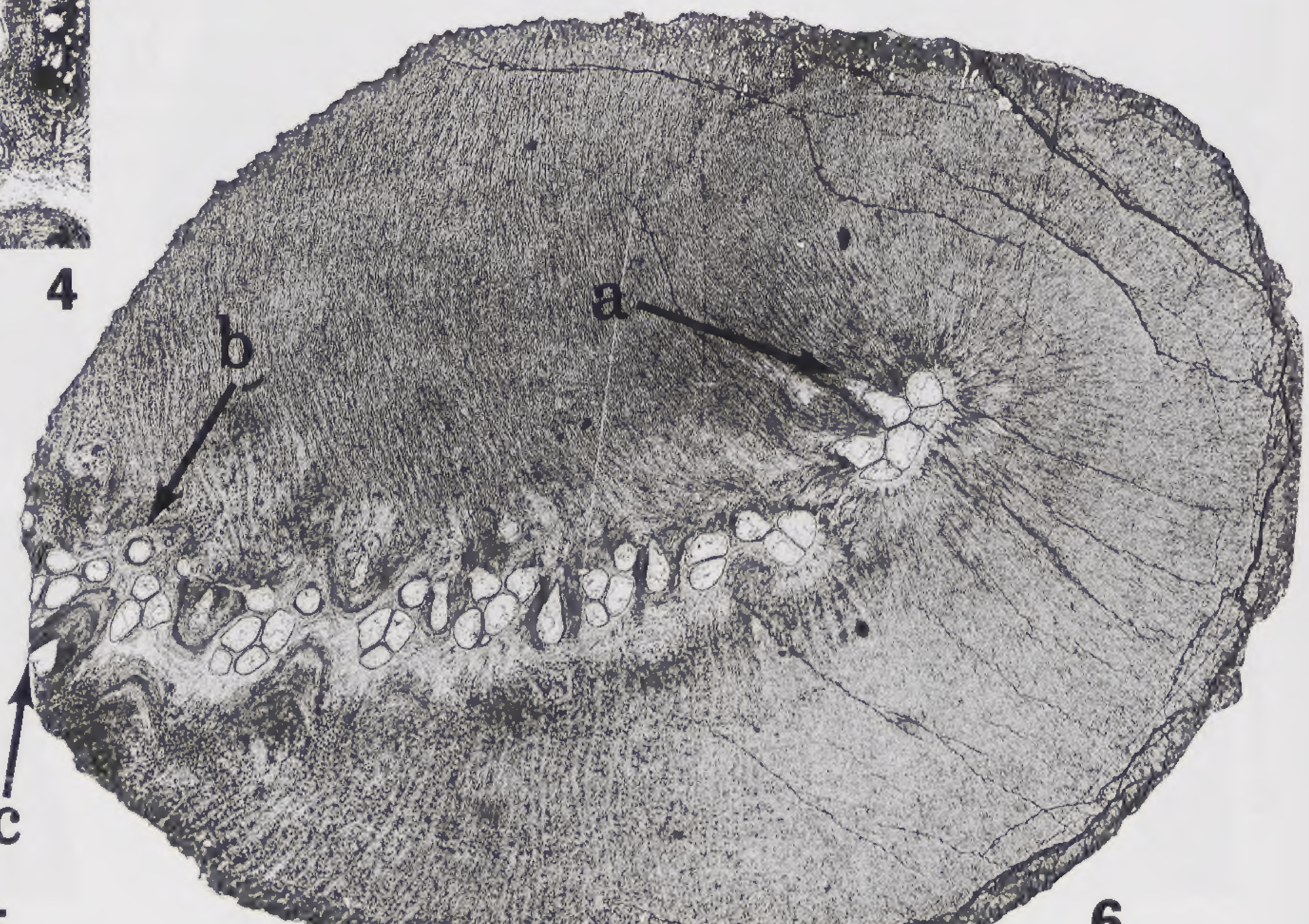

6

EXPLANATION OF PLATE 62

Figure Page

1–6. ***Archimedes valmeyeri,*** new species 133

1. Paratype, UI X-6981. FY77, shallow to very shallow tangential section illustrating typical aperture outline (arrow **a**), extension of aperture into fenestrule (arrow **b**) in shallow view causing inflection in fenestrule outline, incomplete peristome (arrow **c**) open at proximal to proximal–adaxial edge (arrow **d**), keel (arrow **e**), and nodes (arrow **f**) positioned atop keel, ×70.

2–5. Holotype, UI X-6987. 2. AI28, mid shallow to deep tangential section. Note typical autozooecial chamber outline in mid tangential view (arrow **a**), chamber outline in deep section near reverse-wall budding-site (arrow **b**), and longitudinal striae (arrow **c**) comosed of granular skeletal material which is continuous with reverse microstylets (arrow **d**), ×40; 3. AI40, shallow to very shallow tangential section illustrating chamber outline in shallow tangential view (arrow **a**), lamellar skeleton plugging aperture (arrow **b**) exhibiting expanded peristome, longitudinal ridge across dissepiment (arrow **c**), keel (arrow **d**), and node (arrow **e**) developing atop keel, ×70; 4. AI40, shallow to deep tangential section showing typical mesh symmetry of this species. Note site of branch bifurcation (arrow **a**) and fenestrule partially plugged by lamellar skeleton (arrow **b**). Such plugging is common in mesh near axis, ×40; 5. AI40, mid tangential section illustrating heterozooecia (ovicells?) consisting of lamellar skeleton partially infilling fenestrule (arrow **a**) with perforation (arrow **b**) in center of infilling, ×70.

6. Paratype, UI X-6989. AI91, transverse section of central axis illustrating sinistral spiraling of axial section. When viewed toward distal end of axis, if lateral branches develop to the left of central axial branch (arrow **a**), spiraling is sinistral. Zoarial mesh flattens toward edge of spiral into tangential view showing aperture openings (arrow **b**) and fenestrules (arrow **c**) typical of this orientation. Note thick lamellar skeleton forming central spiral axis, ×20.

EXPLANATION OF PLATE 63

Figure Page

1–10. ***Fenestralia sanctiludovici*** Prout, 1858a 138

1. Holotype, ISGS (ISM) 4486-1, obverse exterior surface of zoarial fragment exhibiting slight ontogenetic thickening and moderately poor preservation. Note fenestrule (arrow **a**) and variation in fenestrule outlines, longitudinal ridge across obverse dissepiment surface (arrow **b**) and site of branch bifurcation (arrow **c**), ×18.

2–10. Paratype, ISGS (ISM) 4486-2. Large, moderately ontogenetically thickened zoarial fragment. 2. Obverse exterior surface illustrating thickened lamellar skeleton covering apertures (arrow **a**), causing thickening of keel (arrow **b**) and partially covering both keel and nodes (arrow **c**). Note zoarial support developed at lateral edge of zoarium (arrow **d**), ×18; 3. Side view of obverse exterior branch surface illustrating orientation of adaxial (arrow **a**) and abaxial (arrow **b**) autozooecial apertures across branch surface; also note keel (arrow **c**), and nodal (arrow **d**) development atop keel, ×35; 4. Reverse exterior zoarial surface showing site of branch bifurcation (arrow **a**) and microstylets (arrow **b**) across reverse zoarial surface, ×18; 5. FSL89, deep longitudinal section near center of branch, obverse to left, illustrating adaxial chamber outline (arrow **a**) in this view, abaxial chamber (arrow **b**) budding from edge of adaxial chamber, and granular skeletal layer (arrow **c**) continuous around autozooecial chambers, and with reverse microstylets (arrow **d**), ×70; 6. FSL41, shallow longitudinal section, obverse to left, showing reverse (arrow **a**) and obverse (arrow **b**) ends of abaxial autozooecial chambers, ×70; 7. FSL48, shallow to mid longitudinal section, obverse to right, illustrating typical abaxial chamber outline in mid longitudinal view (arrow **a**) capped by terminal diaphragm, and abaxial chamber outline in shallow longitudinal view (arrow **b**), ×40; 8. FSL33, transverse section showing mid axial wall (arrow **a**) separating adaxial autozooecia, abaxial two rows of chamber axial walls (arrow **b**), and granular skeletal layer (arrow **c**) continuous around autozooecial chambers, and with reverse longitudinal striae (arrow **d**), microstylets (arrow **e**), and obverse nodes (arrow **f**), ×70; 9. FSL86, transverse section showing terminal diaphragm (arrow) capping adaxial aperture that exhibits typical attitudinal relationship to plane of obverse surface, ×70; 10. FSL89, transverse section illustrating attitudinal relationship of adaxial (arrow **a**) and abaxial (arrow **b**) apertures relative to plane of obverse surface; also shown is continuity of granular skeletal layer across dissepiment (arrow **c**) between branches, ×70.

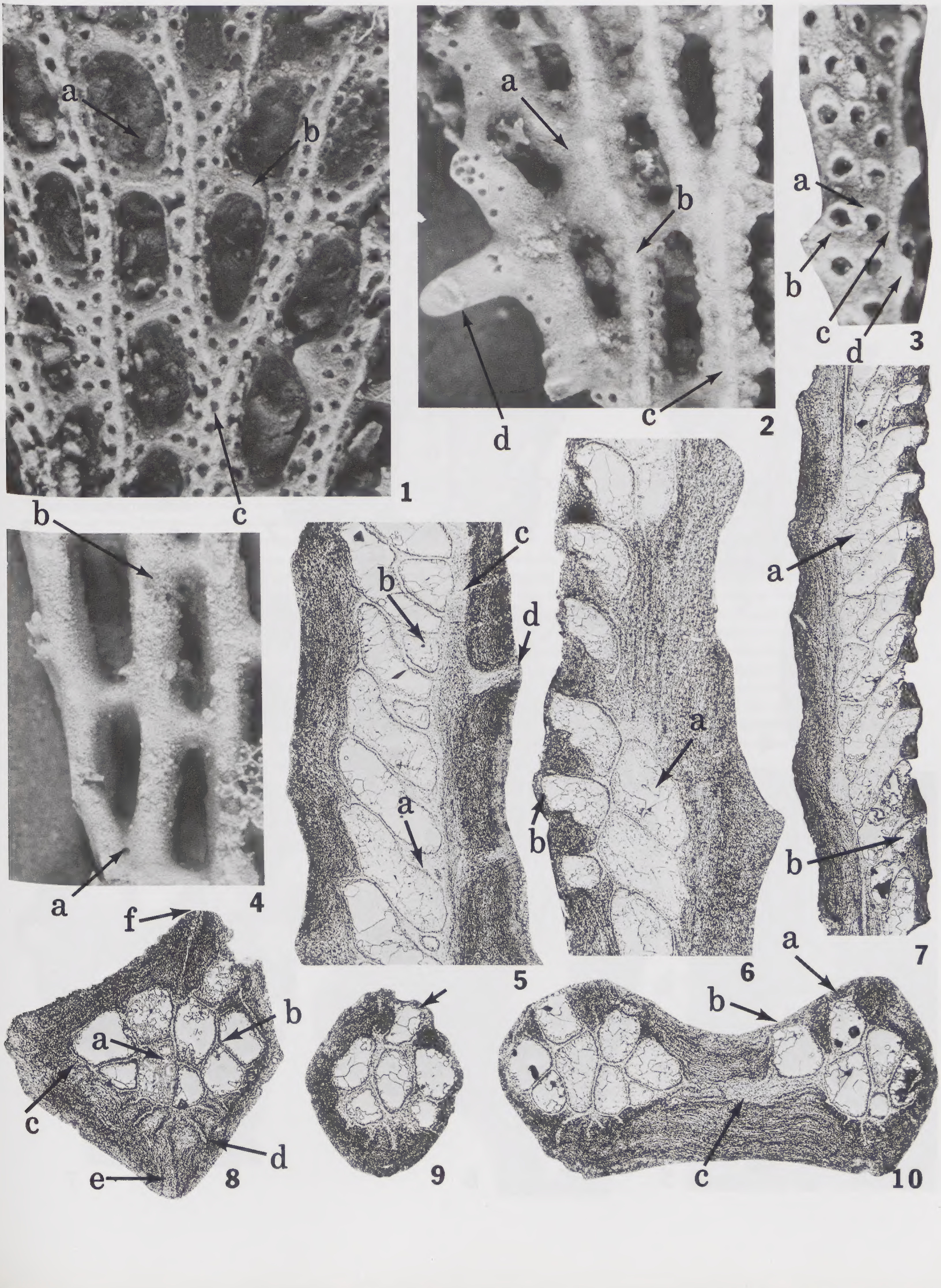
a
b
c
1
a
b
c
d
2
a
b
c
d
3
b
a
4
b
c
d
a
5
a
b
6
a
b
7
f
a
b
c
d
e
8
9
a
b
c
10

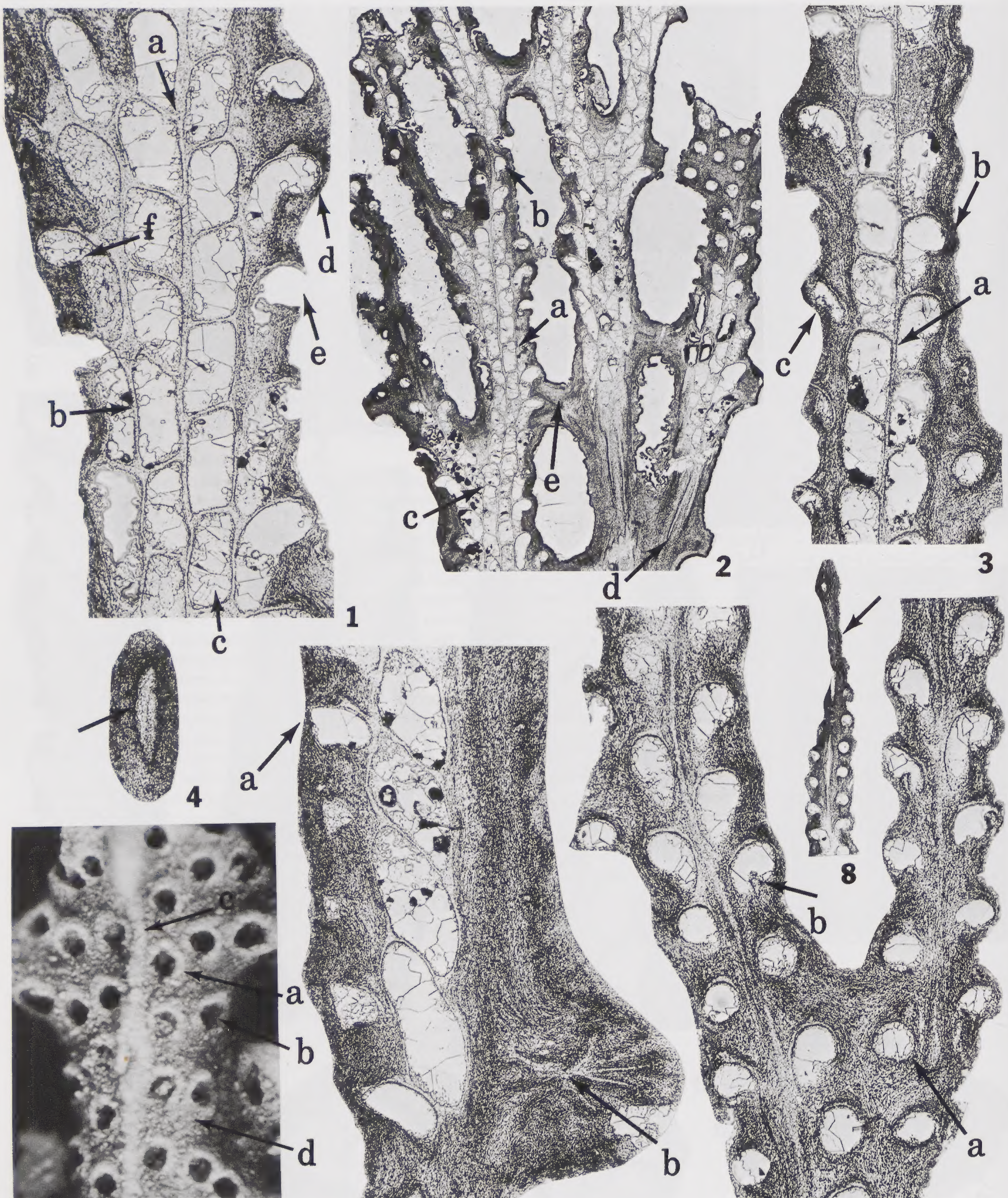
a
f
d
e
b
c
1
b
a
e
c
d
2
b
a
c
3
4
a
c
a
b
d
5
6
b
b
a
7
8

EXPLANATION OF PLATE 64

Figure		Page
1–8.	***Fenestralia sanctiludovici*** Prout, 1858a	138

Paratype, ISGS (ISM) 4486-2. 1. FSL75, mid to shallow tangential section illustrating mid axial wall (arrow **a**) and abaxial wall (arrow **b**) exhibiting typical appearance in this view, rectangular to slightly parallelogram-shaped outline of autozooecial chambers in mid tangential view (arrow **c**), outline of abaxial chambers in shallow tangential view (arrow **d**) and abaxial aperture opening (arrow **e**), and short superior hemiseptum at proximal edge of vestibule (arrow **f**), ×70. 2. FSL75, shallow to deep tangential section illustrating adaxial autozooecial chamber outline in mid (arrow **a**) and shallow (arrow **b**) tangential views, site of branch bifurcation (arrow **c**) and chamber outline at that site, and longitudinal striae (arrow **d**) continuous with granular skeletal layer surrounding autozooecial chambers and extending across dissepiment (arrow **e**), ×20; 3. FSL81, mid to mid shallow tangential section illustrating mid axial wall (arrow **a**), mid shallow adaxial chamber outline (arrow **b**), and inflection into fenestrule opening of abaxial apertures (arrow **c**), ×60; 4. FSL27, node with central core of granular skeletal material (arrow), ×70; 5. Obverse exterior view of well-preserved zoarial surface illustrating adaxial (arrow **a**) and abaxial (arrow **b**) attitudinal relationship of aperture relative to branch surface, keel (arrow **c**) with nodes positioned atop, and small obverse stylets (arrow **d**), ×45; 6. FSL86, very shallow to shallow longitudinal section, obverse to left, showing chamber outlines in this view, attitudinal relationship of aperture to plane of obverse surface (arrow **a**), and continuity of granular skeleton across dissepiment (arrow **b**), ×70; 7. FSL80, shallow tangential section at site of branch bifurcation illustrating thin peristome surrounding aperture (arrow **a**), and short superior hemiseptum at proximal edge of aperture opening (arrow **b**), ×70; 8. FSL27, shallow tangential section showing thick keel (arrow) covered with lamellar skeletal material atop which nodes with granular skeletal cores occur, ×20.

EXPLANATION OF PLATE 65

Figure | Page
1–9. ***Polypora gracilis*** Prout, 1860 144

1, 3–9. Figured specimen, UI X-6919. Large, well-preserved zoarial fragment. 1. Obverse exterior surface illustrating aperture (arrow **a**) surrounded by apertural stylets, intermediate-size stylets (arrow **b**) anastomosing around apertures along obverse branch surface, extensions of apertures into fenestrule causing inflection in fenestrule outline (arrow **c**), site of branch bifurcation (arrow **d**), large stellate node (arrow **e**), and longitudinal ridges across dissepiment obverse surface (arrow **f**), ×8; 3. PO56, mid to deep longitudinal section, obverse to left, illustrating granular skeletal layer (arrow **a**) continuous around autozooecial chamber and with macrostylets (arrow **b**), ×40; 4. PO51, transverse section showing two branches separated by fenestrule opening (arrow) filled with sediment, ×40; 5. PO56, mid to deep longitudinal section, obverse to left, illustrating typical chamber outline (arrow **a**) with aperture opening toward middle of branch, edge of more laterally positioned chamber (arrow **b**), peristome continuous with apertural stylets, and all connected with inner granular skeletal layer (arrow **c**), and obverse node (arrow **d**), ×70; 6. PO56, shallow to mid longitudinal section, obverse to left, showing autozooecial chamber exhibiting typical outline in mid longitudinal view (arrow **a**), edge of chamber near reverse-wall budding-site (arrow **b**), and well-developed obverse stylets (arrow **c**) continuous with inner granular skeleton, ×70; 7. PO4, shallow to deep tangential section illustrating typical adaxial chamber outline in mid tangential view (arrow **a**), abaxial chamber outline in mid tangential view (arrow **b**), and chamber outline near reverse-wall budding-site (arrow **c**). Note aperture position at site of branch bifurcation (arrow **d**), longitudinal ridges across obverse dissepiment surface (arrow **e**) and large fenestrule (arrow **f**), ×20; 8. PO5, transverse section showing attitudinal relationship of adaxial (arrow **a**) and abaxial (arrow **b**) aperture openings to plane of obverse surface, and obverse node (arrow **c**) continuous with inner granular skeletal layer, ×70; 9. PO56, mid shallow longitudinal section, obverse to left, illustrating chamber outline in this view (arrow **a**), and apertural stylets (arrow **b**), ×70.

2. Figured specimen, UI X-6920. Enlarged obverse and reverse surfaces of a zoarial fragment exhibiting pronounced ontogenetic thickening. Shown are longitudinal striae (arrow **a**) extending along reverse branch surface and across dissepiment (arrow **b**), and macrostylets (arrow **c**) developed atop reverse longitudinal striae. Note aperture (arrow **d**) plugged by lamellar skeleton added during ontogenetic thickening, ×30.

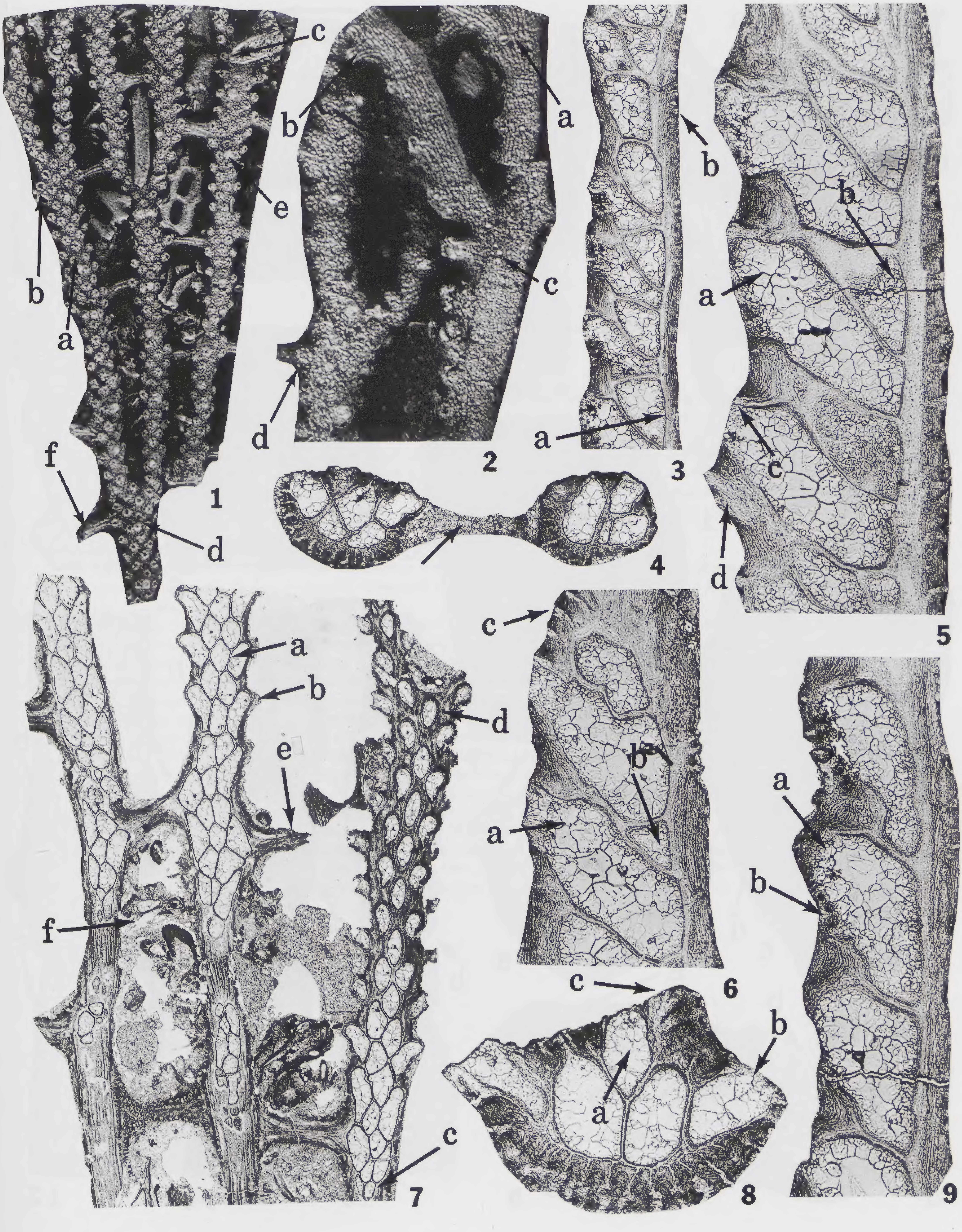
c
b
a
e
b
a
f
d
1
b
a
c
d
2
b
a
3
b
a
c
d
5
4
a
b
d
e
f
c
7
c
b
a
6
c
b
a
8
a
b
9

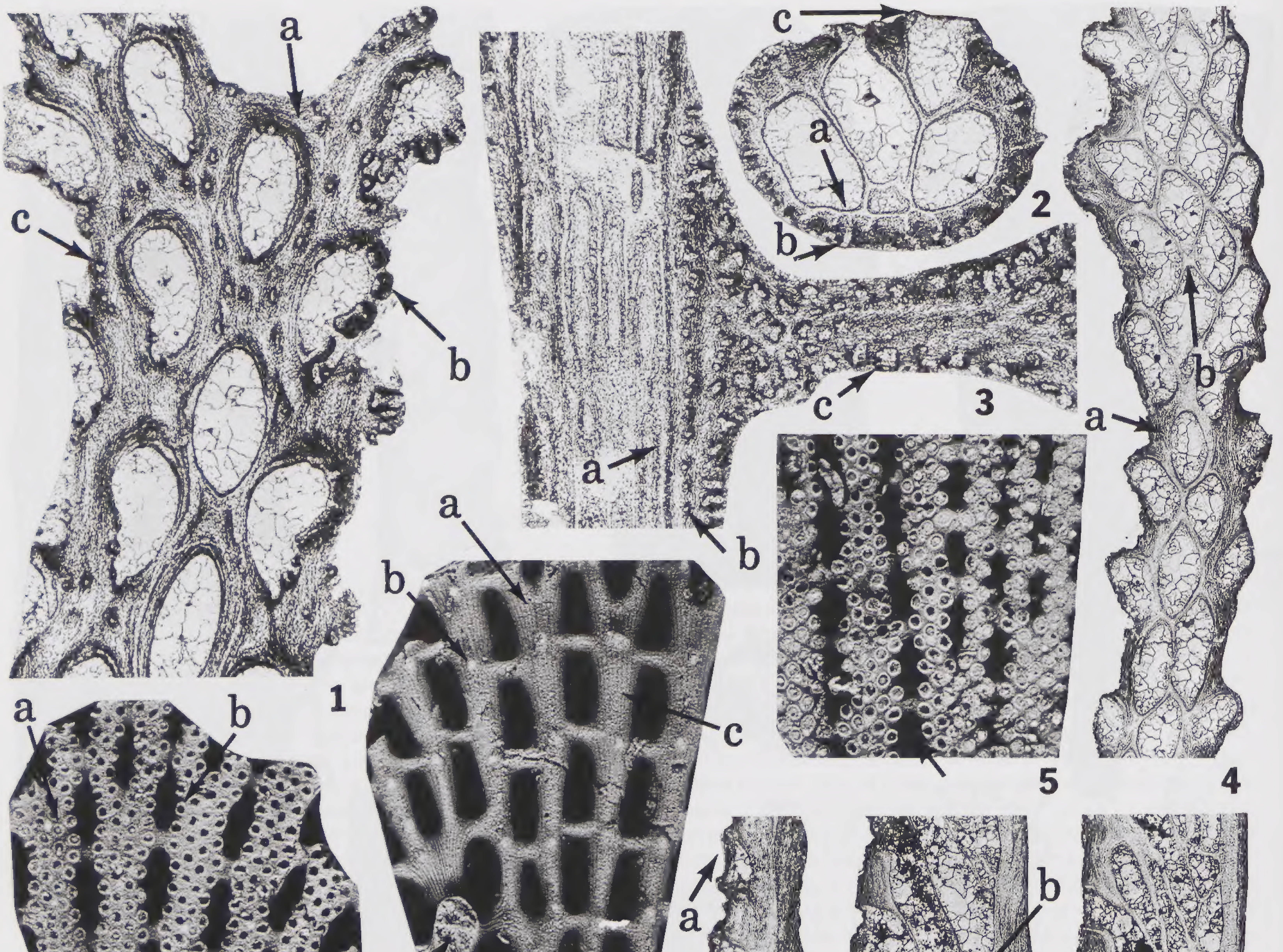
1
a
b
c
2
a
b
c
3
a
b
c
4
a
b
5
6
a
b
c
d
7
a
b
c
d
8
9
a
b
c
d
10
a
b
11
a
b
c
12
a
b
c

EXPLANATION OF PLATE 66

Figure | Page

1–4. ***Polypora gracilis*** Prout, 1860 144
Figured specimen, UI X-6919. 1. PO4, shallow tangential section showing peristome surrounding aperture (arrow **a**), with peristomal projections expanding outward to become apertural stylets (arrow **b**), and intermediate-size stylets (arrow **c**) developed across obverse surface, × 70; 2. PO5, transverse section showing granular skeletal layer continuous around autozooecial chambers (arrow **a**), with reverse macrostylets (arrow **b**), and apertural stylets (arrow **c**), ×70; 3. PO4, deep tangential section showing longitudinal striae (arrow **a**) of granular skeletal material, macrostylets (arrow **b**) developed as extensions of these striae and as extensions of striae extending across dissepiment (arrow **c**), ×70; 4. PO18, mid shallow to shallow tangential section. Note increased angularity, to accomodate fit into available space, of autozooecial chamber going from shallow (arrow **a**) to mid shallow (arrow **b**) tangential view, ×40.

5–12. ***Polypora varsoviensis*** Prout, 1858a 146

5. Figured specimen, UI X-7022. Obverse exterior surface of moderately ontogenetically thickened zoarial fragment containing numerous apertures capped by centrally thickened terminal diaphragms. Note extension of apertures into fenestrule openings and onto edge of dissepiment (arrow), ×8.

6–12. Figured specimen, UI X-6907. Large, well-preserved zoarial fragment. 6. Obverse exterior surface showing centrally thickened terminal diaphragm (arrow **a**) capping aperture, aperture not capped by terminal diaphragm (arrow **b**), obverse node (arrow **c**), and pronounced branch thickening proximal (arrow **d**), and thinning distal to site of branch bifurcation, ×8; 7. Reverse exterior surface illustrating longitudinal striae (arrow **a**) atop which develop reverse microstylets, macrostylets (arrow **b**) typically located at site of branch–dissepiment junction, branch thickening proximal to site of branch bifurcation (arrow **c**), and zoarial support (arrow **d**) developed from reverse branch surface, ×8; 8. PO90, transverse section showing typical attitudinal relationship of aperture to plane of obverse surface and part of centrally thickened terminal diaphragm (arrow), ×70; 9. PO90, transverse section of two branches immediately distal to site of branch bifurcation. Note attitudinal relationship of adaxial (arrow **a**) and abaxial (arrow **b**) apertures relative to plane of obverse surface, granular skeletal layer surrounding autozooecial chambers (arrow **c**) and continuous with longitudinal striae (arrow **d**), ×70; 10. PO80, mid shallow to shallow longitudinal section, obverse to left, showing aperture opening at abaxial branch edge (arrow **a**) and mid chamber outline of abaxial autozooecial chamber (arrow **b**), ×40; 11. PO82, deep longitudinal section, obverse to left, showing chamber outline in this view (arrow **a**) and near reverse-wall budding-site (arrow **b**), also note aperture opening onto branch center (arrow **c**), ×40; 12. PO82, mid longitudinal section, obverse to left, illustrating typical autozooecial chamber outline in this view (arrow **a**) as well as continuity of granular skeletal layer along reverse wall (arrow **b**), and with reverse macrostylets (arrow **c**), ×40.

EXPLANATION OF PLATE 67

Figure Page

1–6. ***Polypora varsoviensis*** Prout, 1858a 146

1. Figured specimen, UI X-7022. Enlarged obverse exterior surface of well-preserved zoarial fragment illustrating typical outline of aperture (arrow **a**), obverse node (arrow **b**), and ridge across dissepiment surface (arrow **c**), ×20.

2–6. Figured specimen, UI X-6907. 2. PO77, mid to deep tangential section showing adaxial autozooecial chamber outline near reverse-wall budding-site (arrow **a**), adaxial chamber outline in mid tangential view (arrow **b**), and abaxial chamber outline in same view (arrow **c**). Note longitudinal striae composed of granular skeletal material (arrow **d**), and microstylets developing as extensions of striae along branch (arrow **e**) and dissepiment (arrow **f**) surfaces, ×20; 3. PO80, mid to shallow longitudinal section, obverse to left, showing typical abaxial autozooecial chamber outline in this view (arrow), ×70; 4. PO83, shallow tangential section illustrating peristome surrounding aperture that exhibits a typical apertural outline (arrow **a**), apertural stylets developed atop peristome (arrow **b**), and obverse node (arrow **c**), ×70; 5. PO87, mid to mid shallow tangential section showing typical autozooecial chamber outline in mid (arrow **a**) and mid shallow (arrow **b**) tangential views, also note continuity of granular skeletal material across dissepiment (arrow **c**), ×40; 6. PO87, shallow to mid tangential section. Note inflection in fenestrule outline caused by extension of apertures into opening (arrow **a**) in shallow tangential view and lack of such inflections in mid tangential view (arrow **b**); also shown is recessed dissepiment near obverse surface (arrow **c**) with continuity of dissepiment evident between branches in mid tangential section (arrow **d**), ×20.

7, 8. ***Polypora spininodata*** Ulrich, 1890 149

Figured specimen, UI X-7017. PA43. 7. Transverse section showing attitudinal relationship of abaxial (arrow **a**) and adaxial (arrow **b**) apertures relative to plane of obverse surface; also shown is granular skeletal layer continuous with peristome (arrow **b**). Note granular skeletal layer surrounding autozooecial chambers and continuous with longitudinal striae (arrow **c**) and reverse microstylets (arrow **d**), ×40; 8. Transverse section illustrating centrally thickened terminal diaphragm capping aperture (arrow **a**), and continuity of granular skeletal material across dissepiment between branches (arrow **b**), ×40.

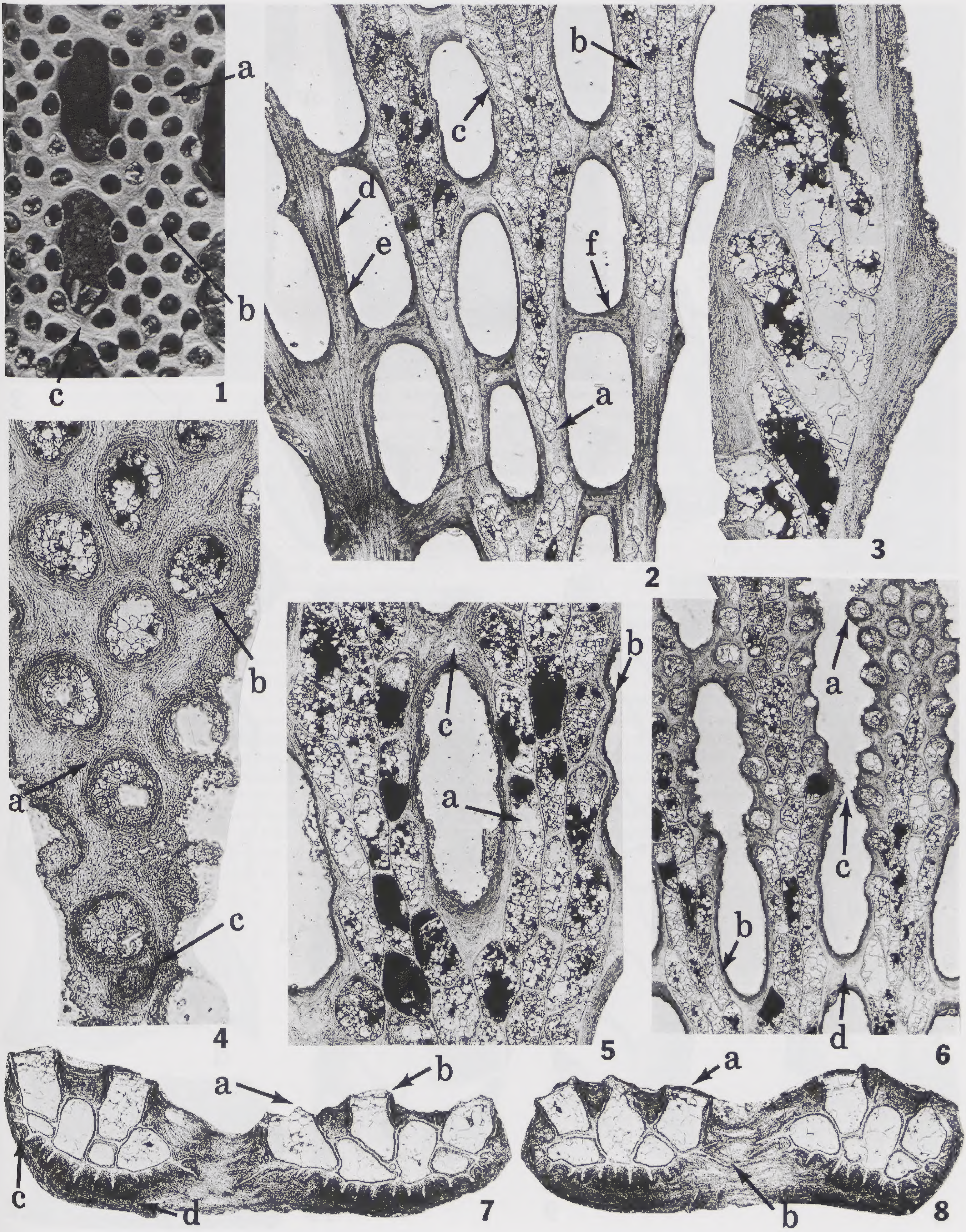
1
2
3
4
5
6
7
8

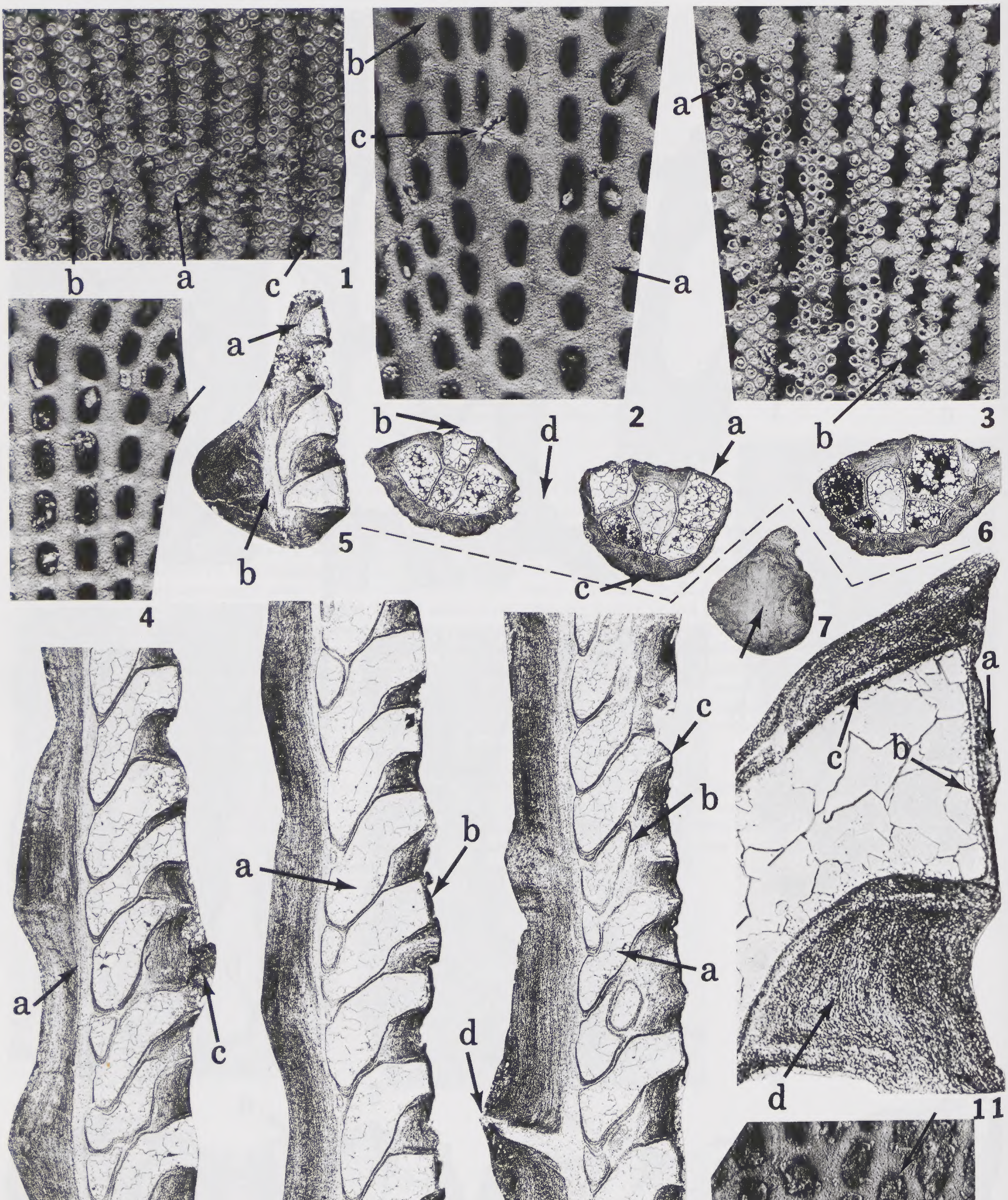
1
2
3
4
5
6
7
8
9
10
11
12
a
b
c
d

EXPLANATION OF PLATE 68

Figure Page

1–12. ***Polypora spininodata*** Ulrich, 1890 ... 149

1, 11, 12. Figured specimen, UI X-7017. Large, moderately ontogenetically thickened zoarial fragment. 1. Obverse exterior surface illustrating centrally thickened terminal diaphragm capping aperture (arrow **a**) at thickened branch area proximal to site of branch bifurcation, pronounced extension of apertures onto dissepiment surface (arrow **b**), and nodes (arrow **c**) along obverse branch surface, ×8; 11. PA41, greatly enlarged longitudinal section, obverse to right, illustrating centrally thickened terminal diaphragm (arrow **a**) with granular skeleton forming inner apertural plug (arrow **b**) apparently continuous with inner granular skeletal layer (arrow **c**). Note thickened lamellar skeletal material (arrow **d**) infilling area between zones of granular skeleton, ×200; 12. Reverse exterior surface showing typical fenestrule outline (arrow), ×8.

2, 3. Figured specimen, UI X-7018. 2. Reverse exterior surface containing branch exhibiting pronounced thickening proximal (arrow **a**) and thinning distal to site of branch bifurcation, longitudinal striae and microstylets developing atop striae (arrow **b**), and reverse zoarial support (arrow **c**) forming on reverse surface near site of branch bifurcation, ×8; 3. Obverse exterior surface illustrating aperture not capped by terminal diaphragm (arrow **a**), and extension of abaxial aperture opening (arrow **b**) into fenestrule opening, ×8.

4, 6. Figured specimen, UI X-7019. 4. Reverse exterior surface showing macrostylet development (arrow) typically at site of branch–dissepiment junction, ×8; 6. PO68, transverse section. Note attitudinal relationship of abaxial (arrow **a**) and adaxial (arrow **b**) autozooecial chambers, both capped by centrally thickened terminal diaphragms, to plane of obverse surface; also note well-developed longitudinal striae of granular skeletal material (arrow **c**), and spacing between branches (arrow **d**) across fenestrule opening, ×40.

5, 7–10. Figured specimen, UI X-6921. 5. PA21, shallow longitudinal section, obverse to right, illustrating aperture extending into fenestrule in shallow longitudinal view (arrow **a**), and continuity of granular skeletal material across dissepiment (arrow **b**), ×40; 7. PA21, transverse section of dissepiment, obverse to right, showing continuity of granular skeletal material (arrow) through middle of dissepiment, ×40; 8. PA23, mid to deep longitudinal section, obverse to right. Note granular skeletal layer continuous around autozooecial chambers, with reverse chamber wall (arrow **a**) and reverse microstylets (arrow **b**); also shown is edge of obverse node (arrow **c**), ×40; 9. PA26, mid longitudinal section, obverse to right, illustrating typical chamber outline in this view (arrow **a**) and centrally thickened terminal diaphragm capping aperture (arrow **b**), ×40; 10. PA26, mid to deep longitudinal section, obverse to right, showing variable chamber outline (arrows **a** and **b**) toward center of branch, and continuity of granular skeleton with peristome (arrow **c**) and with large reverse macrostylets (arrow **d**), ×40.

EXPLANATION OF PLATE 69

Figure Page

1–7. ***Polypora spininodata*** Ulrich, 1890 149

1–3, 7. Figured specimen, UI X-6921. 1. PA31, shallow to deep tangential section showing typical mesh symmetry. Note extension of aperture into fenestrule in shallow tangential view causing inflection in fenestrule outline (arrow **a**), lack of such inflections in mid tangential view (arrow **b**), and pronounced increase in fenestrule size, particularly width, near reverse wall (arrow **c**), ×20; 2. PA31, shallow to mid tangential section showing abaxial autozooecial chamber outline in mid (arrow **a**) and mid shallow (arrow **b**) tangential views, and site of branch bifurcation (arrow **c**), ×20; 3. PA29, very shallow tangential section illustrating typical aperture outline (arrow **a**), peristome surrounding aperture (arrow **b**), apertural stylets (arrow **c**) developing at lateral edge of peristome, and stellate nodes (arrow **d**) along obverse zoarial surface, ×75; 7. PA21, shallow to mid shallow longitudinal section, obverse to right, showing aperture opening into fenestrule at abaxial branch edge (arrow **a**), and diaphragm capping aperture in shallow longitudinal sectional view (arrow **b**), ×40.

4, 5. Figured specimen, UI X-6913. Highly ontogenetically thickened zoarial fragment. 4. PO69, mid to deep tangential section showing continuity of granular skeletal material with reverse macrostylets (arrow **a**), and lamellar skeleton covering macrostylets in deeper tangential view (arrow **b**). Note macrostylet location near site of branch–dissepiment junction, ×25; 5. PO74, shallow to mid tangential section illustrating typical adaxial (arrow **a**) and abaxial (arrow **b**) chamber outline in mid tangential view, adaxial (arrow **c**) and abaxial (arrow **d**) aperture outlines, continuity of granular skeleton across dissepiments (arrow **e**), and thickened lamellar skeletal layer (arrow **f**) partially filling fenestrules inside which microstylets develop, ×25.

6. Figured specimen, UI X-7017. PA47, mid to deep tangential section of slightly ontogenetically thickened zoarial fragment showing typical chamber outline near reverse-wall budding-site (arrow **a**), longitudinal striae (arrow **b**) continuous with granular skeletal layer from which reverse microstylets (arrow **c**) and macrostylets (arrow **d**) develop, ×20.

8, 9. ***Polypora simulatrix*** Ulrich, 1890 151

Figured specimen, UI X-6922. 8. PI43, mid shallow longitudinal section, obverse to right, showing typical autozooecial chamber outline (arrow) in this view, ×20; 9. PI27, transverse section of branch showing abaxial (arrow **a**) and adaxial (arrow **b**) attitudinal relationship of aperture to plane of obverse surface. Note continuity of granular skeletal material with peristome (arrow **a**) and apertural stylets (arrow **b**), ×60.

10. ***Polypora spininodata*** Ulrich, 1890 149

Figured specimen, UI X-6911. PO49, shallow tangential section illustrating apertural stylets (arrow **a**) and extension of apertures onto dissepiments (arrow **b**), ×40.

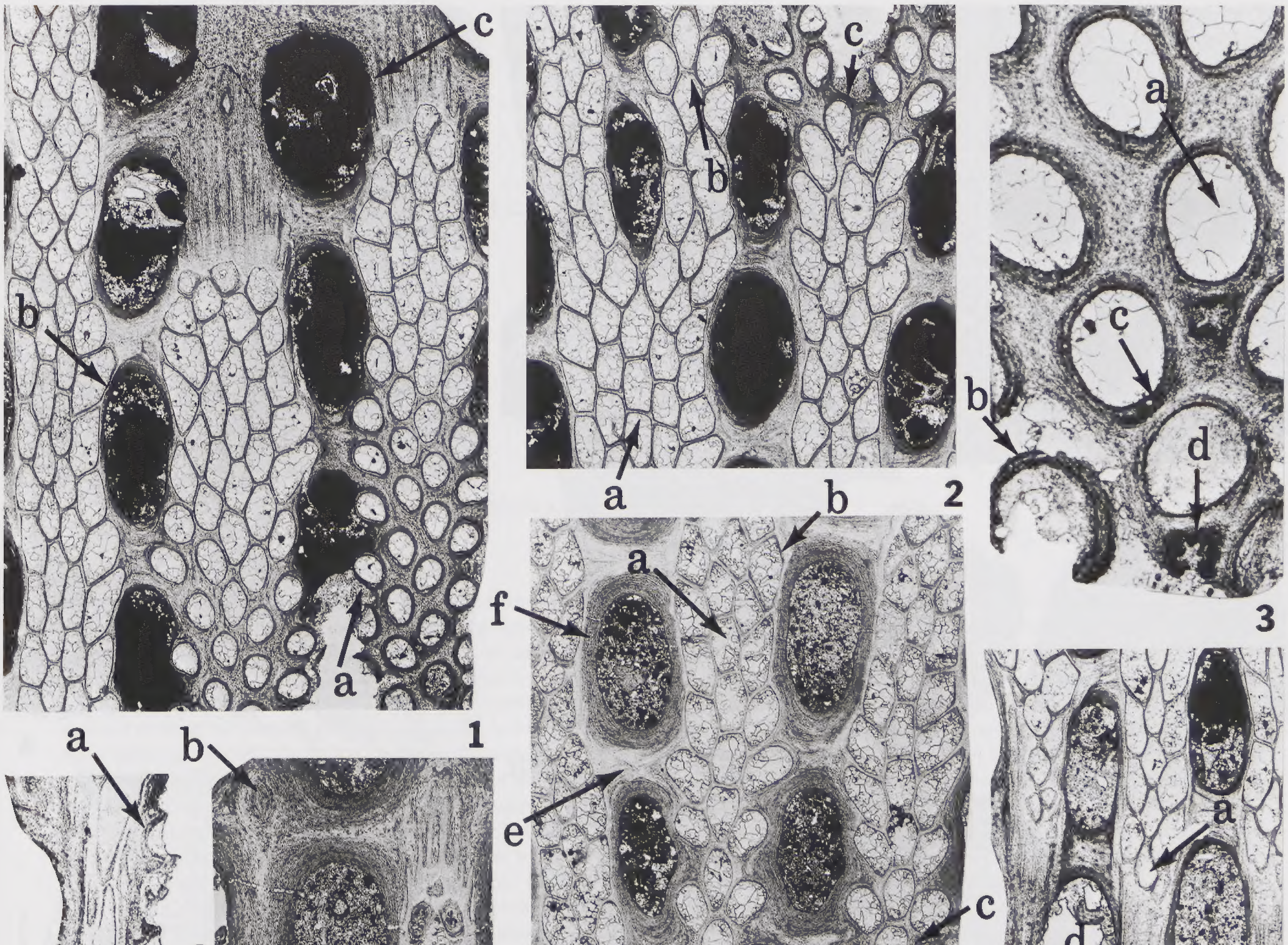
1 2 3 4 5 6 7 8 9 10

1
2
3
4
5
6
7
8
9
10
11
12
a
b
c

EXPLANATION OF PLATE 70

Figure Page

1–12. ***Polypora simulatrix*** Ulrich, 1890 151

Figured specimen, UI X-6922. Well-preserved, moderately large zoarial fragment. 1. Obverse exterior surface showing aperture position at site of branch bifurcation (arrow **a**) and longitudinal ridges extending across dissepiment (arrow **b**), ×15; 2. Obverse exterior surface; note typical outlines of adaxial (arrow **a**) and abaxial (arrow **b**) autozooecial apertures, both capped by centrally thickened terminal diaphragms and surrounded by apertural stylets, and stylets (arrow **c**) occurring between and anastomosing around apertures and nodes, ×15; 3. Obverse exterior surface illustrating adaxial aperture (arrow **a**) surrounded by apertural stylets and not capped by terminal diaphragm, and obverse node (arrow **b**), ×15; 4. PI37, shallow mid longitudinal section, obverse to right, showing centrally thickened terminal diaphragm (arrow **a**) and granular skeletal layer (arrow **b**) continuous with reverse wall, around autozooecial chambers, and with reverse microstylets, ×60; 5. PI35, transverse section of zoarial support illustrating core of granular skeletal material (arrow) continuous with small stylets at edge of support, ×60; 6. PI35, transverse section of dissepiment, obverse to right, showing aperture opening onto edge of dissepiment (arrow **a**), and continuity of granular skeletal material across middle of dissepiment between branches (arrow **b**), ×60; 7. PI35, mid longitudinal section, obverse to right, illustrating typical autozooecial chamber outline in this view (arrow **a**), and continuity of granular skeletal layer with peristome (arrow **b**), ×40; 8. PI35, very shallow to shallow longitudinal section, obverse to right, showing changing autozooecial chamber outline from very shallow (arrow **a**) to shallow (arrow **b**) longitudinal view, ×60; 9. PI29, transverse section of branch showing typical attitudinal relationship of adaxial aperture to plane of obverse surface (arrow **a**), and zoarial support with core of granular skeletal material (arrow **b**) extending from reverse branch surface, ×60; 10. PI44, mid to deep longitudinal section, obverse to right, showing typical chamber outline in deep longitudinal view (arrow **a**), and obverse node (arrow **b**) of granular skeletal material, ×40; 11. PI45, mid longitudinal section, obverse to right, showing typical chamber outline in this view (arrow) with aperture capped by diaphragm, ×40; 12. PI45, shallow to mid longitudinal section, obverse to right, showing adaxial edge of apertural stylets (arrow), ×40.

EXPLANATION OF PLATE 71

Figure Page

1–4. ***Polypora simulatrix*** Ulrich, 1890 151

Figured specimen, UI X-6922. 1. PI48, shallow to deep tangential section illustrating typical outline of adaxial chambers in mid (arrow **a**) and shallow (arrow **b**) tangential view, abaxial chambers in mid (arrow **c**) and shallow (arrow **d**) tangential view, continuity of granular skeleton across dissepiment (arrow **e**) and site of branch bifurcation (arrow **f**), ×20; 2. PI32, mid shallow tangential section showing chamber outline in this view (arrow), ×60; 3. PI48, shallow tangential section illustrating aperture surrounded by apertural stylets (arrow **a**), and obverse stylet (arrow **b**) and nodal (arrow **c**) development, ×60; 4. PI48, deep tangential section showing chamber outline near reverse-wall budding-site (arrow **a**), and granular skeletal layer continuous with longitudinal striae (arrow **b**), and microstylets (arrow **c**) developing atop and as extensions of striae (arrow **c**), ×60.

5–9. ***Polypora retrorsa*** Ulrich, 1890 154

Figured specimen, UI X-6908. 5. Enlarged obverse exterior surface showing autozooecial aperture (arrow **a**) exhibiting slight inflection into fenestrule, aperture (arrow **b**) developed well onto edge of dissepiment, and site of branch bifurcation (arrow **c**), ×20; 6. PI17, mid longitudinal section, obverse to left, illustrating typical autozooecial chamber outline in this view (arrow **a**), and thick granular skeletal layer continuous around autozooecial chambers, with reverse wall (arrow **b**) and reverse microstylets (arrow **c**), ×40; 7. PI21, mid longitudinal section, obverse to left. Note typical autozooecial chamber outline in this view (arrow **a**), and continuity of granular skeletal layer with obverse stylets (arrow **b**), ×70; 8. PI63, transverse section illustrating zoarial base (arrow) from which colony developed and in which is contained the ancestrula of this zoarium, ×20; 9. Obverse exterior surface showing typical aperture outline (arrow) with aperture surrounded by incomplete peristome and containing apertural stylets, ×20.

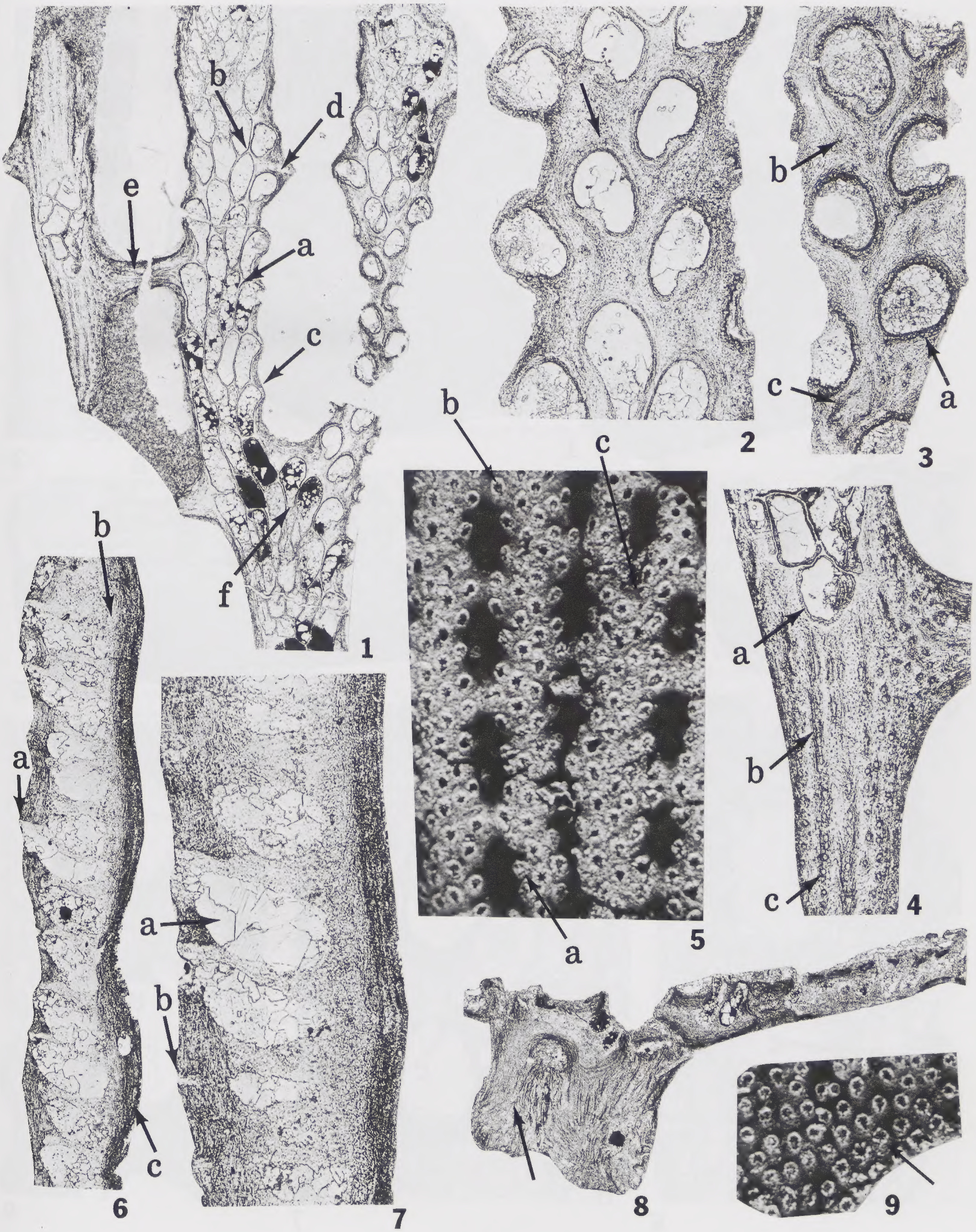

b
d
e
a
c
f
1
2
b
c
a
3
b
c
a
5
a
b
c
4
b
a
c
6
a
b
7
8
9

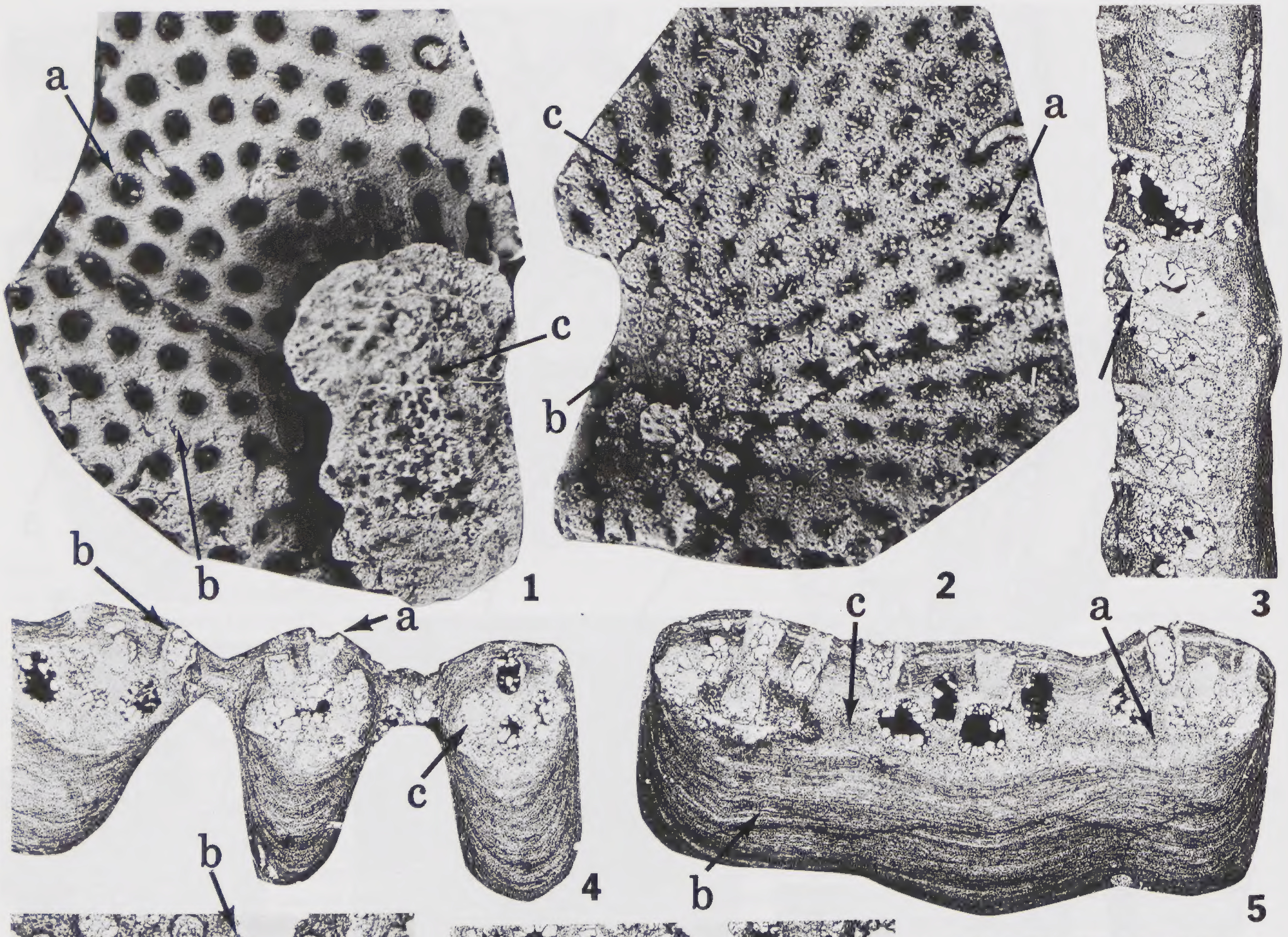
a
c
b
1
c
a
b
2
3
b
a
c
4
c
a
b
5
b
a
c
6
a
b
c
d
7
b
a
c
8

EXPLANATION OF PLATE 72

Figure Page

1–8. ***Polypora retrorsa*** Ulrich, 1890 154

Figured specimen, UI X-6908. Large, moderately complete, well-preserved zoarial fragment. 1. Reverse exterior surface illustrating typical fenestrule shape as observed from reverse surface (arrow **a**), site of branch bifurcation (arrow **b**), and base of zoarium (arrow **c**) containing ancestrula, ×1; 2. Obverse exterior surface illustrating slight inflection in fenestrule outline caused by extension of abaxial aperture edge into opening (arrow **a**), thickening of lamellar skeleton at proximal end of zoarium completely plugging fenestrules (arrow **b**), and site of branch bifurcation (arrow **c**), ×1; 3. PI21, mid to deep longitudinal section, obverse to left, showing typical autozooecial chamber outline in mid longitudinal view (arrow), ×40; 4. PI8, transverse section showing attitudinal relationship of adaxial (arrow **a**) and abaxial (arrow **b**) apertures to plane of obverse surface. Note thickened granular skeletal material around autozooecial chambers, and rounded chambers (arrow **c**) in transverse section, ×40; 5. PI6, transverse section showing continuity of granular skeletal layer (arrow **a**) around autozooecial chambers, with reverse microstylets (arrow **b**), and across dissepiment (arrow **c**) between branches, ×40; 6. PI67, shallow to mid shallow tangential section illustrating incomplete peristome surrounding aperture that exhibits a typical outline (arrow **a**), apertural stylets (arrow **b**), and obverse stylets (arrow **c**), ×40; 7. PI67, deep mid to mid shallow tangential section showing typical bilobate chamber outline in mid shallow (arrow **a**) and ovate outline in mid (arrow **b**) tangential views. Note pronounced extension of autozooecial chambers onto dissepiment (arrow **c**), and rounded chamber shape (arrow **d**) in deep mid tangential section, ×40; 8. PI62, mid to deep tangential section illustrating autozooecial chamber outline near reverse-wall budding-site (arrow **a**), and poorly defined longitudinal striae (arrow **b**) of thickened granular skeletal material which expands outward to become reverse microstylets (arrow **c**), ×40.

INDEX

Note: Page numbers are in light face; plate numbers are in **bold** face type; pages on which principal discussions occur are in *italics*. **F** and **B** indicate the foldouts inside the front and back covers, respectively.

AAB [distance between aperture centers across branch]
defined .... **F,B**
illustrated 35
ABB [distance between aperture centers between branches]
defined .... **F,B**
illustrated 35
abundant (*defined*) 156
ACA [angle between distal end of axis and axial whorl]
defined .... **F,B**
illustrated 36
ADB [distance between aperture centers along branch]
defined .... **F,B**
illustrated 35
Aequifenestella Termier and Termier, 1971 23
AF [number of aperture openings per fenestrule length]
defined .... **F,B**
illustrated 35
Afghanistan 18,23
AL [aperture length]
defined .... **F,B**
illustrated 35,37,38
Alternifenestella Termier and Termier, 1971 23,24
AMNH [American Museum of Natural History, New York, NY] *40*,133
angle between distal end of axis and axial whorl [**ACA**]
defined .... **F,B**
illustrated 36
Anstey and Perry (1970) 19,34
Anstey and Perry (1973) 19,34
antiqua, Fenestella 17
Apertostella, n. gen. 7,29–31,33,34,39,40,90,*97*, 98,101,103,106,108,124
crassata, n. sp. .... **36,37** 7,39,97,98,*101*,102–104,156,158,159,227,228
foramenmajor, n. sp. .... **35,36** 7,39,98,*99*,101, 156,158,226,227
venusta, n. sp. .... **38,39** 7,39,98,*104*,106, 156,158,159,229,230
aperture length [**AL**]
defined .... **F,B**
illustrated 35,37,38
aperture width [**AW**]
defined .... **F,B**
illustrated 35,37
Appalachian Revolution 15
Appalachian State University, Boone, NC 7
aprilae, Hemitrypa .... **44,45** 7,39,108,*114*,116, 156,158,159,235,236
Archaefenestella Miller, 1962 23,24
Archimedes Hall, 1858 .... **F**,18,27,29–31,33,34,36,39,40, 54,56,*122*,124,127,133,136
distans Condra and Elias, 1944 126
grandis Ulrich, 1890 124,127,130
halli Condra and Elias, 1944 127,130
meekanus Condra and Elias, 1944 126
negligens Ulrich, 1890 .... **50,51,52** 39,*124*,125–127, 156,158,159,241-243
owenanus (Hall, 1857b) .... **52,53,54,55,56** 39,124, *127*,130,133,136,156,158,159,243–247
reversa Hall, 1858 124,130,133
terebriformis Condra and Elias, 1944 126
valmeyeri, n. sp. .... **60,61,62** 7,39,124,*133*,134, 136,156,158,159,251–253
welleri Condra and Elias, 1944 130,133
wortheni (Hall, 1857b) .... **56,57,58,59,60** 39,71,122, 124,127,*130*,131,133,156,158,159,247–251
Archimedes limestone 124
Arrow Rock 1:24,000 quadrangle (1971) 176
aspera, Hemitrypa .... **46,47** 39,108,*116*,117, 119,156,158,237,238
Astrova and Morozova (1956) 16,39
Atherton and Palmer (1979) 10–12,158
Augusta Northwest (locality 1) 9,*172*
Ausich (1978) 168,169
Ausich (1980) 160,168,169
Australia 22,61
autozooecial chamber depth [**CD**]
defined .... **F,B**
illustrated 37,38
autozooecial chamber length [**CL**]
defined .... **F,B**
illustrated 37,38
AW [aperture width]
defined .... **F,B**
illustrated 35,37
AZO® 10

Banastella, n. gen. 7,28,30,32,34,39,40,68,71,*72*,73, 76,79,81,83,85,88,141,151
biseriata (Ulrich, 1890) .... **26,27** 39,73,*83*,84, 85,156,158,159,217,218
cingulata (Ulrich, 1890) .... **20,21** 39,73,*77*,78,79, 83,156,158,211,212
delicata, n. sp. ... **27,28** 7,39,73,*86*,88,156,158,218,219
guensburgi, n. sp. ..... **18,19,20** 7,19–21,37,39,72,*73*,74, 76,83,156,158,159,166,209–211
limitaris (Ulrich, 1890) .... **24,25** 39,73,*81*,82,83, 156,158,159,215,216
mediocreforma, n. sp. .... **22,23** 7,39,73,*79*,80, 81,83,156,158,213,214
Bancroft (1986a) 22,25,27
Bancroft (1986b) 27
Banta, McKinney, and Zimmer (1974) 166
Bassler (1953) 16,17,22,142
Baxter (1960) 14
Baxter (1972) 11
Belfast Formation 14
Bell (1932) 15
Beltrees–Melville Anticline 15,16
Benchmark on State Highway 369 (locality 33) 9,*175*
Bentonsport, Iowa (locality 2; measured section 1) 9,157–159,*172*,*177*

biseriata,
Banastella ...... **26,27** 39,73,*83*,84,85, 156,158,159,217,218
Polypora 73,83,151
Blake (1975) 16,17
Blake (1980) 17,31
Blake (1983) 31
Blake, D. B. 7,39
Boardman (1975) 31,161
Boardman and Cheetham (1969) 22,31
Boardman and Cheetham (1983) 22
Boardman and Utgaard (1964) 10
Boardman, R. S. 7,18
Bonaparte 1:24,000 quadrangle (1968) 172
Borden Delta 10,14
Borden Siltstone Formation 14
Bilyeu Member 14
Borg (1926) 16
Bork and Perry (1967) 19,34
Braem (1940) 162
branch width [**WB**]
defined ...... **F,B**
illustrated 35,37,38
Branner (1888) 11
Briggs Branch (locality 37) 9,*175*
Brighton 1:62,500 quadrangle (1925) 175
Buel Branch 173
Buel Branch (locality 14; measured section 9) 9,157–159,*173*,*180*
Bugula turrita 162
Bullivant (1968a) 161,162,164
Bullivant (1968b) 160,162,163
Burckle (1960) 41,56,127,138
Burlington Group 11
Burlington Limestone Formation 10,11,14,88
Busk (1852) 16
Butts (1915) 12

Cahokia 1:24,000 quadrangle (1954) 176
Campbell (1961) 22
Canton, Missouri—A (locality 17) 9,*174*
Canton, Missouri—B (locality 18) 9,*174*
Canton, Missouri—C (locality 19) 9,*174*
Cap au Gres Faulted Flexure 15,16
Carozzi (1972) 10
Carper, H. 7
Carrollton Anticline 15
Carrollton, Illinois (locality 32) 9,*175*
Cavernella Morozova, 1974 23–25
Cavusgnathus unicornis–Apatognathus Zone 12
CD [autozooecial chamber depth]
defined ...... **F,B**
illustrated 37,38
Cervella Chronic, 1949 22
chamber lateral-wall budding-angle [**LA**]
defined ...... **F,B**
illustrated 37,38
chamber reverse-wall budding-angle [**RA**]
defined ...... **F,B**
illustrated 37,38
Cheetham, A. H. 7
Chester
Group 56,126
Series 11

Choteau Formation 11,14
Chronic (1949) 22
Cincinnati Arch–Nashville Dome 10
cingulata,
Banastella ... **20,21** 39,73,*77*,78,79,83,156,158,211,212
Fenestella 77
CL [autozooecial chamber length]
defined ...... **F,B**
illustrated 37,38
Cole (1961) 16
Collinson (1964) 12,14
Collinson, Scott, and Rexroad (1962) 12,14,174
Columbia Roadcut (locality 48; measured section 22) 9,157–159,*176*,*183*
Columbia Syncline 16
common (*defined*) 156
compressa, Fenestella 97
Condra and Elias (1944) 17,18,41,45,47,56,124,126,127,129,130,133
coniunctistyla, Laxifenestella ...... **5,6,7** 7,39,49,*50*,52, 53,56,156,158,196–198
Connell (1975) 160
Cook (1977) 22,166
County Road U (locality 42) 9,*175*
Cragwold Road (locality 47; measured section 21) 9,56,58,72,79,95,97,111,136,149,157–159,*176*,*184*
crassata, Apertostella ...... **36,37** 7,39,97,98,*101*, 102–104,156,158,159,227,228
crawfordsvillensis, Dictyoclostus 12
Crisia eburnea Lamouroux, 1812 163
Crockford (1944) 22–24,28,30,32,39–41,61,62,65,97
Cryptosula pallasiana (Moll, 1803) 165,166
Cubifenestella, n. gen. 7,29–31,33,34,39–41,*88*,90,92,97,98
globodensata, n. sp. ...... **33,34** 7,39,90,92,94,*95*, 97,156,158,224,225
rudis (Ulrich, 1890) ...... **29,30** 39,83,88,*90*, 92,94,156,158,220,221
usitata, n. sp. ...... **31,32** 7,19–21,38,39,90,*92*, 93–95,97,156,158,222,223
Cuffey (1967) 19,34
Cuffey (1973) 16,17
Cuiver River 175
Cuiver River (locality 39) 9,*175*
Cumings (1901) 14
Cumings (1904) 17
Cumings (1905) 17
Cumings (1906) 39,41,44–47,49,56,68,90,156,193,194
Cumings (1922) 12
Cumings, E. R. 53
Cyclopora Prout, 1858a 12
Cycloporella Ulrich, 1889 12

Dales (1957) 160
DBC [distance between branch centers]
defined ...... **F,B**
illustrated 35
DCA [maximum diameter of central axis]
defined ...... **F,B**
illustrated 36
Deer Lick Anticline 15
delicata, Banastella ...... **27,28** 7,39,73,*86*,88, 156,158,218,219
dendroides, Polypora 142

Dennis Hollow at Valmeyer (locality 49; measured section 23) 9,45,47,49,54,56,58,60,61,65,67,72,76,79,81,88,92,95,97, 114,116,119,136,146,149,156–159,*176*,*185*
Des Moines River 9,173
diameter of macrostylets on reverse branch surface [**RSL**]
defined ..... **F**,**B**
illustrated 35
diameter of microstylets of reverse branch surface [**RSS**]
illustrated 35
defined ..... **F**,**B**
diameter of nodes along obverse branch surface [**DN**]
defined ..... **F**,**B**
illustrated 35
diameter of nodes on dissepiments [**DND**]
defined ..... **F**,**B**
illustrated 35
diameter of stylets on obverse surface [**DSO**]
defined ..... **F**,**B**
illustrated 35
diameter of stylets surrounding aperture [**SAD**]
defined ..... **F**,**B**
illustrated 35,37
Diamond (1978) 160
Dictyoclostus crawfordsvillensis (Hall, 1858) 12
dissepiment width [**WD**]
defined ..... **F**,**B**
illustrated 35,37,38
distance between aperture centers across branch [**AAB**]
defined ..... **F**,**B**
illustrated 35
distance between aperture centers along branch [**ADB**]
defined ..... **F**,**B**
illustrated 35
distance between aperture centers between branches [**ABB**]
defined ..... **F**,**B**
illustrated 35
distance between branch centers [**DBC**]
defined ..... **F**,**B**
illustrated 35
distance between node centers along obverse branch surface [**SNB**]
defined ..... **F**,**B**
illustrated 35
distans, Archimedes 126
DN [diameter of nodes along obverse branch surface]
defined ..... **F**,**B**
illustrated 35
DND [diameter of nodes on dissepiments]
defined ..... **F**,**B**
illustrated 35
Dogaddanella Ganesan, 1972 22
Drake–White Hall Anticline 15
DSO [diameter of stylets on obverse surface]
defined ..... **F**,**B**
illustrated 35
Dunaeva and Morozova (1974) 16,17
duplaris, Minilya 61,62
Dupo Quarry (locality 44) 9,*176*
Dussart (1964) 162

Eastern Interior Basin 10
eburnea, Crisia 163
Edmondson (1965) 160
Ehrenberg (1831) 163
Elias (1964) 90,92
Elias and Condra (1957) **F**,16,18,23,41,56,61,68
Endothyra Phillips, 1841 15
Engel (1975) 22
Engelmann (1847) 15
England 23,106,108
Epotuf® 10
erkovae, Fenestella 67
Europe 19
Exfenestella Morozova, 1974 ..... 23–25,27,28, 30,32,34,39,40,*67*,68,72
exigua (Ulrich, 1890) ..... **16,17,18** 39,67,*68*,70–72, 101,156,158,159,207–209
exigua,
Exfenestella ..... **16,17,18** 39,67,*68*,70–72, 101,156,158,159,207–209
Fenestella 68
exigua springerensis, Fenestella 68

Fabifenestella Morozova, 1974 23–25
Fabricius (1780) 163
Family
Acanthocladiidae Zittel, 1880 17
Arthrostylidae Ulrich, 1888 17
Diploporidae Vine, 1884 17
Fenestellidae King, 1849 ..... 16,17,29,34,39,*40*,156
Hyphasmoporidae Vine, 1884 17
Melicerititidae d'Orbigny, 1852 16
Phylloporinidae Dunaeva and Morozova, 1974 16,17
Polyporidae Vine, 1884 ..... 17,30,34,39,*136*,156
Rhabdomesontidae Vine, 1884 17
Fenestella Lonsdale, 1839 ..... **F**,17–25,27,40,61,71,85,113
antiqua Lonsdale, 1839 17
cingulata Ulrich, 1890 77
compressa Ulrich, 1890 97
erkovae (Shulga-Nesterenko, 1951) 67
exigua Ulrich, 1890 68
exigua springerensis Elias and Condra, 1957 68
filistriata Ulrich, 1890 88
funicula Ulrich, 1890 76,94,95
hemitrypa Prout, 1859 111,113
iowensis Elias, 1964 90,92
limitaris Ulrich, 1890 81,83
medvedkensis Shulga-Nesterenko, 1951 40
multispinosa Ulrich, 1890 47
owenana Hall, 1857b 127
plumosa Prout, 1860 113
regalis Ulrich, 1890 76,88
rudiformis Elias, 1964 90,92
rudis Ulrich, 1890 41,83,88,90,92
sarytshevae (Shulga-Nesterenko, 1951) 49
serratula Ulrich, 1890 41,56
stocktonensis Condra and Elias, 1944 45,47
subantiqua d'Orbigny, 1839 25
submicroporata Shulga-Nesterenko, 1952 41,45
tenax Ulrich, 1888 40,41
tenuissima Cumings, 1906 45,47
triserialis Ulrich, 1890 65,67
wortheni Hall, 1857b 130
Fenestella (*Archimedes*) Hall, 1857b 124
wortheni Hall, 1857b 122
fenestelliformis, Synocladia(?) 26
Fenestralia Prout, 1858a 27,29–31,33,34,39,*137*,141
sancti-ludovici Prout 138
sanctiludovici Prout, 1858a ..... **63,64** 39,137,*138*,140, 141,156,158,159,254,255
St. Ludovici Prout, 1858a 138

Fenestralia? *sancti-ludovici* Prout 138
Fenestrapora Frederiks, 1915 22
Fenestrellina d'Orbigny, 1849 22,61
multispinosa (Ulrich) 47
filistriata, Fenestella 88
Fishhook Anticline 15
Flabelliporella Simpson, 1895a 142
Flabelliporina Simpson, 1895a 22
Flexifenestella Morozova, 1974 23–25,50
fluctuata, Laxifenestella .... **11,12,13** 7,39,50,53,56,*58*, 59,60,156,158,159,202–204
Flustrellidra hispida Fabricius, 1780 163
Foote Mineral Co. 173
foramenmajor, Apertostella .... **35,36** 7,39,98, *99*,101,156,158,226,227
Forest City Basin 15
Fort Payne Formation 14
Frederiks (1915) 22
Frederiks (1920) 142
funicula, Fenestella 76,94,95
FWT [thickness of front-wall (obverse-wall) laminated layer]
defined .... F,B
illustrated 37,38

Ganesan (1972) 22
Gautier (1970) 22,31
Gautier (1972) 22
Genevieve Stage 11
Geode Glen (locality 11; measured section 7) 9,58,72, 85,101,111,114,119,121,122,127,133,148,149,151,153,157–159,*173,179*
Gerster Formation 39
Gilead Syncline 15
globodensata, Cubifenestella .... **33,34** 7,39,90,92, 94,*95*,97,156,158,224,225
Gnathodus texanus–Taphrognathus conodont Zone of Collinson, Scott, and Rexroad (1962) 12
Gordon, C. H. (1895) 12
Gordon, D. P. (1974) 161
gracilis,
Polypora .... **65,66** 39,143,*144*,146,153,156, 158,159,256,257
Polypora(?) 144
gracilis (cf.), *Polypora* 144
grandis, Archimedes 124,127,130
Grays Quarry (locality 9; measured section 5) 9,157–159,*173,178*
Guensburg, T. 7,73
guensburgi, Banastella ..... **18,19,20** 7,19–21,37,39,72,*73*, 74,76,83,156,158,159,166,209–211

Hageman (1987) 7,39
Hageman, S. 7
Hall (1847) 17
Hall (1852) 17
Hall (1857a) 11,12
Hall (1857b) 17,39,71,122,124,127,129–131,133,156,243–251
Hall (1858) 12,18,27,29–31,33,36,39,40,56,122,124,130,133,136
Hall (1864) 14
Hall (1883) 17
Hall (1885) 17
halli, Archimedes 127,130
halliana, Polypora 146
Hamilton 1:24,000 quadrangle (1964) 173
Hamilton–Warsaw Roadcut (locality 10; measured section 6) 9,45,49,54,67,83,92,95,101,104,106,111,114,119,127,130, 151,157–159,*173,179*
Hannibal Shale 11
Hardin (1960) 160
Hardin Syncline 15
Harris and Parker (1964) 11,172
Harrodsburg Limestone Formation 11,12,14
Hemitrypa Phillips, 1841 .... **F**,23,27,29–31,33, 34,36,39,40,103,*106*,108,116,119,121,124
aprilae, n. sp. .... **44,45** 7,39,108,*114*, 116,156,158,159,235,236
aspera Ulrich, 1890 .... **46,47** 39,108,*116*,117, 119,156,158,237,238
hemitrypa (Prout, 1859) .... **41,42,43** 39,108,*111*, 113,114,121,122,156,158,232–234
hemitrypa nodulosa Ulrich, 1890 114
hibernicia McCoy, 1844 27
nodulosa 114
oculata Phillips, 1841 106
pateriformis Ulrich, 1890 108,110
perstriata Ulrich, 1890 .... **39,40,41** 39,106, *108*,109–111,113,156,158,230–232
plumosa (Prout, 1860) 113
proutana Ulrich, 1890 111,113
proutana vermifera Ulrich, 1890 119,122
vermifera (Ulrich, 1890) .... **47,48,49** 39,108, *119*,120–122,156,158,238–240
hemitrypa,
Fenestella 111,113
Hemitrypa .... **41,42,43** 39,108,*111*,113,114, 121,122,156,158,232–234
Henry, D. 7
hibernicia, Hemitrypa 27
hispida, Flustrellidra 163
Holtsclaw Sandstone 12
Hoover, P. 7
Hopkins and Siebenthal (1897) 14
Horowitz (1968) 19,34
Horowitz, A. 7
Hutchinson (1959) 160
Hyman (1959) 161,162

Ignotifenestella Morozova, 1974 23,24
Illinois 9,11,173
Adams Co. 14,173,174
Alton 15,138,141
Appanoose 127
Beardstown 8
Brown Co. 15,174
Calhoun Co. 15
Champaign 72
Columbia 138,176
Grafton 15
Greene Co. 15,174,175
Hamilton 173
Hancock Co. 14,172,173
Geode Glen at Warsaw 12,14,173
Henderson Co. 151
Jersey Co. 15,127,130,175
Madison Co. 15
McDonough Co. 15
Monroe Co. 16,56,67,68,83,111,138,146,176
Dennis Hollow at Valmeyer 11,16,47,60
Mt. Sterling 83,106,122

Illinois
Nauvoo 8,56,77,90,116,119,144,146,151,153
Niota 172
Pike Co. 15
Pulaski Co., Ullin 14
Quincy 15,127
Scott Co. 175
Sonora Quarry near Nauvoo 14
southeastern 14,15
southern 14,15
St. Clair Co. 16,176
Urbana 72
Valmeyer 8,15,65,72,76,79,81,85,88,95,97,116,133,136,176
Versailles 174
Warsaw 15,56,61,71,83,90,92,101,104,106,111, 119,130,133,138,141,142,144,146,148,149,151,153,173
west-central 14
western 14,15
White Hall 15,97,104,136
Illinois Basin 10,14,15,88,160,176
Illinois Highway
3 176
156 176
167 175
369 175
Illinois River 8,9,15
Indiana 12
Dark Hollow near Bloomington 53
Hamilton Co. 14
Harrodsburg 12
Washington Co., Salem 14
Indiana University, Bloomington, IN 7,53
Interstate Route
44 176
270 176
Iowa 9,15,173
Augusta 172
Belfast 14
Bentonsport 15,81,90,106,108,110,116,119,124,126,151,153,172
Burlington 88
Des Moines Co. 172
eastern 8
Keokuk 9,15,56,67,77,81,83,90,92,101,104,106,108, 110,111,116,119,124,126,127,144,146,151,153,154,156
Lacy Keosauqua Park 172
Lee Co. 173
Soap Creek at Keokuk 11
southeastern 14
southern 12
Van Buren Co. 172
Iowa Terminal (locality 5; measured section 2) 9,157–159,*173*,*177*
iowensis, Fenestella 90,92
Ireland 18,142
ISGS [Illinois State Geological Survey, Champaign, IL] 7,8,11,13,*40*,45,58,83,85,92,111,114,119,122,127,129,130, 133,141,146,151,241–243,247,254,255
ISM [Illinois State Museum, Champaign, IL] 18,*40*

Jackson and Cheetham (1990) 33
Jerseyville 1:62,500 quadrangle (1930) 175

Kaisin (1942) 47
Kent, L. 7
Kentucky 12,15
Caldwell Co. 56
Crittenden Co. 56
Kings Mountain 65,88,97,144,146
Lyon Co. 56
Sloan's Valley 56
Keokuk 1:24,000 quadrangle (1964) 173
Keokuk Group 11,56,77,81,106,108,110,111,116, 119,124,127,144,148,151,153,154,156
Keokuk Industrial (locality 6; measured section 3) 9,127,130,157–159,*173*,*177*
Keokuk Limestone Formation 11–14,56,67, 73,77,81,83,88,90,92,98,104,106,108,113,116,127,130, 144,149,151,154,156,158–160,163,172–181,183–185
Montrose Chert Member 12
Short Creek Oolite Member 12
Keokuk West (locality 8) 9,*173*
keokuk, Orthotetes 12
Keosauqua 1:24,00 quadrangle (1968) 172
Keyes (1894) 56,77,81,83,90,108,111,116,127,130,133, 138,146,149,151,154
Keyes (1895) 12,14
Keyes, C. R. 108
Kibbe Station 173
Kinderhookian Series 11,138
King (1849) 17,39,40,156
King (1850) 17
Kirkwood 1:24,000 quadrangle (1954) 176
Klein, G. D. 7
Knight-Jones and Moyse (1961) 160
Kodabromide® 10
Kodak® 10
Koenig (1958) 56,90
Kolata, D. R. 7
Kritesville Syncline 15

La Grange (locality 16; measured section 11) 9,157–159,*174*,*181*
La Grange 1:24,000 quadrangle (1950) 174
LA [chamber lateral-wall budding-angle]
defined .... **F**,**B**
illustrated 37,38
Lacy Keosauqua (locality 3) 9,12,*172*
Lamouroux (1812) 163
Langenheim, R. L. 7
Laudon (1948) 11,12
Laxifenestella Morozova, 1974 .... 23–25,27,28,30,32, 34,39–41,*49*,50,53,124
coniunctistyla, n. sp. .... **5,6,7** 7,39,49,*50*,52, 53,56,156,158,196–198
fluctuata, n. sp. .... **11,12,13** 7,39,50,53,56, *58*,59,60,156,158,159,202–204
maculasimilis, n. sp. .... **7,8,9** 7,39,50,53,*54*, 56,156,158,198–200
serratula (Ulrich, 1890) .... **9,10,11** 39,45,50,53,*56*, 57,58,156,158,200–202
length of fenestrule opening [**LF**]
defined .... **F**,**B**
illustrated 35,37,38
LeSueur (*unpublished*) 124
Levifenestella Miller, 1961a 22
Levinsen (1925) 16
Levinton (1972) 160
LF [length of fenestrule opening]

defined .... **F**,**B**
illustrated 35,37,38
limitaris,
Banastella .... **24,25** 39,73,*81*,82,83,156, 158,159,215,216
Fenestella 81,83
Lincoln Anticline 15
Lincoln Co. (MO) road U 175
Lincoln Fold 15,16
Lineback (1966) 14
Lisbon, Missouri (locality 43) 9,*176*
Little Whitaker Creek 174
Little Whitaker Creek (locality 23; measured section 15) 9,157–159,*174*,*182*
Localities:
1: Augusta Northwest 9,*172*
2: Bentonsport, Iowa (measured section 1) 9,157–159,*172*,*177*
3: Lacy Keosauqua 9,12,*172*
4: Niota, Illinois 9,*172*
5: Iowa Terminal (measured section 2) 9,157–159,*173*,*177*
6: Keokuk Industrial (measured section 3) 9,127,130,157–159,*173*,*177*
7: White Hollow (measured section 4) 9,157–159,*173*,*178*
8: Keokuk West 9,*173*
9: Grays Quarry (measured section 5) 9,157–159,*173*,*178*
10: Hamilton–Warsaw Roadcut (measured section 6) 9,45,49,54,67,83,92,95,101, 104,106,111,114,119,127,130,151,157–159,*173*,*179*
11: Geode Glen (measured section 7) 9,58,72,85,101, 111,114,119,121,122,127,133,148, 149,151,153,157–159,*173*,*179*
12: Warsaw East 9,*173*
13: Soap Factory Hollow (measured section 8) 9,157–159,*173*,*180*
14: Buel Branch (measured section 9) 9,157–159,*173*,*180*
15: Sand Branch (measured section 10) 9,12,157–159,*174*,*180*
16: La Grange (measured section 11) 9,157–159,*174*,*181*
17: Canton, Missouri—A 9,*174*
18: Canton, Missouri—B 9,*174*
19: Canton, Missouri—C 9,*174*
20: Mount Sterling (measured section 12) 9,97,157–159,*174*,*181*
21: McKee Creek (measured section 13) 9,12,157–159,*174*,*181*
22: Versailles West (measured section 14) 9,12,157–159,*174*,*182*
23: Little Whitaker Creek (measured section 15) 9,157–159,*174*,*182*
24: White Hall—A 9,47,*174*
25: White Hall—B 9,47,*174*
26: White Hall—C (measured section 16) 9,47,157–159,*174*,*182*
27: White Hall—D (measured section 17) 9,47,157–159,*174*,*182*
28: White Hall—E 9,47,*175*
29: White Hall—F (measured section 18) 9,47,133,157–159,*175*,*182*
30: White Hall—G 9,47,*175*
31: White Hall—H 9,47,*175*
32: Carrollton, Illinois 9,*175*
33: Benchmark on State Highway 369 .... 9,*175*
34: Otter Branch (measured section 19) 9,157–159,*175*,*183*
35: McClusky West 9,*175*
36: South Fork Otter Creek 9,*175*
37: Briggs Branch 9,*175*
38: Piasa Creek 9,*175*
39: Cuiver River 9,*175*
40: Troy Roadcut (measured section 20) ... 9,157–159,*175*,*183*
41: Moscow Mills 9,*175*
42: County Road U 9,*175*
43: Lisbon, Missouri 9,*176*
44: Dupo Quarry (locality 44) 9,*176*
45: Meramec River Bend 9,*176*
46: Marshall Road 9,*176*
47: Cragwold Road (measured section 21) 9,56,58,72,79,95,97,111,136,149,157–159,*176*,*184*
48: Columbia Roadcut (measured section 22) 9,157–159,*176*,*183*
49: Dennis Hollow at Valmeyer (measured section 23) 9,45,47,49,54,56,58,60,61,65,67,72,76,79,81,88,92,95,97, 114,116,119,136,146,149,156–159,*176*,*185*
Loculiporina Elias and Condra, 1957 23
logani, Spirifer 12
Lonsdale (1839) 17,18,23,24,40,61,71,85,113
LRM [reticulate meshwork spacing parallel to direction of branch growth]
defined .... **F**,**B**
illustrated 36
Lutaud (1955) 161
Lutaud (1973) 161

maccoyana, Polypora 146,153
maculasimilis, Laxifenestella .... **7,8,9** 7,39,50,53, *54*,56,156,158,198–200
Malaya 144
Marcus (1924) 16
Marischal (1965) 160
Marshall Road 176
Marshall Road (locality 46) 9,*176*
Mary Knott 1:24,000 quadrangle (1972) 175
Massachusetts, Woods Hole 163
MAW [maximum chamber width]
defined .... **F**,**B**
illustrated 37,38
maximum chamber width [**MAW**]
defined .... **F**,**B**
illustrated 37,38
maximum diameter of central axis [**DCA**]
defined .... **F**,**B**
illustrated 36
maximum width of ovicell in mid tangential view [**WOT**] (*defined*) .... **F**,**B**
Maxville Limestone 146
McClusky West (locality 35) 9,*175*
McCoy (1844) 17,27,29–31,33,39,73,85,137,142
McFarlan (1942) 47
McKee and Weir (1953) 10
McKee Creek 174
McKee Creek (locality 21; measured section 13) 9,12,157–159,*174*,*181*
McKinney (1977) 166
McKinney (1979) 124
McKinney (1980) 8,21,25,27,28,38
McKinney and Gault (1980) 124
McKinney, F. K. 7
McNair (1937) 16
McQueen, Hinchey, and Aid (1941) 15

Measured Sections:
1: Bentonsport, Iowa (locality 2) 9,157–159,*172,177*
2: Iowa Terminal (locality 5) 9,157–159,*173,177*
3: Keokuk Industrial (locality 6) ... 9,127,130,157–159,*173,177*
4: White Hollow (locality 7) 9,157–159,*173,178*
5: Grays Quarry (locality 9) 9,157–159,*173,178*
6: Hamilton–Warsaw Roadcut (locality 10) ....
... 9,45,49,54,67,83,92,95,101,104,106,111,114,119,127,130, 151,157–159,*173,179*
7: Geode Glen (locality 11) 9,58,72,85,101,111, 114,119,121,122,127,133,148,149,151,153,157–159,*173,179*
8: Soap Factory Hollow (locality 13) 9,157–159,*173,180*
9: Buel Branch (locality 14) 9,157–159,*173,180*
10: Sand Branch (locality 15) 9,12,157–159,*174,180*
11: La Grange (locality 16) 9,157–159,*174,181*
12: Mount Sterling (locality 20) 9,97,157–159,*174,181*
13: McKee Creek (locality 21) 9,12,157–159,*174,181*
14: Versailles West (locality 22) 9,12,157–159,*174,182*
15: Little Whitaker Creek (locality 23) 9,157–159,*174,182*
16: White Hall—C (locality 26) 9,47,157–159,*174,182*
17: White Hall—D (locality 27) 9,47,157–159,*174,182*
18: White Hall—F (locality 29) 9,47,133,157–159,*175,182*
19: Otter Branch (locality 34) 9,157–159,*175,183*
20: Troy Roadcut (locality 40) 9,157–159,*175,183*
21: Cragwold Road (locality 47) ....
.... 9,56,58,72,79,95,97,111,136,149,157–159,*176,184*
22: Columbia Roadcut (locality 48) 9,157–159,*176,183*
23: Dennis Hollow at Valmeyer (locality 49) ....
.... 9,45,47,49,54,56,58,60,61,65,67,72,76,79,81,88,92,95,97, 114,116,119,136,146,149,156–159,*176,185*
mediocreforma, Banastella .... **22,23** 7,39,73,*79*, 80,81,83,156,158,213,214
medvedkensis, Fenestella 40
Meek and Worthen (1860) 12
meekanus, Archimedes 126
Meepen Syncline 15
Mendon 1:62,500 quadrangle (1946) 173,174
Meramec River 176
Meramec River Bend (locality 45) 9,*176*
Meramecian Group 11
Meramecian Series 11,13,49,61,126,176–185
Meredosia 1:62,500 quadrangle (1928) 174
Meremac [*see* Meramec]
Meremec [*see* Meramec]
meshwork formula of Condra and Elias (1944) 18,58
Meyer and Macurda (1977) 160
Michigan River 10,11
micrometric formula of Miller (1961a) *et seq.* 18,58
Miller, S. A. (1889) 130
Miller, T. G. (1961a) 18,22
Miller, T. G. (1961b) 18,22
Miller, T. G. (1962) 23,24,47
Minilya Crockford, 1944 ... 22–24,28,30,32,34,39–41,*61*,62,65,97
duplaris Crockford, 1944 61,62
paratriserialis, n. sp. .... **14,15** 7,39,62,*65*, 66,67,156,158,205,206
sivonella, n. sp. .... **13,14** 7,39,61,*62*,65,67,97, 156,158,159,164,204,205
minimum chamber width [**MIW**]
defined .... **F,B**
illustrated 37,38
Mirandifenestella Termier and Termier, 1971 23
Mirifenestella Morozova, 1974 23,24
Mississippi Arch 15
Mississippi River 8,9,12,15,16,18,49,173,176
Mississippi River Arch 10
Mississippian stratotype 8,10
Missouri 8,9,15,16,173
eastern 12
Howard Co. 8,176
La Grange 130
Lewis Co. 174
Lincoln Co. 15,175
Lisbon 176
Meramec 137
Moscow Mills 175
St. Francisville 90,127
St. Louis 9,12,15,65,72,76,79,81,85,88,95,97,111, 116,136,138,141,176
St. Louis Co., Barrett's Station 83,111,113,138,146
Troy 16,175
Wayland 130
Missouri Geological Survey 11
Missouri Highway
47 175
61 175
Missouri River 9,176
MIW [minimum chamber width]
defined .... **F,B**
illustrated 37,38
Moll (1803) 165
Monroe City Syncline 16
Moore (1933) 11
Morozova (1962) 17,19,22
Morozova (1970a) 19,22,23
Morozova (1970b) 19,20,22
Morozova (1973) 19,22
Morozova (1974) 8,18,19,22–25,27–30,32,39–41, 49,50,61,62,67,68,72,90,124
Moscow Mills (locality 41) 9,*175*
Mount Sterling (locality 20; measured section 12) ....
.... 9,97,157–159,*174,181*
Mount Sterling 1:62,500 quadrangle (1926) 174
Mullin (1963) 160
multispinosa,
Fenestella 47
Fenestrellina 47
Rectifenestella .... **4,5** 39,41,44,45,*47*, 49,156,158,195,196

negligens, Archimedes .... **50,51,52** 39,*124*, 125–127,156,158,159,241-243
Nekhoroshev (1926) 18,41,47
Nekhoroshev (1928) 19,22
Nekhoroshev (1932) 19,22
Nekhoroshev (1949) 19,22
Nekhoroshev (1953) 19,22
Nekhoroshev (1956) 19,22
Nekhoroshev (1960) 22,61
Nekhoroshev, V. P. 19
Nevada, northeastern 39
Nicholson and Lydekker (1889) 17
Nickles and Bassler (1900) 22
Nielsen (1970) 161
Nielsen and Pedersen (1979) 161
Nikiforova (1927) 47
Nikiforova (1933) 19,47
Nikiforova (1935) 19

Nikiforova (1938) 19
Nikiforova, A. I. 19
Niota 1:24,000 quadrangle (1964) 172
Niota, Illinois (locality 4) 9,*172*
nobilis, Utropora 25
number of aperture openings per fenestrule length [AF]
illustrated 35
defined .... **F,B**
number of stylets surrounding aperture [SA]
defined .... **F,B**
illustrated 35
Nutwood Anticline 15
Nye, Dean, and Hinds (1972) 10

oculata, Hemitrypa 106
Ohio 40
Newtonville 146
Richfield 144
Sciotoville 144
OL [ovicell length]
defined .... **F,B**
illustrated 35
d'Orbigny (1839) 25
d'Orbigny (1848–1852) 16,17,22
Order
Cheilostomata Busk, 1852 16
Cryptostomata Vine, 1884 16,17,31,39
Cyclostomata 17
Cystoporata 17
Trepostomata Ulrich, 1882 16,17
Orthotetes keokuk (Weller, 1914) 12
Osagean Group 11
Osagean Series 11,13,49,61,126,177–181,183–185
Osgood Fund 8
Osgood Prize 8
Otter Branch (locality 34; measured section 19) 9,157–159,*175,183*
Otter Creek 175
Otter Creek Syncline 15
ovicell length [**OL**]
defined .... **F,B**
illustrated 35
ovicell width [**OW**]
defined .... **F,B**
illustrated 35
OW [ovicell width]
defined .... **F,B**
illustrated 35
Owen (1838) 17,124
Owen (1842) 17,124
Owen (1852) 11
owenana, Fenestella 127
owenanus, Archimedes .... **52,53,54,55,56** 39,124, *127*,130,133,136,156,158,159,243–247
Ozark Dome 10,15
Ozark Uplift 15

pallasiana, Cryptosula 165,166
Palmolive® 10
Parafenestella Miller, 1961b 22
paratriserialis, Minilya .... **14,15** 7,39,62, *65*,66,67,156,158,205,206
Parsons and Le Brasseur (1970) 162
pateriformis, Hemitrypa 108,110
Payson Anticline 15
Permofenestella Morozova, 1974 23,24,25
perstriata, Hemitrypa .... **39,40,41** 39,106,*108*, 109–111,113,156,158,230–232
Phillips (1836) 17
Phillips (1841) .. 15,17,23,27,29–31,33,36,39,40,103,106,108,119
Phyllopora King, 1849 17
Piasa Creek 175
Piasa Creek (locality 38) 9,*175*
Pittsfield Anticline 15
plumosa,
Fenestella 113
Hemitrypa 113
Počta (1894) 17,21,25
Polyfenestella Bancroft, 1986a 22,26
Polypora McCoy, 1844 .... 17,27,29–31,33,34,39,73,85,137,141,*142*,146
biseriata Ulrich, 1890 73,83,151
dendroides McCoy, 1844 142
gracilis Prout, 1860 .... **65,66** 39,143,*144*, 146,153,156,158,159,256,257
cf. *gracilis* Prout 144
halliana Prout, 1860 146
maccoyana Ulrich, 1890 146,153
retrorsa Ulrich, 1890 .... **71,72** 39,144, *154*,156,158,159,262,263
simulatrix Ulrich, 1890 .... **69,70,71** 39,143, 144,148,*151*,152,153,156,158,260–262
spininodata Ulrich, 1890 .... **67,68,69** 39,143,144, 148,*149*,151,156,158,258–260
Varsouviensis Prout 146
Varsouviensis? Prout 146
varsoviensis Prout, 1858a .... **66,67** 39,85,142,143, *146*,147,148,151,156,158,257,258
Polypora(?) *gracilis* Prout 144
Polyporella Simpson, 1895a 142
Polyporina Fredriks, 1920 142
Potter and Pryor (1961) 10
PRI [Paleontological Research Institution, Ithaca, NY] 7,8
Prout (1858a) 12,17,27,29–31,33,39,85, 137,138,140–142,146–148,156,254,255,257,258
Prout (1858b) 17
Prout (1859) 17,39,108,111,113,146,156,232–234
Prout (1860) 39,113,144,146,156,256,257
Prout (1866) 17,144
proutana, Hemitrypa 111,113
proutana vermifera, Hemitrypa 119,122
Proutella Ulrich, 1889 12
Pryor and Sable (1974) 11
Ptylopora McCoy, 1844 17

RA [chamber reverse-wall budding-angle]
defined .... **F,B**
illustrated 37,38
Ramp Creek Limestone 14
rare (*defined*) 156
Rarifenestella Morozova, 1974 23,25
Rectifenestella Morozova, 1974 .... 23–25,27,28,30,32,34,39,*40*,41,42,90,124
multispinosa (Ulrich, 1890) .... **4,5** 39,41,44,45, *47*,49,156,158,195,196
tenax (Ulrich, 1888) .... **1,2** 39,*41*,42,44, 45,47,49,58,156,158,192,193

Rectifenestella Morozova, 1974
tenuissima (Cumings, 1906) .... **2,3** 39,41,42,44, *45*,46,47,49,156,158,159,193,194
regalis, Fenestella 76,88
"*Retepora Archimedes*" of Owen (1842) 124
reticulate meshwork spacing parallel to direction of branch growth [**LRM**]
defined .... **F,B**
illustrated 36
reticulate meshwork spacing perpendicular to direction of branch growth [**WRM**]
defined .... **F,B**
illustrated 36
retrorsa, Polypora .... **71,72** 39,144,*154*, 156,158,159,262,263
reversa, Archimedes 124,130,133
Rexroad and Collinson (1965) 12
Rhabdomesidea 17
Rhodes, Austin, and Druce (1969) 12
Rhombofenestella Termier and Termier, 1971 23,61
Roodhouse 1:62,500 quadrangle (1924) 174,175
Ross (1964) 16,17
Rotaia subtrigona (Meek and Worthen, 1860) 12
RSL [diameter of macrostylets on reverse branch surface]
defined .... **F,B**
illustrated 35
RSS [diameter of microstylets on reverse branch surface]
defined .... **F,B**
illustrated 35
Rubey (1952) 15
rudiformis, Fenestella 90,92
rudis,
Cubifenestella .... **29,30** 39,83,88,*90*, 92,94,156,158,220,221
Fenestella 41,83,88,90,92
Rugofenestella Termier and Termier, 1971 23
RWT [thickness of reverse-wall laminated layer]
defined .... **F,B**
illustrated 37,38

SA [number of stylets surrounding aperture]
defined .... **F,B**
illustrated 35
SAD [diameter of stylets surrounding aperture]
defined .... **F,B**
illustrated 35,37
Sakagami (1970) 144
Salem Limestone Formation 11–16,53,73,90,92,97,98, 141,159,174–176,180,181,183,184
Chalfin Member 14
Fults Member 14
Kidd Member 14
Rocher Member 14
sancti-ludovici, Fenestralia 138
sanctiludovici,
Fenestralia .... **63,64** 39,137,*138*,140, 141,156,158,159,254,255
Fenestralia? 138
Sand Branch (locality 15; measured section 10) 9,12,157–159,*174*,*180*
Sand Branch Creek 174
Sandberg, P. 7
Sangamon Arch 15
sarytschevae, Fenestella 49
Schoener (1974) 160,169,171
Schoener (1982) 160
Scotland, Midland Valley 26
Second *Archimedes* Limestone 111,113
Seminary Creek 175
serratula,
Fenestella 41,56
Laxifenestella .... **9,10,11** 39,45,50,53, *56*,57,58,156,158,200–202
Sheldon, Sutcliffe, and Prakash (1973) 162
Shepherd College, Shepherdstown, WV 7
Faculty Minigrant Fund 8
Foundation 8
Shishova (1968) 16
Shulga-Nesterenko (1936) 19
Shulga-Nesterenko (1941) 19,22
Shulga-Nesterenko (1949) 19,22
Shulga-Nesterenko (1951) 19,22,40,47,49,67
Shulga-Nesterenko (1952) 19,22,41,45
Shulga-Nesterenko (1955) 19,22
Shulga-Nesterenko (1960) 16,17
Silen and Harmelin (1974) 31
Simpson (1895a) 22,142
Simpson (1895b) 138
simulatrix, Polypora .... **69,70,71** 39,143,144,148, *151*,152,153,156,158,260–262
Sivon, P. 7,62
sivonella, Minilya .... **13,14** 7,39,61,*62*,65, 67,97,156,158,159,164,204,205
Smith (1981) 160
SNB [distance between node centers along obverse branch surface]
defined .... **F,B**
illustrated 35
Snyder (1987) 163
Snyder and Kepler (1987) 39
Snyder, C. 8
Soap Factory Hollow (locality 13; measured section 8) 9,157–159,*173*,*180*
Sonora Formation 11–15,159,172–174,177,179
Sonora Sandstone 14
South Fork Otter Creek (locality 36) 9,*175*
spacing of macrostylets along reverse branch surface [**SSL**]
defined .... **F,B**
illustrated 35
spacing of microstylets along reverse branch surface [**SSS**]
defined .... **F,B**
illustrated 35
spacing of stylets along obverse branch surface [**SSO**]
defined .... **F,B**
illustrated 35
spacing of whorls along central axis [**WSC**]
defined .... **F,B**
illustrated 36
Spergen Hill Limestone 14
Spergen Limestone 14,159,172,173
spininodata, Polypora .... **67,68,69** 39,143, 144,148,*149*,151,156,158,258–260
Spinofenestella Termier and Termier, 1971 23,24
Spirifer logani Hall, 1858 12
Spoon Formation 15
Springville Formation 14
SSL [spacing of macrostylets along reverse branch surface]
defined .... **F,B**
illustrated 35

SSO [spacing of stylets along obverse branch surface]
defined ... **F,B**
illustrated ... 35
SSS [spacing of microstylets along reverse branch surface]
defined ... **F,B**
illustrated ... 35
St. Charles 1:62,500 quadrangle (1954) ... 175
St. Genevieve
Formation ... 11
Group ... 11
St. Louis
Group ... 11,138,141
Limestone Formation ... 11–15,47,56, 73,83,90,98,138,141,146,159,173,176,177,179
St. Ludovici, Fenestralia ... 138
Ste. Genevieve Limestone ... 15
Stockdale (1929) ... 14
Stockdale (1939) ... 14
stocktonensis, Fenestella ... 45,47
Strathmann (1971) ... 162,164
Strathmann (1973) ... 160–164,167
subantiqua, Fenestella ... 25
Subfamily
Fenestellinae ... 17
Goniocladiinae ... 17
Polyporinae ... 17
submicroporata, Fenestella ... 41,45
Suborder
Fenestelloidea Astrova and Morozova, 1956 ... 16,17,21,22,27,39
Ptilodictyoidea Astrova and Morozova, 1956 ... 16,17
Rhabdomesoidea Astrova and Morozova, 1956 ... 16,17
subtrigona, Rotaia ... 12
Swann (1963) ... 11
Sweeney, D. ... 7
Synocladia King, 1849 ... 17
Synocladia(?) *fenestelliformis* Young, 1881 ... 26

Taphrognathus varians–Apatognathus Zone ... 12
Taphrognathus varians–Cavusgnathus–Apatognathus Zone of Rhodes, Austin, and Druce (1969) ... 12
Tavener-Smith (1965) ... 18,34
Tavener-Smith (1966) ... 18
Tavener-Smith (1973) ... 18,22,47
Tavener-Smith and Williams (1972) ... 16,17
Tavener-Smith, R. ... 19
TB [thickness of branch]
defined ... **F,B**
illustrated ... 37,38
tenax,
Fenestella ... 40,41
Rectifenestella ... **1,2** ... 39,*41*,42,44, 45,47,49,58,156,158,192,193
Tennessee ... 15
tenuissima,
Fenestella ... 45,47
Rectifenestella ... **2,3** ... 39,41,42,44,*45*,46,47,49, 156,158,159,193,194
terebriformis, Archimedes ... 126
Termier and Termier (1971) ... 8,18,23,24,61
Texas, west ... 18,23
Thailand ... 144
thickness of branch [**TB**]
defined ... **F,B**
illustrated ... 37,38
thickness of chamber lateral-wall granular layer [**TLW**]
defined ... **F,B**
illustrated ... 37,38
thickness of front-wall (obverse wall) laminated layer [**FWT**]
defined ... **F,B**
illustrated ... 37,38
thickness of reverse-wall granular layer [**TRW**]
defined ... **F,B**
illustrated ... 37,38
thickness of reverse-wall laminated layer [**RWT**]
defined ... **F,B**
illustrated ... 37,38
TLW [thickness of chamber lateral-wall granular layer]
defined ... **F,B**
illustrated ... 37,38
Transcontinental Arch ... 10
Treworgy (1981) ... 15
triserialis, Fenestella ... 65,67
Trizna (1939) ... 19
Trizna (1950) ... 19
Trizna (1958) ... 19,41,47,56,68,83,90,111,146,149
Trizna and Kautsan (1951) ... 19
Troy 1:24,000 quadrangle (1972) ... 175
Troy Roadcut (locality 40; measured section 20) ... 9,157–159,*175*,*183*
Troy–Brussels Syncline ... 15
TRW [thickness of reverse-wall granular layer]
defined ... **F,B**
illustrated ... 37,38
Turpaeva (1957) ... 160
turrita, Bugula ... 162

UI X [University of Illinois, Urbana, IL] ... 7,*40*,45, 47,49,54,56,58,60,61,65,67,72,76,79,81,83,85,88, 92,95,97,101,104,106,111,114,116,119,122,127,130,133,136, 146,149,151,153,156,192–253,256–263
Ullen Formation [*see* Ullin Limestone Formation]
Ullin Limestone Formation ... 11,13–15
Ulrich (1882) ... 16,18
Ulrich (1888) ... 17–19,39–42,47,49,58,144,156,192,193
Ulrich (1890) ... **F**,8,12,16–19,22,39,41,44,45,47,50,53, 56–58,65,67,68,70,71,73,76–78,81–85,88,90,92,94,95, 97,101,106,108–111,113,114,116,117,119–122,124–127, 130,133,138,141,144,146,148,149,151–154,156,173, 195,196,200–202,207–209,211,212,215–218, 220,221,230–232,237–243,258–263
Ulrich (1893) ... 17-19
Ulrich (1904) ... 11
Ulrich, E. O. ... 39,40,53,65,106,108,122,129
USGS [United States Geological Survey, Reston, VA] ... 8,11,13
U. S. Highway 61 ... 173,174
usitata, Cubifenestella ... **31,32** ... 7,19–21,38, 39,90,*92*,93–95,97,156,158,222,223
USNM [United States National Museum of Natural History, Smithsonian Institution, Washington, DC] ... 7,18,*40*,45,49,58,65,92,111,114,119,146
U. S. S. R. ... 19
Altai ... 19
Armenia ... 19
Bashkiria ... 19
Kazakhstan ... 19
Kunwrak Vain ... 149

U. S. S. R.
Kuzbass 19
Russian Platform 40,49,67
Turkestan 19
Utgaard and Perry (1960) 22
Utropora Počta, 1894 21,25,27
nobilis (Barrande *in* Počta, 1894) 25

Valmeyer 1:24,000 quadrangle (1954) 176
Valmeyer Anticline 16
Valmeyeran Series ... 11,13,16,31,73,90,98,122,126,138,177–185
valmeyeri, Archimedes .... **60,61,62** 7,39,124,*133*, 134,136,156,158,159,251–253
Van Tuyl (1925) 11,12,14,130,133
Varsouviensis, Polypora 146
Varsouviensis?, *Polypora* 146
varsoviensis, Polypora .... **66,67** 39,85,142,143, *146*,147,148,151,156,158,257,258
VD [vestibule depth]
defined .... **F,B**
illustrated 37,38
venusta, Apertostella .... **38,39** 7,39,98,*104*, 106,156,158,159,229,230
Vermeij (1977) 160
vermifera, Hemitrypa .... **47,48,49** 39,108, *119*,120–122,156,158,238–240
Versailles Anticline 15
Versailles West (locality 22; measured section 14) 9,12,157–159,*174,182*
verticillatum, Zoobotryon 162
vestibule depth [**VD**]
defined .... **F,B**
illustrated 37,38
Vine (1880) 17
Vine (1884) 16,17,39,136,156
Vine (1886) 17

Waagen and Pichl (1885) 17
Walker (1962) 10
Wanless (1957) 11
Warsaw 1:24,000 quadrangle (1964) 173
Warsaw Anticline 15
Warsaw Dome 15
Warsaw East (locality 12) 9,*173*
Warsaw Formation 7–17,26,27,29,31,34–37,39–41,47,49,50, 53,56,58,60,65,67,68,71–73,76,79,81,83,85,88,90,92, 95,97,98,104,106,108,111,116,119,121,122,124,127, 130,133,136–138,141–144,146,148,149,151, 153,156,158–160,162,163,165–185
Garret Mill Sandstone Member 12
Somerset Shale Member 12
Wildie Sandstone Member 12
Warsaw Shale 11,13
Wass (1966) 23,61
Waterloo 1:62,500 quadrangle (1955) 176
Waterloo–Dupo Anticline 16
Waters (1891) 16
Waters (1904) 162
Waverly Group 40,144
WB [branch width]
defined .... **F,B**
illustrated 35,37,38
WD [dissepiment width]
defined .... **F,B**
illustrated 35,37,38
Weller, J. M. (1934) 12
Weller, J. M., *et al.* (1948) 11
Weller, J. M., and Sutton (1940) 11,12
Weller, S. (1908) 11,12,14
Weller, S. (1914) 11,12
Weller, S. (1926) 12
welleri, Archimedes 130,133
WF [width of fenestrule opening]
defined .... **F,B**
illustrated 35
Whitaker Creek 174,175
White Hall—A (locality 24) 9,47,*174*
White Hall—B (locality 25) 9,47,*174*
White Hall—C (locality 26; measured section 16) 9,47,157–159,*174,182*
White Hall—D (locality 27; measured section 17) 9,47,157–159,*174,182*
White Hall—E (locality 28) 9,47,*175*
White Hall—F (locality 29; measured section 18) 9,47,133,157–159,*175,182*
White Hall—G (locality 30) 9,47,*175*
White Hall—H (locality 31) 9,47,*175*
White Hollow (locality 7; measured section 4) 9,157–159,*173,178*
Whitfield (1891) 146
Whitfield (1895) 146
Whiting and Stevenson (1965) 15
width of fenestrule opening [**WF**]
defined .... **F,B**
illustrated 35
width of keel [**WK**]
defined .... **F,B**
illustrated 35
width of peristome [**WP**]
defined .... **F,B**
illustrated 35
Wiens (1977) 160
Willman *et al.* (1975) 15
Wills (1971) 12–14
Winston (1976) 162
Winston (1977) 160–166,169,170
Winston (1978) 166
Winston (1982) 160,165
Wisconsin Arch 10
WK [width of keel]
defined .... **F,B**
illustrated 35
Worthen (1866) 11
Worthen (1870) 12
Worthen, Shaw, and Meek (1873) 12
wortheni,
Archimedes .... **56,57,58,59,60** 39,71, 122,124,127,*130*,131,133,156,158,159,247–251
Fenestella 130
Fenestella (*Archimedes*) 122
Worthenopora Ulrich, 1889 12
WOT [maximum width of ovicell in mid tangential view] (*defined*) .... **F,B**
WP [width of peristome]
defined .... **F,B**
illustrated 35

WRM [reticulate meshwork spacing perpendicular to direction of branch growth]
defined .... **F,B**
illustrated 36
WSC [spacing of whorls along central axis]
defined .... **F,B**
illustrated 36

Young (1881) 26

Zittel (1880) 17
Zoobotryon Ehrenberg, 1831 163
verticillatum 162

Table 8a.—Continued.

Outline of **Exterior Description**

1. Zoarial characters
   A. robustness (*delicate* [fragile, zoaria frequently broken and small] → *intermediate* [moderate number of large zoaria present, resist breakage better than delicate forms] → *robust* [zoaria typically large, highly resistant to breakage])
   B. outward expansion (flat, obversely or reversely curved, undulating, cup-shaped, or spiralling from central axis)
   C. mesh spacing (*close* [**WF** < **WB**] → *intermediate* [**WF** ≅ **WB**] → *open* [**WF** > **WB**])
   D. astogenetic thickening of the zoarial skeleton (slight, moderate, or pronounced)
   E. mesh uniformity (regular or irregular)
   F. secondary features (*e.g.,* central axis, reticulate meshwork)
   G. dimensions of secondary features
   H. probable size and shape of mature colonies
2. Branch characters
   A. robustness (*delicate* [fragile, frequently crushed, thin width and depth] → *intermediate* [moderate preservation, width and depth intermediate] → *robust* [wide, thick, typically well-preserved]
   B. width (*narrow* [<0.30 mm] → *intermediate* [0.30–0.39 mm] → *wide* [>0.39 mm], and *constant* [CV < 15] or *variable* [CV > 15])
   C. proximodistal trace (straight, sinuous [bending toward sites of dissepiment emplacement], or locally broadly curved)
   D. spacing (*close* [**DBC** < 2.0 × **WB**] → *intermediate* [**DBC** 2.0–2.5 × **WB**] → *wide* [**DBC** < 2.5 × **WB**])
   E. distance between adjacent branch centers (*regular* [CV < 20] or *irregular* [CV > 20])
   F. texture (smooth or granular, and effects of astogeny thereon)
   G. surface profile (*e.g., rounded* [∩], *flat* [−], or *angular* [∧])
   H. keels (if present)
      1. whether they are single or multiple, and the number across branch surface
      2. width (*narrow* [<0.05 mm] → *intermediate* [0.05–0.15 mm] → *wide* [>0.15 mm, or <0.5 × **WB**])
      3. degree of development
      4. linear characteristics (continuous or intermittent, straight or anastomosing)
      5. position along branch (at branch midline or curving around apertures)
      6. effect on obverse surface profile
      7. effects of astogeny
   I. nodes (if present)
      1. emplacement (monoserial or biserial)
      2. degree of development (poorly developed, intermediate, or well-developed)
      3. size (*small* [<0.07 mm] → *intermediate* [0.07–0.12 mm] → *large* [>0.12 mm])
      4. shape (*e.g.,* circular, ovate [includes direction of elongation], stellate [number of lobes])
      5. uniformity of size and shape (*regular* [CV < 25] or *variable* [CV > 25])
      6. location (on branch, on keel, and in a straight line or anastomosing)
      7. number per fenestrule (includes range and mode)
      8. spacing interval (*close* [<0.25 mm] → *intermediate* [0.25–0.80 mm] → *wide* [>0.80 mm]) and uniformity (*even* [CV < 25] or *uneven* [CV > 25])
      9. effects of astogeny
   J. stylets
      1. size (*small* [<0.01 mm] → *intermediate* [0.01–0.02 mm] → *large* [>0.02 mm])
      2. uniformity of size and position (*regular* [CV < 20] or *irregular* [CV > 20])
      3. location across branch surface
      4. effects of astogeny
   K. texture (smooth or granular, and effects of astogeny)
   L. longitudinal striae
      1. number (few, intermediate, or numerous)
      2. spacing (close, intermediate, or wide)
      3. effects of astogeny
   M. microstylets
      1. relative size (*small* [<0.018 mm] → *intermediate* [0.018–0.026 mm] → *large* [>0.026 mm])
      2. location and spacing across branch surface
      3. size (*regular* [CV < 20] or *variable* [CV > 20])
      4. effects of astogeny
   N. macrostylets
      1. relative size (*small* [<0.05 mm] → *intermediate* [0.05–0.08 mm] → *large* [>0.08 mm])
      2. shape (*e.g.,* circular, ovate, or irregular)
      3. uniformity of size and shape (*regular* [CV < 25] or *variable* [CV > 25])
      4. location on branch surface
      5. spacing (regular or variable)
      6. effects of astogeny

Table 8a.—Continued.

   O. rows of autozooecia
      1. number across normal branch surface
      2. number and extent proximal to sites of branch bifurcation
   P. changes in branch thickness
      1. thickening proximal to bifurcation (slight, moderate, or pronounced)
      2. thinning distal to bifurcation (slight, moderate, or pronounced)
   Q. heterozooecia (if present)
      1. type (*e.g.,* ovicells, parazooecia, cyclozooecia, caverns, or microzooecia)
      2. size and emplacement
3. Dissepiments
   A. width
      1. overall width (*thin* [<0.5 × **WB**] → *intermediate* [0.5–1.0 × **WB**] → *wide* [>1.0 × **WB**])
      2. width relative to branch
      3. uniformity (*constant* [CV < 20] or *variable* [CV > 20])
   B. length
      1. overall length (*short* [**WF** ≪ **WB**] → *intermediate* [**WF** ≅ **WB**] → *long* [**WF** ≫ **WB**])
      2. uniformity (*constant* [CV < 20] or *variable* [CV > 20])
   C. emplacement (at regular or irregular intervals)
   D. shape (medially thinned, flaring at branch contact, or uniform, and degree of deformation, if any)
   E. positioning relative to reference planes
      1. obverse surface (even, recessed, or highly recessed)
      2. reverse surface (even, recessed, highly recessed)
   F. overall astogenetic thickening (degree and effect)
   G. ornamentation
      1. obverse surface (longitudinal striae [number and position] and stylets [size and position])
      2. reverse surface (longitudinal striae [size and position] and stylets [size and position])
   H. texture
      1. obverse (smooth or granular, and effects of astogeny thereon)
      2. reverse (smooth or granular, and effects of astogeny thereon)
   I. emplacement relative to branch length (perpendicular or at a variable angle)
   J. aperture emplacement relative to dissepiment–branch contact (position and symmetry)
4. Fenestrules[1]
   A. relative size (*small* [length <0.4 mm; width <0.24 mm] → *intermediate* [length 0.4–0.9 mm; width 0.24–0.34 mm] → *large* [length >0.9 mm; width >0.34 mm])
   B. shape (*e.g.,* elliptical, ovate, rectangular, or square)
   C. direction of elongation (proximodistal or perpendicular to branch growth)
   D. consistency of size (length, width) and shape (*regular* [CV < 20] or *variable* [CV > 20])
   E. variation in shape and size of fenestrules on obverse and reverse surfaces of zoarium
   F. mean **WF** : **WB**; differences between obverse and reverse surface noted
   G. changes in shape and size toward proximal end of zoarium, and effects of astogeny
   H. **WF** : **LF** (and range if highly variable) and uniformity of this ratio (*regular* [CV < 20] or *variable* [CV > 20])
   I. number of apertures per fenestrule length (range and mode)
   J. **ADB** : **AAB**, **ADB** : **ABB**, and **ADB** : **ABB** and relative variability of these ratios (*constant* [CV < 10] or *variable* [CV > 10])
5. Aperture
   A. relative size (*small* [length <0.09 mm; width <0.07 mm] → *intermediate* [length 0.09–0.15 mm; width 0.07–0.12 mm] → *large* [length >0.15 mm; width >0.12 mm])
   B. shape
      1. circular
      2. ovate (direction of elongation, distal enlargement, and **AL** : **AW** as applicable)
      3. elliptical (direction of elongation, distal enlargement, and **AL** : **AW** as applicable)
      4. uniformity (*uniform* [CV < 10] or *variable* [CV > 10])
   C. attitudinal relationship of aperture to plane of obverse surface (parallel, inclined into fenestrule, or perpendicular)
   D. peristome (if present)
      1. relative width (*thin* [<0.025 mm] → *intermediate* [0.025–0.050 mm] → *wide* [>0.050 mm])
      2. degree of development (poorly developed, intermediate, or well-developed)
      3. complete or incomplete (if incomplete, location of peristomal gap)
      4. stylet development in peristomal gap, and association of stylets with peristome
   E. stylets surrounding aperture (*e.g.,* number, size [*small* → *intermediate* → *large*], constant or variable)
   F. projection into fenestrule and degree of inflection in fenestrule
   G. terminal diaphragm (of uniform thickness or centrally thickened, and area of occurrence)

[1] Caution: if **WF** : **WB** is large for colonies with extremely small **WB**, the following distinctions may not apply.

Table 8a.—Continued.

6. Zoarial supports
   A. placement (on reverse surface or on zoarial edges)
   B. degree of development

Outline of **Interior Description**

1. Branch
   A. shape in transverse-section (*e.g.,* elliptical, ovate, circular, semicircular, rhombic, polygonal)
   B. direction of elongation (obverse–reverse, or parallel to zoarial surface)
   C. branch thickness (*shallow* [<0.30 mm] → *medium* [0.30–0.39 mm] → *thick* [>0.39 mm], *regular* [CV < 15] or *variable* [CV > 15])
2. Autozooecial living chamber
   A. relative size (*small* [length <0.20 mm; depth <0.10 mm; maximum width <0.10 mm; minimum width <0.07 mm] → *intermediate* [length 0.20–0.48 mm; depth 0.10–0.20 mm; maximum width 0.10–0.15 mm; minimum width 0.07–0.12 mm] → *large* [length >0.48 mm; depth >0.20 mm; maximum width >0.15 mm; minimum width >0.12 mm])
   B. emplacement at or near budding-site (monoserial, biserial [alternating or adjacent], or polyserial [alternating or adjacent])
   C. axial wall trace (straight, sinuous [irregular], sinuous [extending toward and connecting with proximal and distal lateral chamber walls], or zigzag [extending diagonally across entire branch, lateral chamber walls short or absent]) and change in axial wall shape from reverse to obverse chamber surface
   D. orientation of autozooecial chamber elongation (elongate proximodistally parallel to reverse wall, parallel to proximal and distal lateral chamber walls, or length and depth equal [*i.e.,* a cubic chamber])
   E. chamber outline near reverse wall (*e.g.,* triangular, rectangular, square, ovate, elliptical, circular, pentagonal, parallelogram-shaped, diamond-shaped)
   F. chamber outline in mid chamber (*e.g.,* triangular, rectangular, square, ovate, elliptical, circular, pentagonal, parallelogram-shaped, diamond-shaped)
   G. chamber outline near obverse surface (*e.g.,* triangular, rectangular, square, ovate, elliptical, circular, pentagonal, parallelogram-shaped, diamond-shaped), orientation of outline, and causes of irregularities in shape
   H. chamber shape uniformity (highly uniform, uniform, moderately uniform, moderately variable, variable, or highly variable)
   I. location of aperture relative to chamber
   J. vestibules (if present)
      1. degree of development
      2. length (*short* [<0.06 mm] → *intermediate* [0.06–0.12 mm] → *long* [>0.12 mm])
      3. variability of length (*constant* [CV < 15] or *variable* [CV > 15])
   K. chamber ratios (**MIW** : **MAW**, **MAW** : **CD**, **CD** : **CL**), and variability of dimensions (*constant* [CV < 10] or *variable* [CV > 10])
   L. hemisepta (if present) (degree of development, shape, and positioning of superior and inferior hemisepta)
   M. uniformity of (*constant* [CV < 10] or *variable* [CV > 10]) and mean chamber lateral-wall budding-angle
   N. uniformity of (*constant* [CV < 10] or *variable* [CV > 10]) and mean chamber reverse-wall budding-angle
   O. heterozooecia (if present) (type [ovicells, parazooecia, cyclozooecia, caverns, microzooecia], size, and emplacement)
   P. description of three-dimensional shape
3. Skeletal microstructure
   A. granular layer
      1. relative thickness (thin, intermediate, or thick), and degree of development
      2. continuity with nodes, stylets, longitudinal striae, keels, peristomes, and apertural stylets, and ornamentation and features of dissepiments
      3. relative thickness of reverse and lateral walls
      4. astogenetic effects
   B. lamellar layer
      1. relative thickness (thin, intermediate, or thick) and degree of development
      2. astogenetic effects

Table 8b.—Definitions and abbreviations of the 44 fenestellid and polyporid zooecial and zoarial characters measured in this study. Characters 6 and 19 are simple numbers; character 29, 41, and 42 are measured in °; all other characters are measured in mm.

Exterior characters:

1. **WB**: *branch width* (not measured at branch bifurcation).
2. **DBC**: *distance between branch centers* (not measured at branch bifurcation).
3. **WD**: *dissepiment width* (measured parallel to branch growth direction).
4. **LF**: *length of fenestrule opening* (measured proximodistally).
5. **WF**: *width of fenestrule opening* (measured perpendicular to branch length).
6. **AF**: *number of aperture openings per fenestrule length* (measured between dissepiment centers).
7. **AL**: *aperture length* (measured proximodistally).
8. **AW**: *aperture width* (measured perpendicular to length).
9. **ADB**: *distance between aperture centers along branch.*
10. **AAB**: *distance between aperture centers across branch.*
11. **ABB**: *distance between aperture centers between branches.*
12. **DN**: *diameter of nodes along obverse branch surface.*
13. **DND**: *diameter of nodes on dissepiments.*
14. **SNB**: *distance between node centers along obverse branch surface.*
15. **WK**: *width of keel.*
16. **DSO**: *diameter of stylets on obverse surface.*
17. **SSO**: *spacing of stylets along obverse branch surface.*
18. **WP**: *width of peristome* (measured at distal end of aperture).
19. **SA**: *number of stylets surrounding aperture.*
20. **SAD**: *diameter of small stylets surrounding aperture.*
21. **RSL**: *diameter of macrostylets on reverse branch surface.*
22. **RSS**: *diameter of microstylets on reverse branch surface.*
23. **SSL**: *spacing of macrostylets along reverse branch surface.*
24. **SSS**: *spacing of microstylets along reverse branch surface.*
25. **LRM**: *reticulate meshwork spacing parallel to direction of branch growth.*
26. **WRM**: *reticulate meshwork spacing perpendicular to direction of branch growth.*
27. **WSC**: *spacing of whorls along central axis* (spire).
28. **DCA**: *maximum diameter of central axis.*
29. **ACA**: *angle between distal end of axis and axial whorl.*
30. **OL**: *ovicell length* (measured proximodistally).
31. **OW**: *ovicell width* (measured perpendicular to ovicell length).

Interior characters:

32. **TRW**: *thickness of reverse-wall granular layer.*
33. **TLW**: *thickness of chamber lateral-wall granular layer.*
34. **FWT**: *thickness of front-wall (obverse-wall) laminated layer.*
35. **RWT**: *thickness of reverse-wall laminated layer.*
36. **CL**: *autozooecial chamber length* (maximum dimension measured down the middle of the chamber).
37. **CD**: *autozooecial chamber depth* (measured from obverse to reverse surface, perpendicular to chamber length).
38. **MAW**: *maximum chamber width* (measured across the branch).
39. **MIW**: *minimum chamber width* (measured across the branch).
40. **VD**: *vestibule depth* (where significant).
41. **RA**: *chamber reverse-wall budding-angle* (an acute angle).
42. **LA**: *chamber lateral-wall budding-angle* (angle between aperture opening and plane defined by center of branch surface. In species with more than two rows of zooecia, use **LA-1** for adaxial zooecia and **LA-2** for abaxial zooecia).
43. **TB**: *thickness of branch* (measured in obverse–reverse direction).
44. **WOT**: *maximum width of ovicell in mid tangential view.*

PREPARATION OF MANUSCRIPTS

Palaeontographica Americana currently appears irregularly, on an average of about one monograph each year. This series is a publication outlet for significant longer paleontological monographs for which high quality photographic illustrations and the large quarto format are a requisite.

Manuscripts submitted for publication in this monograph series must be typewritten, and double-spaced *throughout* (including direct quotations and references). All manuscripts should contain a table of contents, lists of text-figures and (or) tables, and a short, informative abstract that includes names of all new taxa. Format should follow that of recent numbers in the series. All measurements must be stated in the metric system, alone or in addition to the English system equivalent. The maximum dimensions for photographic plates are 178 mm × 229 mm (7″ × 9″; outlined on this page). Single-page text-figures should be drafted for reproduction as single column (82 mm; 3¼″) or full page (178 mm; 7″) width, but arrangements can be made to publish text-figures that must be larger. Any lettering in illustrations should follow the recommendations of Collinson (1962).

Authors must provide three (3) copies of the text and accompanying illustrative material. The text and line-drawings may be reproduced xerographically, but glossy prints at publication scale must be supplied for all half-tone illustrations and photographic plates. These prints should be identified clearly on the back.

All dated text-citations must be referenced. Additional references may be listed separately if their importance can be demonstrated by a short general comment, or individual annotations. Referenced publication titles must be spelled out in their entirety. Citations of illustrations within the monograph bear initial capitals (*e.g.*, Plate, Text-figure), but citations of illustrations in other articles appear in lower-case letters (*e.g.*, plate, text-figure).

Original plate photomounts should have oversize cardboard backing and strong tracing paper overlays. These photomounts should be retained by the author until the manuscript has been formally accepted for publication. Explanations of text-figures should be interleaved on separate numbered pages within the text, and the approximate position of the text-figure in the text should be indicated. Explanations of plates follow the Bibliography.

Authors are requested to enclose $10 with each manuscript submitted, to cover costs of postage during the review process.

Collinson, J.

1962. *Size of lettering for text-figures.* Journal of Paleontology, vol. 36, p. 1402.

Gilbert Dennison Harris
(1864 - 1952)

Founder of *Palaeontographica Americana* (1916)

ISBN 0-87710-419-0